NASA Technical Paper 3542

Internal Performance of Highly Integrated Deployable Exhaust Nozzles Applicable to Advanced Short-Takeoff and Vertical-Landing Aircraft

Scott C. Asbury, Mary L. Mason, and Milton Lamb

October 1995

NASA Technical Paper 3542

Internal Performance of Highly Integrated Deployable Exhaust Nozzles Applicable to Advanced Short-Takeoff and Vertical-Landing Aircraft

Scott C. Asbury, Mary L. Mason, and Milton Lamb
Langley Research Center • Hampton, Virginia

National Aeronautics and Space Administration
Langley Research Center • Hampton, Virginia 23681-0001

October 1995

Available electronically at the following URL address: http://techreports.larc.nasa.gov/ltrs/ltrs.html

Printed copies available from the following:

NASA Center for AeroSpace Information
800 Elkridge Landing Road
Linthicum Heights, MD 21090-2934
(301) 621-0390

National Technical Information Service (NTIS)
5285 Port Royal Road
Springfield, VA 22161-2171
(703) 487-4650

Abstract

An investigation was conducted in the Jet-Exit Test Facility of the Langley 16-Foot Transonic Tunnel to evaluate the internal performance of highly integrated deployable exhaust nozzles (HIDEN) applicable to advanced short-takeoff and vertical-landing tactical aircraft. This investigation studied the performance of four HIDEN nozzle concepts in both the forward (thrust) and vertical (lift) operation modes. Two plenum designs with different offtake duct geometries varied the vertical distance between the plenum centerline and bearing plane surface centerline. Four plenum centerbodies with interchangeable blockers were tested to simulate engine fan- and core-mounted nozzle installations. All tests were conducted with no external flow and nozzle pressure ratio (NPR) was varied from 1.5 to approximately 6.0. Results indicate that the HIDEN nozzle concept has internal performance characteristics comparable to thrust-vectoring convergent-divergent nozzles. However, the exhaust flow was slightly underturned with each nozzle design, which resulted in a cosine thrust loss. Nozzles installed on the offset plenum had higher internal performance than the same nozzles installed on the centerline plenum throughout the entire NPR range investigated. Changing operation mode had only small effects on internal performance characteristics. Centerbody and blocker effects were also small.

Introduction

Operational requirements for the next generation of tactical aircraft will emphasize increased flexibility and affordability over current designs. Economic considerations will necessitate aircraft capable of meeting multimission, multiservice, and multinational requirements while maintaining the highest possible combat effectiveness. Therefore, tactical aircraft mission and performance goals are likely to include short-takeoff and vertical-landing (STOVL) capability, supersonic cruise at dry power (supercruise), and low-observable (stealth) characteristics. Stealth and supercruise will assure survivability by reducing the target acquisition envelope of threat missiles and guarantee lethality by providing an aircraft with a first shot advantage. The STOVL capability will offer increased basing flexibility and high sortie rates not possible with conventional takeoff and landing (CTOL) aircraft.

The operational benefits of STOVL capability have been demonstrated by the subsonic Harrier aircraft (refs. 1 to 4). With the ability to operate from small, makeshift strips, the Harrier does not require vulnerable airfields and can reposition closer to a changing line of battle (ref. 1). Unfortunately, aircraft control in hover dictated propulsion system requirements for the Harrier (i.e., high bypass ratio, low specific thrust) that were counterproductive to efficient high-speed performance (ref. 2). Design tradeoffs resulting from the STOVL requirement have left the Harrier lacking the necessary maneuverability, supersonic performance, and stealth characteristics that are critical to future combat effectiveness.

Recent advances in engine technology that enable higher specific thrust for high bypass-ratio engines have overcome many of the penalties previously associated with STOVL propulsion systems. Considerable effort by engine and airframe companies has been applied to develop aircraft and propulsion system concepts suitable for supersonic advanced short-takeoff and vertical-landing (ASTOVL) applications (refs. 5 and 6). One ASTOVL engine design is the tandem-fan engine concept, which was the focus of the Supersonic Tandem-Fan V/STOL Ground Demonstrator Study that was funded by the United States Navy and initiated in 1982. Under this study, a derivative of the tandem-fan engine called the hybrid-fan vectored thrust (HFVT) concept was developed (ref. 7). The HFVT concept requires that flow from the forward fan be discharged through a pair of ventral nozzles for STOVL, transition, and possibly throughout significant portions of the subsonic flight envelope. The remaining exhaust flow is discharged through a single thrust-vectoring nozzle at the rear of the engine. When the ventral nozzles are no longer needed, an internal flow diverter valve routes the forward fan air to the aft fan and closes the air supply to the ventral nozzles. Critical to the success of the HFVT concept is the development of a ventral nozzle system that not only possesses good performance during STOVL and subsonic operations, but is also capable of adopting a low drag, low observable profile during high-speed flight.

One of the ventral nozzle concepts developed as a result of the supersonic tandem-fan study was the highly integrated deployable exhaust nozzle (HIDEN). This ingenious design takes advantage of geometric characteristics inherent to thrust-vectoring ventral nozzles. Each

nozzle is stowed by simply rotating about its main bearing. An artist's concept of a typical HIDEN installation is shown in figure 1. The relatively simple stowing and deploying capability requires that the relationship between fundamental geometric parameters be maintained. Nozzle geometry, engine offtake duct geometry, and fuselage mold lines must all be manipulated to achieve a balance between minimum stowed volume, minimum weight, and acceptable performance. A drawing of the HIDEN concept installed in the fan section of the HFVT engine is presented in figure 2.

To evaluate the internal performance of the HIDEN concept, an investigation was conducted at static (no external flow) conditions in the Jet-Exit Test Facility of the Langley 16-Foot Transonic Tunnel. Four convergent nozzle designs were tested in the forward (thrust) and vertical (lift) operation modes. Two plenum designs with offtake duct geometries that varied the vertical distance between the plenum (engine) centerline and the bearing plane surface centerline were tested. Four plenum centerbodies with interchangeable blockers were tested to investigate engine fan- and core-mounted ventral nozzle installations. High-pressure air was used to simulate jet exhaust flow at nozzle pressure ratios (NPR's) from 1.5 to approximately 6.0.

The research presented in this report is the result of a cooperative effort between Rolls-Royce, Inc. and NASA. Program funding was provided by NASA, Rolls-Royce, and the United Kingdom Defence Research Agency. The HIDEN concept and model hardware were designed and developed by Rolls-Royce. The investigation was conducted by the staff of the Component Integration Branch at the Langley Research Center in Hampton, Virginia.

Symbols

All forces and moments (with the exception of resultant thrust) are referenced to the model centerline (body axis). The model (balance) moment reference center was located at model station (MS) 5.500. A discussion of the data reduction procedure, the definitions of the force and moment terms, and the propulsion relationships used herein can be found in reference 8.

A core centerbody length, in.

A_t measured geometric nozzle throat area, in^2

F_A measured thrust along body axis, positive in forward direction, lbf

F_i ideal isentropic gross thrust,

$$w_p\sqrt{\frac{R_j T_{t,j}}{g^2}\frac{2\gamma}{\gamma-1}\left[1-\left(\frac{1}{\mathrm{NPR}}\right)^{(\gamma-1)/\gamma}\right]}, \text{ lbf}$$

F_N measured normal force, positive upward, lbf

F_{RR} used to compute δ_{RR} for a single nozzle, $\sqrt{\frac{1}{2}}F_N$ in thrust mode, $\sqrt{\frac{1}{2}}F_A$ in lift mode, lbf

F_r resultant thrust, $\sqrt{F_A^2+F_N^2+F_S^2}$, lbf

F_S measured side force, positive to right when looking upstream, lbf

g acceleration due to gravity, 32.174 ft/sec^2

L length of instrumented ramp, in.

l_s streamline length from bearing plane to nozzle exit, in.

NPR nozzle pressure ratio, $p_{t,j}/p_a$

p local static pressure, psi

p_a ambient pressure, psi

$p_{t,j}$ average jet total pressure, psi

R_j gas constant (for $\gamma = 1.3997$), 1716 ft^2/sec^2-°R

s distance along streamline measured from bearing plane, in.

$T_{t,j}$ jet total temperature, °R

w_i ideal isentropic weight-flow rate,

$$A_t p_{t,j}\left(\frac{2}{\gamma+1}\right)^{\frac{\gamma+1}{2(\gamma-1)}}\sqrt{\frac{\gamma g^2}{T_{t,j}R_j}} \text{ for NPR} > 1.89,$$

$$A_t p_{t,j}\left(\frac{1}{\mathrm{NPR}}\right)^{\frac{1}{\gamma}}\sqrt{\frac{2g\gamma}{(\gamma-1)T_{t,j}R_j}\left[1-\left(\frac{1}{\mathrm{NPR}}\right)^{\sqrt{(\gamma-1)/\gamma}}\right]}$$

for NPR ≤ 1.89, lbf/sec

w_p measured weight-flow rate, lbf/sec

X, Y, Z coordinates, in.

x length along instrumented ramp, in.

γ ratio of specific heats, 1.3997 for air

δ_{RR} computed exhaust flow angle, $\tan^{-1}\left(\frac{\sqrt{2}F_N}{F_A}\right)$ in thrust mode, $90° - \tan^{-1}\left(\frac{\sqrt{2}F_A}{F_N}\right)$ in lift mode, deg

ϕ flow turning angle in nozzle, deg

Model Component Designations:

B_F flat blocker

B_N no blocker

B_T tapered blocker

C_F fan centerbody

C_L long-core centerbody

C_M	medium-core centerbody
C_S	short-core centerbody
L	lift mode
N_1	1.8 CR D-shaped nozzles
N_2	1.4 CR D-shaped nozzles
N_3	1.4 CR Pegasus nozzles
N_4	1.4 CR submerged nozzles
P_C	centerline plenum
P_O	offset plenum
T	thrust mode

Abbreviations:

ASTOVL	advanced short takeoff and vertical landing
C-D	convergent-divergent
CR	contraction ratio
CTOL	conventional takeoff and landing
HFVT	hybrid-fan vectored thrust
HIDEN	highly integrated deployable exhaust nozzle
MS	model station, in.
STOVL	short takeoff and vertical landing
V/STOL	vertical/short takeoff and landing
WL	waterline

Description of Test Facility

This investigation was conducted in the Jet-Exit Test Facility of the Langley 16-Foot Transonic Tunnel. Tests are conducted in a large room where the jet from a dual-flow single-engine propulsion simulation system vents to the atmosphere through an acoustically treated exhaust passage. A control room is remotely located from the test room and a closed-circuit television is used to observe the model when the jet is operating. The Jet-Exit Test Facility has an air control system that is similar to that of the 16-Foot Transonic Tunnel and includes valves, filters, and a heat exchanger to maintain the jet flow at a constant stagnation temperature. The air system utilizes the same clean, dry air supply that is used by the 16-Foot Transonic Tunnel (ref. 9).

Dual-Flow Single-Engine Propulsion Simulation System

The HIDEN model was tested on a dual-flow single-engine propulsion simulation system consisting of an axisymmetric air-powered model mounted on a six-component strain-gauge balance (fig. 3). An external high-pressure air system supplies the simulator with a continuous flow of clean, dry air at a constant stagnation temperature of about 540°R inside the HIDEN plenum. This high-pressure air was varied during the jet simulation to approximately 80 psi in the HIDEN nozzles.

Independently controlled primary and secondary flow systems provide pressurized air to isolated plenum chambers on the dual-flow system through two pairs of semirigid, thin-walled (0.021-in. wall thickness), 1-in. diameter, S-shaped, stainless steel tubes (S-tubes). These tubes provide flexible connections that transfer air from the nonmetric to the metric (supported by the force balance) part of the system. The geometric design of the airflow system minimizes any balance force and moment tares that can be generated by flexure of the S-tubes as air pressure is increased or by transfer of axial momentum as pressurized air passes into the plenum. The primary and the secondary air systems can be used separately or combined for dual-flow operation. For the current investigation, only the primary air system was used.

High-pressure air supplied to the primary plenum is delivered by a 15 lbf/sec air system that contains dual in-line venturis for weight-flow measurements. From the primary plenum, air is discharged radially into an annular low-pressure duct (on the model centerline) through eight equally spaced sonic nozzles. The primary airflow then passes over a bullet fairing and through an annular choke plate (primarily used as a flow straightener) before entering the HIDEN plenum at model station (MS) 18.370. Flow characteristics are measured in the HIDEN plenum at MS 19.370 by static-pressure, total-pressure, and total-temperature instrumentation before the flow enters the offtake ducts and exhausts through the HIDEN nozzles to sea level static conditions.

Highly Integrated Deployable Exhaust Nozzle Concept

The HIDEN concept is a design for thrust-vectoring ventral nozzles that can be stowed within an airframe by rotating the nozzles about their main bearing (fig. 2). This concept requires a highly integrated engine and airframe because the stowing and deploying capabilities of HIDEN nozzles must maintain the relationship between fundamental geometric parameters. The area required by the bearing plane inside the fuselage affects the weight and the volume of the installation and the Mach number of flow entering the nozzle. Nozzle geometry and fuselage mold lines must be manipulated to achieve a balance between minimum stowed volume, minimum weight, and acceptable performance. Optimal flow quality at the nozzle bearing plane is critical to overall exhaust-system performance. Unlike nozzles for engines with plenum chamber burning, HIDEN nozzles are not intended to be augmented. Engines with plenum chamber burning have a colander positioned upstream of the nozzle bearing plane to stabilize the combustion flame and to serve as a

flow conditioning device. The HIDEN nozzles, however, are subject to all upstream flow disturbances caused by flow switching valves, bypass ducts, and blockers.

Highly Integrated Deployable Exhaust Nozzle Model

The subscale model hardware that was tested during this investigation simulated the internal flow path of the HIDEN concept and consisted of the components necessary to assemble fan- and core-mounted nozzle installations in the thrust and the lift operation modes. The model consisted of two plenums, four pairs of nozzles, four centerbodies, and four blockers. Additional hardware included adapters to the dual-flow system on the upstream side of the plenum and adapters to the twin-engine calibration equipment of reference 9 on the downstream side of the plenum.

The HIDEN plenum was attached to the dual-flow system at the facility adapter and the bullet fairing (fig. 3). Photographs of the HIDEN hardware installed on the propulsion simulation system are presented in figures 4 and 5. The facility adapter mated to the primary plenum and acted as a seal for the secondary plenum. The bullet fairing provided a smooth transition from the primary system balance and bullet assembly to the HIDEN model hardware and provided a convenient surface for mounting the choke plate (fig. 3). The internal diameter of the primary flow path at the attachment plane was 5.064 in.

Plenums

The vertical position of the HIDEN offtake duct from the plenum centerline was expected to have a significant impact on flow quality at the nozzle bearing plane. Therefore, two plenum designs that varied the vertical distance between the plenum centerline and the bearing plane surface centerline were tested. The offset plenum (fig. 4) had the bearing plane surface centerline positioned below the plenum centerline; whereas, the centerline plenum (fig. 5) had the bearing plane surface centerline positioned at the plenum centerline. The centerline plenum was designed to minimize the moment arm between the balance moment center and the thrust axis when the nozzles were operating in the thrust mode, thereby minimizing the amount of pitching moment generated. Sketches showing the offset and the centerline plenum geometries are presented in figures 6 and 7, respectively. Both plenums had offtake duct droop and trail angles of 45° each (see fig. 6(b) and fig. 7(d)), which were representative of a typical HIDEN installation between the engine and aircraft fuselage.

The offset plenum assembly consisted of the offset plenum, offtake ducts, offtake duct sleeves, instrumented sleeves or spacer rings, and a pair of HIDEN nozzles (fig. 6). The offtake ducts extended from the plenum at droop and trail angles of 45°, which required the flow to turn a true angle of 54.74° from the plenum centerline to the nozzle bearing plane. The offtake duct centerlines intersect the plenum centerline and the bearing plane surfaces lay below the horizontal centerline plane of the plenum (fig. 6(b)). The internal intersections of the offset plenum and the offtake ducts were given a minimum curvature that was approximately 15 percent of the offtake duct diameter. An offtake duct sleeve (fig. 6(c)) was bolted to the downstream face of each offtake duct and was designed to accept either an instrumented spacer ring, an instrumented sleeve, or a blanking plate for model pressurization. Static-pressure measurements taken in the instrumented sleeves and instrumented spacer rings were used to determine the pressure distribution at each bearing plane and to evaluate flow symmetry between the left and the right offtake ducts. The 1.8 contraction ratio (CR) nozzles were tested with instrumented spacer rings installed between the offtake duct sleeves and the nozzles. The 1.4 CR nozzles were tested with the instrumented sleeves, which reduced the offtake duct diameter to match the nozzle bearing plane surface geometry (fig. 6(a)).

The centerline plenum had offtake ducts positioned as high on the plenum as possible (fig. 7). The offtake ducts extended from each side of the plenum with 45° of droop and trail angle and had a constant-diameter bend of 35.26° (which resulted in a required flow turning angle of 80.26° from the plenum centerline to the nozzle bearing plane). The offtake ducts were positioned so that the centerline of the bearing plane surface lay in the same horizontal plane as the centerline of the plenum (fig. 7(d)). The intersection of the offtake ducts and the plenum was fairly sharp, with the curvature less than 3 percent of the offtake duct diameter. The downstream face of each offtake duct accepted either an instrumented spacer ring or a blanking plate for model pressurization (fig. 7(a)). The curved offtake duct geometry prevented installation of the instrumented sleeves and therefore, the 1.4 CR nozzles were not tested on the centerline plenum.

Nozzles

Photographs of the four HIDEN nozzles tested are presented in figure 8 and geometric details of each nozzle are presented in figure 9. Design specifications for the HIDEN nozzles are summarized in the following chart.

Coordinates defining the nozzle internal flow path and turning vane geometries are presented for each

Nozzle	A_l, in^2	ϕ, deg	Scarf angle, deg	Splay angle, deg
1.8 CR D-shaped	4.022	54.74	19.67	0
1.4 CR D-shaped	4.022	54.74	19.67	0
1.4 CR Pegasus	4.078	54.74	19.67	0
1.4 CR submerged	4.022	42.24	29.74	12.5

nozzle as sets of spline data in tables 1 to 4. Each nozzle is defined by a set of splines in planes parallel to the symmetry plane and by a set of vertical splines which run from the bearing plane to the nozzle exit. These splines were used to define a meshed surface that described the aerodynamic nozzle shape. Computational fluid dynamics was used to design the shape and the location of the turning vanes for the D-shaped and submerged nozzles, while the turning vanes in the Pegasus nozzles were based on the current turning vane design in the Rolls-Royce Pegasus engine.

Three of the HIDEN nozzles were designed with common specifications tailored to a specific fuselage integration. The 1.8 CR D-shaped nozzles (fig. 9(a)), the 1.4 CR D-shaped nozzles (fig. 9(b)), and the 1.4 CR Pegasus nozzles (fig. 9(c)) were designed to turn the flow 54.74° from the bearing plane to the nozzle thrust plane to produce pure axial force (Splay angle = 0°). Each of these configurations had a scarf angle of 19.67°. The scarf angle was designed to position the nozzle exit plane parallel to a nominal fuselage surface when the nozzle was rotated to the stowed position. (See fig. 2(b).)

The 1.8 CR D-shaped nozzles (fig. 9(a)) had a contraction ratio of 1.8 from the bearing plane to the D-shaped exit plane. The nozzle geometry was designed to minimize the size of the hole in the fuselage that would be required for rotation of the nozzles about the main bearing. Two turning vanes were installed in each nozzle to span approximately half the internal flow field. The outer turning vane extended downstream along the nozzle centerline and the inner turning vane extended along the quarter line. (See fig. 9(a).) The vanes were positioned so that the leading edges were near the start of the nozzle turn and the trailing edges were located at the nozzle exit.

The 1.4 CR D-shaped nozzles (fig. 9(b)) were designed to evaluate the effect of contraction ratio (or bearing-plane diameter) on nozzle performance. The nozzle and turning vane geometries were identical to those of the 1.8 CR D-shaped nozzles from a plane just upstream of the leading edge of the turning vanes to the exit plane. Nozzle geometry upstream of the turning vanes was changed from the 1.8 CR D-shaped nozzle geometry to set the 1.4 contraction ratio.

The 1.4 CR Pegasus nozzles (fig. 9(c)) were designed with two turning vanes spaced equally across the internal flow path. Nozzle exit shape and vane positions were designed for compatibility with the curren Rolls-Royce Pegasus engine nozzle design. From a plane upstream of the leading edge of the turning vanes to the nozzle exit plane, the inner and the outer flow channels between the vanes had a semielliptical cross section and the middle channel had a rectangular cross section.

The 1.4 CR submerged nozzles (fig. 9(d)) incorporated a different design criteria from the other nozzl configurations. In actual application, these nozzles woul be partially submerged inside the aircraft fuselage. I thrust mode, the jet would exhaust along a ramp tha formed the side fuselage boundary; in the stowed mode the ramp would cover the nozzle exit. A typical installation of the submerged nozzles in the fan section of th HFVT engine is shown in figure 9(e). To model the partially submerged orientation, the 1.4 CR submerge nozzles were designed with a reduced nozzle flow turning angle $\phi = 42.24°$, which imposed a nozzle spla angle of 12.5°. (For the other nozzles, $\phi = 54.74°$ an Splay angle = 0°.) This nozzle design had a super elliptical exit geometry, a single turning vane, and a scar angle of 29.74°.

Centerbodies

To evaluate the effect of offtake duct position or performance, four axial locations of the offtake duc openings were simulated by using interchangeable centerbodies. Geometric details of the fan and core centerbodies are presented in figure 10(a) and typica centerbody installations are shown in figure 10(b). The centerbodies were bolted to the downstream face of the system choke plate (fig. 3) and were designed to simulate engine fan- and core-mounted nozzle installations. The fan centerbody simulated a forward engine fan-mounted nozzle and the three core centerbodies simulated af engine core-mounted nozzles.

The fan centerbody extended the full length of the plenum from the choke plate to the model blanking plate. This centerbody had a cylindrical shape with a constant diameter of 2.727 in. The diameter was chosen to provide a nominal Mach number of 0.35 at the instrumented charging plane upstream of the duct and nozzle assembly (MS 19.370 in fig. 3).

Each core centerbody was a constant-diameter cylinder with a tapered truncated cone at the downstream end. The diameter of the cylindrical section was 2.727 in., identical to the fan centerbody diameter. The tapered end

had a 20° boattail angle to simulate a turbine exit cone. The long-core centerbody was designed to span the length of the plenum from the choke plate to the tapered blocker. (See fig. 3.) The short-core centerbody was designed to position the start of the cone boattail radius near the downstream edge of the instrumented rakes. The length of the medium-core centerbody was designed to be the average length of the long-core and the short-core centerbodies.

Blockers

Two blockers, a flat concept and a tapered concept, were designed for the fan and the core centerbodies. The fan blocker geometries are presented in figure 11(a) and the core blocker geometries are presented in figure 11(b). Typical fan and core blocker installations are presented in figure 11(c). The blockers were designed to close the cavity between the centerbody and the end of the plenum to the most downstream intersection point between the plenum wall and the offtake ducts (fig. 3). Each blocker was bolted to the upstream face of the plenum end cap and inserted into the end of the plenum. The fan and the core blockers were similar, except that the fan blockers had an opening to allow the fan centerbody through each blocker. A no-blocker configuration was also tested for each centerbody. These configurations were assembled without a blocker section so that a cavity between the offtake ducts and the end cap was formed within the plenum.

The flat blocker concept provided a surface perpendicular to the plenum centerline which inhibited downstream internal flow within the plenum. The tapered blocker concept provided an angled surface to block the internal flow. The tapered fan blocker had a taper half angle of 32.35°; the tapered core blocker had a taper half angle of 45°.

Instrumentation

All forces and moments were measured by a six-component strain-gauge balance located on the centerline of the propulsion simulation system (fig. 3). The weight-flow rate of high-pressure air supplied to the model was calculated from static-pressures and temperatures measured at the dual in-line venturis. Flow conditions in the HIDEN plenum were determined by total-pressure, static-pressure, and total-temperature measurements taken at MS 19.370. Each HIDEN plenum was equipped with eight static-pressure taps, four total-pressure rakes with five probes each, and seven iron-constantan thermocouples (four in the centerline plenum and three in the offset plenum) (figs. 6(b) and 7(b)). Flow total pressure and temperature were determined by the average of these measurements.

Static pressures were measured upstream of each nozzle by orifices located in an instrumented spacer ring (fig. 12(a)) on 1.8 CR nozzle assemblies and in an instrumented sleeve (fig. 12(b)) on 1.4 CR nozzle assemblies. The left (looking upstream) nozzle of each pair was equipped with static-pressure taps on the internal surfaces between the start of the turning vanes and the nozzle exit. The orifice locations for each of the nozzles are given in figure 13. As shown in figure 13, a coordinate system was chosen to define the position of the static taps in each nozzle along an approximate flow streamline located in the plane of $Z = -0.350$ in. Each tap was located a distance s along the length of the streamline, l_s. For the inner wall taps, l_s approximated the contour length of the nozzle inner wall at the plane of $Z = -0.350$ in. For the channel taps (see figs. 13(b) to 13(d)), which are located on the interior surface of the nozzle, l_s consisted of a straight line fairing from the bearing plane, through the tap locations (projected onto the plane of $Z = -0.350$ in.) to the nozzle exit. Because only one tap was located in each channel of the 1.8 CR D-shaped nozzle, an s/l_s location based on the last tap of the inner wall was chosen for the channel taps and no l_s was calculated (fig. 13(a)).

A ramp, which simulated a fuselage side, was bolted to the downstream face of the plenum blanking plate and was instrumented to measure pressures downstream of the exit of the left submerged nozzle during thrust mode operation. A sketch showing the geometry of the ramp and the location of the pressure taps is presented in figure 14. Figure 4(a) shows a photograph of the submerged nozzle with the instrumented ramp installed. During this investigation, all total pressures were measured with individual pressure transducers, while all static pressures were measured with electronically scanning pressure devices.

Flow Visualization

Nozzle internal flow visualization was obtained by using a mixture of linseed oil, tempera paint, and kerosene. The paint mixture was brushed onto the model surface across the flow direction so that a predetermined paint pattern inside the nozzle could not be misinterpreted as flow streamlines. The propulsion simulation system was then turned on. The jetflow evaporated the kerosene, which left a residue showing the surface flow patterns inside the nozzle. Data were obtained for each HIDEN nozzle in thrust mode at nominal NPR = 4.0. Although analysis based on this type of flow visualization is fairly subjective, it can provide insight into the flow behavior on and near the painted surfaces (ref. 10).

Data Reduction

Each data point is the average steady-state value computed from 50 frames of data taken at a rate of 10 frames per second. All data were taken in ascending order of $p_{t,j}$. Balance measurements were initially corrected for model weight tares and isolated-balance component interactions. Additional calibrations of the balance installed in the dual-flow system were performed to determine jet-off installation tares and to measure the effects of model pressurization and nozzle throat area. Although the S-tube geometry in the air system was designed to minimize balance effects due to pressurization and flow transfer, small tares resulted as the S-tubes deformed slightly under pressure. These tares were determined by testing single-engine calibration nozzles with known performance over ranges of expected internal pressure and external forces and moments. The jet-off and momentum and pressurization corrections were then applied to fully correct the balance data.

Two twin-engine calibration adapter assemblies were fabricated with the HIDEN model hardware to perform additional balance calibrations (fig. 15). The calibration adapters were attached to the downstream end of the offtake duct sleeves on the offset plenum or to the offtake ducts on the centerline plenum. The twin-engine calibration nozzles discussed in reference 9 were attached to the downstream end of the calibration adapters. The combination of droop and trail angles facilitates balance calibrations, because the twin-engine calibration nozzles can be rotated 120° about the bearing plane to provide either pure axial force (thrust mode) or pure normal force (lift mode). Comparisons between the thrust and lift mode calibration data were used extensively during the data reduction and analysis process. A detailed description of the procedures used for data reduction and analysis in this investigation can be found in reference 8.

Four basic nozzle internal performance parameters are used in the presentation of results: the internal thrust ratio (F_A/F_i in thrust mode, F_N/F_i in lift mode), the resultant thrust ratio F_r/F_i, the discharge coefficient w_p/w_i, and the computed exhaust flow angle δ_{RR}.

The internal thrust ratio is the ratio of the measured nozzle thrust to ideal isentropic thrust. Ideal thrust F_i is based on measured weight flow w_p, jet total pressure $p_{t,j}$, and jet total temperature $T_{t,j}$. The resultant thrust ratio F_r/F_i is the resultant thrust divided by the ideal isentropic thrust. Resultant thrust is obtained from the measured axial, normal, and side components of the jet resultant force. The internal thrust ratio includes a reduction in thrust that results from the flow underturning or overturning what is produced by the nozzles, whereas the resultant thrust F_r does not. Losses included in both terms are the result of friction and pressure drags associated with the plenum and nozzle internal geometry.

The nozzle discharge coefficient w_p/w_i is the ratio of measured weight-flow rate from upstream venturi measurements to ideal weight-flow rate, which is calculated from the measured nozzle throat area A_t and total-pressure and temperature measurements taken inside the plenum. Discharge coefficient is a measure of the nozzle efficiency in passing weight flow, and in an actual engine should be held constant to assure efficient engine operation.

The parameter δ_{RR} is the computed exhaust flow angle for each nozzle that ideally, for nozzles with no splay angle, should be 0° in thrust mode and 90° in lift mode. Values of δ_{RR} that are not ideal result in an effective cosine thrust loss that occurs when the exhaust flow exits the nozzles misaligned with the nominal (thrust or lift) plane. In thrust mode operation, the definition of δ_{RR} is based on the assumption that a side force is generated by the nozzles that is equal to the measured normal force because the nozzles lie in a 45° droop plane (fig. 16(a)). The side force measured by the balance is approximately zero due to the symmetry of the two nozzles about the plenum. Flow underturning is indicated by positive values of δ_{RR} and flow overturning is indicated by negative values of δ_{RR}. In lift mode operation, the definition of δ_{RR} is based on the assumption that a side force is generated by the nozzle that is equal to the axial force because the nozzles lie in a 45° trail plane. Flow underturning is indicated by values of δ_{RR} less than 90° and flow overturning is indicated by values of δ_{RR} greater than 90°.

Presentation of Results

The results of this investigation are presented in both tabular and plotted forms. Basic nozzle internal performance data for each configuration tested are presented in tables 5 to 24. Nozzle internal static-pressure ratios $p/p_{t,j}$ are given in tables 25 to 124 for each model configuration tested. Nozzle internal static-pressure ratios $p/p_{t,j}$ are plotted in the vicinity of the turning vanes. Static-pressure ratios for the first tap along the nozzle inner wall were not plotted, but their values can be found in the tables. During discussion of the results, comparisons of nozzle internal performance are made with percentage change from isentropic conditions.

Comparison plots and flow visualization for selected configurations are presented in figures 17 to 35 as follows:

Figure

HIDEN nozzles in thrust mode on the offset plenum with short-core centerbody and no blocker showing
Internal performance characteristics 17
Nozzle internal static-pressure distributions 18
Flow visualization inside the HIDEN nozzles; nominal NPR = 4.0 19
Effect of CR and NPR on offtake duct static-pressure ratios for D-shaped nozzle 20

1.8 CR D-shaped nozzles with short-core centerbody and no blocker showing
Effect of plenum type on performance 21
Effect of plenum type on offtake duct static-pressure ratios; nominal NPR = 4.0 22

1.8 CR D-shaped nozzles installed on the offset plenum showing
Effect of operation mode on performance 23
Effect of operation mode on offtake duct static-pressure ratios; nominal NPR = 4.0 24

1.8 CR D-shaped nozzles installed on the centerline plenum showing
Effect of operation mode on performance 25
Effect of operation mode on offtake duct static-pressure ratios; nominal NPR = 4.0 26

1.8 CR D-shaped nozzles in thrust mode installed on the offset plenum showing
Effect of centerbody type on performance 27
Effect of centerbody type on offtake duct static-pressure ratios; nominal NPR = 4.0 28

1.8 CR D-shaped nozzles in thrust mode installed on the centerline plenum showing
Effect of centerbody type on performance 29
Effect of centerbody type on offtake duct static-pressure ratios; nominal NPR = 4.0 30

1.8 CR D-shaped nozzles in thrust mode installed on the offset plenum showing
Effect of blocker type on performance 31
Effect of blocker type on offtake duct static-pressure ratios; nominal NPR = 4.0 32

1.8 CR D-shaped nozzles in thrust mode installed on the centerline plenum showing
Effect of blocker type on performance 33
Effect of blocker type on offtake duct static-pressure ratios; nominal NPR = 4.0 34

1.4 CR submerged nozzles in thrust mode installed on the offset plenum with fan centerbody showing
Instrumented-ramp static-pressure ratios 35

Results and Discussion

Unless stated otherwise, the effect of nozzle geometry will be discussed for HIDEN nozzles installed on the offset plenum in thrust mode with short-core centerbody and no blocker. The effects of plenum geometry, centerbody geometry, blocker geometry, and operation mode (thrust or lift) will be discussed in subsequent sections.

Effect of Nozzle Geometry

The internal performance characteristics of HIDEN nozzles installed on the offset plenum in thrust mode are summarized in figure 17. Internal thrust ratio F_A/F_i, resultant thrust ratio F_r/F_i, discharge coefficient w_p/w_i, and computed exhaust flow angle δ_{RR} are presented as a function of nozzle pressure ratio (NPR). Internal and resultant thrust ratios for each nozzle increased to a maximum value between NPR's of 3.0 and 4.0, then decreased with increasing NPR. This pattern of increase and decrease suggests an effective expansion ratio greater than 1.0 for HIDEN nozzles, although the nozzles were designed with no geometric internal divergence. This pattern implies that the physical throat formed inside the nozzle. As a result, HIDEN nozzle thrust ratio trends are similar to low expansion ratio convergent-divergent (C-D) nozzles (ref. 11). Typically, C-D nozzle thrust ratios increase with increasing NPR until a maximum value is reached near the design NPR (the NPR required for fully expanded flow at the nozzle exit). Thrust levels then decrease with increasing NPR because of losses associated with nozzle underexpansion effects.

A physical throat location upstream of the nozzle exit is confirmed by internal static-pressure distributions plotted for each instrumented nozzle in figure 18. Static-pressure distributions $p/p_{t,j}$ are presented as a function of the nondimensionalized orifice location s/l_s for each NPR investigated. Sonic conditions are reflected by a $p/p_{t,j}$ value of 0.528. It is apparent from these pressure distributions that the physical throat formed upstream of the exit ($p/p_{t,j} \leq 0.528$ at $s/l_s < 1.000$) in each HIDEN nozzle tested and that the location of the throat varied somewhat with NPR. This result is understandable, as several factors (including local flow separation on the nozzle inner wall or turning vanes) could have resulted in a local minimum area in the channels between the vanes and nozzle walls. Such factors would cause the physical throat to form inside the nozzle and result in performance characteristics typical of a C-D nozzle.

Peak resultant thrust ratios measured for HIDEN nozzles ranged from 0.94 for the submerged nozzles to 0.96 for the 1.8 CR D-shaped nozzles (fig. 17). These values are 3 percent to 5 percent lower than peak thrust-ratio levels for a typical C-D nozzle, which can experience peak thrust efficiency of approximately 0.99 at optimum (fully expanded flow at the nozzle exit) conditions (ref. 11). The lower thrust performance levels of HIDEN nozzles may be partially attributed to total-pressure losses between the model instrumentation plane (MS 19.370) and the nozzle bearing plane. Calculations performed in reference 7 for the offset plenum with nozzles in thrust mode indicated that total-pressure losses upstream of the nozzle bearing plane diminished thrust efficiency (or thrust ratio) by approximately 3 percent at peak performance levels. Accounting for this total-pressure loss would indicate that HIDEN nozzles themselves have thrust-ratio performance from 0.97 to 0.99, which is comparable to other C-D nozzle designs (ref. 11).

Discharge-coefficient w_p/w_i levels presented in figure 17 for HIDEN nozzles ranged from 0.87 to 0.93, which is somewhat low for high performance propulsion systems. Discharge coefficient was relatively constant at NPR's above 2.5, but varied at lower NPR's. The static-pressure distributions in figure 18 show some variation in the location of the nozzle throat at low NPR's, which results in the variation in discharge coefficient noted at NPR's below 2.5. The low values of discharge coefficient for HIDEN nozzles are partially attributed to the 3 percent total-pressure loss within the plenum system, which was discussed in reference 7. Total pressure measured at the instrumentation plane was used to calculate w_i, which leads to an artificially high value (as it did not reflect the 3-percent total-pressure loss) and thus, to a low value of discharge coefficient.

All HIDEN nozzles produced positive values of δ_{RR} in thrust mode operation, and therefore, each nozzle underturned the exhaust flow slightly. The cosine thrust losses ranged from 4° to about 10° for the 1.8 CR D-shaped, 1.4 CR D-shaped, and Pegasus nozzles, but ranged from 17° to about 21° for the submerged nozzles. When δ_{RR} values for the submerged nozzles are adjusted for splay angle (recall that the submerged nozzles were designed with a 12.5° splay angle), δ_{RR} values are comparable to other HIDEN nozzle designs.

The 1.8 CR D-shaped nozzles. The 1.8 CR D-shaped nozzles had the highest thrust ratios of the four HIDEN nozzle designs that were investigated (fig. 17). Peak internal and resultant thrust-ratio performance (0.956 and 0.958, respectively) occurred between NPR's of 3.5 and 4.0, which indicates an effective expansion ratio (ratio of nozzle exit area to nozzle throat area) of about 1.2. Discharge-coefficient levels ranged from 0.91 to 0.92 and were relatively constant at NPR's above 2.0. The 1.8 CR D-shaped nozzles had the lowest values of δ_{RR}, which indicates that it was the most effective of the four HIDEN nozzle designs at turning the exhaust flow.

Although static-pressure instrumentation inside the instrumented 1.8 CR D-shaped nozzle was sparse, static-pressure distributions in figure 18(a) support an internal throat location and show evidence of supersonic flow inside the nozzle. The decreasing pressures on the nozzle inner wall indicate that the exhaust flow accelerated around the tight radius turn near the nozzle exit.

Surface flow visualization inside a 1.8 CR D-shaped nozzle at nominal NPR of 4.0 is shown in figure 19(a). A view of the flow patterns inside the nozzle halves shows generally smooth streamlines from the bearing plane to the nozzle exit with little indication of separated or vortical flow inside the nozzle. Flow entering the bottom of the nozzle was drawn into the lower pressure regions at the nozzle outer wall, which caused nearly vertical streamlines just downstream of the nozzle bearing plane. The flow on the upper and lower surfaces of the turning vanes was well behaved, with little evidence of spanwise flow on these surfaces.

The 1.4 CR D-shaped nozzles. The 1.4 CR D-shaped nozzles had values of internal and resultant thrust ratio that were as much as 1.5 percent lower than the 1.8 CR D-shaped nozzles at low NPR's; however, these differences decreased with increasing NPR (fig. 17). Discharge-coefficient levels for this nozzle design ranged from 0.90 to 0.91 (approximately 0.5 percent to 1.0 percent lower than the 1.8 CR D-shaped nozzles) and were relatively constant at NPR's above 2.0. The differences in performance between the 1.4 CR D-shaped nozzles and the 1.8 CR D-shaped

nozzles result from the reduction in bearing-plane diameter that occurred for the 1.4 CR D-shaped nozzles. The reduction in bearing-plane diameter increased the Mach number of the flow entering the nozzles and reduced the area contraction from the bearing plane to the nozzle exit. A complete discussion of the effects of contraction ratio on performance will be presented in a subsequent section.

Peak internal and resultant thrust-ratio performance (0.951 and 0.954, respectively) for the 1.4 CR D-shaped nozzles occurred between NPR's of 3.5 and 4.0, which indicates an effective expansion ratio of about 1.2. This expansion ratio is the same as the 1.8 CR D-shaped nozzles. This similarity is not unexpected because the 1.4 CR D-shaped nozzle geometry from the turning vanes to the exit was identical to the 1.8 CR D-shaped nozzles. The lower thrust performance of this nozzle design had little effect on turning performance as the values of δ_{RR} were nearly the same as the 1.8 CR D-shaped nozzles.

Static-pressure instrumentation inside the 1.4 CR D-shaped nozzle was more extensive than in the 1.8 CR D-shaped nozzle, and therefore, the pressure measurements give better indication of the flow characteristics inside the 1.4 CR D-shaped nozzle (fig. 18(b)). Flow along the nozzle inner wall was supersonic near $s/l_s \approx 0.85$ and accelerated up to $s/l_s \approx 0.92$. Beyond $s/l_s \approx 0.92$, the flow either separated from the wall (at low NPR's) or recompressed (decelerated). Turning supersonic flow inside the nozzle probably resulted in some of the performance losses noted for this design. Static pressures measured inside the nozzle channels indicate generally smooth acceleration of the flow through the turning vanes to the nozzle exit.

Surface flow visualization inside a 1.4 CR D-shaped nozzle at nominal NPR of 4.0 is shown in figure 19(b). Comparison of figures 19(a) and 19(b) shows that the flow patterns inside the 1.4 CR D-shaped nozzle are less benign than flow patterns inside the 1.8 CR D-shaped nozzle. As was the case for the 1.8 CR D-shaped nozzle, flow entering the bottom of the 1.4 CR D-shaped nozzle was drawn into the lower pressure regions at the nozzle outer wall. The streamlines just downstream of the nozzle bearing plane were nearly vertical, but appear to have a slight upstream component near the location of the nozzle outer wall. A vortex is also indicated inside the nozzle, as the vertical streamlines terminate in a small region where the paint was removed by the flow. Downstream of this area, the flow behaved in a manner similar to the 1.8 CR D-shaped nozzle, perhaps illustrating why the turning performance of the 1.4 CR D-shaped nozzle was nearly the same as the 1.8 CR D-shaped nozzle, although the thrust performance was lower.

The 1.4 CR Pegasus nozzles. The 1.4 CR Pegasus nozzles had lower values of internal and resultant thrust ratio than either of the D-shaped nozzle designs (fig. 17). Thrust-ratio performance was typically 1 percent lower than the 1.4 CR D-shaped nozzles. Peak internal and resultant thrust-ratio performance (0.941 and 0.947, respectively) for the Pegasus nozzles occurred between NPR's of 4.0 and 4.5, which indicates an effective expansion ratio of about 1.3. Discharge-coefficient values for the Pegasus nozzles varied more with NPR than any other HIDEN nozzle design and w_p/w_i did not stabilize until NPR reached approximately 2.5. Values of δ_{RR} for the Pegasus nozzles ranged from 7° to about 10°, which indicates that this nozzle design was less effective at turning the exhaust flow than either of the D-shaped nozzle designs. The differences in turning performance between the Pegasus nozzles and the D-shaped nozzles generally decreased with increasing NPR.

Internal static-pressure distributions for the instrumented Pegasus nozzle are presented in figure 18(c). Static-pressure distributions on the nozzle inner wall indicate that the flow separated from the tight radius turn of the inner wall at $s/l_s \approx 0.90$. This flow separation appears to be the case throughout most of the NPR range and is at least partially responsible for the poor thrust and turning performance of the Pegasus nozzles. As was the case for the 1.4 CR D-shaped nozzle, static-pressures measured inside the Pegasus nozzle indicate generally smooth acceleration of the flow through the turning vanes with the exception of the outer channel. The static-pressure ratio curves for the Pegasus nozzle flatten in the outer channel between $s/l_s = 0.839$ and $s/l_s = 0.912$, which indicates little flow acceleration occurred in this region.

Surface flow visualization inside the Pegasus nozzle at nominal NPR of 4.0 is presented in figure 19(c). The flow patterns near the entrance of the Pegasus nozzle have characteristics similar to the patterns in the 1.4 CR D-shaped nozzle. A vortex is indicated in the Pegasus nozzle near the outer wall, just downstream of the bearing plane. The higher Mach number flow in the Pegasus nozzle and the rapid flow acceleration on the nozzle inner wall is indicated by an area where a large amount of paint has been removed by the flow. Near the location of the turning vanes, the flow patterns are unlike either of the D-shaped nozzles. Flow in the Pegasus nozzle approached the inner turning vane at a very high angle of attack, which resulted in a separation bubble on the upper surface of the inner turning vane. In the middle channel, a distinct line can be seen that runs between the leading edge of the outer turning vane to the midpoint of the inner turning vane. Distinct streamlines are apparent upstream of this line but not downstream. This pattern could indicate that a vortex formed in this region. The

lack of uniform streamlines on the turning vanes and the likelihood of a vortex between the turning vanes reflects the poor turning and the poor thrust performance of the Pegasus nozzle.

The 1.4 CR submerged nozzles. The 1.4 CR submerged nozzles had the lowest internal and resultant thrust ratios of the four HIDEN nozzle designs (fig. 17). By design, most of the thrust reduction results from the 12.5° splay angle (fig. 9), which generates a cosine thrust loss. At NPR's below 3.0, resultant thrust ratio was comparable to the other nozzles, but as NPR increased, thrust levels decreased at a substantially faster rate than the other HIDEN nozzles. Peak internal and resultant thrust-ratio performance (0.918 and 0.941, respectively) for the submerged nozzles occurred near a NPR of 3.0, which indicates an effective nozzle expansion ratio of 1.1. The rapid drop in thrust-ratio performance with increasing NPR is the result of greater nozzle underexpansion losses occurring for the submerged nozzles. Note that this nozzle design has the lowest effective expansion ratio of the four HIDEN nozzle designs tested. Discharge-coefficient levels for this nozzle ranged from 0.92 to 0.93 and were slightly higher than the other HIDEN nozzles. The submerged nozzles were designed with reduced turning angles, indicated by δ_{RR} values between 17° and 21°, and a simpler geometric transition from the bearing plane to the nozzle exit, which probably minimized losses inside the submerged nozzles. Adjusting δ_{RR} for the designed 12.5° splay angle results in flow underturning between 4° and 8°, which is comparable to the δ_{RR} values for the D-shaped nozzles.

Internal static-pressure distributions for the instrumented submerged nozzle are presented in figure 18(d). Static-pressure ratios on the nozzle inner wall indicate that flow separation probably occurred at NPR's below 2.5. This separation was most severe at low NPR's and likely contributed to the decreased amount of flow turning (higher δ_{RR}).

Surface flow visualization inside a submerged nozzle at nominal NPR of 4.0 is shown in figure 19(d). The flow patterns in the submerged nozzle are more uniform than in the Pegasus nozzle, as indicated by smooth streamlines throughout the nozzle. The higher velocity flow in the nozzle outer channel, which was indicated by the static-pressure distributions, appears as an area in the nozzle where a large portion of the paint has been removed by the flow. Patterns are characteristic of attached flow on the nozzle inner wall, which was indicated by the static-pressure distributions at NPR = 4.0. Flow on the upper surface of the nozzle turning vane was relatively uniform, as little spanwise flow was indicated by flow patterns.

Effect of Nozzle Contraction Ratio

The effect of nozzle contraction ratio (bearing-plane diameter) on internal performance characteristics can be determined by comparing the performance of the D-shaped nozzles (fig. 17). Recall that these nozzles were designed with identical geometry from a plane just upstream of the turning vanes to the nozzle exit. The 1.4 CR D-shaped nozzle design was different from the 1.8 CR D-shaped nozzle design from the bearing plane to a plane just upstream of the turning vanes to allow the reduction in bearing-plane diameter. As shown in figure 17, the 1.4 CR D-shaped nozzles had internal and resultant thrust-ratio performance that was as much as 1.5 percent lower than the 1.8 CR D-shaped nozzles at low NPR's. The 1.4 CR D-shaped nozzles also had discharge-coefficient levels approximately 0.5 percent lower than the 1.8 CR D-shaped nozzles. The differences in turning performance between the 1.8 CR and 1.4 CR D-shaped nozzles were small, typically less than 0.5°.

The reduction in bearing-plane diameter that occurred with the 1.4 CR D-shaped nozzles required the installation of a sleeve into the offtake duct, which forced the flow to accelerate to higher Mach numbers. This acceleration is evident in figure 20(a), where higher Mach numbers (lower static pressure) at the nozzle bearing plane are indicated around the circumference of the duct for the 1.4 CR. Note that NPR had little effect on offtake duct static-pressure ratios (fig. 20(b)). The higher Mach numbers entering the nozzle and the loss of some area contraction between the bearing plane and nozzle exit likely contributed to the performance losses noted for the 1.4 CR D-shaped nozzles. In actual application, the weight savings of the reduced contraction-ratio nozzle could possibly offset the small penalty in thrust performance that resulted from the reduction in contraction ratio.

Effect of Plenum Geometry

The effects of plenum geometry on nozzle performance and on offtake duct static-pressure ratios are presented in figures 21 and 22, respectively. Results are presented for the 1.8 CR D-shaped nozzles, which had the highest performance of the four nozzle designs tested, installed on each plenum with short-core centerbody and no blocker. The effect of plenum geometry presented here is typical of other configurations.

During thrust mode operation, nozzles installed on the offset plenum exhibited higher thrust-ratio and

discharge-coefficient values than the same nozzles installed on the centerline plenum (fig. 21(a)). Differences in thrust-ratio performance were as large as 2 percent between plenum configurations; these differences decreased with increasing NPR. Discharge coefficient was approximately 2 percent higher for the offset plenum installation and this difference remained essentially constant across the entire NPR range. Nozzles installed on the offset plenum also had lower values of δ_{RR} over the entire NPR range, which indicates that nozzles installed on the offset plenum were more effective at turning the exhaust flow.

The superior performance of nozzles installed on the offset plenum can be partially attributed to rounded duct intersections in the offset plenum and to the lower total flow turning angles required in the offset plenum. The intersections of the offset plenum with the offtake ducts were designed with a minimum curvature that was 15 percent of the offtake duct diameter. The intersections of the centerline plenum with the offtake ducts were relatively sharp and were designed with a curvature that was less than 3 percent of the offtake duct diameter. The sharp radius at the centerline plenum and offtake duct intersection probably resulted in local flow separation in the centerline plenum offtake duct, which increased the amount of turbulent flow entering the nozzles. The centerline plenum design also requires a total flow turning angle of 80.26° from the plenum centerline to the nozzle bearing plane; the equivalent turning angle on the offset plenum is 54.74°. The larger internal flow turning angle of the centerline plenum accelerated flow to higher internal Mach numbers at the nozzle bearing plane and likely contributed to higher losses in nozzle performance. Higher internal Mach numbers in the centerline plenum are confirmed by offtake duct static-pressure ratios in figure 22(a), which indicate lower static pressure (higher Mach numbers) in the offtake ducts. Undoubtedly, higher Mach numbers and more turbulent flow entering the nozzles would contribute to the losses in nozzle performance noted in figure 21. As indicated in figure 21, these effects on internal and resultant thrust ratios become less important at higher NPR's, while the effects on discharge coefficient and nozzle flow turning angle remain nearly constant.

The effects of plenum geometry on HIDEN nozzle performance in lift mode are presented in figure 21(b). A complete discussion of lift-mode effects is presented in the following section. Lift-mode performance trends are similar to the thrust-mode results for the two plenum geometries. Nozzles installed on the offset plenum produced higher thrust and discharge-coefficient levels and had δ_{RR} values closer to 90° than nozzles installed on the centerline plenum throughout the entire NPR range investigated. Thrust losses (from 1 percent to 4 percent) and discharge-coefficient losses (about 3 percent) due to the centerline plenum geometry were larger in lift mode than in thrust mode, but δ_{RR} differences were actually smaller. Static-pressure ratios at the nozzle bearing plane indicate significantly higher Mach numbers entering the nozzles on the centerline plenum during lift mode operation (when compared with thrust mode), as shown in figures 22(a) and 22(b). This increase in Mach number likely accounted for additional losses in performance that were noted for the centerline plenum configuration during lift mode operation.

Effect of Operation Mode

Offset plenum. The effect of operation mode (thrust or lift) on performance of the 1.8 CR D-shaped nozzles installed on the offset plenum is presented in figure 23. Overall, the differences in performance due to changing from one operation mode to the other were small. Slightly higher performance did occur in lift mode, although the differences in F_r/F_i and w_p/w_i between the two operation modes were less than 1 percent and 0.5 percent, respectively. Perhaps the most notable feature of the HIDEN concept is the fact that the nozzles can transition from thrust mode to lift mode with little effect on discharge coefficient. Such a result is desirable, because large changes in discharge coefficient would affect engine operation. The most significant effect of operation mode was on δ_{RR}, or the ability of the nozzles to turn the flow to the axial force direction in thrust mode and the normal force direction in lift mode. As shown in figure 23, the nozzles were slightly better at turning the exhaust flow in lift mode, where values of δ_{RR} were between 86° and 90° (which indicates maximum flow underturning of 4°). In thrust mode, values of δ_{RR} were between 4° and 8° (flow underturning as high as 8°).

The effect of operation mode on offtake duct static-pressure ratios is presented in figure 24 for the offset plenum. Changing the nozzles from thrust mode to lift mode had little effect on offtake duct static-pressure ratios. As discussed previously, the plenum and offtake duct intersection was rounded on the offset plenum to minimize flow distortion in the offtake ducts. This rounding caused minimal changes in offtake duct static-pressure ratios when the nozzle operation mode was changed.

Centerline plenum. The effect of operation mode on performance of the 1.8 CR D-shaped nozzles installed on the centerline plenum is presented in figure 25. As was the case with the offset plenum, the differences in performance due to changing from one operation mode to the other were small. Typical variations in F_r/F_i and w_p/w_i between operation modes were less than 1 percent. The effect of operation mode on δ_{RR} was the same for the

centerline plenum and the offset plenum; superior flow turning occurred for the lift mode configuration.

The effect of operation mode on offtake duct static-pressure ratios for centerline plenum configurations is presented in figure 26. Changing the nozzles from thrust mode to lift mode resulted in lower static-pressure ratios (higher Mach numbers) predominately at the nozzle inner wall. The orientation of the nozzle on the offtake duct affects the position of the nozzle bearing plane in relation to the plenum centerline. Rotating the nozzle from thrust mode to lift mode influenced the characteristics of the flow entering the nozzle and contributed to the differences in performance indicated in figure 25.

Effect of Centerbody Geometry

Offset plenum. The effect of centerbody geometry on performance of 1.8 CR D-shaped nozzles in thrust mode installed on the offset plenum is presented in figure 27. For each blocker configuration, the effect of varying centerbody type was small. Typical variations in resultant thrust ratio and discharge coefficient were less than 1 percent and values of δ_{RR} varied 0.5° or less. With no blocker installed, nozzle performance was highest for the short-core centerbody configuration (fig. 27(a)). The fan centerbody configuration had the highest performance with either the flat blocker (fig. 27(b)) or tapered blocker (fig. 27(c)) installed. Similarly, varying centerbody type had little influence on offtake duct static-pressure ratios for the offset plenum (fig. 28).

Centerline plenum. The effect of centerbody geometry on performance of 1.8 CR D-shaped nozzles installed on the centerline plenum is presented in figure 29. With no blocker installed, the centerbody geometry only slightly affected nozzle performance, which was also the case for the offset plenum configuration. Variations in thrust ratios and discharge coefficient were less than 1 percent, with the short-core centerbody configuration demonstrating slightly higher performance than the other centerbody configurations. Variations in δ_{RR} for the no-blocker configurations were typically less than 1°.

The most significant effects of centerbody geometry on performance occurred with the flat blocker installed (fig. 29(b)). The fan centerbody configuration produced the highest F_r/F_i and w_p/w_i values of the four centerbody configurations, but was the least effective configuration at turning the exhaust flow. The long-core centerbody configuration produced the lowest thrust levels but had the best flow turning (lowest δ_{RR} values). Resultant thrust ratios for the fan centerbody configuration were approximately 3 percent higher than the long-core centerbody configuration at NPR = 1.50, but the differences decreased to 1 percent at NPR = 6.0. Discharge-coefficient variation with centerbody configuration showed similar trends and ranged from approximately 0.85 for the long-core centerbody to 0.91 for the fan centerbody. The apparent discrepancy in the effect of centerbody type on performance between the centerline plenum and offset plenum geometry is somewhat perplexing. However, this result does indicate the sensitivity of the flow characteristics at the entrance of the nozzles to changes in geometry of the offtake duct system.

The effect of centerbody geometry on HIDEN nozzle performance with the tapered blocker installed is presented in figure 29(c) for long-core and fan centerbody configurations. The differences in performance between the long-core and fan centerbody configurations were typically small and their performance levels ($F_r/F_i \approx 0.96$ and $w_p/w_i \approx 0.91$) were slightly higher than the centerbody and blocker configurations tested on the centerline plenum. Therefore, utilizing the tapered blockers to help turn the exhaust flow from the plenum centerline to the offtake duct centerline helped reduce losses and increase nozzle performance.

The effect of centerbody geometry on offtake duct static-pressure ratios are presented in figure 30 for the no-blocker, flat blocker, and tapered blocker configurations. As would be expected, little effect of centerbody type on offtake duct static-pressure ratios was found for the no-blocker (fig. 30(a)) and tapered blocker (fig. 30(c)) configurations. However, there were changes in offtake duct static-pressure ratios for the flat blocker configuration, which had the most significant effects of centerbody type on nozzle performance (fig. 30(b)). The medium- and long-core centerbody configurations, which had the lowest performance of any of the centerbody and blocker configurations, had slightly higher Mach numbers at the nozzle bearing plane. The higher Mach numbers probably increased losses in the system and reduced nozzle performance as indicated in figure 30(b).

Effect of Blocker Geometry

Offset plenum. The effect of blocker geometry on performance of 1.8 CR D-shaped nozzles in thrust mode installed on the offset plenum is presented in figure 31. Installing the flat blocker typically resulted in slight losses (less than 1 percent) in resultant thrust ratio F_r/F_i and discharge coefficient w_p/w_i for the short-core, medium-core, and long-core centerbody configurations. These performance losses are largest for the short-core centerbody and tend to decrease with increasing centerbody length. In fact, the fan centerbody configuration shows a slight increase in thrust-ratio and discharge-coefficient values with the flat blocker installed. The long-core and fan centerbody configurations had the

highest values of F_r/F_i and w_p/w_i with the tapered blocker installed, while δ_{RR} showed only small changes between blocker configurations. As shown in figure 32, changing blocker type had no effect on offtake duct static-pressure ratios.

Centerline plenum. The effect of blocker geometry on performance of the 1.8 CR D-shaped nozzles in thrust mode installed on the centerline plenum is presented in figure 33. Similar to the centerbodies, the effects of blocker geometry on performance are more significant for the centerline plenum than for the offset plenum. Installing the flat blocker reduced the thrust ratios and discharge coefficient across the entire NPR range investigated. Variations in F_r/F_i and w_p/w_i were typically less than 1 percent for the short-core (fig. 33(a)) and medium-core (fig. 33(b)) centerbody configurations, but were as high as 2.5 percent for the long-core centerbody configuration. Although nozzle performance was reduced when the flat blocker was installed, nozzle turning performance was increased by approximately 1° on the short-core (fig. 33(a)) and medium-core (fig. 33(b)) configurations and by 2° on the long-core centerbody configuration (fig. 33(c)). Installing the flat blocker reduced the volume inside the plenum, which resulted in higher plenum Mach numbers near the offtake ducts. As discussed previously, the higher Mach numbers inside the offtake ducts likely contribute to higher total-pressure, friction, and boundary layer losses, thereby reducing nozzle performance. The increased Mach numbers for the flat blocker configurations are indicated in figure 34 by lower offtake duct static-pressure ratios. Apparently, the centerline plenum was more susceptible to losses, which resulted from reduced volume in the plenum (i.e., the insertion of a blocker), possibly because of the sharpness of the offtake ducts. Recall that the offset plenum was given an offtake duct and plenum intersection curvature that was 15 percent of the offtake duct diameter, while the centerline plenum had an intersection curvature that was approximately 3 percent of the offtake duct diameter. This fact may contribute to the differences in observed performance. Another factor could be the location of the offtake ducts themselves. The geometry of the centerline plenum may have made critical differences in flow conditions that resulted in the performance differences observed here.

The effects of inserting the tapered blocker into the centerline plenum are presented in figures 33(c) and 33(d) for the long-core and fan centerbodies, respectively. The tapered blocker configuration had higher F_r/F_i and w_p/w_i performance than the no-blocker and flat blocker configurations across the entire NPR range investigated. This higher performance indicates that the tapered blocker configurations minimized performance losses when compared with the other blocker configurations. Values of δ_{RR} were comparable to the other blocker configurations except for the long-core centerbody and flat blocker configuration, which had approximately 2° higher turning performance than the other configurations.

Instrumented-Ramp Static-Pressure Distributions

A ramp (fig. 14), which simulated a fuselage side, was bolted to the downstream face of the offset plenum blanking plate (see fig. 4(a)) and contained instrumentation to measure static pressure downstream of the left submerged nozzle during thrust mode operation. The leading edge of the ramp was positioned flush to the nozzle exit at the nozzle inner wall. Note that from $x/L = 0.000$ to $x/L = 0.497$ the ramp surface was parallel to the submerged nozzle splay angle of 12.5°. Downstream of $x/L = 0.497$ the ramp surface canted away from the nozzle exhaust by 12.5° to position the ramp surface parallel to the plenum centerline.

Static-pressure distributions on the instrumented ramp with the fan centerbody installed in the offset plenum for various blocker configurations are presented in figure 35. Comparison of figures 35(a), 35(b), and 35(c) indicates little effect of blocker type on instrumented-ramp static-pressure distributions. As the flow exits the nozzle, an initial overexpansion is indicated by static-pressure ratios up to $x/L \approx 0.2$. This initial overexpansion is a result of the sharp turn along the nozzle inner wall. At NPR's below 2.5, the flow is probably separated from the ramp surface (indicated by the flat static-pressure distributions and $p/p_{t,j}$ values approximately equal to 1/NPR). However, at NPR's above 2.2, an oscillation in local static pressure occurs along the ramp. Such behavior is indicative of alternating regions of expansion and compression beginning with a Prandtl-Meyer expansion fan at the nozzle exit. This behavior continues along the ramp until $x/L \approx 0.7$ where the flow is probably separated from the ramp surface as indicated by a flattening of the static-pressure distributions. Similar trends in surface pressure data have been reported for a two-dimensional wedge nozzle in reference 12.

Conclusions

An investigation was conducted in the Jet-Exit Test Facility of the Langley 16-Foot Transonic Tunnel to evaluate the internal performance characteristics of highly integrated deployable exhaust nozzles (HIDEN) applicable to advanced short-takeoff and vertical-landing tactical aircraft. Four nozzle designs were tested in the forward (thrust) and vertical (lift) operation modes. Two plenum designs with different offtake duct geometries

were selected to vary the vertical distance between the plenum (engine) centerline and the bearing plane surface centerline. Four plenum centerbodies, along with interchangeable blockers, were tested to investigate engine fan- and core-mounted nozzle installations. The test was conducted with no external flow, and nozzle pressure ratio was varied from 1.5 to approximately 6.0. The results of this investigation indicate the following conclusions:

1. The 1.8 contraction ratio (CR) D-shaped nozzles had the highest resultant thrust ratio (0.96) of the four HIDEN nozzle designs tested. Up to 3 percent of the thrust efficiency loss measured for the nozzles was attributed to losses in total pressure occurring upstream of the nozzle bearing plane. The HIDEN nozzles themselves performed comparable to thrust-vectoring convergent-divergent nozzles.

2. All four HIDEN nozzles underturned the exhaust flow from a minimum of 4° on the 1.8 CR D-shaped nozzles to 9° on the submerged nozzles.

3. The decrease in CR from the 1.8 D-shaped nozzles to the 1.4 D-shaped nozzles caused a decrease in resultant thrust ratio of less than 1 percent in thrust mode. In actual application, the potential weight savings from the smaller contraction ratio nozzle may overcome this loss in performance.

4. The 1.4 CR submerged nozzles had the highest discharge coefficient (0.93) of the four HIDEN nozzle designs tested. This result was attributed to reduced flow turning requirement of the submerged nozzles, as well as the comparatively simpler geometric transition from bearing plane to nozzle exit.

5. The offset plenum resulted in higher levels of nozzle performance than the centerline plenum. This higher performance is attributed to the larger radius of the offset plenum at the offtake ducts and the smaller total flow turning angle from the plenum centerline to the nozzle bearing plane.

6. Changing operation mode had only small effects on internal performance characteristics. Hence, engine operation would not be effected by nozzle operating mode.

7. Centerbody and blocker effects were small (typically less than 1 percent). These differences due to changes in centerbody and blocker geometry probably result from Mach number differences at the entrance to the offtake ducts.

NASA Langley Research Center
Hampton, VA 23681-0001
August 24, 1995

References

1. Jackson, Paul: Harrier. *World Airpower J.*, vol. 6, 1991, p. 46.

2. Appleyard, George M.: Propulsion/Aerodynamic Integration in ASTOVL Combat Aircraft. *Proceedings of the International Powered Lift Conference*, P-203, SAE, 1988, pp. 337–348. (Available as SAE Paper 87233.)

3. Hamilton, D. A.; and Richardson, S. D.: V/STOL Advantages for Ground Attack. AIAA-88-4478, Sept. 1988.

4. Brown, David M.: Supersonic STOVL Conceptual Design of a Fighter/Attack Aircraft. AIAA-89-2112, July–Aug. 1989.

5. Deckert, W. H.; and Franklin, J. A.: *Powered-Lift Aircraft Technology*. NASA SP-501, 1989.

6. Bucknell, R. L.: STOVL Engine/Airframe Integration. AIAA-87-1711, June 1987.

7. Taylor, John G.; Asbury, Scott C.; Mason, Mary L.; and Lamb, Milton: Internal Performance of Highly Integrated Deployable Exhaust Nozzles. AIAA-93-2570, June 1993.

8. Mercer, Charles E.; Berrier, Bobby L.; Capone, Francis J.; and Grayston, Alan M.: *Data Reduction Formulas for the 16-Foot Transonic Tunnel—NASA Langley Research Center, Revision 2*. NASA TM-107646, 1992. (Supersedes NASA TM-86319, Rev. 1.)

9. Capone, Francis J.; Bangert, Linda S.; Asbury, Scott C.; Mills, Charles T. L.; and Bare, E. Ann: *The NASA Langley 16-Foot Transonic Tunnel—Historical Overview, Facility Description, Calibration, Flow Characteristics, and Test Capabilities*. NASA TP-3521, 1995.

10. Maltby, R. L.; and Keating, R. F. A., compilers: The Surface Oil Flow Technique for Use in Low Speed Wind Tunnels. *Flow Visualization in Wind Tunnels Using Indicators*. AGARDograph 70, Apr. 1962, pp. 29–38.

11. Berrier, Bobby L.; and Re, Richard J.: *Investigation of Convergent-Divergent Nozzles Applicable to Reduced-Power Supersonic Cruise Aircraft*. NASA TP-1766, 1980.

12. Carson, George T., Jr.; and Mason, Mary L.: *Experimental and Analytical Investigation of a Nonaxisymmetric Wedge Nozzle at Static Conditions*. NASA TP-1188, 1978.

Table 1. Coordinates Defining Internal Flow Path and Turning Vane Geometry of 1.8 CR D-Shaped Nozzles

(a) Nozzle internal flow path

Spline 1		
X, in.	Y, in.	Z, in.
−2.472	1.748	.000
−2.443	1.799	.000
−2.425	1.854	.000
−2.416	1.912	.000
−2.417	1.971	.000
−2.417	2.029	.000
−2.417	2.088	.000
−2.417	2.146	.000
−2.417	2.204	.000
−2.417	2.263	.000
−2.417	2.321	.000
−2.417	2.380	.000
−2.416	2.438	.000
−2.412	2.497	.000
−2.406	2.555	.000
−2.397	2.612	.000
−2.385	2.670	.000
−2.371	2.727	.000
−2.354	2.783	.000
−2.335	2.838	.000
−2.313	2.892	.000
−2.289	2.945	.000
−2.262	2.997	.000
−2.233	3.048	.000
−2.202	3.098	.000
−2.169	3.145	.000
−2.133	3.192	.000
−2.096	3.237	.000
−2.056	3.280	.000
−2.015	3.321	.000
−1.972	3.361	.000
−1.927	3.398	.000
−1.880	3.434	.000
−1.832	3.467	.000
−1.783	3.498	.000
−1.732	3.526	.000
−1.679	3.553	.000
−1.626	3.577	.000
−1.572	3.599	.000
−1.517	3.618	.000
−1.461	3.635	.000
−1.404	3.649	.000
−1.347	3.661	.000
−1.289	3.670	.000
−1.231	3.676	.000
−1.173	3.680	.000
−1.114	3.681	.000
−1.056	3.680	.000
−.997	3.681	.000
−.939	3.681	.000
−.880	3.681	.000

Spline 2		
X, in.	Y, in.	Z, in.
−2.403	1.699	.500
−2.370	1.746	.500
−2.348	1.799	.500
−2.342	1.857	.500
−2.346	1.914	.500
−2.353	1.971	.500
−2.359	2.029	.500
−2.365	2.086	.500
−2.368	2.144	.500
−2.370	2.201	.500
−2.371	2.259	.500
−2.369	2.316	.500
−2.367	2.374	.500
−2.363	2.431	.500
−2.357	2.489	.500
−2.349	2.546	.500
−2.339	2.602	.500
−2.327	2.659	.500
−2.313	2.714	.500
−2.295	2.769	.500
−2.275	2.823	.500
−2.252	2.876	.500
−2.225	2.927	.500
−2.196	2.977	.500
−2.164	3.025	.500
−2.131	3.071	.500
−2.094	3.116	.500
−2.056	3.159	.500
−2.016	3.201	.500
−1.974	3.241	.500
−1.931	3.279	.500
−1.887	3.315	.500
−1.840	3.349	.500
−1.793	3.382	.500
−1.745	3.413	.500
−1.695	3.442	.500
−1.644	3.469	.500
−1.592	3.494	.500
−1.539	3.516	.500
−1.485	3.537	.500
−1.430	3.555	.500
−1.375	3.570	.500
−1.319	3.584	.500
−1.262	3.595	.500
−1.205	3.604	.500
−1.148	3.612	.500
−1.091	3.617	.500
−1.033	3.621	.500
−.976	3.624	.500
−.918	3.626	.500
−.861	3.626	.500

Spline 3		
X, in.	Y, in.	Z, in.
−2.164	1.530	1.000
−2.136	1.579	1.000
−2.117	1.631	1.000
−2.108	1.687	1.000
−2.108	1.743	1.000
−2.115	1.798	1.000
−2.126	1.853	1.000
−2.138	1.908	1.000
−2.151	1.962	1.000
−2.162	2.017	1.000
−2.172	2.072	1.000
−2.180	2.128	1.000
−2.185	2.184	1.000
−2.189	2.240	1.000
−2.190	2.296	1.000
−2.189	2.352	1.000
−2.185	2.408	1.000
−2.179	2.463	1.000
−2.170	2.518	1.000
−2.158	2.573	1.000
−2.143	2.627	1.000
−2.125	2.680	1.000
−2.104	2.732	1.000
−2.080	2.782	1.000
−2.052	2.831	1.000
−2.022	2.878	1.000
−1.988	2.923	1.000
−1.953	2.966	1.000
−1.915	3.008	1.000
−1.875	3.047	1.000
−1.834	3.085	1.000
−1.791	3.121	1.000
−1.746	3.155	1.000
−1.700	3.187	1.000
−1.653	3.217	1.000
−1.605	3.245	1.000
−1.556	3.272	1.000
−1.506	3.297	1.000
−1.455	3.321	1.000
−1.403	3.342	1.000
−1.351	3.362	1.000
−1.298	3.381	1.000
−1.244	3.397	1.000
−1.190	3.412	1.000
−1.136	3.425	1.000
−1.081	3.437	1.000
−1.026	3.446	1.000
−.970	3.453	1.000
−.914	3.459	1.000
−.859	3.462	1.000
−.803	3.463	1.000

Spline 4		
X, in.	Y, in.	Z, in.
−1.934	1.367	1.250
−1.906	1.415	1.250
−1.887	1.468	1.250
−1.876	1.522	1.250
−1.876	1.578	1.250
−1.884	1.633	1.250
−1.899	1.686	1.250
−1.918	1.739	1.250
−1.937	1.791	1.250
−1.956	1.844	1.250
−1.974	1.896	1.250
−1.990	1.949	1.250
−2.003	2.003	1.250
−2.014	2.058	1.250
−2.021	2.113	1.250
−2.027	2.169	1.250
−2.030	2.224	1.250
−2.030	2.280	1.250
−2.028	2.335	1.250
−2.024	2.391	1.250
−2.017	2.446	1.250
−2.008	2.501	1.250
−1.995	2.555	1.250
−1.979	2.608	1.250
−1.960	2.661	1.250
−1.936	2.711	1.250
−1.908	2.759	1.250
−1.877	2.805	1.250
−1.843	2.849	1.250
−1.806	2.891	1.250
−1.767	2.930	1.250
−1.726	2.968	1.250
−1.683	3.003	1.250
−1.639	3.037	1.250
−1.594	3.069	1.250
−1.547	3.099	1.250
−1.499	3.128	1.250
−1.450	3.154	1.250
−1.401	3.179	1.250
−1.350	3.202	1.250
−1.298	3.224	1.250
−1.246	3.243	1.250
−1.194	3.261	1.250
−1.140	3.277	1.250
−1.087	3.292	1.250
−1.033	3.304	1.250
−.978	3.315	1.250
−.923	3.323	1.250
−.868	3.329	1.250
−.812	3.333	1.250
−.756	3.334	1.250

Table 1. Continued

(a) Continued

Spline 5		
X, in.	Y, in.	Z, in.
-1.236	.874	1.514
-1.211	.912	1.515
-1.187	.951	1.517
-1.166	.991	1.521
-1.147	1.032	1.526
-1.130	1.074	1.533
-1.117	1.117	1.542
-1.106	1.160	1.553
-1.098	1.203	1.565
-1.093	1.246	1.579
-1.091	1.289	1.594
-1.091	1.332	1.610
-1.093	1.374	1.627
-1.096	1.416	1.644
-1.102	1.458	1.662
-1.108	1.499	1.681
-1.115	1.540	1.699
-1.122	1.581	1.718
-1.130	1.622	1.737
-1.138	1.663	1.755
-1.145	1.704	1.773
-1.152	1.746	1.791
-1.158	1.787	1.808
-1.163	1.830	1.825
-1.166	1.872	1.840
-1.167	1.916	1.855
-1.166	1.959	1.868
-1.163	2.003	1.880
-1.158	2.047	1.890
-1.149	2.092	1.898
-1.139	2.136	1.904
-1.126	2.179	1.909
-1.112	2.222	1.911
-1.095	2.265	1.911
-1.076	2.306	1.908
-1.055	2.346	1.903
-1.032	2.385	1.895
-1.008	2.423	1.886
-.982	2.459	1.875
-.955	2.493	1.864
-.925	2.526	1.851
-.894	2.556	1.838
-.860	2.584	1.825
-.825	2.610	1.812
-.788	2.634	1.799
-.749	2.655	1.788
-.708	2.672	1.777
-.666	2.686	1.769
-.622	2.696	1.762
-.577	2.702	1.758
-.531	2.704	1.757

Spline 6		
X, in.	Y, in.	Z, in.
-.539	.381	1.250
-.517	.415	1.250
-.499	.452	1.250
-.486	.490	1.250
-.476	.530	1.250
-.469	.570	1.250
-.466	.611	1.250
-.465	.651	1.250
-.466	.692	1.250
-.469	.733	1.250
-.473	.773	1.250
-.477	.814	1.250
-.482	.854	1.250
-.486	.895	1.250
-.490	.935	1.250
-.493	.976	1.250
-.497	1.016	1.250
-.501	1.057	1.250
-.507	1.097	1.250
-.513	1.137	1.250
-.520	1.177	1.250
-.527	1.217	1.250
-.535	1.257	1.250
-.543	1.297	1.250
-.552	1.337	1.250
-.561	1.377	1.250
-.570	1.416	1.250
-.579	1.456	1.250
-.588	1.496	1.250
-.597	1.536	1.250
-.605	1.575	1.250
-.614	1.615	1.250
-.621	1.655	1.250
-.628	1.695	1.250
-.635	1.735	1.250
-.640	1.776	1.250
-.643	1.816	1.250
-.646	1.857	1.250
-.646	1.898	1.250
-.646	1.938	1.250
-.642	1.979	1.250
-.636	2.019	1.250
-.623	2.058	1.250
-.603	2.093	1.250
-.577	2.124	1.250
-.546	2.151	1.250
-.512	2.173	1.250
-.475	2.190	1.250
-.436	2.202	1.250
-.396	2.210	1.250
-.356	2.212	1.250

Spline 7		
X, in.	Y, in.	Z, in.
-.308	.218	1.000
-.285	.256	1.000
-.269	.298	1.000
-.259	.342	1.000
-.254	.386	1.000
-.254	.431	1.000
-.256	.475	1.000
-.262	.520	1.000
-.269	.564	1.000
-.278	.608	1.000
-.289	.651	1.000
-.302	.693	1.000
-.315	.736	1.000
-.328	.779	1.000
-.342	.822	1.000
-.355	.864	1.000
-.368	.907	1.000
-.381	.950	1.000
-.394	.992	1.000
-.407	1.035	1.000
-.420	1.078	1.000
-.433	1.121	1.000
-.445	1.163	1.000
-.458	1.206	1.000
-.471	1.249	1.000
-.484	1.292	1.000
-.497	1.335	1.000
-.510	1.377	1.000
-.523	1.420	1.000
-.537	1.462	1.000
-.551	1.505	1.000
-.565	1.547	1.000
-.579	1.590	1.000
-.592	1.632	1.000
-.605	1.675	1.000
-.617	1.718	1.000
-.627	1.762	1.000
-.635	1.806	1.000
-.641	1.850	1.000
-.645	1.895	1.000
-.645	1.939	1.000
-.642	1.984	1.000
-.634	2.028	1.000
-.618	2.069	1.000
-.593	2.106	1.000
-.562	2.139	1.000
-.526	2.165	1.000
-.486	2.185	1.000
-.444	2.200	1.000
-.400	2.209	1.000
-.355	2.212	1.000

Spline 8		
X, in.	Y, in.	Z, in.
-.069	.049	.500
-.045	.092	.500
-.031	.139	.500
-.023	.188	.500
-.021	.237	.500
-.024	.286	.500
-.031	.335	.500
-.042	.383	.500
-.057	.430	.500
-.075	.476	.500
-.093	.521	.500
-.112	.567	.500
-.130	.613	.500
-.149	.658	.500
-.169	.703	.500
-.188	.749	.500
-.207	.794	.500
-.227	.839	.500
-.246	.885	.500
-.265	.930	.500
-.284	.975	.500
-.302	1.021	.500
-.320	1.067	.500
-.338	1.113	.500
-.356	1.159	.500
-.374	1.205	.500
-.392	1.250	.500
-.409	1.296	.500
-.427	1.342	.500
-.445	1.388	.500
-.464	1.434	.500
-.482	1.479	.500
-.501	1.525	.500
-.520	1.570	.500
-.539	1.616	.500
-.557	1.662	.500
-.576	1.707	.500
-.594	1.753	.500
-.612	1.799	.500
-.627	1.846	.500
-.638	1.894	.500
-.644	1.943	.500
-.642	1.992	.500
-.631	2.040	.500
-.609	2.084	.500
-.578	2.123	.500
-.541	2.155	.500
-.498	2.180	.500
-.453	2.198	.500
-.405	2.208	.500
-.355	2.212	.500

Table 1. Continued

(a) Continued

Spline 9		
X, in.	Y, in.	Z, in.
.000	.000	.000
.026	.044	.000
.044	.091	.000
.053	.141	.000
.055	.191	.000
.048	.242	.000
.032	.290	.000
.014	.337	.000
-.006	.384	.000
-.026	.430	.000
-.045	.477	.000
-.064	.524	.000
-.084	.571	.000
-.103	.618	.000
-.122	.664	.000
-.142	.711	.000
-.161	.758	.000
-.180	.805	.000
-.200	.852	.000
-.219	.898	.000
-.238	.945	.000
-.258	.992	.000
-.277	1.039	.000
-.296	1.086	.000
-.316	1.133	.000
-.335	1.179	.000
-.354	1.226	.000
-.374	1.273	.000
-.393	1.320	.000
-.413	1.367	.000
-.432	1.413	.000
-.451	1.460	.000
-.471	1.507	.000
-.490	1.554	.000
-.509	1.601	.000
-.529	1.648	.000
-.548	1.694	.000
-.567	1.741	.000
-.587	1.788	.000
-.607	1.834	.000
-.626	1.882	.000
-.640	1.930	.000
-.643	1.981	.000
-.634	2.030	.000
-.613	2.077	.000
-.583	2.118	.000
-.545	2.151	.000
-.502	2.178	.000
-.455	2.197	.000
-.406	2.208	.000
-.355	2.212	.000

Spline 10		
X, in.	Y, in.	Z, in.
.000	.000	.000
-.001	.000	.047
-.002	.002	.095
-.005	.004	.142
-.010	.007	.190
-.015	.011	.237
-.022	.015	.284
-.030	.021	.330
-.039	.027	.377
-.049	.035	.422
-.060	.043	.468
-.073	.052	.513
-.087	.061	.557
-.102	.072	.601
-.118	.083	.645
-.135	.095	.687
-.153	.108	.729
-.172	.122	.771
-.192	.136	.811
-.214	.151	.851
-.236	.167	.890
-.259	.183	.928
-.284	.200	.965
-.309	.218	1.001
-.335	.237	1.036
-.362	.256	1.071
-.390	.276	1.104
-.419	.296	1.136
-.448	.317	1.166
-.479	.338	1.196
-.510	.360	1.225
-.541	.383	1.252
-.574	.406	1.278
-.607	.429	1.303
-.641	.453	1.327
-.675	.477	1.349
-.710	.502	1.370
-.745	.527	1.389
-.781	.552	1.408
-.817	.578	1.424
-.854	.604	1.440
-.891	.630	1.454
-.929	.657	1.466
-.966	.683	1.477
-1.005	.710	1.487
-1.043	.737	1.495
-1.081	.765	1.502
-1.120	.792	1.507
-1.158	.819	1.511
-1.197	.847	1.513
-1.236	.874	1.514

Spline 11		
X, in.	Y, in.	Z, in.
-.187	.821	.000
-.187	.821	.041
-.188	.822	.083
-.189	.822	.125
-.191	.823	.166
-.193	.824	.208
-.196	.825	.249
-.200	.827	.290
-.204	.828	.332
-.208	.830	.373
-.214	.833	.414
-.219	.835	.455
-.226	.838	.496
-.233	.841	.537
-.240	.844	.578
-.249	.848	.619
-.258	.852	.659
-.267	.856	.699
-.278	.860	.739
-.289	.865	.779
-.300	.870	.819
-.313	.876	.858
-.326	.882	.897
-.340	.887	.936
-.355	.894	.974
-.370	.901	1.012
-.386	.908	1.050
-.403	.915	1.087
-.421	.923	1.123
-.440	.931	1.160
-.459	.939	1.196
-.480	.948	1.231
-.501	.958	1.265
-.524	.967	1.298
-.548	.978	1.330
-.575	.990	1.360
-.602	1.002	1.389
-.632	1.014	1.416
-.662	1.028	1.440
-.694	1.042	1.463
-.727	1.056	1.484
-.762	1.071	1.502
-.797	1.086	1.517
-.833	1.102	1.531
-.870	1.118	1.542
-.907	1.134	1.551
-.945	1.151	1.558
-.982	1.167	1.563
-1.020	1.184	1.567
-1.058	1.200	1.569
-1.097	1.217	1.569

Spline 12		
X, in.	Y, in.	Z, in.
-.449	1.456	.000
-.450	1.456	.041
-.450	1.456	.082
-.451	1.456	.124
-.452	1.456	.165
-.454	1.457	.206
-.456	1.457	.247
-.458	1.457	.288
-.461	1.458	.329
-.464	1.459	.370
-.467	1.459	.412
-.470	1.460	.453
-.474	1.461	.494
-.478	1.462	.535
-.482	1.463	.576
-.487	1.464	.617
-.492	1.464	.658
-.497	1.466	.698
-.502	1.467	.739
-.508	1.468	.780
-.514	1.469	.821
-.520	1.470	.862
-.526	1.472	.902
-.532	1.473	.943
-.539	1.474	.984
-.545	1.476	1.024
-.552	1.477	1.065
-.559	1.479	1.106
-.566	1.480	1.146
-.573	1.482	1.187
-.581	1.483	1.227
-.588	1.485	1.268
-.597	1.486	1.308
-.607	1.488	1.348
-.618	1.491	1.387
-.633	1.494	1.426
-.650	1.497	1.463
-.671	1.502	1.499
-.695	1.507	1.532
-.722	1.512	1.562
-.752	1.519	1.590
-.784	1.525	1.615
-.818	1.532	1.637
-.853	1.540	1.657
-.890	1.547	1.675
-.927	1.555	1.689
-.966	1.563	1.702
-1.005	1.571	1.712
-1.045	1.579	1.719
-1.085	1.588	1.723
-1.125	1.596	1.725

Table 1. Continued

(a) Continued

Spline 13		
X, in.	Y, in.	Z, in.
-.644	1.967	.000
-.644	1.967	.043
-.644	1.967	.086
-.644	1.967	.130
-.644	1.967	.173
-.644	1.967	.216
-.644	1.967	.259
-.644	1.967	.303
-.644	1.967	.346
-.644	1.967	.389
-.644	1.967	.432
-.644	1.967	.476
-.644	1.967	.519
-.644	1.967	.562
-.644	1.967	.605
-.644	1.967	.649
-.644	1.967	.692
-.644	1.967	.735
-.644	1.967	.778
-.644	1.967	.822
-.644	1.967	.865
-.644	1.967	.908
-.644	1.967	.951
-.644	1.967	.995
-.644	1.967	1.038
-.644	1.967	1.081
-.644	1.967	1.124
-.644	1.967	1.168
-.644	1.967	1.211
-.644	1.967	1.254
-.644	1.967	1.297
-.644	1.967	1.340
-.646	1.967	1.384
-.651	1.967	1.427
-.658	1.967	1.469
-.670	1.967	1.511
-.686	1.967	1.551
-.706	1.967	1.589
-.729	1.967	1.626
-.755	1.967	1.661
-.784	1.967	1.693
-.815	1.967	1.723
-.848	1.967	1.751
-.883	1.967	1.776
-.919	1.967	1.799
-.958	1.967	1.819
-.997	1.967	1.837
-1.038	1.967	1.851
-1.080	1.967	1.861
-1.123	1.967	1.868
-1.166	1.967	1.870

Spline 14		
X, in.	Y, in.	Z, in.
-.630	2.040	.000
-.630	2.040	.044
-.630	2.040	.087
-.630	2.040	.131
-.630	2.040	.175
-.630	2.040	.219
-.630	2.040	.263
-.630	2.040	.306
-.630	2.040	.350
-.630	2.040	.394
-.630	2.040	.438
-.630	2.040	.482
-.630	2.040	.525
-.630	2.040	.569
-.630	2.040	.613
-.630	2.040	.657
-.630	2.040	.701
-.630	2.040	.744
-.630	2.040	.788
-.630	2.040	.832
-.630	2.040	.876
-.630	2.040	.919
-.630	2.040	.963
-.630	2.040	1.007
-.630	2.040	1.051
-.630	2.040	1.095
-.630	2.040	1.138
-.630	2.040	1.182
-.630	2.040	1.226
-.630	2.040	1.270
-.630	2.040	1.314
-.630	2.040	1.357
-.631	2.040	1.401
-.635	2.041	1.445
-.642	2.043	1.488
-.654	2.045	1.530
-.669	2.048	1.571
-.688	2.052	1.610
-.710	2.057	1.648
-.735	2.062	1.683
-.762	2.068	1.717
-.792	2.074	1.749
-.824	2.081	1.778
-.858	2.088	1.805
-.893	2.095	1.829
-.931	2.103	1.851
-.970	2.111	1.870
-1.010	2.119	1.885
-1.051	2.128	1.896
-1.094	2.137	1.903
-1.136	2.146	1.906

Spline 15		
X, in.	Y, in.	Z, in.
-.590	2.110	.000
-.590	2.110	.044
-.590	2.110	.087
-.590	2.110	.131
-.590	2.110	.175
-.590	2.110	.219
-.590	2.110	.263
-.590	2.110	.306
-.590	2.110	.350
-.590	2.110	.394
-.590	2.110	.438
-.590	2.110	.481
-.590	2.110	.525
-.590	2.110	.569
-.590	2.110	.613
-.590	2.110	.656
-.590	2.110	.700
-.590	2.110	.744
-.590	2.110	.788
-.590	2.110	.831
-.590	2.110	.875
-.590	2.110	.919
-.590	2.110	.963
-.590	2.110	1.007
-.590	2.110	1.050
-.590	2.110	1.094
-.590	2.110	1.138
-.590	2.110	1.182
-.590	2.110	1.225
-.590	2.110	1.269
-.590	2.110	1.313
-.591	2.110	1.357
-.594	2.112	1.400
-.600	2.114	1.444
-.608	2.117	1.487
-.619	2.122	1.528
-.634	2.129	1.569
-.652	2.137	1.608
-.673	2.146	1.646
-.696	2.156	1.681
-.722	2.167	1.715
-.749	2.178	1.747
-.779	2.191	1.777
-.810	2.205	1.804
-.843	2.219	1.829
-.878	2.234	1.851
-.914	2.250	1.870
-.952	2.266	1.885
-.990	2.283	1.897
-1.030	2.300	1.904
-1.070	2.317	1.907

Spline 16		
X, in.	Y, in.	Z, in.
-.534	2.159	.000
-.534	2.159	.043
-.534	2.159	.086
-.534	2.159	.129
-.534	2.159	.172
-.534	2.159	.215
-.534	2.159	.258
-.534	2.159	.301
-.534	2.159	.345
-.534	2.159	.388
-.534	2.159	.431
-.534	2.159	.474
-.534	2.159	.517
-.534	2.159	.560
-.534	2.159	.603
-.534	2.159	.646
-.534	2.159	.689
-.534	2.159	.732
-.534	2.159	.775
-.534	2.160	.818
-.534	2.160	.861
-.534	2.160	.905
-.534	2.160	.947
-.534	2.160	.991
-.534	2.160	1.034
-.534	2.160	1.077
-.534	2.160	1.120
-.534	2.160	1.163
-.534	2.160	1.206
-.534	2.160	1.249
-.535	2.160	1.292
-.537	2.162	1.335
-.541	2.165	1.378
-.547	2.170	1.420
-.555	2.177	1.462
-.566	2.185	1.503
-.580	2.197	1.542
-.596	2.210	1.580
-.614	2.224	1.616
-.634	2.241	1.650
-.656	2.259	1.683
-.680	2.278	1.713
-.705	2.299	1.741
-.732	2.320	1.767
-.760	2.343	1.790
-.790	2.367	1.811
-.820	2.392	1.828
-.852	2.417	1.842
-.884	2.444	1.853
-.917	2.470	1.860
-.951	2.498	1.862

Table 1. Continued

(a) Continued

Spline 17		
X, in.	Y, in.	Z, in.
-.449	2.198	.000
-.449	2.198	.042
-.449	2.198	.084
-.449	2.198	.126
-.449	2.198	.168
-.449	2.198	.210
-.449	2.198	.252
-.449	2.198	.294
-.449	2.198	.336
-.449	2.198	.379
-.449	2.198	.421
-.449	2.198	.463
-.449	2.198	.505
-.449	2.198	.547
-.449	2.198	.589
-.449	2.198	.631
-.449	2.198	.673
-.449	2.198	.715
-.449	2.198	.757
-.449	2.198	.799
-.449	2.198	.841
-.449	2.198	.883
-.449	2.198	.925
-.449	2.198	.967
-.449	2.198	1.009
-.449	2.198	1.051
-.449	2.198	1.094
-.449	2.198	1.136
-.449	2.198	1.178
-.449	2.198	1.220
-.449	2.199	1.262
-.451	2.201	1.304
-.454	2.205	1.345
-.459	2.213	1.387
-.467	2.223	1.427
-.475	2.236	1.466
-.486	2.251	1.503
-.499	2.269	1.539
-.514	2.289	1.573
-.530	2.312	1.605
-.547	2.336	1.635
-.565	2.362	1.662
-.585	2.389	1.687
-.605	2.418	1.710
-.626	2.448	1.731
-.648	2.479	1.749
-.671	2.511	1.764
-.694	2.544	1.776
-.718	2.578	1.785
-.742	2.612	1.791
-.766	2.646	1.793

Spline 18		
X, in.	Y, in.	Z, in.
-.355	2.212	.000
-.355	2.212	.041
-.355	2.212	.082
-.355	2.212	.123
-.355	2.212	.164
-.355	2.212	.205
-.355	2.212	.247
-.355	2.212	.288
-.355	2.212	.329
-.355	2.212	.370
-.355	2.212	.411
-.355	2.212	.452
-.355	2.212	.493
-.355	2.212	.534
-.355	2.212	.575
-.355	2.212	.616
-.355	2.212	.657
-.355	2.212	.698
-.355	2.212	.740
-.355	2.212	.781
-.355	2.212	.822
-.355	2.212	.863
-.355	2.212	.904
-.355	2.212	.945
-.355	2.212	.986
-.355	2.212	1.028
-.355	2.212	1.068
-.355	2.212	1.110
-.355	2.212	1.151
-.355	2.212	1.192
-.355	2.212	1.233
-.356	2.214	1.274
-.357	2.218	1.315
-.360	2.225	1.355
-.364	2.236	1.395
-.369	2.249	1.433
-.374	2.265	1.470
-.381	2.284	1.507
-.389	2.306	1.541
-.397	2.329	1.573
-.407	2.356	1.603
-.417	2.384	1.631
-.428	2.414	1.656
-.439	2.447	1.679
-.451	2.480	1.699
-.464	2.515	1.717
-.477	2.552	1.731
-.490	2.589	1.742
-.504	2.627	1.750
-.517	2.665	1.755
-.531	2.704	1.757

Spline 19		
X, in.	Y, in.	Z, in.
-2.473	1.748	.000
-2.472	1.748	.047
-2.470	1.746	.095
-2.466	1.744	.142
-2.463	1.741	.190
-2.457	1.737	.237
-2.451	1.733	.284
-2.442	1.727	.330
-2.434	1.721	.377
-2.423	1.713	.422
-2.412	1.705	.468
-2.399	1.696	.513
-2.386	1.687	.557
-2.370	1.676	.601
-2.355	1.665	.645
-2.338	1.653	.687
-2.319	1.640	.729
-2.300	1.626	.771
-2.279	1.612	.811
-2.259	1.597	.851
-2.236	1.581	.890
-2.213	1.565	.928
-2.188	1.548	.965
-2.164	1.530	1.001
-2.137	1.511	1.036
-2.111	1.492	1.071
-2.083	1.472	1.104
-2.053	1.452	1.136
-2.024	1.431	1.166
-1.994	1.410	1.196
-1.963	1.388	1.225
-1.931	1.365	1.252
-1.898	1.342	1.278
-1.866	1.319	1.303
-1.832	1.295	1.327
-1.798	1.271	1.349
-1.763	1.246	1.370
-1.727	1.221	1.389
-1.692	1.196	1.408
-1.655	1.170	1.424
-1.618	1.144	1.440
-1.581	1.118	1.454
-1.543	1.091	1.466
-1.506	1.065	1.477
-1.467	1.038	1.487
-1.429	1.011	1.495
-1.391	.984	1.502
-1.352	.956	1.507
-1.314	.929	1.511
-1.275	.902	1.513
-1.236	.874	1.514

Spline 20		
X, in.	Y, in.	Z, in.
-2.442	1.802	.000
-2.440	1.801	.047
-2.437	1.800	.094
-2.433	1.798	.141
-2.428	1.796	.188
-2.421	1.793	.235
-2.414	1.789	.282
-2.405	1.785	.328
-2.394	1.781	.374
-2.383	1.776	.419
-2.369	1.770	.465
-2.356	1.765	.509
-2.341	1.758	.554
-2.325	1.751	.598
-2.309	1.744	.641
-2.290	1.736	.684
-2.270	1.727	.726
-2.250	1.719	.768
-2.230	1.709	.809
-2.206	1.700	.850
-2.184	1.689	.890
-2.160	1.679	.929
-2.135	1.668	.968
-2.108	1.656	1.005
-2.080	1.644	1.041
-2.049	1.631	1.076
-2.019	1.618	1.110
-1.989	1.605	1.143
-1.957	1.591	1.175
-1.924	1.577	1.206
-1.892	1.562	1.236
-1.856	1.547	1.265
-1.822	1.532	1.293
-1.786	1.517	1.320
-1.749	1.501	1.346
-1.712	1.485	1.370
-1.676	1.468	1.394
-1.637	1.452	1.416
-1.599	1.435	1.437
-1.558	1.418	1.457
-1.518	1.400	1.475
-1.479	1.383	1.492
-1.437	1.365	1.507
-1.395	1.347	1.521
-1.354	1.329	1.533
-1.312	1.310	1.544
-1.269	1.292	1.553
-1.226	1.273	1.560
-1.184	1.254	1.565
-1.139	1.235	1.568
-1.096	1.217	1.569

Table 1. Continued

(a) Continued

Spline 21		
X, in.	Y, in.	Z, in.
-2.423	1.866	.000
-2.421	1.866	.047
-2.418	1.865	.094
-2.413	1.864	.141
-2.409	1.863	.187
-2.401	1.862	.234
-2.395	1.860	.280
-2.386	1.859	.326
-2.376	1.857	.372
-2.365	1.854	.418
-2.354	1.852	.463
-2.339	1.849	.508
-2.326	1.846	.553
-2.310	1.843	.598
-2.294	1.840	.642
-2.277	1.836	.685
-2.260	1.832	.728
-2.240	1.828	.771
-2.220	1.824	.813
-2.198	1.820	.855
-2.176	1.815	.896
-2.153	1.810	.937
-2.130	1.805	.977
-2.105	1.800	1.017
-2.079	1.795	1.056
-2.052	1.789	1.094
-2.024	1.783	1.131
-1.996	1.777	1.168
-1.965	1.771	1.204
-1.935	1.765	1.240
-1.905	1.758	1.274
-1.873	1.752	1.309
-1.841	1.745	1.342
-1.808	1.738	1.375
-1.775	1.731	1.407
-1.740	1.724	1.438
-1.704	1.717	1.469
-1.669	1.709	1.498
-1.633	1.702	1.526
-1.594	1.694	1.554
-1.557	1.686	1.580
-1.518	1.678	1.604
-1.477	1.669	1.627
-1.436	1.661	1.648
-1.393	1.652	1.667
-1.350	1.643	1.684
-1.306	1.634	1.698
-1.262	1.625	1.709
-1.217	1.615	1.718
-1.172	1.606	1.723
-1.126	1.596	1.725

Spline 22		
X, in.	Y, in.	Z, in.
-2.418	1.967	.000
-2.416	1.967	.048
-2.415	1.967	.096
-2.412	1.967	.144
-2.407	1.967	.192
-2.403	1.967	.240
-2.395	1.967	.288
-2.389	1.967	.336
-2.379	1.967	.383
-2.369	1.967	.430
-2.358	1.967	.477
-2.347	1.967	.524
-2.332	1.967	.570
-2.318	1.967	.616
-2.303	1.967	.662
-2.287	1.967	.707
-2.270	1.967	.752
-2.251	1.967	.797
-2.231	1.967	.841
-2.211	1.967	.885
-2.191	1.967	.928
-2.168	1.967	.971
-2.145	1.967	1.013
-2.122	1.967	1.055
-2.097	1.967	1.096
-2.070	1.967	1.137
-2.045	1.967	1.178
-2.017	1.967	1.217
-1.990	1.967	1.257
-1.960	1.967	1.296
-1.931	1.967	1.334
-1.901	1.967	1.372
-1.871	1.967	1.409
-1.839	1.967	1.445
-1.808	1.967	1.482
-1.775	1.967	1.517
-1.742	1.967	1.551
-1.707	1.967	1.585
-1.670	1.967	1.617
-1.635	1.967	1.649
-1.597	1.967	1.680
-1.560	1.967	1.709
-1.521	1.967	1.738
-1.481	1.967	1.766
-1.440	1.967	1.792
-1.399	1.967	1.816
-1.354	1.967	1.835
-1.309	1.967	1.850
-1.262	1.967	1.861
-1.214	1.967	1.868
-1.166	1.967	1.870

Spline 23		
X, in.	Y, in.	Z, in.
-2.417	2.412	.000
-2.416	2.412	.050
-2.415	2.412	.100
-2.413	2.411	.149
-2.408	2.410	.199
-2.404	2.409	.249
-2.399	2.408	.298
-2.393	2.407	.347
-2.384	2.405	.397
-2.376	2.404	.446
-2.367	2.401	.495
-2.356	2.399	.543
-2.344	2.397	.591
-2.330	2.394	.639
-2.315	2.391	.687
-2.299	2.388	.734
-2.283	2.384	.781
-2.266	2.381	.827
-2.247	2.377	.873
-2.226	2.372	.919
-2.207	2.368	.964
-2.184	2.364	1.008
-2.160	2.358	1.051
-2.134	2.353	1.093
-2.107	2.348	1.135
-2.079	2.342	1.177
-2.052	2.336	1.217
-2.022	2.330	1.257
-1.993	2.324	1.297
-1.963	2.318	1.336
-1.931	2.311	1.374
-1.900	2.304	1.411
-1.867	2.297	1.448
-1.833	2.290	1.485
-1.799	2.283	1.520
-1.764	2.276	1.554
-1.728	2.269	1.588
-1.691	2.261	1.621
-1.655	2.253	1.654
-1.616	2.246	1.686
-1.579	2.238	1.717
-1.539	2.229	1.746
-1.500	2.221	1.775
-1.457	2.213	1.801
-1.415	2.204	1.826
-1.372	2.195	1.848
-1.327	2.185	1.867
-1.281	2.176	1.883
-1.233	2.166	1.895
-1.185	2.156	1.903
-1.137	2.146	1.906

Spline 24		
X, in.	Y, in.	Z, in.
-2.326	2.859	.000
-2.326	2.859	.051
-2.323	2.859	.101
-2.320	2.857	.152
-2.316	2.856	.202
-2.311	2.853	.252
-2.306	2.851	.302
-2.299	2.848	.352
-2.290	2.844	.402
-2.281	2.840	.451
-2.270	2.835	.501
-2.258	2.830	.549
-2.246	2.825	.598
-2.231	2.819	.646
-2.217	2.812	.694
-2.200	2.805	.742
-2.183	2.798	.789
-2.166	2.790	.835
-2.147	2.782	.882
-2.127	2.773	.927
-2.105	2.764	.972
-2.083	2.754	1.016
-2.061	2.744	1.060
-2.037	2.734	1.104
-2.011	2.723	1.146
-1.985	2.712	1.188
-1.959	2.700	1.229
-1.931	2.688	1.270
-1.902	2.676	1.309
-1.872	2.663	1.348
-1.842	2.650	1.386
-1.810	2.636	1.424
-1.778	2.622	1.460
-1.745	2.608	1.496
-1.711	2.593	1.530
-1.677	2.578	1.564
-1.643	2.563	1.597
-1.607	2.547	1.629
-1.569	2.531	1.660
-1.531	2.515	1.690
-1.494	2.499	1.718
-1.456	2.482	1.746
-1.415	2.465	1.773
-1.376	2.447	1.799
-1.335	2.430	1.823
-1.294	2.412	1.847
-1.253	2.394	1.868
-1.208	2.375	1.885
-1.163	2.355	1.897
-1.118	2.336	1.904
-1.072	2.315	1.907

Table 1. Continued

(a) Concluded

Spline 25		
X, in.	Y, in.	Z, in.
−1.992	3.343	.000
−1.991	3.342	.049
−1.989	3.340	.098
−1.985	3.337	.147
−1.979	3.333	.195
−1.974	3.328	.244
−1.967	3.322	.292
−1.957	3.315	.340
−1.949	3.308	.387
−1.937	3.299	.434
−1.927	3.290	.481
−1.915	3.280	.528
−1.902	3.270	.574
−1.889	3.259	.620
−1.874	3.248	.665
−1.860	3.236	.711
−1.844	3.224	.756
−1.829	3.211	.801
−1.814	3.198	.845
−1.797	3.185	.890
−1.781	3.171	.933
−1.763	3.157	.977
−1.744	3.142	1.020
−1.725	3.126	1.062
−1.704	3.110	1.104
−1.684	3.093	1.145
−1.663	3.076	1.185
−1.640	3.058	1.225
−1.618	3.039	1.265
−1.595	3.020	1.303
−1.570	3.001	1.341
−1.546	2.980	1.378
−1.519	2.960	1.415
−1.494	2.939	1.450
−1.468	2.917	1.485
−1.441	2.895	1.520
−1.412	2.873	1.554
−1.385	2.850	1.587
−1.356	2.827	1.620
−1.327	2.803	1.652
−1.298	2.779	1.682
−1.266	2.754	1.711
−1.235	2.729	1.739
−1.203	2.703	1.764
−1.170	2.675	1.788
−1.135	2.647	1.809
−1.100	2.619	1.827
−1.063	2.589	1.842
−1.027	2.559	1.853
−.988	2.529	1.860
−.951	2.498	1.862

Spline 26		
X, in.	Y, in.	Z, in.
−1.464	3.633	.000
−1.464	3.632	.046
−1.463	3.630	.092
−1.460	3.627	138
−1.457	3.622	.184
−1.453	3.616	.229
−1.448	3.609	.275
−1.442	3.602	.320
−1.436	3.593	.365
−1.429	3.583	.409
−1.421	3.572	.454
−1.413	3.561	.498
−1.404	3.548	.541
−1.395	3.536	.585
−1.386	3.522	.628
−1.377	3.508	.670
−1.366	3.494	.713
−1.355	3.479	.755
−1.344	3.463	.798
−1.333	3.448	.840
−1.322	3.432	.881
−1.311	3.415	.923
−1.300	3.399	.964
−1.286	3.382	1.005
−1.275	3.364	1.046
−1.262	3.345	1.086
−1.248	3.326	1.126
−1.233	3.306	1.165
−1.219	3.285	1.203
−1.203	3.264	1.241
−1.189	3.242	1.279
−1.171	3.219	1.316
−1.155	3.196	1.352
−1.139	3.172	1.387
−1.120	3.147	1.422
−1.103	3.122	1.456
−1.085	3.095	1.489
−1.065	3.069	1.522
−1.047	3.041	1.554
−1.026	3.013	1.584
−1.006	2.985	1.615
−.985	2.956	1.644
−.965	2.926	1.672
−.943	2.895	1.697
−.920	2.862	1.721
−.895	2.828	1.741
−.871	2.793	1.759
−.845	2.758	1.773
−.820	2.721	1.783
−.793	2.684	1.790
−.766	2.646	1.793

Spline 27		
X, in.	Y, in.	Z, in.
−.880	3.681	.000
−.880	3.680	.044
−.880	3.679	.088
−.879	3.677	.132
−.878	3.674	.175
−.876	3.670	.219
−.874	3.665	.263
−.873	3.660	.306
−.870	3.654	.350
−.868	3.647	.393
−.865	3.639	.436
−.863	3.631	.479
−.859	3.621	.522
−.855	3.611	.564
−.852	3.601	.607
−.847	3.589	.649
−.843	3.577	.691
−.838	3.564	.733
−.833	3.550	.774
−.828	3.536	.815
−.824	3.521	.856
−.817	3.506	.897
−.812	3.490	.937
−.807	3.473	.977
−.799	3.456	1.017
−.793	3.438	1.057
−.786	3.419	1.096
−.779	3.399	1.135
−.772	3.379	1.173
−.765	3.358	1.210
−.757	3.336	1.247
−.748	3.313	1.284
−.741	3.289	1.320
−.732	3.265	1.355
−.723	3.239	1.390
−.713	3.213	1.424
−.703	3.187	1.458
−.693	3.159	1.491
−.683	3.131	1.523
−.673	3.102	1.554
−.662	3.072	1.585
−.652	3.042	1.614
−.640	3.010	1.643
−.629	2.977	1.669
−.617	2.942	1.692
−.603	2.905	1.711
−.589	2.866	1.727
−.576	2.827	1.740
−.560	2.786	1.749
−.546	2.745	1.755
−.531	2.704	1.757

Table 1. Concluded

(b) Outer turning vane

X, in.	Y, in.	Z, in.
-.885	2.093	.000
-.890	2.118	.000
-.894	2.144	.000
-.895	2.169	.000
-.895	2.195	.000
-.892	2.221	.000
-.887	2.246	.000
-.878	2.270	.000
-.868	2.294	.000
-.854	2.316	.000
-.838	2.336	.000
-.820	2.355	.000
-.800	2.371	.000
-.779	2.385	.000
-.756	2.398	.000
-.733	2.408	.000
-.708	2.417	.000
-.684	2.425	.000
-.658	2.430	.000
-.633	2.435	.000
-.607	2.438	.000
-.582	2.439	.000
-.447	2.439	.000
-.437	2.435	.000
-.432	2.424	.000
-.437	2.414	.000

X, in.	Y, in.	Z, in.
-.447	2.409	.000
-.473	2.408	.000
-.499	2.405	.000
-.525	2.399	.000
-.550	2.392	.000
-.575	2.384	.000
-.599	2.374	.000
-.623	2.362	.000
-.646	2.350	.000
-.668	2.336	.000
-.689	2.321	.000
-.712	2.304	.000
-.731	2.288	.000
-.750	2.270	.000
-.767	2.251	.000
-.783	2.232	.000
-.799	2.211	.000
-.813	2.189	.000
-.826	2.166	.000
-.837	2.142	.000
-.848	2.117	.000
-.856	2.092	.000
-.862	2.084	.000
-.871	2.081	.000
-.880	2.085	.000

(c) Inner turning vane

X, in.	Y, in.	Z, in.
-1.417	2.183	.000
-1.430	2.230	.000
-1.439	2.278	.000
-1.445	2.326	.000
-1.446	2.374	.000
-1.443	2.423	.000
-1.435	2.471	.000
-1.421	2.517	.000
-1.402	2.562	.000
-1.378	2.604	.000
-1.349	2.643	.000
-1.317	2.679	.000
-1.280	2.711	.000
-1.242	2.741	.000
-1.202	2.769	.000
-1.160	2.793	.000
-1.116	2.814	.000
-1.071	2.832	.000
-1.024	2.846	.000
-.977	2.856	.000
-.929	2.863	.000
-.880	2.865	.000
-.599	2.865	.000
-.589	2.860	.000
-.584	2.850	.000
-.589	2.839	.000

X, in.	Y, in.	Z, in.
-.599	2.835	.000
-.785	2.835	.000
-.831	2.833	.000
-.877	2.826	.000
-.922	2.816	.000
-.966	2.801	.000
-1.009	2.783	.000
-1.049	2.760	.000
-1.088	2.735	.000
-1.125	2.707	.000
-1.160	2.677	.000
-1.194	2.645	.000
-1.225	2.611	.000
-1.253	2.574	.000
-1.280	2.536	.000
-1.303	2.497	.000
-1.324	2.455	.000
-1.342	2.413	.000
-1.357	2.369	.000
-1.369	2.324	.000
-1.378	2.279	.000
-1.384	2.233	.000
-1.388	2.187	.000
-1.392	2.177	.000
-1.401	2.172	.000
-1.411	2.175	.000

Table 2. Coordinates Defining Internal Flow Path and Turning Vane Geometry of 1.4 CR D-Shaped Nozzles

(a) Nozzle internal flow path

Spline 1		
X, in.	Y, in.	Z, in.
−2.501	1.397	.000
−2.471	1.454	.000
−2.455	1.517	.000
−2.452	1.581	.000
−2.452	1.645	.000
−2.452	1.710	.000
−2.452	1.774	.000
−2.452	1.839	.000
−2.452	1.903	.000
−2.452	1.968	.000
−2.452	2.032	.000
−2.452	2.096	.000
−2.452	2.161	.000
−2.452	2.225	.000
−2.452	2.290	.000
−2.452	2.354	.000
−2.449	2.419	.000
−2.443	2.483	.000
−2.434	2.546	.000
−2.422	2.610	.000
−2.407	2.672	.000
−2.388	2.734	.000
−2.367	2.795	.000
−2.342	2.854	.000
−2.315	2.913	.000
−2.284	2.970	.000
−2.251	3.025	.000
−2.216	3.079	.000
−2.177	3.130	.000
−2.136	3.180	.000
−2.093	3.228	.000
−2.048	3.273	.000
−2.000	3.317	.000
−1.950	3.357	.000
−1.898	3.396	.000
−1.844	3.431	.000
−1.789	3.464	.000
−1.732	3.494	.000
−1.674	3.522	.000
−1.614	3.546	.000
−1.553	3.567	.000
−1.491	3.586	.000
−1.429	3.601	.000
−1.366	3.613	.000
−1.302	3.622	.000
−1.238	3.628	.000
−1.173	3.631	.000
−1.109	3.631	.000
−1.044	3.631	.000
−.980	3.631	.000
−.915	3.631	.000

Spline 2		
X, in.	Y, in.	Z, in.
−2.482	1.384	.250
−2.451	1.440	.250
−2.432	1.502	.250
−2.424	1.565	.250
−2.424	1.629	.250
−2.428	1.694	.250
−2.432	1.758	.250
−2.435	1.822	.250
−2.436	1.886	.250
−2.437	1.950	.250
−2.439	2.014	.250
−2.441	2.079	.250
−2.442	2.143	.250
−2.443	2.207	.250
−2.443	2.271	.250
−2.441	2.335	.250
−2.437	2.400	.250
−2.430	2.463	.250
−2.422	2.527	.250
−2.410	2.590	.250
−2.396	2.653	.250
−2.378	2.715	.250
−2.358	2.776	.250
−2.334	2.835	.250
−2.307	2.893	.250
−2.276	2.950	.250
−2.243	3.005	.250
−2.207	3.058	.250
−2.168	3.109	.250
−2.127	3.158	.250
−2.083	3.206	.250
−2.038	3.251	.250
−1.990	3.294	.250
−1.940	3.334	.250
−1.889	3.372	.250
−1.835	3.408	.250
−1.780	3.441	.250
−1.724	3.472	.250
−1.666	3.500	.250
−1.607	3.524	.250
−1.546	3.546	.250
−1.484	3.564	.250
−1.422	3.579	.250
−1.359	3.591	.250
−1.295	3.600	.250
−1.231	3.607	.250
−1.167	3.611	.250
−1.103	3.614	.250
−1.039	3.616	.250
−.975	3.617	.250
−.911	3.617	.250

Spline 3		
X, in.	Y, in.	Z, in.
−2.422	1.341	.500
−2.390	1.397	.500
−2.369	1.457	.500
−2.358	1.519	.500
−2.358	1.583	.500
−2.365	1.647	.500
−2.374	1.710	.500
−2.380	1.773	.500
−2.384	1.837	.500
−2.387	1.900	.500
−2.390	1.964	.500
−2.394	2.028	.500
−2.397	2.091	.500
−2.400	2.155	.500
−2.402	2.219	.500
−2.402	2.282	.500
−2.401	2.346	.500
−2.396	2.410	.500
−2.389	2.473	.500
−2.379	2.536	.500
−2.366	2.598	.500
−2.350	2.660	.500
−2.331	2.721	.500
−2.308	2.780	.500
−2.281	2.838	.500
−2.251	2.894	.500
−2.217	2.948	.500
−2.181	3.001	.500
−2.142	3.051	.500
−2.100	3.099	.500
−2.057	3.146	.500
−2.011	3.190	.500
−1.963	3.232	.500
−1.913	3.272	.500
−1.862	3.310	.500
−1.809	3.345	.500
−1.755	3.379	.500
−1.699	3.409	.500
−1.642	3.437	.500
−1.583	3.463	.500
−1.524	3.486	.500
−1.463	3.506	.500
−1.402	3.523	.500
−1.340	3.537	.500
−1.277	3.549	.500
−1.214	3.558	.500
−1.151	3.565	.500
−1.087	3.570	.500
−1.024	3.574	.500
−.960	3.576	.500
−.896	3.576	.500

Spline 4		
X, in.	Y, in.	Z, in.
−2.313	1.264	.750
−2.281	1.319	.750
−2.259	1.378	.750
−2.247	1.440	.750
−2.246	1.503	.750
−2.254	1.566	.750
−2.267	1.628	.750
−2.279	1.690	.750
−2.289	1.752	.750
−2.296	1.815	.750
−2.302	1.878	.750
−2.308	1.941	.750
−2.314	2.004	.750
−2.319	2.067	.750
−2.325	2.130	.750
−2.328	2.193	.750
−2.331	2.256	.750
−2.330	2.319	.750
−2.327	2.382	.750
−2.320	2.445	.750
−2.311	2.508	.750
−2.298	2.569	.750
−2.281	2.630	.750
−2.260	2.690	.750
−2.236	2.749	.750
−2.208	2.805	.750
−2.176	2.860	.750
−2.140	2.912	.750
−2.102	2.962	.750
−2.061	3.010	.750
−2.018	3.056	.750
−1.972	3.100	.750
−1.924	3.142	.750
−1.875	3.181	.750
−1.824	3.219	.750
−1.772	3.254	.750
−1.718	3.287	.750
−1.663	3.318	.750
−1.606	3.346	.750
−1.549	3.373	.750
−1.490	3.397	.750
−1.431	3.418	.750
−1.371	3.438	.750
−1.310	3.454	.750
−1.248	3.469	.750
−1.186	3.481	.750
−1.124	3.491	.750
−1.061	3.499	.750
−.998	3.504	.750
−.935	3.508	.750
−.872	3.509	.750

Table 2. Continued

(a) Continued

Spline 5		
X, in.	Y, in.	Z, in.
−2.133	1.137	1.000
−2.102	1.192	1.000
−2.082	1.252	1.000
−2.071	1.314	1.000
−2.070	1.377	1.000
−2.079	1.440	1.000
−2.094	1.501	1.000
−2.112	1.561	1.000
−2.131	1.621	1.000
−2.148	1.682	1.000
−2.161	1.744	1.000
−2.171	1.806	1.000
−2.181	1.868	1.000
−2.189	1.931	1.000
−2.198	1.993	1.000
−2.207	2.056	1.000
−2.214	2.118	1.000
−2.220	2.181	1.000
−2.223	2.244	1.000
−2.223	2.307	1.000
−2.220	2.370	1.000
−2.212	2.433	1.000
−2.201	2.495	1.000
−2.186	2.556	1.000
−2.166	2.616	1.000
−2.143	2.675	1.000
−2.115	2.731	1.000
−2.084	2.786	1.000
−2.049	2.839	1.000
−2.011	2.889	1.000
−1.970	2.936	1.000
−1.926	2.982	1.000
−1.880	3.025	1.000
−1.832	3.066	1.000
−1.782	3.104	1.000
−1.730	3.141	1.000
−1.677	3.175	1.000
−1.623	3.206	1.000
−1.567	3.236	1.000
−1.510	3.263	1.000
−1.452	3.288	1.000
−1.393	3.310	1.000
−1.333	3.331	1.000
−1.273	3.349	1.000
−1.212	3.366	1.000
−1.151	3.380	1.000
−1.089	3.392	1.000
−1.027	3.401	1.000
−.964	3.408	1.000
−.901	3.412	1.000
−.838	3.414	1.000

Spline 6		
X, in.	Y, in.	Z, in.
−1.794	.897	1.250
−1.766	.955	1.250
−1.755	1.019	1.250
−1.757	1.083	1.250
−1.767	1.147	1.250
−1.783	1.209	1.250
−1.804	1.271	1.250
−1.827	1.331	1.250
−1.853	1.390	1.250
−1.879	1.449	1.250
−1.906	1.508	1.250
−1.931	1.567	1.250
−1.954	1.627	1.250
−1.974	1.688	1.250
−1.992	1.750	1.250
−2.008	1.813	1.250
−2.021	1.876	1.250
−2.034	1.939	1.250
−2.044	2.003	1.250
−2.053	2.067	1.250
−2.060	2.131	1.250
−2.063	2.195	1.250
−2.064	2.260	1.250
−2.061	2.324	1.250
−2.054	2.389	1.250
−2.044	2.452	1.250
−2.029	2.515	1.250
−2.009	2.576	1.250
−1.984	2.636	1.250
−1.954	2.693	1.250
−1.919	2.747	1.250
−1.879	2.798	1.250
−1.837	2.846	1.250
−1.791	2.892	1.250
−1.742	2.934	1.250
−1.692	2.974	1.250
−1.640	3.012	1.250
−1.586	3.048	1.250
−1.530	3.080	1.250
−1.473	3.111	1.250
−1.415	3.139	1.250
−1.356	3.165	1.250
−1.296	3.188	1.250
−1.235	3.209	1.250
−1.173	3.228	1.250
−1.111	3.245	1.250
−1.048	3.258	1.250
−.984	3.269	1.250
−.920	3.278	1.250
−.856	3.283	1.250
−.792	3.284	1.250

Spline 7		
X, in.	Y, in.	Z, in.
−1.411	.627	1.335
−1.383	.669	1.337
−1.358	.712	1.342
−1.335	.757	1.351
−1.315	.802	1.362
−1.297	.847	1.376
−1.281	.892	1.392
−1.267	.938	1.410
−1.256	.983	1.429
−1.246	1.028	1.450
−1.238	1.073	1.472
−1.232	1.117	1.495
−1.227	1.162	1.519
−1.224	1.206	1.543
−1.221	1.250	1.568
−1.220	1.294	1.593
−1.219	1.338	1.618
−1.218	1.382	1.643
−1.218	1.427	1.667
−1.218	1.471	1.690
−1.218	1.517	1.713
−1.217	1.562	1.735
−1.217	1.608	1.757
−1.216	1.654	1.777
−1.215	1.701	1.797
−1.213	1.748	1.815
−1.211	1.795	1.832
−1.208	1.843	1.848
−1.204	1.892	1.863
−1.199	1.940	1.876
−1.193	1.989	1.888
−1.185	2.038	1.897
−1.174	2.087	1.904
−1.160	2.136	1.909
−1.143	2.183	1.911
−1.123	2.230	1.910
−1.101	2.275	1.906
−1.077	2.319	1.899
−1.051	2.361	1.889
−1.023	2.402	1.878
−.992	2.440	1.865
−.960	2.476	1.851
−.925	2.510	1.836
−.888	2.541	1.822
−.848	2.569	1.807
−.806	2.594	1.794
−.762	2.615	1.782
−.715	2.631	1.772
−.667	2.644	1.764
−.617	2.652	1.758
−.566	2.654	1.757

Spline 8		
X, in.	Y, in.	Z, in.
−1.028	.356	1.250
−1.004	.390	1.250
−.980	.423	1.250
−.956	.457	1.250
−.933	.491	1.250
−.909	.525	1.250
−.886	.559	1.250
−.864	.594	1.250
−.843	.629	1.250
−.823	.665	1.250
−.804	.702	1.250
−.786	.740	1.250
−.770	.778	1.250
−.756	.816	1.250
−.743	.856	1.250
−.732	.895	1.250
−.721	.935	1.250
−.712	.976	1.250
−.704	1.016	1.250
−.697	1.057	1.250
−.691	1.098	1.250
−.686	1.139	1.250
−.682	1.180	1.250
−.679	1.221	1.250
−.676	1.262	1.250
−.674	1.304	1.250
−.672	1.345	1.250
−.671	1.386	1.250
−.671	1.427	1.250
−.671	1.469	1.250
−.671	1.510	1.250
−.671	1.551	1.250
−.672	1.593	1.250
−.673	1.634	1.250
−.674	1.675	1.250
−.675	1.717	1.250
−.676	1.758	1.250
−.677	1.799	1.250
−.678	1.840	1.250
−.679	1.882	1.250
−.679	1.923	1.250
−.674	1.964	1.250
−.660	2.003	1.250
−.640	2.039	1.250
−.615	2.072	1.250
−.584	2.099	1.250
−.549	2.122	1.250
−.512	2.139	1.250
−.473	2.152	1.250
−.432	2.160	1.250
−.391	2.163	1.250

Table 2. Continued

(a) Continued

Spline 9		
X, in.	Y, in.	Z, in.
-.689	.116	1.000
-.665	.154	1.000
-.644	.193	1.000
-.627	.235	1.000
-.613	.278	1.000
-.603	.321	1.000
-.597	.366	1.000
-.595	.411	1.000
-.595	.455	1.000
-.597	.500	1.000
-.598	.545	1.000
-.599	.590	1.000
-.600	.635	1.000
-.601	.680	1.000
-.603	.725	1.000
-.604	.769	1.000
-.605	.814	1.000
-.606	.859	1.000
-.607	.904	1.000
-.608	.949	1.000
-.609	.994	1.000
-.609	1.038	1.000
-.610	1.083	1.000
-.611	1.128	1.000
-.613	1.173	1.000
-.615	1.218	1.000
-.617	1.263	1.000
-.620	1.307	1.000
-.624	1.352	1.000
-.629	1.397	1.000
-.633	1.441	1.000
-.638	1.486	1.000
-.642	1.531	1.000
-.647	1.575	1.000
-.652	1.620	1.000
-.656	1.664	1.000
-.660	1.709	1.000
-.664	1.754	1.000
-.668	1.798	1.000
-.673	1.843	1.000
-.677	1.888	1.000
-.678	1.933	1.000
-.670	1.977	1.000
-.653	2.018	1.000
-.629	2.056	1.000
-.597	2.088	1.000
-.562	2.115	1.000
-.522	2.135	1.000
-.479	2.150	1.000
-.435	2.159	1.000
-.391	2.162	1.000

Spline 10		
X, in.	Y, in.	Z, in.
-.509	-.011	.750
-.484	.029	.750
-.465	.073	.750
-.452	.118	.750
-.444	.165	.750
-.444	.213	.750
-.449	.260	.750
-.455	.307	.750
-.461	.355	.750
-.467	.402	.750
-.474	.449	.750
-.480	.496	.750
-.486	.543	.750
-.492	.590	.750
-.498	.637	.750
-.504	.685	.750
-.510	.732	.750
-.516	.779	.750
-.522	.826	.750
-.529	.873	.750
-.535	.920	.750
-.540	.968	.750
-.546	1.015	.750
-.552	1.062	.750
-.558	1.109	.750
-.565	1.156	.750
-.571	1.203	.750
-.578	1.250	.750
-.584	1.297	.750
-.592	1.344	.750
-.599	1.391	.750
-.606	1.438	.750
-.614	1.485	.750
-.621	1.532	.750
-.629	1.579	.750
-.636	1.626	.750
-.643	1.673	.750
-.651	1.720	.750
-.658	1.767	.750
-.666	1.814	.750
-.673	1.861	.750
-.679	1.908	.750
-.675	1.956	.750
-.661	2.001	.750
-.638	2.043	.750
-.607	2.079	.750
-.571	2.109	.750
-.529	2.132	.750
-.485	2.149	.750
-.438	2.159	.750
-.391	2.162	.750

Spline 11		
X, in.	Y, in.	Z, in.
-.400	-.088	.500
-.375	-.046	.500
-.356	.000	.500
-.345	.048	.500
-.342	.097	.500
-.348	.146	.500
-.357	.195	.500
-.366	.243	.500
-.375	.292	.500
-.384	.340	.500
-.393	.389	.500
-.403	.437	.500
-.412	.486	.500
-.421	.534	.500
-.430	.583	.500
-.439	.631	.500
-.448	.680	.500
-.458	.728	.500
-.467	.777	.500
-.476	.825	.500
-.485	.874	.500
-.494	.922	.500
-.503	.971	.500
-.513	1.019	.500
-.522	1.068	.500
-.531	1.116	.500
-.540	1.165	.500
-.547	1.214	.500
-.557	1.262	.500
-.568	1.310	.500
-.577	1.358	.500
-.586	1.407	.500
-.595	1.455	.500
-.604	1.504	.500
-.613	1.552	.500
-.623	1.601	.500
-.632	1.649	.500
-.641	1.698	.500
-.650	1.746	.500
-.659	1.795	.500
-.669	1.843	.500
-.677	1.892	.500
-.678	1.941	.500
-.666	1.989	.500
-.644	2.034	.500
-.614	2.073	.500
-.576	2.105	.500
-.534	2.130	.500
-.488	2.148	.500
-.440	2.159	.500
-.391	2.162	.500

Spline 12		
X, in.	Y, in.	Z, in.
-.340	-.131	.250
-.315	-.087	.250
-.297	-.040	.250
-.288	.010	.250
-.289	.060	.250
-.298	.110	.250
-.309	.159	.250
-.319	.208	.250
-.330	.257	.250
-.340	.307	.250
-.351	.356	.250
-.361	.405	.250
-.372	.454	.250
-.382	.504	.250
-.393	.553	.250
-.403	.602	.250
-.414	.651	.250
-.424	.701	.250
-.435	.750	.250
-.445	.799	.250
-.456	.848	.250
-.466	.898	.250
-.477	.947	.250
-.487	.996	.250
-.498	1.045	.250
-.508	1.095	.250
-.519	1.144	.250
-.529	1.193	.250
-.540	1.242	.250
-.550	1.292	.250
-.561	1.341	.250
-.571	1.390	.250
-.582	1.439	.250
-.592	1.489	.250
-.603	1.538	.250
-.613	1.587	.250
-.624	1.636	.250
-.634	1.686	.250
-.645	1.735	.250
-.655	1.784	.250
-.666	1.833	.250
-.676	1.883	.250
-.678	1.933	.250
-.668	1.983	.250
-.648	2.028	.250
-.617	2.069	.250
-.580	2.102	.250
-.537	2.128	.250
-.490	2.147	.250
-.441	2.158	.250
-.391	2.162	.250

Table 2. Continued

(a) Continued

Spline 13		
X, in.	Y, in.	Z, in.
-.321	-.144	.000
-.296	-.100	.000
-.279	-.052	.000
-.272	-.002	.000
-.275	.049	.000
-.285	.098	.000
-.296	.148	.000
-.307	.197	.000
-.318	.247	.000
-.328	.296	.000
-.339	.346	.000
-.350	.395	.000
-.361	.445	.000
-.372	.494	.000
-.383	.544	.000
-.394	.593	.000
-.404	.643	.000
-.415	.692	.000
-.426	.742	.000
-.437	.791	.000
-.448	.841	.000
-.459	.890	.000
-.469	.940	.000
-.480	.989	.000
-.491	1.039	.000
-.502	1.088	.000
-.513	1.138	.000
-.524	1.187	.000
-.535	1.237	.000
-.545	1.286	.000
-.556	1.336	.000
-.567	1.385	.000
-.578	1.435	.000
-.589	1.484	.000
-.600	1.534	.000
-.610	1.583	.000
-.621	1.633	.000
-.632	1.682	.000
-.643	1.732	.000
-.654	1.781	.000
-.665	1.831	.000
-.675	1.880	.000
-.678	1.931	.000
-.669	1.980	.000
-.648	2.027	.000
-.618	2.067	.000
-.581	2.101	.000
-.538	2.128	.000
-.491	2.147	.000
-.441	2.158	.000
-.391	2.162	.000

Spline 14		
X, in.	Y, in.	Z, in.
-.321	-.144	.000
-.322	-.144	.042
-.323	-.143	.084
-.326	-.141	.126
-.330	-.138	.167
-.334	-.135	.209
-.340	-.131	.250
-.347	-.126	.291
-.355	-.120	.332
-.364	-.114	.372
-.374	-.106	.413
-.385	-.099	.452
-.398	-.090	.491
-.411	-.081	.530
-.425	-.071	.568
-.440	-.060	.606
-.456	-.049	.643
-.473	-.037	.680
-.491	-.024	.715
-.510	-.011	.750
-.529	.003	.785
-.550	.018	.818
-.571	.033	.851
-.593	.048	.883
-.616	.065	.914
-.640	.082	.944
-.665	.099	.973
-.690	.117	1.001
-.716	.135	1.029
-.743	.154	1.055
-.770	.174	1.080
-.798	.193	1.104
-.827	.214	1.127
-.856	.234	1.149
-.886	.255	1.170
-.916	.277	1.190
-.947	.298	1.208
-.978	.321	1.225
-1.010	.343	1.241
-1.042	.366	1.256
-1.074	.388	1.270
-1.107	.412	1.282
-1.140	.435	1.293
-1.173	.458	1.303
-1.207	.482	1.311
-1.241	.506	1.319
-1.275	.530	1.325
-1.309	.554	1.329
-1.343	.578	1.332
-1.377	.602	1.334
-1.411	.627	1.335

Spline 15		
X, in.	Y, in.	Z, in.
-.375	.510	.000
-.375	.510	.039
-.375	.510	.077
-.376	.511	.116
-.378	.512	.155
-.380	.513	.194
-.383	.514	.232
-.386	.516	.271
-.391	.518	.309
-.395	.520	.348
-.401	.523	.386
-.407	.526	.424
-.413	.529	.462
-.421	.533	.500
-.429	.537	.538
-.438	.542	.575
-.447	.546	.612
-.457	.552	.649
-.468	.557	.686
-.480	.563	.723
-.492	.569	.759
-.505	.576	.795
-.519	.583	.830
-.534	.590	.865
-.549	.598	.900
-.565	.606	.934
-.583	.615	.968
-.601	.624	1.001
-.619	.633	1.034
-.639	.643	1.066
-.659	.653	1.097
-.681	.664	1.127
-.704	.675	1.157
-.727	.687	1.185
-.752	.700	1.211
-.779	.713	1.236
-.807	.727	1.260
-.835	.742	1.281
-.865	.756	1.301
-.895	.772	1.320
-.927	.787	1.337
-.958	.803	1.352
-.991	.820	1.366
-1.024	.836	1.378
-1.057	.853	1.389
-1.091	.870	1.398
-1.124	.887	1.405
-1.159	.904	1.411
-1.193	.921	1.415
-1.228	.939	1.417
-1.262	.956	1.417

Spline 16		
X, in.	Y, in.	Z, in.
-.532	1.223	.000
-.531	1.223	.040
-.531	1.223	.080
-.532	1.223	.120
-.532	1.223	.160
-.533	1.223	.200
-.534	1.223	.240
-.536	1.224	.280
-.537	1.224	.320
-.539	1.225	.360
-.542	1.225	.400
-.544	1.226	.440
-.547	1.227	.480
-.550	1.228	.520
-.554	1.229	.559
-.558	1.230	.599
-.562	1.231	.639
-.566	1.232	.679
-.571	1.233	.718
-.576	1.235	.758
-.582	1.236	.798
-.588	1.238	.837
-.594	1.239	.877
-.601	1.241	.916
-.608	1.243	.956
-.615	1.245	.995
-.623	1.247	1.034
-.631	1.249	1.073
-.640	1.252	1.112
-.649	1.254	1.151
-.659	1.257	1.190
-.669	1.260	1.228
-.681	1.263	1.266
-.695	1.267	1.304
-.711	1.271	1.340
-.730	1.276	1.375
-.752	1.282	1.408
-.776	1.288	1.439
-.803	1.296	1.468
-.831	1.303	1.495
-.861	1.311	1.520
-.893	1.320	1.543
-.925	1.329	1.565
-.959	1.338	1.584
-.994	1.347	1.601
-1.030	1.357	1.617
-1.066	1.367	1.630
-1.103	1.377	1.640
-1.141	1.387	1.649
-1.180	1.397	1.654
-1.218	1.407	1.656

Table 2. Continued

(a) Continued

Spline 17		
X, in.	Y, in.	Z, in.
-.679	1.917	.000
-.679	1.917	.043
-.679	1.917	.086
-.679	1.917	.130
-.679	1.917	.173
-.679	1.917	.216
-.679	1.917	.259
-.679	1.917	.303
-.679	1.917	.346
-.679	1.917	.389
-.679	1.917	.432
-.679	1.917	.476
-.679	1.917	.519
-.679	1.917	.562
-.679	1.917	.605
-.679	1.917	.649
-.679	1.917	.692
-.679	1.917	.735
-.679	1.917	.778
-.679	1.917	.822
-.679	1.917	.865
-.679	1.917	.908
-.679	1.917	.951
-.679	1.917	.995
-.679	1.917	1.038
-.679	1.917	1.081
-.679	1.917	1.124
-.679	1.917	1.168
-.679	1.917	1.211
-.679	1.917	1.254
-.679	1.917	1.297
-.679	1.917	1.341
-.681	1.917	1.384
-.686	1.917	1.427
-.694	1.917	1.469
-.705	1.917	1.511
-.721	1.917	1.551
-.741	1.917	1.590
-.764	1.917	1.626
-.790	1.917	1.661
-.819	1.917	1.693
-.850	1.917	1.723
-.883	1.917	1.751
-.918	1.917	1.776
-.955	1.917	1.799
-.993	1.917	1.820
-1.033	1.917	1.837
-1.073	1.917	1.851
-1.115	1.917	1.861
-1.158	1.917	1.868
-1.201	1.917	1.870

Spline 18		
X, in.	Y, in.	Z, in.
-.666	1.991	.000
-.666	1.991	.044
-.666	1.991	.088
-.666	1.991	.131
-.666	1.991	.175
-.666	1.991	.219
-.666	1.991	.263
-.666	1.991	.307
-.666	1.991	.350
-.666	1.991	.394
-.666	1.991	.438
-.666	1.991	.482
-.666	1.991	.525
-.666	1.991	.569
-.666	1.991	.613
-.666	1.991	.657
-.666	1.991	.701
-.666	1.991	.744
-.666	1.991	.788
-.666	1.991	.832
-.666	1.991	.876
-.666	1.991	.920
-.666	1.991	.963
-.666	1.991	1.007
-.666	1.991	1.051
-.666	1.991	1.095
-.666	1.991	1.138
-.666	1.991	1.182
-.666	1.991	1.226
-.665	1.991	1.270
-.665	1.990	1.314
-.665	1.990	1.357
-.667	1.991	1.401
-.670	1.992	1.445
-.678	1.993	1.488
-.689	1.995	1.530
-.704	1.999	1.571
-.723	2.003	1.610
-.745	2.007	1.648
-.770	2.012	1.683
-.798	2.018	1.717
-.827	2.024	1.749
-.859	2.031	1.778
-.893	2.038	1.805
-.929	2.045	1.829
-.966	2.053	1.851
-1.005	2.061	1.870
-1.045	2.070	1.885
-1.086	2.078	1.896
-1.129	2.087	1.903
-1.172	2.096	1.906

Spline 19		
X, in.	Y, in.	Z, in.
-.625	2.060	.000
-.625	2.060	.044
-.625	2.060	.088
-.625	2.060	.131
-.625	2.060	.175
-.625	2.060	.219
-.625	2.060	.263
-.625	2.060	.306
-.625	2.060	.350
-.625	2.060	.394
-.625	2.060	.438
-.625	2.060	.481
-.625	2.060	.525
-.625	2.060	.569
-.625	2.060	.613
-.625	2.060	.657
-.625	2.060	.700
-.625	2.060	.744
-.625	2.060	.788
-.625	2.060	.832
-.625	2.060	.875
-.625	2.060	.919
-.625	2.060	.963
-.625	2.060	1.007
-.625	2.060	1.050
-.625	2.060	1.094
-.625	2.060	1.138
-.625	2.060	1.182
-.625	2.060	1.225
-.625	2.060	1.269
-.626	2.060	1.313
-.627	2.061	1.357
-.630	2.062	1.400
-.635	2.064	1.444
-.643	2.068	1.487
-.655	2.073	1.529
-.670	2.079	1.569
-.688	2.087	1.608
-.708	2.096	1.646
-.732	2.106	1.682
-.757	2.117	1.715
-.784	2.129	1.747
-.814	2.142	1.777
-.845	2.155	1.804
-.878	2.169	1.829
-.913	2.184	1.851
-.949	2.200	1.870
-.987	2.216	1.886
-1.026	2.233	1.897
-1.065	2.250	1.904
-1.105	2.267	1.907

Spline 20		
X, in.	Y, in.	Z, in.
-.569	2.110	.000
-.569	2.110	.043
-.569	2.110	.086
-.569	2.110	.129
-.569	2.110	.172
-.569	2.110	.215
-.569	2.110	.258
-.569	2.110	.302
-.569	2.110	.345
-.569	2.110	.388
-.569	2.110	.431
-.569	2.110	.474
-.569	2.110	.517
-.569	2.110	.560
-.569	2.110	.603
-.569	2.110	.646
-.569	2.110	.689
-.569	2.110	.732
-.569	2.110	.775
-.569	2.110	.818
-.569	2.110	.861
-.569	2.110	.905
-.569	2.110	.948
-.569	2.110	.991
-.569	2.110	1.034
-.569	2.110	1.077
-.569	2.110	1.120
-.569	2.110	1.163
-.569	2.110	1.206
-.569	2.110	1.249
-.570	2.110	1.292
-.572	2.112	1.335
-.576	2.115	1.378
-.582	2.120	1.420
-.590	2.127	1.462
-.601	2.136	1.503
-.615	2.147	1.542
-.631	2.160	1.580
-.649	2.175	1.616
-.669	2.191	1.650
-.692	2.209	1.683
-.715	2.228	1.713
-.741	2.249	1.741
-.767	2.271	1.767
-.795	2.293	1.790
-.825	2.317	1.811
-.855	2.342	1.828
-.887	2.368	1.843
-.919	2.394	1.853
-.952	2.421	1.860
-.986	2.448	1.862

Table 2. Continued

(a) Continued

Spline 21		
X, in.	Y, in.	Z, in.
-.485	2.149	.000
-.485	2.149	.042
-.485	2.149	.084
-.485	2.149	.126
-.485	2.149	.168
-.485	2.149	.210
-.485	2.149	.252
-.485	2.149	.294
-.485	2.149	.336
-.485	2.149	.379
-.485	2.149	.421
-.485	2.149	.463
-.485	2.149	.505
-.485	2.149	.547
-.485	2.149	.589
-.485	2.149	.631
-.485	2.149	.673
-.485	2.149	.715
-.485	2.149	.757
-.485	2.149	.799
-.485	2.149	.841
-.485	2.149	.883
-.485	2.149	.925
-.485	2.149	.967
-.485	2.149	1.009
-.485	2.149	1.052
-.485	2.149	1.094
-.485	2.149	1.136
-.485	2.149	1.178
-.485	2.149	1.220
-.485	2.149	1.262
-.486	2.151	1.304
-.489	2.156	1.345
-.495	2.163	1.387
-.502	2.173	1.427
-.511	2.186	1.466
-.522	2.201	1.503
-.534	2.219	1.539
-.549	2.240	1.573
-.565	2.262	1.605
-.582	2.286	1.635
-.600	2.312	1.662
-.620	2.340	1.687
-.640	2.369	1.710
-.661	2.399	1.731
-.683	2.430	1.749
-.706	2.462	1.764
-.729	2.495	1.776
-.753	2.528	1.785
-.777	2.562	1.791
-.801	2.596	1.793

Spline 22		
X, in.	Y, in.	Z, in.
-.391	2.162	.000
-.391	2.162	.041
-.391	2.162	.082
-.391	2.162	.123
-.391	2.162	.164
-.391	2.162	.205
-.391	2.162	.247
-.391	2.162	.288
-.391	2.162	.329
-.391	2.162	.370
-.391	2.162	.411
-.391	2.162	.452
-.391	2.162	.493
-.391	2.162	.534
-.391	2.162	.575
-.391	2.162	.616
-.391	2.162	.657
-.391	2.162	.699
-.391	2.162	.740
-.391	2.162	.781
-.391	2.162	.822
-.391	2.162	.863
-.391	2.162	.904
-.391	2.162	.945
-.391	2.162	.986
-.391	2.162	1.028
-.391	2.162	1.068
-.391	2.162	1.110
-.391	2.162	1.151
-.391	2.162	1.192
-.391	2.162	1.233
-.391	2.164	1.274
-.393	2.168	1.315
-.395	2.175	1.355
-.399	2.186	1.395
-.404	2.199	1.433
-.410	2.215	1.470
-.416	2.234	1.507
-.424	2.256	1.541
-.433	2.280	1.573
-.442	2.306	1.603
-.452	2.334	1.631
-.463	2.365	1.657
-.474	2.397	1.679
-.487	2.431	1.699
-.499	2.466	1.717
-.512	2.502	1.731
-.525	2.539	1.742
-.539	2.577	1.750
-.553	2.616	1.755
-.566	2.654	1.757

Spline 23		
X, in.	Y, in.	Z, in.
-2.501	1.397	.000
-2.501	1.397	.042
-2.499	1.396	.084
-2.496	1.394	.126
-2.493	1.391	.167
-2.488	1.388	.209
-2.482	1.384	.250
-2.475	1.379	.291
-2.467	1.373	.332
-2.458	1.367	.372
-2.448	1.360	.413
-2.437	1.352	.452
-2.425	1.343	.491
-2.412	1.334	.530
-2.398	1.324	.568
-2.382	1.313	.606
-2.366	1.302	.643
-2.349	1.290	.680
-2.332	1.277	.715
-2.313	1.264	.750
-2.293	1.250	.785
-2.273	1.236	.818
-2.251	1.221	.851
-2.229	1.205	.883
-2.206	1.189	.914
-2.182	1.172	.944
-2.157	1.154	.973
-2.132	1.136	1.001
-2.106	1.118	1.029
-2.079	1.099	1.055
-2.052	1.080	1.080
-2.024	1.060	1.104
-1.995	1.040	1.127
-1.966	1.019	1.149
-1.936	.998	1.170
-1.906	.977	1.190
-1.875	.955	1.208
-1.844	.933	1.225
-1.812	.910	1.241
-1.780	.888	1.256
-1.748	.865	1.270
-1.715	.842	1.282
-1.682	.818	1.293
-1.649	.795	1.303
-1.615	.771	1.311
-1.582	.747	1.319
-1.548	.723	1.325
-1.514	.699	1.329
-1.480	.675	1.332
-1.445	.651	1.334
-1.411	.627	1.335

Spline 24		
X, in.	Y, in.	Z, in.
-2.452	1.554	.000
-2.451	1.553	.043
-2.448	1.552	.085
-2.444	1.550	.128
-2.439	1.547	.170
-2.432	1.544	.212
-2.425	1.541	.254
-2.417	1.537	.296
-2.407	1.532	.337
-2.397	1.527	.378
-2.386	1.521	.419
-2.373	1.514	.460
-2.359	1.508	.499
-2.345	1.500	.539
-2.329	1.493	.578
-2.313	1.484	.617
-2.295	1.475	.654
-2.277	1.466	.692
-2.257	1.456	.729
-2.237	1.446	.765
-2.216	1.436	.800
-2.194	1.424	.835
-2.171	1.413	.869
-2.147	1.401	.903
-2.123	1.389	.936
-2.097	1.376	.967
-2.071	1.363	.998
-2.044	1.349	1.029
-2.016	1.335	1.058
-1.988	1.321	1.087
-1.959	1.306	1.114
-1.929	1.291	1.141
-1.899	1.276	1.167
-1.868	1.260	1.192
-1.836	1.245	1.216
-1.804	1.228	1.239
-1.771	1.212	1.260
-1.737	1.195	1.281
-1.703	1.178	1.300
-1.669	1.160	1.318
-1.634	1.143	1.335
-1.598	1.125	1.351
-1.562	1.107	1.366
-1.526	1.089	1.379
-1.489	1.070	1.391
-1.452	1.052	1.401
-1.415	1.033	1.408
-1.377	1.014	1.414
-1.339	.995	1.417
-1.301	.975	1.418
-1.262	.956	1.417

Table 2. Continued

(a) Continued

Spline 25		
X, in.	Y, in.	Z, in.
−2.452	1.740	.000
−2.451	1.739	.045
−2.449	1.739	.091
−2.445	1.738	.136
−2.440	1.736	.181
−2.435	1.735	.226
−2.428	1.733	.271
−2.420	1.731	.315
−2.411	1.729	.360
−2.401	1.726	.404
−2.390	1.723	.448
−2.377	1.720	.491
−2.364	1.716	.534
−2.350	1.712	.577
−2.334	1.708	.620
−2.318	1.704	.662
−2.301	1.699	.704
−2.282	1.694	.745
−2.263	1.689	.785
−2.243	1.683	.826
−2.222	1.678	.865
−2.200	1.672	.905
−2.177	1.666	.943
−2.153	1.659	.981
−2.128	1.653	1.019
−2.103	1.646	1.056
−2.077	1.639	1.092
−2.049	1.631	1.127
−2.022	1.624	1.162
−1.993	1.616	1.197
−1.963	1.608	1.230
−1.933	1.600	1.263
−1.902	1.592	1.295
−1.871	1.583	1.327
−1.839	1.574	1.357
−1.806	1.566	1.387
−1.772	1.556	1.416
−1.737	1.547	1.444
−1.701	1.538	1.470
−1.665	1.528	1.496
−1.628	1.518	1.520
−1.591	1.508	1.543
−1.552	1.497	1.565
−1.514	1.487	1.586
−1.474	1.476	1.606
−1.433	1.465	1.623
−1.392	1.454	1.636
−1.349	1.443	1.646
−1.306	1.431	1.653
−1.262	1.419	1.656
−1.218	1.407	1.656

Spline 26		
X, in.	Y, in.	Z, in.
−2.452	1.917	.000
−2.452	1.917	.048
−2.450	1.917	.096
−2.447	1.917	.144
−2.443	1.917	.193
−2.437	1.917	.240
−2.431	1.917	.288
−2.423	1.917	.336
−2.415	1.917	.383
−2.405	1.917	.430
−2.394	1.917	.477
−2.381	1.917	.524
−2.368	1.917	.570
−2.354	1.917	.616
−2.338	1.917	.662
−2.322	1.917	.707
−2.305	1.917	.752
−2.286	1.917	.797
−2.267	1.917	.841
−2.247	1.917	.885
−2.225	1.917	.928
−2.203	1.917	.971
−2.180	1.917	1.013
−2.156	1.917	1.055
−2.132	1.917	1.096
−2.106	1.917	1.137
−2.080	1.917	1.178
−2.053	1.917	1.217
−2.025	1.917	1.257
−1.996	1.917	1.296
−1.967	1.917	1.334
−1.937	1.917	1.372
−1.906	1.917	1.409
−1.875	1.917	1.445
−1.843	1.917	1.482
−1.810	1.917	1.517
−1.776	1.917	1.551
−1.742	1.917	1.585
−1.706	1.917	1.617
−1.670	1.917	1.649
−1.633	1.917	1.680
−1.595	1.917	1.709
−1.556	1.917	1.738
−1.516	1.917	1.766
−1.476	1.917	1.792
−1.434	1.917	1.816
−1.390	1.917	1.835
−1.344	1.917	1.850
−1.297	1.917	1.861
−1.249	1.917	1.868
−1.201	1.917	1.870

Spline 27		
X, in.	Y, in.	Z, in.
−2.452	2.362	.000
−2.451	2.362	.050
−2.450	2.362	.100
−2.447	2.361	.149
−2.444	2.361	.199
−2.440	2.360	.249
−2.434	2.359	.298
−2.428	2.357	.348
−2.420	2.356	.397
−2.411	2.354	.446
−2.401	2.352	.495
−2.390	2.350	.543
−2.378	2.347	.591
−2.365	2.344	.639
−2.351	2.341	.687
−2.335	2.338	.734
−2.318	2.335	.781
−2.301	2.331	.827
−2.282	2.327	.873
−2.262	2.323	.919
−2.241	2.318	.964
−2.219	2.314	1.008
−2.194	2.309	1.051
−2.169	2.303	1.093
−2.142	2.298	1.135
−2.115	2.292	1.177
−2.087	2.286	1.217
−2.058	2.280	1.257
−2.028	2.274	1.297
−1.998	2.268	1.336
−1.966	2.261	1.374
−1.934	2.255	1.412
−1.902	2.248	1.448
−1.868	2.241	1.485
−1.834	2.234	1.520
−1.798	2.226	1.554
−1.763	2.219	1.588
−1.726	2.211	1.621
−1.689	2.204	1.654
−1.652	2.196	1.686
−1.614	2.188	1.717
−1.574	2.180	1.746
−1.534	2.171	1.775
−1.493	2.163	1.801
−1.451	2.154	1.826
−1.407	2.145	1.848
−1.362	2.136	1.867
−1.316	2.126	1.883
−1.268	2.116	1.895
−1.220	2.106	1.903
−1.172	2.096	1.906

Spline 28		
X, in.	Y, in.	Z, in.
−2.361	2.810	.000
−2.360	2.809	.051
−2.359	2.809	.101
−2.356	2.808	.152
−2.352	2.806	.202
−2.347	2.804	.252
−2.341	2.801	.302
−2.333	2.798	.352
−2.325	2.794	.402
−2.316	2.790	.451
−2.305	2.786	.501
−2.293	2.781	.550
−2.281	2.775	.598
−2.267	2.769	.646
−2.252	2.763	.694
−2.236	2.756	.742
−2.219	2.748	.789
−2.201	2.740	.835
−2.182	2.732	.882
−2.162	2.723	.927
−2.141	2.714	.972
−2.119	2.705	1.017
−2.096	2.695	1.060
−2.072	2.684	1.104
−2.047	2.673	1.146
−2.021	2.662	1.188
−1.994	2.651	1.229
−1.966	2.638	1.270
−1.937	2.626	1.309
−1.908	2.613	1.348
−1.877	2.600	1.386
−1.846	2.586	1.424
−1.814	2.572	1.460
−1.781	2.558	1.496
−1.747	2.544	1.530
−1.712	2.529	1.564
−1.677	2.513	1.597
−1.641	2.498	1.629
−1.604	2.482	1.660
−1.567	2.466	1.690
−1.529	2.449	1.718
−1.490	2.432	1.746
−1.451	2.415	1.773
−1.411	2.398	1.799
−1.370	2.380	1.823
−1.329	2.362	1.847
−1.287	2.344	1.868
−1.244	2.325	1.885
−1.199	2.306	1.897
−1.153	2.286	1.904
−1.106	2.266	1.907

Table 2. Continued

(a) Concluded

Spline 29		
X, in.	Y, in.	Z, in.
-2.026	3.293	.000
-2.026	3.292	.049
-2.023	3.291	.098
-2.020	3.288	.147
-2.015	3.284	.195
-2.009	3.279	.244
-2.001	3.273	.292
-1.993	3.266	.340
-1.984	3.258	.387
-1.973	3.250	.434
-1.962	3.241	.481
-1.950	3.231	.528
-1.937	3.220	.574
-1.924	3.210	.620
-1.910	3.198	.666
-1.895	3.186	.711
-1.880	3.174	.756
-1.865	3.161	.801
-1.849	3.149	.845
-1.832	3.135	.890
-1.816	3.122	.933
-1.798	3.107	.977
-1.780	3.092	1.020
-1.760	3.077	1.062
-1.740	3.060	1.104
-1.719	3.044	1.145
-1.698	3.026	1.185
-1.676	3.008	1.225
-1.653	2.990	1.265
-1.629	2.971	1.303
-1.605	2.951	1.341
-1.580	2.931	1.378
-1.555	2.910	1.415
-1.529	2.889	1.450
-1.502	2.867	1.485
-1.475	2.845	1.520
-1.448	2.823	1.554
-1.420	2.801	1.588
-1.392	2.777	1.620
-1.362	2.754	1.652
-1.333	2.730	1.682
-1.302	2.705	1.711
-1.270	2.679	1.739
-1.238	2.653	1.764
-1.205	2.626	1.788
-1.170	2.598	1.809
-1.135	2.569	1.827
-1.099	2.540	1.842
-1.061	2.509	1.853
-1.024	2.479	1.860
-.986	2.448	1.862

Spline 30		
X, in.	Y, in.	Z, in.
-1.500	3.583	.000
-1.500	3.583	.046
-1.498	3.581	.092
-1.496	3.577	.138
-1.492	3.573	.184
-1.488	3.567	.230
-1.483	3.560	.275
-1.478	3.552	.320
-1.471	3.543	.365
-1.464	3.533	.409
-1.457	3.522	.454
-1.449	3.511	.498
-1.440	3.499	.541
-1.431	3.486	.585
-1.422	3.472	.628
-1.412	3.458	.670
-1.401	3.444	.713
-1.391	3.429	.755
-1.380	3.414	.798
-1.369	3.398	.840
-1.358	3.382	.881
-1.346	3.366	.923
-1.334	3.349	.964
-1.322	3.332	1.005
-1.309	3.314	1.046
-1.296	3.295	1.086
-1.283	3.276	1.126
-1.269	3.256	1.165
-1.254	3.236	1.203
-1.239	3.214	1.241
-1.223	3.192	1.279
-1.207	3.170	1.316
-1.191	3.146	1.352
-1.173	3.122	1.387
-1.156	3.097	1.422
-1.138	3.072	1.456
-1.120	3.046	1.489
-1.101	3.019	1.522
-1.081	2.992	1.554
-1.061	2.964	1.585
-1.041	2.935	1.615
-1.021	2.906	1.644
-.999	2.876	1.672
-.977	2.845	1.697
-.954	2.812	1.721
-.930	2.779	1.741
-.906	2.744	1.759
-.880	2.708	1.773
-.854	2.671	1.784
-.828	2.634	1.790
-.986	2.448	1.862
-.801	2.596	1.793

Spline 31		
X, in.	Y, in.	Z, in.
-.915	3.631	.000
-.915	3.630	.044
-.915	3.629	.088
-.914	3.627	.132
-.913	3.624	.175
-.912	3.620	.219
-.910	3.616	.263
-.908	3.610	.306
-.906	3.604	.350
-.904	3.597	.393
-.901	3.589	.436
-.898	3.581	.479
-.894	3.572	.522
-.891	3.562	.564
-.887	3.551	.607
-.883	3.539	.649
-.878	3.527	.691
-.874	3.514	.733
-.869	3.501	.774
-.864	3.486	.815
-.859	3.472	.856
-.853	3.456	.897
-.847	3.440	.937
-.841	3.423	.977
-.835	3.406	1.017
-.829	3.388	1.057
-.822	3.369	1.096
-.815	3.350	1.135
-.808	3.329	1.173
-.800	3.308	1.210
-.792	3.286	1.248
-.784	3.263	1.284
-.776	3.239	1.320
-.767	3.215	1.356
-.758	3.190	1.390
-.749	3.164	1.424
-.739	3.137	1.458
-.729	3.109	1.491
-.719	3.081	1.523
-.709	3.052	1.554
-.698	3.023	1.585
-.687	2.992	1.614
-.676	2.961	1.643
-.664	2.927	1.669
-.651	2.892	1.692
-.638	2.855	1.711
-.624	2.817	1.727
-.610	2.777	1.740
-.596	2.737	1.749
-.581	2.696	1.755
-.566	2.654	1.757

Table 2. Concluded

(b) Outer turning vane

X, in.	Y, in.	Z, in.
-.920	2.043	.000
-.925	2.068	.000
-.929	2.094	.000
-.930	2.120	.000
-.930	2.145	.000
-.927	2.171	.000
-.922	2.196	.000
-.914	2.221	.000
-.903	2.244	.000
-.889	2.266	.000
-.873	2.286	.000
-.855	2.305	.000
-.835	2.321	.000
-.814	2.336	.000
-.791	2.348	.000
-.768	2.359	.000
-.744	2.367	.000
-.719	2.375	.000
-.694	2.381	.000
-.668	2.385	.000
-.643	2.388	.000
-.617	2.390	.000
-.483	2.390	.000
-.472	2.385	.000
-.468	2.375	.000
-.472	2.364	.000

X, in.	Y, in.	Z, in.
-.483	2.360	.000
-.509	2.358	.000
-.535	2.355	.000
-.560	2.350	.000
-.585	2.343	.000
-.610	2.334	.000
-.634	2.324	.000
-.658	2.313	.000
-.681	2.300	.000
-.703	2.286	.000
-.724	2.271	.000
-.747	2.254	.000
-.766	2.238	.000
-.785	2.220	.000
-.802	2.201	.000
-.818	2.182	.000
-.834	2.161	.000
-.848	2.139	.000
-.861	2.116	.000
-.873	2.092	.000
-.883	2.067	.000
-.891	2.042	.000
-.897	2.034	.000
-.906	2.031	.000
-.915	2.035	.000

(c) Inner turning vane

X, in.	Y, in.	Z, in.
-1.452	2.133	.000
-1.465	2.180	.000
-1.474	2.228	.000
-1.480	2.276	.000
-1.481	2.325	.000
-1.478	2.373	.000
-1.470	2.421	.000
-1.456	2.467	.000
-1.437	2.512	.000
-1.413	2.554	.000
-1.384	2.594	.000
-1.352	2.630	.000
-1.315	2.662	.000
-1.277	2.691	.000
-1.237	2.719	.000
-1.195	2.743	.000
-1.151	2.764	.000
-1.106	2.782	.000
-1.060	2.796	.000
-1.012	2.807	.000
-.964	2.813	.000
-.915	2.815	.000
-.635	2.815	.000
-.624	2.811	.000
-.620	2.800	.000
-.624	2.789	.000

X, in.	Y, in.	Z, in.
-.635	2.785	.000
-.820	2.785	.000
-.867	2.783	.000
-.912	2.777	.000
-.958	2.766	.000
-1.001	2.751	.000
-1.044	2.733	.000
-1.084	2.711	.000
-1.123	2.685	.000
-1.160	2.657	.000
-1.196	2.628	.000
-1.229	2.595	.000
-1.260	2.561	.000
-1.289	2.525	.000
-1.315	2.487	.000
-1.338	2.447	.000
-1.359	2.405	.000
-1.377	2.363	.000
-1.392	2.319	.000
-1.404	2.274	.000
-1.414	2.229	.000
-1.420	2.183	.000
-1.423	2.137	.000
-1.427	2.127	.000
-1.436	2.123	.000
-1.446	2.125	.000

Table 3. Coordinates Defining Internal Flow Path and Turning Vane Geometry of 1.4 CR Pegasus Nozzles

(a) Nozzle internal flow path

Spline 1		
X, in.	Y, in.	Z, in.
-2.180	1.542	.000
-2.149	1.599	.000
-2.134	1.663	.000
-2.131	1.728	.000
-2.131	1.794	.000
-2.131	1.859	.000
-2.131	1.925	.000
-2.131	1.990	.000
-2.131	2.056	.000
-2.132	2.121	.000
-2.133	2.187	.000
-2.133	2.252	.000
-2.134	2.317	.000
-2.134	2.383	.000
-2.134	2.448	.000
-2.132	2.514	.000
-2.128	2.579	.000
-2.123	2.644	.000
-2.116	2.709	.000
-2.106	2.774	.000
-2.094	2.838	.000
-2.078	2.902	.000
-2.060	2.965	.000
-2.038	3.027	.000
-2.013	3.087	.000
-1.985	3.146	.000
-1.954	3.204	.000
-1.921	3.260	.000
-1.884	3.314	.000
-1.845	3.367	.000
-1.803	3.417	.000
-1.758	3.464	.000
-1.710	3.509	.000
-1.660	3.551	.000
-1.607	3.590	.000
-1.552	3.625	.000
-1.494	3.656	.000
-1.435	3.683	.000
-1.373	3.706	.000
-1.310	3.724	.000
-1.247	3.739	.000
-1.182	3.751	.000
-1.118	3.760	.000
-1.052	3.767	.000
-.987	3.771	.000
-.922	3.774	.000
-.856	3.775	.000
-.791	3.776	.000
-.725	3.776	.000
-.660	3.775	.000
-.594	3.775	.000

Spline 2		
X, in.	Y, in.	Z, in.
-1.992	1.409	.750
-1.962	1.468	.750
-1.947	1.534	.750
-1.945	1.601	.750
-1.956	1.667	.750
-1.974	1.732	.750
-1.998	1.795	.750
-2.024	1.857	.750
-2.048	1.919	.750
-2.065	1.984	.750
-2.073	2.051	.750
-2.079	2.118	.750
-2.084	2.185	.750
-2.087	2.252	.750
-2.089	2.319	.750
-2.090	2.386	.750
-2.089	2.454	.750
-2.086	2.521	.750
-2.081	2.588	.750
-2.073	2.654	.750
-2.063	2.721	.750
-2.050	2.787	.750
-2.034	2.852	.750
-2.015	2.916	.750
-1.993	2.980	.750
-1.968	3.042	.750
-1.940	3.103	.750
-1.909	3.163	.750
-1.875	3.221	.750
-1.838	3.277	.750
-1.798	3.331	.750
-1.755	3.383	.750
-1.710	3.432	.750
-1.661	3.478	.750
-1.609	3.521	.750
-1.555	3.560	.750
-1.497	3.595	.750
-1.437	3.625	.750
-1.375	3.650	.750
-1.311	3.670	.750
-1.245	3.686	.750
-1.179	3.699	.750
-1.113	3.708	.750
-1.046	3.715	.750
-.979	3.719	.750
-.912	3.722	.750
-.845	3.723	.750
-.777	3.724	.750
-.710	3.724	.750
-.643	3.723	.750
-.576	3.723	.750

Spline 3		
X, in.	Y, in.	Z, in.
-1.473	1.042	1.250
-1.453	1.113	1.250
-1.470	1.185	1.250
-1.497	1.254	1.250
-1.528	1.320	1.250
-1.563	1.386	1.250
-1.600	1.450	1.250
-1.638	1.513	1.250
-1.678	1.575	1.250
-1.720	1.636	1.250
-1.765	1.695	1.250
-1.810	1.753	1.250
-1.854	1.812	1.250
-1.896	1.873	1.250
-1.929	1.940	1.250
-1.947	2.011	1.250
-1.957	2.084	1.250
-1.965	2.158	1.250
-1.970	2.231	1.250
-1.974	2.305	1.250
-1.975	2.379	1.250
-1.973	2.453	1.250
-1.969	2.527	1.250
-1.961	2.600	1.250
-1.950	2.673	1.250
-1.936	2.746	1.250
-1.918	2.817	1.250
-1.896	2.888	1.250
-1.871	2.957	1.250
-1.841	3.025	1.250
-1.809	3.091	1.250
-1.772	3.156	1.250
-1.732	3.218	1.250
-1.688	3.277	1.250
-1.640	3.333	1.250
-1.588	3.386	1.250
-1.532	3.434	1.250
-1.472	3.477	1.250
-1.409	3.514	1.250
-1.341	3.545	1.250
-1.271	3.568	1.250
-1.199	3.585	1.250
-1.126	3.596	1.250
-1.053	3.604	1.250
-.979	3.609	1.250
-.905	3.611	1.250
-.831	3.613	1.250
-.757	3.613	1.250
-.684	3.612	1.250
-.610	3.611	1.250
-.536	3.611	1.250

Spline 4		
X, in.	Y, in.	Z, in.
-1.090	.771	1.335
-1.059	.822	1.340
-1.035	.875	1.355
-1.017	.929	1.375
-1.004	.982	1.399
-.997	1.035	1.426
-.995	1.089	1.454
-.996	1.142	1.481
-1.000	1.196	1.507
-1.007	1.251	1.532
-1.017	1.306	1.554
-1.029	1.360	1.576
-1.044	1.415	1.596
-1.062	1.469	1.616
-1.081	1.523	1.634
-1.103	1.576	1.652
-1.126	1.628	1.670
-1.151	1.680	1.687
-1.175	1.733	1.703
-1.197	1.787	1.718
-1.215	1.843	1.731
-1.228	1.901	1.740
-1.237	1.960	1.746
-1.242	2.020	1.750
-1.245	2.080	1.752
-1.248	2.140	1.752
-1.248	2.200	1.751
-1.247	2.260	1.749
-1.243	2.320	1.747
-1.236	2.379	1.744
-1.226	2.439	1.742
-1.212	2.497	1.740
-1.194	2.554	1.739
-1.171	2.610	1.739
-1.145	2.664	1.740
-1.114	2.715	1.743
-1.079	2.765	1.745
-1.041	2.811	1.747
-.999	2.854	1.748
-.954	2.893	1.748
-.905	2.929	1.746
-.853	2.959	1.741
-.799	2.983	1.734
-.743	3.002	1.724
-.685	3.015	1.712
-.627	3.024	1.700
-.568	3.030	1.688
-.509	3.034	1.677
-.450	3.035	1.668
-.390	3.036	1.662
-.330	3.036	1.660

Table 3. Continued

(a) Continued

Spline 5		
X, in.	Y, in.	Z, in.
-.707	.500	1.250
-.679	.538	1.250
-.651	.576	1.250
-.623	.613	1.250
-.596	.651	1.250
-.570	.691	1.250
-.546	.731	1.250
-.524	.773	1.250
-.503	.815	1.250
-.485	.858	1.250
-.467	.901	1.250
-.451	.946	1.250
-.436	.990	1.250
-.422	1.035	1.250
-.408	1.080	1.250
-.394	1.125	1.250
-.380	1.169	1.250
-.366	1.214	1.250
-.353	1.259	1.250
-.340	1.305	1.250
-.329	1.350	1.250
-.319	1.396	1.250
-.310	1.442	1.250
-.304	1.489	1.250
-.300	1.536	1.250
-.300	1.583	1.250
-.304	1.630	1.250
-.314	1.676	1.250
-.329	1.720	1.250
-.351	1.762	1.250
-.377	1.801	1.250
-.406	1.838	1.250
-.435	1.875	1.250
-.464	1.912	1.250
-.491	1.951	1.250
-.513	1.992	1.250
-.530	2.036	1.250
-.536	2.082	1.250
-.533	2.129	1.250
-.522	2.175	1.250
-.505	2.218	1.250
-.481	2.259	1.250
-.453	2.296	1.250
-.420	2.330	1.250
-.383	2.359	1.250
-.344	2.386	1.250
-.304	2.410	1.250
-.262	2.431	1.250
-.219	2.449	1.250
-.174	2.462	1.250
-.127	2.467	1.250

Spline 6		
X, in.	Y, in.	Z, in.
-.188	.133	.750
-.161	.176	.750
-.137	.221	.750
-.117	.267	.750
-.100	.315	.750
-.087	.364	.750
-.076	.413	.750
-.068	.463	.750
-.062	.514	.750
-.059	.564	.750
-.057	.615	.750
-.056	.665	.750
-.056	.716	.750
-.057	.767	.750
-.059	.817	.750
-.060	.868	.750
-.062	.919	.750
-.064	.969	.750
-.065	1.020	.750
-.066	1.071	.750
-.067	1.121	.750
-.069	1.172	.750
-.070	1.223	.750
-.073	1.273	.750
-.077	1.324	.750
-.081	1.374	.750
-.088	1.424	.750
-.097	1.474	.750
-.108	1.524	.750
-.123	1.572	.750
-.142	1.619	.750
-.164	1.665	.750
-.191	1.708	.750
-.221	1.748	.750
-.254	1.787	.750
-.287	1.825	.750
-.320	1.864	.750
-.351	1.904	.750
-.379	1.946	.750
-.401	1.992	.750
-.413	2.041	.750
-.413	2.092	.750
-.402	2.141	.750
-.383	2.188	.750
-.355	2.230	.750
-.320	2.266	.750
-.279	2.296	.750
-.234	2.321	.750
-.187	2.340	.750
-.138	2.352	.750
-.088	2.357	.750

Spline 7		
X, in.	Y, in.	Z, in.
.000	.000	.000
.029	.044	.000
.054	.091	.000
.076	.139	.000
.095	.188	.000
.110	.239	.000
.122	.291	.000
.131	.343	.000
.138	.395	.000
.143	.448	.000
.145	.501	.000
.147	.553	.000
.147	.606	.000
.147	.659	.000
.145	.712	.000
.143	.765	.000
.140	.818	.000
.137	.870	.000
.133	.923	.000
.129	.976	.000
.124	1.029	.000
.119	1.081	.000
.112	1.134	.000
.103	1.186	.000
.093	1.238	.000
.081	1.289	.000
.067	1.340	.000
.050	1.390	.000
.031	1.440	.000
.009	1.488	.000
-.015	1.535	.000
-.042	1.580	.000
-.071	1.624	.000
-.103	1.667	.000
-.137	1.707	.000
-.172	1.747	.000
-.208	1.785	.000
-.244	1.825	.000
-.278	1.865	.000
-.309	1.908	.000
-.334	1.954	.000
-.352	2.004	.000
-.358	2.057	.000
-.351	2.109	.000
-.333	2.159	.000
-.305	2.203	.000
-.267	2.241	.000
-.222	2.269	.000
-.174	2.290	.000
-.122	2.302	.000
-.070	2.306	.000

Spline 8		
X, in.	Y, in.	Z, in.
.000	.000	.000
-.001	.001	.042
-.003	.002	.084
-.006	.004	.126
-.009	.006	.167
-.013	.009	.209
-.019	.013	.250
-.026	.018	.291
-.034	.024	.332
-.043	.031	.373
-.053	.038	.413
-.065	.046	.452
-.077	.054	.492
-.090	.063	.530
-.104	.073	.569
-.119	.084	.606
-.135	.095	.643
-.152	.107	.680
-.170	.120	.715
-.189	.133	.750
-.208	.147	.785
-.229	.162	.818
-.250	.177	.851
-.272	.193	.883
-.295	.209	.914
-.319	.226	.944
-.344	.243	.973
-.369	.261	1.002
-.395	.279	1.029
-.422	.298	1.055
-.449	.318	1.080
-.477	.338	1.104
-.506	.358	1.127
-.535	.378	1.149
-.565	.399	1.170
-.595	.421	1.190
-.626	.443	1.208
-.657	.465	1.225
-.689	.487	1.241
-.721	.510	1.256
-.753	.533	1.270
-.786	.556	1.282
-.819	.579	1.293
-.852	.603	1.303
-.886	.626	1.311
-.920	.650	1.319
-.953	.674	1.325
-.988	.698	1.329
-1.022	.722	1.332
-1.056	.747	1.334
-1.090	.771	1.335

Table 3. Continued

(a) Continued

Spline 9		
X, in.	Y, in.	Z, in.
.111	.243	.000
.110	.244	.042
.108	.245	.084
.105	.247	.126
.101	.250	.167
.096	.253	.209
.089	.257	.250
.082	.261	.291
.073	.266	.332
.064	.272	.373
.053	.279	.413
.041	.286	.452
.029	.293	.492
.015	.302	.530
.000	.311	.569
-.015	.320	.606
-.032	.330	.644
-.050	.341	.680
-.068	.352	.716
-.088	.364	.751
-.108	.376	.786
-.129	.389	.820
-.152	.403	.853
-.175	.417	.885
-.198	.431	.916
-.223	.446	.947
-.248	.461	.977
-.274	.477	1.006
-.301	.494	1.033
-.329	.511	1.059
-.358	.528	1.085
-.387	.546	1.110
-.416	.563	1.134
-.446	.582	1.157
-.476	.600	1.179
-.507	.619	1.201
-.538	.638	1.221
-.570	.657	1.241
-.602	.677	1.260
-.635	.696	1.278
-.668	.716	1.295
-.701	.736	1.310
-.735	.757	1.325
-.769	.778	1.338
-.803	.799	1.349
-.838	.820	1.358
-.874	.841	1.365
-.909	.863	1.370
-.945	.885	1.373
-.981	.907	1.374
-1.017	.928	1.375

Spline 10		
X, in.	Y, in.	Z, in.
.147	.553	.000
.146	.554	.042
.143	.555	.085
.140	.557	.127
.136	.559	.169
.130	.562	.211
.123	.565	.252
.115	.569	.294
.106	.574	.335
.096	.579	.376
.084	.585	.416
.072	.591	.456
.059	.598	.496
.045	605	.535
.029	.613	.574
.013	.621	.612
-.004	.629	.649
-.022	.639	.687
-.041	.648	.723
-.061	.658	.759
-.082	.669	.795
-.104	.679	.829
-.126	.691	.864
-.149	.702	.897
-.173	.714	.930
-.197	.727	.962
-.223	.739	.994
-.249	.752	1.025
-.276	.766	1.054
-.303	.780	1.083
-.331	.794	1.112
-.359	.808	1.140
-.388	.822	1.168
-.417	.837	1.195
-.447	.852	1.221
-.477	.867	1.247
-.507	.882	1.272
-.538	.898	1.297
-.569	.913	1.321
-.601	.929	1.344
-.633	.946	1.365
-.667	.962	1.386
-.701	.979	1.404
-.736	.997	1.421
-.771	1.015	1.435
-.808	1.033	1.446
-.845	1.052	1.455
-.882	1.071	1.461
-.920	1.089	1.466
-.957	1.108	1.471
-.995	1.127	1.474

Spline 11		
X, in.	Y, in.	Z, in.
.135	.906	.000
.133	.907	044
.131	.908	.087
.128	.909	.131
.123	.911	.174
.117	.913	.217
.110	.916	.260
.100	.920	.303
.090	.924	.345
.080	.928	.387
.068	.933	.429
.055	.938	.471
.041	.943	.512
.026	.949	.552
.009	.955	.592
-.008	.962	.632
-.026	.969	.671
-.044	.976	.710
-.064	.984	.748
-.084	.992	.786
-.104	1.000	.824
-.126	1.008	.861
-.147	1.016	.898
-.170	1.025	.935
-.192	1.034	.971
-.216	1.043	1.007
-.240	1.053	1.042
-.264	1.062	1.077
-.289	1.072	1.112
-.314	1.082	1.146
-.340	1.092	1.180
-.367	1.102	1.213
-.393	1.113	1.246
-.421	1.123	1.278
-.449	1.134	1.310
-.477	1.145	1.341
-.507	1.157	1.371
-.538	1.169	1.399
-.570	1.182	1.426
-.603	1.195	1.451
-.638	1.208	1.474
-.674	1.222	1.494
-.711	1.237	1.512
-.749	1.252	1.528
-.788	1.267	1.541
-.827	1.282	1.552
-.867	1.298	1.561
-.907	1.313	1.568
-.948	1.329	1.573
-.989	1.345	1.575
-1.029	1.361	1.576

Spline 12		
X, in.	Y, in.	Z, in.
.082	1.288	.000
.080	1.289	.046
.078	1.289	.092
.074	1.290	.139
.070	1.291	.185
.065	1.293	.231
.058	1.294	.276
.051	1.296	.322
.043	1.299	.368
.034	1.301	.413
.024	1.304	.458
.013	1.307	.503
-.001	1.310	.547
-.016	1.314	.591
-.031	1.319	.634
-.048	1.323	.677
-.065	1.328	.720
-.082	1.332	.762
-.101	1.337	.804
-.120	1.342	.846
-.139	1.348	.888
-.159	1.353	.929
-.179	1.358	.971
-.199	1.364	1.012
-.218	1.369	1.054
-.238	1.374	1.096
-.258	1.380	1.137
-.279	1.385	1.178
-.301	1.391	1.218
-.323	1.397	1.258
-.347	1.404	1.297
-.373	1.410	1.335
-.400	1.418	1.372
-.428	1.425	1.408
-.458	1.433	1.442
-.490	1.442	1.474
-.524	1.451	1.504
-.560	1.461	1.532
-.598	1.471	1.556
-.638	1.482	1.577
-.679	1.493	1.595
-.721	1.504	1.609
-.764	1.516	1.621
-.808	1.528	1.632
-.852	1.539	1.641
-.896	1.551	1.648
-.940	1.563	1.654
-.985	1.575	1.658
-1.029	1.587	1.662
-1.074	1.599	1.663
-1.119	1.611	1.664

Table 3. Continued

(a) Continued

Spline 13		
X, in.	Y, in.	Z, in.
-.123	1.692	.000
-.123	1.692	.047
-.124	1.692	.095
-.125	1.692	.142
-.127	1.692	.189
-.129	1.692	.237
-.131	1.693	.284
-.135	1.693	.331
-.139	1.694	.379
-.143	1.694	.426
-.148	1.695	.473
-.153	1.696	.520
-.159	1.697	.567
-.165	1.698	.614
-.172	1.699	.661
-.179	1.700	.708
-.187	1.701	.754
-.196	1.702	.801
-.205	1.703	.847
-.215	1.705	.894
-.226	1.706	.940
-.238	1.708	.986
-.251	1.710	1.031
-.265	1.711	1.076
-.280	1.714	1.121
-.296	1.716	1.166
-.313	1.718	1.210
-.331	1.721	1.254
-.353	1.724	1.296
-.376	1.727	1.337
-.401	1.731	1.377
-.428	1.734	1.416
-.456	1.738	1.454
-.486	1.742	1.490
-.518	1.747	1.525
-.552	1.752	1.558
-.588	1.757	1.588
-.626	1.762	1.616
-.665	1.768	1.641
-.707	1.774	1.663
-.751	1.780	1.681
-.795	1.786	1.695
-.841	1.792	1.706
-.887	1.799	1.713
-.934	1.805	1.718
-.981	1.812	1.721
-1.028	1.818	1.723
-1.075	1.825	1.725
-1.122	1.831	1.728
-1.169	1.838	1.730
-1.215	1.845	1.731

Spline 14		
X, in.	Y, in.	Z, in.
-.358	2.062	.000
-.358	2.062	.045
-.359	2.062	.090
-.360	2.062	.135
-.361	2.062	.180
-.363	2.062	.225
-.365	2.062	.270
-.367	2.062	.315
-.370	2.062	.360
-.374	2.062	.405
-.378	2.062	.449
-.382	2.062	.494
-.386	2.062	.539
-.392	2.062	.584
-.397	2.062	.628
-.403	2.062	.673
-.410	2.062	.717
-.417	2.062	.762
-.424	2.062	.806
-.432	2.062	.851
-.441	2.062	.895
-.450	2.062	.939
-.460	2.062	.983
-.470	2.062	1.027
-.481	2.062	1.070
-.493	2.062	1.114
-.505	2.062	1.157
-.518	2.062	1.200
-.532	2.062	1.243
-.547	2.062	1.285
-.563	2.062	1.327
-.580	2.062	1.369
-.598	2.062	1.410
-.618	2.062	1.451
-.638	2.062	1.491
-.661	2.062	1.530
-.685	2.062	1.567
-.711	2.062	1.604
-.740	2.062	1.639
-.771	2.062	1.671
-.806	2.062	1.700
-.844	2.062	1.724
-.885	2.062	1.742
-.930	2.062	1.750
-.975	2.062	1.751
-1.020	2.062	1.752
-1.065	2.062	1.752
-1.110	2.062	1.752
-1.155	2.062	1.752
-1.200	2.062	1.752
-1.245	2.062	1.752

Spline 15		
X, in.	Y, in.	Z, in.
-.306	2.202	.000
-.306	2.202	.046
-.306	2.202	.092
-.307	2.203	.138
-.309	2.203	.185
-.311	2.204	.231
-.313	2.205	.277
-.315	2.206	.323
-.318	2.207	.369
-.321	2.209	.415
-.325	2.210	.461
-.329	2.212	.507
-.334	2.214	.553
-.339	2.216	.598
-.344	2.219	.644
-.350	2.221	.690
-.357	2.224	.736
-.364	2.227	.781
-.371	2.230	.826
-.379	2.234	.872
-.387	2.237	.917
-.396	2.241	.962
-.406	2.245	1.007
-.416	2.250	1.052
-.427	2.255	1.096
-.439	2.260	1.141
-.451	2.265	1.185
-.464	2.271	1.229
-.479	2.277	1.272
-.494	2.283	1.315
-.510	2.290	1.358
-.527	2.298	1.400
-.545	2.306	1.442
-.565	2.314	1.483
-.586	2.324	1.522
-.610	2.334	1.561
-.635	2.345	1.598
-.662	2.357	1.633
-.693	2.370	1.665
-.726	2.384	1.694
-.763	2.400	1.717
-.802	2.417	1.732
-.844	2.436	1.738
-.887	2.454	1.739
-.929	2.472	1.739
-.971	2.491	1.739
-1.014	2.509	1.739
-1.056	2.527	1.739
-1.098	2.546	1.739
-1.141	2.564	1.739
-1.183	2.582	1.739

Spline 16		
X, in.	Y, in.	Z, in.
-.190	2.284	.000
-.190	2.284	.046
-.191	2.284	.091
-.191	2.285	.137
-.192	2.286	.182
-.194	2.287	.228
-.195	2.289	.274
-.197	2.291	.319
-.199	2.293	.365
-.201	2.295	.410
-.204	2.298	.456
-.206	2.301	.501
-.210	2.305	.546
-.213	2.308	.592
-.217	2.312	.637
-.221	2.317	.682
-.225	2.321	.727
-.230	2.326	.772
-.235	2.332	.817
-.241	2.338	.862
-.247	2.344	.907
-.253	2.351	.952
-.259	2.358	.996
-.266	2.365	1.041
-.273	2.372	1.085
-.281	2.381	1.130
-.289	2.390	1.174
-.299	2.400	1.217
-.309	2.411	1.260
-.321	2.423	1.302
-.334	2.437	1.344
-.348	2.452	1.385
-.363	2.468	1.425
-.379	2.485	1.464
-.396	2.504	1.502
-.414	2.523	1.539
-.433	2.544	1.575
-.454	2.566	1.609
-.476	2.589	1.641
-.500	2.614	1.671
-.525	2.642	1.697
-.553	2.671	1.718
-.583	2.703	1.731
-.614	2.736	1.738
-.645	2.769	1.738
-.676	2.803	1.738
-.707	2.836	1.739
-.738	2.869	1.739
-.769	2.903	1.739
-.801	2.936	1.739
-.832	2.969	1.739

Table 3. Continued

(a) Continued

Spline 17		
X, in.	Y, in.	Z, in.
-.133	2.300	.000
-.133	2.301	.044
-.134	2.301	.088
-.134	2.302	.131
-.135	2.303	.175
-.136	2.304	.219
-.137	2.306	.262
-.138	2.308	.306
-.139	2.310	.350
-.141	2.313	.393
-.143	2.316	.437
-.145	2.319	.481
-.147	2.322	.524
-.150	2.326	.568
-.153	2.331	.611
-.156	2.335	.655
-.159	2.340	.698
-.162	2.346	.741
-.166	2.352	.784
-.170	2.358	.827
-.174	2.365	.871
-.179	2.372	.913
-.183	2.379	.956
-.188	2.387	.999
-.194	2.395	1.042
-.200	2.404	1.084
-.206	2.414	1.126
-.212	2.424	1.168
-.219	2.435	1.210
-.227	2.447	1.252
-.235	2.461	1.292
-.245	2.475	1.332
-.255	2.491	1.372
-.266	2.508	1.411
-.277	2.526	1.449
-.290	2.545	1.486
-.303	2.566	1.522
-.317	2.589	1.557
-.332	2.613	1.590
-.349	2.639	1.621
-.367	2.667	1.649
-.387	2.699	1.672
-.409	2.733	1.688
-.432	2.770	1.694
-.456	2.807	1.694
-.480	2.843	1.694
-.503	2.880	1.694
-.527	2.917	1.694
-.550	2.954	1.694
-.574	2.991	1.694
-.597	3.028	1.694

Spline 18		
X, in.	Y, in.	Z, in.
-.070	2.306	.000
-.070	2.307	.042
-.070	2.307	.084
-.070	2.308	.126
-.070	2.309	.168
-.071	2.310	.210
-.072	2.312	.251
-.072	2.314	.293
-.073	2.316	.335
-.074	2.319	.377
-.075	2.322	.419
-.076	2.325	.461
-.077	2.328	.502
-.079	2.332	.544
-.080	2.337	.586
-.082	2.341	.627
-.084	2.346	.669
-.086	2.352	.710
-.088	2.357	.752
-.090	2.363	.793
-.092	2.370	.835
-.095	2.377	.876
-.098	2.385	.917
-.100	2.392	.958
-.103	2.401	.999
-.107	2.410	1.040
-.110	2.419	1.080
-.114	2.430	1.121
-.117	2.440	1.161
-.122	2.452	1.201
-.126	2.464	1.241
-.131	2.477	1.281
-.136	2.491	1.320
-.141	2.506	1.359
-.147	2.522	1.397
-.153	2.540	1.435
-.160	2.559	1.471
-.167	2.579	1.507
-.175	2.602	1.542
-.184	2.627	1.574
-.194	2.655	1.604
-.205	2.686	1.629
-.218	2.721	1.649
-.231	2.759	1.658
-.246	2.799	1.660
-.260	2.838	1.660
-.274	2.878	1.660
-.288	2.917	1.660
-.302	2.957	1.660
-.316	2.996	1.660
-.330	3.036	1.660

Spline 19		
X, in.	Y, in.	Z, in.
-2.180	1.542	.000
-2.179	1.541	.042
-2.177	1.539	.084
-2.175	1.538	.126
-2.171	1.535	.167
-2.167	1.532	.209
-2.161	1.528	.250
-2.154	1.523	.291
-2.146	1.518	.332
-2.137	1.511	.373
-2.127	1.504	.413
-2.116	1.496	.452
-2.104	1.487	.492
-2.091	1.478	.530
-2.076	1.468	.569
-2.061	1.458	.606
-2.045	1.446	.643
-2.028	1.434	.680
-2.011	1.422	.715
-1.992	1.408	.750
-1.972	1.394	.785
-1.951	1.380	.818
-1.930	1.365	.851
-1.908	1.349	.883
-1.885	1.333	.914
-1.861	1.316	.944
-1.836	1.298	.973
-1.811	1.281	1.002
-1.785	1.262	1.029
-1.758	1.243	1.055
-1.731	1.224	1.080
-1.703	1.204	1.104
-1.674	1.184	1.127
-1.645	1.163	1.149
-1.615	1.142	1.170
-1.585	1.121	1.190
-1.554	1.099	1.208
-1.523	1.077	1.225
-1.491	1.055	1.241
-1.459	1.032	1.256
-1.427	1.009	1.270
-1.394	.986	1.282
-1.361	.963	1.293
-1.328	.939	1.303
-1.294	.915	1.311
-1.261	.891	1.319
-1.227	.867	1.325
-1.193	.843	1.329
-1.159	.819	1.332
-1.124	.795	1.334
-1.090	.771	1.335

Spline 20		
X, in.	Y, in.	Z, in.
-2.144	1.613	.000
-2.143	1.613	.042
-2.142	1.611	.084
-2.139	1.610	.126
-2.134	1.607	.168
-2.129	1.604	.210
-2.123	1.600	.252
-2.115	1.595	.293
-2.106	1.590	.334
-2.097	1.584	.375
-2.086	1.578	.415
-2.075	1.571	.455
-2.063	1.564	.495
-2.049	1.555	.534
-2.035	1.547	.573
-2.019	1.537	.611
-2.003	1.527	.648
-1.986	1.517	.685
-1.968	1.506	.722
-1.949	1.494	.758
-1.929	1.482	.793
-1.908	1.469	.827
-1.886	1.456	.861
-1.863	1.442	.894
-1.840	1.428	.926
-1.816	1.413	.957
-1.791	1.398	.988
-1.765	1.383	1.017
-1.737	1.366	1.045
-1.710	1.349	1.072
-1.681	1.332	1.098
-1.653	1.315	1.123
-1.623	1.297	1.148
-1.593	1.279	1.172
-1.563	1.260	1.194
-1.532	1.241	1.216
-1.500	1.222	1.236
-1.469	1.203	1.256
-1.436	1.183	1.275
-1.404	1.163	1.293
-1.370	1.143	1.309
-1.337	1.123	1.324
-1.302	1.102	1.338
-1.268	1.081	1.349
-1.233	1.059	1.359
-1.197	1.038	1.365
-1.161	1.016	1.370
-1.125	.994	1.373
-1.089	.972	1.374
-1.053	.950	1.375
-1.017	.928	1.375

Table 3. Continued

(a) Continued

Spline 21		
X, in.	Y, in.	Z, in.
−2.131	1.699	.000
−2.129	1.698	.043
−2.126	1.696	.086
−2.122	1.694	.128
−2.116	1.691	.171
−2.109	1.688	.213
−2.102	1.684	.255
−2.094	1.680	.297
−2.085	1.675	.339
−2.075	1.670	.381
−2.065	1.665	.422
−2.053	1.659	.463
−2.041	1.653	.504
−2.028	1.647	.544
−2.014	1.640	.584
−1.999	1.632	.624
−1.984	1.624	.663
−1.967	1.616	.702
−1.950	1.607	.740
−1.932	1.598	.778
−1.913	1.589	.816
−1.894	1.579	.853
−1.873	1.569	.889
−1.852	1.558	.925
−1.830	1.547	.960
−1.807	1.535	.994
−1.783	1.523	1.028
−1.758	1.511	1.061
−1.733	1.498	1.093
−1.706	1.485	1.124
−1.679	1.471	1.155
−1.652	1.457	1.184
−1.623	1.443	1.213
−1.594	1.428	1.241
−1.564	1.413	1.268
−1.534	1.398	1.294
−1.503	1.383	1.319
−1.471	1.367	1.343
−1.438	1.350	1.366
−1.405	1.333	1.387
−1.370	1.316	1.406
−1.335	1.298	1.423
−1.299	1.280	1.438
−1.262	1.262	1.450
−1.225	1.243	1.459
−1.187	1.224	1.465
−1.148	1.204	1.469
−1.110	1.185	1.472
−1.072	1.166	1.473
−1.033	1.147	1.474
−.995	1.127	1.474

Spline 22		
X, in.	Y, in.	Z, in.
−2.131	1.791	.000
−2.128	1.790	.044
−2.124	1.789	.087
−2.119	1.787	.131
−2.113	1.784	.174
−2.106	1.781	.217
−2.099	1.778	.260
−2.092	1.776	.303
−2.084	1.773	.346
−2.076	1.770	.389
−2.067	1.766	.431
−2.056	1.762	.474
−2.046	1.758	.516
−2.035	1.754	.558
−2.023	1.749	.600
−2.011	1.744	.641
−1.997	1.739	.683
−1.983	1.733	.724
−1.968	1.728	.765
−1.953	1.722	.805
−1.937	1.715	.845
−1.920	1.709	.885
−1.903	1.702	.925
−1.884	1.695	.964
−1.865	1.687	1.002
−1.845	1.680	1.040
−1.825	1.672	1.078
−1.804	1.663	1.116
−1.782	1.655	1.152
−1.759	1.646	1.189
−1.735	1.636	1.224
−1.709	1.626	1.258
−1.682	1.616	1.290
−1.653	1.605	1.321
−1.624	1.593	1.352
−1.594	1.581	1.381
−1.562	1.569	1.409
−1.530	1.556	1.435
−1.497	1.543	1.460
−1.462	1.530	1.483
−1.426	1.516	1.505
−1.390	1.502	1.524
−1.352	1.487	1.540
−1.313	1.472	1.552
−1.273	1.456	1.562
−1.233	1.440	1.568
−1.192	1.424	1.572
−1.151	1.409	1.575
−1.111	1.393	1.576
−1.070	1.377	1.576
−1.029	1.361	1.576

Spline 23		
X, in.	Y, in.	Z, in.
−2.131	1.884	.000
−2.129	1.883	.044
−2.127	1.883	.088
−2.123	1.882	.132
−2.119	1.880	.177
−2.113	1.879	.220
−2.108	1.878	.264
−2.103	1.876	.308
−2.098	1.875	.352
−2.092	1.873	.396
−2.085	1.871	.440
−2.077	1.869	.483
−2.070	1.867	.527
−2.062	1.865	.570
−2.054	1.863	.614
−2.045	1.861	.657
−2.035	1.858	.700
−2.025	1.855	.743
−2.014	1.852	.786
−2.003	1.849	.829
−1.992	1.846	.871
−1.979	1.843	.914
−1.966	1.839	.956
−1.953	1.836	.998
−1.938	1.832	1.040
−1.923	1.828	1.081
−1.908	1.824	1.122
−1.891	1.819	1.163
−1.874	1.815	1.203
−1.855	1.809	1.243
−1.834	1.804	1.282
−1.811	1.798	1.319
−1.787	1.791	1.355
−1.761	1.784	1.391
−1.734	1.777	1.425
−1.705	1.769	1.458
−1.675	1.761	1.489
−1.643	1.752	1.518
−1.609	1.743	1.545
−1.573	1.734	1.570
−1.536	1.724	1.592
−1.497	1.713	1.611
−1.457	1.702	1.625
−1.416	1.691	1.637
−1.374	1.680	1.646
−1.332	1.669	1.653
−1.289	1.657	1.658
−1.247	1.646	1.661
−1.204	1.634	1.663
−1.161	1.623	1.664
−1.119	1.611	1.664

Spline 24		
X, in.	Y, in.	Z, in.
−2.131	1.973	.000
−2.131	1.973	.045
−2.130	1.972	.089
−2.128	1.972	.134
−2.125	1.972	.179
−2.122	1.971	.223
−2.119	1.971	.268
−2.116	1.971	.312
−2.112	1.970	.357
−2.108	1.970	.401
−2.104	1.969	.446
−2.098	1.968	.490
−2.093	1.967	.534
−2.088	1.967	.579
−2.081	1.966	.623
−2.075	1.965	.667
−2.068	1.964	.711
−2.060	1.963	.755
−2.052	1.962	.799
−2.043	1.960	.843
−2.034	1.959	.887
−2.024	1.958	.930
−2.014	1.956	.974
−2.003	1.955	1.017
−1.991	1.953	1.060
−1.979	1.951	1.103
−1.966	1.950	1.146
−1.952	1.948	1.188
−1.938	1.946	1.230
−1.922	1.943	1.272
−1.904	1.941	1.313
−1.886	1.938	1.354
−1.866	1.936	1.394
−1.845	1.933	1.433
−1.823	1.930	1.471
−1.799	1.926	1.509
−1.773	1.923	1.545
−1.746	1.919	1.580
−1.716	1.915	1.614
−1.684	1.910	1.644
−1.648	1.905	1.671
−1.609	1.900	1.691
−1.567	1.894	1.706
−1.524	1.888	1.716
−1.481	1.882	1.723
−1.437	1.875	1.727
−1.392	1.869	1.729
−1.348	1.863	1.729
−1.304	1.857	1.730
−1.260	1.851	1.731
−1.215	1.845	1.731

Table 3. Continued

(a) Continued

Spline 25		
X, in.	Y, in.	Z, in.
-2.131	2.062	.000
-2.131	2.062	.045
-2.130	2.062	.090
-2.129	2.062	.135
-2.128	2.062	.180
-2.126	2.062	.225
-2.124	2.062	.270
-2.122	2.062	.315
-2.119	2.062	.360
-2.115	2.062	.405
-2.111	2.062	.449
-2.107	2.062	.494
-2.103	2.062	.539
-2.097	2.062	.584
-2.092	2.062	.628
-2.086	2.062	.673
-2.079	2.062	.717
-2.072	2.062	.762
-2.065	2.062	.806
-2.057	2.062	.851
-2.048	2.062	.895
-2.039	2.062	.939
-2.029	2.062	.983
-2.019	2.062	1.027
-2.008	2.062	1.070
-1.996	2.062	1.114
-1.984	2.062	1.157
-1.971	2.062	1.200
-1.957	2.062	1.243
-1.942	2.062	1.285
-1.926	2.062	1.327
-1.909	2.062	1.369
-1.891	2.062	1.410
-1.871	2.062	1.451
-1.851	2.062	1.491
-1.828	2.062	1.530
-1.804	2.062	1.567
-1.778	2.062	1.604
-1.749	2.062	1.639
-1.718	2.062	1.671
-1.683	2.062	1.700
-1.645	2.062	1.724
-1.604	2.062	1.742
-1.560	2.062	1.750
-1.515	2.062	1.751
-1.470	2.062	1.752
-1.425	2.062	1.752
-1.380	2.062	1.752
-1.335	2.062	1.752
-1.290	2.062	1.752
-1.245	2.062	1.752

Spline 26		
X, in.	Y, in.	Z, in.
-2.061	2.963	.000
-2.060	2.963	.046
-2.060	2.963	.092
-2.059	2.962	.138
-2.058	2.962	.185
-2.056	2.961	.231
-2.054	2.960	.277
-2.051	2.959	.323
-2.048	2.958	.369
-2.045	2.956	.415
-2.041	2.955	.461
-2.037	2.953	.507
-2.032	2.951	.553
-2.027	2.949	.598
-2.022	2.946	.644
-2.016	2.944	.690
-2.010	2.941	.736
-2.003	2.938	.781
-1.995	2.935	.826
-1.987	2.931	.872
-1.979	2.928	.917
-1.970	2.924	.962
-1.960	2.919	1.007
-1.950	2.915	1.052
-1.939	2.910	1.096
-1.927	2.905	1.141
-1.915	2.900	1.185
-1.902	2.894	1.229
-1.888	2.888	1.272
-1.873	2.881	1.315
-1.857	2.875	1.358
-1.840	2.867	1.400
-1.821	2.859	1.442
-1.801	2.851	1.483
-1.780	2.841	1.522
-1.757	2.831	1.561
-1.732	2.820	1.598
-1.704	2.808	1.633
-1.674	2.795	1.665
-1.640	2.781	1.694
-1.604	2.765	1.717
-1.564	2.748	1.732
-1.522	2.729	1.738
-1.480	2.711	1.739
-1.437	2.693	1.739
-1.395	2.674	1.739
-1.353	2.656	1.739
-1.310	2.638	1.739
-1.268	2.619	1.739
-1.225	2.601	1.739
-1.183	2.582	1.739

Spline 27		
X, in.	Y, in.	Z, in.
-1.481	3.663	.000
-1.481	3.663	.046
-1.481	3.662	.092
-1.480	3.662	.139
-1.479	3.660	.185
-1.478	3.659	.231
-1.476	3.658	.277
-1.474	3.656	.323
-1.472	3.653	.369
-1.470	3.651	.416
-1.467	3.648	.462
-1.464	3.645	.508
-1.461	3.641	.554
-1.457	3.637	.600
-1.453	3.633	.645
-1.449	3.629	.691
-1.444	3.624	.737
-1.439	3.618	.783
-1.434	3.613	.828
-1.428	3.607	.874
-1.422	3.600	.919
-1.416	3.593	.964
-1.409	3.586	1.009
-1.401	3.578	1.054
-1.393	3.569	1.099
-1.385	3.560	1.143
-1.376	3.551	1.188
-1.367	3.540	1.232
-1.356	3.530	1.276
-1.345	3.518	1.319
-1.334	3.505	1.362
-1.321	3.492	1.404
-1.308	3.478	1.446
-1.293	3.462	1.487
-1.278	3.446	1.527
-1.261	3.427	1.566
-1.242	3.408	1.604
-1.222	3.386	1.639
-1.199	3.362	1.671
-1.174	3.335	1.699
-1.146	3.305	1.722
-1.116	3.273	1.735
-1.084	3.239	1.738
-1.053	3.205	1.738
-1.021	3.172	1.738
-.990	3.138	1.739
-.958	3.104	1.739
-.927	3.070	1.739
-.895	3.037	1.739
-.863	3.003	1.739
-.832	2.969	1.739

Spline 28		
X, in.	Y, in.	Z, in.
-1.067	3.765	.000
-1.067	3.765	.044
-1.067	3.764	.088
-1.066	3.763	.132
-1.065	3.762	.176
-1.064	3.761	.220
-1.063	3.759	.264
-1.062	3.757	.308
-1.060	3.754	.352
-1.058	3.751	.396
-1.056	3.748	.440
-1.054	3.745	.483
-1.052	3.741	.527
-1.049	3.737	.571
-1.046	3.732	.615
-1.043	3.727	.658
-1.040	3.722	.702
-1.036	3.716	.745
-1.032	3.710	.789
-1.028	3.703	.832
-1.023	3.696	.875
-1.018	3.689	.918
-1.013	3.680	.961
-1.008	3.672	1.004
-1.002	3.663	1.047
-.996	3.653	1.089
-.989	3.642	1.132
-.982	3.631	1.174
-.974	3.620	1.215
-.967	3.607	1.257
-.958	3.594	1.298
-.950	3.581	1.339
-.940	3.566	1.379
-.930	3.550	1.419
-.919	3.533	1.459
-.908	3.515	1.497
-.895	3.495	1.534
-.881	3.473	1.570
-.866	3.450	1.603
-.849	3.423	1.634
-.830	3.394	1.661
-.809	3.361	1.682
-.787	3.325	1.693
-.763	3.288	1.694
-.739	3.251	1.694
-.716	3.213	1.694
-.692	3.176	1.694
-.668	3.139	1.694
-.645	3.102	1.694
-.621	3.065	1.694
-.597	3.028	1.694

Table 3. Continued

(a) Concluded

Spline 29		
X, in.	*Y*, in.	*Z*, in.
-.594	3.775	.000
-.594	3.775	.042
-.594	3.774	.084
-.594	3.774	.126
-.594	3.772	.168
-.593	3.771	.210
-.592	3.769	.252
-.592	3.767	.294
-.591	3.765	.336
-.590	3.762	.378
-.589	3.759	.420
-.588	3.756	.462
-.586	3.752	.504
-.585	3.748	.545
-.583	3.744	.587
-.582	3.739	.629
-.580	3.734	.671
-.578	3.729	.712
-.576	3.723	.754
-.573	3.716	.795
-.571	3.710	.837
-.569	3.702	.878
-.566	3.695	.919
-.563	3.687	.960
-.560	3.678	1.001
-.556	3.669	1.042
-.553	3.659	1.083
-.549	3.648	1.123
-.545	3.637	1.164
-.541	3.626	1.204
-.537	3.613	1.244
-.532	3.600	1.283
-.527	3.585	1.322
-.521	3.570	1.361
-.515	3.553	1.399
-.509	3.535	1.437
-.502	3.516	1.473
-.494	3.495	1.509
-.486	3.472	1.543
-.477	3.446	1.575
-.467	3.418	1.605
-.456	3.386	1.630
-.443	3.351	1.649
-.429	3.313	1.658
-.415	3.273	1.660
-.401	3.233	1.660
-.387	3.194	1.660
-.373	3.154	1.660
-.358	3.115	1.660
-.344	3.075	1.660
-.330	3.036	1.660

Table 3. Concluded

(b) Outer turning vane

X, in.	Y, in.	Z, in.
-.961	2.249	.000
-.970	2.289	.000
-.975	2.330	.000
-.978	2.371	.000
-.977	2.411	.000
-.973	2.452	.000
-.965	2.492	.000
-.952	2.531	.000
-.936	2.569	.000
-.915	2.604	.000
-.890	2.636	.000
-.862	2.666	.000
-.831	2.693	.000
-.797	2.716	.000
-.762	2.736	.000
-.725	2.754	.000
-.686	2.768	.000
-.647	2.780	.000
-.607	2.790	.000
-.567	2.798	.000
-.527	2.803	.000
-.486	2.806	.000
-.259	2.806	.000
-.248	2.801	.000
-.244	2.791	.000
-.248	2.780	.000

X, in.	Y, in.	Z, in.
-.259	2.776	.000
-.302	2.774	.000
-.345	2.769	.000
-.388	2.761	.000
-.430	2.750	.000
-.471	2.737	.000
-.512	2.721	.000
-.551	2.702	.000
-.589	2.682	.000
-.626	2.659	.000
-.662	2.634	.000
-.696	2.608	.000
-.729	2.579	.000
-.760	2.549	.000
-.790	2.517	.000
-.817	2.483	.000
-.842	2.448	.000
-.865	2.411	.000
-.885	2.372	.000
-.903	2.333	.000
-.919	2.292	.000
-.932	2.251	.000
-.936	2.242	.000
-.946	2.238	.000
-.956	2.241	.000

(c) Inner turning vane

X, in.	Y, in.	Z, in.
-1.417	2.868	.000
-1.410	2.916	.000
-1.399	2.965	.000
-1.383	3.011	.000
-1.362	3.056	.000
-1.334	3.096	.000
-1.300	3.132	.000
-1.262	3.164	.000
-1.221	3.191	.000
-1.177	3.215	.000
-1.132	3.234	.000
-1.085	3.249	.000
-1.037	3.261	.000
-.988	3.270	.000
-.940	3.277	.000
-.890	3.282	.000
-.841	3.286	.000
-.792	3.289	.000
-.743	3.292	.000
-.693	3.294	.000
-.644	3.295	.000
-.594	3.295	.000
-.434	3.295	.000
-.423	3.291	.000
-.419	3.280	.000
-.423	3.270	.000

X, in.	Y, in.	Z, in.
-.434	3.265	.000
-.491	3.265	.000
-.542	3.264	.000
-.590	3.262	.000
-.638	3.258	.000
-.687	3.252	.000
-.735	3.245	.000
-.783	3.235	.000
-.830	3.224	.000
-.877	3.212	.000
-.924	3.197	.000
-.970	3.180	.000
-1.014	3.161	.000
-1.059	3.140	.000
-1.101	3.117	.000
-1.143	3.092	.000
-1.183	3.064	.000
-1.222	3.034	.000
-1.259	3.003	.000
-1.294	2.969	.000
-1.327	2.933	.000
-1.359	2.896	.000
-1.388	2.857	.000
-1.396	2.851	.000
-1.406	2.852	.000
-1.414	2.858	.000

Table 4. Coordinates Defining Internal Flow Path and Turning Vane Geometry of 1.4 CR Submerged Nozzles

(a) Nozzle internal flow path

Spline 1		
X, in.	Y, in.	Z, in.
-2.180	1.542	.000
-2.155	1.578	.000
-2.131	1.616	.000
-2.108	1.654	.000
-2.086	1.693	.000
-2.064	1.732	.000
-2.043	1.771	.000
-2.022	1.810	.000
-2.001	1.849	.000
-1.979	1.888	.000
-1.957	1.927	.000
-1.935	1.965	.000
-1.911	2.003	.000
-1.886	2.040	.000
-1.860	2.076	.000
-1.832	2.111	.000
-1.803	2.145	.000
-1.772	2.177	.000
-1.739	2.207	.000
-1.706	2.236	.000
-1.671	2.264	.000
-1.635	2.290	.000
-1.598	2.315	.000
-1.560	2.339	.000
-1.522	2.362	.000
-1.483	2.383	.000
-1.443	2.403	.000
-1.403	2.422	.000
-1.362	2.441	.000
-1.321	2.458	.000
-1.280	2.474	.000
-1.238	2.490	.000
-1.196	2.505	.000
-1.154	2.519	.000
-1.111	2.533	.000
-1.069	2.546	.000
-1.026	2.558	.000
-.983	2.570	.000
-.940	2.581	.000
-.897	2.592	.000
-.854	2.603	.000
-.810	2.613	.000
-.767	2.622	.000
-.723	2.632	.000
-.680	2.642	.000
-.636	2.651	.000
-.593	2.661	.000
-.549	2.671	.000
-.506	2.680	.000
-.462	2.690	.000
-.419	2.700	.000

Spline 2		
X, in.	Y, in.	Z, in.
-2.090	1.478	.531
-2.066	1.514	.531
-2.042	1.552	.531
-2.021	1.590	.531
-2.000	1.628	.531
-1.980	1.668	.531
-1.962	1.707	.531
-1.943	1.747	.531
-1.926	1.787	.531
-1.908	1.827	.531
-1.889	1.867	.531
-1.870	1.907	.531
-1.850	1.946	.531
-1.829	1.984	.531
-1.806	2.022	.531
-1.781	2.058	.531
-1.754	2.093	.531
-1.726	2.126	.531
-1.696	2.158	.531
-1.664	2.188	.531
-1.631	2.218	.531
-1.597	2.245	.531
-1.562	2.272	.531
-1.526	2.297	.531
-1.490	2.321	.531
-1.452	2.344	.531
-1.414	2.366	.531
-1.376	2.387	.531
-1.337	2.407	.531
-1.297	2.426	.531
-1.257	2.444	.531
-1.217	2.462	.531
-1.176	2.478	.531
-1.136	2.494	.531
-1.094	2.510	.531
-1.053	2.525	.531
-1.012	2.539	.531
-.970	2.552	.531
-.928	2.565	.531
-.886	2.578	.531
-.844	2.590	.531
-.802	2.602	.531
-.759	2.614	.531
-.717	2.625	.531
-.674	2.636	.531
-.632	2.647	.531
-.589	2.658	.531
-.547	2.669	.531
-.504	2.680	.531
-.462	2.690	.531
-.419	2.700	.531

Spline 3		
X, in.	Y, in.	Z, in.
-1.750	1.238	1.062
-1.728	1.274	1.062
-1.709	1.313	1.062
-1.693	1.353	1.062
-1.682	1.394	1.062
-1.673	1.436	1.062
-1.666	1.479	1.062
-1.662	1.521	1.062
-1.658	1.564	1.062
-1.655	1.607	1.062
-1.652	1.650	1.062
-1.648	1.692	1.062
-1.643	1.735	1.062
-1.636	1.777	1.062
-1.626	1.819	1.062
-1.614	1.860	1.062
-1.598	1.900	1.062
-1.579	1.939	1.062
-1.558	1.976	1.062
-1.534	2.011	1.062
-1.507	2.046	1.062
-1.480	2.078	1.062
-1.451	2.110	1.062
-1.420	2.140	1.062
-1.389	2.170	1.062
-1.358	2.199	1.062
-1.326	2.228	1.062
-1.293	2.255	1.062
-1.259	2.282	1.062
-1.225	2.308	1.062
-1.191	2.334	1.062
-1.155	2.358	1.062
-1.120	2.382	1.062
-1.084	2.405	1.062
-1.047	2.428	1.062
-1.010	2.450	1.062
-.973	2.471	1.062
-.936	2.492	1.062
-.898	2.512	1.062
-.859	2.532	1.062
-.821	2.550	1.062
-.782	2.568	1.062
-.742	2.586	1.062
-.703	2.602	1.062
-.663	2.618	1.062
-.623	2.634	1.062
-.583	2.649	1.062
-.542	2.664	1.062
-.502	2.677	1.062
-.461	2.689	1.062
-.419	2.700	1.062

Spline 4		
X, in.	Y, in.	Z, in.
-1.439	1.017	1.265
-1.413	1.048	1.267
-1.390	1.081	1.270
-1.372	1.117	1.273
-1.357	1.155	1.277
-1.347	1.193	1.281
-1.340	1.233	1.286
-1.335	1.272	1.291
-1.334	1.312	1.296
-1.334	1.352	1.301
-1.335	1.392	1.307
-1.337	1.432	1.312
-1.338	1.472	1.317
-1.339	1.512	1.323
-1.339	1.552	1.328
-1.337	1.592	1.333
-1.331	1.632	1.338
-1.322	1.671	1.342
-1.310	1.709	1.346
-1.293	1.745	1.350
-1.272	1.780	1.353
-1.248	1.812	1.355
-1.222	1.843	1.357
-1.195	1.872	1.359
-1.166	1.900	1.361
-1.136	1.927	1.362
-1.105	1.953	1.363
-1.073	1.978	1.364
-1.041	2.002	1.365
-1.008	2.025	1.366
-.974	2.047	1.366
-.940	2.069	1.367
-.905	2.090	1.367
-.871	2.110	1.367
-.835	2.129	1.367
-.800	2.148	1.367
-.764	2.167	1.367
-.728	2.186	1.367
-.692	2.204	1.367
-.656	2.222	1.366
-.620	2.240	1.366
-.584	2.258	1.366
-.548	2.276	1.366
-.512	2.294	1.365
-.476	2.312	1.365
-.440	2.331	1.365
-.405	2.350	1.365
-.370	2.369	1.365
-.334	2.389	1.365
-.299	2.409	1.365
-.264	2.428	1.365

Table 4. Continued

(a) Continued

Spline 5		
X, in.	Y, in.	Z, in.
-1.090	.771	1.335
-1.070	.801	1.335
-1.052	.833	1.337
-1.036	.866	1.338
-1.022	.900	1.341
-1.010	.935	1.344
-1.001	.970	1.348
-.993	1.006	1.352
-.988	1.042	1.357
-.983	1.078	1.362
-.980	1.114	1.367
-.978	1.151	1.373
-.976	1.187	1.379
-.975	1.223	1.385
-.974	1.259	1.391
-.972	1.296	1.397
-.970	1.332	1.402
-.966	1.368	1.408
-.960	1.404	1.412
-.952	1.440	1.417
-.941	1.474	1.420
-.927	1.508	1.423
-.910	1.541	1.424
-.890	1.572	1.425
-.868	1.601	1.425
-.844	1.629	1.425
-.819	1.655	1.423
-.792	1.680	1.422
-.764	1.704	1.420
-.734	1.726	1.417
-.704	1.747	1.415
-.673	1.766	1.412
-.642	1.785	1.409
-.610	1.803	1.406
-.578	1.820	1.403
-.545	1.836	1.400
-.512	1.852	1.396
-.478	1.866	1.393
-.444	1.880	1.390
-.410	1.894	1.387
-.376	1.906	1.384
-.341	1.919	1.381
-.307	1.930	1.378
-.272	1.942	1.375
-.237	1.952	1.373
-.201	1.963	1.371
-.166	1.972	1.369
-.131	1.982	1.367
-.095	1.991	1.366
-.059	1.999	1.365
-.023	2.007	1.365

Spline 6		
X, in.	Y, in.	Z, in.
-.742	.524	1.265
-.724	.551	1.265
-.708	.578	1.267
-.693	.607	1.269
-.680	.636	1.271
-.668	.665	1.275
-.658	.695	1.279
-.649	.725	1.283
-.641	.756	1.288
-.635	.786	1.294
-.629	.817	1.301
-.624	.848	1.307
-.620	.879	1.314
-.617	.910	1.321
-.613	.941	1.328
-.609	.971	1.335
-.604	1.002	1.342
-.599	1.033	1.348
-.593	1.064	1.354
-.585	1.094	1.359
-.575	1.124	1.363
-.563	1.154	1.366
-.550	1.183	1.367
-.534	1.211	1.368
-.517	1.237	1.368
-.498	1.263	1.369
-.477	1.287	1.369
-.454	1.309	1.370
-.430	1.330	1.370
-.405	1.350	1.370
-.378	1.367	1.371
-.351	1.384	1.371
-.323	1.400	1.371
-.295	1.415	1.372
-.267	1.429	1.372
-.238	1.443	1.372
-.209	1.457	1.372
-.180	1.469	1.372
-.150	1.482	1.372
-.121	1.493	1.371
-.091	1.504	1.371
-.061	1.515	1.370
-.030	1.524	1.370
.000	1.533	1.369
.031	1.542	1.368
.062	1.550	1.368
.093	1.558	1.367
.124	1.565	1.366
.155	1.573	1.366
.186	1.580	1.365
.217	1.587	1.365

Spline 7		
X, in.	Y, in.	Z, in.
-.430	.304	1.062
-.413	.328	1.062
-.398	.352	1.062
-.382	.377	1.062
-.368	.402	1.062
-.355	.428	1.062
-.342	.454	1.062
-.331	.481	1.062
-.321	.508	1.062
-.311	.535	1.062
-.302	.563	1.062
-.293	.590	1.062
-.285	.618	1.062
-.278	.646	1.062
-.271	.674	1.062
-.266	.703	1.062
-.261	.731	1.062
-.257	.760	1.062
-.253	.789	1.062
-.250	.818	1.062
-.248	.847	1.062
-.245	.876	1.062
-.241	.904	1.062
-.237	.933	1.062
-.231	.961	1.062
-.224	.990	1.062
-.215	1.017	1.062
-.205	1.044	1.062
-.192	1.070	1.062
-.177	1.095	1.062
-.160	1.118	1.062
-.141	1.140	1.062
-.120	1.160	1.062
-.097	1.179	1.062
-.073	1.195	1.062
-.048	1.209	1.062
-.022	1.222	1.062
.005	1.234	1.062
.032	1.244	1.062
.059	1.253	1.062
.087	1.261	1.062
.115	1.269	1.062
.143	1.275	1.062
.172	1.281	1.062
.200	1.286	1.062
.229	1.290	1.062
.258	1.295	1.062
.286	1.299	1.062
.315	1.304	1.062
.344	1.309	1.062
.372	1.315	1.062

Spline 8		
X, in.	Y, in.	Z, in.
-.090	.064	.531
-.074	.089	.531
-.060	.116	.531
-.049	.144	.531
-.042	.174	.531
-.038	.203	.531
-.037	.234	.531
-.038	.264	.531
-.040	.294	.531
-.043	.324	.531
-.046	.354	.531
-.049	.384	.531
-.052	.414	.531
-.056	.444	.531
-.059	.474	.531
-.062	.504	.531
-.066	.534	.531
-.070	.564	.531
-.074	.594	.531
-.078	.624	.531
-.082	.654	.531
-.085	.684	.531
-.088	.714	.531
-.091	.744	.531
-.093	.774	.531
-.094	.804	.531
-.093	.835	.531
-.090	.865	.531
-.085	.894	.531
-.079	.924	.531
-.071	.953	.531
-.062	.982	.531
-.050	1.010	.531
-.038	1.037	.531
-.023	1.064	.531
-.007	1.089	.531
.011	1.114	.531
.030	1.137	.531
.051	1.159	.531
.073	1.180	.531
.096	1.199	.531
.120	1.217	.531
.146	1.233	.531
.172	1.248	.531
.199	1.261	.531
.227	1.273	.531
.255	1.284	.531
.284	1.293	.531
.313	1.301	.531
.342	1.309	.531
.372	1.315	.531

Table 4. Continued

(a) Continued

Spline 9		
X, in.	Y, in.	Z, in.
.000	.000	.000
.016	.026	.000
.029	.054	.000
.039	.083	.000
.046	.113	.000
.049	.143	.000
.048	.174	.000
.044	.205	.000
.039	.235	.000
.034	.265	.000
.029	.295	.000
.023	.326	.000
.018	.356	.000
.013	.386	.000
.008	.416	.000
.002	.447	.000
-.003	.477	.000
-.008	.507	.000
-.013	.538	.000
-.019	.568	.000
-.024	.598	.000
-.029	.628	.000
-.034	.659	.000
-.040	.689	.000
-.044	.719	.000
-.048	.750	.000
-.049	.780	.000
-.049	.811	.000
-.047	.842	.000
-.043	.872	.000
-.037	.902	.000
-.030	.932	.000
-.021	.962	.000
-.011	.990	.000
.002	1.019	.000
.015	1.046	.000
.031	1.073	.000
.048	1.098	.000
.066	1.123	.000
.086	1.147	.000
.107	1.169	.000
.129	1.190	.000
.152	1.210	.000
.177	1.229	.000
.202	1.246	.000
.229	1.261	.000
.256	1.275	.000
.284	1.288	.000
.313	1.299	.000
.342	1.308	.000
.372	1.315	.000

Spline 10		
X, in.	Y, in.	Z, in.
.000	.000	.000
-.001	.000	.042
-.002	.002	.084
-.005	.003	.126
-.009	.006	.167
-.013	.009	.209
-.019	.014	.250
-.026	.019	.291
-.034	.024	.332
-.043	.031	.372
-.053	.038	.413
-.064	.046	.452
-.077	.054	.491
-.090	.063	.530
-.104	.073	.568
-.119	.084	.606
-.135	.095	.643
-.152	.107	.680
-.170	.120	.715
-.189	.133	.750
-.208	.147	.785
-.229	.162	.818
-.250	.177	.851
-.272	.193	.883
-.295	.209	.914
-.319	.226	.944
-.344	.243	.973
-.369	.261	1.001
-.395	.279	1.029
-.422	.298	1.055
-.449	.318	1.080
-.477	.338	1.104
-.506	.358	1.127
-.535	.378	1.149
-.565	.399	1.170
-.595	.421	1.190
-.626	.443	1.208
-.657	.465	1.225
-.689	.487	1.241
-.721	.510	1.256
-.753	.533	1.270
-.786	.556	1.282
-.819	.579	1.293
-.852	.603	1.303
-.886	.626	1.311
-.920	.650	1.319
-.953	.674	1.325
-.988	.698	1.329
-1.022	.722	1.332
-1.056	.747	1.334
-1.090	.771	1.335

Spline 11		
X, in.	Y, in.	Z, in.
.011	.397	.000
.011	.397	.041
.009	.398	.083
.007	.399	.124
.004	.402	.166
.000	.404	.207
-.004	.407	.248
-.009	.411	.289
-.015	.415	.330
-.022	.420	.371
-.029	.425	.411
-.037	.430	.451
-.046	.437	.491
-.055	.444	.531
-.066	.451	.571
-.077	.459	.610
-.089	.467	.649
-.102	.476	.687
-.115	.486	.725
-.130	.496	.763
-.145	.507	.800
-.161	.518	.837
-.177	.530	.873
-.195	.542	.908
-.213	.555	.943
-.233	.569	.977
-.253	.583	1.010
-.274	.598	1.043
-.296	.614	1.074
-.320	.631	1.103
-.346	.649	1.131
-.372	.667	1.157
-.399	.687	1.182
-.428	.707	1.204
-.457	.727	1.225
-.487	.749	1.244
-.518	.770	1.261
-.549	.793	1.277
-.581	.815	1.291
-.613	.838	1.303
-.646	.861	1.314
-.679	.884	1.324
-.712	.908	1.332
-.746	.932	1.340
-.779	.955	1.346
-.813	.979	1.351
-.846	1.003	1.356
-.880	1.027	1.360
-.914	1.050	1.363
-.948	1.074	1.364
-.981	1.098	1.365

Spline 12		
X, in.	Y, in.	Z, in.
-.047	.842	.000
-.047	.842	.042
-.048	.843	.084
-.049	.844	.126
-.051	.845	.167
-.054	.847	.209
-.056	.849	.251
-.060	.851	.293
-.064	.854	.334
-.068	.857	.376
-.073	.860	.417
-.078	.864	.459
-.084	.868	.500
-.090	.873	.541
-.097	.878	.582
-.105	.883	.623
-.113	.889	.664
-.122	.895	.704
-.131	.901	.745
-.141	.908	.785
-.151	.916	.825
-.162	.924	.864
-.174	.932	.904
-.186	.941	.943
-.199	.950	.982
-.213	.959	1.020
-.227	.970	1.058
-.243	.981	1.095
-.260	.993	1.132
-.279	1.006	1.166
-.301	1.021	1.199
-.325	1.038	1.229
-.350	1.056	1.257
-.378	1.076	1.282
-.407	1.096	1.304
-.437	1.118	1.323
-.469	1.140	1.339
-.501	1.163	1.353
-.534	1.186	1.365
-.567	1.210	1.375
-.601	1.234	1.383
-.635	1.257	1.390
-.668	1.281	1.395
-.702	1.305	1.400
-.736	1.329	1.405
-.770	1.354	1.409
-.805	1.378	1.413
-.839	1.402	1.416
-.873	1.426	1.418
-.907	1.450	1.420
-.941	1.474	1.420

Table 4. Continued

(a) Continued

Spline 13		
X, in.	Y, in.	Z, in.
.024	1.061	.000
.024	1.062	.041
.023	1.062	.083
.022	1.063	.124
.021	1.064	.165
.019	1.066	.206
.017	1.068	.248
.014	1.070	.289
.012	1.072	.330
.009	1.075	.371
.005	1.078	.412
.001	1.082	.453
-.003	1.086	.494
-.008	1.090	.535
-.013	1.094	.576
-.018	1.099	.616
-.024	1.104	.657
-.030	1.109	.698
-.036	1.115	.738
-.043	1.121	.778
-.050	1.128	.819
-.058	1.134	.859
-.065	1.141	.899
-.074	1.149	.938
-.082	1.157	.978
-.091	1.165	1.018
-.101	1.173	1.057
-.111	1.182	1.096
-.123	1.193	1.134
-.137	1.205	1.171
-.153	1.220	1.206
-.173	1.237	1.238
-.194	1.257	1.268
-.218	1.278	1.294
-.243	1.301	1.317
-.270	1.325	1.337
-.298	1.350	1.353
-.328	1.376	1.367
-.357	1.403	1.378
-.387	1.430	1.386
-.418	1.457	1.392
-.448	1.485	1.396
-.479	1.512	1.399
-.510	1.540	1.402
-.541	1.567	1.405
-.571	1.595	1.408
-.602	1.622	1.411
-.633	1.650	1.413
-.663	1.677	1.415
-.694	1.705	1.416
-.725	1.732	1.417

Spline 14		
X, in.	Y, in.	Z, in.
.174	1.227	.000
.174	1.227	.041
.174	1.227	.082
.174	1.228	.123
.173	1.229	.164
.172	1.229	.205
.171	1.230	.246
.170	1.232	.287
.169	1.233	.328
.168	1.234	.369
.167	1.236	.410
.165	1.238	.451
.164	1.240	.492
.162	1.242	.533
.160	1.244	.574
.159	1.246	.614
.157	1.248	.655
.155	1.250	.696
.153	1.253	.737
.151	1.255	.778
.149	1.258	.819
.146	1.260	.860
.144	1.263	.901
.142	1.266	.942
.140	1.268	.982
.138	1.270	1.023
.136	1.273	1.064
.132	1.278	1.105
.125	1.286	1.144
.116	1.297	1.183
.103	1.312	1.219
.088	1.331	1.252
.069	1.352	1.281
.049	1.377	1.307
.026	1.404	1.328
.003	1.432	1.346
-.022	1.462	1.360
-.048	1.493	1.368
-.074	1.524	1.372
-.100	1.556	1.374
-.126	1.587	1.376
-.153	1.618	1.377
-.179	1.650	1.378
-.205	1.681	1.380
-.232	1.713	1.381
-.258	1.744	1.382
-.284	1.776	1.383
-.310	1.807	1.384
-.337	1.839	1.384
-.363	1.870	1.385
-.389	1.902	1.385

Spline 15		
X, in.	Y, in.	Z, in.
.372	1.315	.000
.372	1.315	.041
.372	1.315	.081
.372	1.315	.122
.372	1.315	.163
.372	1.315	.203
.372	1.315	.244
.372	1.315	.284
.372	1.315	.325
.372	1.315	.366
.372	1.315	.406
.372	1.315	.447
.372	1.315	.488
.372	1.315	.528
.372	1.315	.569
.372	1.315	.610
.372	1.315	.650
.372	1.315	.691
.372	1.315	.731
.372	1.315	.772
.372	1.315	.813
.372	1.315	.853
.372	1.315	.894
.372	1.315	.935
.372	1.315	.975
.372	1.315	1.016
.372	1.315	1.057
.371	1.317	1.097
.367	1.323	1.137
.361	1.334	1.176
.352	1.350	1.212
.341	1.369	1.246
.328	1.393	1.277
.313	1.419	1.303
.296	1.449	1.326
.278	1.480	1.343
.258	1.514	1.356
.239	1.549	1.363
.218	1.584	1.365
.198	1.619	1.365
.178	1.655	1.365
.158	1.690	1.365
.138	1.725	1.365
.118	1.760	1.365
.097	1.796	1.365
.077	1.831	1.365
.057	1.866	1.365
.037	1.902	1.365
.017	1.937	1.365
-.003	1.972	1.365
-.023	2.007	1.365

Spline 16		
X, in.	Y, in.	Z, in.
-2.180	1.542	.000
-2.180	1.541	.042
-2.178	1.540	.084
-2.175	1.538	.126
-2.172	1.536	.167
-2.167	1.532	.209
-2.161	1.528	.250
-2.154	1.523	.291
-2.146	1.517	.332
-2.137	1.511	.372
-2.127	1.504	.413
-2.116	1.496	.452
-2.104	1.488	.491
-2.091	1.478	.530
-2.076	1.468	.568
-2.061	1.458	.606
-2.045	1.446	.643
-2.028	1.434	.680
-2.011	1.422	.715
-1.992	1.408	.750
-1.972	1.394	.785
-1.951	1.380	.818
-1.930	1.365	.851
-1.908	1.349	.883
-1.885	1.333	.914
-1.861	1.316	.944
-1.836	1.298	.973
-1.811	1.281	1.001
-1.785	1.262	1.029
-1.758	1.243	1.055
-1.731	1.224	1.080
-1.703	1.204	1.104
-1.674	1.184	1.127
-1.645	1.163	1.149
-1.615	1.142	1.170
-1.585	1.121	1.190
-1.554	1.099	1.208
-1.523	1.077	1.225
-1.491	1.055	1.241
-1.459	1.032	1.256
-1.427	1.009	1.270
-1.394	.986	1.282
-1.361	.963	1.293
-1.328	.939	1.303
-1.294	.915	1.311
-1.261	.891	1.319
-1.227	.867	1.325
-1.193	.843	1.329
-1.159	.819	1.332
-1.124	.795	1.334
-1.090	.771	1.335

Table 4. Continued

(a) Continued

Spline 17		
X, in.	Y, in.	Z, in.
-2.012	1.827	.000
-2.012	1.827	.042
-2.010	1.826	.083
-2.008	1.824	.125
-2.004	1.822	.166
-2.000	1.818	.207
-1.994	1.815	.249
-1.988	1.810	.289
-1.981	1.805	.330
-1.973	1.800	.371
-1.965	1.794	.411
-1.955	1.787	.451
-1.945	1.779	.491
-1.933	1.771	.530
-1.921	1.763	.569
-1.908	1.753	.607
-1.894	1.743	.645
-1.879	1.733	.682
-1.864	1.722	.720
-1.847	1.711	.756
-1.830	1.698	.792
-1.812	1.686	.827
-1.794	1.673	.862
-1.774	1.659	.896
-1.754	1.644	.930
-1.732	1.629	.962
-1.710	1.614	.994
-1.687	1.598	1.025
-1.664	1.581	1.054
-1.639	1.563	1.083
-1.614	1.545	1.111
-1.587	1.527	1.137
-1.560	1.508	1.162
-1.532	1.488	1.186
-1.503	1.467	1.208
-1.474	1.447	1.229
-1.444	1.425	1.248
-1.413	1.403	1.265
-1.381	1.381	1.281
-1.349	1.358	1.295
-1.317	1.336	1.308
-1.284	1.312	1.319
-1.251	1.289	1.329
-1.218	1.266	1.338
-1.185	1.242	1.345
-1.151	1.218	1.351
-1.117	1.194	1.356
-1.083	1.170	1.360
-1.049	1.146	1.363
-1.015	1.122	1.364
-.981	1.098	1.365

Spline 18		
X, in.	Y, in.	Z, in.
-1.836	2.107	.000
-1.835	2.107	.041
-1.834	2.106	.081
-1.833	2.105	.122
-1.830	2.103	.162
-1.827	2.101	.202
-1.823	2.098	.243
-1.819	2.095	.283
-1.814	2.091	.323
-1.808	2.087	.363
-1.802	2.083	.403
-1.795	2.078	.442
-1.787	2.072	.482
-1.779	2.067	.521
-1.770	2.060	.560
-1.760	2.053	.599
-1.750	2.046	.637
-1.739	2.038	.676
-1.727	2.030	.714
-1.715	2.022	.751
-1.703	2.013	.789
-1.690	2.004	.826
-1.676	1.994	.863
-1.661	1.984	.899
-1.646	1.973	.935
-1.630	1.961	.971
-1.613	1.950	1.006
-1.596	1.937	1.040
-1.577	1.924	1.074
-1.558	1.910	1.107
-1.538	1.896	1.139
-1.516	1.881	1.169
-1.493	1.864	1.199
-1.469	1.847	1.226
-1.444	1.829	1.252
-1.417	1.811	1.277
-1.389	1.791	1.298
-1.360	1.770	1.318
-1.330	1.749	1.335
-1.299	1.727	1.350
-1.268	1.705	1.363
-1.236	1.683	1.374
-1.204	1.660	1.384
-1.172	1.637	1.393
-1.139	1.614	1.400
-1.106	1.591	1.407
-1.073	1.568	1.412
-1.040	1.544	1.415
-1.007	1.521	1.418
-.974	1.498	1.420
-.941	1.474	1.420

Spline 19		
X, in.	Y, in.	Z, in.
-1.463	2.393	.000
-1.463	2.393	.040
-1.462	2.393	.080
-1.461	2.392	.120
-1.460	2.391	.160
-1.458	2.389	.200
-1.455	2.387	.239
-1.453	2.384	.279
-1.450	2.382	.319
-1.446	2.378	.359
-1.442	2.375	.398
-1.438	2.371	.438
-1.433	2.366	.477
-1.427	2.362	.517
-1.422	2.357	.556
-1.415	2.351	.595
-1.409	2.345	.634
-1.402	2.339	.673
-1.394	2.332	.711
-1.386	2.325	.750
-1.378	2.317	.788
-1.369	2.309	.826
-1.360	2.301	.864
-1.350	2.292	.902
-1.339	2.283	.939
-1.329	2.273	.977
-1.317	2.263	1.014
-1.305	2.252	1.050
-1.292	2.240	1.086
-1.277	2.227	1.121
-1.261	2.213	1.154
-1.243	2.197	1.186
-1.224	2.179	1.217
-1.203	2.161	1.245
-1.180	2.140	1.271
-1.156	2.119	1.294
-1.131	2.096	1.315
-1.104	2.072	1.333
-1.077	2.048	1.349
-1.049	2.022	1.362
-1.020	1.997	1.373
-.991	1.971	1.382
-.962	1.945	1.389
-.933	1.918	1.395
-.903	1.892	1.400
-.873	1.865	1.405
-.844	1.839	1.409
-.814	1.812	1.413
-.784	1.786	1.415
-.755	1.759	1.416
-.725	1.732	1.417

Spline 20		
X, in.	Y, in.	Z, in.
-.954	2.578	.000
-.954	2.578	.040
-.954	2.577	.080
-.954	2.577	.121
-.953	2.576	.161
-.952	2.575	.201
-.952	2.574	.241
-.951	2.573	.281
-.949	2.572	.322
-.948	2.570	.362
-.947	2.568	.402
-.945	2.566	.442
-.943	2.564	.482
-.941	2.562	.522
-.939	2.559	.562
-.937	2.557	.603
-.934	2.554	.643
-.932	2.551	.683
-.929	2.547	.723
-.926	2.544	.763
-.923	2.540	.803
-.920	2.536	.842
-.917	2.532	.882
-.913	2.528	.922
-.909	2.524	.962
-.906	2.519	1.002
-.901	2.514	1.041
-.896	2.507	1.081
-.888	2.499	1.119
-.879	2.487	1.156
-.866	2.472	1.192
-.851	2.455	1.225
-.835	2.434	1.255
-.816	2.412	1.283
-.795	2.387	1.306
-.772	2.360	1.325
-.748	2.331	1.341
-.724	2.302	1.353
-.698	2.271	1.360
-.673	2.241	1.365
-.647	2.210	1.368
-.621	2.179	1.371
-.596	2.148	1.374
-.570	2.117	1.377
-.544	2.087	1.379
-.518	2.056	1.381
-.493	2.025	1.382
-.467	1.994	1.383
-.441	1.963	1.384
-.415	1.932	1.385
-.389	1.902	1.385

Table 4. Continued

(a) Concluded

Spline 21		
X, in.	Y, in.	Z, in.
-.419	2.700	.000
-.419	2.700	.041
-.419	2.700	.081
-.419	2.700	.122
-.419	2.700	.163
-.419	2.700	.203
-.419	2.700	.244
-.419	2.700	.284
-.419	2.700	.325
-.419	2.700	.366
-.419	2.700	.406
-.419	2.700	.447
-.419	2.700	.488
-.419	2.700	.528
-.419	2.700	.569
-.419	2.700	.610
-.419	2.700	.650
-.419	2.700	.691
-.419	2.700	.731
-.419	2.700	.772
-.419	2.700	.813
-.419	2.700	.853
-.419	2.700	.894
-.419	2.700	.935
-.419	2.699	.975
-.419	2.700	1.016
-.419	2.700	1.057
-.418	2.698	1.097
-.414	2.691	1.137
-.408	2.680	1.176
-.399	2.665	1.212
-.388	2.646	1.246
-.375	2.622	1.277
-.359	2.596	1.303
-.343	2.566	1.326
-.324	2.534	1.343
-.305	2.501	1.356
-.285	2.466	1.363
-.265	2.431	1.365
-.245	2.396	1.365
-.225	2.360	1.365
-.205	2.325	1.365
-.185	2.290	1.365
-.165	2.254	1.365
-.144	2.219	1.365
-.124	2.184	1.365
-.104	2.149	1.365
-.084	2.113	1.365
-.064	2.078	1.365
-.044	2.043	1.365
-.023	2.007	1.365

Table 4. Concluded

(b) Turning vane

X, in.	Y, in.	Z, in.
-.575	1.228	.000
-.566	1.255	.000
-.557	1.283	.000
-.547	1.310	.000
-.536	1.337	.000
-.524	1.364	.000
-.511	1.390	.000
-.497	1.416	.000
-.482	1.441	.000
-.466	1.466	.000
-.449	1.490	.000
-.431	1.512	.000
-.411	1.534	.000
-.391	1.555	.000
-.369	1.575	.000
-.346	1.594	.000
-.323	1.611	.000
-.298	1.626	.000
-.272	1.640	.000
-.245	1.652	.000
-.218	1.662	.000
-.190	1.669	.000
.118	1.738	.000
.130	1.736	.000
.136	1.726	.000
.134	1.715	.000

X, in.	Y, in.	Z, in.
.125	1.708	.000
.085	1.699	.000
.046	1.688	.000
.006	1.676	.000
-.033	1.662	.000
-.071	1.646	.000
-.109	1.630	.000
-.146	1.611	.000
-.183	1.592	.000
-.218	1.570	.000
-.253	1.548	.000
-.286	1.524	.000
-.318	1.498	.000
-.348	1.471	.000
-.377	1.442	.000
-.404	1.412	.000
-.430	1.381	.000
-.455	1.349	.000
-.479	1.316	.000
-.502	1.282	.000
-.525	1.249	.000
-.548	1.215	.000
-.557	1.209	.000
-.567	1.210	.000
-.574	1.217	.000

Table 5. Internal Static Performance of 1.8 CR D-Shaped Nozzles Installed on Centerline Plenum With Short-Core Centerbody

(a) No blocker

Configuration $P_C C_S B_N N_1 T$

NPR	F_r/F_i	F_A/F_i	F_N/F_i	F_S/F_i	w_p/w_i	δ_{RR}, deg
1.50	0.8857	0.8813	0.0851	-0.0234	0.8848	7.78
1.80	0.9082	0.9047	0.0752	-0.0227	0.8944	6.71
2.00	0.9196	0.9168	0.0697	-0.0175	0.8990	6.14
2.20	0.9269	0.9241	0.0696	-0.0176	0.9012	6.08
2.51	0.9377	0.9346	0.0758	-0.0143	0.9023	6.55
2.99	0.9482	0.9444	0.0843	-0.0113	0.9030	7.19
3.50	0.9542	0.9500	0.0890	-0.0105	0.9031	7.55
4.00	0.9548	0.9502	0.0935	-0.0119	0.9026	7.92
4.50	0.9548	0.9498	0.0968	-0.0095	0.9024	8.20
5.01	0.9538	0.9486	0.0998	-0.0096	0.9022	8.47
6.01	0.9487	0.9431	0.1023	-0.0084	0.9009	8.72

Configuration $P_C C_S B_N N_1 L$

NPR	F_r/F_i	F_A/F_i	F_N/F_i	F_S/F_i	w_p/w_i	δ_{RR}, deg
1.52	0.8761	0.0701	0.8726	-0.0322	0.8802	86.75
1.81	0.9002	0.0606	0.8976	-0.0327	0.8864	87.27
2.02	0.9128	0.0520	0.9108	-0.0307	0.8910	87.69
2.22	0.9251	0.0500	0.9233	-0.0287	0.8930	87.81
2.51	0.9357	0.0556	0.9336	-0.0295	0.8935	87.59
3.01	0.9453	0.0667	0.9425	-0.0298	0.8946	87.14
3.52	0.9506	0.0746	0.9472	-0.0299	0.8947	86.81
4.00	0.9520	0.0787	0.9483	-0.0297	0.8945	86.64
4.51	0.9506	0.0845	0.9464	-0.0284	0.8947	86.39

(b) Flat blocker

Configuration $P_C C_S B_F N_1 T$

NPR	F_r/F_i	F_A/F_i	F_N/F_i	F_S/F_i	w_p/w_i	δ_{RR}, deg
1.50	0.8773	0.8730	0.0852	-0.0175	0.8732	7.86
1.82	0.9011	0.8983	0.0694	-0.0109	0.8832	6.24
2.01	0.9131	0.9110	0.0616	-0.0104	0.8884	5.47
2.20	0.9206	0.9187	0.0576	-0.0105	0.8906	5.07
2.51	0.9320	0.9297	0.0655	-0.0075	0.8927	5.69
3.01	0.9443	0.9412	0.0753	-0.0070	0.8936	6.46
3.52	0.9500	0.9464	0.0827	-0.0067	0.8945	7.05
4.00	0.9516	0.9475	0.0873	-0.0059	0.8944	7.42
4.52	0.9511	0.9468	0.0899	-0.0050	0.8940	7.64
5.01	0.9505	0.9460	0.0922	-0.0048	0.8935	7.85
6.03	0.9458	0.9409	0.0964	-0.0044	0.8927	8.25

Configuration $P_C C_S B_F N_1 L$

NPR	F_r/F_i	F_A/F_i	F_N/F_i	F_S/F_i	w_p/w_i	δ_{RR}, deg
1.50	0.8736	0.0743	0.8699	-0.0313	0.8785	86.55
1.80	0.8959	0.0669	0.8929	-0.0297	0.8855	86.97
2.00	0.9116	0.0585	0.9092	-0.0284	0.8898	87.39
2.22	0.9223	0.0546	0.9202	-0.0299	0.8924	87.60
2.51	0.9330	0.0594	0.9307	-0.0273	0.8940	87.41
3.01	0.9450	0.0709	0.9419	-0.0268	0.8941	86.95
3.52	0.9496	0.0782	0.9459	-0.0279	0.8940	86.65
4.02	0.9516	0.0839	0.9475	-0.0273	0.8940	86.42
4.52	0.9508	0.0891	0.9462	-0.0276	0.8938	86.19
4.77	0.9520	0.0900	0.9474	-0.0268	0.8929	86.16

Table 6. Internal Static Performance of 1.8 CR D-Shaped Nozzles Installed on Centerline Plenum With Medium-Core Centerbody

(a) No blocker

Configuration $P_C C_M B_N N_1 T$

NPR	F_r/F_i	F_A/F_i	F_N/F_i	F_S/F_i	w_p/w_i	δ_{RR}, deg
1.52	0.8850	0.8803	0.0889	-0.0181	0.8776	8.13
1.80	0.9051	0.9017	0.0766	-0.0165	0.8868	6.85
2.02	0.9172	0.9144	0.0695	-0.0171	0.8921	6.14
2.20	0.9246	0.9220	0.0675	-0.0164	0.8944	5.91
2.50	0.9360	0.9329	0.0746	-0.0124	0.8955	6.45
3.00	0.9478	0.9439	0.0848	-0.0117	0.8965	7.24
3.51	0.9527	0.9483	0.0906	-0.0108	0.8968	7.70
4.01	0.9542	0.9494	0.0949	-0.0100	0.8968	8.04
4.50	0.9535	0.9484	0.0981	-0.0095	0.8969	8.32
5.01	0.9514	0.9461	0.0994	-0.0090	0.8967	8.45
6.01	0.9485	0.9430	0.1019	-0.0084	0.8958	8.69

Configuration $P_C C_M B_N N_1 L$

NPR	F_r/F_i	F_A/F_i	F_N/F_i	F_S/F_i	w_p/w_i	δ_{RR}, deg
1.50	0.8725	0.0737	0.8689	-0.0301	0.8782	86.57
1.80	0.9001	0.0639	0.8974	-0.0280	0.8839	87.12
2.00	0.9171	0.0558	0.9149	-0.0293	0.8885	87.53
2.21	0.9275	0.0525	0.9255	-0.0317	0.8910	87.71
2.51	0.9369	0.0585	0.9345	-0.0306	0.8919	87.46
3.01	0.9471	0.0710	0.9440	-0.0285	0.8929	86.95
3.51	0.9539	0.0790	0.9502	-0.0276	0.8931	86.64
4.01	0.9544	0.0841	0.9503	-0.0273	0.8931	86.42
4.50	0.9543	0.0887	0.9498	-0.0276	0.8931	86.22
4.65	0.9535	0.0892	0.9489	-0.0270	0.8931	86.20

(b) Flat blocker

Configuration $P_C C_M B_F N_1 T$

NPR	F_r/F_i	F_A/F_i	F_N/F_i	F_S/F_i	w_p/w_i	δ_{RR}, deg
1.51	0.8649	0.8608	0.0811	-0.0197	0.8623	7.59
1.80	0.8887	0.8855	0.0745	-0.0156	0.8721	6.78
2.01	0.9052	0.9029	0.0644	-0.0115	0.8781	5.76
2.21	0.9157	0.9137	0.0585	-0.0115	0.8813	5.18
2.51	0.9266	0.9243	0.0644	-0.0093	0.8829	5.62
3.01	0.9394	0.9364	0.0744	-0.0066	0.8839	6.41
3.51	0.9465	0.9430	0.0810	-0.0065	0.8846	6.93
4.01	0.9479	0.9439	0.0865	-0.0043	0.8847	7.38
4.50	0.9495	0.9453	0.0890	-0.0049	0.8847	7.58
5.00	0.9490	0.9445	0.0923	-0.0045	0.8842	7.87
5.99	0.9449	0.9401	0.0949	-0.0040	0.8838	8.12

Configuration $P_C C_M B_F N_1 L$

NPR	F_r/F_i	F_A/F_i	F_N/F_i	F_S/F_i	w_p/w_i	δ_{RR}, deg
1.50	0.8607	0.0754	0.8569	-0.0284	0.8692	86.44
1.79	0.8883	0.0694	0.8851	-0.0292	0.8746	86.83
2.00	0.9074	0.0569	0.9052	-0.0270	0.8828	87.45
2.20	0.9184	0.0545	0.9163	-0.0282	0.8850	87.59
2.50	0.9264	0.0581	0.9242	-0.0263	0.8858	87.45
3.01	0.9435	0.0705	0.9405	-0.0269	0.8868	86.97
3.51	0.9481	0.0785	0.9444	-0.0262	0.8870	86.64
4.02	0.9509	0.0847	0.9468	-0.0260	0.8873	86.38
4.53	0.9501	0.0904	0.9454	-0.0259	0.8872	86.13
4.79	0.9498	0.0913	0.9451	-0.0251	0.8870	86.09

Table 7. Internal Static Performance of 1.8 CR D-Shaped Nozzles Installed on Centerline Plenum With Long-Core Centerbody

(a) No blocker

Configuration $P_C C_L B_N N_1 T$

NPR	F_r/F_i	F_A/F_i	F_N/F_i	F_S/F_i	w_p/w_i	δ_{RR}, deg
1.51	0.8813	0.8759	0.0965	-0.0169	0.8744	8.86
1.81	0.9018	0.8981	0.0805	-0.0136	0.8843	7.23
2.01	0.9134	0.9103	0.0739	-0.0147	0.8894	6.55
2.20	0.9227	0.9196	0.0740	-0.0123	0.8919	6.49
2.49	0.9334	0.9301	0.0781	-0.0116	0.8934	6.77
3.00	0.9456	0.9413	0.0888	-0.0102	0.8944	7.60
3.50	0.9519	0.9473	0.0931	-0.0095	0.8946	7.91
4.00	0.9532	0.9482	0.0971	-0.0082	0.8949	8.24
4.52	0.9539	0.9485	0.1008	-0.0087	0.8946	8.55
5.01	0.9525	0.9470	0.1020	-0.0085	0.8943	8.66
6.02	0.9481	0.9421	0.1056	-0.0079	0.8937	9.01

Configuration $P_C C_L B_N N_1 L$

NPR	F_r/F_i	F_A/F_i	F_N/F_i	F_S/F_i	w_p/w_i	δ_{RR}, deg
1.50	0.8700	0.0768	0.8661	-0.0308	0.8786	86.41
1.80	0.8962	0.0673	0.8931	-0.0319	0.8850	86.95
2.01	0.9134	0.0597	0.9109	-0.0304	0.8892	87.35
2.20	0.9253	0.0578	0.9230	-0.0293	0.8914	87.47
2.50	0.9338	0.0624	0.9312	-0.0300	0.8922	87.29
3.01	0.9458	0.0738	0.9425	-0.0289	0.8932	86.83
3.50	0.9507	0.0811	0.9469	-0.0274	0.8935	86.53
4.00	0.9515	0.0879	0.9471	-0.0268	0.8934	86.24
4.52	0.9524	0.0923	0.9476	-0.0259	0.8934	86.06
4.68	0.9523	0.0935	0.9474	-0.0259	0.8929	86.01

(b) Flat blocker

Configuration $P_C C_L B_F N_1 T$

NPR	F_r/F_i	F_A/F_i	F_N/F_i	F_S/F_i	w_p/w_i	δ_{RR}, deg
1.51	0.8543	0.8504	0.0796	-0.0160	0.8486	7.54
1.82	0.8832	0.8806	0.0667	-0.0108	0.8619	6.11
2.00	0.8973	0.8955	0.0557	-0.0094	0.8679	5.03
2.20	0.9080	0.9063	0.0538	-0.0062	0.8714	4.80
2.51	0.9212	0.9196	0.0550	-0.0050	0.8736	4.84
3.01	0.9349	0.9328	0.0633	-0.0046	0.8743	5.48
3.51	0.9415	0.9388	0.0700	-0.0032	0.8743	6.02
4.00	0.9447	0.9418	0.0736	-0.0021	0.8749	6.31
4.50	0.9459	0.9428	0.0772	-0.0029	0.8734	6.60
5.01	0.9456	0.9422	0.0800	-0.0023	0.8737	6.85
6.01	0.9419	0.9382	0.0837	-0.0020	0.8723	7.19

Configuration $P_C C_L B_F N_1 L$

NPR	F_r/F_i	F_A/F_i	F_N/F_i	F_S/F_i	w_p/w_i	δ_{RR}, deg
1.50	0.8535	0.0759	0.8496	-0.0285	0.8644	86.39
1.81	0.8894	0.0715	0.8862	-0.0247	0.8736	86.74
2.00	0.9038	0.0617	0.9013	-0.0244	0.8786	87.23
2.21	0.9143	0.0575	0.9122	-0.0244	0.8806	87.45
2.50	0.9256	0.0618	0.9232	-0.0244	0.8817	87.29
3.00	0.9411	0.0747	0.9378	-0.0244	0.8828	86.78
3.51	0.9455	0.0829	0.9415	-0.0246	0.8820	86.44
4.00	0.9493	0.0898	0.9447	-0.0237	0.8820	86.15
4.49	0.9476	0.0954	0.9425	-0.0222	0.8814	85.91
4.76	0.9482	0.0978	0.9428	-0.0226	0.8810	85.80

Table 7. Concluded

(c) Tapered blocker

Configuration $P_C C_L B_T N_1 T$

NPR	F_r/F_i	F_A/F_i	F_N/F_i	F_S/F_i	w_p/w_i	δ_{RR}, deg
1.50	0.8876	0.8834	0.0853	-0.0146	0.8823	7.77
1.80	0.9099	0.9067	0.0757	-0.0139	0.8905	6.74
2.01	0.9212	0.9185	0.0686	-0.0129	0.8952	6.03
2.21	0.9291	0.9267	0.0661	-0.0125	0.8976	5.76
2.51	0.9390	0.9360	0.0734	-0.0104	0.8989	6.33
3.01	0.9502	0.9466	0.0833	-0.0073	0.8998	7.09
3.51	0.9540	0.9499	0.0882	-0.0071	0.9004	7.48
4.00	0.9551	0.9507	0.0916	-0.0075	0.9007	7.76
4.51	0.9558	0.9511	0.0947	-0.0067	0.9007	8.02
5.00	0.9538	0.9488	0.0975	-0.0064	0.9005	8.27
5.99	0.9489	0.9437	0.0996	-0.0056	0.8997	8.49

Configuration $P_C C_L B_T N_1 L$

NPR	F_r/F_i	F_A/F_i	F_N/F_i	F_S/F_i	w_p/w_i	δ_{RR}, deg
1.51	0.8721	0.0763	0.8682	-0.0315	0.8859	86.44
1.81	0.9037	0.0682	0.9007	-0.0279	0.8906	86.94
2.00	0.9171	0.0579	0.9148	-0.0291	0.8948	87.44
2.20	0.9270	0.0570	0.9248	-0.0298	0.8967	87.51
2.51	0.9348	0.0609	0.9323	-0.0292	0.8977	87.36
3.00	0.9484	0.0730	0.9451	-0.0274	0.8985	86.88
3.50	0.9523	0.0811	0.9485	-0.0266	0.8989	86.54
4.00	0.9531	0.0859	0.9488	-0.0267	0.8990	86.34
4.51	0.9538	0.0907	0.9491	-0.0266	0.8989	86.14
4.76	0.9543	0.0923	0.9495	-0.0253	0.8980	86.07

Table 8. Internal Static Performance of 1.8 CR D-Shaped Nozzles Installed on Centerline Plenum With Fan Centerbody

(a) No blocker

Configuration $P_C C_F B_N N_1 T$

NPR	F_r/F_i	F_A/F_i	F_N/F_i	F_S/F_i	w_p/w_i	δ_{RR}, deg
1.50	0.8775	0.8732	0.0845	-0.0227	0.8740	7.80
1.80	0.8991	0.8964	0.0684	-0.0167	0.8824	6.16
2.01	0.9135	0.9110	0.0658	-0.0118	0.8881	5.83
2.20	0.9226	0.9201	0.0669	-0.0084	0.8906	5.87
2.51	0.9337	0.9309	0.0712	-0.0061	0.8919	6.17
3.01	0.9462	0.9428	0.0799	-0.0047	0.8929	6.83
3.51	0.9511	0.9473	0.0855	-0.0040	0.8928	7.28
4.00	0.9531	0.9487	0.0917	-0.0030	0.8940	7.79
4.51	0.9535	0.9489	0.0938	-0.0027	0.8936	7.96
5.00	0.9525	0.9475	0.0969	-0.0026	0.8934	8.23
6.00	0.9476	0.9423	0.1000	-0.0022	0.8934	8.53

Configuration $P_C C_F B_N N_1 L$

NPR	F_r/F_i	F_A/F_i	F_N/F_i	F_S/F_i	w_p/w_i	δ_{RR}, deg
1.52	0.8747	0.0743	0.8711	-0.0291	0.8818	86.55
1.82	0.9017	0.0655	0.8988	-0.0305	0.8882	87.05
2.01	0.9137	0.0586	0.9113	-0.0292	0.8925	87.40
2.20	0.9242	0.0570	0.9220	-0.0283	0.8944	87.50
2.52	0.9326	0.0604	0.9303	-0.0260	0.8954	87.37
3.00	0.9455	0.0727	0.9424	-0.0266	0.8959	86.88
3.51	0.9509	0.0817	0.9470	-0.0263	0.8963	86.51
4.00	0.9523	0.0847	0.9482	-0.0252	0.8961	86.39
4.50	0.9526	0.0901	0.9480	-0.0242	0.8958	86.15
4.92	0.9524	0.0925	0.9475	-0.0247	0.8955	86.05

(b) Flat blocker

Configuration $P_C C_F B_F N_1 T$

NPR	F_r/F_i	F_A/F_i	F_N/F_i	F_S/F_i	w_p/w_i	δ_{RR}, deg
1.50	0.8837	0.8782	0.0968	-0.0149	0.8776	8.86
1.81	0.9056	0.9020	0.0796	-0.0161	0.8869	7.11
1.99	0.9163	0.9135	0.0709	-0.0152	0.8916	6.26
2.22	0.9265	0.9238	0.0697	-0.0127	0.8947	6.09
2.50	0.9363	0.9332	0.0747	-0.0102	0.8958	6.46
3.00	0.9476	0.9438	0.0845	-0.0084	0.8970	7.21
3.51	0.9526	0.9483	0.0906	-0.0073	0.8977	7.70
4.01	0.9543	0.9494	0.0959	-0.0076	0.8978	8.13
4.51	0.9543	0.9492	0.0979	-0.0070	0.8977	8.30
5.00	0.9522	0.9471	0.0984	-0.0054	0.8976	8.36
5.98	0.9486	0.9432	0.1015	-0.0048	0.8969	8.66

Configuration $P_C C_F B_F N_1 L$

NPR	F_r/F_i	F_A/F_i	F_N/F_i	F_S/F_i	w_p/w_i	δ_{RR}, deg
1.51	0.8775	0.0823	0.8731	-0.0295	0.8850	86.19
1.81	0.9028	0.0726	0.8994	-0.0310	0.8903	86.73
2.00	0.9159	0.0632	0.9133	-0.0295	0.8944	87.20
2.22	0.9262	0.0612	0.9237	-0.0285	0.8971	87.32
2.52	0.9363	0.0648	0.9337	-0.0270	0.8977	87.19
3.00	0.9489	0.0759	0.9455	-0.0258	0.8986	86.75
3.51	0.9536	0.0843	0.9495	-0.0258	0.8989	86.41
4.00	0.9545	0.0891	0.9500	-0.0246	0.8988	86.21
4.51	0.9549	0.0926	0.9501	-0.0247	0.8985	86.06
4.90	0.9541	0.0957	0.9490	-0.0247	0.8981	85.92

Table 8. Concluded

(c) Tapered blocker

Configuration $P_C C_F B_T N_1 T$

NPR	F_r/F_i	F_A/F_i	F_N/F_i	F_S/F_i	w_p/w_i	δ_{RR}, deg
1.51	0.8944	0.8896	0.0913	-0.0189	0.8885	8.25
1.79	0.9101	0.9066	0.0784	-0.0151	0.8958	6.97
2.01	0.9230	0.9204	0.0675	-0.0154	0.9002	5.92
2.20	0.9304	0.9278	0.0684	-0.0134	0.9028	5.95
2.51	0.9407	0.9377	0.0749	-0.0107	0.9035	6.44
3.01	0.9510	0.9472	0.0843	-0.0085	0.9045	7.17
3.50	0.9561	0.9517	0.0908	-0.0081	0.9048	7.68
3.99	0.9573	0.9526	0.0938	-0.0079	0.9050	7.93
4.51	0.9562	0.9513	0.0964	-0.0070	0.9050	8.16
5.01	0.9552	0.9500	0.0987	-0.0069	0.9046	8.36
5.99	0.9502	0.9447	0.1016	-0.0063	0.9039	8.64

Configuration $P_C C_F B_T N_1 L$

NPR	F_r/F_i	F_A/F_i	F_N/F_i	F_S/F_i	w_p/w_i	δ_{RR}, deg
1.51	0.8800	0.0767	0.8762	-0.0282	0.8882	86.46
1.81	0.9068	0.0682	0.9037	-0.0296	0.8933	86.94
2.00	0.9192	0.0608	0.9167	-0.0305	0.8967	87.31
2.21	0.9277	0.0586	0.9254	-0.0278	0.8987	87.44
2.50	0.9366	0.0644	0.9340	-0.0261	0.8999	87.21
3.01	0.9489	0.0762	0.9455	-0.0268	0.9004	86.74
3.49	0.9547	0.0830	0.9507	-0.0254	0.9010	86.47
3.99	0.9552	0.0885	0.9508	-0.0254	0.9009	86.23
4.51	0.9551	0.0938	0.9502	-0.0242	0.9007	86.01
4.91	0.9544	0.0966	0.9492	-0.0240	0.9003	85.88

Table 9. Internal Static Performance of 1.8 CR D-Shaped Nozzles Installed on Offset Plenum With Short-Core Centerbody

(a) No blocker

Configuration $P_OC_SB_NN_1T$

NPR	F_r/F_i	F_A/F_i	F_N/F_i	F_S/F_i	w_p/w_i	δ_{RR}, deg
1.50	0.9044	0.9016	0.0701	-0.0122	0.9075	6.28
1.80	0.9236	0.9219	0.0545	-0.0084	0.9118	4.77
2.01	0.9330	0.9318	0.0466	-0.0056	0.9154	4.04
2.19	0.9396	0.9384	0.0469	-0.0057	0.9183	4.04
2.50	0.9468	0.9453	0.0520	-0.0040	0.9193	4.45
3.01	0.9559	0.9538	0.0627	-0.0021	0.9201	5.32
3.51	0.9583	0.9556	0.0713	0.0003	0.9200	6.02
4.02	0.9583	0.9552	0.0763	-0.0005	0.9203	6.45
4.51	0.9571	0.9538	0.0788	0.0005	0.9194	6.67
5.01	0.9548	0.9514	0.0807	0.0012	0.9187	6.84
6.00	0.9497	0.9459	0.0848	0.0008	0.9176	7.23

Configuration $P_OC_SB_NN_1L$

NPR	F_r/F_i	F_A/F_i	F_N/F_i	F_S/F_i	w_p/w_i	δ_{RR}, deg
1.50	0.9125	0.0517	0.9104	-0.0321	0.9127	87.70
1.80	0.9316	0.0398	0.9303	-0.0297	0.9163	88.27
2.00	0.9428	0.0332	0.9418	-0.0291	0.9193	88.57
2.20	0.9481	0.0341	0.9470	-0.0309	0.9215	88.54
2.50	0.9536	0.0414	0.9523	-0.0303	0.9226	88.24
3.00	0.9588	0.0541	0.9568	-0.0303	0.9228	87.71
3.50	0.9611	0.0628	0.9586	-0.0298	0.9229	87.35
4.00	0.9617	0.0694	0.9588	-0.0284	0.9226	87.07
4.51	0.9600	0.0744	0.9567	-0.0275	0.9220	86.85
4.70	0.9577	0.0758	0.9543	-0.0289	0.9217	86.79

(b) Flat blocker

Configuration $P_OC_SB_FN_1T$

NPR	F_r/F_i	F_A/F_i	F_N/F_i	F_S/F_i	w_p/w_i	δ_{RR}, deg
1.52	0.8948	0.8918	0.0726	-0.0126	0.8992	6.57
1.80	0.9149	0.9133	0.0527	-0.0088	0.9054	4.66
2.00	0.9265	0.9254	0.0450	-0.0040	0.9102	3.93
2.20	0.9324	0.9313	0.0446	-0.0058	0.9119	3.87
2.51	0.9407	0.9395	0.0472	-0.0055	0.9136	4.07
2.99	0.9505	0.9487	0.0591	-0.0026	0.9139	5.03
3.53	0.9536	0.9513	0.0668	-0.0013	0.9142	5.67
4.00	0.9537	0.9511	0.0710	-0.0010	0.9130	6.02
4.49	0.9545	0.9515	0.0755	0.0003	0.9132	6.40
5.01	0.9527	0.9495	0.0788	-0.0001	0.9121	6.70
6.03	0.9473	0.9436	0.0829	0.0007	0.9108	7.08

Configuration $P_OC_SB_FN_1L$

NPR	F_r/F_i	F_A/F_i	F_N/F_i	F_S/F_i	w_p/w_i	δ_{RR}, deg
1.51	0.9002	0.0508	0.8982	-0.0314	0.9001	87.71
1.80	0.9220	0.0434	0.9205	-0.0295	0.9072	88.09
1.99	0.9314	0.0352	0.9302	-0.0308	0.9103	88.47
2.21	0.9382	0.0342	0.9370	-0.0326	0.9136	88.52
2.50	0.9487	0.0409	0.9473	-0.0316	0.9141	88.25
2.99	0.9579	0.0544	0.9558	-0.0324	0.9145	87.70
3.50	0.9609	0.0633	0.9583	-0.0318	0.9143	87.33
4.02	0.9567	0.0709	0.9536	-0.0305	0.9135	86.99
4.51	0.9557	0.0744	0.9523	-0.0303	0.9128	86.84
4.75	0.9551	0.0773	0.9515	-0.0298	0.9124	86.71

Table 10. Internal Static Performance of 1.8 CR D-Shaped Nozzles Installed on Offset Plenum With Medium-Core Centerbody

(a) No blocker

Configuration $P_OC_MB_NN_1T$

NPR	F_r/F_i	F_A/F_i	F_N/F_i	F_S/F_i	w_p/w_i	δ_{RR}, deg
1.51	0.9006	0.8982	0.0644	-0.0137	0.9016	5.79
1.81	0.9191	0.9176	0.0525	-0.0099	0.9070	4.62
2.01	0.9278	0.9267	0.0455	-0.0073	0.9108	3.97
2.21	0.9352	0.9340	0.0459	-0.0056	0.9127	3.97
2.50	0.9423	0.9408	0.0540	-0.0052	0.9136	4.64
3.01	0.9525	0.9503	0.0649	-0.0015	0.9141	5.52
3.52	0.9555	0.9527	0.0729	0.0003	0.9139	6.18
4.01	0.9553	0.9522	0.0776	0.0001	0.9142	6.57
4.50	0.9555	0.9520	0.0814	0.0011	0.9135	6.89
5.00	0.9532	0.9496	0.0829	0.0007	0.9130	7.04
5.99	0.9489	0.9448	0.0878	0.0015	0.9118	7.49

Configuration $P_OC_MB_NN_1L$

NPR	F_r/F_i	F_A/F_i	F_N/F_i	F_S/F_i	w_p/w_i	δ_{RR}, deg
1.51	0.9092	0.0494	0.9073	-0.0301	0.9060	87.79
1.79	0.9268	0.0398	0.9254	-0.0306	0.9096	88.26
2.00	0.9378	0.0311	0.9368	-0.0293	0.9134	88.66
2.21	0.9437	0.0315	0.9427	-0.0303	0.9149	88.65
2.51	0.9508	0.0379	0.9496	-0.0296	0.9156	88.38
3.01	0.9581	0.0522	0.9561	-0.0306	0.9154	87.79
3.51	0.9574	0.0588	0.9551	-0.0299	0.9155	87.51
4.00	0.9573	0.0654	0.9546	-0.0289	0.9153	87.23
4.50	0.9572	0.0713	0.9541	-0.0287	0.9146	86.98
4.76	0.9567	0.0726	0.9536	-0.0278	0.9142	86.92

(b) Flat blocker

Configuration $P_OC_MB_FN_1T$

NPR	F_r/F_i	F_A/F_i	F_N/F_i	F_S/F_i	w_p/w_i	δ_{RR}, deg
1.52	0.8916	0.8887	0.0703	-0.0139	0.8962	6.38
1.80	0.9121	0.9104	0.0543	-0.0100	0.9018	4.82
2.01	0.9238	0.9225	0.0465	-0.0084	0.9055	4.08
2.20	0.9308	0.9297	0.0435	-0.0080	0.9080	3.79
2.53	0.9408	0.9395	0.0496	-0.0047	0.9092	4.27
3.02	0.9499	0.9479	0.0621	-0.0018	0.9098	5.29
3.51	0.9534	0.9510	0.0673	-0.0002	0.9097	5.71
4.01	0.9543	0.9515	0.0729	0.0011	0.9094	6.18
4.51	0.9533	0.9502	0.0768	0.0001	0.9092	6.52
5.02	0.9512	0.9478	0.0804	0.0013	0.9087	6.84
6.01	0.9467	0.9428	0.0852	0.0019	0.9076	7.28

Configuration $P_OC_MB_FN_1L$

NPR	F_r/F_i	F_A/F_i	F_N/F_i	F_S/F_i	w_p/w_i	δ_{RR}, deg
1.52	0.8895	0.0539	0.8874	-0.0302	0.9015	87.54
1.79	0.9173	0.0428	0.9158	-0.0309	0.9049	88.11
2.02	0.9313	0.0336	0.9302	-0.0299	0.9090	88.54
2.20	0.9395	0.0337	0.9384	-0.0306	0.9106	88.54
2.51	0.9473	0.0406	0.9459	-0.0314	0.9115	88.26
3.00	0.9545	0.0532	0.9525	-0.0309	0.9115	87.74
3.50	0.9586	0.0621	0.9560	-0.0307	0.9116	87.37
4.01	0.9573	0.0690	0.9543	-0.0297	0.9118	87.07
4.52	0.9586	0.0741	0.9553	-0.0293	0.9114	86.86
4.77	0.9568	0.0762	0.9533	-0.0297	0.9107	86.77

Table 11. Internal Static Performance of 1.8 CR D-Shaped Nozzles Installed on Offset Plenum With Long-Core Centerbody

(a) No blocker

Configuration $P_OC_LB_NN_1T$

NPR	F_r/F_i	F_A/F_i	F_N/F_i	F_S/F_i	w_p/w_i	δ_{RR}, deg
1.50	0.8980	0.8952	0.0690	-0.0144	0.8977	6.22
1.81	0.9176	0.9159	0.0547	-0.0082	0.9040	4.82
2.00	0.9277	0.9263	0.0508	-0.0038	0.9079	4.44
2.21	0.9350	0.9335	0.0521	-0.0040	0.9100	4.51
2.50	0.9423	0.9407	0.0545	-0.0016	0.9111	4.68
3.00	0.9522	0.9499	0.0656	0.0008	0.9112	5.58
3.50	0.9554	0.9528	0.0709	0.0014	0.9118	6.01
4.00	0.9562	0.9532	0.0758	0.0000	0.9114	6.42
4.50	0.9552	0.9519	0.0803	0.0013	0.9112	6.80
5.00	0.9531	0.9495	0.0826	0.0025	0.9103	7.02
6.00	0.9489	0.9450	0.0861	0.0023	0.9090	7.34

Configuration $P_OC_LB_NN_1L$

NPR	F_r/F_i	F_A/F_i	F_N/F_i	F_S/F_i	w_p/w_i	δ_{RR}, deg
1.50	0.8998	0.0479	0.8981	-0.0289	0.9021	87.84
1.81	0.9220	0.0348	0.9209	-0.0274	0.9064	88.47
2.00	0.9367	0.0280	0.9359	-0.0251	0.9097	88.79
2.20	0.9402	0.0272	0.9394	-0.0291	0.9115	88.83
2.49	0.9490	0.0353	0.9479	-0.0289	0.9117	88.49
2.98	0.9555	0.0486	0.9539	-0.0290	0.9117	87.94
3.53	0.9561	0.0575	0.9539	-0.0289	0.9122	87.56
4.01	0.9573	0.0638	0.9547	-0.0281	0.9116	87.30
4.53	0.9557	0.0697	0.9527	-0.0277	0.9111	87.04
4.75	0.9555	0.0717	0.9524	-0.0284	0.9109	86.95

(b) Flat blocker

Configuration $P_OC_LB_FN_1T$

NPR	F_r/F_i	F_A/F_i	F_N/F_i	F_S/F_i	w_p/w_i	δ_{RR}, deg
1.50	0.8937	0.8903	0.0767	-0.0120	0.8983	6.95
1.81	0.9150	0.9132	0.0552	-0.0104	0.9042	4.89
2.00	0.9229	0.9217	0.0478	-0.0075	0.9080	4.19
2.21	0.9321	0.9309	0.0470	-0.0058	0.9098	4.08
2.50	0.9405	0.9388	0.0555	-0.0053	0.9107	4.78
3.00	0.9494	0.9471	0.0664	-0.0015	0.9110	5.66
3.51	0.9531	0.9503	0.0731	-0.0007	0.9109	6.21
4.00	0.9548	0.9515	0.0793	0.0009	0.9106	6.72
4.50	0.9538	0.9503	0.0824	0.0012	0.9102	6.99
5.00	0.9518	0.9479	0.0857	0.0013	0.9096	7.29
6.00	0.9470	0.9428	0.0887	0.0026	0.9079	7.58

Configuration $P_OC_LB_FN_1L$

NPR	F_r/F_i	F_A/F_i	F_N/F_i	F_S/F_i	w_p/w_i	δ_{RR}, deg
1.51	0.9051	0.0539	0.9029	-0.0320	0.9039	87.58
1.80	0.9235	0.0419	0.9222	-0.0251	0.9068	88.16
2.02	0.9318	0.0330	0.9308	-0.0266	0.9102	88.56
2.20	0.9379	0.0333	0.9368	-0.0293	0.9119	88.56
2.50	0.9490	0.0395	0.9477	-0.0288	0.9126	88.31
3.00	0.9582	0.0516	0.9564	-0.0289	0.9125	87.82
3.51	0.9590	0.0616	0.9566	-0.0287	0.9126	87.39
3.99	0.9582	0.0677	0.9554	-0.0273	0.9122	87.13
4.51	0.9559	0.0740	0.9526	-0.0270	0.9117	86.85
4.77	0.9572	0.0754	0.9538	-0.0272	0.9111	86.80

Table 11. Concluded

(c) Tapered blocker

Configuration $P_OC_LB_TN_1T$

NPR	F_r/F_i	F_A/F_i	F_N/F_i	F_S/F_i	w_p/w_i	δ_{RR}, deg
1.50	0.9036	0.9002	0.0773	-0.0128	0.9054	6.92
1.81	0.9184	0.9164	0.0598	-0.0071	0.9097	5.27
2.01	0.9311	0.9297	0.0492	-0.0080	0.9126	4.28
2.21	0.9365	0.9353	0.0482	-0.0048	0.9150	4.17
2.50	0.9454	0.9437	0.0564	-0.0044	0.9154	4.83
3.01	0.9542	0.9518	0.0664	-0.0028	0.9159	5.64
3.53	0.9563	0.9534	0.0750	-0.0018	0.9161	6.35
4.00	0.9560	0.9528	0.0778	-0.0008	0.9158	6.59
4.53	0.9558	0.9523	0.0820	-0.0003	0.9152	6.95
5.00	0.9537	0.9500	0.0843	-0.0001	0.9151	7.15
6.00	0.9491	0.9449	0.0893	0.0004	0.9132	7.61

Configuration $P_OC_LB_TN_1L$

NPR	F_r/F_i	F_A/F_i	F_N/F_i	F_S/F_i	w_p/w_i	δ_{RR}, deg
1.50	0.9051	0.0486	0.9033	-0.0312	0.9071	87.82
1.80	0.9242	0.0394	0.9228	-0.0311	0.9104	88.27
2.00	0.9371	0.0329	0.9360	-0.0298	0.9126	88.57
2.21	0.9428	0.0332	0.9418	-0.0286	0.9150	88.57
2.50	0.9500	0.0381	0.9488	-0.0287	0.9149	88.37
3.00	0.9575	0.0509	0.9556	-0.0304	0.9152	87.84
3.51	0.9589	0.0606	0.9566	-0.0285	0.9153	87.43
4.01	0.9593	0.0671	0.9565	-0.0289	0.9147	87.16
4.51	0.9565	0.0718	0.9534	-0.0280	0.9143	86.95
4.76	0.9553	0.0739	0.9520	-0.0276	0.9140	86.86

Table 12. Internal Static Performance of 1.8 CR D-Shaped Nozzles Installed on Offset Plenum With Fan Centerbody

(a) No blocker

Configuration $P_OC_FB_NN_1T$

NPR	F_r/F_i	F_A/F_i	F_N/F_i	F_S/F_i	w_p/w_i	δ_{RR}, deg
1.51	0.8944	0.8917	0.0682	-0.0110	0.8961	6.17
1.81	0.9165	0.9148	0.0542	-0.0073	0.9032	4.79
2.01	0.9267	0.9255	0.0470	-0.0051	0.9076	4.11
2.21	0.9329	0.9320	0.0413	-0.0051	0.9094	3.59
2.52	0.9419	0.9406	0.0489	-0.0038	0.9106	4.21
3.00	0.9504	0.9486	0.0589	-0.0002	0.9108	5.02
3.52	0.9539	0.9515	0.0678	-0.0001	0.9111	5.75
4.02	0.9552	0.9523	0.0742	0.0019	0.9105	6.29
4.51	0.9541	0.9509	0.0770	0.0028	0.9100	6.53
5.00	0.9523	0.9490	0.0793	0.0033	0.9095	6.74
5.99	0.9477	0.9440	0.0835	0.0041	0.9080	7.13

Configuration $P_OC_FB_NN_1L$

NPR	F_r/F_i	F_A/F_i	F_N/F_i	F_S/F_i	w_p/w_i	δ_{RR}, deg
1.51	0.9003	0.0507	0.8984	-0.0298	0.9024	87.72
1.80	0.9159	0.0395	0.9145	-0.0300	0.9048	88.25
2.01	0.9317	0.0329	0.9306	-0.0292	0.9085	88.57
2.19	0.9373	0.0314	0.9362	-0.0317	0.9110	88.64
2.50	0.9474	0.0394	0.9460	-0.0310	0.9116	88.31
3.01	0.9556	0.0530	0.9536	-0.0299	0.9118	87.75
3.52	0.9579	0.0617	0.9555	-0.0302	0.9115	87.39
4.00	0.9567	0.0685	0.9538	-0.0285	0.9114	87.09
4.52	0.9544	0.0736	0.9511	-0.0297	0.9107	86.87
4.77	0.9556	0.0758	0.9521	-0.0287	0.9101	86.78

(b) Flat blocker

Configuration $P_OC_FB_FN_1T$

NPR	F_r/F_i	F_A/F_i	F_N/F_i	F_S/F_i	w_p/w_i	δ_{RR}, deg
1.50	0.9028	0.8996	0.0747	-0.0150	0.9060	6.69
1.80	0.9205	0.9186	0.0593	-0.0104	0.9097	5.22
2.00	0.9300	0.9285	0.0514	-0.0091	0.9125	4.48
2.21	0.9376	0.9362	0.0496	-0.0085	0.9153	4.29
2.50	0.9450	0.9434	0.0549	-0.0066	0.9160	4.71
3.01	0.9528	0.9504	0.0675	-0.0043	0.9161	5.73
3.50	0.9560	0.9531	0.0743	-0.0022	0.9161	6.29
4.00	0.9572	0.9540	0.0783	-0.0020	0.9159	6.62
4.51	0.9555	0.9520	0.0823	-0.0009	0.9152	6.97
5.00	0.9539	0.9501	0.0854	-0.0013	0.9148	7.25
6.01	0.9487	0.9445	0.0887	-0.0006	0.9138	7.56

Configuration $P_OC_FB_FN_1L$

NPR	F_r/F_i	F_A/F_i	F_N/F_i	F_S/F_i	w_p/w_i	δ_{RR}, deg
1.51	0.9031	0.0524	0.9010	-0.0328	0.9085	87.64
1.80	0.9260	0.0404	0.9246	-0.0282	0.9106	88.23
2.02	0.9349	0.0336	0.9338	-0.0291	0.9132	88.54
2.21	0.9411	0.0337	0.9400	-0.0295	0.9149	88.55
2.50	0.9514	0.0397	0.9501	-0.0290	0.9152	88.31
3.00	0.9569	0.0525	0.9551	-0.0279	0.9154	87.77
3.52	0.9601	0.0611	0.9578	-0.0289	0.9155	87.42
4.00	0.9587	0.0675	0.9559	-0.0271	0.9152	87.14
4.50	0.9578	0.0726	0.9546	-0.0271	0.9148	86.92
4.77	0.9565	0.0753	0.9531	-0.0269	0.9143	86.80

Table 12. Concluded

(c) Tapered blocker

Configuration $P_OC_FB_TN_IT$

NPR	F_r/F_i	F_A/F_i	F_N/F_i	F_S/F_i	w_p/w_i	δ_{RR}, deg
1.51	0.9087	0.9055	0.0756	-0.0119	0.9102	6.73
1.81	0.9265	0.9245	0.0600	-0.0084	0.9129	5.24
2.02	0.9346	0.9333	0.0482	-0.0059	0.9156	4.18
2.22	0.9404	0.9390	0.0524	-0.0045	0.9178	4.51
2.52	0.9467	0.9450	0.0565	-0.0040	0.9186	4.84
3.01	0.9549	0.9526	0.0658	-0.0014	0.9189	5.58
3.50	0.9577	0.9550	0.0717	-0.0007	0.9186	6.06
4.01	0.9575	0.9544	0.0770	-0.0016	0.9185	6.51
4.53	0.9566	0.9533	0.0795	-0.0001	0.9180	6.73
5.01	0.9543	0.9507	0.0825	-0.0008	0.9175	7.00
6.01	0.9490	0.9451	0.0866	0.0011	0.9162	7.38

Configuration $P_OC_FB_TN_IL$

NPR	F_r/F_i	F_A/F_i	F_N/F_i	F_S/F_i	w_p/w_i	δ_{RR}, deg
1.51	0.9074	0.0516	0.9055	-0.0294	0.9082	87.69
1.80	0.9249	0.0389	0.9237	-0.0280	0.9108	88.29
1.99	0.9362	0.0315	0.9353	-0.0270	0.9134	88.64
2.21	0.9450	0.0317	0.9441	-0.0282	0.9158	88.64
2.50	0.9494	0.0369	0.9482	-0.0292	0.9159	88.43
3.00	0.9574	0.0510	0.9557	-0.0279	0.9160	87.84
3.48	0.9600	0.0587	0.9577	-0.0288	0.9161	87.52
4.01	0.9591	0.0652	0.9565	-0.0273	0.9157	87.24
4.52	0.9586	0.0716	0.9556	-0.0263	0.9157	86.97
4.77	0.9561	0.0738	0.9529	-0.0269	0.9148	86.86

Table 13. Internal Static Performance of 1.4 CR D-Shaped Nozzles Installed on Offset Plenum With Short-Core Centerbody

(a) No blocker

Configuration $P_OC_SB_NN_2T$

NPR	F_r/F_i	F_A/F_i	F_N/F_i	F_S/F_i	w_p/w_i	δ_{RR}, deg
1.50	0.8912	0.8881	0.0734	-0.0121	0.9047	6.67
1.80	0.9094	0.9075	0.0580	-0.0080	0.9064	5.17
2.01	0.9193	0.9180	0.0468	-0.0072	0.9088	4.12
2.20	0.9284	0.9270	0.0495	-0.0074	0.9103	4.32
2.50	0.9390	0.9372	0.0571	-0.0080	0.9111	4.92
3.00	0.9491	0.9468	0.0657	-0.0055	0.9117	5.61
3.51	0.9529	0.9500	0.0737	-0.0046	0.9118	6.26
3.99	0.9540	0.9507	0.0786	-0.0042	0.9118	6.66
4.51	0.9538	0.9502	0.0823	-0.0041	0.9113	6.98
5.01	0.9518	0.9480	0.0845	-0.0036	0.9106	7.19
6.01	0.9468	0.9426	0.0883	-0.0028	0.9097	7.54

Configuration $P_OC_SB_NN_2L$

NPR	F_r/F_i	F_A/F_i	F_N/F_i	F_S/F_i	w_p/w_i	δ_{RR}, deg
1.50	0.8883	0.0592	0.8857	-0.0334	0.9052	87.29
1.80	0.9114	0.0461	0.9097	-0.0327	0.9048	87.95
2.00	0.9213	0.0407	0.9198	-0.0314	0.9082	88.21
2.20	0.9288	0.0399	0.9274	-0.0316	0.9094	88.26
2.50	0.9391	0.0487	0.9373	-0.0320	0.9103	87.90
2.99	0.9493	0.0623	0.9467	-0.0313	0.9106	87.34
3.50	0.9526	0.0720	0.9494	-0.0305	0.9105	86.93
4.00	0.9544	0.0788	0.9506	-0.0303	0.9100	86.64
4.51	0.9538	0.0829	0.9497	-0.0299	0.9095	86.47
4.76	0.9538	0.0852	0.9495	-0.0297	0.9088	86.37

(b) Flat blocker

Configuration $P_OC_SB_FN_2T$

NPR	F_r/F_i	F_A/F_i	F_N/F_i	F_S/F_i	w_p/w_i	δ_{RR}, deg
1.51	0.8777	0.8745	0.0741	-0.0143	0.8938	6.83
1.80	0.9021	0.9000	0.0598	-0.0118	0.8990	5.37
2.00	0.9138	0.9125	0.0484	-0.0103	0.9021	4.29
2.20	0.9215	0.9203	0.0446	-0.0114	0.9042	3.92
2.51	0.9333	0.9317	0.0523	-0.0102	0.9051	4.54
3.01	0.9443	0.9422	0.0622	-0.0087	0.9057	5.33
3.51	0.9486	0.9460	0.0700	-0.0064	0.9060	5.97
4.00	0.9499	0.9468	0.0767	-0.0064	0.9054	6.54
4.49	0.9501	0.9467	0.0806	-0.0054	0.9044	6.86
5.01	0.9487	0.9450	0.0832	-0.0049	0.9051	7.10
6.00	0.9446	0.9406	0.0870	-0.0041	0.9040	7.46

Configuration $P_OC_SB_FN_2L$

NPR	F_r/F_i	F_A/F_i	F_N/F_i	F_S/F_i	w_p/w_i	δ_{RR}, deg
1.51	0.8800	0.0608	0.8774	-0.0310	0.8909	87.20
1.80	0.9043	0.0462	0.9026	-0.0316	0.8922	87.92
2.01	0.9175	0.0420	0.9159	-0.0342	0.8983	88.14
2.20	0.9266	0.0412	0.9250	-0.0346	0.9000	88.20
2.50	0.9362	0.0486	0.9344	-0.0320	0.8999	87.90
3.01	0.9501	0.0638	0.9474	-0.0323	0.9006	87.27
3.51	0.9521	0.0725	0.9488	-0.0326	0.9002	86.91
4.00	0.9537	0.0789	0.9500	-0.0302	0.8999	86.64
4.49	0.9533	0.0842	0.9490	-0.0307	0.9004	86.41
4.76	0.9526	0.0862	0.9482	-0.0303	0.8992	86.32

Table 14. Internal Static Performance of 1.4 CR D-Shaped Nozzles Installed on Offset Plenum With Medium-Core Centerbody

(a) No blocker

Configuration $P_OC_MB_NN_2T$

NPR	F_r/F_i	F_A/F_i	F_N/F_i	F_S/F_i	w_p/w_i	δ_{RR}, deg
1.51	0.8850	0.8820	0.0717	-0.0110	0.8988	6.56
1.80	0.9048	0.9029	0.0579	-0.0099	0.9014	5.18
2.00	0.9154	0.9142	0.0474	-0.0090	0.9035	4.19
2.20	0.9248	0.9235	0.0492	-0.0086	0.9056	4.31
2.50	0.9356	0.9339	0.0549	-0.0079	0.9056	4.75
3.00	0.9456	0.9433	0.0661	-0.0052	0.9061	5.66
3.50	0.9512	0.9482	0.0760	-0.0045	0.9063	6.46
4.00	0.9521	0.9486	0.0817	-0.0034	0.9062	6.94
4.50	0.9523	0.9485	0.0847	-0.0033	0.9058	7.20
5.01	0.9506	0.9466	0.0874	-0.0027	0.9054	7.44
5.97	0.9464	0.9420	0.0912	-0.0022	0.9041	7.80

Configuration $P_OC_MB_NN_2L$

NPR	F_r/F_i	F_A/F_i	F_N/F_i	F_S/F_i	w_p/w_i	δ_{RR}, deg
1.50	0.8922	0.0579	0.8897	-0.0328	0.8981	87.37
1.80	0.9111	0.0455	0.9095	-0.0304	0.8992	87.98
2.00	0.9197	0.0381	0.9184	-0.0310	0.9021	88.32
2.19	0.9275	0.0369	0.9262	-0.0316	0.9032	88.39
2.50	0.9386	0.0456	0.9370	-0.0318	0.9038	88.03
3.01	0.9497	0.0586	0.9474	-0.0311	0.9040	87.50
3.51	0.9535	0.0681	0.9506	-0.0297	0.9039	87.10
4.00	0.9534	0.0742	0.9501	-0.0301	0.9036	86.84
4.50	0.9521	0.0796	0.9483	-0.0297	0.9030	86.60
4.75	0.9511	0.0819	0.9471	-0.0302	0.9023	86.50

(b) Flat blocker

Configuration $P_OC_MB_FN_2T$

NPR	F_r/F_i	F_A/F_i	F_N/F_i	F_S/F_i	w_p/w_i	δ_{RR}, deg
1.51	0.8764	0.8731	0.0750	-0.0112	0.8920	6.92
1.80	0.8984	0.8968	0.0526	-0.0097	0.8957	4.75
2.00	0.9114	0.9102	0.0453	-0.0085	0.8990	4.02
2.20	0.9205	0.9193	0.0453	-0.0084	0.9003	3.98
2.51	0.9310	0.9296	0.0506	-0.0074	0.9012	4.40
3.00	0.9426	0.9405	0.0631	-0.0061	0.9015	5.42
3.50	0.9485	0.9458	0.0707	-0.0041	0.9019	6.03
4.00	0.9497	0.9467	0.0762	-0.0035	0.9017	6.50
4.50	0.9496	0.9461	0.0808	-0.0025	0.9015	6.89
5.00	0.9477	0.9440	0.0835	-0.0029	0.9012	7.13
6.00	0.9444	0.9403	0.0884	-0.0022	0.9003	7.57

Configuration $P_OC_MB_FN_2L$

NPR	F_r/F_i	F_A/F_i	F_N/F_i	F_S/F_i	w_p/w_i	δ_{RR}, deg
1.50	0.8761	0.0594	0.8736	-0.0287	0.8916	87.25
1.81	0.8964	0.0479	0.8947	-0.0277	0.8937	87.83
2.00	0.9107	0.0412	0.9093	-0.0290	0.8965	88.17
2.20	0.9227	0.0395	0.9213	-0.0314	0.8980	88.26
2.50	0.9357	0.0479	0.9339	-0.0329	0.8991	87.92
3.00	0.9474	0.0620	0.9448	-0.0321	0.8990	87.34
3.52	0.9530	0.0716	0.9498	-0.0307	0.8990	86.95
4.00	0.9546	0.0773	0.9510	-0.0300	0.8988	86.71
4.50	0.9540	0.0831	0.9499	-0.0301	0.8985	86.46
4.75	0.9532	0.0848	0.9489	-0.0305	0.8979	86.39

Table 15. Internal Static Performance of 1.4 CR D-Shaped Nozzles Installed on Offset Plenum With Long-Core Centerbody

(a) No blocker

Configuration $P_OC_LB_NN_2T$

NPR	F_r/F_i	F_A/F_i	F_N/F_i	F_S/F_i	w_p/w_i	δ_{RR}, deg
1.51	0.8838	0.8805	0.0755	-0.0122	0.8952	6.92
1.80	0.9033	0.9012	0.0611	-0.0104	0.8984	5.48
2.00	0.9148	0.9134	0.0493	-0.0091	0.9008	4.37
2.21	0.9237	0.9224	0.0477	-0.0088	0.9022	4.18
2.51	0.9338	0.9322	0.0536	-0.0066	0.9030	4.65
3.01	0.9448	0.9424	0.0669	-0.0051	0.9036	5.73
3.51	0.9505	0.9476	0.0740	-0.0044	0.9038	6.30
4.00	0.9514	0.9482	0.0778	-0.0041	0.9037	6.62
4.51	0.9509	0.9473	0.0822	-0.0029	0.9035	6.99
5.00	0.9499	0.9461	0.0849	-0.0019	0.9030	7.23
6.01	0.9456	0.9414	0.0895	-0.0017	0.9020	7.65

Configuration $P_OC_LB_NN_2L$

NPR	F_r/F_i	F_A/F_i	F_N/F_i	F_S/F_i	w_p/w_i	δ_{RR}, deg
1.51	0.8873	0.0570	0.8849	-0.0331	0.8934	87.39
1.81	0.9094	0.0436	0.9078	-0.0305	0.8956	88.06
2.01	0.9217	0.0376	0.9204	-0.0312	0.8980	88.35
2.21	0.9288	0.0365	0.9275	-0.0315	0.8999	88.41
2.50	0.9399	0.0440	0.9384	-0.0319	0.9000	88.10
3.01	0.9481	0.0583	0.9458	-0.0310	0.9001	87.50
3.50	0.9531	0.0674	0.9502	-0.0309	0.9002	87.13
4.01	0.9529	0.0738	0.9496	-0.0297	0.8998	86.85
4.50	0.9524	0.0790	0.9487	-0.0301	0.8997	86.63
4.74	0.9520	0.0810	0.9481	-0.0302	0.8991	86.54

(b) Flat blocker

Configuration $P_OC_LB_FN_2T$

NPR	F_r/F_i	F_A/F_i	F_N/F_i	F_S/F_i	w_p/w_i	δ_{RR}, deg
1.51	0.8787	0.8754	0.0756	-0.0131	0.8939	6.96
1.80	0.9008	0.8989	0.0565	-0.0113	0.8977	5.08
2.01	0.9132	0.9118	0.0484	-0.0097	0.9001	4.29
2.20	0.9206	0.9193	0.0486	-0.0080	0.9016	4.27
2.50	0.9317	0.9300	0.0566	-0.0072	0.9021	4.92
3.01	0.9443	0.9419	0.0671	-0.0056	0.9027	5.75
3.51	0.9484	0.9455	0.0744	-0.0040	0.9024	6.35
3.99	0.9495	0.9461	0.0800	-0.0028	0.9022	6.82
4.51	0.9501	0.9463	0.0849	-0.0027	0.9019	7.23
5.00	0.9488	0.9448	0.0874	-0.0016	0.9013	7.46
6.00	0.9440	0.9396	0.0910	-0.0015	0.9002	7.80

Configuration $P_OC_LB_FN_2L$

NPR	F_r/F_i	F_A/F_i	F_N/F_i	F_S/F_i	w_p/w_i	δ_{RR}, deg
1.50	0.8815	0.0590	0.8789	-0.0324	0.8943	87.28
1.81	0.9013	0.0463	0.8997	-0.0278	0.8959	87.91
2.01	0.9167	0.0388	0.9155	-0.0286	0.8985	88.28
2.20	0.9252	0.0385	0.9239	-0.0305	0.9002	88.31
2.50	0.9363	0.0458	0.9347	-0.0300	0.9005	88.02
2.80	0.9408	0.0558	0.9386	-0.0304	0.9006	87.59
3.01	0.9453	0.0604	0.9429	-0.0298	0.9008	87.41
3.51	0.9500	0.0705	0.9469	-0.0303	0.9004	86.99
4.01	0.9505	0.0771	0.9469	-0.0299	0.9002	86.70
4.51	0.9494	0.0817	0.9454	-0.0300	0.8998	86.51
4.75	0.9509	0.0835	0.9468	-0.0286	0.8992	86.43

Table 15. Concluded

(c) Tapered blocker

Configuration $P_OC_LB_TN_2T$

NPR	F_r/F_i	F_A/F_i	F_N/F_i	F_S/F_i	w_p/w_i	δ_{RR}, deg
1.50	0.8855	0.8812	0.0862	-0.0134	0.9012	7.88
1.80	0.9071	0.9046	0.0662	-0.0094	0.9041	5.91
2.00	0.9173	0.9157	0.0539	-0.0102	0.9059	4.75
2.21	0.9264	0.9249	0.0520	-0.0097	0.9073	4.55
2.51	0.9361	0.9342	0.0592	-0.0086	0.9081	5.12
3.00	0.9474	0.9448	0.0697	-0.0069	0.9078	5.95
3.50	0.9512	0.9481	0.0764	-0.0058	0.9075	6.51
4.00	0.9523	0.9489	0.0807	-0.0045	0.9073	6.86
4.50	0.9523	0.9485	0.0847	-0.0041	0.9071	7.19
5.01	0.9502	0.9461	0.0874	-0.0042	0.9067	7.44
6.01	0.9457	0.9413	0.0914	-0.0035	0.9055	7.82

Configuration $P_OC_LB_TN_2L$

NPR	F_r/F_i	F_A/F_i	F_N/F_i	F_S/F_i	w_p/w_i	δ_{RR}, deg
1.50	0.8808	0.0582	0.8782	-0.0340	0.8975	87.32
1.80	0.9030	0.0470	0.9013	-0.0291	0.8977	87.89
2.00	0.9198	0.0415	0.9185	-0.0284	0.9010	88.17
2.20	0.9248	0.0383	0.9236	-0.0291	0.9024	88.32
2.50	0.9381	0.0455	0.9366	-0.0297	0.9027	88.03
3.00	0.9497	0.0601	0.9474	-0.0302	0.9029	87.43
3.51	0.9519	0.0695	0.9490	-0.0283	0.9027	87.03
4.01	0.9541	0.0759	0.9506	-0.0291	0.9025	86.77
4.49	0.9527	0.0805	0.9488	-0.0288	0.9021	86.57
4.76	0.9529	0.0827	0.9488	-0.0285	0.9012	86.47

Table 16. Internal Static Performance of 1.4 CR D-Shaped Nozzles Installed on Offset Plenum With Fan Centerbody

(a) No blocker

Configuration $P_OC_FB_NN_2T$

NPR	F_r/F_i	F_A/F_i	F_N/F_i	F_S/F_i	w_p/w_i	δ_{RR}, deg
1.51	0.8811	0.8775	0.0774	-0.0139	0.8906	7.11
1.80	0.9014	0.8994	0.0592	-0.0074	0.8953	5.32
2.00	0.9142	0.9128	0.0509	-0.0053	0.8981	4.51
2.20	0.9238	0.9224	0.0493	-0.0054	0.8998	4.33
2.51	0.9326	0.9309	0.0560	-0.0042	0.9008	4.86
3.00	0.9450	0.9427	0.0662	-0.0042	0.9015	5.67
3.50	0.9495	0.9467	0.0718	-0.0029	0.9014	6.13
4.01	0.9505	0.9473	0.0778	-0.0023	0.9016	6.63
4.51	0.9504	0.9469	0.0811	-0.0017	0.9018	6.91
5.01	0.9498	0.9460	0.0839	-0.0015	0.9012	7.15
6.01	0.9453	0.9412	0.0880	-0.0012	0.9002	7.53

Configuration $P_OC_FB_NN_2L$

NPR	F_r/F_i	F_A/F_i	F_N/F_i	F_S/F_i	w_p/w_i	δ_{RR}, deg
1.51	0.8797	0.0592	0.8771	-0.0343	0.8920	87.27
1.80	0.9033	0.0452	0.9016	-0.0315	0.8944	87.97
2.01	0.9215	0.0397	0.9201	-0.0305	0.8977	88.25
2.20	0.9296	0.0392	0.9283	-0.0309	0.8987	88.29
2.50	0.9401	0.0463	0.9384	-0.0316	0.8993	88.00
3.01	0.9485	0.0618	0.9460	-0.0311	0.8997	87.36
3.50	0.9513	0.0708	0.9481	-0.0315	0.8994	86.98
4.00	0.9519	0.0773	0.9483	-0.0292	0.8997	86.70
4.51	0.9521	0.0820	0.9481	-0.0300	0.8990	86.50
4.75	0.9528	0.0840	0.9486	-0.0293	0.8986	86.42

(b) Flat blocker

Configuration $P_OC_FB_FN_2T$

NPR	F_r/F_i	F_A/F_i	F_N/F_i	F_S/F_i	w_p/w_i	δ_{RR}, deg
1.50	0.8859	0.8825	0.0752	-0.0145	0.9000	6.88
1.80	0.9050	0.9029	0.0598	-0.0121	0.9024	5.35
2.00	0.9174	0.9162	0.0456	-0.0103	0.9048	4.02
2.21	0.9261	0.9249	0.0474	-0.0087	0.9064	4.15
2.50	0.9364	0.9346	0.0563	-0.0091	0.9068	4.87
3.00	0.9462	0.9439	0.0653	-0.0081	0.9071	5.59
3.50	0.9507	0.9478	0.0740	-0.0068	0.9075	6.30
4.00	0.9528	0.9494	0.0802	-0.0062	0.9076	6.81
4.50	0.9523	0.9487	0.0831	-0.0054	0.9071	7.06
5.01	0.9508	0.9468	0.0870	-0.0045	0.9067	7.40
5.99	0.9459	0.9416	0.0897	-0.0041	0.9055	7.67

Configuration $P_OC_FB_FN_2L$

NPR	F_r/F_i	F_A/F_i	F_N/F_i	F_S/F_i	w_p/w_i	δ_{RR}, deg
1.51	0.8858	0.0617	0.8831	-0.0309	0.8984	87.17
1.80	0.9044	0.0481	0.9027	-0.0291	0.8993	87.84
2.01	0.9224	0.0401	0.9210	-0.0299	0.9020	88.24
2.20	0.9299	0.0412	0.9286	-0.0290	0.9033	88.20
2.50	0.9386	0.0479	0.9369	-0.0311	0.9034	87.93
3.00	0.9496	0.0612	0.9471	-0.0303	0.9036	87.39
3.50	0.9503	0.0703	0.9472	-0.0296	0.9037	86.99
3.99	0.9535	0.0764	0.9499	-0.0295	0.9036	86.75
4.50	0.9520	0.0817	0.9481	-0.0281	0.9035	86.51
4.76	0.9527	0.0833	0.9487	-0.0277	0.9026	86.45

Table 16. Concluded

(c) Tapered blocker

Configuration $P_OC_FB_TN_2T$

NPR	F_r/F_i	F_A/F_i	F_N/F_i	F_S/F_i	w_p/w_i	δ_{RR}, deg
1.50	0.8877	0.8838	0.0817	-0.0175	0.9040	7.45
1.81	0.9076	0.9053	0.0625	-0.0120	0.9056	5.58
2.00	0.9187	0.9174	0.0490	-0.0090	0.9073	4.32
2.20	0.9272	0.9256	0.0534	-0.0103	0.9084	4.66
2.50	0.9375	0.9357	0.0576	-0.0090	0.9092	4.98
3.01	0.9480	0.9457	0.0663	-0.0073	0.9094	5.66
3.50	0.9525	0.9495	0.0749	-0.0068	0.9096	6.37
4.01	0.9534	0.9501	0.0792	-0.0054	0.9095	6.72
4.51	0.9528	0.9491	0.0833	-0.0049	0.9092	7.08
5.00	0.9513	0.9474	0.0860	-0.0044	0.9089	7.31
6.01	0.9466	0.9423	0.0900	-0.0042	0.9077	7.69

Configuration $P_OC_FB_TN_2L$

NPR	F_r/F_i	F_A/F_i	F_N/F_i	F_S/F_i	w_p/w_i	δ_{RR}, deg
1.51	0.8839	0.0610	0.8813	-0.0309	0.9002	87.20
1.80	0.9032	0.0465	0.9016	-0.0291	0.9005	87.91
2.02	0.9200	0.0398	0.9187	-0.0281	0.9045	88.25
2.20	0.9312	0.0383	0.9299	-0.0303	0.9046	88.33
2.50	0.9393	0.0460	0.9376	-0.0308	0.9049	88.01
3.02	0.9500	0.0613	0.9476	-0.0302	0.9052	87.38
3.52	0.9526	0.0706	0.9495	-0.0298	0.9049	86.99
4.01	0.9546	0.0769	0.9511	-0.0287	0.9048	86.73
4.49	0.9543	0.0822	0.9503	-0.0287	0.9042	86.50
4.76	0.9536	0.0844	0.9495	-0.0283	0.9038	86.41

Table 17. Internal Static Performance of 1.4 CR Pegasus Nozzles Installed on Offset Plenum With Short-Core Centerbody

(a) No blocker

Configuration $P_OC_SB_NN_3T$

NPR	F_r/F_i	F_A/F_i	F_N/F_i	F_S/F_i	w_p/w_i	δ_{RR}, deg
1.51	0.8861	0.8804	0.1002	-0.0067	0.8663	9.14
1.80	0.9039	0.8989	0.0950	-0.0069	0.8860	8.51
2.01	0.9144	0.9102	0.0879	-0.0049	0.8987	7.78
2.20	0.9229	0.9187	0.0878	-0.0049	0.9055	7.69
2.50	0.9307	0.9269	0.0849	-0.0045	0.9115	7.38
3.00	0.9395	0.9350	0.0916	-0.0028	0.9155	7.89
3.50	0.9443	0.9391	0.0989	-0.0027	0.9169	8.47
4.00	0.9465	0.9410	0.1020	-0.0028	0.9182	8.71
4.51	0.9465	0.9406	0.1052	-0.0023	0.9186	8.99
5.02	0.9445	0.9383	0.1076	-0.0022	0.9186	9.21
6.02	0.9401	0.9339	0.1080	-0.0016	0.9178	9.29

Configuration $P_OC_SB_NN_3L$

NPR	F_r/F_i	F_A/F_i	F_N/F_i	F_S/F_i	w_p/w_i	δ_{RR}, deg
1.50	0.8870	0.0905	0.8819	-0.0284	0.8680	85.85
1.81	0.9048	0.0858	0.9003	-0.0282	0.8882	86.15
2.01	0.9157	0.0821	0.9117	-0.0269	0.9002	86.36
2.20	0.9249	0.0811	0.9209	-0.0290	0.9068	86.44
2.50	0.9374	0.0835	0.9332	-0.0288	0.9116	86.38
3.00	0.9426	0.0915	0.9377	-0.0284	0.9153	86.05
3.51	0.9464	0.0993	0.9407	-0.0274	0.9172	85.73
4.00	0.9473	0.1042	0.9412	-0.0264	0.9180	85.52
4.51	0.9461	0.1074	0.9396	-0.0262	0.9177	85.38
4.76	0.9459	0.1093	0.9393	-0.0261	0.9175	85.30

(b) Flat blocker

Configuration $P_OC_SB_FN_3T$

NPR	F_r/F_i	F_A/F_i	F_N/F_i	F_S/F_i	w_p/w_i	δ_{RR}, deg
1.51	0.8796	0.8740	0.0979	-0.0134	0.8502	9.00
1.79	0.8978	0.8932	0.0908	-0.0082	0.8766	8.18
2.00	0.9084	0.9042	0.0870	-0.0077	0.8901	7.75
2.19	0.9176	0.9138	0.0837	-0.0059	0.8971	7.38
2.48	0.9267	0.9229	0.0826	-0.0067	0.9038	7.21
2.98	0.9372	0.9328	0.0907	-0.0063	0.9069	7.83
3.50	0.9411	0.9363	0.0948	-0.0059	0.9092	8.15
4.00	0.9435	0.9382	0.0996	-0.0054	0.9093	8.54
4.50	0.9430	0.9375	0.1016	-0.0044	0.9103	8.71
5.01	0.9428	0.9369	0.1048	-0.0043	0.9099	8.99
6.02	0.9391	0.9330	0.1070	-0.0033	0.9095	9.21

Configuration $P_OC_SB_FN_3L$

NPR	F_r/F_i	F_A/F_i	F_N/F_i	F_S/F_i	w_p/w_i	δ_{RR}, deg
1.49	0.8728	0.0817	0.8681	-0.0395	0.8501	86.19
1.81	0.8979	0.0840	0.8932	-0.0346	0.8771	86.19
2.00	0.9078	0.0812	0.9036	-0.0324	0.8888	86.36
2.51	0.9293	0.0832	0.9250	-0.0327	0.9015	86.36
3.00	0.9366	0.0912	0.9316	-0.0319	0.9051	86.04
3.52	0.9408	0.0986	0.9351	-0.0309	0.9059	85.74
4.00	0.9434	0.1038	0.9371	-0.0303	0.9062	85.52
4.52	0.9442	0.1079	0.9375	-0.0295	0.9074	85.35
4.75	0.9438	0.1087	0.9371	-0.0298	0.9073	85.31

Table 18. Internal Static Performance of 1.4 CR Pegasus Nozzles Installed on Offset Plenum With Medium-Core Centerbody

(a) No blocker

Configuration $P_OC_MB_NN_3T$

NPR	F_r/F_i	F_A/F_i	F_N/F_i	F_S/F_i	w_p/w_i	δ_{RR}, deg
1.52	0.8820	0.8770	0.0935	-0.0072	0.8629	8.57
1.81	0.8999	0.8953	0.0905	-0.0054	0.8817	8.13
2.01	0.9092	0.9048	0.0889	-0.0055	0.8939	7.91
2.20	0.9176	0.9133	0.0890	-0.0055	0.9004	7.85
2.50	0.9274	0.9233	0.0868	-0.0039	0.9051	7.57
2.99	0.9358	0.9312	0.0922	-0.0041	0.9089	7.97
3.52	0.9422	0.9367	0.1013	-0.0019	0.9104	8.69
4.00	0.9438	0.9380	0.1039	-0.0017	0.9112	8.90
4.51	0.9439	0.9379	0.1059	-0.0016	0.9119	9.07
5.02	0.9422	0.9359	0.1084	-0.0018	0.9118	9.30
6.01	0.9388	0.9324	0.1099	-0.0008	0.9109	9.46

Configuration $P_OC_MB_NN_3L$

NPR	F_r/F_i	F_A/F_i	F_N/F_i	F_S/F_i	w_p/w_i	δ_{RR}, deg
1.50	0.8809	0.0905	0.8756	-0.0331	0.8605	85.82
1.80	0.8994	0.0852	0.8948	-0.0306	0.8794	86.15
2.00	0.9103	0.0808	0.9062	-0.0310	0.8913	86.39
2.20	0.9184	0.0791	0.9145	-0.0312	0.8981	86.50
2.50	0.9288	0.0813	0.9248	-0.0301	0.9030	86.44
3.00	0.9355	0.0886	0.9308	-0.0287	0.9063	86.15
3.50	0.9406	0.0978	0.9350	-0.0283	0.9078	85.77
4.01	0.9430	0.1023	0.9371	-0.0278	0.9089	85.59
4.50	0.9455	0.1055	0.9392	-0.0275	0.9088	85.46
4.74	0.9428	0.1071	0.9364	-0.0267	0.9084	85.38

(b) Flat blocker

Configuration $P_OC_MB_FN_3T$

NPR	F_r/F_i	F_A/F_i	F_N/F_i	F_S/F_i	w_p/w_i	δ_{RR}, deg
1.51	0.8764	0.8705	0.1008	-0.0096	0.8551	9.30
1.81	0.8948	0.8900	0.0916	-0.0071	0.8760	8.28
2.00	0.9059	0.9017	0.0871	-0.0054	0.8881	7.78
2.21	0.9152	0.9109	0.0878	-0.0055	0.8955	7.76
2.50	0.9247	0.9206	0.0868	-0.0035	0.8998	7.59
3.00	0.9348	0.9303	0.0918	-0.0031	0.9039	7.94
3.50	0.9400	0.9349	0.0984	-0.0034	0.9055	8.47
4.00	0.9432	0.9377	0.1013	-0.0023	0.9066	8.68
4.51	0.9433	0.9375	0.1042	-0.0015	0.9069	8.93
5.00	0.9420	0.9360	0.1053	-0.0011	0.9068	9.04
6.02	0.9383	0.9321	0.1072	-0.0010	0.9063	9.24

Configuration $P_OC_MB_FN_3L$

NPR	F_r/F_i	F_A/F_i	F_N/F_i	F_S/F_i	w_p/w_i	δ_{RR}, deg
1.50	0.8770	0.0898	0.8717	-0.0354	0.8521	85.83
1.80	0.9006	0.0838	0.8961	-0.0323	0.8730	86.22
2.00	0.9081	0.0820	0.9038	-0.0328	0.8844	86.33
2.20	0.9203	0.0803	0.9162	-0.0327	0.8924	86.45
2.50	0.9284	0.0825	0.9242	-0.0312	0.8970	86.39
3.01	0.9377	0.0899	0.9329	-0.0307	0.9009	86.10
3.51	0.9398	0.0974	0.9342	-0.0309	0.9023	85.78
3.99	0.9435	0.1029	0.9374	-0.0297	0.9028	85.56
4.51	0.9444	0.1068	0.9379	-0.0292	0.9030	85.39
4.75	0.9424	0.1079	0.9357	-0.0293	0.9026	85.34

Table 19. Internal Static Performance of 1.4 CR Pegasus Nozzles Installed on Offset Plenum With Long-Core Centerbody

(a) No blocker

Configuration $P_OC_LB_NN_3T$

NPR	F_r/F_i	F_A/F_i	F_N/F_i	F_S/F_i	w_p/w_i	δ_{RR}, deg
1.52	0.8814	0.8757	0.1001	-0.0065	0.8584	9.18
1.81	0.8964	0.8915	0.0930	-0.0022	0.8775	8.39
2.00	0.9081	0.9035	0.0913	-0.0012	0.8896	8.14
2.20	0.9165	0.9123	0.0875	-0.0019	0.8968	7.73
2.49	0.9260	0.9220	0.0859	-0.0005	0.9015	7.50
3.00	0.9355	0.9311	0.0908	-0.0004	0.9052	7.85
3.50	0.9408	0.9357	0.0973	-0.0014	0.9074	8.37
4.02	0.9433	0.9377	0.1021	-0.0013	0.9083	8.76
4.51	0.9435	0.9377	0.1044	-0.0013	0.9088	8.95
5.01	0.9416	0.9355	0.1067	-0.0001	0.9086	9.16
6.01	0.9382	0.9319	0.1081	-0.0005	0.9075	9.32

Configuration $P_OC_LB_NN_3L$

NPR	F_r/F_i	F_A/F_i	F_N/F_i	F_S/F_i	w_p/w_i	δ_{RR}, deg
1.52	0.8798	0.0863	0.8750	-0.0318	0.8583	86.01
1.80	0.8993	0.0834	0.8949	-0.0299	0.8760	86.23
2.01	0.9121	0.0779	0.9083	-0.0304	0.8880	86.53
2.20	0.9216	0.0778	0.9178	-0.0293	0.8946	86.57
2.51	0.9315	0.0809	0.9275	-0.0290	0.8996	86.47
3.00	0.9394	0.0881	0.9348	-0.0281	0.9026	86.19
3.50	0.9445	0.0960	0.9392	-0.0285	0.9039	85.87
4.00	0.9420	0.1010	0.9361	-0.0274	0.9049	85.64
4.52	0.9421	0.1053	0.9358	-0.0269	0.9049	85.45
4.75	0.9428	0.1061	0.9364	-0.0273	0.9046	85.42

(b) Flat blocker

Configuration $P_OC_LB_FN_3T$

NPR	F_r/F_i	F_A/F_i	F_N/F_i	F_S/F_i	w_p/w_i	δ_{RR}, deg
1.51	0.8815	0.8750	0.1064	-0.0038	0.8592	9.76
1.81	0.8975	0.8920	0.0990	-0.0034	0.8781	8.92
2.00	0.9069	0.9020	0.0938	-0.0055	0.8898	8.36
2.20	0.9178	0.9132	0.0916	-0.0025	0.8969	8.08
2.50	0.9256	0.9213	0.0892	-0.0012	0.9011	7.80
3.01	0.9359	0.9311	0.0949	-0.0003	0.9046	8.20
3.52	0.9416	0.9362	0.1006	-0.0005	0.9059	8.64
4.00	0.9432	0.9373	0.1054	0.0000	0.9067	9.03
4.50	0.9433	0.9373	0.1062	0.0008	0.9069	9.10
5.01	0.9422	0.9358	0.1095	0.0005	0.9071	9.40
6.00	0.9384	0.9318	0.1115	0.0012	0.9060	9.60

Configuration $P_OC_LB_FN_3L$

NPR	F_r/F_i	F_A/F_i	F_N/F_i	F_S/F_i	w_p/w_i	δ_{RR}, deg
1.51	0.8795	0.0899	0.8742	-0.0340	0.8583	85.84
1.81	0.8971	0.0856	0.8925	-0.0271	0.8774	86.12
2.00	0.9095	0.0805	0.9055	-0.0296	0.8879	86.40
2.20	0.9201	0.0798	0.9162	-0.0287	0.8954	86.48
2.50	0.9273	0.0814	0.9233	-0.0281	0.9002	86.43
3.00	0.9364	0.0890	0.9318	-0.0278	0.9031	86.14
3.51	0.9407	0.0974	0.9352	-0.0277	0.9047	85.79
4.01	0.9431	0.1028	0.9371	-0.0264	0.9051	85.57
4.51	0.9425	0.1065	0.9361	-0.0265	0.9051	85.40
4.76	0.9430	0.1077	0.9365	-0.0258	0.9048	85.35

Table 19. Concluded

(c) Tapered blocker

Configuration $P_OC_LB_TN_3T$

NPR	F_r/F_i	F_A/F_i	F_N/F_i	F_S/F_i	w_p/w_i	δ_{RR}, deg
1.53	0.8869	0.8809	0.1027	-0.0101	0.8666	9.36
1.80	0.9026	0.8977	0.0932	-0.0078	0.8841	8.36
2.02	0.9138	0.9092	0.0912	-0.0058	0.8969	8.07
2.20	0.9218	0.9174	0.0901	-0.0060	0.9024	7.91
2.51	0.9308	0.9263	0.0907	-0.0043	0.9076	7.88
3.00	0.9385	0.9337	0.0938	-0.0035	0.9106	8.08
3.51	0.9441	0.9386	0.1018	-0.0032	0.9126	8.72
4.02	0.9453	0.9395	0.1050	-0.0027	0.9133	8.98
4.50	0.9450	0.9389	0.1073	-0.0026	0.9133	9.18
5.02	0.9438	0.9375	0.1085	-0.0024	0.9137	9.29
6.02	0.9396	0.9330	0.1117	-0.0019	0.9127	9.61

Configuration $P_OC_LB_TN_3L$

NPR	F_r/F_i	F_A/F_i	F_N/F_i	F_S/F_i	w_p/w_i	δ_{RR}, deg
1.50	0.8821	0.0897	0.8770	-0.0310	0.8596	85.86
1.80	0.9025	0.0871	0.8978	-0.0300	0.8787	86.08
2.00	0.9075	0.0829	0.9032	-0.0298	0.8897	86.29
2.19	0.9189	0.0811	0.9149	-0.0284	0.8966	86.41
2.52	0.9279	0.0824	0.9238	-0.0285	0.9023	86.39
3.00	0.9365	0.0910	0.9317	-0.0271	0.9051	86.05
3.50	0.9435	0.0981	0.9380	-0.0272	0.9063	85.77
3.99	0.9449	0.1031	0.9389	-0.0265	0.9071	85.56
4.50	0.9420	0.1066	0.9355	-0.0267	0.9071	85.39
4.76	0.9439	0.1074	0.9374	-0.0264	0.9067	85.37

Table 20. Internal Static Performance of 1.4 CR Pegasus Nozzles Installed on Offset Plenum With Fan Centerbody

(a) No blocker

Configuration $P_OC_FB_NN_3T$

NPR	F_r/F_i	F_A/F_i	F_N/F_i	F_S/F_i	w_p/w_i	δ_{RR}, deg
1.51	0.8773	0.8716	0.1000	-0.0058	0.8539	9.22
1.81	0.8968	0.8919	0.0933	-0.0041	0.8751	8.42
2.00	0.9071	0.9027	0.0886	-0.0031	0.8876	7.90
2.20	0.9153	0.9110	0.0881	-0.0018	0.8951	7.79
2.50	0.9254	0.9213	0.0876	-0.0020	0.9004	7.66
3.01	0.9356	0.9309	0.0939	-0.0014	0.9041	8.11
3.51	0.9418	0.9365	0.0998	-0.0014	0.9062	8.57
4.00	0.9427	0.9371	0.1031	-0.0010	0.9070	8.85
4.51	0.9433	0.9374	0.1054	-0.0007	0.9075	9.03
5.02	0.9417	0.9358	0.1055	-0.0007	0.9068	9.06
5.99	0.9377	0.9315	0.1076	-0.0001	0.9057	9.27

Configuration $P_OC_FB_NN_3L$

NPR	F_r/F_i	F_A/F_i	F_N/F_i	F_S/F_i	w_p/w_i	δ_{RR}, deg
1.50	0.8796	0.0910	0.8743	-0.0327	0.8541	85.79
1.80	0.9000	0.0856	0.8954	-0.0329	0.8733	86.13
2.00	0.9105	0.0823	0.9062	-0.0327	0.8854	86.33
2.19	0.9196	0.0801	0.9155	-0.0325	0.8923	86.46
2.50	0.9273	0.0820	0.9231	-0.0312	0.8979	86.40
3.00	0.9385	0.0897	0.9337	-0.0293	0.9015	86.11
3.49	0.9403	0.0970	0.9348	-0.0297	0.9029	85.80
4.00	0.9431	0.1028	0.9371	-0.0290	0.9035	85.57
4.51	0.9426	0.1069	0.9361	-0.0282	0.9036	85.38
4.75	0.9431	0.1083	0.9364	-0.0286	0.9033	85.33

(b) Flat blocker

Configuration $P_OC_FB_FN_3T$

NPR	F_r/F_i	F_A/F_i	F_N/F_i	F_S/F_i	w_p/w_i	δ_{RR}, deg
1.50	0.8838	0.8773	0.1059	-0.0140	0.8647	9.69
1.80	0.9009	0.8955	0.0975	-0.0082	0.8833	8.75
2.01	0.9104	0.9055	0.0937	-0.0077	0.8952	8.33
2.21	0.9200	0.9154	0.0922	-0.0060	0.9019	8.11
2.50	0.9295	0.9250	0.0917	-0.0054	0.9067	7.98
3.00	0.9386	0.9335	0.0976	-0.0043	0.9102	8.41
3.51	0.9429	0.9373	0.1024	-0.0032	0.9119	8.79
4.00	0.9448	0.9389	0.1061	-0.0028	0.9128	9.08
4.50	0.9452	0.9391	0.1075	-0.0026	0.9130	9.20
5.00	0.9430	0.9367	0.1092	-0.0025	0.9132	9.36
6.01	0.9393	0.9328	0.1100	-0.0022	0.9118	9.47

Configuration $P_OC_FB_FN_3L$

NPR	F_r/F_i	F_A/F_i	F_N/F_i	F_S/F_i	w_p/w_i	δ_{RR}, deg
1.50	0.8754	0.0875	0.8705	-0.0312	0.8609	85.93
1.80	0.8979	0.0843	0.8934	-0.0293	0.8793	86.18
2.01	0.9112	0.0831	0.9069	-0.0284	0.8904	86.29
2.20	0.9189	0.0803	0.9150	-0.0274	0.8972	86.45
2.50	0.9284	0.0825	0.9243	-0.0281	0.9020	86.39
3.01	0.9370	0.0900	0.9323	-0.0279	0.9053	86.09
3.50	0.9431	0.0976	0.9376	-0.0279	0.9068	85.79
3.99	0.9446	0.1031	0.9385	-0.0270	0.9075	85.56
4.50	0.9431	0.1069	0.9366	-0.0260	0.9077	85.39
4.76	0.9448	0.1080	0.9383	-0.0256	0.9074	85.35

Table 20. Concluded

(c) Tapered blocker

Configuration $P_OC_FB_TN_3T$

NPR	F_r/F_i	F_A/F_i	F_N/F_i	F_S/F_i	w_p/w_i	δ_{RR}, deg
1.51	0.8841	0.8779	0.1038	-0.0125	0.8660	9.49
1.80	0.9023	0.8969	0.0979	-0.0089	0.8849	8.78
2.00	0.9127	0.9078	0.0942	-0.0067	0.8972	8.35
2.20	0.9220	0.9177	0.0890	-0.0067	0.9045	7.81
2.51	0.9296	0.9252	0.0906	-0.0046	0.9089	7.88
3.00	0.9393	0.9345	0.0952	-0.0037	0.9122	8.20
3.51	0.9437	0.9382	0.1015	-0.0027	0.9141	8.70
4.00	0.9459	0.9400	0.1053	-0.0031	0.9148	9.00
4.51	0.9447	0.9386	0.1075	-0.0016	0.9151	9.20
5.01	0.9441	0.9379	0.1084	-0.0018	0.9148	9.28
6.01	0.9396	0.9331	0.1100	-0.0012	0.9138	9.46

Configuration $P_OC_FB_TN_3L$

NPR	F_r/F_i	F_A/F_i	F_N/F_i	F_S/F_i	w_p/w_i	δ_{RR}, deg
1.50	0.8821	0.0887	0.8800	-0.0328	0.8604	85.92
1.80	0.8950	0.0830	0.8906	-0.0303	0.8781	86.23
2.00	0.9149	0.0819	0.9108	-0.0291	0.8900	86.36
2.20	0.9198	0.0803	0.9158	-0.0294	0.8973	86.45
2.50	0.9302	0.0823	0.9261	-0.0288	0.9023	86.40
3.00	0.9397	0.0904	0.9349	-0.0283	0.9059	86.09
3.50	0.9440	0.0979	0.9385	-0.0275	0.9073	85.78
4.00	0.9448	0.1030	0.9388	-0.0266	0.9081	85.56
4.51	0.9448	0.1030	0.9388	-0.0266	0.9081	85.56
4.75	0.9444	0.1075	0.9379	-0.0261	0.9079	85.37

Table 21. Internal Static Performance of 1.4 CR Submerged Nozzles Installed on Offset Plenum With Short-Core Centerbody

(a) No blocker

Configuration $P_OC_SB_NN_4T$

NPR	F_r/F_i	F_A/F_i	F_N/F_i	F_S/F_i	w_p/w_i	δ_{RR}, deg
1.50	0.8913	0.8622	0.2253	-0.0136	0.9276	20.28
1.80	0.9083	0.8802	0.2241	-0.0069	0.9206	19.80
2.01	0.9176	0.8933	0.2095	-0.0052	0.9239	18.35
2.20	0.9276	0.9066	0.1964	-0.0077	0.9254	17.04
2.50	0.9350	0.9126	0.2035	-0.0062	0.9261	17.50
3.00	0.9406	0.9163	0.2125	-0.0058	0.9268	18.16
3.51	0.9398	0.9143	0.2174	-0.0059	0.9267	18.59
4.00	0.9386	0.9119	0.2224	-0.0052	0.9264	19.03
4.50	0.9365	0.9092	0.2245	-0.0043	0.9253	19.25
5.01	0.9328	0.9051	0.2258	-0.0046	0.9254	19.43
6.00	0.9255	0.8972	0.2272	-0.0044	0.9239	19.70

Configuration $P_OC_SB_NN_4L$

NPR	F_r/F_i	F_A/F_i	F_N/F_i	F_S/F_i	w_p/w_i	δ_{RR}, deg
1.51	0.8953	0.2132	0.8689	-0.0330	0.9275	80.16
1.81	0.9131	0.2122	0.8875	-0.0339	0.9217	80.40
2.00	0.9227	0.2032	0.8995	-0.0319	0.9249	80.93
2.20	0.9333	0.1908	0.9131	-0.0304	0.9257	81.59
2.50	0.9379	0.1990	0.9161	-0.0288	0.9267	81.27
3.00	0.9422	0.2109	0.9179	-0.0270	0.9271	80.77
3.49	0.9402	0.2188	0.9140	-0.0261	0.9276	80.39
4.00	0.9392	0.2234	0.9119	-0.0250	0.9276	80.17
4.51	0.9364	0.2273	0.9081	-0.0250	0.9265	79.96
5.00	0.9322	0.2289	0.9034	-0.0247	0.9266	79.84

(b) Flat blocker

Configuration $P_OC_SB_FN_4T$

NPR	F_r/F_i	F_A/F_i	F_N/F_i	F_S/F_i	w_p/w_i	δ_{RR}, deg
1.51	0.8714	0.8444	0.2145	-0.0153	0.9059	19.76
1.81	0.8949	0.8687	0.2148	-0.0088	0.9071	19.28
2.01	0.9082	0.8853	0.2025	-0.0058	0.9130	17.92
2.20	0.9162	0.8967	0.1884	-0.0028	0.9138	16.55
2.50	0.9281	0.9069	0.1967	-0.0074	0.9159	17.05
3.00	0.9329	0.9099	0.2057	-0.0071	0.9141	17.73
3.49	0.9342	0.9096	0.2126	-0.0061	0.9147	18.29
4.02	0.9337	0.9078	0.2182	-0.0066	0.9148	18.77
4.50	0.9310	0.9047	0.2198	-0.0060	0.9140	18.96
5.00	0.9283	0.9015	0.2214	-0.0059	0.9132	19.15
6.01	0.9220	0.8945	0.2236	-0.0049	0.9124	19.47

Configuration $P_OC_SB_FN_4L$

NPR	F_r/F_i	F_A/F_i	F_N/F_i	F_S/F_i	w_p/w_i	δ_{RR}, deg
1.51	0.8802	0.2143	0.8530	-0.0352	0.9132	79.93
1.81	0.8971	0.2150	0.8702	-0.0357	0.9128	80.09
2.00	0.9121	0.2065	0.8878	-0.0331	0.9163	80.66
2.49	0.9300	0.2003	0.9076	-0.0328	0.9190	81.13
3.00	0.9377	0.2107	0.9132	-0.0306	0.9192	80.73
3.51	0.9386	0.2192	0.9121	-0.0306	0.9192	80.36
4.02	0.9359	0.2239	0.9083	-0.0281	0.9194	80.11
4.51	0.9341	0.2280	0.9054	-0.0289	0.9183	79.90
4.98	0.9314	0.2289	0.9024	-0.0279	0.9183	79.83

Table 22. Internal Static Performance of 1.4 CR Submerged Nozzles Installed on Offset Plenum With Medium-Core Centerbody

(a) No blocker

Configuration $P_OC_MB_NN_4T$

NPR	F_r/F_i	F_A/F_i	F_N/F_i	F_S/F_i	w_p/w_i	δ_{RR}, deg
1.51	0.8857	0.8568	0.2239	-0.0107	0.9223	20.28
1.81	0.9017	0.8746	0.2193	-0.0071	0.9161	19.53
2.00	0.9136	0.8890	0.2106	-0.0053	0.9182	18.53
2.20	0.9226	0.9014	0.1963	-0.0076	0.9193	17.12
2.51	0.9308	0.9087	0.2011	-0.0066	0.9200	17.38
3.01	0.9371	0.9130	0.2111	-0.0059	0.9202	18.11
3.50	0.9384	0.9129	0.2175	-0.0051	0.9200	18.62
4.01	0.9369	0.9099	0.2234	-0.0045	0.9198	19.15
4.51	0.9350	0.9078	0.2241	-0.0042	0.9192	19.25
5.00	0.9311	0.9033	0.2261	-0.0042	0.9191	19.49
6.01	0.9249	0.8965	0.2276	-0.0037	0.9179	19.75

Configuration $P_OC_MB_NN_4L$

NPR	F_r/F_i	F_A/F_i	F_N/F_i	F_S/F_i	w_p/w_i	δ_{RR}, deg
1.50	0.8853	0.2087	0.8597	-0.0322	0.9236	80.26
1.81	0.9016	0.2070	0.8769	-0.0334	0.9164	80.52
2.00	0.9137	0.1977	0.8915	-0.0313	0.9184	81.09
2.21	0.9241	0.1869	0.9044	-0.0312	0.9197	81.69
2.50	0.9310	0.1949	0.9099	-0.0297	0.9204	81.39
3.01	0.9386	0.2077	0.9149	-0.0276	0.9206	80.88
3.50	0.9371	0.2153	0.9117	-0.0260	0.9208	80.52
3.99	0.9358	0.2198	0.9093	-0.0256	0.9206	80.30
4.51	0.9342	0.2240	0.9066	-0.0253	0.9203	80.09
5.00	0.9316	0.2264	0.9034	-0.0241	0.9201	79.95

(b) Flat blocker

Configuration $P_OC_MB_FN_4T$

NPR	F_r/F_i	F_A/F_i	F_N/F_i	F_S/F_i	w_p/w_i	δ_{RR}, deg
1.51	0.8753	0.8483	0.2154	-0.0132	0.9141	19.75
1.81	0.8936	0.8675	0.2142	-0.0085	0.9087	19.24
2.00	0.9041	0.8817	0.1999	-0.0045	0.9115	17.78
2.20	0.9150	0.8957	0.1867	-0.0053	0.9132	16.43
2.51	0.9253	0.9045	0.1952	-0.0054	0.9139	16.97
3.00	0.9324	0.9091	0.2068	-0.0044	0.9141	17.83
3.52	0.9345	0.9096	0.2144	-0.0044	0.9141	18.44
4.01	0.9333	0.9074	0.2183	-0.0037	0.9140	18.79
4.50	0.9312	0.9047	0.2206	-0.0035	0.9136	19.03
5.00	0.9288	0.9013	0.2242	-0.0026	0.9129	19.38
6.00	0.9223	0.8945	0.2245	-0.0027	0.9117	19.54

Configuration $P_OC_MB_FN_4L$

NPR	F_r/F_i	F_A/F_i	F_N/F_i	F_S/F_i	w_p/w_i	δ_{RR}, deg
1.51	0.8773	0.2082	0.8516	-0.0325	0.9139	80.19
1.80	0.8976	0.2080	0.8726	-0.0317	0.9103	80.43
2.01	0.9105	0.2023	0.8872	-0.0329	0.9127	80.84
2.21	0.9211	0.1903	0.9007	-0.0299	0.9145	81.50
2.50	0.9303	0.1960	0.9089	-0.0297	0.9147	81.33
3.00	0.9349	0.2087	0.9109	-0.0295	0.9153	80.80
3.52	0.9357	0.2171	0.9098	-0.0276	0.9156	80.42
4.01	0.9350	0.2222	0.9078	-0.0270	0.9153	80.18
4.51	0.9320	0.2253	0.9039	-0.0266	0.9148	80.00
5.01	0.9309	0.2275	0.9023	-0.0262	0.9144	79.89

Table 23. Internal Static Performance of 1.4 CR Submerged Nozzles Installed on Offset Plenum With Long-Core Centerbody

(a) No blocker

Configuration $P_OC_LB_NN_4T$

NPR	F_r/F_i	F_A/F_i	F_N/F_i	F_S/F_i	w_p/w_i	δ_{RR}, deg
1.50	0.8830	0.8542	0.2234	-0.0112	0.9166	20.29
1.80	0.8976	0.8703	0.2197	-0.0052	0.9111	19.65
2.00	0.9088	0.8853	0.2053	-0.0057	0.9138	18.16
2.21	0.9193	0.8993	0.1907	-0.0062	0.9148	16.69
2.50	0.9285	0.9069	0.1990	-0.0051	0.9155	17.24
2.99	0.9351	0.9116	0.2080	-0.0052	0.9157	17.88
3.51	0.9363	0.9113	0.2150	-0.0041	0.9155	18.45
4.00	0.9347	0.9085	0.2197	-0.0042	0.9155	18.88
4.51	0.9328	0.9060	0.2221	-0.0040	0.9150	19.12
5.00	0.9304	0.9029	0.2247	-0.0035	0.9145	19.39
6.00	0.9244	0.8963	0.2263	-0.0029	0.9131	19.65

Configuration $P_OC_LB_NN_4L$

NPR	F_r/F_i	F_A/F_i	F_N/F_i	F_S/F_i	w_p/w_i	δ_{RR}, deg
1.51	0.8811	0.2069	0.8558	-0.0329	0.9180	80.30
1.81	0.8979	0.2062	0.8733	-0.0317	0.9126	80.52
2.01	0.9171	0.1987	0.8948	-0.0299	0.9153	81.08
2.20	0.9240	0.1857	0.9047	-0.0286	0.9166	81.74
2.51	0.9307	0.1941	0.9098	-0.0285	0.9170	81.42
3.00	0.9368	0.2061	0.9135	-0.0277	0.9171	80.94
3.50	0.9366	0.2145	0.9114	-0.0261	0.9176	80.55
4.01	0.9369	0.2198	0.9104	-0.0249	0.9173	80.31
4.50	0.9337	0.2232	0.9063	-0.0247	0.9168	80.12
5.01	0.9314	0.2253	0.9034	-0.0248	0.9163	80.00

(b) Flat blocker

Configuration $P_OC_LB_FN_4T$

NPR	F_r/F_i	F_A/F_i	F_N/F_i	F_S/F_i	w_p/w_i	δ_{RR}, deg
1.51	0.8819	0.8524	0.2258	-0.0130	0.9196	20.54
1.81	0.8975	0.8697	0.2214	-0.0090	0.9130	19.80
2.01	0.9109	0.8874	0.2052	-0.0069	0.9156	18.11
2.21	0.9206	0.8993	0.1965	-0.0073	0.9163	17.17
2.50	0.9291	0.9068	0.2022	-0.0061	0.9166	17.50
3.01	0.9364	0.9117	0.2137	-0.0049	0.9169	18.34
3.51	0.9370	0.9109	0.2198	-0.0044	0.9166	18.84
4.00	0.9354	0.9080	0.2247	-0.0037	0.9163	19.29
4.50	0.9339	0.9058	0.2271	-0.0025	0.9160	19.52
5.01	0.9311	0.9028	0.2279	-0.0030	0.9154	19.65
6.01	0.9245	0.8957	0.2289	-0.0025	0.9138	19.87

Configuration $P_OC_LB_FN_4L$

NPR	F_r/F_i	F_A/F_i	F_N/F_i	F_S/F_i	w_p/w_i	δ_{RR}, deg
1.51	0.8815	0.2101	0.8556	-0.0282	0.9182	80.15
1.81	0.8976	0.2084	0.8726	-0.0283	0.9122	80.41
2.00	0.9130	0.2020	0.8900	-0.0285	0.9146	80.88
2.20	0.9215	0.1870	0.9019	-0.0274	0.9159	81.66
2.51	0.9307	0.1968	0.9093	-0.0265	0.9168	81.30
2.99	0.9336	0.2083	0.9097	-0.0249	0.9169	80.80
3.51	0.9358	0.2172	0.9099	-0.0245	0.9167	80.42
4.01	0.9338	0.2231	0.9065	-0.0237	0.9166	80.13
4.50	0.9329	0.2264	0.9048	-0.0231	0.9161	79.97
5.00	0.9303	0.2286	0.9015	-0.0226	0.9159	79.83

Table 23. Concluded

(c) Tapered blocker

Configuration $P_OC_LB_TN_4T$

NPR	F_r/F_i	F_A/F_i	F_N/F_i	F_S/F_i	w_p/w_i	δ_{RR}, deg
1.51	0.8855	0.8575	0.2205	-0.0157	0.9233	19.98
1.81	0.9013	0.8735	0.2217	-0.0112	0.9167	19.75
2.00	0.9136	0.8890	0.2101	-0.0091	0.9188	18.48
2.20	0.9239	0.9030	0.1951	-0.0092	0.9200	16.99
2.50	0.9312	0.9089	0.2021	-0.0089	0.9202	17.46
3.00	0.9376	0.9132	0.2123	-0.0071	0.9205	18.20
3.50	0.9392	0.9131	0.2199	-0.0061	0.9206	18.81
4.01	0.9368	0.9098	0.2232	-0.0058	0.9204	19.14
4.51	0.9352	0.9076	0.2255	-0.0052	0.9200	19.36
4.99	0.9316	0.9034	0.2276	-0.0047	0.9195	19.61
6.01	0.9257	0.8969	0.2294	-0.0044	0.9176	19.89

Configuration $P_OC_LB_TN_4L$

NPR	F_r/F_i	F_A/F_i	F_N/F_i	F_S/F_i	w_p/w_i	δ_{RR}, deg
1.51	0.8873	0.2075	0.8621	-0.0314	0.9241	80.34
1.81	0.9048	0.2070	0.8802	-0.0307	0.9184	80.56
1.99	0.9137	0.2007	0.8909	-0.0286	0.9202	80.95
2.20	0.9228	0.1865	0.9032	-0.0291	0.9211	81.69
2.51	0.9318	0.1957	0.9106	-0.0280	0.9218	81.36
3.00	0.9364	0.2087	0.9125	-0.0259	0.9222	80.81
3.51	0.9371	0.2158	0.9115	-0.0249	0.9224	80.50
3.99	0.9363	0.2212	0.9095	-0.0244	0.9221	80.24
4.51	0.9329	0.2250	0.9050	-0.0234	0.9217	80.03
4.76	0.9336	0.2266	0.9054	-0.0230	0.9211	79.96

Table 24. Internal Static Performance of 1.4 CR Submerged Nozzles Installed on Offset Plenum With Fan Centerbody

(a) No blocker

Configuration $P_OC_FB_NN_4T$

NPR	F_r/F_i	F_A/F_i	F_N/F_i	F_S/F_i	w_p/w_i	δ_{RR}, deg
1.51	0.8757	0.8493	0.2129	-0.0117	0.9136	19.52
1.80	0.8928	0.8675	0.2111	-0.0080	0.9096	18.99
2.01	0.9070	0.8835	0.2053	-0.0047	0.9133	18.19
2.20	0.9180	0.8980	0.1906	-0.0048	0.9140	16.71
2.51	0.9268	0.9054	0.1979	-0.0055	0.9148	17.18
3.01	0.9344	0.9109	0.2079	-0.0045	0.9152	17.89
3.50	0.9362	0.9110	0.2158	-0.0035	0.9151	18.52
4.00	0.9341	0.9083	0.2182	-0.0042	0.9148	18.76
4.50	0.9323	0.9053	0.2227	-0.0036	0.9144	19.18
5.01	0.9298	0.9023	0.2245	-0.0038	0.9140	19.38
6.01	0.9237	0.8957	0.2254	-0.0026	0.9119	19.59

Configuration $P_OC_FB_NN_4L$

NPR	F_r/F_i	F_A/F_i	F_N/F_i	F_S/F_i	w_p/w_i	δ_{RR}, deg
1.50	0.8807	0.2083	0.8551	-0.0312	0.9157	80.22
1.80	0.8978	0.2075	0.8728	-0.0344	0.9126	80.46
2.00	0.9111	0.2009	0.8882	-0.0304	0.9147	80.91
2.20	0.9193	0.1898	0.8989	-0.0307	0.9160	81.51
2.50	0.9291	0.1964	0.9076	-0.0301	0.9168	81.30
3.00	0.9335	0.2091	0.9093	-0.0291	0.9173	80.77
3.50	0.9350	0.2169	0.9091	-0.0271	0.9174	80.42
4.00	0.9346	0.2218	0.9075	-0.0268	0.9169	80.20
4.49	0.9330	0.2254	0.9050	-0.0257	0.9165	80.01
4.75	0.9318	0.2270	0.9034	-0.0259	0.9158	79.92

(b) Flat blocker

Configuration $P_OC_FB_FN_4T$

NPR	F_r/F_i	F_A/F_i	F_N/F_i	F_S/F_i	w_p/w_i	δ_{RR}, deg
1.50	0.8861	0.8572	0.2241	-0.0149	0.9237	20.29
1.80	0.9027	0.8748	0.2224	-0.0125	0.9166	19.77
2.00	0.9142	0.8890	0.2126	-0.0101	0.9193	18.68
2.21	0.9233	0.9022	0.1961	-0.0070	0.9202	17.09
2.50	0.9323	0.9096	0.2042	-0.0096	0.9206	17.61
3.00	0.9385	0.9137	0.2140	-0.0077	0.9208	18.32
3.51	0.9396	0.9133	0.2210	-0.0064	0.9207	18.89
4.00	0.9382	0.9110	0.2241	-0.0063	0.9206	19.18
4.50	0.9356	0.9075	0.2274	-0.0056	0.9201	19.51
5.00	0.9327	0.9041	0.2291	-0.0052	0.9199	19.72
6.01	0.9256	0.8968	0.2293	-0.0048	0.9184	19.88

Configuration $P_OC_FB_FN_4L$

NPR	F_r/F_i	F_A/F_i	F_N/F_i	F_S/F_i	w_p/w_i	δ_{RR}, deg
1.50	0.8847	0.2061	0.8599	-0.0271	0.9265	80.38
1.80	0.9007	0.2091	0.8757	-0.0278	0.9200	80.42
2.00	0.9156	0.2029	0.8925	-0.0265	0.9214	80.87
2.20	0.9247	0.1896	0.9046	-0.0272	0.9222	81.57
2.50	0.9333	0.1979	0.9117	-0.0260	0.9228	81.27
3.00	0.9384	0.2101	0.9142	-0.0257	0.9233	80.77
3.50	0.9376	0.2172	0.9118	-0.0239	0.9231	80.44
4.01	0.9365	0.2227	0.9093	-0.0231	0.9230	80.18
4.50	0.9343	0.2259	0.9063	-0.0230	0.9227	80.00
4.76	0.9335	0.2270	0.9052	-0.0228	0.9221	79.94

Table 24. Concluded

(c) Tapered blocker

Configuration $P_OC_FB_TN_4T$

NPR	F_r/F_i	F_A/F_i	F_N/F_i	F_S/F_i	w_p/w_i	δ_{RR}, deg
1.50	0.8878	0.8592	0.2230	-0.0165	0.9263	20.16
1.80	0.9037	0.8762	0.2206	-0.0136	0.9195	19.60
2.00	0.9156	0.8908	0.2117	-0.0107	0.9211	18.57
2.20	0.9248	0.9039	0.1950	-0.0089	0.9217	16.97
2.51	0.9329	0.9105	0.2027	-0.0088	0.9224	17.47
2.99	0.9391	0.9147	0.2122	-0.0089	0.9221	18.16
3.50	0.9393	0.9135	0.2186	-0.0074	0.9222	18.69
4.00	0.9376	0.9107	0.2227	-0.0073	0.9219	19.07
4.50	0.9353	0.9077	0.2254	-0.0064	0.9214	19.35
4.99	0.9320	0.9039	0.2268	-0.0053	0.9207	19.54

Configuration $P_OC_FB_TN_4L$

NPR	F_r/F_i	F_A/F_i	F_N/F_i	F_S/F_i	w_p/w_i	δ_{RR}, deg
1.50	0.8879	0.2045	0.8636	-0.0287	0.9283	80.49
1.80	0.9042	0.2055	0.8801	-0.0287	0.9218	80.63
2.00	0.9172	0.1992	0.8949	-0.0273	0.9235	81.06
2.20	0.9260	0.1861	0.9067	-0.0263	0.9239	81.74
2.51	0.9337	0.1956	0.9126	-0.0257	0.9249	81.38
3.00	0.9392	0.2079	0.9156	-0.0242	0.9249	80.88
3.51	0.9377	0.2170	0.9119	-0.0233	0.9249	80.45
4.00	0.9365	0.2221	0.9095	-0.0234	0.9247	80.20
4.50	0.9348	0.2253	0.9070	-0.0225	0.9243	80.04
4.76	0.9330	0.2264	0.9048	-0.0229	0.9236	79.96

Table 25. Static-Pressure Ratios in Nozzle and Instrumented Spacers for Configuration $P_C C_S B_N N_1 T$

Inner wall

Static-pressure ratios at s/l_s of -

NPR	0.429	0.858	0.913	0.937	0.956	0.972
1.50	0.927	0.623	0.497	0.515	0.566	0.598
1.80	0.916	0.573	0.385	0.419	0.457	0.464
2.00	0.915	0.566	0.361	0.394	0.435	0.400
2.20	0.915	0.563	0.355	0.385	0.429	0.386
2.51	0.915	0.563	0.352	0.385	0.427	0.382
2.99	0.915	0.564	0.351	0.388	0.426	0.379
3.50	0.916	0.564	0.350	0.392	0.424	0.378
4.00	0.915	0.562	0.348	0.399	0.423	0.377
4.50	0.915	0.562	0.347	0.403	0.422	0.376
5.01	0.916	0.563	0.347	0.403	0.421	0.376
6.01	0.915	0.560	0.345	0.403	0.419	0.376

Inner channel

Static-pressure ratios at s/l_s of -

	0.972
	0.556
	0.465
	0.445
	0.439
	0.441
	0.443
	0.441
	0.439
	0.438
	0.436
	0.433

Outer channel

Static-pressure ratios at s/l_s of -

NPR	0.972
1.50	0.684
1.80	0.579
2.00	0.535
2.20	0.508
2.51	0.457
2.99	0.425
3.50	0.425
4.00	0.425
4.50	0.425
5.01	0.425
6.01	0.425

Left instrumented spacer

Static-pressure ratios at ϕ, deg, of -

NPR	0	45	90	135	180	225	270	315
1.50	0.821	0.843	0.893	0.942	0.953	0.920	0.863	0.831
1.80	0.798	0.823	0.880	0.936	0.947	0.909	0.845	0.807
2.00	0.795	0.820	0.878	0.934	0.946	0.907	0.843	0.803
2.20	0.794	0.819	0.877	0.935	0.946	0.907	0.842	0.802
2.51	0.795	0.820	0.878	0.935	0.947	0.908	0.842	0.802
2.99	0.795	0.820	0.879	0.936	0.947	0.908	0.843	0.802
3.50	0.796	0.821	0.879	0.937	0.948	0.908	0.843	0.803
4.00	0.796	0.821	0.879	0.936	0.948	0.909	0.843	0.802
4.50	0.797	0.821	0.879	0.936	0.948	0.909	0.843	0.802
5.01	0.797	0.822	0.879	0.937	0.948	0.910	0.843	0.802
6.01	0.797	0.821	0.878	0.936	0.948	0.910	0.843	0.802

Right instrumented spacer

Static-pressure ratios at ϕ, deg, of -

0	45	90	135	180	225	270	315
0.816	0.830	0.872	0.908	0.945	0.944	0.901	0.840
0.791	0.807	0.854	0.895	0.937	0.936	0.888	0.819
0.788	0.803	0.851	0.893	0.937	0.935	0.886	0.816
0.786	0.802	0.851	0.893	0.936	0.935	0.885	0.815
0.786	0.802	0.850	0.894	0.937	0.935	0.885	0.815
0.787	0.803	0.851	0.894	0.938	0.935	0.886	0.816
0.787	0.803	0.851	0.895	0.938	0.936	0.886	0.816
0.787	0.803	0.851	0.895	0.938	0.935	0.885	0.815
0.788	0.804	0.851	0.895	0.939	0.936	0.885	0.816
0.788	0.803	0.851	0.895	0.938	0.935	0.885	0.816
0.788	0.803	0.851	0.896	0.939	0.935	0.886	0.816

Table 26. Static-Pressure Ratios in Nozzle and Instrumented Spacers for Configuration $P_C C_S B_N N_1 L$

Inner wall

Static-pressure ratios at s/l_s of -

NPR	0.429	0.858	0.913	0.937	0.956	0.972
1.52	0.883	0.688	0.581	0.540	0.573	0.599
1.81	0.871	0.647	0.509	0.433	0.464	0.480
2.02	0.870	0.638	0.491	0.394	0.425	0.417
2.22	0.870	0.634	0.481	0.373	0.408	0.380
2.51	0.869	0.633	0.479	0.367	0.404	0.364
3.01	0.871	0.634	0.479	0.366	0.405	0.362
3.52	0.871	0.634	0.480	0.367	0.405	0.360
4.00	0.872	0.633	0.478	0.369	0.404	0.359
4.51	0.872	0.633	0.478	0.372	0.403	0.358

Inner channel

Static-pressure ratios at s/l_s of -

	0.972
	0.562
	0.462
	0.427
	0.409
	0.407
	0.412
	0.416
	0.416
	0.415

Outer channel

Static-pressure ratios at s/l_s of -

NPR	0.972
1.52	0.671
1.81	0.578
2.02	0.540
2.22	0.518
2.51	0.490
3.01	0.435
3.52	0.406
4.00	0.406
4.51	0.406

Left instrumented spacer

Static-pressure ratios at ϕ, deg, of -

NPR	0	45	90	135	180	225	270	315
1.52	0.821	0.831	0.854	0.868	0.869	0.876	0.858	0.828
1.81	0.803	0.815	0.839	0.853	0.856	0.864	0.842	0.809
2.02	0.801	0.814	0.836	0.851	0.854	0.863	0.841	0.807
2.22	0.800	0.814	0.835	0.851	0.853	0.863	0.840	0.806
2.51	0.800	0.815	0.835	0.851	0.853	0.863	0.839	0.806
3.01	0.802	0.817	0.836	0.852	0.854	0.864	0.841	0.807
3.52	0.801	0.817	0.836	0.852	0.854	0.864	0.841	0.807
4.00	0.802	0.818	0.836	0.853	0.855	0.865	0.841	0.808
4.51	0.802	0.818	0.837	0.853	0.856	0.866	0.842	0.808

Right instrumented spacer

Static-pressure ratios at ϕ, deg, of -

0	45	90	135	180	225	270	315
0.826	0.828	0.857	0.883	0.876	0.870	0.864	0.833
0.809	0.811	0.842	0.871	0.863	0.857	0.849	0.817
0.807	0.809	0.839	0.870	0.862	0.856	0.847	0.815
0.807	0.809	0.839	0.869	0.862	0.855	0.847	0.814
0.807	0.809	0.839	0.869	0.862	0.855	0.846	0.814
0.808	0.810	0.839	0.869	0.862	0.856	0.847	0.815
0.809	0.811	0.839	0.870	0.863	0.856	0.848	0.815
0.809	0.811	0.839	0.870	0.862	0.856	0.847	0.815
0.809	0.811	0.838	0.870	0.862	0.856	0.848	0.815

Table 27. Static-Pressure Ratios in Nozzle and Instrumented Spacers for Configuration $P_C C_S B_F N_1 T$

Inner wall

Static-pressure ratios at s/l_s of -

NPR	0.429	0.858	0.913	0.937	0.956	0.972
1.50	0.919	0.653	0.518	0.499	0.570	0.604
1.82	0.906	0.601	0.416	0.364	0.452	0.471
2.01	0.905	0.595	0.399	0.328	0.420	0.413
2.20	0.904	0.595	0.396	0.303	0.398	0.387
2.51	0.905	0.591	0.388	0.301	0.396	0.373
3.01	0.906	0.590	0.385	0.298	0.396	0.370
3.52	0.905	0.591	0.386	0.296	0.392	0.365
4.00	0.907	0.590	0.383	0.298	0.393	0.365
4.52	0.907	0.589	0.383	0.301	0.391	0.364
5.01	0.908	0.590	0.382	0.297	0.386	0.363
6.03	0.908	0.588	0.380	0.309	0.385	0.363

Inner channel

Static-pressure ratios at s/l_s of -

	0.972
	0.553
	0.440
	0.405
	0.381
	0.383
	0.387
	0.386
	0.389
	0.388
	0.382
	0.384

Outer channel

Static-pressure ratios at s/l_s of -

NPR	0.972
1.50	0.686
1.82	0.576
2.01	0.536
2.20	0.508
2.51	0.458
3.01	0.427
3.52	0.428
4.00	0.428
4.52	0.429
5.01	0.429
6.03	0.429

Left instrumented spacer

Static-pressure ratios at ϕ, deg, of -

NPR	0	45	90	135	180	225	270	315
1.50	0.813	0.839	0.891	0.931	0.937	0.913	0.860	0.819
1.82	0.787	0.815	0.876	0.921	0.929	0.900	0.843	0.792
2.01	0.784	0.813	0.874	0.920	0.927	0.898	0.841	0.788
2.20	0.782	0.812	0.874	0.921	0.927	0.896	0.840	0.787
2.51	0.784	0.813	0.873	0.920	0.927	0.899	0.840	0.787
3.01	0.784	0.813	0.874	0.922	0.929	0.900	0.841	0.788
3.52	0.786	0.814	0.875	0.924	0.930	0.900	0.842	0.788
4.00	0.787	0.814	0.875	0.924	0.931	0.902	0.842	0.789
4.52	0.786	0.815	0.875	0.923	0.931	0.902	0.842	0.788
5.01	0.786	0.815	0.875	0.924	0.931	0.902	0.842	0.788
6.03	0.787	0.815	0.875	0.924	0.931	0.903	0.842	0.789

Right instrumented spacer

Static-pressure ratios at ϕ, deg, of -

0	45	90	135	180	225	270	315
0.809	0.825	0.871	0.898	0.939	0.938	0.898	0.836
0.781	0.800	0.853	0.883	0.928	0.930	0.883	0.813
0.778	0.796	0.851	0.882	0.928	0.928	0.882	0.811
0.777	0.795	0.849	0.884	0.929	0.928	0.881	0.811
0.777	0.796	0.851	0.883	0.927	0.928	0.881	0.811
0.778	0.796	0.852	0.883	0.928	0.929	0.882	0.811
0.780	0.797	0.852	0.886	0.930	0.930	0.883	0.812
0.779	0.798	0.853	0.884	0.929	0.930	0.883	0.812
0.779	0.797	0.853	0.884	0.928	0.929	0.882	0.812
0.779	0.798	0.853	0.884	0.928	0.929	0.883	0.812
0.779	0.797	0.853	0.884	0.929	0.930	0.882	0.812

Table 28. Static-Pressure Ratios in Nozzle and Instrumented Spacers for Configuration $P_C C_S B_F N_1 L$

Inner wall

Static-pressure ratios at s/l_s of -

NPR	0.429	0.858	0.913	0.937	0.956	0.972
1.50	0.895	0.670	0.552	0.526	0.574	0.604
1.80	0.883	0.619	0.466	0.413	0.459	0.476
2.00	0.880	0.612	0.448	0.372	0.423	0.414
2.22	0.880	0.608	0.438	0.351	0.408	0.378
2.51	0.880	0.608	0.437	0.345	0.406	0.367
3.01	0.881	0.606	0.435	0.347	0.407	0.365
3.52	0.882	0.607	0.434	0.345	0.406	0.364
4.02	0.883	0.606	0.432	0.344	0.404	0.362
4.52	0.884	0.606	0.430	0.343	0.403	0.362
4.77	0.884	0.605	0.429	0.346	0.402	0.361

Inner channel

Static-pressure ratios at s/l_s of -

	0.972
	0.558
	0.454
	0.420
	0.402
	0.402
	0.409
	0.412
	0.411
	0.408
	0.409

Outer channel

Static-pressure ratios at s/l_s of -

NPR	0.972
1.50	0.677
1.80	0.576
2.00	0.538
2.22	0.512
2.51	0.480
3.01	0.428
3.52	0.418
4.02	0.418
4.52	0.420
4.77	0.420

Left instrumented spacer

Static-pressure ratios at ϕ, deg, of -

NPR	0	45	90	135	180	225	270	315
1.50	0.826	0.840	0.858	0.872	0.877	0.882	0.861	0.829
1.80	0.806	0.822	0.841	0.855	0.861	0.868	0.844	0.809
2.00	0.803	0.820	0.838	0.853	0.859	0.866	0.842	0.805
2.22	0.803	0.821	0.837	0.853	0.859	0.866	0.840	0.805
2.51	0.804	0.821	0.837	0.853	0.859	0.867	0.841	0.806
3.01	0.805	0.823	0.838	0.854	0.860	0.868	0.842	0.806
3.52	0.806	0.824	0.838	0.855	0.862	0.869	0.842	0.806
4.02	0.806	0.824	0.839	0.856	0.862	0.870	0.843	0.807
4.52	0.806	0.825	0.839	0.856	0.864	0.871	0.843	0.807
4.77	0.806	0.825	0.839	0.856	0.863	0.870	0.843	0.807

Right instrumented spacer

Static-pressure ratios at ϕ, deg, of -

0	45	90	135	180	225	270	315
0.833	0.832	0.853	0.892	0.878	0.875	0.869	0.840
0.815	0.814	0.836	0.880	0.863	0.861	0.854	0.822
0.813	0.812	0.833	0.879	0.862	0.859	0.853	0.820
0.813	0.812	0.833	0.879	0.862	0.859	0.853	0.820
0.814	0.813	0.834	0.881	0.863	0.860	0.854	0.821
0.815	0.814	0.834	0.881	0.864	0.861	0.854	0.821
0.816	0.815	0.834	0.883	0.865	0.862	0.856	0.822
0.816	0.816	0.834	0.883	0.865	0.863	0.856	0.823
0.816	0.816	0.832	0.883	0.865	0.863	0.857	0.822
0.816	0.816	0.832	0.882	0.865	0.863	0.856	0.822

Table 29. Static-Pressure Ratios in Nozzle and Instrumented Spacers for Configuration $P_C C_M B_N N_I T$

Inner wall

Static-pressure ratios at s/l_s of -

NPR	0.429	0.858	0.913	0.937	0.956	0.972
1.52	0.921	0.618	0.485	0.499	0.556	0.588
1.80	0.910	0.572	0.382	0.408	0.455	0.463
2.02	0.909	0.566	0.361	0.378	0.430	0.398
2.20	0.909	0.564	0.354	0.369	0.424	0.385
2.50	0.910	0.563	0.352	0.369	0.423	0.380
3.00	0.911	0.565	0.353	0.368	0.421	0.377
3.51	0.911	0.565	0.351	0.375	0.420	0.376
4.01	0.911	0.564	0.349	0.381	0.419	0.375
4.50	0.911	0.566	0.351	0.378	0.415	0.374
5.01	0.912	0.563	0.348	0.390	0.417	0.375
6.01	0.912	0.562	0.346	0.389	0.414	0.374

Inner channel

Static-pressure ratios at s/l_s of -

0.972
0.543
0.458
0.434
0.429
0.430
0.432
0.432
0.430
0.424
0.429
0.426

Outer channel

Static-pressure ratios at s/l_s of -

NPR	0.972
1.52	0.674
1.80	0.574
2.02	0.527
2.20	0.501
2.50	0.449
3.00	0.421
3.51	0.421
4.01	0.421
4.50	0.422
5.01	0.422
6.01	0.423

Left instrumented spacer

Static-pressure ratios at ϕ, deg, of -

NPR	0	45	90	135	180	225	270	315
1.52	0.813	0.837	0.890	0.939	0.946	0.910	0.857	0.823
1.80	0.792	0.818	0.877	0.933	0.940	0.900	0.840	0.802
2.02	0.789	0.816	0.875	0.931	0.939	0.898	0.838	0.798
2.20	0.789	0.815	0.875	0.932	0.940	0.897	0.837	0.798
2.50	0.789	0.815	0.875	0.932	0.941	0.898	0.837	0.797
3.00	0.790	0.816	0.876	0.933	0.942	0.898	0.838	0.799
3.51	0.792	0.817	0.877	0.934	0.942	0.899	0.839	0.799
4.01	0.791	0.817	0.876	0.934	0.942	0.900	0.838	0.799
4.50	0.792	0.817	0.876	0.934	0.942	0.899	0.839	0.799
5.01	0.793	0.818	0.877	0.935	0.943	0.902	0.839	0.800
6.01	0.792	0.818	0.877	0.935	0.944	0.903	0.839	0.800

Right instrumented spacer

Static-pressure ratios at ϕ, deg, of -

0	45	90	135	180	225	270	315
0.807	0.821	0.864	0.895	0.933	0.933	0.891	0.831
0.783	0.799	0.848	0.882	0.925	0.924	0.879	0.811
0.780	0.796	0.845	0.881	0.924	0.924	0.876	0.808
0.778	0.795	0.843	0.880	0.925	0.924	0.876	0.807
0.779	0.796	0.843	0.881	0.925	0.925	0.876	0.807
0.780	0.796	0.844	0.883	0.927	0.925	0.877	0.808
0.780	0.797	0.843	0.884	0.928	0.926	0.878	0.808
0.781	0.798	0.845	0.884	0.928	0.926	0.878	0.809
0.782	0.799	0.844	0.886	0.930	0.927	0.878	0.810
0.782	0.798	0.845	0.884	0.929	0.927	0.878	0.809
0.782	0.798	0.846	0.885	0.930	0.927	0.879	0.810

Table 30. Static-Pressure Ratios in Nozzle and Instrumented Spacers for Configuration $P_C C_M B_N N_1 L$

Inner wall

Static-pressure ratios at s/l_s of -

NPR	0.429	0.858	0.913	0.937	0.956	0.972
1.50	0.889	0.687	0.577	0.541	0.579	0.606
1.80	0.872	0.647	0.507	0.430	0.465	0.482
2.00	0.871	0.637	0.487	0.388	0.424	0.418
2.21	0.870	0.635	0.479	0.368	0.407	0.381
2.51	0.870	0.634	0.476	0.360	0.402	0.364
3.01	0.872	0.634	0.475	0.357	0.404	0.362
3.51	0.873	0.634	0.474	0.358	0.404	0.361
4.01	0.872	0.634	0.476	0.362	0.403	0.359
4.50	0.873	0.633	0.475	0.363	0.402	0.358
4.65	0.873	0.633	0.476	0.366	0.402	0.358

Inner channel

Static-pressure ratios at s/l_s of -

	0.972
	0.567
	0.461
	0.424
	0.406
	0.403
	0.408
	0.412
	0.414
	0.413
	0.414

Outer channel

Static-pressure ratios at s/l_s of -

NPR	0.972
1.50	0.678
1.80	0.580
2.00	0.541
2.21	0.518
2.51	0.485
3.01	0.422
3.51	0.407
4.01	0.407
4.50	0.408
4.65	0.408

Left instrumented spacer

Static-pressure ratios at ϕ, deg, of -

NPR	0	45	90	135	180	225	270	315
1.50	0.825	0.834	0.858	0.867	0.871	0.878	0.858	0.827
1.80	0.805	0.815	0.839	0.849	0.855	0.863	0.840	0.808
2.00	0.802	0.814	0.836	0.847	0.853	0.862	0.838	0.805
2.21	0.802	0.814	0.836	0.847	0.852	0.862	0.837	0.804
2.51	0.803	0.815	0.835	0.848	0.853	0.863	0.837	0.805
3.01	0.804	0.817	0.837	0.848	0.854	0.864	0.838	0.806
3.51	0.805	0.818	0.837	0.849	0.855	0.866	0.839	0.806
4.01	0.805	0.818	0.837	0.849	0.855	0.865	0.839	0.806
4.50	0.806	0.819	0.837	0.850	0.855	0.866	0.840	0.807
4.65	0.806	0.819	0.837	0.849	0.855	0.865	0.840	0.807

Right instrumented spacer

Static-pressure ratios at ϕ, deg, of -

0	45	90	135	180	225	270	315
0.825	0.827	0.857	0.885	0.876	0.869	0.863	0.835
0.805	0.807	0.839	0.871	0.862	0.853	0.846	0.817
0.802	0.805	0.837	0.869	0.860	0.851	0.844	0.814
0.802	0.805	0.836	0.869	0.860	0.850	0.844	0.814
0.802	0.805	0.836	0.869	0.859	0.851	0.844	0.814
0.803	0.806	0.837	0.869	0.861	0.852	0.845	0.814
0.804	0.807	0.837	0.870	0.861	0.852	0.845	0.815
0.805	0.808	0.837	0.871	0.862	0.852	0.846	0.815
0.805	0.808	0.837	0.871	0.862	0.853	0.846	0.816
0.805	0.809	0.838	0.872	0.862	0.853	0.846	0.816

Table 31. Static-Pressure Ratios in Nozzle and Instrumented Spacers for Configuration $P_C C_M B_F N_1 T$

Inner wall

Static-pressure ratios at s/l_s of -

NPR	0.429	0.858	0.913	0.937	0.956	0.972
1.51	0.917	0.647	0.501	0.479	0.560	0.597
1.80	0.904	0.602	0.414	0.361	0.457	0.483
2.01	0.903	0.594	0.392	0.317	0.415	0.421
2.21	0.902	0.590	0.384	0.290	0.389	0.387
2.51	0.902	0.591	0.383	0.273	0.375	0.370
3.01	0.903	0.590	0.380	0.264	0.371	0.361
3.51	0.904	0.589	0.378	0.265	0.373	0.359
4.01	0.905	0.588	0.377	0.264	0.371	0.357
4.50	0.905	0.587	0.377	0.270	0.374	0.357
5.00	0.906	0.587	0.374	0.273	0.373	0.356
5.99	0.906	0.585	0.373	0.281	0.370	0.356

Inner channel

Static-pressure ratios at s/l_s of -

	0.972
	0.540
	0.440
	0.395
	0.367
	0.352
	0.351
	0.356
	0.358
	0.363
	0.364
	0.364

Outer channel

Static-pressure ratios at s/l_s of -

NPR	0.972
1.51	0.678
1.80	0.580
2.01	0.534
2.21	0.500
2.51	0.445
3.01	0.427
3.51	0.427
4.01	0.428
4.50	0.428
5.00	0.428
5.99	0.428

Left instrumented spacer

Static-pressure ratios at ϕ, deg, of -

NPR	0	45	90	135	180	225	270	315
1.51	0.806	0.834	0.885	0.926	0.933	0.906	0.855	0.814
1.80	0.782	0.812	0.870	0.916	0.924	0.893	0.836	0.787
2.01	0.778	0.808	0.867	0.914	0.923	0.890	0.833	0.782
2.21	0.777	0.807	0.867	0.915	0.923	0.890	0.832	0.781
2.51	0.778	0.807	0.867	0.916	0.923	0.890	0.833	0.782
3.01	0.779	0.808	0.868	0.917	0.924	0.891	0.833	0.782
3.51	0.781	0.809	0.869	0.918	0.926	0.893	0.834	0.783
4.01	0.781	0.809	0.869	0.918	0.927	0.894	0.834	0.783
4.50	0.781	0.810	0.869	0.919	0.928	0.895	0.834	0.783
5.00	0.781	0.809	0.869	0.919	0.927	0.895	0.835	0.783
5.99	0.781	0.810	0.869	0.919	0.928	0.897	0.835	0.783

Right instrumented spacer

Static-pressure ratios at ϕ, deg, of -

0	45	90	135	180	225	270	315
0.798	0.817	0.865	0.888	0.928	0.931	0.890	0.827
0.772	0.793	0.848	0.873	0.917	0.922	0.876	0.806
0.768	0.789	0.845	0.871	0.916	0.921	0.874	0.803
0.766	0.788	0.845	0.870	0.916	0.920	0.873	0.802
0.767	0.787	0.844	0.872	0.916	0.921	0.873	0.802
0.767	0.788	0.845	0.871	0.916	0.921	0.874	0.803
0.768	0.789	0.846	0.873	0.917	0.922	0.875	0.803
0.768	0.789	0.847	0.872	0.916	0.922	0.875	0.804
0.768	0.789	0.847	0.872	0.916	0.922	0.876	0.804
0.768	0.789	0.848	0.872	0.916	0.922	0.875	0.805
0.768	0.789	0.848	0.873	0.916	0.922	0.875	0.806

Table 32. Static-Pressure Ratios in Nozzle and Instrumented Spacers for Configuration $P_C C_M B_F N_I L$

Inner wall

Static-pressure ratios at s/l_s of -

NPR	0.429	0.858	0.913	0.937	0.956	0.972
1.50	0.889	0.672	0.566	0.545	0.583	0.609
1.79	0.873	0.620	0.482	0.436	0.470	0.488
2.00	0.872	0.608	0.457	0.394	0.427	0.420
2.20	0.871	0.605	0.448	0.376	0.410	0.382
2.50	0.871	0.603	0.444	0.369	0.406	0.365
3.01	0.872	0.604	0.444	0.369	0.406	0.362
3.51	0.873	0.603	0.442	0.370	0.406	0.361
4.02	0.873	0.602	0.441	0.373	0.405	0.360
4.53	0.874	0.602	0.440	0.372	0.403	0.360
4.79	0.874	0.602	0.440	0.373	0.403	0.360

Inner channel

Static-pressure ratios at s/l_s of -

0.972
0.572
0.467
0.429
0.413
0.410
0.413
0.416
0.416
0.414
0.414

Outer channel

Static-pressure ratios at s/l_s of -

NPR	0.972
1.50	0.675
1.79	0.578
2.00	0.533
2.20	0.505
2.50	0.469
3.01	0.429
3.51	0.425
4.02	0.425
4.53	0.425
4.79	0.426

Left instrumented spacer

Static-pressure ratios at ϕ, deg, of -

NPR	0	45	90	135	180	225	270	315
1.50	0.824	0.838	0.856	0.866	0.872	0.877	0.856	0.824
1.79	0.802	0.818	0.835	0.848	0.854	0.860	0.835	0.801
2.00	0.801	0.817	0.833	0.847	0.853	0.860	0.835	0.799
2.20	0.801	0.818	0.832	0.846	0.852	0.859	0.833	0.798
2.50	0.802	0.819	0.832	0.846	0.853	0.860	0.833	0.798
3.01	0.803	0.821	0.833	0.847	0.854	0.861	0.834	0.800
3.51	0.804	0.822	0.833	0.848	0.855	0.862	0.835	0.799
4.02	0.805	0.822	0.834	0.848	0.856	0.863	0.835	0.800
4.53	0.805	0.823	0.834	0.849	0.856	0.863	0.836	0.800
4.79	0.805	0.823	0.834	0.850	0.856	0.863	0.836	0.800

Right instrumented spacer

Static-pressure ratios at ϕ, deg, of -

0	45	90	135	180	225	270	315
0.832	0.830	0.846	0.891	0.881	0.875	0.869	0.839
0.812	0.810	0.825	0.876	0.866	0.858	0.851	0.818
0.811	0.809	0.823	0.877	0.865	0.858	0.850	0.817
0.810	0.809	0.822	0.876	0.866	0.857	0.850	0.816
0.811	0.809	0.823	0.877	0.867	0.858	0.850	0.817
0.812	0.811	0.824	0.878	0.868	0.859	0.852	0.818
0.813	0.812	0.823	0.879	0.870	0.861	0.852	0.819
0.814	0.813	0.824	0.880	0.871	0.862	0.853	0.820
0.814	0.814	0.823	0.880	0.872	0.862	0.853	0.820
0.815	0.814	0.824	0.880	0.873	0.862	0.854	0.820

Table 33. Static-Pressure Ratios in Nozzle and Instrumented Spacers for Configuration $P_C C_L B_N N_1 T$

Inner wall

Static-pressure ratios at s/l_s of -

NPR	0.429	0.858	0.913	0.937	0.956	0.972
1.51	0.917	0.626	0.489	0.488	0.558	0.593
1.81	0.906	0.579	0.386	0.382	0.454	0.468
2.01	0.904	0.572	0.367	0.348	0.426	0.405
2.20	0.904	0.570	0.361	0.333	0.415	0.385
2.49	0.904	0.570	0.358	0.328	0.412	0.378
3.00	0.906	0.570	0.357	0.330	0.411	0.374
3.50	0.906	0.570	0.355	0.336	0.410	0.373
4.00	0.906	0.569	0.354	0.343	0.409	0.372
4.52	0.907	0.569	0.354	0.350	0.408	0.372
5.01	0.908	0.569	0.353	0.354	0.407	0.372
6.02	0.908	0.568	0.352	0.358	0.404	0.371

Inner channel

Static-pressure ratios at s/l_s of -

	0.972
	0.543
	0.449
	0.421
	0.409
	0.410
	0.413
	0.415
	0.414
	0.413
	0.412
	0.410

Outer channel

Static-pressure ratios at s/l_s of -

NPR	0.972
1.51	0.676
1.81	0.575
2.01	0.530
2.20	0.501
2.49	0.444
3.00	0.418
3.50	0.419
4.00	0.419
4.52	0.420
5.01	0.420
6.02	0.420

Left instrumented spacer

Static-pressure ratios at ϕ, deg, of -

NPR	0	45	90	135	180	225	270	315
1.51	0.811	0.835	0.890	0.937	0.941	0.903	0.858	0.824
1.81	0.789	0.815	0.876	0.931	0.935	0.891	0.841	0.801
2.01	0.785	0.812	0.874	0.929	0.933	0.888	0.838	0.797
2.20	0.784	0.811	0.873	0.930	0.933	0.888	0.837	0.796
2.49	0.785	0.811	0.874	0.930	0.934	0.888	0.837	0.797
3.00	0.786	0.813	0.874	0.931	0.935	0.889	0.838	0.798
3.50	0.787	0.813	0.875	0.932	0.936	0.890	0.838	0.797
4.00	0.788	0.814	0.875	0.933	0.937	0.891	0.839	0.798
4.52	0.788	0.814	0.876	0.933	0.938	0.891	0.838	0.799
5.01	0.788	0.814	0.876	0.933	0.938	0.892	0.839	0.799
6.02	0.788	0.814	0.876	0.933	0.938	0.892	0.838	0.799

Right instrumented spacer

Static-pressure ratios at ϕ, deg, of -

0	45	90	135	180	225	270	315
0.807	0.824	0.864	0.890	0.929	0.932	0.891	0.829
0.783	0.801	0.848	0.876	0.919	0.922	0.877	0.809
0.779	0.797	0.844	0.874	0.918	0.921	0.875	0.805
0.778	0.796	0.843	0.873	0.918	0.921	0.874	0.805
0.778	0.797	0.843	0.874	0.919	0.922	0.874	0.805
0.779	0.797	0.843	0.875	0.921	0.923	0.875	0.806
0.780	0.798	0.845	0.876	0.922	0.924	0.876	0.807
0.780	0.798	0.845	0.877	0.922	0.924	0.876	0.807
0.780	0.799	0.844	0.877	0.922	0.924	0.876	0.807
0.781	0.799	0.844	0.877	0.922	0.924	0.877	0.808
0.781	0.799	0.844	0.877	0.923	0.924	0.877	0.808

Table 34. Static-Pressure Ratios in Nozzle and Instrumented Spacers for Configuration $P_C C_L B_N N_1 L$

Inner wall
Static-pressure ratios at s/l_s of -

NPR	0.429	0.858	0.913	0.937	0.956	0.972
1.50	0.888	0.690	0.579	0.542	0.579	0.606
1.80	0.874	0.643	0.498	0.426	0.462	0.479
2.01	0.872	0.635	0.479	0.385	0.423	0.415
2.20	0.873	0.630	0.468	0.363	0.407	0.380
2.50	0.873	0.630	0.467	0.357	0.403	0.365
3.01	0.874	0.630	0.467	0.357	0.406	0.363
3.50	0.874	0.630	0.467	0.358	0.406	0.362
4.00	0.875	0.631	0.467	0.358	0.405	0.360
4.52	0.875	0.631	0.468	0.361	0.404	0.359
4.68	0.874	0.631	0.469	0.362	0.403	0.359

Inner channel
Static-pressure ratios at s/l_s of -

	0.972
1.50	0.565
1.80	0.457
2.01	0.421
2.20	0.405
2.50	0.403
3.01	0.410
3.50	0.414
4.00	0.415
4.52	0.414
4.68	0.413

Outer channel
Static-pressure ratios at s/l_s of -

NPR	0.972
1.50	0.680
1.80	0.581
2.01	0.542
2.20	0.521
2.50	0.485
3.01	0.420
3.50	0.407
4.00	0.407
4.52	0.407
4.68	0.407

Left instrumented spacer
Static-pressure ratios at ϕ, deg, of -

NPR	0	45	90	135	180	225	270	315
1.50	0.824	0.833	0.858	0.863	0.871	0.879	0.856	0.827
1.80	0.805	0.814	0.839	0.846	0.855	0.865	0.839	0.806
2.01	0.802	0.813	0.837	0.844	0.853	0.864	0.836	0.803
2.20	0.802	0.814	0.836	0.844	0.853	0.864	0.836	0.803
2.50	0.803	0.815	0.836	0.844	0.853	0.864	0.836	0.803
3.01	0.804	0.816	0.837	0.845	0.854	0.865	0.837	0.804
3.50	0.805	0.818	0.837	0.846	0.855	0.866	0.837	0.805
4.00	0.805	0.818	0.838	0.846	0.855	0.867	0.838	0.805
4.52	0.805	0.818	0.838	0.846	0.855	0.867	0.838	0.805
4.68	0.805	0.818	0.837	0.846	0.854	0.866	0.837	0.805

Right instrumented spacer
Static-pressure ratios at ϕ, deg, of -

0	45	90	135	180	225	270	315
0.825	0.827	0.858	0.890	0.881	0.868	0.864	0.836
0.806	0.808	0.841	0.877	0.868	0.853	0.847	0.818
0.803	0.807	0.839	0.876	0.865	0.851	0.845	0.815
0.803	0.805	0.838	0.875	0.864	0.849	0.845	0.814
0.803	0.806	0.839	0.876	0.865	0.850	0.845	0.815
0.804	0.807	0.839	0.876	0.866	0.851	0.846	0.815
0.805	0.808	0.840	0.878	0.867	0.852	0.847	0.816
0.805	0.808	0.840	0.878	0.867	0.851	0.846	0.816
0.806	0.809	0.840	0.878	0.867	0.853	0.847	0.817
0.805	0.809	0.840	0.878	0.867	0.852	0.847	0.816

Table 35. Static-Pressure Ratios in Nozzle and Instrumented Spacers for Configuration $P_C C_L B_F N_1 T$

Inner wall

Static-pressure ratios at s/l_s of -

NPR	0.429	0.858	0.913	0.937	0.956	0.972
1.51	0.911	0.669	0.521	0.474	0.569	0.606
1.82	0.897	0.623	0.440	0.354	0.457	0.486
2.00	0.895	0.616	0.424	0.315	0.414	0.431
2.20	0.895	0.613	0.415	0.282	0.380	0.391
2.51	0.894	0.612	0.412	0.255	0.354	0.362
3.01	0.894	0.613	0.411	0.233	0.335	0.344
3.51	0.895	0.613	0.410	0.221	0.325	0.337
4.00	0.895	0.613	0.410	0.218	0.324	0.334
4.50	0.895	0.613	0.410	0.214	0.318	0.329
5.01	0.896	0.612	0.409	0.216	0.321	0.329
6.01	0.896	0.612	0.408	0.211	0.314	0.323

Inner channel

Static-pressure ratios at s/l_s of -

0.972
0.547
0.437
0.392
0.355
0.327
0.307
0.297
0.298
0.294
0.300
0.295

Outer channel

Static-pressure ratios at s/l_s of -

NPR	0.972
1.51	0.678
1.82	0.570
2.00	0.526
2.20	0.492
2.51	0.438
3.01	0.424
3.51	0.424
4.00	0.424
4.50	0.425
5.01	0.425
6.01	0.426

Left instrumented spacer

Static-pressure ratios at ϕ, deg, of -

NPR	0	45	90	135	180	225	270	315
1.51	0.801	0.829	0.880	0.913	0.920	0.895	0.850	0.806
1.82	0.774	0.805	0.862	0.900	0.908	0.880	0.828	0.778
2.00	0.769	0.801	0.859	0.898	0.906	0.877	0.824	0.773
2.20	0.769	0.801	0.859	0.898	0.906	0.876	0.824	0.772
2.51	0.769	0.801	0.858	0.898	0.906	0.877	0.824	0.772
3.01	0.770	0.802	0.858	0.899	0.907	0.876	0.825	0.772
3.51	0.770	0.802	0.858	0.899	0.907	0.877	0.825	0.771
4.00	0.771	0.802	0.859	0.899	0.907	0.877	0.825	0.772
4.50	0.770	0.802	0.858	0.899	0.907	0.876	0.825	0.771
5.01	0.771	0.802	0.858	0.900	0.908	0.878	0.825	0.771
6.01	0.771	0.802	0.858	0.899	0.908	0.877	0.825	0.771

Right instrumented spacer

Static-pressure ratios at ϕ, deg, of -

0	45	90	135	180	225	270	315
0.799	0.814	0.862	0.885	0.923	0.926	0.885	0.826
0.771	0.788	0.841	0.869	0.910	0.915	0.867	0.802
0.766	0.783	0.838	0.866	0.908	0.914	0.864	0.797
0.763	0.781	0.837	0.865	0.907	0.912	0.864	0.796
0.763	0.780	0.837	0.865	0.908	0.913	0.864	0.796
0.763	0.780	0.837	0.865	0.907	0.913	0.864	0.796
0.763	0.780	0.838	0.865	0.907	0.913	0.864	0.796
0.763	0.781	0.838	0.866	0.907	0.913	0.865	0.796
0.763	0.780	0.837	0.865	0.906	0.912	0.864	0.796
0.763	0.780	0.838	0.866	0.907	0.913	0.865	0.796
0.763	0.780	0.838	0.866	0.907	0.913	0.864	0.796

Table 36. Static-Pressure Ratios in Nozzle and Instrumented Spacers for Configuration $P_C C_L B_F N_1 L$

Inner wall

Static-pressure ratios at s/l_s of -

NPR	0.429	0.858	0.913	0.937	0.956	0.972
1.50	0.884	0.666	0.565	0.552	0.582	0.606
1.81	0.869	0.612	0.477	0.447	0.465	0.478
2.00	0.867	0.603	0.457	0.416	0.430	0.420
2.21	0.868	0.597	0.443	0.401	0.414	0.381
2.50	0.868	0.596	0.440	0.398	0.412	0.367
3.00	0.870	0.596	0.439	0.400	0.413	0.366
3.51	0.871	0.593	0.435	0.405	0.412	0.365
4.00	0.872	0.592	0.434	0.410	0.411	0.364
4.49	0.872	0.592	0.434	0.413	0.410	0.364
4.76	0.872	0.592	0.434	0.413	0.409	0.364

Inner channel

Static-pressure ratios at s/l_s of -

	0.972
	0.573
	0.467
	0.438
	0.425
	0.423
	0.428
	0.431
	0.430
	0.430
	0.429

Outer channel

Static-pressure ratios at s/l_s of -

NPR	0.972
1.50	0.671
1.81	0.566
2.00	0.525
2.21	0.489
2.50	0.456
3.00	0.436
3.51	0.435
4.00	0.435
4.49	0.436
4.76	0.436

Left instrumented spacer

Static-pressure ratios at ϕ, deg, of -

NPR	0	45	90	135	180	225	270	315
1.50	0.816	0.837	0.851	0.861	0.865	0.874	0.846	0.816
1.81	0.794	0.818	0.830	0.844	0.847	0.858	0.826	0.794
2.00	0.791	0.816	0.827	0.841	0.846	0.856	0.824	0.791
2.21	0.791	0.817	0.827	0.841	0.845	0.857	0.823	0.790
2.50	0.792	0.817	0.827	0.842	0.845	0.857	0.823	0.790
3.00	0.793	0.819	0.828	0.842	0.847	0.860	0.824	0.791
3.51	0.795	0.820	0.828	0.843	0.847	0.861	0.824	0.790
4.00	0.795	0.821	0.829	0.843	0.847	0.861	0.824	0.790
4.49	0.795	0.821	0.828	0.844	0.847	0.861	0.824	0.790
4.76	0.796	0.821	0.828	0.844	0.847	0.861	0.823	0.790

Right instrumented spacer

Static-pressure ratios at ϕ, deg, of -

0	45	90	135	180	225	270	315
0.831	0.811	0.841	0.887	0.875	0.869	0.862	0.835
0.812	0.788	0.821	0.874	0.859	0.853	0.844	0.814
0.809	0.786	0.819	0.873	0.858	0.851	0.842	0.812
0.809	0.785	0.817	0.873	0.858	0.850	0.841	0.811
0.810	0.785	0.817	0.873	0.858	0.850	0.842	0.811
0.811	0.786	0.819	0.875	0.859	0.852	0.843	0.812
0.812	0.786	0.818	0.877	0.861	0.853	0.844	0.813
0.813	0.787	0.818	0.877	0.861	0.854	0.844	0.813
0.814	0.787	0.817	0.878	0.862	0.854	0.845	0.814
0.814	0.787	0.817	0.878	0.863	0.855	0.845	0.814

Table 37. Static-Pressure Ratios in Nozzle and Instrumented Spacers for Configuration $P_C C_L B_T N_I T$

Inner wall

Static-pressure ratios at s/l_s of -

NPR	0.429	0.858	0.913	0.937	0.956	0.972
1.50	0.915	0.640	0.506	0.489	0.567	0.601
1.80	0.902	0.592	0.408	0.364	0.460	0.477
2.01	0.901	0.586	0.389	0.320	0.423	0.413
2.21	0.901	0.584	0.383	0.299	0.405	0.388
2.51	0.901	0.584	0.380	0.289	0.400	0.379
3.01	0.902	0.584	0.379	0.289	0.401	0.375
3.51	0.903	0.583	0.377	0.293	0.402	0.374
4.00	0.903	0.584	0.378	0.298	0.400	0.372
4.51	0.905	0.584	0.377	0.303	0.399	0.372
5.00	0.905	0.583	0.376	0.312	0.398	0.373
5.99	0.906	0.582	0.374	0.321	0.396	0.372

Inner channel

Static-pressure ratios at s/l_s of -

	0.972
1.50	0.551
1.80	0.449
2.01	0.408
2.21	0.389
2.51	0.385
3.01	0.391
3.51	0.397
4.00	0.398
4.51	0.397
5.00	0.400
5.99	0.397

Outer channel

Static-pressure ratios at s/l_s of -

NPR	0.972
1.50	0.683
1.80	0.578
2.01	0.535
2.21	0.510
2.51	0.474
3.01	0.421
3.51	0.422
4.00	0.423
4.51	0.424
5.00	0.424
5.99	0.425

Left instrumented spacer

Static-pressure ratios at ϕ, deg, of -

NPR	0	45	90	135	180	225	270	315
1.50	0.818	0.842	0.895	0.941	0.942	0.913	0.865	0.828
1.80	0.795	0.821	0.881	0.933	0.936	0.902	0.848	0.805
2.01	0.792	0.818	0.879	0.932	0.934	0.900	0.845	0.801
2.21	0.791	0.818	0.878	0.932	0.935	0.900	0.845	0.800
2.51	0.792	0.818	0.879	0.933	0.936	0.900	0.846	0.800
3.01	0.793	0.819	0.880	0.934	0.937	0.901	0.846	0.801
3.51	0.795	0.820	0.880	0.935	0.938	0.903	0.847	0.801
4.00	0.795	0.821	0.881	0.936	0.939	0.903	0.848	0.802
4.51	0.795	0.821	0.881	0.935	0.939	0.904	0.848	0.801
5.00	0.796	0.821	0.881	0.936	0.940	0.905	0.848	0.802
5.99	0.796	0.822	0.881	0.937	0.941	0.906	0.849	0.802

Right instrumented spacer

Static-pressure ratios at ϕ, deg, of -

0	45	90	135	180	225	270	315
0.811	0.821	0.870	0.896	0.933	0.933	0.894	0.836
0.787	0.798	0.853	0.883	0.925	0.924	0.880	0.815
0.784	0.796	0.850	0.881	0.924	0.923	0.878	0.812
0.783	0.795	0.850	0.881	0.924	0.923	0.878	0.813
0.784	0.796	0.851	0.882	0.925	0.924	0.879	0.813
0.785	0.797	0.851	0.882	0.925	0.925	0.880	0.813
0.786	0.798	0.852	0.883	0.926	0.925	0.881	0.815
0.787	0.798	0.853	0.884	0.927	0.926	0.881	0.815
0.788	0.799	0.853	0.885	0.928	0.926	0.882	0.816
0.788	0.799	0.853	0.884	0.928	0.926	0.882	0.816
0.788	0.799	0.854	0.885	0.928	0.926	0.882	0.816

Table 38. Static-Pressure Ratios in Nozzle and Instrumented Spacers for Configuration $P_C C_L B_T N_1 L$

Inner wall

Static-pressure ratios at s/l_s of -

NPR	0.429	0.858	0.913	0.937	0.956	0.972
1.51	0.904	0.671	0.548	0.524	0.567	0.598
1.81	0.892	0.626	0.468	0.410	0.453	0.468
2.00	0.891	0.618	0.449	0.374	0.423	0.406
2.20	0.891	0.615	0.440	0.356	0.412	0.378
2.51	0.892	0.615	0.438	0.350	0.411	0.370
3.00	0.893	0.616	0.438	0.350	0.413	0.369
3.50	0.894	0.615	0.437	0.353	0.413	0.367
4.00	0.894	0.615	0.438	0.355	0.411	0.365
4.51	0.894	0.616	0.438	0.358	0.410	0.364
4.76	0.894	0.615	0.438	0.360	0.409	0.363

Inner channel

Static-pressure ratios at s/l_s of -

	0.972
1.51	0.553
1.81	0.450
2.00	0.421
2.20	0.407
2.51	0.409
3.00	0.417
3.50	0.422
4.00	0.421
4.51	0.420
4.76	0.418

Outer channel

Static-pressure ratios at s/l_s of -

NPR	0.972
1.51	0.677
1.81	0.579
2.00	0.543
2.20	0.521
2.51	0.481
3.00	0.421
3.50	0.410
4.00	0.409
4.51	0.409
4.76	0.409

Left instrumented spacer

Static-pressure ratios at ϕ, deg, of -

NPR	0	45	90	135	180	225	270	315
1.51	0.832	0.840	0.864	0.873	0.882	0.892	0.865	0.834
1.81	0.814	0.823	0.846	0.856	0.868	0.878	0.849	0.815
2.00	0.813	0.822	0.844	0.855	0.867	0.877	0.847	0.812
2.20	0.812	0.822	0.843	0.854	0.866	0.877	0.846	0.811
2.51	0.813	0.823	0.844	0.854	0.867	0.878	0.847	0.812
3.00	0.815	0.825	0.845	0.856	0.868	0.879	0.848	0.813
3.50	0.816	0.826	0.846	0.856	0.869	0.880	0.848	0.813
4.00	0.816	0.827	0.846	0.857	0.870	0.880	0.849	0.814
4.51	0.817	0.827	0.846	0.857	0.870	0.881	0.849	0.814
4.76	0.817	0.827	0.846	0.858	0.870	0.881	0.849	0.814

Right instrumented spacer

Static-pressure ratios at ϕ, deg, of -

0	45	90	135	180	225	270	315
0.832	0.834	0.863	0.896	0.886	0.875	0.871	0.836
0.814	0.816	0.847	0.885	0.873	0.861	0.856	0.818
0.813	0.815	0.845	0.884	0.872	0.860	0.855	0.816
0.813	0.814	0.845	0.884	0.872	0.859	0.854	0.816
0.813	0.815	0.845	0.885	0.873	0.859	0.855	0.816
0.814	0.816	0.846	0.886	0.874	0.861	0.856	0.817
0.815	0.817	0.847	0.888	0.875	0.862	0.857	0.818
0.816	0.818	0.847	0.888	0.875	0.862	0.858	0.819
0.817	0.819	0.848	0.889	0.877	0.863	0.858	0.820
0.817	0.819	0.848	0.889	0.876	0.863	0.858	0.820

Table 39. Static-Pressure Ratios in Nozzle and Instrumented Spacers for Configuration $P_C C_F B_N N_1 T$

Inner wall

Static-pressure ratios at s/l_s of -

NPR	0.429	0.858	0.913	0.937	0.956	0.972
1.50	0.906	0.651	0.519	0.492	0.569	0.601
1.80	0.898	0.589	0.410	0.380	0.462	0.481
2.01	0.898	0.574	0.376	0.340	0.425	0.416
2.20	0.897	0.570	0.367	0.320	0.407	0.389
2.51	0.897	0.570	0.365	0.305	0.396	0.374
3.01	0.897	0.571	0.365	0.304	0.393	0.368
3.51	0.897	0.576	0.372	0.299	0.388	0.364
4.00	0.899	0.572	0.363	0.307	0.391	0.365
4.51	0.900	0.573	0.364	0.312	0.388	0.364
5.00	0.900	0.571	0.363	0.318	0.388	0.365
6.00	0.903	0.569	0.357	0.328	0.388	0.366

Inner channel

Static-pressure ratios at s/l_s of -

	0.972
	0.552
	0.453
	0.418
	0.398
	0.388
	0.387
	0.384
	0.389
	0.388
	0.389
	0.391

Outer channel

Static-pressure ratios at s/l_s of -

NPR	0.972
1.50	0.680
1.80	0.581
2.01	0.537
2.20	0.513
2.51	0.469
3.01	0.422
3.51	0.419
4.00	0.420
4.51	0.421
5.00	0.422
6.00	0.423

Left instrumented spacer

Static-pressure ratios at ϕ, deg, of -

NPR	0	45	90	135	180	225	270	315
1.50	0.809	0.833	0.890	0.931	0.927	0.898	0.866	0.817
1.80	0.786	0.812	0.875	0.927	0.928	0.894	0.845	0.796
2.01	0.783	0.809	0.872	0.926	0.928	0.893	0.842	0.792
2.20	0.782	0.809	0.872	0.927	0.928	0.893	0.841	0.791
2.51	0.783	0.809	0.872	0.927	0.928	0.893	0.842	0.791
3.01	0.784	0.810	0.873	0.927	0.928	0.893	0.842	0.792
3.51	0.785	0.811	0.873	0.926	0.927	0.892	0.843	0.791
4.00	0.786	0.812	0.874	0.929	0.930	0.895	0.843	0.793
4.51	0.786	0.812	0.874	0.929	0.931	0.896	0.843	0.793
5.00	0.786	0.812	0.875	0.930	0.932	0.897	0.844	0.793
6.00	0.786	0.813	0.875	0.932	0.935	0.900	0.845	0.794

Right instrumented spacer

Static-pressure ratios at ϕ, deg, of -

0	45	90	135	180	225	270	315
0.809	0.820	0.867	0.900	0.931	0.932	0.892	0.833
0.781	0.794	0.854	0.878	0.911	0.919	0.877	0.810
0.778	0.791	0.852	0.875	0.910	0.918	0.875	0.807
0.777	0.790	0.852	0.875	0.910	0.918	0.875	0.807
0.777	0.790	0.853	0.876	0.911	0.919	0.875	0.807
0.778	0.791	0.853	0.876	0.911	0.919	0.876	0.808
0.778	0.791	0.852	0.878	0.912	0.918	0.876	0.808
0.780	0.793	0.855	0.879	0.913	0.920	0.879	0.809
0.780	0.793	0.855	0.879	0.914	0.921	0.878	0.810
0.781	0.793	0.856	0.879	0.914	0.921	0.879	0.810
0.781	0.794	0.857	0.879	0.915	0.922	0.879	0.810

Table 40. Static-Pressure Ratios in Nozzle and Instrumented Space Configuration $P_C C_F B_N N_I L$

Inner wall

Static-pressure ratios at s/l_s of -

NPR	0.429	0.858	0.913	0.937	0.956	0.972
1.52	0.885	0.672	0.571	0.548	0.576	0.601
1.82	0.873	0.622	0.486	0.445	0.463	0.475
2.01	0.872	0.613	0.465	0.413	0.429	0.417
2.20	0.873	0.608	0.454	0.398	0.416	0.382
2.52	0.873	0.607	0.449	0.391	0.412	0.367
3.00	0.874	0.606	0.448	0.393	0.413	0.366
3.51	0.874	0.607	0.448	0.396	0.412	0.364
4.00	0.874	0.606	0.448	0.401	0.411	0.363
4.50	0.873	0.606	0.449	0.404	0.409	0.362
4.92	0.873	0.608	0.452	0.405	0.408	0.362

Inner channel

Static-pressure ratios at s/l_s of -

	0.972
	0.568
	0.466
	0.437
	0.425
	0.423
	0.427
	0.429
	0.428
	0.428
	0.426

Outer channel

Static-pressure ratios at s/l_s of -

NPR	0.972
1.52	0.673
1.82	0.577
2.01	0.541
2.20	0.522
2.52	0.482
3.00	0.419
3.51	0.405
4.00	0.405
4.50	0.406
4.92	0.405

Left instrumented spacer

Static-pressure ratios at ϕ, deg. of -

NPR	0	45	90	135	180	225	270	315
1.52	0.826	0.835	0.854	0.867	0.869	0.879	0.854	0.827
1.82	0.809	0.819	0.839	0.852	0.856	0.868	0.839	0.809
2.01	0.807	0.817	0.836	0.850	0.854	0.867	0.836	0.806
2.20	0.807	0.817	0.836	0.850	0.854	0.867	0.836	0.806
2.52	0.807	0.818	0.836	0.850	0.854	0.869	0.837	0.806
3.00	0.809	0.819	0.837	0.851	0.855	0.869	0.837	0.807
3.51	0.810	0.821	0.838	0.852	0.856	0.870	0.838	0.807
4.00	0.810	0.821	0.838	0.852	0.856	0.870	0.838	0.807
4.50	0.810	0.821	0.837	0.852	0.856	0.870	0.837	0.807
4.92	0.810	0.821	0.838	0.852	0.856	0.870	0.838	0.807

Right instrumented spacer

Static-pressure ratios at ϕ, deg. of -

0	45	90	135	180	225	270	315
0.833	0.831	0.861	0.893	0.887	0.877	0.869	0.840
0.816	0.815	0.846	0.880	0.874	0.864	0.853	0.822
0.814	0.813	0.844	0.878	0.872	0.862	0.852	0.820
0.814	0.812	0.844	0.878	0.871	0.862	0.851	0.820
0.814	0.813	0.843	0.878	0.871	0.862	0.852	0.820
0.815	0.814	0.844	0.878	0.870	0.862	0.852	0.821
0.816	0.815	0.844	0.879	0.870	0.863	0.853	0.822
0.817	0.815	0.844	0.879	0.871	0.864	0.854	0.823
0.817	0.816	0.844	0.881	0.871	0.864	0.854	0.824
0.818	0.816	0.844	0.881	0.872	0.864	0.854	0.823

Table 41. Static-Pressure Ratios in Nozzle and Instrumented Spacers for Configuration $P_C C_F B_F N_I T$

Inner wall

Static-pressure ratios at s/l_s of -

NPR	0.429	0.858	0.913	0.937	0.956	0.972
1.50	0.918	0.633	0.493	0.477	0.566	0.600
1.81	0.906	0.586	0.393	0.356	0.461	0.479
1.99	0.904	0.585	0.381	0.314	0.425	0.426
2.22	0.904	0.579	0.370	0.286	0.398	0.392
2.50	0.904	0.579	0.368	0.272	0.388	0.379
3.00	0.906	0.581	0.368	0.264	0.386	0.373
3.51	0.906	0.581	0.367	0.266	0.388	0.371
4.01	0.907	0.582	0.367	0.266	0.385	0.369
4.51	0.907	0.583	0.369	0.268	0.382	0.367
5.00	0.908	0.581	0.367	0.277	0.383	0.369
5.98	0.908	0.582	0.367	0.282	0.378	0.368

Inner channel

Static-pressure ratios at s/l_s of -

0.972
0.548
0.447
0.405
0.376
0.367
0.368
0.374
0.375
0.373
0.378
0.374

Outer channel

Static-pressure ratios at s/l_s of -

NPR	0.972
1.50	0.684
1.81	0.579
1.99	0.537
2.22	0.506
2.50	0.452
3.00	0.424
3.51	0.424
4.01	0.425
4.51	0.425
5.00	0.426
5.98	0.427

Left instrumented spacer

Static-pressure ratios at ϕ, deg. of -

NPR	0	45	90	135	180	225	270	315
1.50	0.815	0.838	0.894	0.943	0.943	0.906	0.864	0.828
1.81	0.791	0.817	0.879	0.935	0.935	0.893	0.846	0.804
1.99	0.787	0.814	0.877	0.932	0.932	0.890	0.844	0.800
2.22	0.787	0.814	0.876	0.933	0.933	0.891	0.843	0.799
2.50	0.787	0.814	0.877	0.933	0.933	0.891	0.843	0.799
3.00	0.789	0.815	0.878	0.934	0.935	0.893	0.844	0.800
3.51	0.789	0.816	0.878	0.935	0.935	0.894	0.845	0.800
4.01	0.790	0.816	0.879	0.935	0.936	0.895	0.845	0.801
4.51	0.790	0.816	0.879	0.935	0.936	0.895	0.845	0.800
5.00	0.790	0.817	0.879	0.936	0.937	0.896	0.846	0.801
5.98	0.791	0.817	0.880	0.936	0.938	0.898	0.847	0.801

Right instrumented spacer

Static-pressure ratios at ϕ, deg. of -

0	45	90	135	180	225	270	315
0.809	0.826	0.867	0.890	0.931	0.934	0.894	0.832
0.784	0.804	0.849	0.876	0.922	0.925	0.880	0.810
0.781	0.801	0.846	0.875	0.922	0.925	0.879	0.808
0.779	0.800	0.846	0.874	0.921	0.924	0.878	0.807
0.780	0.800	0.846	0.875	0.922	0.924	0.878	0.807
0.781	0.801	0.847	0.875	0.922	0.926	0.880	0.808
0.782	0.802	0.848	0.877	0.924	0.927	0.880	0.809
0.782	0.802	0.849	0.877	0.924	0.927	0.881	0.809
0.783	0.803	0.849	0.878	0.924	0.927	0.881	0.810
0.783	0.802	0.850	0.877	0.924	0.927	0.881	0.810
0.783	0.802	0.851	0.878	0.924	0.928	0.881	0.810

Table 42. Static-Pressure Ratios in Nozzle and Instrumented Spacers for Configuration $P_C C_F B_F N_1 L$

Inner wall
Static-pressure ratios at s/l_s of -

NPR	0.429	0.858	0.913	0.937	0.956	0.972
1.51	0.895	0.674	0.558	0.532	0.569	0.597
1.81	0.884	0.629	0.479	0.427	0.457	0.473
2.00	0.883	0.620	0.457	0.391	0.425	0.410
2.22	0.883	0.617	0.450	0.374	0.413	0.377
2.52	0.883	0.616	0.448	0.369	0.412	0.369
3.00	0.887	0.614	0.441	0.369	0.415	0.369
3.51	0.885	0.616	0.447	0.372	0.413	0.366
4.00	0.885	0.616	0.446	0.375	0.412	0.364
4.51	0.886	0.616	0.446	0.378	0.410	0.363
4.90	0.886	0.616	0.447	0.380	0.409	0.363

Inner channel
Static-pressure ratios at s/l_s of -

	0.972
	0.557
	0.457
	0.427
	0.415
	0.415
	0.424
	0.426
	0.426
	0.423
	0.422

Outer channel
Static-pressure ratios at s/l_s of -

NPR	0.972
1.51	0.674
1.81	0.580
2.00	0.543
2.22	0.520
2.52	0.480
3.00	0.418
3.51	0.406
4.00	0.406
4.51	0.406
4.90	0.406

Left instrumented spacer
Static-pressure ratios at ϕ, deg, of -

NPR	0	45	90	135	180	225	270	315
1.51	0.829	0.837	0.863	0.865	0.876	0.886	0.859	0.830
1.81	0.812	0.820	0.848	0.849	0.862	0.874	0.844	0.811
2.00	0.810	0.818	0.846	0.848	0.861	0.873	0.841	0.808
2.22	0.810	0.819	0.846	0.848	0.861	0.874	0.841	0.809
2.52	0.811	0.819	0.846	0.849	0.861	0.874	0.842	0.809
3.00	0.812	0.821	0.848	0.850	0.864	0.876	0.843	0.810
3.51	0.813	0.822	0.848	0.850	0.863	0.876	0.843	0.810
4.00	0.813	0.822	0.848	0.851	0.863	0.876	0.843	0.811
4.51	0.813	0.822	0.848	0.851	0.863	0.877	0.843	0.811
4.90	0.814	0.823	0.848	0.851	0.864	0.877	0.844	0.811

Right instrumented spacer
Static-pressure ratios at ϕ, deg, of -

0	45	90	135	180	225	270	315
0.830	0.830	0.862	0.896	0.887	0.870	0.870	0.836
0.812	0.812	0.847	0.884	0.875	0.856	0.854	0.819
0.811	0.811	0.846	0.882	0.873	0.854	0.853	0.817
0.810	0.811	0.845	0.882	0.874	0.854	0.853	0.817
0.812	0.811	0.845	0.883	0.874	0.854	0.853	0.817
0.813	0.813	0.845	0.882	0.873	0.855	0.853	0.818
0.814	0.814	0.845	0.884	0.874	0.856	0.854	0.819
0.814	0.814	0.845	0.884	0.875	0.857	0.855	0.820
0.815	0.815	0.845	0.885	0.875	0.858	0.856	0.821
0.815	0.815	0.845	0.885	0.875	0.858	0.856	0.821

Table 43. Static-Pressure Ratios in Nozzle and Instrumented Spacers for Configuration $P_C C_F B_T N_I T$

Inner wall

Static-pressure ratios at s/l_s of -

NPR	0.429	0.858	0.913	0.937	0.956	0.972
1.51	0.915	0.619	0.490	0.489	0.561	0.591
1.79	0.905	0.571	0.386	0.389	0.462	0.472
2.01	0.903	0.565	0.363	0.345	0.432	0.399
2.20	0.903	0.568	0.362	0.323	0.421	0.385
2.51	0.904	0.564	0.356	0.321	0.421	0.380
3.01	0.905	0.565	0.355	0.322	0.420	0.377
3.50	0.906	0.566	0.355	0.324	0.418	0.375
3.99	0.906	0.567	0.355	0.329	0.415	0.375
4.51	0.907	0.569	0.357	0.335	0.412	0.375
5.01	0.908	0.569	0.357	0.341	0.411	0.375
5.99	0.909	0.569	0.357	0.342	0.406	0.374

Inner channel

Static-pressure ratios at s/l_s of -

0.972
0.545
0.459
0.427
0.412
0.416
0.422
0.422
0.420
0.418
0.416
0.412

Outer channel

Static-pressure ratios at s/l_s of -

NPR	0.972
1.51	0.673
1.79	0.575
2.01	0.524
2.20	0.495
2.51	0.429
3.01	0.417
3.50	0.418
3.99	0.419
4.51	0.420
5.01	0.420
5.99	0.422

Left instrumented spacer

Static-pressure ratios at ϕ, deg, of -

NPR	0	45	90	135	180	225	270	315
1.51	0.814	0.838	0.894	0.943	0.945	0.902	0.858	0.829
1.79	0.793	0.821	0.883	0.937	0.940	0.892	0.843	0.810
2.01	0.791	0.819	0.880	0.936	0.938	0.890	0.840	0.806
2.20	0.790	0.818	0.881	0.935	0.938	0.889	0.840	0.805
2.51	0.791	0.819	0.881	0.937	0.940	0.891	0.841	0.806
3.01	0.793	0.820	0.882	0.938	0.941	0.891	0.841	0.807
3.50	0.793	0.821	0.882	0.938	0.943	0.892	0.842	0.807
3.99	0.794	0.821	0.883	0.939	0.943	0.893	0.842	0.807
4.51	0.794	0.821	0.883	0.939	0.943	0.894	0.843	0.807
5.01	0.795	0.822	0.883	0.939	0.944	0.895	0.843	0.807
5.99	0.795	0.822	0.883	0.940	0.944	0.896	0.844	0.807

Right instrumented spacer

Static-pressure ratios at ϕ, deg, of -

0	45	90	135	180	225	270	315
0.809	0.826	0.864	0.889	0.939	0.937	0.895	0.833
0.787	0.806	0.848	0.877	0.931	0.929	0.884	0.814
0.783	0.803	0.845	0.874	0.930	0.928	0.881	0.811
0.784	0.804	0.845	0.877	0.932	0.930	0.883	0.813
0.784	0.804	0.846	0.876	0.931	0.930	0.882	0.812
0.785	0.805	0.847	0.877	0.933	0.931	0.883	0.813
0.786	0.805	0.848	0.877	0.933	0.931	0.884	0.814
0.787	0.806	0.849	0.878	0.934	0.931	0.885	0.814
0.787	0.806	0.849	0.879	0.934	0.932	0.885	0.815
0.787	0.806	0.849	0.879	0.934	0.932	0.885	0.815
0.788	0.806	0.850	0.879	0.935	0.932	0.885	0.815

Table 44. Static-Pressure Ratios in Nozzle and Instrumented Spacers for Configuration $P_C C_F B_T N_1 L$

Inner wall
Static-pressure ratios at s/l_s of -

NPR	0.429	0.858	0.913	0.937	0.956	0.972
1.51	0.906	0.691	0.556	0.510	0.563	0.595
1.81	0.896	0.649	0.478	0.388	0.447	0.462
2.00	0.895	0.642	0.463	0.350	0.417	0.403
2.21	0.895	0.639	0.457	0.334	0.407	0.380
2.50	0.896	0.637	0.452	0.328	0.409	0.375
3.01	0.897	0.638	0.454	0.326	0.410	0.373
3.49	0.898	0.638	0.453	0.327	0.412	0.371
3.99	0.898	0.637	0.453	0.326	0.411	0.368
4.51	0.898	0.637	0.453	0.331	0.409	0.367
4.91	0.898	0.636	0.453	0.333	0.409	0.367

Inner channel
Static-pressure ratios at s/l_s of -

	0.972
	0.547
	0.440
	0.407
	0.395
	0.398
	0.407
	0.415
	0.416
	0.415
	0.415

Outer channel
Static-pressure ratios at s/l_s of -

NPR	0.972
1.51	0.679
1.81	0.580
2.00	0.543
2.21	0.521
2.50	0.480
3.01	0.414
3.49	0.408
3.99	0.408
4.51	0.408
4.91	0.408

Left instrumented spacer
Static-pressure ratios at ϕ, deg, of -

NPR	0	45	90	135	180	225	270	315
1.51	0.832	0.835	0.869	0.866	0.876	0.892	0.863	0.832
1.81	0.814	0.819	0.854	0.851	0.862	0.880	0.848	0.814
2.00	0.812	0.817	0.851	0.848	0.861	0.879	0.846	0.811
2.21	0.812	0.818	0.851	0.848	0.860	0.879	0.845	0.812
2.50	0.813	0.819	0.851	0.849	0.861	0.881	0.846	0.812
3.01	0.814	0.820	0.852	0.849	0.861	0.881	0.846	0.813
3.49	0.815	0.821	0.853	0.850	0.863	0.882	0.847	0.813
3.99	0.815	0.822	0.853	0.851	0.863	0.882	0.847	0.813
4.51	0.816	0.822	0.853	0.851	0.863	0.882	0.848	0.814
4.91	0.816	0.822	0.853	0.851	0.863	0.882	0.848	0.814

Right instrumented spacer
Static-pressure ratios at ϕ, deg, of -

0	45	90	135	180	225	270	315
0.832	0.832	0.865	0.896	0.888	0.869	0.872	0.833
0.815	0.814	0.849	0.884	0.875	0.854	0.857	0.814
0.813	0.812	0.848	0.882	0.873	0.852	0.855	0.812
0.813	0.812	0.847	0.883	0.874	0.852	0.855	0.812
0.814	0.813	0.848	0.883	0.874	0.852	0.856	0.813
0.815	0.814	0.848	0.884	0.875	0.853	0.857	0.814
0.816	0.815	0.849	0.885	0.875	0.854	0.857	0.815
0.817	0.816	0.849	0.886	0.876	0.854	0.858	0.816
0.817	0.816	0.848	0.886	0.877	0.855	0.858	0.816
0.818	0.817	0.849	0.887	0.877	0.856	0.858	0.817

Table 45. Static-Pressure Ratios in Nozzle and Instrumented Spacers for Configuration $P_O C_S B_N N_I T$

Inner wall

Static-pressure ratios at s/l_s of -

NPR	0.429	0.858	0.913	0.937	0.956	0.972
1.50	0.932	0.652	0.531	0.528	0.557	0.564
1.80	0.925	0.609	0.447	0.435	0.466	0.460
2.01	0.925	0.602	0.426	0.408	0.443	0.435
2.19	0.926	0.601	0.419	0.397	0.436	0.430
2.50	0.926	0.600	0.418	0.399	0.442	0.430
3.01	0.927	0.601	0.417	0.404	0.448	0.429
3.51	0.927	0.600	0.415	0.412	0.448	0.426
4.02	0.928	0.601	0.413	0.413	0.444	0.424
4.51	0.927	0.599	0.412	0.419	0.443	0.423
5.01	0.928	0.598	0.411	0.420	0.442	0.421
6.00	0.928	0.597	0.409	0.418	0.439	0.420

Inner channel

Static-pressure ratios at s/l_s of -

0.972
0.596
0.469
0.410
0.389
0.383
0.380
0.378
0.377
0.377
0.377
0.376

Outer channel

Static-pressure ratios at s/l_s of -

NPR	0.972
1.50	0.686
1.80	0.586
2.01	0.553
2.19	0.532
2.50	0.509
3.01	0.441
3.51	0.437
4.02	0.439
4.51	0.438
5.01	0.436
6.00	0.434

Left instrumented spacer

Static-pressure ratios at ϕ, deg, of -

NPR	0	45	90	135	180	225	270	315
1.50	0.853	0.856	0.898	0.941	0.947	0.937	0.899	0.855
1.80	0.838	0.840	0.886	0.935	0.942	0.932	0.888	0.841
2.01	0.838	0.839	0.885	0.934	0.942	0.932	0.887	0.839
2.19	0.837	0.839	0.885	0.935	0.943	0.932	0.887	0.839
2.50	0.839	0.840	0.886	0.935	0.944	0.933	0.888	0.840
3.01	0.839	0.841	0.886	0.936	0.945	0.934	0.888	0.840
3.51	0.841	0.841	0.886	0.937	0.946	0.934	0.888	0.840
4.02	0.841	0.841	0.885	0.937	0.946	0.935	0.888	0.840
4.51	0.842	0.841	0.885	0.936	0.947	0.935	0.888	0.840
5.01	0.843	0.841	0.886	0.937	0.947	0.935	0.889	0.841
6.00	0.843	0.841	0.885	0.937	0.947	0.935	0.888	0.839

Right instrumented spacer

Static-pressure ratios at ϕ, deg, of -

0	45	90	135	180	225	270	315
0.837	0.848	0.896	0.936	0.944	0.931	0.896	0.853
0.819	0.832	0.884	0.929	0.938	0.925	0.884	0.836
0.817	0.830	0.884	0.930	0.938	0.924	0.884	0.834
0.818	0.831	0.885	0.931	0.940	0.926	0.885	0.835
0.818	0.832	0.885	0.932	0.941	0.927	0.886	0.835
0.819	0.834	0.886	0.934	0.943	0.929	0.887	0.836
0.820	0.835	0.887	0.935	0.944	0.929	0.888	0.837
0.821	0.837	0.888	0.936	0.945	0.931	0.889	0.838
0.820	0.836	0.888	0.935	0.944	0.930	0.888	0.837
0.820	0.835	0.886	0.935	0.944	0.930	0.888	0.837
0.820	0.836	0.887	0.936	0.945	0.930	0.888	0.837

Table 46. Static-Pressure Ratios in Nozzle and Instrumented Spacers for Configuration $P_OC_SB_NN_1L$

Inner wall
Static-pressure ratios at s/l_s of -

NPR	0.429	0.858	0.913	0.937	0.956	0.972
1.50	0.924	0.658	0.549	0.547	0.567	0.573
1.80	0.917	0.612	0.473	0.463	0.480	0.473
2.00	0.917	0.606	0.455	0.438	0.454	0.443
2.20	0.918	0.603	0.446	0.427	0.445	0.432
2.50	0.918	0.603	0.444	0.427	0.447	0.431
3.00	0.919	0.603	0.441	0.428	0.451	0.430
3.50	0.920	0.603	0.440	0.434	0.451	0.427
4.00	0.919	0.602	0.440	0.439	0.450	0.426
4.51	0.920	0.602	0.436	0.437	0.447	0.424
4.70	0.920	0.601	0.435	0.437	0.446	0.423

Inner channel
Static-pressure ratios at s/l_s of -

	0.972
1.50	0.596
1.80	0.481
2.00	0.427
2.20	0.392
2.50	0.381
3.00	0.379
3.50	0.378
4.00	0.378
4.51	0.377
4.70	0.377

Outer channel
Static-pressure ratios at s/l_s of -

NPR	0.972
1.50	0.680
1.80	0.577
2.00	0.539
2.20	0.515
2.50	0.479
3.00	0.434
3.50	0.432
4.00	0.434
4.51	0.433
4.70	0.432

Left instrumented spacer
Static-pressure ratios at ϕ, deg, of -

NPR	0	45	90	135	180	225	270	315
1.50	0.833	0.851	0.893	0.936	0.938	0.927	0.894	0.850
1.80	0.818	0.838	0.882	0.931	0.935	0.922	0.885	0.835
2.00	0.817	0.838	0.881	0.930	0.934	0.921	0.884	0.835
2.20	0.817	0.838	0.882	0.931	0.935	0.922	0.884	0.834
2.50	0.818	0.839	0.882	0.931	0.936	0.923	0.884	0.835
3.00	0.818	0.841	0.883	0.931	0.937	0.923	0.885	0.836
3.50	0.818	0.841	0.883	0.932	0.938	0.924	0.885	0.836
4.00	0.818	0.842	0.883	0.932	0.938	0.924	0.884	0.836
4.51	0.818	0.842	0.883	0.932	0.939	0.923	0.885	0.836
4.70	0.818	0.842	0.883	0.932	0.939	0.924	0.886	0.837

Right instrumented spacer
Static-pressure ratios at ϕ, deg, of -

	0	45	90	135	180	225	270	315
1.50	0.840	0.847	0.890	0.926	0.936	0.930	0.893	0.851
1.80	0.826	0.834	0.880	0.920	0.931	0.925	0.883	0.837
2.00	0.824	0.833	0.880	0.920	0.931	0.924	0.881	0.835
2.20	0.825	0.834	0.880	0.921	0.932	0.925	0.882	0.836
2.50	0.826	0.836	0.881	0.922	0.934	0.927	0.884	0.836
3.00	0.826	0.835	0.881	0.922	0.933	0.927	0.884	0.836
3.50	0.827	0.837	0.882	0.923	0.934	0.928	0.885	0.837
4.00	0.828	0.838	0.883	0.924	0.935	0.929	0.886	0.838
4.51	0.828	0.837	0.883	0.923	0.934	0.928	0.886	0.838
4.70	0.828	0.838	0.882	0.923	0.934	0.929	0.886	0.838

Table 47. Static-Pressure Ratios in Nozzle and Instrumented Spacers for Configuration $P_0C_SB_FN_1T$

Inner wall

Static-pressure ratios at s/l_s of -

NPR	0.429	0.858	0.913	0.937	0.956	0.972
1.52	0.932	0.648	0.519	0.514	0.546	0.554
1.80	0.925	0.609	0.441	0.426	0.462	0.459
2.00	0.925	0.602	0.421	0.398	0.440	0.434
2.20	0.925	0.601	0.416	0.390	0.435	0.429
2.51	0.925	0.600	0.415	0.392	0.440	0.430
2.99	0.926	0.600	0.413	0.398	0.447	0.428
3.53	0.926	0.599	0.411	0.405	0.446	0.425
4.00	0.926	0.598	0.410	0.412	0.443	0.423
4.49	0.926	0.598	0.407	0.413	0.441	0.421
5.01	0.926	0.597	0.406	0.413	0.439	0.420
6.03	0.926	0.596	0.404	0.411	0.437	0.418

Inner channel

Static-pressure ratios at s/l_s of -

	0.972
	0.584
	0.467
	0.408
	0.387
	0.381
	0.379
	0.377
	0.377
	0.376
	0.375
	0.374

Outer channel

Static-pressure ratios at s/l_s of -

NPR	0.972
1.52	0.677
1.80	0.585
2.00	0.551
2.20	0.529
2.51	0.498
2.99	0.444
3.53	0.444
4.00	0.443
4.49	0.442
5.01	0.441
6.03	0.440

Left instrumented spacer

Static-pressure ratios at ϕ, deg, of -

NPR	0	45	90	135	180	225	270	315
1.52	0.849	0.853	0.896	0.941	0.948	0.935	0.897	0.851
1.80	0.835	0.839	0.886	0.936	0.944	0.930	0.886	0.837
2.00	0.833	0.838	0.885	0.935	0.943	0.930	0.886	0.836
2.20	0.834	0.838	0.885	0.936	0.944	0.930	0.886	0.836
2.51	0.833	0.839	0.885	0.936	0.944	0.930	0.886	0.835
2.99	0.836	0.840	0.885	0.936	0.945	0.932	0.887	0.837
3.53	0.837	0.840	0.886	0.937	0.946	0.933	0.887	0.838
4.00	0.838	0.840	0.885	0.937	0.946	0.933	0.887	0.838
4.49	0.840	0.840	0.885	0.937	0.947	0.933	0.887	0.838
5.01	0.841	0.840	0.885	0.937	0.947	0.933	0.887	0.838
6.03	0.842	0.840	0.883	0.937	0.947	0.933	0.887	0.838

Right instrumented spacer

Static-pressure ratios at ϕ, deg, of -

0	45	90	135	180	225	270	315
0.825	0.833	0.890	0.930	0.941	0.934	0.897	0.859
0.807	0.818	0.879	0.924	0.936	0.928	0.888	0.843
0.805	0.820	0.879	0.925	0.937	0.928	0.887	0.841
0.804	0.816	0.878	0.925	0.936	0.928	0.886	0.841
0.807	0.818	0.880	0.926	0.938	0.929	0.887	0.841
0.805	0.818	0.878	0.927	0.938	0.929	0.887	0.841
0.806	0.820	0.879	0.928	0.939	0.930	0.888	0.842
0.807	0.818	0.877	0.927	0.938	0.929	0.887	0.843
0.806	0.821	0.879	0.928	0.939	0.930	0.888	0.842
0.806	0.819	0.877	0.927	0.939	0.929	0.887	0.842
0.804	0.819	0.877	0.927	0.938	0.929	0.887	0.842

Table 48. Static-Pressure Ratios in Nozzle and Instrumented Spacers for Configuration $P_0C_SB_FN_1L$

Inner wall

Static-pressure ratios at s/l_s of -

NPR	0.429	0.858	0.913	0.937	0.956	0.972
1.51	0.924	0.657	0.546	0.543	0.563	0.569
1.80	0.914	0.612	0.479	0.472	0.485	0.477
1.99	0.915	0.605	0.459	0.446	0.459	0.447
2.21	0.916	0.602	0.448	0.433	0.448	0.433
2.50	0.916	0.602	0.443	0.428	0.447	0.432
2.99	0.918	0.603	0.441	0.430	0.452	0.430
3.50	0.918	0.602	0.439	0.434	0.452	0.428
4.02	0.917	0.602	0.438	0.436	0.449	0.425
4.51	0.920	0.602	0.434	0.434	0.446	0.423
4.75	0.919	0.601	0.432	0.433	0.445	0.422

Inner channel

Static-pressure ratios at s/l_s of -

	0.972
1.51	0.594
1.80	0.486
1.99	0.433
2.21	0.394
2.50	0.382
2.99	0.380
3.50	0.380
4.02	0.378
4.51	0.377
4.75	0.377

Outer channel

Static-pressure ratios at s/l_s of -

NPR	0.972
1.51	0.675
1.80	0.572
1.99	0.533
2.21	0.504
2.50	0.468
2.99	0.437
3.50	0.438
4.02	0.439
4.51	0.438
4.75	0.438

Left instrumented spacer

Static-pressure ratios at ϕ, deg, of -

NPR	0	45	90	135	180	225	270	315
1.51	0.832	0.850	0.891	0.933	0.936	0.926	0.892	0.847
1.80	0.818	0.837	0.879	0.928	0.932	0.920	0.880	0.833
1.99	0.817	0.836	0.878	0.927	0.932	0.920	0.880	0.832
2.21	0.817	0.837	0.878	0.928	0.934	0.921	0.881	0.832
2.50	0.817	0.838	0.879	0.928	0.934	0.921	0.882	0.832
2.99	0.818	0.840	0.880	0.929	0.936	0.922	0.883	0.833
3.50	0.818	0.841	0.880	0.929	0.937	0.922	0.883	0.833
4.02	0.818	0.841	0.880	0.929	0.937	0.921	0.882	0.834
4.51	0.818	0.842	0.881	0.930	0.938	0.923	0.885	0.834
4.75	0.817	0.841	0.880	0.928	0.937	0.922	0.883	0.833

Right instrumented spacer

Static-pressure ratios at ϕ, deg, of -

0	45	90	135	180	225	270	315
0.839	0.850	0.872	0.900	0.921	0.919	0.886	0.842
0.826	0.836	0.864	0.899	0.921	0.915	0.876	0.829
0.823	0.834	0.862	0.898	0.919	0.914	0.875	0.827
0.824	0.834	0.863	0.899	0.920	0.915	0.876	0.827
0.824	0.835	0.863	0.898	0.920	0.915	0.876	0.826
0.824	0.836	0.864	0.899	0.920	0.915	0.877	0.827
0.824	0.836	0.865	0.899	0.921	0.916	0.878	0.827
0.824	0.836	0.864	0.898	0.921	0.916	0.878	0.827
0.823	0.836	0.862	0.893	0.918	0.915	0.877	0.825
0.824	0.837	0.863	0.898	0.921	0.916	0.878	0.827

Table 49. Static-Pressure Ratios in Nozzle and Instrumented Spacers for Configuration $P_0C_MB_NN_1T$

Inner wall

Static-pressure ratios at s/l_s of -

NPR	0.429	0.858	0.913	0.937	0.956	0.972
1.51	0.927	0.641	0.521	0.523	0.552	0.559
1.81	0.920	0.597	0.437	0.435	0.466	0.459
2.01	0.920	0.591	0.416	0.408	0.443	0.435
2.21	0.920	0.589	0.407	0.401	0.439	0.429
2.50	0.920	0.587	0.404	0.402	0.443	0.429
3.01	0.921	0.587	0.401	0.405	0.447	0.428
3.52	0.922	0.588	0.399	0.411	0.446	0.425
4.01	0.922	0.587	0.398	0.414	0.444	0.424
4.50	0.922	0.587	0.396	0.417	0.442	0.422
5.00	0.922	0.586	0.395	0.417	0.441	0.421
5.99	0.922	0.584	0.392	0.416	0.438	0.419

Inner channel

Static-pressure ratios at s/l_s of -

0.972
0.589
0.467
0.408
0.387
0.382
0.379
0.377
0.377
0.377
0.377
0.376

Outer channel

Static-pressure ratios at s/l_s of -

NPR	0.972
1.51	0.678
1.81	0.584
2.01	0.552
2.21	0.532
2.50	0.513
3.01	0.462
3.52	0.424
4.01	0.424
4.50	0.423
5.00	0.423
5.99	0.422

Left instrumented spacer

Static-pressure ratios at ϕ, deg, of -

NPR	0	45	90	135	180	225	270	315
1.51	0.849	0.850	0.891	0.936	0.942	0.933	0.894	0.850
1.81	0.834	0.835	0.880	0.930	0.938	0.928	0.884	0.835
2.01	0.833	0.833	0.878	0.929	0.938	0.927	0.882	0.833
2.21	0.833	0.833	0.878	0.929	0.938	0.927	0.882	0.833
2.50	0.834	0.834	0.878	0.930	0.940	0.928	0.883	0.833
3.01	0.836	0.834	0.878	0.931	0.941	0.929	0.882	0.834
3.52	0.837	0.835	0.878	0.932	0.942	0.930	0.883	0.834
4.01	0.838	0.835	0.878	0.931	0.942	0.930	0.883	0.835
4.50	0.838	0.836	0.879	0.932	0.943	0.931	0.883	0.835
5.00	0.839	0.836	0.878	0.932	0.943	0.931	0.883	0.835
5.99	0.840	0.836	0.878	0.932	0.943	0.931	0.883	0.835

Right instrumented spacer

Static-pressure ratios at ϕ, deg, of -

0	45	90	135	180	225	270	315
0.834	0.846	0.893	0.934	0.942	0.930	0.893	0.848
0.817	0.831	0.882	0.928	0.937	0.923	0.882	0.832
0.815	0.830	0.882	0.928	0.938	0.923	0.880	0.830
0.815	0.830	0.881	0.928	0.938	0.923	0.881	0.830
0.816	0.830	0.881	0.929	0.939	0.923	0.881	0.830
0.816	0.831	0.882	0.930	0.939	0.924	0.882	0.830
0.816	0.832	0.882	0.931	0.941	0.926	0.882	0.831
0.817	0.833	0.883	0.931	0.941	0.926	0.882	0.831
0.817	0.832	0.882	0.931	0.941	0.925	0.882	0.831
0.817	0.833	0.882	0.932	0.942	0.926	0.883	0.831
0.816	0.832	0.882	0.931	0.942	0.925	0.882	0.831

Table 50. Static-Pressure Ratios in Nozzle and Instrumented Spacers for Configuration $P_OC_MB_NN_IL$

Inner wall

Static-pressure ratios at s/l_s of -

NPR	0.429	0.858	0.913	0.937	0.956	0.972
1.51	0.918	0.648	0.551	0.554	0.573	0.575
1.79	0.910	0.600	0.474	0.473	0.488	0.478
2.00	0.909	0.592	0.454	0.449	0.461	0.446
2.21	0.909	0.588	0.442	0.437	0.450	0.433
2.51	0.909	0.587	0.438	0.436	0.450	0.431
3.01	0.909	0.586	0.436	0.441	0.453	0.430
3.51	0.909	0.586	0.435	0.444	0.453	0.428
4.00	0.909	0.586	0.435	0.445	0.451	0.427
4.50	0.910	0.585	0.433	0.444	0.450	0.426
4.76	0.910	0.585	0.433	0.444	0.449	0.426

Inner channel

Static-pressure ratios at s/l_s of -

	0.972
	0.598
	0.487
	0.429
	0.392
	0.382
	0.380
	0.380
	0.379
	0.379
	0.379

Outer channel

Static-pressure ratios at s/l_s of -

NPR	0.972
1.51	0.678
1.79	0.582
2.00	0.542
2.21	0.520
2.51	0.491
3.01	0.437
3.51	0.426
4.00	0.427
4.50	0.427
4.76	0.427

Left instrumented spacer

Static-pressure ratios at ϕ, deg, of -

NPR	0	45	90	135	180	225	270	315
1.51	0.830	0.845	0.888	0.932	0.937	0.923	0.891	0.847
1.79	0.813	0.831	0.876	0.926	0.932	0.917	0.881	0.832
2.00	0.812	0.831	0.875	0.926	0.932	0.917	0.879	0.831
2.21	0.811	0.831	0.874	0.926	0.932	0.917	0.880	0.830
2.51	0.811	0.831	0.875	0.926	0.933	0.917	0.880	0.831
3.01	0.811	0.832	0.875	0.927	0.934	0.918	0.881	0.831
3.51	0.811	0.833	0.875	0.927	0.934	0.918	0.880	0.832
4.00	0.811	0.833	0.875	0.927	0.934	0.918	0.880	0.832
4.50	0.811	0.833	0.875	0.927	0.934	0.918	0.880	0.832
4.76	0.811	0.833	0.875	0.927	0.934	0.918	0.880	0.832

Right instrumented spacer

Static-pressure ratios at ϕ, deg, of -

0	45	90	135	180	225	270	315
0.838	0.845	0.888	0.923	0.933	0.929	0.889	0.848
0.822	0.831	0.877	0.916	0.927	0.922	0.878	0.833
0.822	0.830	0.878	0.916	0.928	0.923	0.878	0.831
0.821	0.829	0.876	0.916	0.927	0.922	0.878	0.831
0.821	0.829	0.877	0.916	0.928	0.922	0.878	0.831
0.821	0.830	0.878	0.917	0.928	0.923	0.878	0.831
0.822	0.831	0.878	0.918	0.929	0.923	0.879	0.831
0.822	0.832	0.879	0.917	0.930	0.923	0.879	0.831
0.822	0.831	0.878	0.917	0.929	0.923	0.879	0.831
0.822	0.832	0.879	0.917	0.929	0.923	0.879	0.831

Table 51. Static-Pressure Ratios in Nozzle and Instrumented Spacers for Configuration $P_0C_MB_FN_1T$

Inner wall

Static-pressure ratios at s/l_s of -

NPR	0.429	0.858	0.913	0.937	0.956	0.972
1.52	0.926	0.643	0.512	0.505	0.544	0.554
1.80	0.917	0.601	0.429	0.409	0.457	0.455
2.01	0.916	0.594	0.408	0.378	0.430	0.429
2.20	0.918	0.592	0.401	0.367	0.424	0.422
2.53	0.918	0.591	0.399	0.369	0.430	0.424
3.02	0.918	0.590	0.397	0.376	0.436	0.423
3.51	0.919	0.590	0.396	0.382	0.437	0.422
4.01	0.919	0.589	0.396	0.391	0.436	0.420
4.51	0.920	0.589	0.395	0.394	0.434	0.419
5.02	0.920	0.588	0.394	0.397	0.433	0.417
6.01	0.920	0.587	0.392	0.397	0.430	0.415

Inner channel

Static-pressure ratios at s/l_s of -

	0.972
	0.586
	0.466
	0.405
	0.385
	0.379
	0.377
	0.375
	0.374
	0.374
	0.374
	0.373

Outer channel

Static-pressure ratios at s/l_s of -

NPR	0.972
1.52	0.677
1.80	0.585
2.01	0.553
2.20	0.531
2.53	0.509
3.02	0.456
3.51	0.433
4.01	0.433
4.51	0.433
5.02	0.432
6.01	0.431

Left instrumented spacer

Static-pressure ratios at ϕ, deg, of -

NPR	0	45	90	135	180	225	270	315
1.52	0.846	0.849	0.889	0.935	0.941	0.930	0.891	0.847
1.80	0.831	0.834	0.877	0.928	0.936	0.924	0.880	0.832
2.01	0.830	0.832	0.876	0.927	0.936	0.923	0.879	0.831
2.20	0.830	0.833	0.876	0.928	0.937	0.924	0.879	0.830
2.53	0.832	0.833	0.876	0.929	0.938	0.925	0.880	0.831
3.02	0.833	0.834	0.876	0.929	0.939	0.926	0.881	0.832
3.51	0.834	0.834	0.876	0.929	0.940	0.927	0.881	0.833
4.01	0.835	0.835	0.876	0.930	0.940	0.927	0.881	0.833
4.51	0.835	0.835	0.877	0.930	0.940	0.927	0.881	0.833
5.02	0.836	0.835	0.877	0.930	0.940	0.928	0.881	0.833
6.01	0.837	0.835	0.877	0.930	0.941	0.928	0.881	0.833

Right instrumented spacer

Static-pressure ratios at ϕ, deg, of -

0	45	90	135	180	225	270	315
0.824	0.842	0.892	0.930	0.943	0.934	0.895	0.850
0.808	0.827	0.880	0.924	0.937	0.927	0.885	0.834
0.805	0.825	0.879	0.923	0.937	0.926	0.883	0.831
0.805	0.825	0.879	0.924	0.938	0.926	0.883	0.831
0.805	0.825	0.879	0.925	0.938	0.927	0.884	0.832
0.805	0.826	0.879	0.926	0.939	0.928	0.885	0.832
0.806	0.826	0.879	0.926	0.939	0.928	0.885	0.832
0.805	0.826	0.879	0.926	0.940	0.928	0.885	0.833
0.806	0.827	0.880	0.926	0.940	0.928	0.886	0.833
0.806	0.827	0.879	0.926	0.940	0.928	0.886	0.834
0.805	0.827	0.879	0.926	0.940	0.928	0.885	0.833

Table 52. Static-Pressure Ratios in Nozzle and Instrumented Spacers for Configuration $P_OC_MB_FN_IL$

Inner wall
Static-pressure ratios at s/l_s of -

NPR	0.429	0.858	0.913	0.937	0.956	0.972
1.52	0.914	0.646	0.557	0.562	0.580	0.580
1.52	0.914	0.645	0.555	0.560	0.578	0.579
1.79	0.906	0.598	0.484	0.489	0.498	0.487
2.02	0.905	0.587	0.459	0.463	0.469	0.451
2.20	0.905	0.585	0.450	0.452	0.459	0.438
2.51	0.906	0.583	0.444	0.450	0.457	0.435
3.00	0.906	0.584	0.443	0.451	0.458	0.433
3.50	0.907	0.584	0.442	0.452	0.457	0.432
4.01	0.907	0.584	0.442	0.453	0.456	0.430
4.52	0.907	0.583	0.439	0.451	0.454	0.429
4.77	0.907	0.583	0.437	0.449	0.453	0.428

Inner channel
Static-pressure ratios at s/l_s of -

	0.972
	0.599
	0.597
	0.493
	0.429
	0.396
	0.384
	0.383
	0.382
	0.382
	0.381
	0.380

Outer channel
Static-pressure ratios at s/l_s of -

NPR	0.972
1.52	0.673
1.52	0.671
1.79	0.576
2.02	0.528
2.20	0.504
2.51	0.468
3.00	0.440
3.50	0.438
4.01	0.439
4.52	0.438
4.77	0.437

Left instrumented spacer
Static-pressure ratios at ϕ, deg, of -

NPR	0	45	90	135	180	225	270	315
1.52	0.828	0.846	0.882	0.929	0.936	0.922	0.886	0.843
1.52	0.828	0.846	0.881	0.929	0.936	0.922	0.887	0.843
1.79	0.813	0.831	0.870	0.923	0.931	0.915	0.876	0.828
2.02	0.811	0.831	0.869	0.922	0.931	0.915	0.875	0.827
2.20	0.811	0.831	0.869	0.923	0.932	0.915	0.875	0.826
2.51	0.812	0.832	0.870	0.924	0.933	0.917	0.877	0.827
3.00	0.812	0.833	0.871	0.924	0.933	0.917	0.877	0.828
3.50	0.812	0.833	0.872	0.926	0.934	0.918	0.878	0.829
4.01	0.812	0.834	0.872	0.926	0.935	0.918	0.877	0.829
4.52	0.812	0.834	0.872	0.926	0.935	0.918	0.879	0.829
4.77	0.811	0.834	0.872	0.926	0.935	0.918	0.879	0.830

Right instrumented spacer
Static-pressure ratios at ϕ, deg, of -

0	45	90	135	180	225	270	315
0.842	0.845	0.877	0.919	0.932	0.924	0.885	0.846
0.842	0.845	0.877	0.919	0.932	0.924	0.886	0.846
0.827	0.830	0.866	0.912	0.926	0.917	0.874	0.831
0.825	0.828	0.865	0.912	0.925	0.916	0.873	0.830
0.825	0.827	0.865	0.911	0.925	0.916	0.873	0.829
0.825	0.829	0.866	0.912	0.926	0.917	0.874	0.830
0.826	0.830	0.868	0.913	0.927	0.918	0.875	0.830
0.826	0.831	0.867	0.913	0.927	0.918	0.876	0.830
0.826	0.831	0.868	0.914	0.928	0.919	0.877	0.830
0.826	0.832	0.867	0.913	0.927	0.918	0.877	0.830
0.827	0.832	0.866	0.912	0.927	0.918	0.877	0.830

Table 53. Static-Pressure Ratios in Nozzle and Instrumented Spacers for Configuration $P_O C_L B_N N_1 T$

Inner wall

Static-pressure ratios at s/l_s of -

NPR	0.429	0.858	0.913	0.937	0.956	0.972
1.50	0.926	0.643	0.527	0.528	0.558	0.564
1.81	0.918	0.597	0.441	0.438	0.469	0.462
2.00	0.918	0.589	0.420	0.414	0.447	0.437
2.21	0.918	0.587	0.412	0.405	0.440	0.430
2.50	0.919	0.587	0.408	0.402	0.442	0.429
3.00	0.918	0.585	0.406	0.411	0.447	0.428
3.50	0.919	0.587	0.404	0.412	0.446	0.425
4.00	0.920	0.587	0.402	0.413	0.443	0.423
4.50	0.920	0.586	0.400	0.415	0.441	0.422
5.00	0.919	0.584	0.399	0.419	0.441	0.421
6.00	0.920	0.583	0.396	0.417	0.438	0.419

Inner channel

Static-pressure ratios at s/l_s of -

0.972
0.592
0.469
0.414
0.388
0.380
0.379
0.377
0.377
0.376
0.376
0.375

Outer channel

Static-pressure ratios at s/l_s of -

NPR	0.972
1.50	0.681
1.81	0.583
2.00	0.551
2.21	0.530
2.50	0.507
3.00	0.456
3.50	0.425
4.00	0.427
4.50	0.427
5.00	0.423
6.00	0.424

Left instrumented spacer

Static-pressure ratios at ϕ, deg, of -

NPR	0	45	90	135	180	225	270	315
1.50	0.849	0.849	0.889	0.935	0.943	0.931	0.892	0.849
1.81	0.834	0.833	0.877	0.928	0.939	0.925	0.881	0.833
2.00	0.832	0.831	0.875	0.928	0.938	0.924	0.879	0.831
2.21	0.833	0.831	0.875	0.928	0.938	0.925	0.880	0.831
2.50	0.833	0.831	0.875	0.928	0.939	0.926	0.879	0.830
3.00	0.835	0.832	0.876	0.929	0.939	0.926	0.880	0.831
3.50	0.836	0.833	0.876	0.930	0.940	0.927	0.880	0.831
4.00	0.835	0.833	0.875	0.929	0.940	0.927	0.879	0.830
4.50	0.837	0.834	0.876	0.930	0.941	0.927	0.880	0.831
5.00	0.838	0.834	0.876	0.931	0.941	0.927	0.880	0.832
6.00	0.838	0.834	0.875	0.931	0.942	0.928	0.880	0.832

Right instrumented spacer

Static-pressure ratios at ϕ, deg, of -

0	45	90	135	180	225	270	315
0.829	0.842	0.889	0.935	0.944	0.929	0.892	0.847
0.809	0.824	0.877	0.928	0.938	0.922	0.880	0.829
0.807	0.823	0.876	0.928	0.938	0.921	0.877	0.827
0.806	0.822	0.876	0.929	0.938	0.921	0.878	0.826
0.808	0.824	0.877	0.929	0.938	0.922	0.878	0.826
0.807	0.824	0.876	0.929	0.939	0.922	0.877	0.826
0.810	0.826	0.877	0.930	0.940	0.923	0.878	0.827
0.811	0.827	0.878	0.929	0.940	0.924	0.879	0.827
0.811	0.828	0.878	0.930	0.941	0.924	0.879	0.828
0.809	0.826	0.877	0.930	0.941	0.923	0.878	0.827
0.809	0.827	0.877	0.930	0.941	0.923	0.878	0.827

Table 54. Static-Pressure Ratios in Nozzle and Instrumented Spacers for Configuration $P_0C_LB_NN_1L$

Inner wall
Static-pressure ratios at s/l_s of -

NPR	0.429	0.858	0.913	0.937	0.956	0.972
1.50	0.921	0.652	0.539	0.536	0.561	0.569
1.81	0.913	0.603	0.454	0.447	0.470	0.465
2.00	0.911	0.596	0.437	0.426	0.450	0.440
2.20	0.911	0.593	0.426	0.413	0.440	0.429
2.49	0.912	0.592	0.422	0.413	0.442	0.428
2.98	0.911	0.591	0.422	0.419	0.447	0.427
3.53	0.911	0.590	0.424	0.428	0.447	0.425
4.01	0.912	0.590	0.421	0.429	0.445	0.423
4.53	0.912	0.589	0.419	0.429	0.443	0.422
4.75	0.912	0.589	0.418	0.429	0.442	0.421

Inner channel
Static-pressure ratios at s/l_s of -

	0.972
1.50	0.596
1.81	0.472
2.00	0.419
2.20	0.388
2.49	0.379
2.98	0.377
3.53	0.377
4.01	0.376
4.53	0.375
4.75	0.375

Outer channel
Static-pressure ratios at s/l_s of -

NPR	0.972
1.50	0.679
1.81	0.576
2.00	0.539
2.20	0.518
2.49	0.490
2.98	0.433
3.53	0.427
4.01	0.426
4.53	0.427
4.75	0.427

Left instrumented spacer
Static-pressure ratios at ϕ, deg, of -

NPR	0	45	90	135	180	225	270	315
1.50	0.829	0.845	0.886	0.930	0.935	0.921	0.889	0.846
1.81	0.811	0.829	0.873	0.923	0.930	0.914	0.878	0.830
2.00	0.809	0.828	0.872	0.922	0.929	0.913	0.876	0.828
2.20	0.808	0.828	0.872	0.923	0.929	0.913	0.877	0.827
2.49	0.808	0.828	0.872	0.923	0.930	0.914	0.877	0.828
2.98	0.808	0.829	0.872	0.924	0.931	0.915	0.877	0.828
3.53	0.808	0.829	0.872	0.924	0.931	0.914	0.876	0.829
4.01	0.808	0.830	0.872	0.924	0.931	0.914	0.877	0.829
4.53	0.807	0.830	0.872	0.924	0.932	0.914	0.877	0.829
4.75	0.807	0.830	0.872	0.924	0.932	0.915	0.878	0.829

Right instrumented spacer
Static-pressure ratios at ϕ, deg, of -

0	45	90	135	180	225	270	315
0.838	0.844	0.880	0.916	0.928	0.927	0.886	0.844
0.821	0.827	0.867	0.908	0.921	0.919	0.874	0.827
0.820	0.826	0.868	0.909	0.922	0.919	0.874	0.826
0.819	0.825	0.867	0.908	0.922	0.919	0.874	0.826
0.819	0.824	0.866	0.907	0.920	0.918	0.873	0.825
0.819	0.826	0.867	0.908	0.922	0.919	0.874	0.826
0.820	0.827	0.870	0.910	0.923	0.920	0.875	0.826
0.820	0.827	0.869	0.909	0.923	0.920	0.875	0.826
0.819	0.826	0.869	0.909	0.923	0.920	0.875	0.826
0.819	0.827	0.869	0.909	0.923	0.920	0.875	0.826

Table 55. Static-Pressure Ratios in Nozzle and Instrumented Spacers for Configuration $P_O C_L B_F N_I T$

Inner wall

Static-pressure ratios at s/l_s of -

NPR	0.429	0.858	0.913	0.937	0.956	0.972
1.50	0.926	0.662	0.524	0.506	0.547	0.560
1.81	0.917	0.616	0.438	0.389	0.447	0.451
2.00	0.917	0.609	0.420	0.354	0.417	0.424
2.21	0.917	0.607	0.413	0.341	0.409	0.416
2.50	0.917	0.604	0.411	0.343	0.416	0.418
3.00	0.917	0.604	0.409	0.345	0.424	0.418
3.51	0.917	0.602	0.408	0.352	0.427	0.417
4.00	0.917	0.601	0.407	0.359	0.425	0.415
4.50	0.918	0.601	0.406	0.363	0.423	0.413
5.00	0.917	0.600	0.406	0.366	0.421	0.411
6.00	0.916	0.598	0.404	0.369	0.419	0.408

Inner channel

Static-pressure ratios at s/l_s of -

0.972
0.596
0.464
0.406
0.385
0.380
0.376
0.374
0.373
0.373
0.372
0.371

Outer channel

Static-pressure ratios at s/l_s of -

NPR	0.972
1.50	0.687
1.81	0.587
2.00	0.555
2.21	0.534
2.50	0.514
3.00	0.464
3.51	0.432
4.00	0.430
4.50	0.430
5.00	0.430
6.00	0.427

Left instrumented spacer

Static-pressure ratios at ϕ, deg, of -

NPR	0	45	90	135	180	225	270	315
1.50	0.846	0.848	0.887	0.931	0.937	0.927	0.891	0.847
1.81	0.829	0.831	0.875	0.923	0.931	0.920	0.878	0.829
2.00	0.828	0.830	0.873	0.922	0.931	0.919	0.876	0.828
2.21	0.828	0.830	0.873	0.922	0.932	0.920	0.876	0.827
2.50	0.828	0.830	0.873	0.922	0.932	0.920	0.876	0.828
3.00	0.830	0.831	0.873	0.922	0.933	0.920	0.877	0.828
3.51	0.831	0.831	0.873	0.923	0.934	0.922	0.877	0.828
4.00	0.832	0.832	0.873	0.923	0.934	0.921	0.877	0.829
4.50	0.833	0.832	0.874	0.924	0.934	0.922	0.878	0.829
5.00	0.833	0.831	0.873	0.924	0.934	0.921	0.877	0.829
6.00	0.834	0.831	0.873	0.923	0.933	0.920	0.877	0.829

Right instrumented spacer

Static-pressure ratios at ϕ, deg, of -

0	45	90	135	180	225	270	315
0.837	0.850	0.896	0.937	0.946	0.934	0.896	0.850
0.818	0.832	0.883	0.930	0.939	0.925	0.883	0.832
0.817	0.831	0.883	0.929	0.939	0.924	0.881	0.830
0.816	0.831	0.881	0.929	0.939	0.925	0.881	0.829
0.816	0.831	0.882	0.929	0.939	0.925	0.880	0.829
0.816	0.832	0.882	0.930	0.940	0.926	0.881	0.830
0.817	0.832	0.882	0.930	0.940	0.926	0.881	0.830
0.817	0.833	0.882	0.930	0.941	0.927	0.882	0.830
0.817	0.833	0.882	0.930	0.941	0.926	0.882	0.830
0.817	0.833	0.882	0.930	0.941	0.926	0.881	0.830
0.816	0.833	0.882	0.930	0.941	0.925	0.881	0.829

Table 56. Static-Pressure Ratios in Nozzle and Instrumented Spacers for Configuration $P_OC_LB_FN_IL$

Inner wall

Static-pressure ratios at s/l_s of -

NPR	0.429	0.858	0.913	0.937	0.956	0.972
1.51	0.912	0.650	0.543	0.540	0.566	0.571
1.80	0.903	0.604	0.465	0.452	0.478	0.471
2.02	0.902	0.594	0.441	0.421	0.448	0.437
2.20	0.902	0.591	0.432	0.410	0.440	0.427
2.50	0.902	0.590	0.428	0.408	0.440	0.426
3.00	0.902	0.589	0.426	0.411	0.443	0.424
3.51	0.903	0.588	0.424	0.418	0.443	0.422
3.99	0.903	0.587	0.426	0.424	0.442	0.421
4.51	0.903	0.586	0.423	0.423	0.440	0.420
4.77	0.903	0.586	0.422	0.422	0.439	0.419

Inner channel

Static-pressure ratios at s/l_s of -

	0.972
	0.598
	0.484
	0.417
	0.388
	0.378
	0.377
	0.376
	0.376
	0.375
	0.375

Outer channel

Static-pressure ratios at s/l_s of -

NPR	0.972
1.51	0.676
1.80	0.578
2.02	0.536
2.20	0.516
2.50	0.485
3.00	0.438
3.51	0.435
3.99	0.436
4.51	0.435
4.77	0.435

Left instrumented spacer

Static-pressure ratios at ϕ, deg, of -

NPR	0	45	90	135	180	225	270	315
1.51	0.824	0.845	0.883	0.924	0.934	0.922	0.890	0.842
1.80	0.808	0.830	0.870	0.917	0.929	0.916	0.880	0.826
2.02	0.805	0.829	0.869	0.916	0.929	0.914	0.879	0.824
2.20	0.804	0.829	0.869	0.917	0.929	0.915	0.879	0.824
2.50	0.805	0.830	0.869	0.918	0.930	0.915	0.879	0.824
3.00	0.805	0.830	0.870	0.918	0.931	0.916	0.879	0.825
3.51	0.806	0.831	0.870	0.919	0.932	0.917	0.880	0.826
3.99	0.806	0.831	0.870	0.919	0.932	0.917	0.879	0.826
4.51	0.805	0.831	0.870	0.919	0.932	0.916	0.879	0.826
4.77	0.805	0.831	0.870	0.919	0.932	0.916	0.879	0.826

Right instrumented spacer

Static-pressure ratios at ϕ, deg, of -

0	45	90	135	180	225	270	315
0.839	0.843	0.889	0.925	0.933	0.927	0.888	0.847
0.823	0.828	0.878	0.918	0.926	0.919	0.878	0.834
0.821	0.826	0.877	0.917	0.926	0.919	0.876	0.831
0.821	0.826	0.877	0.918	0.926	0.919	0.877	0.831
0.821	0.826	0.878	0.918	0.927	0.919	0.877	0.831
0.822	0.827	0.878	0.918	0.927	0.919	0.877	0.831
0.822	0.828	0.878	0.919	0.928	0.919	0.877	0.831
0.822	0.829	0.878	0.919	0.928	0.920	0.878	0.831
0.822	0.828	0.878	0.919	0.928	0.920	0.878	0.831
0.822	0.828	0.877	0.918	0.928	0.919	0.878	0.831

Table 57. Static-Pressure Ratios in Nozzle and Instrumented Spacers for Configuration $P_O C_L B_T N_I T$

Inner wall

Static-pressure ratios at s/l_s of -

NPR	0.429	0.858	0.913	0.937	0.956	0.972
1.50	0.926	0.644	0.520	0.517	0.552	0.560
1.81	0.918	0.598	0.429	0.421	0.461	0.455
2.01	0.917	0.591	0.410	0.395	0.439	0.433
2.21	0.918	0.589	0.402	0.386	0.434	0.427
2.50	0.918	0.588	0.400	0.387	0.438	0.427
3.01	0.919	0.588	0.397	0.392	0.444	0.426
3.53	0.919	0.588	0.396	0.400	0.444	0.424
4.00	0.920	0.588	0.395	0.405	0.441	0.422
4.53	0.920	0.586	0.392	0.408	0.439	0.420
5.00	0.921	0.586	0.390	0.407	0.437	0.419
6.00	0.921	0.584	0.387	0.405	0.434	0.416

Inner channel

Static-pressure ratios at s/l_s of -

	0.972
1.50	0.592
1.81	0.462
2.01	0.404
2.21	0.384
2.50	0.380
3.01	0.377
3.53	0.376
4.00	0.375
4.53	0.374
5.00	0.374
6.00	0.373

Outer channel

Static-pressure ratios at s/l_s of -

NPR	0.972
1.50	0.683
1.81	0.583
2.01	0.552
2.21	0.530
2.50	0.512
3.01	0.452
3.53	0.433
4.00	0.433
4.53	0.432
5.00	0.431
6.00	0.430

Left instrumented spacer

Static-pressure ratios at ϕ, deg, of -

NPR	0	45	90	135	180	225	270	315
1.50	0.848	0.850	0.890	0.939	0.945	0.932	0.893	0.850
1.81	0.833	0.834	0.879	0.933	0.942	0.927	0.882	0.834
2.01	0.832	0.833	0.877	0.933	0.941	0.926	0.880	0.832
2.21	0.832	0.833	0.877	0.933	0.942	0.926	0.880	0.831
2.50	0.833	0.833	0.877	0.933	0.942	0.927	0.880	0.832
3.01	0.835	0.834	0.877	0.934	0.943	0.927	0.881	0.832
3.53	0.836	0.835	0.878	0.935	0.944	0.929	0.882	0.833
4.00	0.837	0.835	0.878	0.935	0.944	0.929	0.882	0.833
4.53	0.838	0.836	0.878	0.935	0.946	0.929	0.882	0.834
5.00	0.838	0.836	0.878	0.936	0.946	0.929	0.883	0.834
6.00	0.839	0.836	0.878	0.936	0.946	0.929	0.882	0.834

Right instrumented spacer

Static-pressure ratios at ϕ, deg, of -

0	45	90	135	180	225	270	315
0.837	0.849	0.895	0.935	0.943	0.935	0.895	0.848
0.821	0.835	0.884	0.929	0.938	0.929	0.885	0.833
0.819	0.833	0.883	0.928	0.938	0.929	0.883	0.830
0.819	0.833	0.884	0.928	0.938	0.930	0.884	0.831
0.819	0.833	0.883	0.928	0.939	0.930	0.884	0.830
0.820	0.834	0.884	0.929	0.940	0.931	0.884	0.831
0.821	0.836	0.885	0.930	0.941	0.932	0.885	0.832
0.821	0.836	0.884	0.930	0.941	0.931	0.885	0.832
0.821	0.835	0.884	0.930	0.941	0.931	0.885	0.831
0.821	0.836	0.884	0.930	0.941	0.931	0.885	0.832
0.820	0.835	0.883	0.929	0.940	0.930	0.884	0.831

Table 58. Static-Pressure Ratios in Nozzle and Instrumented Spacers for Configuration $P_O C_L B_T N_1 L$

Inner wall
Static-pressure ratios at s/l_s of -

NPR	0.429	0.858	0.913	0.937	0.956	0.972
1.50	0.918	0.652	0.550	0.552	0.570	0.576
1.80	0.910	0.604	0.469	0.467	0.481	0.474
2.00	0.909	0.596	0.448	0.443	0.457	0.444
2.21	0.909	0.593	0.439	0.432	0.446	0.431
2.50	0.910	0.592	0.434	0.430	0.446	0.430
3.00	0.910	0.591	0.432	0.434	0.450	0.428
3.51	0.911	0.591	0.432	0.439	0.451	0.427
4.01	0.911	0.590	0.430	0.440	0.449	0.425
4.51	0.910	0.590	0.428	0.440	0.447	0.424
4.76	0.911	0.590	0.429	0.440	0.447	0.424

Inner channel
Static-pressure ratios at s/l_s of -

NPR	0.972
1.50	0.600
1.80	0.482
2.00	0.427
2.21	0.391
2.50	0.381
3.00	0.379
3.51	0.379
4.01	0.377
4.51	0.377
4.76	0.377

Outer channel
Static-pressure ratios at s/l_s of -

NPR	0.972
1.50	0.677
1.80	0.574
2.00	0.536
2.21	0.510
2.50	0.477
3.00	0.433
3.51	0.433
4.01	0.433
4.51	0.433
4.76	0.434

Left instrumented spacer
Static-pressure ratios at ϕ, deg, of -

NPR	0	45	90	135	180	225	270	315
1.50	0.829	0.846	0.885	0.930	0.934	0.922	0.890	0.845
1.80	0.813	0.832	0.873	0.924	0.929	0.915	0.879	0.829
2.00	0.811	0.831	0.871	0.922	0.929	0.914	0.877	0.827
2.21	0.811	0.831	0.872	0.923	0.929	0.914	0.877	0.827
2.50	0.811	0.832	0.872	0.922	0.930	0.914	0.877	0.827
3.00	0.812	0.833	0.872	0.923	0.931	0.916	0.878	0.828
3.51	0.812	0.834	0.873	0.924	0.932	0.916	0.878	0.829
4.01	0.811	0.834	0.873	0.924	0.932	0.916	0.879	0.829
4.51	0.811	0.834	0.872	0.924	0.933	0.916	0.879	0.830
4.76	0.812	0.834	0.873	0.924	0.933	0.916	0.879	0.829

Right instrumented spacer
Static-pressure ratios at ϕ, deg, of -

0	45	90	135	180	225	270	315
0.843	0.847	0.889	0.924	0.933	0.929	0.889	0.847
0.828	0.832	0.879	0.917	0.927	0.922	0.878	0.832
0.826	0.831	0.877	0.915	0.926	0.921	0.876	0.830
0.826	0.831	0.878	0.916	0.928	0.922	0.877	0.830
0.826	0.831	0.878	0.916	0.927	0.921	0.877	0.829
0.826	0.832	0.878	0.916	0.927	0.922	0.877	0.829
0.827	0.832	0.879	0.917	0.928	0.923	0.877	0.830
0.826	0.833	0.878	0.916	0.928	0.922	0.877	0.830
0.826	0.833	0.878	0.917	0.928	0.922	0.877	0.830
0.826	0.833	0.879	0.917	0.929	0.923	0.878	0.830

Table 59. Static-Pressure Ratios in Nozzle and Instrumented Spacers for Configuration $P_0C_FB_NN_1T$

Inner wall

Static-pressure ratios at s/l_s of -

NPR	0.429	0.858	0.913	0.937	0.956	0.972
1.51	0.927	0.647	0.526	0.523	0.553	0.561
1.81	0.919	0.602	0.444	0.434	0.465	0.458
2.01	0.917	0.596	0.425	0.408	0.442	0.434
2.21	0.917	0.593	0.416	0.399	0.436	0.427
2.52	0.917	0.593	0.414	0.400	0.440	0.427
3.00	0.918	0.592	0.412	0.405	0.444	0.425
3.52	0.919	0.594	0.411	0.408	0.443	0.423
4.02	0.919	0.592	0.408	0.413	0.441	0.421
4.51	0.918	0.591	0.408	0.416	0.439	0.420
5.00	0.919	0.590	0.405	0.416	0.438	0.419
5.99	0.919	0.589	0.403	0.415	0.436	0.417

Inner channel

Static-pressure ratios at s/l_s of -

0.972
0.590
0.466
0.410
0.386
0.379
0.377
0.376
0.375
0.374
0.374
0.373

Outer channel

Static-pressure ratios at s/l_s of -

NPR	0.972
1.51	0.679
1.81	0.582
2.01	0.546
2.21	0.527
2.52	0.506
3.00	0.445
3.52	0.427
4.02	0.426
4.51	0.424
5.00	0.424
5.99	0.424

Left instrumented spacer

Static-pressure ratios at ϕ, deg, of -

NPR	0	45	90	135	180	225	270	315
1.51	0.848	0.847	0.889	0.934	0.941	0.929	0.891	0.848
1.81	0.833	0.831	0.877	0.928	0.935	0.922	0.879	0.832
2.01	0.831	0.830	0.875	0.927	0.934	0.921	0.877	0.830
2.21	0.831	0.830	0.875	0.927	0.934	0.921	0.877	0.829
2.52	0.833	0.831	0.876	0.928	0.935	0.921	0.878	0.829
3.00	0.834	0.831	0.876	0.928	0.936	0.922	0.878	0.830
3.52	0.834	0.831	0.876	0.928	0.936	0.923	0.878	0.829
4.02	0.836	0.832	0.876	0.929	0.937	0.923	0.878	0.830
4.51	0.837	0.833	0.876	0.929	0.937	0.923	0.878	0.831
5.00	0.838	0.833	0.876	0.930	0.938	0.924	0.879	0.831
5.99	0.838	0.833	0.876	0.930	0.939	0.924	0.879	0.831

Right instrumented spacer

Static-pressure ratios at ϕ, deg, of -

0	45	90	135	180	225	270	315
0.826	0.842	0.889	0.936	0.945	0.931	0.895	0.847
0.809	0.825	0.877	0.929	0.938	0.922	0.882	0.830
0.808	0.825	0.876	0.928	0.937	0.921	0.880	0.828
0.807	0.824	0.875	0.928	0.937	0.922	0.880	0.827
0.808	0.825	0.876	0.929	0.937	0.922	0.880	0.827
0.808	0.825	0.876	0.929	0.937	0.922	0.880	0.827
0.811	0.827	0.877	0.928	0.937	0.922	0.880	0.828
0.809	0.826	0.876	0.929	0.937	0.921	0.880	0.828
0.808	0.826	0.876	0.928	0.937	0.922	0.880	0.827
0.808	0.826	0.875	0.929	0.938	0.921	0.880	0.828
0.807	0.826	0.875	0.930	0.939	0.922	0.880	0.827

Table 60. Static-Pressure Ratios in Nozzle and Instrumented Spacers for Configuration $P_O C_F B_N N_I L$

Inner wall
Static-pressure ratios at s/l_s of -

NPR	0.429	0.858	0.913	0.937	0.956	0.972
1.51	0.921	0.654	0.538	0.533	0.557	0.564
1.80	0.916	0.608	0.446	0.432	0.463	0.459
2.01	0.915	0.601	0.425	0.402	0.439	0.432
2.19	0.914	0.599	0.421	0.396	0.434	0.427
2.50	0.915	0.597	0.416	0.393	0.438	0.427
3.01	0.914	0.598	0.414	0.395	0.443	0.424
3.52	0.915	0.596	0.412	0.403	0.443	0.422
4.00	0.914	0.596	0.415	0.411	0.441	0.420
4.52	0.915	0.595	0.408	0.409	0.437	0.418
4.77	0.915	0.595	0.407	0.408	0.436	0.417

Inner channel
Static-pressure ratios at s/l_s of -

	0.972
	0.592
	0.469
	0.407
	0.386
	0.378
	0.375
	0.374
	0.374
	0.372
	0.372

Outer channel
Static-pressure ratios at s/l_s of -

NPR	0.972
1.51	0.672
1.80	0.579
2.01	0.539
2.19	0.516
2.50	0.483
3.01	0.430
3.52	0.428
4.00	0.430
4.52	0.429
4.77	0.429

Left instrumented spacer
Static-pressure ratios at ϕ, deg, of -

NPR	0	45	90	135	180	225	270	315
1.51	0.826	0.845	0.886	0.928	0.932	0.919	0.886	0.844
1.80	0.809	0.828	0.874	0.919	0.927	0.912	0.878	0.829
2.01	0.807	0.827	0.872	0.919	0.927	0.911	0.877	0.827
2.19	0.806	0.827	0.872	0.919	0.926	0.912	0.876	0.827
2.50	0.806	0.828	0.872	0.919	0.927	0.912	0.876	0.827
3.01	0.806	0.828	0.872	0.919	0.927	0.912	0.877	0.827
3.52	0.806	0.828	0.872	0.920	0.928	0.913	0.877	0.828
4.00	0.806	0.829	0.872	0.919	0.928	0.913	0.876	0.827
4.52	0.806	0.829	0.872	0.920	0.930	0.914	0.877	0.828
4.77	0.805	0.828	0.872	0.920	0.929	0.913	0.877	0.828

Right instrumented spacer
Static-pressure ratios at ϕ, deg, of -

0	45	90	135	180	225	270	315
0.839	0.843	0.881	0.920	0.931	0.926	0.888	0.846
0.824	0.826	0.865	0.910	0.922	0.918	0.877	0.831
0.821	0.824	0.865	0.910	0.923	0.918	0.876	0.829
0.821	0.825	0.867	0.912	0.923	0.919	0.876	0.829
0.821	0.825	0.867	0.912	0.924	0.920	0.877	0.829
0.821	0.826	0.868	0.913	0.924	0.920	0.877	0.829
0.821	0.827	0.868	0.912	0.924	0.919	0.877	0.829
0.820	0.828	0.870	0.913	0.925	0.919	0.877	0.829
0.820	0.826	0.867	0.912	0.924	0.919	0.877	0.829
0.821	0.827	0.867	0.912	0.924	0.919	0.877	0.829

Table 61. Static-Pressure Ratios in Nozzle and Instrumented Spacers for Configuration $P_OC_FB_FN_1T$

Inner wall

Static-pressure ratios at s/l_s of -

NPR	0.429	0.858	0.913	0.937	0.956	0.972
1.50	0.927	0.649	0.527	0.522	0.553	0.561
1.80	0.919	0.604	0.443	0.431	0.463	0.457
2.00	0.918	0.597	0.423	0.405	0.441	0.433
2.21	0.919	0.596	0.415	0.395	0.434	0.427
2.50	0.919	0.595	0.412	0.396	0.439	0.427
3.01	0.919	0.593	0.410	0.403	0.445	0.425
3.50	0.920	0.593	0.408	0.410	0.444	0.423
4.00	0.919	0.594	0.409	0.413	0.441	0.421
4.51	0.921	0.591	0.404	0.416	0.440	0.420
5.00	0.921	0.591	0.402	0.415	0.438	0.418
6.01	0.921	0.589	0.400	0.414	0.436	0.417

Inner channel

Static-pressure ratios at s/l_s of -

	0.972
	0.592
	0.466
	0.408
	0.384
	0.378
	0.377
	0.374
	0.374
	0.374
	0.374
	0.372

Outer channel

Static-pressure ratios at s/l_s of -

NPR	0.972
1.50	0.683
1.80	0.583
2.00	0.550
2.21	0.528
2.50	0.508
3.01	0.444
3.50	0.430
4.00	0.432
4.51	0.430
5.00	0.429
6.01	0.429

Left instrumented spacer

Static-pressure ratios at ϕ, deg, of -

NPR	0	45	90	135	180	225	270	315
1.50	0.849	0.850	0.890	0.935	0.943	0.930	0.891	0.849
1.80	0.833	0.833	0.878	0.929	0.938	0.923	0.880	0.832
2.00	0.832	0.832	0.877	0.929	0.938	0.923	0.878	0.831
2.21	0.832	0.832	0.877	0.929	0.939	0.923	0.879	0.831
2.50	0.834	0.833	0.877	0.930	0.940	0.924	0.879	0.831
3.01	0.835	0.834	0.878	0.930	0.940	0.924	0.879	0.831
3.50	0.837	0.834	0.878	0.931	0.941	0.925	0.880	0.832
4.00	0.837	0.835	0.878	0.931	0.941	0.925	0.880	0.832
4.51	0.838	0.835	0.878	0.932	0.942	0.926	0.880	0.832
5.00	0.839	0.835	0.878	0.932	0.942	0.926	0.880	0.833
6.01	0.839	0.835	0.878	0.932	0.943	0.927	0.880	0.832

Right instrumented spacer

Static-pressure ratios at ϕ, deg, of -

0	45	90	135	180	225	270	315
0.838	0.848	0.893	0.929	0.937	0.930	0.893	0.846
0.821	0.832	0.881	0.921	0.931	0.924	0.881	0.830
0.818	0.831	0.880	0.920	0.930	0.923	0.880	0.828
0.819	0.831	0.881	0.922	0.931	0.924	0.880	0.828
0.819	0.832	0.881	0.922	0.931	0.925	0.881	0.828
0.819	0.832	0.881	0.922	0.932	0.925	0.881	0.828
0.820	0.833	0.881	0.923	0.933	0.926	0.882	0.829
0.821	0.834	0.882	0.924	0.934	0.927	0.882	0.830
0.820	0.834	0.881	0.923	0.933	0.926	0.882	0.829
0.820	0.834	0.882	0.924	0.934	0.926	0.882	0.829
0.820	0.834	0.881	0.924	0.933	0.926	0.881	0.829

Table 62. Static-Pressure Ratios in Nozzle and Instrumented Spacers for Configuration $P_OC_FB_FN_1L$

Inner wall

Static-pressure ratios at s/l_s of -

NPR	0.429	0.858	0.913	0.937	0.956	0.972
1.51	0.924	0.653	0.529	0.525	0.551	0.561
1.80	0.917	0.610	0.453	0.440	0.467	0.463
2.02	0.915	0.601	0.428	0.409	0.441	0.434
2.21	0.916	0.600	0.421	0.398	0.434	0.427
2.50	0.916	0.599	0.418	0.396	0.438	0.427
3.00	0.916	0.598	0.416	0.402	0.445	0.426
3.52	0.916	0.597	0.415	0.410	0.444	0.422
4.00	0.916	0.596	0.414	0.415	0.441	0.420
4.50	0.916	0.596	0.412	0.416	0.439	0.419
4.77	0.916	0.595	0.412	0.416	0.438	0.418

Inner channel

Static-pressure ratios at s/l_s of -

	0.972
	0.591
	0.473
	0.408
	0.386
	0.379
	0.376
	0.374
	0.374
	0.373
	0.374

Outer channel

Static-pressure ratios at s/l_s of -

NPR	0.972
1.51	0.676
1.80	0.577
2.02	0.535
2.21	0.513
2.50	0.479
3.00	0.434
3.52	0.434
4.00	0.434
4.50	0.434
4.77	0.435

Left instrumented spacer

Static-pressure ratios at ϕ, deg, of -

NPR	0	45	90	135	180	225	270	315
1.51	0.827	0.846	0.887	0.927	0.935	0.921	0.891	0.846
1.80	0.810	0.831	0.876	0.920	0.929	0.914	0.880	0.830
2.02	0.808	0.830	0.874	0.919	0.928	0.912	0.878	0.828
2.21	0.808	0.830	0.874	0.919	0.929	0.913	0.878	0.828
2.50	0.808	0.831	0.874	0.920	0.929	0.914	0.879	0.828
3.00	0.808	0.831	0.874	0.921	0.930	0.915	0.879	0.828
3.52	0.808	0.831	0.874	0.922	0.931	0.915	0.879	0.829
4.00	0.808	0.832	0.875	0.922	0.931	0.915	0.879	0.829
4.50	0.808	0.832	0.875	0.922	0.931	0.915	0.879	0.829
4.77	0.808	0.832	0.875	0.922	0.931	0.915	0.880	0.829

Right instrumented spacer

Static-pressure ratios at ϕ, deg, of -

0	45	90	135	180	225	270	315
0.841	0.846	0.891	0.922	0.934	0.931	0.889	0.847
0.824	0.831	0.881	0.916	0.929	0.924	0.879	0.832
0.822	0.829	0.880	0.914	0.928	0.923	0.876	0.830
0.822	0.829	0.879	0.915	0.929	0.923	0.877	0.830
0.823	0.829	0.880	0.915	0.929	0.924	0.877	0.830
0.823	0.831	0.881	0.915	0.930	0.924	0.877	0.830
0.823	0.831	0.880	0.916	0.930	0.924	0.878	0.830
0.823	0.832	0.881	0.915	0.930	0.925	0.878	0.830
0.823	0.832	0.880	0.915	0.930	0.925	0.878	0.830
0.823	0.832	0.881	0.916	0.930	0.925	0.878	0.830

Table 63. Static-Pressure Ratios in Nozzle and Instrumented Spacers for Configuration $P_OC_FB_TN_1T$

Inner wall

Static-pressure ratios at s/l_s of -

NPR	0.429	0.858	0.913	0.937	0.956	0.972
1.51	0.928	0.649	0.528	0.524	0.553	0.561
1.81	0.920	0.606	0.448	0.438	0.467	0.460
2.02	0.918	0.599	0.430	0.416	0.446	0.436
2.22	0.919	0.596	0.422	0.407	0.441	0.430
2.52	0.919	0.598	0.423	0.411	0.444	0.430
3.01	0.918	0.597	0.422	0.418	0.449	0.428
3.50	0.919	0.598	0.423	0.424	0.448	0.426
4.01	0.919	0.598	0.424	0.430	0.447	0.424
4.53	0.918	0.597	0.422	0.429	0.445	0.423
5.01	0.919	0.596	0.421	0.429	0.444	0.422
6.01	0.918	0.593	0.417	0.428	0.442	0.420

Inner channel

Static-pressure ratios at s/l_s of -

	0.972
	0.593
	0.468
	0.410
	0.388
	0.382
	0.380
	0.378
	0.378
	0.378
	0.377
	0.376

Outer channel

Static-pressure ratios at s/l_s of -

NPR	0.972
1.51	0.682
1.81	0.584
2.02	0.550
2.22	0.529
2.52	0.503
3.01	0.447
3.50	0.436
4.01	0.437
4.53	0.436
5.01	0.436
6.01	0.434

Left instrumented spacer

Static-pressure ratios at ϕ, deg, of -

NPR	0	45	90	135	180	225	270	315
1.51	0.849	0.851	0.891	0.940	0.941	0.929	0.893	0.851
1.81	0.834	0.837	0.879	0.934	0.936	0.923	0.882	0.835
2.02	0.833	0.834	0.878	0.932	0.934	0.922	0.880	0.833
2.22	0.833	0.834	0.878	0.933	0.935	0.922	0.880	0.832
2.52	0.834	0.835	0.877	0.933	0.935	0.923	0.880	0.833
3.01	0.836	0.836	0.878	0.933	0.936	0.924	0.880	0.833
3.50	0.836	0.836	0.878	0.933	0.936	0.924	0.880	0.833
4.01	0.837	0.836	0.878	0.933	0.936	0.925	0.880	0.833
4.53	0.837	0.836	0.878	0.933	0.936	0.925	0.880	0.833
5.01	0.838	0.836	0.878	0.934	0.937	0.925	0.880	0.834
6.01	0.838	0.836	0.877	0.934	0.937	0.925	0.880	0.833

Right instrumented spacer

Static-pressure ratios at ϕ, deg, of -

0	45	90	135	180	225	270	315
0.840	0.850	0.895	0.935	0.939	0.933	0.898	0.849
0.824	0.836	0.884	0.928	0.933	0.926	0.886	0.833
0.822	0.834	0.882	0.927	0.932	0.925	0.885	0.832
0.822	0.834	0.882	0.928	0.933	0.925	0.885	0.832
0.822	0.835	0.882	0.929	0.933	0.925	0.885	0.832
0.822	0.835	0.882	0.929	0.934	0.925	0.885	0.832
0.823	0.836	0.882	0.929	0.934	0.926	0.885	0.832
0.823	0.836	0.883	0.930	0.935	0.926	0.885	0.833
0.823	0.836	0.882	0.930	0.935	0.925	0.885	0.833
0.823	0.836	0.882	0.930	0.936	0.925	0.885	0.832
0.822	0.836	0.882	0.930	0.935	0.924	0.884	0.832

Table 64. Static-Pressure Ratios in Nozzle and Instrumented Spacers for Configuration $P_OC_FB_TN_1L$

Inner wall
Static-pressure ratios at s/l_s of -

NPR	0.429	0.858	0.913	0.937	0.956	0.972
1.51	0.924	0.649	0.530	0.527	0.554	0.560
1.80	0.916	0.605	0.449	0.440	0.467	0.462
1.99	0.916	0.598	0.429	0.414	0.445	0.437
2.21	0.916	0.595	0.416	0.399	0.435	0.427
2.50	0.916	0.594	0.414	0.399	0.439	0.427
3.00	0.915	0.594	0.418	0.409	0.447	0.426
3.48	0.916	0.594	0.412	0.411	0.445	0.423
4.01	0.916	0.593	0.411	0.415	0.442	0.421
4.52	0.916	0.592	0.414	0.421	0.442	0.421
4.77	0.916	0.592	0.408	0.416	0.439	0.418

Inner channel
Static-pressure ratios at s/l_s of -

	0.972
	0.590
	0.473
	0.416
	0.385
	0.379
	0.378
	0.375
	0.374
	0.375
	0.374

Outer channel
Static-pressure ratios at s/l_s of -

NPR	0.972
1.51	0.675
1.80	0.576
1.99	0.539
2.21	0.512
2.50	0.479
3.00	0.435
3.48	0.435
4.01	0.435
4.52	0.437
4.77	0.436

Left instrumented spacer
Static-pressure ratios at ϕ, deg, of -

NPR	0	45	90	135	180	225	270	315
1.51	0.829	0.844	0.888	0.931	0.936	0.920	0.891	0.845
1.80	0.813	0.829	0.876	0.925	0.931	0.914	0.881	0.830
1.99	0.811	0.828	0.875	0.924	0.930	0.912	0.880	0.830
2.21	0.810	0.828	0.875	0.925	0.931	0.913	0.880	0.829
2.50	0.810	0.828	0.875	0.925	0.931	0.913	0.880	0.829
3.00	0.810	0.828	0.876	0.926	0.931	0.913	0.879	0.830
3.48	0.810	0.829	0.876	0.927	0.932	0.914	0.880	0.831
4.01	0.809	0.829	0.876	0.927	0.933	0.914	0.880	0.831
4.52	0.809	0.829	0.876	0.927	0.933	0.914	0.880	0.831
4.77	0.809	0.829	0.876	0.928	0.933	0.914	0.881	0.831

Right instrumented spacer
Static-pressure ratios at ϕ, deg, of -

0	45	90	135	180	225	270	315
0.840	0.849	0.890	0.920	0.933	0.933	0.890	0.843
0.825	0.835	0.881	0.913	0.928	0.927	0.880	0.828
0.823	0.833	0.880	0.913	0.926	0.927	0.878	0.826
0.823	0.833	0.880	0.913	0.928	0.927	0.879	0.826
0.822	0.833	0.880	0.913	0.927	0.927	0.879	0.826
0.822	0.834	0.882	0.914	0.929	0.927	0.880	0.827
0.822	0.834	0.881	0.914	0.929	0.927	0.880	0.826
0.822	0.835	0.881	0.913	0.928	0.927	0.880	0.826
0.822	0.835	0.882	0.914	0.929	0.928	0.880	0.826
0.821	0.835	0.881	0.913	0.928	0.927	0.880	0.826

Table 65. Static-Pressure Ratios in Nozzle and Instrumented Sleeves for Configuration $P_0C_SB_NN_2T$

Inner wall

Static-pressure ratios at s/l_s of -

NPR	0.425	0.860	0.914	0.938	0.957	0.973
1.50	0.877	0.438	0.468	0.516	0.556	0.587
1.80	0.863	0.367	0.327	0.397	0.457	0.476
2.01	0.863	0.357	0.289	0.347	0.429	0.448
2.20	0.863	0.355	0.277	0.336	0.422	0.441
2.50	0.863	0.354	0.274	0.342	0.423	0.440
3.00	0.863	0.352	0.272	0.354	0.424	0.439
3.51	0.863	0.351	0.274	0.368	0.425	0.439
3.99	0.863	0.349	0.275	0.373	0.424	0.438
4.51	0.863	0.347	0.282	0.377	0.425	0.441
5.01	0.863	0.345	0.288	0.377	0.425	0.442
6.01	0.862	0.342	0.301	0.378	0.424	0.440

Inner channel

Static-pressure ratios at s/l_s of -

	0.798	0.886	0.923	0.951
1.50	0.905	0.917	0.859	0.750
1.80	0.894	0.901	0.832	0.701
2.01	0.894	0.898	0.827	0.692
2.20	0.894	0.899	0.827	0.691
2.50	0.894	0.899	0.827	0.691
3.00	0.895	0.900	0.826	0.692
3.51	0.895	0.900	0.827	0.692
3.99	0.896	0.901	0.827	0.694
4.51	0.896	0.901	0.827	0.694
5.01	0.896	0.900	0.826	0.694
6.01	0.897	0.901	0.827	0.695

Middle channel

Static-pressure ratios at s/l_s of -

NPR	0.657	0.809	0.873	0.922	0.964	0.982
1.50	0.914	0.887	0.831	0.734	0.642	0.600
1.80	0.905	0.875	0.811	0.697	0.572	0.473
2.01	0.905	0.875	0.810	0.695	0.568	0.461
2.20	0.906	0.876	0.811	0.694	0.568	0.460
2.50	0.906	0.876	0.810	0.693	0.568	0.459
3.00	0.907	0.876	0.810	0.692	0.567	0.458
3.51	0.907	0.876	0.810	0.691	0.566	0.458
3.99	0.908	0.876	0.809	0.690	0.565	0.457
4.51	0.907	0.876	0.809	0.689	0.564	0.457
5.01	0.907	0.874	0.808	0.688	0.563	0.456
6.01	0.907	0.874	0.807	0.687	0.562	0.455

Outer channel

Static-pressure ratios at s/l_s of -

	0.378	0.659	0.780	0.873	0.951
1.50	0.818	0.771	0.722	0.700	0.690
1.80	0.806	0.726	0.640	0.603	0.595
2.01	0.808	0.721	0.621	0.562	0.557
2.20	0.809	0.720	0.618	0.531	0.534
2.50	0.811	0.720	0.617	0.526	0.469
3.00	0.810	0.719	0.615	0.524	0.461
3.51	0.810	0.719	0.615	0.524	0.461
3.99	0.810	0.719	0.616	0.524	0.462
4.51	0.808	0.718	0.614	0.522	0.460
5.01	0.808	0.718	0.615	0.523	0.461
6.01	0.807	0.717	0.613	0.521	0.460

Left instrumented sleeve

Static-pressure ratios at ϕ, deg, of -

NPR	0	45	90	135	180	225	270	315
1.50	0.778	0.787	0.841	0.898	0.923	0.902	0.843	0.798
1.80	0.756	0.765	0.825	0.889	0.915	0.892	0.827	0.778
2.01	0.754	0.763	0.825	0.889	0.915	0.891	0.825	0.777
2.20	0.754	0.763	0.825	0.889	0.915	0.892	0.826	0.777
2.50	0.755	0.763	0.827	0.890	0.916	0.892	0.826	0.778
3.00	0.755	0.762	0.827	0.891	0.917	0.892	0.826	0.778
3.51	0.755	0.763	0.827	0.890	0.917	0.893	0.826	0.779
3.99	0.755	0.763	0.828	0.891	0.917	0.893	0.825	0.779
4.51	0.755	0.763	0.827	0.891	0.917	0.893	0.826	0.779
5.01	0.755	0.763	0.827	0.891	0.917	0.893	0.825	0.779
6.01	0.755	0.763	0.828	0.891	0.918	0.893	0.825	0.779

Right instrumented sleeve

Static-pressure ratios at ϕ, deg, of -

	0	45	90	135	180	225	270	315
1.50	0.806	0.808	0.841	0.897	0.918	0.900	0.843	0.800
1.80	0.786	0.787	0.824	0.886	0.910	0.889	0.825	0.778
2.01	0.785	0.785	0.823	0.886	0.910	0.888	0.824	0.775
2.20	0.785	0.785	0.823	0.886	0.910	0.889	0.824	0.775
2.50	0.786	0.785	0.823	0.887	0.911	0.890	0.824	0.775
3.00	0.787	0.786	0.823	0.889	0.912	0.891	0.825	0.776
3.51	0.787	0.787	0.824	0.890	0.914	0.891	0.825	0.776
3.99	0.788	0.787	0.825	0.890	0.914	0.892	0.825	0.776
4.51	0.788	0.787	0.825	0.890	0.914	0.891	0.825	0.776
5.01	0.788	0.788	0.825	0.890	0.914	0.892	0.825	0.775
6.01	0.787	0.787	0.825	0.890	0.914	0.891	0.825	0.775

Table 66. Static-Pressure Ratios in Nozzle and Instrumented Sleeves for Configuration $P_O C_S B_N N_2 L$

Inner wall

Static-pressure ratios at s/l_s of -

NPR	0.425	0.860	0.914	0.938	0.957	0.973
1.50	0.873	0.475	0.504	0.534	0.564	0.593
1.80	0.857	0.391	0.388	0.433	0.462	0.478
2.00	0.856	0.380	0.358	0.409	0.442	0.451
2.20	0.856	0.377	0.353	0.407	0.439	0.446
2.50	0.856	0.376	0.354	0.412	0.439	0.446
2.99	0.857	0.374	0.352	0.418	0.441	0.445
3.50	0.857	0.373	0.358	0.422	0.440	0.444
4.00	0.857	0.369	0.362	0.422	0.438	0.443
4.51	0.856	0.367	0.371	0.420	0.437	0.443
4.76	0.856	0.366	0.374	0.420	0.437	0.443

Inner channel

Static-pressure ratios at s/l_s of -

0.798	0.886	0.923	0.951
0.893	0.893	0.838	0.735
0.880	0.874	0.806	0.678
0.880	0.871	0.801	0.668
0.878	0.868	0.796	0.665
0.877	0.863	0.791	0.659
0.880	0.867	0.795	0.663
0.880	0.866	0.793	0.662
0.881	0.869	0.797	0.667
0.882	0.869	0.796	0.667
0.881	0.867	0.794	0.666

Middle channel

Static-pressure ratios at s/l_s of -

NPR	0.657	0.809	0.873	0.922	0.964	0.982
1.50	0.901	0.875	0.820	0.728	0.643	0.604
1.80	0.889	0.859	0.795	0.684	0.563	0.468
2.00	0.890	0.858	0.795	0.682	0.559	0.455
2.20	0.889	0.858	0.794	0.681	0.558	0.453
2.50	0.889	0.859	0.794	0.680	0.558	0.451
2.99	0.889	0.858	0.794	0.679	0.557	0.451
3.50	0.889	0.858	0.794	0.678	0.556	0.450
4.00	0.889	0.857	0.793	0.677	0.555	0.449
4.51	0.889	0.857	0.792	0.676	0.554	0.449
4.76	0.889	0.857	0.792	0.675	0.554	0.448

Outer channel

Static-pressure ratios at s/l_s of -

0.378	0.659	0.780	0.873	0.951
0.815	0.770	0.717	0.690	0.685
0.800	0.726	0.629	0.585	0.584
0.801	0.720	0.612	0.535	0.548
0.802	0.720	0.609	0.513	0.503
0.802	0.721	0.612	0.513	0.449
0.805	0.720	0.609	0.511	0.447
0.804	0.719	0.610	0.512	0.448
0.804	0.718	0.607	0.509	0.446
0.803	0.717	0.608	0.509	0.447
0.803	0.717	0.608	0.510	0.448

Left instrumented sleeve

Static-pressure ratios at ϕ, deg, of -

NPR	0	45	90	135	180	225	270	315
1.50	0.782	0.788	0.836	0.894	0.917	0.897	0.840	0.798
1.80	0.762	0.766	0.820	0.884	0.910	0.887	0.824	0.778
2.00	0.761	0.764	0.820	0.885	0.910	0.887	0.823	0.777
2.20	0.760	0.763	0.819	0.884	0.909	0.887	0.823	0.777
2.50	0.761	0.763	0.820	0.885	0.910	0.887	0.822	0.778
2.99	0.762	0.763	0.821	0.887	0.911	0.888	0.823	0.779
3.50	0.762	0.763	0.821	0.887	0.912	0.888	0.823	0.779
4.00	0.761	0.762	0.821	0.887	0.912	0.888	0.824	0.779
4.51	0.761	0.762	0.821	0.887	0.911	0.888	0.823	0.779
4.76	0.761	0.762	0.821	0.887	0.912	0.888	0.823	0.779

Right instrumented sleeve

Static-pressure ratios at ϕ, deg, of -

0	45	90	135	180	225	270	315
0.814	0.810	0.835	0.896	0.914	0.895	0.838	0.801
0.796	0.791	0.817	0.885	0.907	0.884	0.820	0.780
0.796	0.789	0.815	0.884	0.906	0.884	0.818	0.778
0.796	0.789	0.815	0.885	0.906	0.883	0.818	0.778
0.798	0.790	0.815	0.886	0.907	0.885	0.819	0.779
0.799	0.790	0.816	0.887	0.907	0.884	0.818	0.779
0.800	0.791	0.816	0.887	0.908	0.884	0.818	0.779
0.799	0.791	0.816	0.887	0.908	0.884	0.818	0.779
0.800	0.791	0.817	0.888	0.908	0.884	0.818	0.779
0.800	0.791	0.816	0.888	0.907	0.884	0.818	0.778

Table 67. Static-Pressure Ratios in Nozzle and Instrumented Sleeves for Configuration $P_0C_SB_FN_2T$

Inner wall

Static-pressure ratios at s/l_s of -

NPR	0.425	0.860	0.914	0.938	0.957	0.973
1.51	0.876	0.433	0.462	0.512	0.553	0.585
1.80	0.862	0.365	0.323	0.395	0.458	0.479
2.00	0.861	0.354	0.282	0.340	0.425	0.447
2.20	0.862	0.350	0.266	0.320	0.414	0.438
2.51	0.862	0.350	0.259	0.321	0.412	0.435
3.01	0.862	0.348	0.256	0.334	0.416	0.435
3.51	0.862	0.347	0.256	0.346	0.418	0.434
4.00	0.861	0.346	0.259	0.357	0.416	0.434
4.49	0.861	0.344	0.259	0.363	0.418	0.437
5.01	0.861	0.342	0.263	0.363	0.418	0.439
6.00	0.860	0.339	0.276	0.364	0.417	0.438

Inner channel

Static-pressure ratios at s/l_s of -

0.798	0.886	0.923	0.951
0.902	0.913	0.854	0.747
0.891	0.902	0.832	0.702
0.890	0.899	0.828	0.693
0.890	0.899	0.827	0.692
0.891	0.899	0.827	0.692
0.891	0.900	0.827	0.693
0.892	0.901	0.828	0.694
0.891	0.900	0.826	0.693
0.892	0.901	0.827	0.695
0.892	0.901	0.827	0.696
0.892	0.901	0.827	0.697

Middle channel

Static-pressure ratios at s/l_s of -

NPR	0.657	0.809	0.873	0.922	0.964	0.982
1.51	0.910	0.883	0.826	0.730	0.639	0.597
1.80	0.901	0.871	0.806	0.692	0.569	0.471
2.00	0.901	0.871	0.806	0.691	0.566	0.460
2.20	0.902	0.872	0.806	0.691	0.566	0.458
2.51	0.903	0.872	0.806	0.689	0.565	0.457
3.01	0.903	0.873	0.807	0.690	0.565	0.457
3.51	0.904	0.873	0.807	0.689	0.565	0.457
4.00	0.903	0.872	0.805	0.687	0.563	0.455
4.49	0.904	0.872	0.806	0.687	0.563	0.456
5.01	0.904	0.872	0.805	0.686	0.562	0.455
6.00	0.904	0.872	0.805	0.685	0.561	0.454

Outer channel

Static-pressure ratios at s/l_s of -

0.378	0.659	0.780	0.873	0.951
0.821	0.776	0.722	0.695	0.686
0.807	0.732	0.648	0.600	0.591
0.807	0.727	0.633	0.561	0.554
0.807	0.725	0.629	0.542	0.521
0.807	0.724	0.628	0.539	0.477
0.807	0.722	0.625	0.536	0.473
0.806	0.721	0.624	0.536	0.473
0.803	0.721	0.624	0.534	0.472
0.804	0.718	0.621	0.531	0.470
0.802	0.719	0.622	0.531	0.471
0.802	0.716	0.618	0.528	0.468

Left instrumented sleeve

Static-pressure ratios at ϕ, deg, of -

NPR	0	45	90	135	180	225	270	315
1.51	0.774	0.785	0.840	0.897	0.921	0.900	0.839	0.794
1.80	0.752	0.762	0.824	0.888	0.914	0.890	0.824	0.775
2.00	0.751	0.760	0.824	0.887	0.914	0.889	0.823	0.773
2.20	0.751	0.759	0.824	0.888	0.914	0.890	0.823	0.774
2.51	0.751	0.759	0.826	0.889	0.915	0.890	0.824	0.775
3.01	0.752	0.759	0.826	0.889	0.915	0.891	0.824	0.775
3.51	0.753	0.759	0.827	0.890	0.916	0.891	0.824	0.776
4.00	0.751	0.760	0.827	0.890	0.916	0.891	0.823	0.775
4.49	0.753	0.760	0.826	0.890	0.916	0.891	0.824	0.776
5.01	0.752	0.760	0.827	0.890	0.916	0.891	0.824	0.776
6.00	0.752	0.760	0.827	0.890	0.916	0.891	0.823	0.777

Right instrumented sleeve

Static-pressure ratios at ϕ, deg, of -

0	45	90	135	180	225	270	315
0.791	0.810	0.839	0.894	0.913	0.894	0.835	0.781
0.770	0.788	0.822	0.883	0.905	0.883	0.818	0.759
0.768	0.786	0.819	0.882	0.904	0.882	0.816	0.756
0.768	0.785	0.819	0.882	0.905	0.882	0.816	0.756
0.769	0.786	0.819	0.883	0.905	0.883	0.815	0.755
0.770	0.787	0.819	0.884	0.906	0.883	0.815	0.755
0.770	0.788	0.820	0.883	0.906	0.884	0.815	0.754
0.771	0.788	0.820	0.884	0.907	0.884	0.815	0.755
0.770	0.788	0.819	0.883	0.906	0.883	0.812	0.752
0.771	0.788	0.820	0.884	0.907	0.885	0.815	0.755
0.770	0.787	0.821	0.884	0.907	0.884	0.814	0.755

Table 68. Static-Pressure Ratios in Nozzle and Instrumented Sleeves for Configuration $P_0C_SB_FN_2L$

Inner wall
Static-pressure ratios at s/l_s of -

NPR	0.425	0.860	0.914	0.938	0.957	0.973
1.51	0.871	0.476	0.504	0.533	0.562	0.589
1.80	0.857	0.397	0.396	0.438	0.465	0.481
2.01	0.854	0.388	0.375	0.420	0.445	0.453
2.20	0.854	0.383	0.368	0.415	0.441	0.447
2.50	0.855	0.378	0.357	0.413	0.441	0.446
3.01	0.856	0.374	0.354	0.419	0.442	0.446
3.51	0.856	0.372	0.356	0.421	0.440	0.445
4.00	0.854	0.370	0.363	0.421	0.438	0.443
4.49	0.855	0.367	0.370	0.420	0.437	0.443
4.76	0.855	0.365	0.371	0.419	0.437	0.443

Inner channel
Static-pressure ratios at s/l_s of -

0.798	0.886	0.923	0.951
0.886	0.876	0.819	0.717
0.876	0.857	0.789	0.662
0.870	0.847	0.776	0.645
0.873	0.849	0.776	0.645
0.875	0.854	0.782	0.651
0.878	0.857	0.785	0.655
0.879	0.860	0.787	0.657
0.878	0.859	0.786	0.657
0.881	0.863	0.790	0.662
0.880	0.862	0.789	0.662

Middle channel
Static-pressure ratios at s/l_s of -

NPR	0.657	0.809	0.873	0.922	0.964	0.982
1.51	0.895	0.870	0.815	0.723	0.638	0.600
1.80	0.885	0.856	0.792	0.681	0.560	0.467
2.01	0.883	0.854	0.790	0.677	0.554	0.451
2.20	0.884	0.854	0.790	0.677	0.554	0.449
2.50	0.885	0.855	0.791	0.677	0.555	0.448
3.01	0.886	0.855	0.791	0.677	0.554	0.448
3.51	0.886	0.855	0.790	0.675	0.553	0.447
4.00	0.885	0.854	0.789	0.674	0.552	0.447
4.49	0.886	0.854	0.789	0.673	0.552	0.446
4.76	0.886	0.853	0.789	0.672	0.551	0.446

Outer channel
Static-pressure ratios at s/l_s of -

0.378	0.659	0.780	0.873	0.951
0.808	0.767	0.711	0.679	0.677
0.791	0.727	0.636	0.576	0.576
0.787	0.720	0.619	0.530	0.532
0.788	0.718	0.615	0.519	0.481
0.792	0.718	0.614	0.517	0.452
0.794	0.718	0.613	0.516	0.453
0.795	0.718	0.612	0.515	0.452
0.794	0.717	0.612	0.514	0.452
0.795	0.717	0.611	0.513	0.451
0.795	0.717	0.611	0.513	0.452

Left instrumented sleeve
Static-pressure ratios at ϕ, deg, of -

NPR	0	45	90	135	180	225	270	315
1.51	0.783	0.787	0.834	0.892	0.915	0.896	0.836	0.795
1.80	0.764	0.767	0.819	0.882	0.909	0.887	0.821	0.777
2.01	0.762	0.764	0.816	0.881	0.907	0.885	0.818	0.775
2.20	0.762	0.763	0.817	0.881	0.908	0.886	0.818	0.775
2.50	0.763	0.763	0.818	0.882	0.909	0.887	0.820	0.775
3.01	0.764	0.763	0.819	0.883	0.909	0.888	0.821	0.776
3.51	0.763	0.763	0.820	0.884	0.910	0.888	0.822	0.777
4.00	0.762	0.762	0.818	0.883	0.909	0.887	0.820	0.776
4.49	0.763	0.762	0.819	0.883	0.910	0.888	0.822	0.776
4.76	0.763	0.761	0.819	0.883	0.910	0.887	0.821	0.776

Right instrumented sleeve
Static-pressure ratios at ϕ, deg, of -

0	45	90	135	180	225	270	315
0.817	0.805	0.831	0.889	0.899	0.870	0.824	0.805
0.799	0.786	0.813	0.878	0.888	0.855	0.804	0.784
0.799	0.785	0.810	0.878	0.892	0.860	0.802	0.780
0.798	0.783	0.810	0.878	0.891	0.860	0.802	0.779
0.796	0.782	0.810	0.877	0.889	0.855	0.800	0.778
0.798	0.782	0.810	0.878	0.890	0.855	0.801	0.779
0.798	0.783	0.810	0.878	0.889	0.854	0.800	0.778
0.798	0.783	0.810	0.878	0.890	0.856	0.801	0.778
0.798	0.784	0.812	0.880	0.891	0.858	0.801	0.779
0.798	0.783	0.812	0.879	0.891	0.856	0.800	0.778

Table 69. Static-Pressure Ratios in Nozzle and Instrumented Sleeves for Configuration $P_0C_MB_NN_2T$

Inner wall

Static-pressure ratios at s/l_s of -

NPR	0.425	0.860	0.914	0.938	0.957	0.973
1.51	0.872	0.443	0.474	0.521	0.559	0.588
1.80	0.857	0.366	0.344	0.413	0.460	0.479
2.00	0.855	0.353	0.306	0.368	0.432	0.448
2.20	0.856	0.349	0.287	0.348	0.421	0.438
2.50	0.855	0.346	0.281	0.351	0.420	0.437
3.00	0.856	0.344	0.279	0.360	0.420	0.436
3.50	0.856	0.342	0.280	0.368	0.420	0.436
4.00	0.856	0.340	0.285	0.373	0.420	0.436
4.50	0.855	0.338	0.293	0.376	0.422	0.439
5.01	0.855	0.336	0.299	0.375	0.422	0.440
5.97	0.854	0.333	0.308	0.376	0.420	0.439

Inner channel

Static-pressure ratios at s/l_s of -

0.798	0.886	0.923	0.951
0.902	0.916	0.858	0.751
0.890	0.902	0.832	0.703
0.889	0.898	0.828	0.694
0.890	0.898	0.827	0.692
0.889	0.899	0.828	0.693
0.890	0.901	0.829	0.695
0.890	0.902	0.830	0.696
0.891	0.902	0.830	0.697
0.891	0.903	0.830	0.698
0.892	0.902	0.830	0.698
0.892	0.902	0.829	0.699

Middle channel

Static-pressure ratios at s/l_s of -

NPR	0.657	0.809	0.873	0.922	0.964	0.982
1.51	0.912	0.888	0.832	0.736	0.643	0.601
1.80	0.903	0.876	0.812	0.698	0.573	0.475
2.00	0.902	0.875	0.811	0.696	0.569	0.463
2.20	0.903	0.875	0.811	0.695	0.568	0.460
2.50	0.904	0.876	0.811	0.695	0.568	0.459
3.00	0.904	0.876	0.811	0.694	0.568	0.459
3.50	0.905	0.877	0.811	0.693	0.567	0.459
4.00	0.906	0.876	0.811	0.692	0.566	0.458
4.50	0.906	0.876	0.811	0.692	0.565	0.458
5.01	0.906	0.875	0.810	0.690	0.564	0.457
5.97	0.905	0.874	0.808	0.689	0.562	0.456

Outer channel

Static-pressure ratios at s/l_s of -

0.378	0.659	0.780	0.873	0.951
0.810	0.766	0.722	0.701	0.691
0.794	0.717	0.639	0.612	0.600
0.792	0.710	0.609	0.570	0.563
0.795	0.709	0.605	0.533	0.539
0.794	0.706	0.600	0.511	0.487
0.794	0.706	0.599	0.509	0.450
0.794	0.705	0.598	0.507	0.447
0.794	0.705	0.598	0.507	0.448
0.793	0.704	0.597	0.506	0.447
0.793	0.704	0.597	0.506	0.448
0.792	0.703	0.597	0.505	0.448

Left instrumented sleeve

Static-pressure ratios at ϕ, deg, of -

NPR	0	45	90	135	180	225	270	315
1.51	0.776	0.786	0.836	0.894	0.919	0.898	0.839	0.795
1.80	0.753	0.763	0.819	0.884	0.911	0.887	0.823	0.775
2.00	0.751	0.761	0.818	0.883	0.909	0.886	0.822	0.773
2.20	0.751	0.761	0.819	0.884	0.911	0.887	0.821	0.773
2.50	0.751	0.761	0.819	0.884	0.911	0.887	0.821	0.774
3.00	0.752	0.761	0.820	0.885	0.912	0.887	0.822	0.774
3.50	0.752	0.761	0.821	0.885	0.913	0.888	0.822	0.775
4.00	0.751	0.761	0.821	0.886	0.913	0.888	0.822	0.775
4.50	0.752	0.761	0.820	0.886	0.913	0.888	0.822	0.775
5.01	0.751	0.761	0.821	0.886	0.913	0.888	0.821	0.775
5.97	0.751	0.761	0.820	0.886	0.912	0.887	0.821	0.775

Right instrumented sleeve

Static-pressure ratios at ϕ, deg, of -

0	45	90	135	180	225	270	315
0.806	0.804	0.839	0.896	0.918	0.899	0.842	0.799
0.784	0.783	0.821	0.884	0.909	0.887	0.824	0.776
0.783	0.780	0.818	0.883	0.907	0.886	0.821	0.773
0.784	0.780	0.819	0.885	0.909	0.887	0.822	0.774
0.783	0.781	0.818	0.884	0.909	0.886	0.821	0.774
0.785	0.781	0.819	0.885	0.910	0.887	0.822	0.774
0.785	0.781	0.819	0.886	0.910	0.887	0.822	0.774
0.785	0.781	0.819	0.886	0.911	0.888	0.822	0.774
0.785	0.782	0.819	0.886	0.910	0.887	0.822	0.774
0.785	0.782	0.819	0.886	0.911	0.888	0.822	0.774
0.784	0.781	0.819	0.885	0.910	0.887	0.821	0.773

Table 70. Static-Pressure Ratios in Nozzle and Instrumented Sleeves for Configuration $P_O C_M B_N N_2 L$

Inner wall

Static-pressure ratios at s/l_s of -

NPR	0.425	0.860	0.914	0.938	0.957	0.973
1.50	0.863	0.485	0.512	0.541	0.569	0.595
1.80	0.847	0.398	0.405	0.444	0.468	0.484
2.00	0.844	0.382	0.372	0.416	0.441	0.452
2.19	0.844	0.377	0.365	0.411	0.436	0.445
2.50	0.844	0.376	0.364	0.413	0.435	0.444
3.01	0.844	0.373	0.367	0.419	0.436	0.444
3.51	0.844	0.372	0.373	0.421	0.435	0.443
4.00	0.844	0.369	0.381	0.421	0.434	0.443
4.50	0.843	0.367	0.387	0.421	0.434	0.442
4.75	0.843	0.365	0.388	0.420	0.434	0.442

Inner channel

Static-pressure ratios at s/l_s of -

0.798	0.886	0.923	0.951
0.891	0.897	0.842	0.739
0.879	0.880	0.813	0.687
0.877	0.877	0.807	0.676
0.876	0.876	0.806	0.675
0.876	0.877	0.807	0.675
0.878	0.878	0.807	0.677
0.878	0.876	0.805	0.675
0.879	0.879	0.807	0.678
0.879	0.878	0.807	0.679
0.879	0.880	0.808	0.680

Middle channel

Static-pressure ratios at s/l_s of -

NPR	0.657	0.809	0.873	0.922	0.964	0.982
1.50	0.899	0.874	0.819	0.728	0.643	0.604
1.80	0.887	0.858	0.794	0.683	0.562	0.471
2.00	0.887	0.857	0.793	0.680	0.557	0.454
2.19	0.886	0.857	0.792	0.680	0.557	0.452
2.50	0.887	0.857	0.793	0.680	0.557	0.450
3.01	0.887	0.857	0.792	0.678	0.556	0.450
3.51	0.887	0.856	0.791	0.676	0.555	0.449
4.00	0.887	0.856	0.791	0.676	0.554	0.448
4.50	0.887	0.856	0.791	0.674	0.553	0.448
4.75	0.887	0.855	0.790	0.674	0.553	0.448

Outer channel

Static-pressure ratios at s/l_s of -

0.378	0.659	0.780	0.873	0.951
0.809	0.764	0.715	0.691	0.685
0.792	0.716	0.626	0.593	0.590
0.791	0.709	0.603	0.542	0.550
0.792	0.707	0.598	0.508	0.523
0.793	0.706	0.597	0.501	0.446
0.792	0.705	0.596	0.501	0.439
0.791	0.705	0.597	0.502	0.440
0.791	0.704	0.596	0.500	0.439
0.790	0.704	0.595	0.499	0.439
0.790	0.703	0.595	0.499	0.439

Left instrumented sleeve

Static-pressure ratios at ϕ, deg, of -

NPR	0	45	90	135	180	225	270	315
1.50	0.779	0.784	0.831	0.890	0.913	0.893	0.838	0.795
1.80	0.756	0.762	0.813	0.879	0.904	0.883	0.821	0.775
2.00	0.754	0.759	0.812	0.878	0.904	0.881	0.820	0.773
2.19	0.754	0.758	0.812	0.878	0.904	0.881	0.819	0.773
2.50	0.754	0.757	0.813	0.879	0.905	0.882	0.820	0.773
3.01	0.754	0.757	0.813	0.880	0.906	0.883	0.820	0.774
3.51	0.754	0.757	0.813	0.880	0.906	0.882	0.820	0.774
4.00	0.754	0.757	0.813	0.881	0.906	0.883	0.820	0.775
4.50	0.754	0.756	0.813	0.880	0.906	0.883	0.820	0.776
4.75	0.754	0.756	0.813	0.881	0.906	0.883	0.820	0.775

Right instrumented sleeve

Static-pressure ratios at ϕ, deg, of -

0	45	90	135	180	225	270	315
0.812	0.807	0.831	0.892	0.912	0.892	0.836	0.799
0.794	0.787	0.812	0.880	0.902	0.880	0.818	0.777
0.792	0.784	0.810	0.879	0.901	0.880	0.816	0.774
0.792	0.784	0.809	0.879	0.901	0.879	0.815	0.774
0.794	0.784	0.810	0.880	0.902	0.879	0.815	0.774
0.794	0.785	0.810	0.880	0.903	0.880	0.816	0.774
0.794	0.785	0.810	0.881	0.903	0.881	0.817	0.775
0.795	0.785	0.810	0.881	0.903	0.880	0.816	0.775
0.795	0.785	0.810	0.881	0.903	0.880	0.816	0.775
0.795	0.784	0.809	0.881	0.903	0.880	0.816	0.774

Table 71. Static-Pressure Ratios in Nozzle and Instrumented Sleeves for Configuration $P_0C_MB_FN_2T$

Inner wall

Static-pressure ratios at s/l_s of -

NPR	0.425	0.860	0.914	0.938	0.957	0.973
1.51	0.871	0.431	0.458	0.518	0.560	0.592
1.80	0.856	0.361	0.336	0.409	0.461	0.485
2.00	0.855	0.348	0.293	0.355	0.422	0.444
2.20	0.854	0.342	0.268	0.325	0.404	0.428
2.51	0.855	0.340	0.249	0.307	0.392	0.419
3.00	0.854	0.338	0.243	0.313	0.391	0.417
3.50	0.854	0.337	0.245	0.325	0.393	0.417
4.00	0.854	0.335	0.246	0.333	0.394	0.419
4.50	0.854	0.333	0.251	0.341	0.398	0.423
5.00	0.854	0.332	0.259	0.344	0.400	0.426
6.00	0.854	0.328	0.271	0.348	0.402	0.428

Inner channel

Static-pressure ratios at s/l_s of -

0.798	0.886	0.923	0.951
0.897	0.916	0.859	0.753
0.884	0.903	0.836	0.707
0.885	0.900	0.831	0.698
0.884	0.900	0.830	0.696
0.884	0.900	0.830	0.696
0.886	0.901	0.829	0.697
0.886	0.901	0.830	0.697
0.886	0.902	0.830	0.698
0.886	0.902	0.830	0.699
0.887	0.901	0.829	0.699
0.888	0.901	0.829	0.699

Middle channel

Static-pressure ratios at s/l_s of -

NPR	0.657	0.809	0.873	0.922	0.964	0.982
1.51	0.909	0.885	0.829	0.734	0.642	0.602
1.80	0.899	0.872	0.807	0.694	0.569	0.473
2.00	0.899	0.871	0.807	0.692	0.566	0.460
2.20	0.899	0.872	0.807	0.691	0.565	0.458
2.51	0.900	0.872	0.807	0.691	0.566	0.457
3.00	0.901	0.873	0.808	0.691	0.565	0.457
3.50	0.902	0.873	0.808	0.690	0.565	0.457
4.00	0.903	0.874	0.809	0.690	0.564	0.457
4.50	0.903	0.874	0.808	0.689	0.563	0.456
5.00	0.903	0.873	0.807	0.688	0.562	0.455
6.00	0.903	0.873	0.807	0.687	0.561	0.455

Outer channel

Static-pressure ratios at s/l_s of -

0.378	0.659	0.780	0.873	0.951
0.813	0.773	0.726	0.701	0.691
0.795	0.725	0.649	0.608	0.597
0.796	0.720	0.629	0.569	0.559
0.795	0.717	0.624	0.543	0.532
0.796	0.716	0.621	0.534	0.485
0.794	0.713	0.618	0.530	0.470
0.794	0.712	0.616	0.529	0.468
0.793	0.711	0.614	0.527	0.467
0.792	0.709	0.612	0.524	0.465
0.791	0.709	0.611	0.523	0.464
0.790	0.707	0.608	0.520	0.462

Left instrumented sleeve

Static-pressure ratios at ϕ, deg, of -

NPR	0	45	90	135	180	225	270	315
1.51	0.772	0.782	0.836	0.892	0.916	0.895	0.837	0.792
1.80	0.748	0.758	0.819	0.881	0.908	0.884	0.821	0.772
2.00	0.746	0.756	0.820	0.881	0.908	0.884	0.819	0.770
2.20	0.745	0.755	0.819	0.881	0.908	0.884	0.819	0.770
2.51	0.746	0.755	0.820	0.882	0.909	0.884	0.820	0.771
3.00	0.747	0.756	0.820	0.882	0.909	0.885	0.820	0.772
3.50	0.747	0.756	0.821	0.883	0.910	0.885	0.820	0.772
4.00	0.747	0.756	0.821	0.883	0.911	0.886	0.820	0.773
4.50	0.747	0.757	0.821	0.883	0.910	0.886	0.820	0.773
5.00	0.748	0.757	0.821	0.883	0.910	0.886	0.820	0.773
6.00	0.748	0.757	0.821	0.884	0.911	0.886	0.820	0.773

Right instrumented sleeve

Static-pressure ratios at ϕ, deg, of -

0	45	90	135	180	225	270	315
0.796	0.803	0.840	0.896	0.916	0.895	0.842	0.796
0.776	0.781	0.822	0.885	0.908	0.884	0.823	0.773
0.774	0.779	0.820	0.884	0.907	0.883	0.822	0.771
0.774	0.778	0.819	0.885	0.907	0.883	0.821	0.770
0.776	0.778	0.820	0.885	0.908	0.883	0.821	0.770
0.775	0.780	0.820	0.886	0.908	0.884	0.821	0.769
0.776	0.780	0.820	0.886	0.909	0.884	0.821	0.769
0.775	0.780	0.821	0.886	0.909	0.884	0.821	0.769
0.775	0.780	0.821	0.886	0.909	0.884	0.820	0.768
0.775	0.780	0.821	0.886	0.909	0.884	0.820	0.768
0.774	0.780	0.821	0.886	0.909	0.884	0.819	0.767

Table 72. Static-Pressure Ratios in Nozzle and Instrumented Sleeves for Configuration $P_O C_M B_F N_2 L$

Inner wall

Static-pressure ratios at s/l_s of -

NPR	0.425	0.860	0.914	0.938	0.957	0.973
1.50	0.860	0.502	0.528	0.553	0.574	0.598
1.81	0.843	0.415	0.430	0.459	0.474	0.489
2.00	0.840	0.399	0.405	0.436	0.450	0.459
2.20	0.840	0.393	0.397	0.430	0.442	0.449
2.50	0.841	0.388	0.393	0.430	0.442	0.448
3.00	0.841	0.385	0.395	0.433	0.442	0.448
3.52	0.841	0.381	0.396	0.433	0.441	0.447
4.00	0.840	0.378	0.401	0.431	0.438	0.444
4.50	0.840	0.374	0.404	0.430	0.438	0.444
4.75	0.840	0.372	0.404	0.429	0.438	0.444

Inner channel

Static-pressure ratios at s/l_s of -

0.798	0.886	0.923	0.951
0.890	0.874	0.819	0.718
0.874	0.854	0.787	0.662
0.873	0.849	0.779	0.651
0.872	0.852	0.781	0.652
0.874	0.856	0.786	0.656
0.876	0.860	0.789	0.660
0.877	0.864	0.792	0.664
0.872	0.855	0.784	0.656
0.875	0.862	0.790	0.662
0.878	0.867	0.796	0.669

Middle channel

Static-pressure ratios at s/l_s of -

NPR	0.657	0.809	0.873	0.922	0.964	0.982
1.50	0.892	0.868	0.813	0.721	0.637	0.600
1.81	0.880	0.850	0.787	0.676	0.555	0.463
2.00	0.879	0.849	0.786	0.672	0.550	0.447
2.20	0.879	0.849	0.785	0.672	0.549	0.445
2.50	0.880	0.850	0.786	0.672	0.550	0.444
3.00	0.881	0.850	0.785	0.671	0.550	0.444
3.52	0.882	0.851	0.786	0.670	0.549	0.444
4.00	0.882	0.851	0.786	0.670	0.549	0.443
4.50	0.883	0.851	0.786	0.669	0.548	0.443
4.75	0.883	0.851	0.785	0.669	0.548	0.443

Outer channel

Static-pressure ratios at s/l_s of -

0.378	0.659	0.780	0.873	0.951
0.804	0.766	0.712	0.679	0.676
0.781	0.721	0.633	0.574	0.575
0.778	0.714	0.616	0.531	0.534
0.779	0.712	0.612	0.517	0.485
0.782	0.713	0.611	0.515	0.452
0.784	0.712	0.609	0.513	0.450
0.786	0.712	0.608	0.512	0.449
0.786	0.714	0.610	0.513	0.450
0.788	0.712	0.607	0.511	0.449
0.789	0.711	0.606	0.509	0.449

Left instrumented sleeve

Static-pressure ratios at ϕ, deg, of -

NPR	0	45	90	135	180	225	270	315
1.50	0.778	0.789	0.826	0.886	0.911	0.893	0.832	0.792
1.81	0.757	0.768	0.808	0.875	0.903	0.882	0.815	0.771
2.00	0.755	0.764	0.807	0.874	0.902	0.880	0.813	0.769
2.20	0.755	0.764	0.807	0.874	0.903	0.881	0.813	0.769
2.50	0.755	0.764	0.808	0.875	0.903	0.881	0.815	0.770
3.00	0.755	0.763	0.809	0.877	0.904	0.882	0.816	0.771
3.52	0.755	0.763	0.810	0.877	0.905	0.883	0.817	0.771
4.00	0.755	0.763	0.810	0.877	0.905	0.881	0.815	0.772
4.50	0.755	0.762	0.810	0.878	0.905	0.882	0.816	0.772
4.75	0.755	0.762	0.810	0.878	0.905	0.883	0.817	0.772

Right instrumented sleeve

Static-pressure ratios at ϕ, deg, of -

0	45	90	135	180	225	270	315
0.817	0.808	0.828	0.889	0.908	0.884	0.825	0.800
0.800	0.788	0.809	0.877	0.899	0.874	0.806	0.777
0.797	0.785	0.807	0.875	0.897	0.871	0.802	0.773
0.797	0.784	0.806	0.876	0.897	0.871	0.802	0.773
0.798	0.785	0.806	0.876	0.898	0.872	0.802	0.773
0.800	0.785	0.806	0.877	0.899	0.872	0.802	0.774
0.800	0.785	0.807	0.878	0.899	0.871	0.801	0.775
0.800	0.785	0.807	0.878	0.900	0.873	0.803	0.775
0.800	0.786	0.807	0.878	0.899	0.872	0.801	0.775
0.800	0.785	0.808	0.878	0.899	0.871	0.800	0.775

Table 73. Static-Pressure Ratios in Nozzle and Instrumented Sleeves for Configuration $P_0C_LB_NN_2T$

Inner wall

Static-pressure ratios at s/l_s of -

NPR	0.425	0.860	0.914	0.938	0.957	0.973
1.51	0.871	0.444	0.475	0.521	0.558	0.588
1.80	0.856	0.367	0.344	0.411	0.461	0.480
2.00	0.853	0.355	0.307	0.366	0.430	0.448
2.21	0.854	0.351	0.293	0.352	0.421	0.438
2.51	0.854	0.348	0.286	0.352	0.418	0.436
3.01	0.853	0.347	0.286	0.364	0.420	0.435
3.51	0.854	0.344	0.283	0.367	0.418	0.434
4.00	0.854	0.342	0.286	0.370	0.417	0.435
4.51	0.853	0.341	0.298	0.375	0.420	0.438
5.00	0.853	0.339	0.304	0.376	0.421	0.440
6.01	0.852	0.335	0.312	0.375	0.418	0.438

Inner channel

Static-pressure ratios at s/l_s of -

0.798	0.886	0.923	0.951
0.902	0.913	0.856	0.749
0.890	0.899	0.831	0.702
0.889	0.896	0.825	0.692
0.889	0.897	0.825	0.691
0.888	0.897	0.824	0.691
0.889	0.899	0.826	0.693
0.889	0.899	0.826	0.693
0.890	0.898	0.825	0.693
0.890	0.901	0.828	0.697
0.891	0.900	0.827	0.696
0.891	0.900	0.827	0.697

Middle channel

Static-pressure ratios at s/l_s of -

NPR	0.657	0.809	0.873	0.922	0.964	0.982
1.51	0.910	0.886	0.830	0.733	0.642	0.600
1.80	0.900	0.872	0.808	0.695	0.571	0.475
2.00	0.900	0.872	0.807	0.692	0.567	0.461
2.21	0.900	0.872	0.807	0.692	0.567	0.459
2.51	0.900	0.871	0.807	0.691	0.566	0.458
3.01	0.901	0.872	0.807	0.691	0.566	0.457
3.51	0.901	0.872	0.806	0.689	0.565	0.457
4.00	0.901	0.871	0.806	0.688	0.563	0.456
4.51	0.903	0.873	0.807	0.689	0.564	0.457
5.00	0.903	0.872	0.806	0.688	0.563	0.455
6.01	0.902	0.871	0.805	0.686	0.561	0.454

Outer channel

Static-pressure ratios at s/l_s of -

0.378	0.659	0.780	0.873	0.951
0.813	0.768	0.720	0.698	0.689
0.798	0.720	0.637	0.606	0.599
0.796	0.713	0.610	0.562	0.560
0.797	0.711	0.604	0.523	0.536
0.798	0.710	0.603	0.511	0.468
0.797	0.708	0.600	0.507	0.448
0.796	0.709	0.602	0.510	0.450
0.796	0.709	0.604	0.511	0.451
0.795	0.706	0.598	0.506	0.447
0.795	0.706	0.599	0.507	0.448
0.794	0.705	0.598	0.505	0.448

Left instrumented sleeve

Static-pressure ratios at ϕ, deg, of -

NPR	0	45	90	135	180	225	270	315
1.51	0.777	0.787	0.835	0.895	0.918	0.896	0.837	0.794
1.80	0.754	0.764	0.818	0.884	0.910	0.885	0.820	0.774
2.00	0.752	0.761	0.817	0.883	0.909	0.884	0.819	0.771
2.21	0.752	0.761	0.817	0.883	0.909	0.884	0.819	0.772
2.51	0.751	0.761	0.818	0.884	0.909	0.885	0.818	0.771
3.01	0.752	0.761	0.818	0.885	0.910	0.886	0.819	0.773
3.51	0.751	0.761	0.819	0.885	0.911	0.885	0.819	0.773
4.00	0.750	0.761	0.819	0.884	0.911	0.886	0.818	0.772
4.51	0.752	0.761	0.818	0.885	0.911	0.886	0.820	0.774
5.00	0.752	0.762	0.818	0.885	0.912	0.886	0.819	0.774
6.01	0.751	0.761	0.818	0.885	0.911	0.885	0.819	0.774

Right instrumented sleeve

Static-pressure ratios at ϕ, deg, of -

0	45	90	135	180	225	270	315
0.799	0.803	0.838	0.895	0.918	0.898	0.840	0.797
0.778	0.779	0.819	0.884	0.909	0.887	0.820	0.772
0.776	0.777	0.817	0.883	0.908	0.885	0.818	0.769
0.776	0.776	0.817	0.883	0.908	0.885	0.818	0.769
0.777	0.777	0.817	0.883	0.909	0.885	0.818	0.769
0.777	0.777	0.817	0.883	0.909	0.886	0.817	0.769
0.779	0.778	0.817	0.885	0.910	0.886	0.819	0.770
0.780	0.778	0.817	0.885	0.910	0.886	0.819	0.771
0.779	0.778	0.817	0.885	0.910	0.886	0.818	0.769
0.778	0.778	0.817	0.884	0.910	0.886	0.817	0.769
0.778	0.777	0.817	0.884	0.910	0.885	0.817	0.769

Table 74. Static-Pressure Ratios in Nozzle and Instrumented Sleeves for Configuration $P_OC_LB_NN_2L$

Inner wall

Static-pressure ratios at s/l_s of -

NPR	0.425	0.860	0.914	0.938	0.957	0.973
1.51	0.867	0.463	0.492	0.526	0.559	0.588
1.81	0.851	0.380	0.373	0.425	0.460	0.476
2.01	0.849	0.368	0.341	0.397	0.437	0.447
2.21	0.849	0.365	0.337	0.395	0.434	0.442
2.50	0.849	0.363	0.332	0.398	0.433	0.442
3.01	0.848	0.362	0.338	0.406	0.434	0.441
3.50	0.848	0.360	0.341	0.410	0.433	0.441
4.01	0.848	0.358	0.352	0.410	0.432	0.441
4.50	0.848	0.356	0.358	0.409	0.432	0.441
4.74	0.848	0.355	0.361	0.409	0.432	0.441

Inner channel

Static-pressure ratios at s/l_s of -

0.798	0.886	0.923	0.951
0.892	0.893	0.837	0.735
0.878	0.873	0.807	0.681
0.876	0.871	0.802	0.673
0.874	0.868	0.798	0.669
0.874	0.870	0.800	0.670
0.875	0.871	0.800	0.671
0.877	0.875	0.804	0.676
0.877	0.875	0.804	0.676
0.877	0.875	0.804	0.677
0.878	0.876	0.806	0.678

Middle channel

Static-pressure ratios at s/l_s of -

NPR	0.657	0.809	0.873	0.922	0.964	0.982
1.51	0.893	0.867	0.815	0.724	0.641	0.603
1.81	0.881	0.852	0.790	0.680	0.561	0.469
2.01	0.880	0.851	0.788	0.677	0.555	0.453
2.21	0.880	0.850	0.787	0.676	0.554	0.449
2.50	0.880	0.850	0.788	0.676	0.554	0.449
3.01	0.881	0.851	0.788	0.675	0.554	0.448
3.50	0.883	0.852	0.789	0.675	0.554	0.448
4.01	0.883	0.852	0.788	0.674	0.553	0.448
4.50	0.883	0.851	0.787	0.673	0.552	0.447
4.74	0.883	0.851	0.787	0.672	0.551	0.447

Outer channel

Static-pressure ratios at s/l_s of -

0.378	0.659	0.780	0.873	0.951
0.808	0.762	0.713	0.687	0.681
0.791	0.715	0.624	0.588	0.585
0.789	0.707	0.601	0.537	0.548
0.789	0.706	0.599	0.507	0.513
0.789	0.704	0.597	0.502	0.443
0.788	0.703	0.597	0.502	0.440
0.788	0.702	0.594	0.500	0.439
0.788	0.701	0.594	0.500	0.439
0.787	0.701	0.594	0.499	0.440
0.787	0.701	0.594	0.499	0.440

Left instrumented sleeve

Static-pressure ratios at ϕ, deg, of -

NPR	0	45	90	135	180	225	270	315
1.51	0.775	0.784	0.828	0.889	0.912	0.892	0.836	0.793
1.81	0.753	0.762	0.812	0.878	0.905	0.882	0.820	0.773
2.01	0.750	0.758	0.810	0.878	0.903	0.880	0.818	0.771
2.21	0.750	0.758	0.810	0.877	0.903	0.879	0.817	0.771
2.50	0.750	0.757	0.810	0.878	0.903	0.880	0.817	0.771
3.01	0.751	0.757	0.810	0.879	0.904	0.880	0.818	0.772
3.50	0.750	0.757	0.811	0.879	0.906	0.881	0.819	0.773
4.01	0.750	0.756	0.811	0.879	0.905	0.881	0.819	0.773
4.50	0.750	0.756	0.811	0.880	0.905	0.881	0.819	0.774
4.74	0.750	0.756	0.811	0.880	0.906	0.881	0.819	0.774

Right instrumented sleeve

Static-pressure ratios at ϕ, deg, of -

0	45	90	135	180	225	270	315
0.811	0.803	0.827	0.890	0.905	0.884	0.829	0.796
0.794	0.784	0.809	0.880	0.897	0.873	0.811	0.775
0.792	0.781	0.806	0.877	0.895	0.870	0.807	0.771
0.792	0.781	0.806	0.879	0.896	0.871	0.809	0.771
0.792	0.781	0.806	0.878	0.896	0.871	0.808	0.771
0.793	0.781	0.805	0.879	0.896	0.871	0.809	0.771
0.793	0.781	0.805	0.879	0.896	0.871	0.809	0.771
0.793	0.781	0.805	0.879	0.897	0.871	0.809	0.771
0.793	0.781	0.805	0.880	0.897	0.871	0.809	0.771
0.793	0.781	0.805	0.880	0.897	0.871	0.809	0.771

Table 75. Static-Pressure Ratios in Nozzle and Instrumented Sleeves for Configuration $P_0C_LB_FN_2T$

Inner wall

Static-pressure ratios at s/l_s of -

NPR	0.425	0.860	0.914	0.938	0.957	0.973
1.51	0.873	0.426	0.449	0.512	0.558	0.591
1.80	0.859	0.360	0.323	0.396	0.455	0.482
2.01	0.857	0.349	0.281	0.337	0.412	0.439
2.20	0.857	0.344	0.257	0.306	0.391	0.421
2.50	0.856	0.341	0.239	0.288	0.378	0.411
3.01	0.856	0.340	0.230	0.292	0.376	0.407
3.51	0.856	0.338	0.229	0.302	0.378	0.406
3.99	0.855	0.337	0.229	0.313	0.380	0.408
4.51	0.855	0.335	0.229	0.319	0.380	0.410
5.00	0.855	0.333	0.232	0.324	0.383	0.414
6.00	0.854	0.330	0.244	0.327	0.385	0.416

Inner channel

Static-pressure ratios at s/l_s of -

0.798	0.886	0.923	0.951
0.893	0.910	0.855	0.752
0.880	0.896	0.829	0.704
0.878	0.893	0.824	0.694
0.878	0.893	0.823	0.693
0.878	0.894	0.824	0.693
0.878	0.895	0.824	0.694
0.878	0.896	0.826	0.695
0.879	0.896	0.825	0.696
0.879	0.896	0.826	0.697
0.880	0.895	0.825	0.697
0.880	0.895	0.825	0.697

Middle channel

Static-pressure ratios at s/l_s of -

NPR	0.657	0.809	0.873	0.922	0.964	0.982
1.51	0.906	0.885	0.833	0.740	0.650	0.607
1.80	0.896	0.873	0.811	0.699	0.576	0.481
2.01	0.896	0.872	0.810	0.696	0.571	0.465
2.20	0.896	0.872	0.810	0.696	0.570	0.463
2.50	0.897	0.873	0.810	0.696	0.570	0.462
3.01	0.898	0.874	0.811	0.695	0.570	0.462
3.51	0.898	0.874	0.811	0.695	0.569	0.461
3.99	0.899	0.873	0.810	0.694	0.568	0.461
4.51	0.899	0.873	0.809	0.693	0.567	0.460
5.00	0.899	0.872	0.809	0.692	0.566	0.459
6.00	0.899	0.872	0.807	0.690	0.564	0.458

Outer channel

Static-pressure ratios at s/l_s of -

0.378	0.659	0.780	0.873	0.951
0.800	0.765	0.728	0.706	0.695
0.777	0.712	0.647	0.615	0.604
0.773	0.703	0.617	0.575	0.566
0.774	0.701	0.609	0.543	0.544
0.775	0.699	0.606	0.524	0.499
0.775	0.698	0.602	0.519	0.463
0.775	0.697	0.601	0.517	0.461
0.774	0.696	0.600	0.516	0.460
0.774	0.696	0.600	0.515	0.459
0.774	0.695	0.599	0.514	0.458
0.773	0.694	0.598	0.512	0.457

Left instrumented sleeve

Static-pressure ratios at ϕ, deg, of -

NPR	0	45	90	135	180	225	270	315
1.51	0.770	0.781	0.835	0.890	0.911	0.892	0.835	0.790
1.80	0.745	0.757	0.818	0.878	0.903	0.881	0.818	0.769
2.01	0.742	0.755	0.816	0.876	0.902	0.879	0.816	0.767
2.20	0.742	0.755	0.816	0.877	0.903	0.880	0.816	0.767
2.50	0.742	0.755	0.817	0.877	0.903	0.880	0.817	0.768
3.01	0.743	0.755	0.817	0.878	0.904	0.881	0.818	0.769
3.51	0.743	0.755	0.818	0.878	0.905	0.881	0.818	0.770
3.99	0.743	0.756	0.818	0.878	0.905	0.881	0.818	0.770
4.51	0.743	0.756	0.818	0.878	0.905	0.881	0.818	0.770
5.00	0.743	0.756	0.818	0.878	0.905	0.881	0.818	0.770
6.00	0.742	0.756	0.818	0.878	0.905	0.881	0.817	0.770

Right instrumented sleeve

Static-pressure ratios at ϕ, deg, of -

0	45	90	135	180	225	270	315
0.806	0.804	0.839	0.898	0.919	0.898	0.843	0.802
0.785	0.781	0.820	0.886	0.910	0.887	0.825	0.778
0.783	0.779	0.818	0.884	0.908	0.886	0.823	0.774
0.784	0.779	0.818	0.885	0.909	0.886	0.823	0.775
0.785	0.780	0.818	0.885	0.909	0.886	0.823	0.774
0.785	0.780	0.818	0.887	0.910	0.887	0.823	0.775
0.785	0.780	0.818	0.887	0.910	0.887	0.823	0.775
0.785	0.779	0.818	0.887	0.910	0.887	0.823	0.774
0.785	0.780	0.818	0.887	0.911	0.887	0.824	0.774
0.785	0.780	0.818	0.887	0.910	0.887	0.823	0.774
0.784	0.779	0.818	0.885	0.910	0.886	0.823	0.773

Table 76. Static-Pressure Ratios in Nozzle and Instrumented Sleeves for Configuration $P_0C_LB_FN_2L$

Inner wall

Static-pressure ratios at s/l_s of -

NPR	0.425	0.860	0.914	0.938	0.957	0.973
1.50	0.858	0.478	0.503	0.539	0.571	0.597
1.81	0.839	0.386	0.376	0.428	0.462	0.482
2.01	0.837	0.371	0.339	0.392	0.431	0.447
2.20	0.837	0.368	0.330	0.385	0.424	0.437
2.50	0.837	0.370	0.337	0.391	0.423	0.437
2.80	0.837	0.363	0.323	0.386	0.420	0.435
3.01	0.837	0.362	0.324	0.388	0.420	0.435
3.51	0.837	0.360	0.327	0.392	0.420	0.435
4.01	0.837	0.357	0.333	0.390	0.419	0.435
4.51	0.836	0.355	0.338	0.389	0.419	0.435
4.75	0.836	0.353	0.340	0.388	0.418	0.435

Inner channel

Static-pressure ratios at s/l_s of -

	0.798	0.886	0.923	0.951
1.50	0.892	0.904	0.849	0.747
1.81	0.877	0.892	0.824	0.698
2.01	0.874	0.888	0.819	0.688
2.20	0.875	0.888	0.817	0.686
2.50	0.872	0.881	0.810	0.679
2.80	0.876	0.894	0.823	0.691
3.01	0.876	0.896	0.825	0.693
3.51	0.876	0.898	0.826	0.695
4.01	0.876	0.899	0.827	0.697
4.51	0.876	0.900	0.828	0.699
4.75	0.876	0.900	0.829	0.699

Middle channel

Static-pressure ratios at s/l_s of -

NPR	0.657	0.809	0.873	0.922	0.964	0.982
1.50	0.896	0.869	0.814	0.723	0.640	0.601
1.81	0.885	0.854	0.788	0.676	0.558	0.462
2.01	0.884	0.853	0.787	0.674	0.553	0.450
2.20	0.884	0.853	0.787	0.674	0.553	0.448
2.50	0.884	0.853	0.787	0.673	0.552	0.446
2.80	0.887	0.855	0.789	0.674	0.553	0.447
3.01	0.888	0.856	0.789	0.674	0.554	0.448
3.51	0.889	0.856	0.790	0.673	0.553	0.447
4.01	0.889	0.857	0.790	0.673	0.553	0.447
4.51	0.890	0.856	0.789	0.672	0.552	0.447
4.75	0.890	0.856	0.789	0.672	0.552	0.447

Outer channel

Static-pressure ratios at s/l_s of -

	0.378	0.659	0.780	0.873	0.951
1.50	0.810	0.770	0.718	0.688	0.682
1.81	0.791	0.722	0.631	0.584	0.582
2.01	0.789	0.715	0.612	0.539	0.545
2.20	0.790	0.714	0.609	0.516	0.506
2.50	0.789	0.714	0.610	0.515	0.454
2.80	0.794	0.711	0.605	0.510	0.448
3.01	0.794	0.710	0.603	0.509	0.447
3.51	0.793	0.709	0.602	0.508	0.447
4.01	0.793	0.707	0.601	0.507	0.446
4.51	0.793	0.707	0.600	0.506	0.446
4.75	0.793	0.706	0.599	0.506	0.446

Left instrumented sleeve

Static-pressure ratios at ϕ, deg, of -

NPR	0	45	90	135	180	225	270	315
1.50	0.774	0.786	0.828	0.882	0.908	0.892	0.837	0.788
1.81	0.750	0.763	0.810	0.870	0.899	0.881	0.820	0.766
2.01	0.747	0.759	0.808	0.869	0.898	0.879	0.817	0.765
2.20	0.748	0.759	0.809	0.870	0.899	0.880	0.818	0.765
2.50	0.750	0.759	0.810	0.871	0.899	0.880	0.817	0.766
2.80	0.748	0.758	0.810	0.871	0.900	0.880	0.819	0.767
3.01	0.749	0.758	0.810	0.871	0.901	0.881	0.820	0.767
3.51	0.748	0.758	0.810	0.872	0.901	0.881	0.820	0.768
4.01	0.748	0.758	0.810	0.872	0.901	0.881	0.820	0.769
4.51	0.748	0.757	0.810	0.872	0.901	0.881	0.820	0.769
4.75	0.747	0.757	0.810	0.872	0.901	0.881	0.820	0.769

Right instrumented sleeve

Static-pressure ratios at ϕ, deg, of -

	0	45	90	135	180	225	270	315
1.50	0.814	0.808	0.831	0.890	0.909	0.893	0.837	0.798
1.81	0.795	0.788	0.813	0.878	0.899	0.881	0.819	0.775
2.01	0.793	0.785	0.810	0.876	0.898	0.880	0.817	0.772
2.20	0.793	0.785	0.810	0.876	0.898	0.880	0.817	0.771
2.50	0.792	0.785	0.810	0.877	0.899	0.881	0.820	0.772
2.80	0.794	0.785	0.809	0.877	0.899	0.880	0.818	0.772
3.01	0.794	0.786	0.809	0.877	0.899	0.881	0.818	0.772
3.51	0.795	0.785	0.809	0.877	0.899	0.881	0.817	0.772
4.01	0.796	0.785	0.809	0.877	0.900	0.881	0.817	0.772
4.51	0.796	0.786	0.809	0.878	0.900	0.880	0.816	0.771
4.75	0.795	0.785	0.809	0.877	0.900	0.880	0.816	0.771

Table 77. Static-Pressure Ratios in Nozzle and Instrumented Sleeves for Configuration $P_0C_LB_TN_2T$

Inner wall

Static-pressure ratios at s/l_s of -

NPR	0.425	0.860	0.914	0.938	0.957	0.973
1.50	0.871	0.435	0.465	0.518	0.560	0.591
1.80	0.856	0.359	0.325	0.398	0.458	0.479
2.00	0.854	0.348	0.286	0.344	0.424	0.445
2.21	0.855	0.343	0.267	0.323	0.412	0.434
2.51	0.855	0.342	0.260	0.323	0.409	0.431
3.00	0.854	0.339	0.255	0.333	0.410	0.430
3.50	0.854	0.337	0.255	0.343	0.411	0.430
4.00	0.854	0.336	0.254	0.351	0.411	0.430
4.50	0.854	0.334	0.255	0.355	0.412	0.432
5.01	0.854	0.331	0.261	0.356	0.413	0.435
6.01	0.854	0.327	0.268	0.355	0.411	0.434

Inner channel

Static-pressure ratios at s/l_s of -

0.798	0.886	0.923	0.951
0.900	0.918	0.861	0.754
0.889	0.904	0.835	0.705
0.887	0.900	0.830	0.695
0.887	0.901	0.830	0.695
0.887	0.902	0.830	0.695
0.887	0.903	0.831	0.697
0.888	0.904	0.831	0.698
0.888	0.905	0.832	0.699
0.889	0.905	0.832	0.700
0.889	0.906	0.832	0.701
0.890	0.906	0.833	0.702

Middle channel

Static-pressure ratios at s/l_s of -

NPR	0.657	0.809	0.873	0.922	0.964	0.982
1.50	0.910	0.885	0.829	0.735	0.645	0.604
1.80	0.901	0.872	0.807	0.693	0.569	0.472
2.00	0.900	0.870	0.805	0.690	0.565	0.460
2.21	0.901	0.871	0.805	0.690	0.565	0.458
2.51	0.901	0.871	0.806	0.690	0.565	0.457
3.00	0.902	0.871	0.806	0.689	0.565	0.456
3.50	0.902	0.871	0.806	0.688	0.564	0.456
4.00	0.903	0.872	0.806	0.688	0.563	0.456
4.50	0.903	0.871	0.805	0.687	0.563	0.455
5.01	0.903	0.872	0.805	0.686	0.562	0.455
6.01	0.904	0.871	0.804	0.685	0.560	0.454

Outer channel

Static-pressure ratios at s/l_s of -

0.378	0.659	0.780	0.873	0.951
0.813	0.771	0.725	0.701	0.692
0.796	0.722	0.643	0.604	0.596
0.795	0.716	0.623	0.562	0.559
0.795	0.715	0.617	0.532	0.534
0.796	0.714	0.616	0.527	0.474
0.794	0.712	0.612	0.524	0.464
0.794	0.711	0.611	0.523	0.464
0.793	0.710	0.610	0.521	0.462
0.793	0.709	0.609	0.521	0.462
0.792	0.709	0.609	0.520	0.462
0.791	0.708	0.608	0.518	0.461

Left instrumented sleeve

Static-pressure ratios at ϕ, deg, of -

NPR	0	45	90	135	180	225	270	315
1.50	0.776	0.784	0.837	0.894	0.919	0.897	0.839	0.794
1.80	0.751	0.760	0.820	0.884	0.912	0.886	0.822	0.773
2.00	0.749	0.757	0.819	0.883	0.911	0.885	0.820	0.771
2.21	0.750	0.757	0.819	0.884	0.912	0.886	0.820	0.771
2.51	0.750	0.757	0.820	0.885	0.912	0.886	0.821	0.772
3.00	0.751	0.757	0.820	0.885	0.913	0.886	0.821	0.773
3.50	0.750	0.757	0.821	0.886	0.914	0.886	0.821	0.773
4.00	0.751	0.757	0.821	0.886	0.914	0.887	0.821	0.774
4.50	0.751	0.758	0.821	0.886	0.914	0.887	0.821	0.774
5.01	0.750	0.758	0.821	0.887	0.914	0.887	0.821	0.774
6.01	0.750	0.758	0.821	0.887	0.914	0.887	0.821	0.774

Right instrumented sleeve

Static-pressure ratios at ϕ, deg, of -

0	45	90	135	180	225	270	315
0.807	0.804	0.841	0.899	0.917	0.899	0.843	0.801
0.787	0.783	0.823	0.888	0.910	0.888	0.827	0.779
0.786	0.781	0.820	0.887	0.909	0.887	0.824	0.777
0.787	0.781	0.820	0.888	0.910	0.887	0.825	0.777
0.788	0.781	0.820	0.889	0.911	0.887	0.825	0.777
0.788	0.781	0.820	0.889	0.910	0.888	0.825	0.777
0.788	0.781	0.820	0.889	0.911	0.888	0.825	0.777
0.788	0.781	0.820	0.889	0.911	0.888	0.825	0.777
0.788	0.781	0.820	0.889	0.911	0.888	0.825	0.776
0.788	0.781	0.820	0.889	0.911	0.888	0.825	0.776
0.787	0.781	0.820	0.888	0.910	0.887	0.824	0.775

Table 78. Static-Pressure Ratios in Nozzle and Instrumented Sleeves for Configuration $P_0C_LB_TN_2L$

Inner wall

Static-pressure ratios at s/l_s of -

NPR	0.425	0.860	0.914	0.938	0.957	0.973
1.50	0.865	0.483	0.513	0.542	0.568	0.594
1.80	0.849	0.393	0.403	0.443	0.465	0.481
2.00	0.847	0.380	0.376	0.421	0.443	0.452
2.20	0.847	0.375	0.365	0.415	0.438	0.445
2.50	0.847	0.373	0.364	0.418	0.438	0.444
3.00	0.846	0.371	0.368	0.424	0.439	0.444
3.51	0.846	0.370	0.375	0.426	0.438	0.443
4.01	0.846	0.368	0.383	0.425	0.437	0.442
4.49	0.846	0.365	0.389	0.424	0.436	0.442
4.76	0.846	0.363	0.389	0.423	0.435	0.441

Inner channel

Static-pressure ratios at s/l_s of -

0.798	0.886	0.923	0.951
0.892	0.877	0.822	0.722
0.878	0.859	0.792	0.668
0.874	0.853	0.783	0.654
0.876	0.855	0.784	0.655
0.876	0.858	0.787	0.658
0.877	0.861	0.790	0.661
0.876	0.860	0.789	0.661
0.879	0.864	0.793	0.665
0.878	0.865	0.793	0.666
0.879	0.866	0.795	0.668

Middle channel

Static-pressure ratios at s/l_s of -

NPR	0.657	0.809	0.873	0.922	0.964	0.982
1.50	0.891	0.865	0.812	0.722	0.639	0.603
1.80	0.878	0.848	0.785	0.675	0.555	0.464
2.00	0.877	0.847	0.785	0.672	0.550	0.448
2.20	0.877	0.847	0.784	0.672	0.550	0.445
2.50	0.878	0.847	0.784	0.671	0.550	0.444
3.00	0.878	0.847	0.784	0.670	0.549	0.444
3.51	0.879	0.847	0.784	0.669	0.548	0.443
4.01	0.880	0.847	0.783	0.668	0.548	0.443
4.49	0.880	0.847	0.783	0.667	0.547	0.443
4.76	0.880	0.847	0.782	0.667	0.547	0.442

Outer channel

Static-pressure ratios at s/l_s of -

0.378	0.659	0.780	0.873	0.951
0.807	0.769	0.713	0.682	0.679
0.788	0.724	0.629	0.578	0.578
0.787	0.717	0.612	0.528	0.542
0.789	0.716	0.608	0.511	0.492
0.791	0.715	0.606	0.509	0.446
0.793	0.714	0.605	0.508	0.445
0.793	0.714	0.605	0.508	0.445
0.794	0.713	0.603	0.506	0.444
0.793	0.712	0.603	0.506	0.445
0.794	0.712	0.602	0.505	0.444

Left instrumented sleeve

Static-pressure ratios at ϕ, deg, of -

NPR	0	45	90	135	180	225	270	315
1.50	0.779	0.788	0.829	0.888	0.912	0.893	0.835	0.793
1.80	0.757	0.765	0.811	0.877	0.903	0.882	0.818	0.772
2.00	0.755	0.762	0.810	0.875	0.902	0.880	0.816	0.770
2.20	0.755	0.762	0.810	0.876	0.903	0.881	0.816	0.770
2.50	0.755	0.761	0.811	0.876	0.904	0.881	0.817	0.771
3.00	0.755	0.761	0.811	0.877	0.904	0.882	0.818	0.772
3.51	0.755	0.761	0.811	0.878	0.905	0.882	0.818	0.773
4.01	0.755	0.760	0.812	0.877	0.905	0.882	0.818	0.773
4.49	0.755	0.760	0.812	0.878	0.905	0.882	0.819	0.773
4.76	0.754	0.760	0.812	0.878	0.905	0.882	0.819	0.773

Right instrumented sleeve

Static-pressure ratios at ϕ, deg, of -

0	45	90	135	180	225	270	315
0.818	0.808	0.832	0.893	0.911	0.892	0.837	0.801
0.800	0.789	0.813	0.881	0.902	0.881	0.820	0.779
0.799	0.786	0.810	0.880	0.902	0.880	0.818	0.777
0.798	0.786	0.810	0.880	0.902	0.879	0.818	0.777
0.800	0.786	0.810	0.881	0.903	0.880	0.818	0.777
0.800	0.786	0.809	0.882	0.903	0.880	0.818	0.777
0.800	0.786	0.809	0.882	0.904	0.881	0.818	0.778
0.800	0.786	0.809	0.882	0.904	0.880	0.818	0.777
0.800	0.786	0.809	0.882	0.903	0.880	0.818	0.777
0.799	0.785	0.809	0.882	0.903	0.880	0.817	0.777

Table 79. Static-Pressure Ratios in Nozzle and Instrumented Sleeves for Configuration $P_0C_FB_NN_2T$

Inner wall

Static-pressure ratios at s/l_s of -

NPR	0.425	0.860	0.914	0.938	0.957	0.973
1.51	0.872	0.446	0.475	0.518	0.556	0.585
1.80	0.857	0.371	0.343	0.408	0.458	0.477
2.00	0.855	0.359	0.307	0.364	0.430	0.447
2.20	0.856	0.355	0.296	0.355	0.424	0.440
2.51	0.855	0.354	0.292	0.360	0.424	0.440
3.00	0.855	0.352	0.291	0.370	0.425	0.438
3.50	0.855	0.351	0.293	0.378	0.424	0.438
4.01	0.855	0.349	0.296	0.382	0.423	0.438
4.51	0.855	0.346	0.300	0.380	0.422	0.439
5.01	0.855	0.344	0.306	0.380	0.422	0.439
6.01	0.854	0.339	0.313	0.380	0.421	0.438

Inner channel

Static-pressure ratios at s/l_s of -

0.798	0.886	0.923	0.951
0.899	0.905	0.849	0.743
0.885	0.890	0.822	0.694
0.884	0.885	0.816	0.682
0.884	0.887	0.816	0.683
0.885	0.887	0.816	0.684
0.884	0.889	0.817	0.685
0.885	0.890	0.818	0.686
0.885	0.890	0.818	0.687
0.886	0.891	0.818	0.688
0.886	0.890	0.818	0.689
0.887	0.891	0.818	0.689

Middle channel

Static-pressure ratios at s/l_s of -

NPR	0.657	0.809	0.873	0.922	0.964	0.982
1.51	0.906	0.882	0.827	0.735	0.645	0.604
1.80	0.895	0.868	0.805	0.695	0.573	0.479
2.00	0.895	0.867	0.804	0.692	0.568	0.463
2.20	0.895	0.867	0.803	0.691	0.567	0.461
2.51	0.896	0.868	0.804	0.691	0.567	0.461
3.00	0.896	0.868	0.804	0.690	0.567	0.459
3.50	0.897	0.868	0.804	0.689	0.566	0.459
4.01	0.897	0.868	0.804	0.688	0.565	0.458
4.51	0.897	0.868	0.803	0.687	0.563	0.457
5.01	0.897	0.867	0.802	0.686	0.563	0.456
6.01	0.897	0.867	0.801	0.684	0.561	0.455

Outer channel

Static-pressure ratios at s/l_s of -

0.378	0.659	0.780	0.873	0.951
0.815	0.769	0.721	0.698	0.688
0.800	0.721	0.635	0.604	0.597
0.800	0.715	0.612	0.556	0.557
0.801	0.713	0.606	0.518	0.539
0.800	0.711	0.604	0.511	0.456
0.799	0.709	0.602	0.509	0.448
0.798	0.709	0.601	0.509	0.449
0.797	0.708	0.601	0.508	0.449
0.797	0.708	0.602	0.509	0.450
0.797	0.707	0.601	0.508	0.450
0.796	0.706	0.600	0.507	0.450

Left instrumented sleeve

Static-pressure ratios at ϕ, deg, of -

NPR	0	45	90	135	180	225	270	315
1.51	0.776	0.786	0.834	0.893	0.917	0.895	0.837	0.793
1.80	0.754	0.763	0.819	0.883	0.909	0.883	0.820	0.773
2.00	0.752	0.761	0.817	0.883	0.908	0.882	0.818	0.771
2.20	0.752	0.761	0.818	0.883	0.908	0.882	0.818	0.771
2.51	0.752	0.760	0.818	0.883	0.909	0.882	0.818	0.772
3.00	0.752	0.760	0.818	0.884	0.909	0.883	0.818	0.772
3.50	0.753	0.760	0.819	0.884	0.910	0.883	0.818	0.773
4.01	0.753	0.760	0.819	0.884	0.909	0.883	0.818	0.773
4.51	0.752	0.760	0.819	0.884	0.909	0.883	0.818	0.773
5.01	0.752	0.760	0.819	0.884	0.909	0.883	0.818	0.773
6.01	0.751	0.760	0.819	0.884	0.910	0.883	0.818	0.773

Right instrumented sleeve

Static-pressure ratios at ϕ, deg, of -

0	45	90	135	180	225	270	315
0.798	0.802	0.840	0.895	0.918	0.899	0.840	0.797
0.779	0.780	0.822	0.885	0.909	0.888	0.821	0.775
0.778	0.779	0.819	0.883	0.907	0.886	0.819	0.771
0.777	0.778	0.818	0.883	0.908	0.886	0.818	0.771
0.778	0.778	0.818	0.883	0.908	0.886	0.819	0.771
0.779	0.779	0.818	0.884	0.908	0.886	0.819	0.771
0.780	0.779	0.819	0.884	0.908	0.886	0.819	0.771
0.780	0.779	0.818	0.884	0.909	0.886	0.819	0.770
0.779	0.779	0.818	0.884	0.909	0.886	0.817	0.770
0.780	0.779	0.818	0.883	0.908	0.886	0.817	0.770
0.777	0.777	0.818	0.883	0.908	0.885	0.816	0.768

Table 80. Static-Pressure Ratios in Nozzle and Instrumented Sleeves for Configuration $P_OC_FB_NN_2L$

Inner wall

Static-pressure ratios at s/l_s of -

NPR	0.425	0.860	0.914	0.938	0.957	0.973
1.51	0.869	0.449	0.480	0.518	0.555	0.585
1.80	0.855	0.370	0.347	0.412	0.458	0.475
2.01	0.852	0.359	0.311	0.373	0.435	0.446
2.20	0.852	0.355	0.302	0.369	0.432	0.442
2.50	0.852	0.354	0.300	0.376	0.432	0.441
3.01	0.851	0.352	0.297	0.385	0.433	0.440
3.50	0.851	0.352	0.304	0.393	0.431	0.439
4.00	0.849	0.352	0.315	0.396	0.430	0.439
4.51	0.850	0.348	0.320	0.396	0.430	0.440
4.75	0.850	0.347	0.324	0.396	0.431	0.440

Inner channel

Static-pressure ratios at s/l_s of -

0.798	0.886	0.923	0.951
0.891	0.890	0.835	0.733
0.878	0.873	0.807	0.681
0.875	0.869	0.801	0.671
0.875	0.869	0.799	0.669
0.875	0.871	0.801	0.672
0.877	0.874	0.803	0.674
0.875	0.873	0.802	0.673
0.872	0.867	0.796	0.668
0.876	0.874	0.803	0.675
0.876	0.873	0.802	0.675

Middle channel

Static-pressure ratios at s/l_s of -

NPR	0.657	0.809	0.873	0.922	0.964	0.982
1.51	0.890	0.865	0.812	0.722	0.640	0.602
1.80	0.879	0.849	0.786	0.677	0.559	0.470
2.01	0.878	0.848	0.785	0.674	0.553	0.450
2.20	0.877	0.847	0.784	0.673	0.552	0.448
2.50	0.878	0.848	0.785	0.673	0.552	0.447
3.01	0.879	0.849	0.785	0.672	0.552	0.447
3.50	0.880	0.849	0.785	0.671	0.551	0.447
4.00	0.879	0.848	0.785	0.670	0.550	0.445
4.51	0.880	0.848	0.784	0.670	0.550	0.445
4.75	0.880	0.848	0.784	0.669	0.549	0.445

Outer channel

Static-pressure ratios at s/l_s of -

0.378	0.659	0.780	0.873	0.951
0.812	0.767	0.713	0.686	0.680
0.796	0.720	0.628	0.587	0.584
0.795	0.713	0.607	0.534	0.546
0.795	0.710	0.604	0.511	0.509
0.796	0.709	0.602	0.508	0.447
0.794	0.707	0.601	0.507	0.445
0.792	0.707	0.601	0.508	0.446
0.791	0.708	0.603	0.509	0.447
0.791	0.706	0.600	0.507	0.446
0.791	0.706	0.601	0.507	0.447

Left instrumented sleeve

Static-pressure ratios at ϕ, deg, of -

NPR	0	45	90	135	180	225	270	315
1.51	0.773	0.783	0.830	0.887	0.912	0.892	0.836	0.791
1.80	0.751	0.761	0.814	0.876	0.903	0.881	0.819	0.771
2.01	0.749	0.758	0.812	0.874	0.902	0.879	0.817	0.769
2.20	0.748	0.757	0.812	0.874	0.902	0.879	0.817	0.768
2.50	0.748	0.756	0.813	0.875	0.903	0.879	0.817	0.770
3.01	0.749	0.756	0.813	0.876	0.903	0.880	0.819	0.771
3.50	0.748	0.756	0.813	0.876	0.903	0.880	0.818	0.771
4.00	0.748	0.755	0.813	0.876	0.902	0.879	0.816	0.771
4.51	0.748	0.755	0.813	0.876	0.904	0.880	0.818	0.771
4.75	0.748	0.755	0.813	0.877	0.904	0.880	0.818	0.772

Right instrumented sleeve

Static-pressure ratios at ϕ, deg, of -

0	45	90	135	180	225	270	315
0.813	0.804	0.830	0.891	0.904	0.882	0.824	0.795
0.796	0.786	0.811	0.882	0.897	0.871	0.807	0.774
0.793	0.783	0.809	0.879	0.896	0.869	0.804	0.770
0.793	0.782	0.808	0.880	0.896	0.870	0.804	0.770
0.794	0.782	0.808	0.880	0.896	0.870	0.804	0.769
0.793	0.783	0.808	0.880	0.897	0.871	0.805	0.770
0.794	0.782	0.808	0.880	0.897	0.870	0.805	0.770
0.793	0.782	0.809	0.881	0.899	0.873	0.809	0.772
0.793	0.782	0.808	0.881	0.897	0.871	0.806	0.771
0.793	0.782	0.808	0.881	0.897	0.871	0.806	0.770

Table 81. Static-Pressure Ratios in Nozzle and Instrumented Sleeves for Configuration $P_0C_FB_FN_2T$

Inner wall

Static-pressure ratios at s/l_s of -

NPR	0.425	0.860	0.914	0.938	0.957	0.973
1.50	0.874	0.443	0.472	0.518	0.557	0.588
1.80	0.859	0.366	0.330	0.397	0.456	0.476
2.00	0.858	0.355	0.292	0.347	0.427	0.446
2.21	0.858	0.352	0.280	0.338	0.421	0.440
2.50	0.858	0.351	0.277	0.344	0.422	0.438
3.00	0.858	0.349	0.275	0.356	0.424	0.438
3.50	0.857	0.347	0.275	0.366	0.424	0.437
4.00	0.857	0.347	0.280	0.373	0.421	0.437
4.50	0.857	0.344	0.281	0.377	0.424	0.439
5.01	0.857	0.341	0.286	0.376	0.424	0.440
5.99	0.856	0.338	0.298	0.377	0.422	0.438

Inner channel

Static-pressure ratios at s/l_s of -

0.798	0.886	0.923	0.951
0.901	0.904	0.847	0.742
0.888	0.887	0.819	0.691
0.887	0.884	0.813	0.680
0.886	0.885	0.813	0.680
0.886	0.885	0.813	0.680
0.887	0.887	0.814	0.682
0.888	0.888	0.815	0.683
0.888	0.886	0.813	0.683
0.889	0.889	0.816	0.686
0.889	0.890	0.817	0.687
0.889	0.890	0.816	0.687

Middle channel

Static-pressure ratios at s/l_s of -

NPR	0.657	0.809	0.873	0.922	0.964	0.982
1.50	0.908	0.883	0.828	0.737	0.648	0.607
1.80	0.897	0.868	0.805	0.694	0.571	0.477
2.00	0.896	0.868	0.804	0.691	0.567	0.462
2.21	0.896	0.868	0.804	0.691	0.567	0.460
2.50	0.897	0.868	0.804	0.690	0.566	0.458
3.00	0.898	0.868	0.804	0.689	0.566	0.458
3.50	0.898	0.869	0.804	0.688	0.565	0.458
4.00	0.898	0.868	0.803	0.687	0.564	0.457
4.50	0.899	0.868	0.803	0.686	0.563	0.457
5.01	0.899	0.868	0.803	0.686	0.562	0.456
5.99	0.899	0.867	0.802	0.684	0.561	0.455

Outer channel

Static-pressure ratios at s/l_s of -

0.378	0.659	0.780	0.873	0.951
0.818	0.772	0.723	0.698	0.690
0.802	0.723	0.638	0.598	0.592
0.801	0.718	0.620	0.555	0.556
0.802	0.717	0.615	0.527	0.529
0.802	0.715	0.614	0.523	0.465
0.800	0.713	0.611	0.521	0.461
0.799	0.713	0.611	0.521	0.460
0.801	0.715	0.615	0.524	0.464
0.798	0.711	0.609	0.518	0.459
0.797	0.711	0.609	0.518	0.460
0.796	0.710	0.607	0.516	0.459

Left instrumented sleeve

Static-pressure ratios at ϕ, deg. of -

NPR	0	45	90	135	180	225	270	315
1.50	0.777	0.786	0.837	0.894	0.918	0.895	0.838	0.794
1.80	0.753	0.762	0.821	0.883	0.910	0.884	0.820	0.773
2.00	0.751	0.759	0.820	0.882	0.909	0.883	0.818	0.771
2.21	0.752	0.759	0.820	0.883	0.910	0.883	0.819	0.771
2.50	0.751	0.759	0.821	0.884	0.910	0.884	0.818	0.772
3.00	0.752	0.759	0.822	0.884	0.911	0.884	0.819	0.772
3.50	0.752	0.760	0.822	0.885	0.911	0.884	0.819	0.773
4.00	0.752	0.759	0.822	0.884	0.911	0.884	0.818	0.773
4.50	0.752	0.759	0.822	0.885	0.912	0.885	0.819	0.773
5.01	0.752	0.759	0.822	0.885	0.912	0.885	0.819	0.774
5.99	0.751	0.759	0.822	0.885	0.912	0.885	0.818	0.773

Right instrumented sleeve

Static-pressure ratios at ϕ, deg. of -

0	45	90	135	180	225	270	315
0.808	0.805	0.838	0.897	0.915	0.898	0.845	0.804
0.787	0.783	0.819	0.886	0.905	0.885	0.827	0.781
0.786	0.782	0.818	0.885	0.905	0.884	0.825	0.779
0.787	0.782	0.818	0.886	0.905	0.884	0.825	0.779
0.788	0.782	0.818	0.886	0.906	0.884	0.825	0.779
0.788	0.782	0.818	0.886	0.906	0.884	0.825	0.778
0.789	0.783	0.818	0.887	0.907	0.885	0.825	0.778
0.789	0.783	0.819	0.888	0.908	0.885	0.825	0.779
0.789	0.783	0.818	0.887	0.907	0.885	0.824	0.778
0.789	0.783	0.818	0.887	0.907	0.885	0.824	0.778
0.788	0.782	0.818	0.886	0.907	0.885	0.823	0.777

Table 82. Static-Pressure Ratios in Nozzle and Instrumented Sleeves for Configuration $P_0C_FB_FN_3L$

Inner wall
Static-pressure ratios at s/l_s of -

NPR	0.429	0.859	0.905	0.926	0.943	0.959
1.50	0.922	0.443	0.467	0.616	0.637	0.650
1.80	0.910	0.307	0.324	0.492	0.509	0.530
2.01	0.906	0.279	0.277	0.423	0.440	0.465
2.20	0.905	0.264	0.247	0.371	0.387	0.415
2.50	0.905	0.251	0.220	0.315	0.331	0.360
3.01	0.904	0.241	0.197	0.254	0.268	0.297
3.50	0.904	0.237	0.187	0.216	0.229	0.256
3.99	0.904	0.236	0.183	0.187	0.198	0.226
4.50	0.904	0.234	0.180	0.162	0.172	0.204
4.76	0.904	0.234	0.180	0.153	0.161	0.195

Inner channel
Static-pressure ratios at s/l_s of -

	0.723	0.837	0.885	0.922	0.953
1.50	0.820	0.802	0.758	0.733	0.720
1.80	0.783	0.761	0.706	0.671	0.649
2.01	0.772	0.747	0.688	0.651	0.625
2.20	0.766	0.740	0.680	0.642	0.614
2.50	0.759	0.732	0.671	0.634	0.606
3.01	0.756	0.729	0.666	0.630	0.603
3.50	0.754	0.726	0.664	0.629	0.602
3.99	0.753	0.725	0.663	0.628	0.601
4.50	0.753	0.725	0.663	0.628	0.601
4.76	0.752	0.724	0.662	0.627	0.601

Middle channel
Static-pressure ratios at s/l_s of -

NPR	0.673	0.817	0.878	0.924	0.963	0.982
1.50	0.817	0.801	0.761	0.717	0.672	0.647
1.80	0.775	0.755	0.703	0.642	0.570	0.526
2.01	0.762	0.740	0.685	0.618	0.534	0.475
2.20	0.756	0.735	0.678	0.610	0.524	0.457
2.50	0.754	0.734	0.677	0.607	0.520	0.452
3.01	0.752	0.732	0.675	0.606	0.519	0.451
3.50	0.752	0.732	0.675	0.606	0.519	0.451
3.99	0.751	0.732	0.675	0.605	0.519	0.451
4.50	0.750	0.732	0.675	0.605	0.519	0.451
4.76	0.750	0.732	0.674	0.605	0.519	0.451

Outer channel
Static-pressure ratios at s/l_s of -

	0.524	0.744	0.839	0.912	0.973	0.986
1.50	0.870	0.777	0.704	0.686	0.637	0.639
1.80	0.843	0.709	0.614	0.588	0.506	0.498
2.01	0.836	0.685	0.582	0.556	0.466	0.433
2.20	0.832	0.672	0.566	0.542	0.455	0.414
2.50	0.832	0.666	0.559	0.535	0.450	0.406
3.01	0.829	0.663	0.555	0.532	0.448	0.404
3.50	0.829	0.662	0.553	0.531	0.447	0.404
3.99	0.827	0.660	0.551	0.530	0.446	0.404
4.50	0.826	0.659	0.550	0.529	0.446	0.404
4.76	0.826	0.659	0.549	0.529	0.445	0.404

Left instrumented sleeve
Static-pressure ratios at ϕ, deg, of -

NPR	0	45	90	135	180	225	270	315
1.50	0.804	0.803	0.846	0.892	0.910	0.898	0.850	0.809
1.80	0.772	0.771	0.821	0.875	0.896	0.882	0.826	0.780
2.01	0.763	0.762	0.814	0.869	0.891	0.876	0.819	0.771
2.20	0.759	0.758	0.811	0.868	0.889	0.875	0.815	0.768
2.50	0.757	0.755	0.809	0.867	0.889	0.874	0.814	0.766
3.01	0.754	0.752	0.807	0.866	0.888	0.873	0.813	0.765
3.50	0.754	0.751	0.807	0.866	0.888	0.873	0.812	0.764
3.99	0.753	0.750	0.806	0.866	0.888	0.873	0.812	0.764
4.50	0.752	0.749	0.806	0.866	0.888	0.872	0.812	0.764
4.76	0.751	0.749	0.805	0.866	0.887	0.872	0.811	0.764

Right instrumented sleeve
Static-pressure ratios at ϕ, deg, of -

	0	45	90	135	180	225	270	315
1.50	0.830	0.816	0.846	0.898	0.910	0.896	0.844	0.811
1.80	0.805	0.789	0.822	0.883	0.896	0.879	0.819	0.782
2.01	0.798	0.782	0.815	0.877	0.892	0.875	0.813	0.774
2.20	0.795	0.778	0.812	0.875	0.890	0.872	0.810	0.770
2.50	0.794	0.776	0.810	0.874	0.890	0.872	0.809	0.768
3.01	0.793	0.775	0.808	0.874	0.889	0.871	0.807	0.767
3.50	0.793	0.774	0.808	0.873	0.889	0.870	0.807	0.767
3.99	0.793	0.773	0.807	0.873	0.888	0.869	0.806	0.766
4.50	0.792	0.773	0.807	0.873	0.888	0.869	0.805	0.766
4.76	0.792	0.772	0.807	0.873	0.888	0.869	0.805	0.766

Table 83. Static-Pressure Ratios in Nozzle and Instrumented Sleeves for Configuration $P_0C_FB_TN_2T$

Inner wall

Static-pressure ratios at s/l_s of -

NPR	0.425	0.860	0.914	0.938	0.957	0.973
1.50	0.873	0.450	0.481	0.524	0.561	0.592
1.81	0.857	0.367	0.338	0.405	0.457	0.475
2.00	0.855	0.358	0.305	0.365	0.433	0.448
2.20	0.855	0.355	0.296	0.359	0.429	0.443
2.50	0.856	0.355	0.296	0.367	0.430	0.442
3.01	0.856	0.355	0.303	0.383	0.433	0.442
3.50	0.857	0.355	0.307	0.390	0.431	0.441
4.01	0.856	0.354	0.316	0.396	0.432	0.442
4.51	0.856	0.352	0.325	0.397	0.432	0.443
5.00	0.856	0.350	0.331	0.397	0.431	0.443
6.01	0.855	0.346	0.338	0.396	0.428	0.440

Inner channel

Static-pressure ratios at s/l_s of -

0.798	0.886	0.923	0.951
0.900	0.889	0.835	0.734
0.885	0.868	0.802	0.676
0.884	0.862	0.794	0.664
0.885	0.862	0.793	0.663
0.885	0.863	0.793	0.663
0.886	0.862	0.792	0.663
0.887	0.866	0.794	0.664
0.887	0.865	0.794	0.664
0.887	0.865	0.793	0.665
0.888	0.864	0.793	0.665
0.888	0.864	0.793	0.666

Middle channel

Static-pressure ratios at s/l_s of -

NPR	0.657	0.809	0.873	0.922	0.964	0.982
1.50	0.904	0.882	0.828	0.735	0.646	0.607
1.81	0.894	0.867	0.805	0.692	0.568	0.473
2.00	0.893	0.867	0.804	0.690	0.564	0.459
2.20	0.894	0.868	0.805	0.690	0.564	0.457
2.50	0.896	0.869	0.806	0.690	0.564	0.456
3.01	0.897	0.870	0.806	0.690	0.564	0.456
3.50	0.899	0.871	0.807	0.689	0.564	0.456
4.01	0.899	0.871	0.807	0.689	0.563	0.455
4.51	0.900	0.871	0.806	0.688	0.562	0.455
5.00	0.900	0.871	0.806	0.687	0.561	0.455
6.01	0.900	0.871	0.805	0.686	0.559	0.453

Outer channel

Static-pressure ratios at s/l_s of -

0.378	0.659	0.780	0.873	0.951
0.821	0.775	0.722	0.698	0.691
0.807	0.727	0.637	0.596	0.591
0.807	0.722	0.622	0.557	0.556
0.808	0.720	0.617	0.528	0.528
0.810	0.720	0.616	0.524	0.463
0.809	0.718	0.613	0.523	0.460
0.810	0.720	0.617	0.526	0.463
0.809	0.718	0.614	0.524	0.462
0.808	0.717	0.613	0.522	0.461
0.808	0.717	0.612	0.521	0.460
0.807	0.716	0.612	0.520	0.460

Left instrumented sleeve

Static-pressure ratios at ϕ, deg, of -

NPR	0	45	90	135	180	225	270	315
1.50	0.778	0.785	0.838	0.897	0.918	0.895	0.838	0.795
1.81	0.755	0.762	0.821	0.886	0.910	0.884	0.820	0.774
2.00	0.753	0.759	0.820	0.885	0.908	0.882	0.818	0.772
2.20	0.752	0.760	0.820	0.885	0.908	0.883	0.818	0.772
2.50	0.753	0.760	0.820	0.886	0.909	0.883	0.818	0.773
3.01	0.754	0.760	0.821	0.886	0.909	0.883	0.818	0.774
3.50	0.753	0.760	0.822	0.886	0.908	0.883	0.818	0.774
4.01	0.754	0.760	0.822	0.886	0.909	0.884	0.818	0.775
4.51	0.754	0.760	0.822	0.887	0.909	0.884	0.818	0.775
5.00	0.754	0.761	0.822	0.887	0.910	0.884	0.818	0.775
6.01	0.753	0.761	0.822	0.887	0.909	0.883	0.817	0.775

Right instrumented sleeve

Static-pressure ratios at ϕ, deg, of -

0	45	90	135	180	225	270	315
0.810	0.806	0.840	0.898	0.915	0.898	0.844	0.805
0.790	0.785	0.822	0.888	0.906	0.886	0.826	0.783
0.789	0.784	0.820	0.886	0.904	0.885	0.824	0.780
0.789	0.783	0.820	0.886	0.905	0.885	0.824	0.780
0.790	0.784	0.820	0.887	0.906	0.886	0.824	0.780
0.791	0.784	0.821	0.888	0.906	0.886	0.824	0.780
0.791	0.785	0.820	0.888	0.907	0.886	0.824	0.780
0.791	0.785	0.821	0.889	0.907	0.886	0.824	0.780
0.791	0.785	0.821	0.888	0.907	0.887	0.824	0.780
0.791	0.785	0.821	0.889	0.907	0.887	0.823	0.779
0.790	0.784	0.821	0.888	0.907	0.886	0.823	0.779

Table 84. Static-Pressure Ratios in Nozzle and Instrumented Sleeves for Configuration $P_0C_FB_TN_2L$

Inner wall

Static-pressure ratios at s/l_s of -

NPR	0.425	0.860	0.914	0.938	0.957	0.973
1.51	0.870	0.464	0.496	0.529	0.560	0.590
1.80	0.856	0.376	0.362	0.421	0.460	0.477
2.02	0.854	0.368	0.335	0.392	0.439	0.449
2.20	0.853	0.362	0.321	0.386	0.436	0.445
2.50	0.853	0.360	0.317	0.390	0.436	0.444
3.02	0.853	0.359	0.321	0.400	0.436	0.443
3.52	0.853	0.355	0.318	0.403	0.434	0.442
4.01	0.852	0.355	0.330	0.405	0.434	0.442
4.49	0.852	0.350	0.333	0.403	0.433	0.442
4.76	0.852	0.349	0.335	0.402	0.433	0.442

Inner channel

Static-pressure ratios at s/l_s of -

0.798	0.886	0.923	0.951
0.889	0.878	0.821	0.722
0.879	0.867	0.799	0.676
0.873	0.855	0.785	0.656
0.876	0.861	0.790	0.661
0.876	0.864	0.793	0.664
0.876	0.862	0.792	0.663
0.877	0.868	0.797	0.669
0.876	0.865	0.794	0.667
0.877	0.869	0.798	0.672
0.877	0.870	0.799	0.673

Middle channel

Static-pressure ratios at s/l_s of -

NPR	0.657	0.809	0.873	0.922	0.964	0.982
1.51	0.891	0.866	0.813	0.722	0.638	0.602
1.80	0.878	0.846	0.784	0.675	0.556	0.467
2.02	0.877	0.847	0.784	0.673	0.550	0.448
2.20	0.876	0.846	0.783	0.672	0.549	0.446
2.50	0.877	0.846	0.783	0.671	0.549	0.445
3.02	0.878	0.847	0.783	0.670	0.549	0.444
3.52	0.877	0.846	0.782	0.668	0.548	0.444
4.01	0.878	0.847	0.782	0.668	0.548	0.443
4.49	0.878	0.846	0.781	0.667	0.547	0.443
4.76	0.878	0.846	0.781	0.666	0.547	0.443

Outer channel

Static-pressure ratios at s/l_s of -

0.378	0.659	0.780	0.873	0.951
0.813	0.774	0.716	0.684	0.680
0.797	0.728	0.635	0.583	0.583
0.795	0.723	0.618	0.531	0.539
0.797	0.720	0.613	0.517	0.493
0.799	0.719	0.611	0.515	0.452
0.798	0.718	0.612	0.516	0.453
0.799	0.717	0.610	0.515	0.452
0.798	0.717	0.611	0.515	0.453
0.798	0.715	0.610	0.514	0.452
0.798	0.715	0.609	0.513	0.452

Left instrumented sleeve

Static-pressure ratios at ϕ, deg, of -

NPR	0	45	90	135	180	225	270	315
1.51	0.778	0.785	0.832	0.890	0.915	0.894	0.839	0.795
1.80	0.756	0.764	0.816	0.880	0.907	0.883	0.824	0.775
2.02	0.754	0.760	0.815	0.880	0.905	0.882	0.821	0.774
2.20	0.753	0.759	0.814	0.879	0.906	0.882	0.821	0.773
2.50	0.753	0.759	0.815	0.880	0.906	0.882	0.821	0.774
3.02	0.753	0.758	0.816	0.881	0.907	0.882	0.822	0.775
3.52	0.753	0.757	0.816	0.881	0.908	0.882	0.822	0.775
4.01	0.752	0.757	0.816	0.881	0.908	0.882	0.822	0.775
4.49	0.752	0.756	0.816	0.882	0.908	0.882	0.822	0.775
4.76	0.752	0.756	0.816	0.882	0.908	0.883	0.822	0.775

Right instrumented sleeve

Static-pressure ratios at ϕ, deg, of -

0	45	90	135	180	225	270	315
0.816	0.805	0.833	0.898	0.914	0.893	0.842	0.805
0.799	0.784	0.815	0.888	0.905	0.881	0.824	0.784
0.798	0.782	0.813	0.887	0.905	0.881	0.823	0.782
0.798	0.781	0.812	0.887	0.904	0.880	0.822	0.781
0.797	0.781	0.813	0.887	0.905	0.880	0.822	0.781
0.798	0.781	0.813	0.887	0.905	0.881	0.823	0.781
0.797	0.781	0.812	0.887	0.905	0.880	0.821	0.781
0.797	0.781	0.812	0.887	0.905	0.880	0.822	0.781
0.796	0.781	0.812	0.888	0.905	0.880	0.821	0.781
0.797	0.780	0.812	0.887	0.905	0.880	0.821	0.781

Table 85. Static-Pressure Ratios in Nozzle and Instrumented Sleeves for Configuration $P_0C_5B_5N_3T$

Inner wall

Static-pressure ratios at s/l_s of -

NPR	0.429	0.859	0.905	0.926	0.943	0.959
1.51	0.935	0.440	0.465	0.621	0.636	0.648
1.80	0.924	0.315	0.331	0.496	0.511	0.530
2.01	0.922	0.281	0.275	0.421	0.437	0.464
2.20	0.921	0.268	0.246	0.370	0.386	0.415
2.50	0.921	0.256	0.220	0.311	0.328	0.359
3.00	0.921	0.247	0.200	0.252	0.267	0.297
3.50	0.920	0.243	0.191	0.216	0.229	0.254
4.00	0.921	0.241	0.186	0.189	0.199	0.224
4.51	0.921	0.239	0.183	0.167	0.175	0.202
5.02	0.921	0.239	0.182	0.150	0.156	0.185
6.02	0.920	0.237	0.180	0.126	0.128	0.162

Inner channel

Static-pressure ratios at s/l_s of -

0.723	0.837	0.885	0.922	0.953
0.848	0.821	0.773	0.741	0.722
0.818	0.784	0.725	0.685	0.657
0.808	0.771	0.709	0.666	0.635
0.800	0.764	0.700	0.658	0.627
0.796	0.758	0.693	0.652	0.622
0.789	0.752	0.687	0.647	0.618
0.786	0.748	0.684	0.645	0.618
0.783	0.748	0.683	0.646	0.618
0.782	0.746	0.682	0.644	0.617
0.780	0.745	0.680	0.643	0.617
0.779	0.745	0.680	0.644	0.617

Middle channel

Static-pressure ratios at s/l_s of -

NPR	0.673	0.817	0.878	0.924	0.963	0.982
1.51	0.828	0.814	0.773	0.729	0.678	0.648
1.80	0.790	0.772	0.721	0.660	0.585	0.535
2.01	0.779	0.759	0.705	0.639	0.554	0.491
2.20	0.776	0.755	0.699	0.631	0.544	0.477
2.50	0.775	0.754	0.697	0.628	0.541	0.472
3.00	0.776	0.753	0.697	0.627	0.540	0.471
3.50	0.776	0.753	0.697	0.627	0.540	0.471
4.00	0.776	0.753	0.697	0.626	0.539	0.471
4.51	0.776	0.753	0.696	0.626	0.539	0.470
5.02	0.775	0.753	0.696	0.625	0.538	0.469
6.02	0.774	0.753	0.695	0.625	0.537	0.469

Outer channel

Static-pressure ratios at s/l_s of -

0.524	0.744	0.839	0.912	0.973	0.986
0.857	0.767	0.697	0.679	0.633	0.634
0.833	0.699	0.607	0.584	0.505	0.495
0.827	0.675	0.574	0.552	0.468	0.432
0.826	0.667	0.563	0.544	0.460	0.418
0.826	0.663	0.557	0.539	0.456	0.414
0.828	0.664	0.558	0.540	0.457	0.414
0.828	0.665	0.558	0.540	0.457	0.414
0.828	0.663	0.556	0.540	0.457	0.415
0.828	0.664	0.556	0.540	0.457	0.415
0.829	0.664	0.555	0.539	0.457	0.415
0.829	0.661	0.551	0.538	0.456	0.416

Left instrumented sleeve

Static-pressure ratios at ϕ, deg. of -

NPR	0	45	90	135	180	225	270	315
1.51	0.808	0.804	0.854	0.903	0.918	0.908	0.855	0.813
1.80	0.776	0.773	0.832	0.889	0.905	0.893	0.832	0.785
2.01	0.767	0.764	0.826	0.885	0.902	0.889	0.825	0.777
2.20	0.764	0.761	0.824	0.883	0.901	0.887	0.823	0.774
2.50	0.762	0.758	0.824	0.883	0.901	0.887	0.822	0.773
3.00	0.761	0.756	0.823	0.883	0.901	0.886	0.820	0.771
3.50	0.760	0.755	0.822	0.882	0.900	0.885	0.818	0.770
4.00	0.759	0.755	0.822	0.882	0.900	0.886	0.817	0.770
4.51	0.759	0.754	0.821	0.882	0.900	0.885	0.817	0.769
5.02	0.758	0.754	0.821	0.881	0.899	0.884	0.816	0.768
6.02	0.757	0.753	0.820	0.881	0.900	0.884	0.816	0.768

Right instrumented sleeve

Static-pressure ratios at ϕ, deg. of -

0	45	90	135	180	225	270	315
0.822	0.815	0.855	0.902	0.913	0.902	0.849	0.808
0.795	0.788	0.831	0.887	0.901	0.886	0.825	0.779
0.788	0.781	0.825	0.883	0.898	0.883	0.819	0.770
0.786	0.778	0.823	0.883	0.897	0.881	0.816	0.768
0.784	0.777	0.822	0.883	0.897	0.881	0.815	0.766
0.785	0.776	0.821	0.883	0.898	0.881	0.815	0.765
0.783	0.775	0.820	0.883	0.898	0.881	0.814	0.764
0.783	0.775	0.820	0.883	0.898	0.881	0.814	0.763
0.783	0.775	0.820	0.883	0.898	0.881	0.814	0.764
0.783	0.774	0.819	0.883	0.898	0.881	0.814	0.764
0.782	0.773	0.819	0.882	0.897	0.880	0.813	0.763

Table 86. Static-Pressure Ratios in Nozzle and Instrumented Sleeves for Configuration $P_O C_S B_N N_3 L$

Inner wall

Static-pressure ratios at s/l_s of -

NPR	0.429	0.859	0.905	0.926	0.943	0.959
1.50	0.927	0.446	0.473	0.621	0.642	0.654
1.81	0.915	0.299	0.317	0.496	0.514	0.532
2.01	0.913	0.270	0.266	0.425	0.444	0.469
2.20	0.912	0.256	0.234	0.371	0.390	0.418
2.50	0.911	0.245	0.209	0.312	0.332	0.362
3.00	0.911	0.237	0.191	0.250	0.269	0.301
3.51	0.910	0.233	0.182	0.212	0.227	0.257
4.00	0.910	0.231	0.178	0.183	0.196	0.229
4.51	0.910	0.230	0.176	0.160	0.171	0.210
4.76	0.910	0.230	0.176	0.151	0.160	0.202

Inner channel

Static-pressure ratios at s/l_s of -

0.723	0.837	0.885	0.922	0.953
0.830	0.809	0.765	0.737	0.721
0.796	0.769	0.711	0.675	0.649
0.781	0.754	0.693	0.655	0.626
0.775	0.746	0.684	0.646	0.616
0.767	0.738	0.675	0.638	0.609
0.761	0.732	0.669	0.633	0.605
0.759	0.729	0.667	0.631	0.605
0.752	0.724	0.662	0.628	0.603
0.754	0.725	0.663	0.629	0.603
0.755	0.726	0.664	0.630	0.604

Middle channel

Static-pressure ratios at s/l_s of -

NPR	0.673	0.817	0.878	0.924	0.963	0.982
1.50	0.822	0.809	0.768	0.725	0.678	0.652
1.81	0.782	0.762	0.710	0.648	0.575	0.529
2.01	0.770	0.750	0.693	0.626	0.541	0.481
2.20	0.765	0.745	0.688	0.618	0.530	0.464
2.50	0.764	0.743	0.685	0.615	0.526	0.459
3.00	0.762	0.742	0.684	0.613	0.525	0.457
3.51	0.761	0.741	0.683	0.613	0.524	0.457
4.00	0.762	0.741	0.683	0.612	0.524	0.456
4.51	0.760	0.740	0.683	0.612	0.523	0.456
4.76	0.760	0.740	0.682	0.611	0.524	0.456

Outer channel

Static-pressure ratios at s/l_s of -

0.524	0.744	0.839	0.912	0.973	0.986
0.867	0.773	0.703	0.684	0.640	0.641
0.841	0.703	0.610	0.585	0.504	0.496
0.836	0.679	0.579	0.554	0.466	0.432
0.835	0.668	0.564	0.542	0.456	0.415
0.835	0.663	0.558	0.536	0.452	0.408
0.836	0.662	0.556	0.535	0.451	0.407
0.834	0.660	0.553	0.534	0.449	0.407
0.835	0.661	0.553	0.534	0.449	0.406
0.834	0.659	0.551	0.533	0.448	0.407
0.834	0.658	0.550	0.533	0.449	0.407

Left instrumented sleeve

Static-pressure ratios at ϕ, deg, of -

NPR	0	45	90	135	180	225	270	315
1.50	0.814	0.806	0.849	0.898	0.915	0.904	0.854	0.815
1.81	0.783	0.775	0.825	0.883	0.901	0.888	0.829	0.786
2.01	0.776	0.767	0.819	0.879	0.898	0.884	0.823	0.778
2.20	0.773	0.763	0.817	0.878	0.897	0.882	0.819	0.775
2.50	0.771	0.761	0.816	0.877	0.896	0.881	0.817	0.773
3.00	0.770	0.758	0.815	0.876	0.896	0.881	0.817	0.772
3.51	0.769	0.757	0.814	0.876	0.896	0.880	0.816	0.771
4.00	0.768	0.755	0.813	0.875	0.895	0.879	0.814	0.771
4.51	0.767	0.755	0.812	0.875	0.895	0.879	0.814	0.771
4.76	0.767	0.755	0.813	0.876	0.895	0.879	0.814	0.771

Right instrumented sleeve

Static-pressure ratios at ϕ, deg, of -

0	45	90	135	180	225	270	315
0.822	0.817	0.846	0.900	0.912	0.897	0.842	0.808
0.796	0.791	0.822	0.884	0.898	0.882	0.817	0.777
0.790	0.785	0.816	0.881	0.895	0.878	0.811	0.770
0.787	0.782	0.813	0.879	0.893	0.876	0.808	0.767
0.787	0.781	0.811	0.878	0.893	0.875	0.806	0.765
0.787	0.781	0.810	0.878	0.893	0.875	0.805	0.764
0.787	0.780	0.809	0.878	0.893	0.874	0.804	0.764
0.787	0.780	0.809	0.879	0.894	0.876	0.805	0.765
0.786	0.779	0.809	0.878	0.893	0.875	0.804	0.764
0.786	0.779	0.809	0.878	0.893	0.874	0.803	0.763

Table 87. Static-Pressure Ratios in Nozzle and Instrumented Sleeves for Configuration $P_0C_5B_FN_3T$

Inner wall

Static-pressure ratios at s/l_s of -

NPR	0.429	0.859	0.905	0.926	0.943	0.959
1.51	0.934	0.440	0.465	0.621	0.636	0.647
1.79	0.925	0.321	0.336	0.500	0.514	0.533
2.00	0.921	0.285	0.279	0.421	0.437	0.464
2.19	0.920	0.269	0.248	0.367	0.383	0.414
2.48	0.920	0.259	0.224	0.311	0.327	0.359
2.98	0.919	0.249	0.203	0.252	0.266	0.297
3.50	0.919	0.244	0.193	0.215	0.227	0.253
4.00	0.919	0.242	0.187	0.187	0.198	0.223
4.50	0.919	0.241	0.185	0.166	0.175	0.201
5.01	0.918	0.240	0.184	0.150	0.156	0.184
6.02	0.918	0.239	0.181	0.124	0.127	0.159

Inner channel

Static-pressure ratios at s/l_s of -

NPR	0.723	0.837	0.885	0.922	0.953
1.51	0.846	0.819	0.771	0.741	0.722
1.79	0.821	0.785	0.726	0.686	0.658
2.00	0.808	0.769	0.707	0.666	0.635
2.19	0.802	0.762	0.699	0.657	0.626
2.48	0.797	0.755	0.691	0.651	0.621
2.98	0.790	0.749	0.685	0.646	0.617
3.50	0.781	0.741	0.678	0.642	0.615
4.00	0.786	0.746	0.682	0.645	0.617
4.50	0.786	0.746	0.682	0.645	0.617
5.01	0.783	0.744	0.681	0.644	0.617
6.02	0.782	0.744	0.680	0.643	0.616

Middle channel

Static-pressure ratios at s/l_s of -

NPR	0.673	0.817	0.878	0.924	0.963	0.982
1.51	0.828	0.814	0.773	0.729	0.678	0.649
1.79	0.790	0.773	0.722	0.662	0.589	0.539
2.00	0.778	0.758	0.704	0.638	0.554	0.491
2.19	0.774	0.754	0.699	0.630	0.544	0.477
2.48	0.772	0.752	0.696	0.628	0.541	0.472
2.98	0.773	0.752	0.696	0.627	0.540	0.471
3.50	0.772	0.750	0.694	0.624	0.537	0.468
4.00	0.774	0.752	0.697	0.627	0.540	0.471
4.50	0.773	0.753	0.697	0.628	0.541	0.471
5.01	0.773	0.752	0.696	0.626	0.540	0.470
6.02	0.772	0.751	0.695	0.626	0.539	0.470

Outer channel

Static-pressure ratios at s/l_s of -

NPR	0.524	0.744	0.839	0.912	0.973	0.986
1.51	0.861	0.775	0.706	0.685	0.638	0.637
1.79	0.832	0.712	0.621	0.595	0.516	0.507
2.00	0.825	0.689	0.589	0.562	0.472	0.441
2.19	0.823	0.679	0.577	0.550	0.462	0.422
2.48	0.823	0.676	0.572	0.546	0.458	0.416
2.98	0.822	0.675	0.569	0.545	0.457	0.415
3.50	0.821	0.676	0.569	0.543	0.456	0.414
4.00	0.823	0.670	0.562	0.542	0.457	0.415
4.50	0.823	0.669	0.561	0.542	0.457	0.416
5.01	0.824	0.669	0.560	0.541	0.457	0.416
6.02	0.824	0.666	0.558	0.540	0.456	0.416

Left instrumented sleeve

Static-pressure ratios at ϕ, deg, of -

NPR	0	45	90	135	180	225	270	315
1.51	0.806	0.804	0.856	0.905	0.917	0.907	0.855	0.812
1.79	0.774	0.773	0.834	0.890	0.905	0.892	0.832	0.784
2.00	0.765	0.763	0.828	0.886	0.901	0.887	0.825	0.775
2.19	0.761	0.759	0.825	0.884	0.900	0.886	0.822	0.772
2.48	0.759	0.757	0.824	0.883	0.899	0.885	0.820	0.770
2.98	0.758	0.754	0.823	0.882	0.899	0.884	0.819	0.768
3.50	0.756	0.755	0.822	0.882	0.898	0.883	0.817	0.766
4.00	0.757	0.752	0.821	0.881	0.899	0.883	0.817	0.767
4.50	0.757	0.751	0.821	0.881	0.899	0.884	0.817	0.767
5.01	0.756	0.750	0.820	0.881	0.898	0.883	0.816	0.766
6.02	0.755	0.750	0.819	0.881	0.898	0.882	0.816	0.766

Right instrumented sleeve

Static-pressure ratios at ϕ, deg, of -

NPR	0	45	90	135	180	225	270	315
1.51	0.815	0.825	0.855	0.902	0.911	0.898	0.845	0.799
1.79	0.785	0.794	0.833	0.888	0.899	0.884	0.824	0.771
2.00	0.778	0.786	0.826	0.883	0.895	0.879	0.816	0.761
2.19	0.774	0.781	0.822	0.881	0.893	0.877	0.812	0.756
2.48	0.773	0.779	0.821	0.881	0.893	0.877	0.812	0.755
2.98	0.771	0.778	0.818	0.879	0.892	0.875	0.808	0.751
3.50	0.773	0.777	0.818	0.880	0.893	0.876	0.808	0.752
4.00	0.770	0.777	0.817	0.878	0.891	0.874	0.805	0.746
4.50	0.770	0.776	0.817	0.878	0.891	0.874	0.804	0.748
5.01	0.769	0.775	0.816	0.877	0.891	0.873	0.804	0.747
6.02	0.767	0.774	0.816	0.877	0.890	0.872	0.802	0.747

Table 88. Static-Pressure Ratios in Nozzle and Instrumented Sleeves for Configuration $P_0C_SB_FN_3L$

Inner wall

Static-pressure ratios at s/l_s of -

NPR	0.429	0.859	0.905	0.926	0.943	0.959
1.49	0.927	0.444	0.468	0.616	0.640	0.654
1.81	0.913	0.300	0.317	0.497	0.513	0.531
2.00	0.909	0.272	0.271	0.430	0.447	0.470
2.51	0.909	0.245	0.214	0.323	0.339	0.364
3.00	0.908	0.234	0.190	0.261	0.277	0.303
3.52	0.908	0.231	0.181	0.217	0.231	0.258
4.00	0.909	0.230	0.178	0.187	0.199	0.229
4.52	0.908	0.229	0.175	0.161	0.171	0.209
4.75	0.909	0.229	0.175	0.152	0.161	0.202

Inner channel

Static-pressure ratios at s/l_s of -

0.723	0.837	0.885	0.922	0.953
0.819	0.802	0.757	0.734	0.721
0.776	0.754	0.698	0.667	0.647
0.758	0.736	0.679	0.646	0.623
0.750	0.726	0.666	0.632	0.606
0.743	0.719	0.658	0.626	0.601
0.743	0.718	0.657	0.625	0.600
0.744	0.719	0.658	0.626	0.601
0.745	0.720	0.658	0.626	0.601
0.745	0.720	0.658	0.626	0.601

Middle channel

Static-pressure ratios at s/l_s of -

NPR	0.673	0.817	0.878	0.924	0.963	0.982
1.49	0.823	0.806	0.765	0.722	0.675	0.650
1.81	0.780	0.756	0.703	0.641	0.568	0.524
2.00	0.767	0.743	0.687	0.618	0.533	0.473
2.51	0.760	0.737	0.679	0.608	0.520	0.452
3.00	0.759	0.736	0.679	0.608	0.519	0.451
3.52	0.758	0.736	0.679	0.607	0.519	0.451
4.00	0.757	0.736	0.678	0.607	0.520	0.451
4.52	0.755	0.735	0.677	0.607	0.519	0.451
4.75	0.755	0.735	0.678	0.607	0.519	0.451

Outer channel

Static-pressure ratios at s/l_s of -

0.524	0.744	0.839	0.912	0.973	0.986
0.868	0.777	0.708	0.687	0.642	0.643
0.842	0.710	0.615	0.587	0.507	0.501
0.837	0.687	0.583	0.553	0.465	0.433
0.834	0.670	0.560	0.532	0.447	0.404
0.833	0.669	0.557	0.530	0.445	0.402
0.833	0.667	0.555	0.530	0.445	0.402
0.831	0.665	0.554	0.529	0.445	0.402
0.831	0.664	0.552	0.529	0.445	0.402
0.831	0.664	0.552	0.529	0.445	0.403

Left instrumented sleeve

Static-pressure ratios at ϕ, deg. of -

NPR	0	45	90	135	180	225	270	315
1.49	0.814	0.808	0.849	0.898	0.914	0.903	0.851	0.812
1.81	0.783	0.775	0.823	0.880	0.900	0.886	0.825	0.782
2.00	0.777	0.766	0.816	0.875	0.895	0.881	0.817	0.776
2.51	0.772	0.760	0.812	0.873	0.894	0.879	0.813	0.771
3.00	0.771	0.757	0.811	0.873	0.894	0.878	0.812	0.770
3.52	0.770	0.756	0.810	0.872	0.893	0.877	0.811	0.769
4.00	0.769	0.755	0.810	0.873	0.894	0.878	0.812	0.768
4.52	0.768	0.754	0.809	0.872	0.893	0.878	0.812	0.768
4.75	0.768	0.755	0.810	0.873	0.894	0.879	0.813	0.769

Right instrumented sleeve

Static-pressure ratios at ϕ, deg. of -

0	45	90	135	180	225	270	315
0.818	0.808	0.841	0.889	0.885	0.861	0.826	0.805
0.795	0.786	0.818	0.879	0.882	0.855	0.800	0.778
0.790	0.781	0.811	0.875	0.880	0.852	0.792	0.771
0.786	0.775	0.807	0.873	0.876	0.847	0.786	0.765
0.786	0.775	0.805	0.873	0.878	0.850	0.786	0.764
0.785	0.773	0.804	0.872	0.876	0.847	0.785	0.763
0.783	0.772	0.804	0.871	0.873	0.844	0.783	0.762
0.785	0.773	0.805	0.873	0.876	0.848	0.784	0.763
0.784	0.773	0.805	0.872	0.875	0.847	0.783	0.763

Table 89. Static-Pressure Ratios in Nozzle and Instrumented Sleeves for Configuration $P_O C_M B_N N_3 T$

Inner wall

Static-pressure ratios at s/l_s of -

NPR	0.429	0.859	0.905	0.926	0.943	0.959
1.52	0.931	0.432	0.458	0.617	0.632	0.643
1.81	0.920	0.319	0.334	0.490	0.505	0.524
2.01	0.917	0.285	0.284	0.421	0.438	0.463
2.20	0.916	0.266	0.253	0.370	0.387	0.415
2.50	0.916	0.252	0.225	0.314	0.330	0.360
2.99	0.916	0.241	0.201	0.256	0.270	0.299
3.52	0.915	0.236	0.187	0.215	0.228	0.254
4.00	0.915	0.234	0.181	0.191	0.201	0.226
4.51	0.915	0.232	0.177	0.170	0.178	0.203
5.02	0.915	0.232	0.176	0.153	0.160	0.187
6.01	0.915	0.230	0.173	0.130	0.134	0.164

Inner channel

Static-pressure ratios at s/l_s of -

NPR	0.723	0.837	0.885	0.922	0.953
1.52	0.851	0.820	0.771	0.739	0.721
1.81	0.821	0.783	0.724	0.685	0.657
2.01	0.811	0.772	0.710	0.668	0.638
2.20	0.805	0.764	0.701	0.661	0.629
2.50	0.799	0.758	0.695	0.655	0.624
2.99	0.794	0.752	0.689	0.651	0.622
3.52	0.791	0.750	0.687	0.650	0.621
4.00	0.789	0.749	0.686	0.649	0.620
4.51	0.787	0.748	0.685	0.648	0.620
5.02	0.785	0.747	0.684	0.648	0.620
6.01	0.784	0.747	0.684	0.647	0.620

Middle channel

Static-pressure ratios at s/l_s of -

NPR	0.673	0.817	0.878	0.924	0.963	0.982
1.52	0.822	0.808	0.770	0.727	0.676	0.646
1.81	0.781	0.763	0.717	0.658	0.585	0.533
2.01	0.768	0.750	0.701	0.638	0.555	0.492
2.20	0.764	0.745	0.695	0.629	0.545	0.478
2.50	0.761	0.742	0.691	0.626	0.540	0.471
2.99	0.762	0.742	0.692	0.625	0.539	0.470
3.52	0.762	0.743	0.692	0.625	0.539	0.470
4.00	0.762	0.742	0.691	0.624	0.539	0.470
4.51	0.762	0.742	0.691	0.624	0.538	0.469
5.02	0.761	0.742	0.690	0.623	0.538	0.469
6.01	0.761	0.742	0.690	0.623	0.537	0.468

Outer channel

Static-pressure ratios at s/l_s of -

NPR	0.524	0.744	0.839	0.912	0.973	0.986
1.52	0.853	0.759	0.688	0.671	0.627	0.630
1.81	0.828	0.686	0.592	0.572	0.499	0.493
2.01	0.822	0.661	0.556	0.542	0.461	0.432
2.20	0.820	0.649	0.540	0.529	0.452	0.413
2.50	0.819	0.642	0.533	0.524	0.448	0.407
2.99	0.820	0.641	0.532	0.524	0.448	0.406
3.52	0.820	0.637	0.528	0.523	0.448	0.406
4.00	0.820	0.637	0.526	0.523	0.449	0.407
4.51	0.820	0.636	0.524	0.522	0.448	0.408
5.02	0.820	0.637	0.524	0.522	0.448	0.407
6.01	0.821	0.634	0.520	0.521	0.448	0.408

Left instrumented sleeve

Static-pressure ratios at ϕ, deg, of -

NPR	0	45	90	135	180	225	270	315
1.52	0.806	0.803	0.849	0.899	0.914	0.903	0.852	0.810
1.81	0.774	0.771	0.825	0.883	0.901	0.887	0.829	0.782
2.01	0.766	0.762	0.820	0.879	0.897	0.884	0.823	0.775
2.20	0.762	0.758	0.817	0.877	0.895	0.882	0.820	0.771
2.50	0.760	0.756	0.815	0.877	0.895	0.881	0.817	0.769
2.99	0.758	0.754	0.814	0.876	0.895	0.881	0.816	0.768
3.52	0.757	0.752	0.813	0.875	0.894	0.880	0.815	0.767
4.00	0.756	0.751	0.813	0.875	0.893	0.879	0.814	0.766
4.51	0.756	0.751	0.812	0.875	0.893	0.880	0.814	0.766
5.02	0.755	0.750	0.812	0.875	0.893	0.879	0.813	0.766
6.01	0.754	0.750	0.811	0.875	0.893	0.879	0.813	0.766

Right instrumented sleeve

Static-pressure ratios at ϕ, deg, of -

0	45	90	135	180	225	270	315
0.819	0.812	0.854	0.900	0.914	0.901	0.848	0.806
0.791	0.784	0.830	0.884	0.899	0.885	0.823	0.776
0.785	0.777	0.824	0.880	0.896	0.882	0.818	0.769
0.782	0.773	0.821	0.879	0.895	0.879	0.815	0.765
0.781	0.772	0.820	0.878	0.894	0.879	0.813	0.763
0.781	0.770	0.818	0.878	0.894	0.877	0.812	0.762
0.780	0.769	0.817	0.877	0.893	0.877	0.811	0.761
0.780	0.768	0.816	0.877	0.893	0.876	0.810	0.761
0.780	0.768	0.816	0.877	0.893	0.876	0.810	0.760
0.779	0.768	0.816	0.877	0.893	0.876	0.810	0.760
0.779	0.767	0.816	0.876	0.893	0.876	0.809	0.760

Table 90. Static-Pressure Ratios in Nozzle and Instrumented Sleeves for Configuration $P_OC_MB_NN_3L$

Inner wall

Static-pressure ratios at s/l_s of -

NPR	0.429	0.859	0.905	0.926	0.943	0.959
1.50	0.921	0.445	0.476	0.625	0.643	0.651
1.80	0.909	0.314	0.333	0.500	0.518	0.533
2.00	0.906	0.277	0.282	0.430	0.449	0.470
2.20	0.904	0.256	0.247	0.374	0.394	0.419
2.50	0.903	0.240	0.217	0.316	0.335	0.362
3.00	0.903	0.229	0.191	0.253	0.272	0.302
3.50	0.903	0.225	0.178	0.214	0.229	0.260
4.01	0.903	0.222	0.172	0.186	0.198	0.229
4.50	0.903	0.221	0.169	0.166	0.177	0.210
4.74	0.903	0.221	0.168	0.159	0.168	0.203

Inner channel

Static-pressure ratios at s/l_s of -

NPR	0.723	0.837	0.885	0.922	0.953
1.50	0.834	0.810	0.765	0.737	0.721
1.80	0.799	0.770	0.714	0.677	0.652
2.00	0.789	0.757	0.697	0.658	0.630
2.20	0.780	0.748	0.687	0.647	0.618
2.50	0.773	0.741	0.678	0.640	0.611
3.00	0.768	0.735	0.673	0.635	0.607
3.50	0.765	0.732	0.670	0.634	0.607
4.01	0.762	0.730	0.668	0.632	0.605
4.50	0.761	0.729	0.667	0.632	0.605
4.74	0.761	0.729	0.667	0.632	0.605

Middle channel

Static-pressure ratios at s/l_s of -

NPR	0.673	0.817	0.878	0.924	0.963	0.982
1.50	0.820	0.807	0.767	0.724	0.676	0.651
1.80	0.778	0.760	0.709	0.649	0.577	0.532
2.00	0.765	0.746	0.691	0.625	0.542	0.483
2.20	0.759	0.740	0.683	0.616	0.529	0.464
2.50	0.756	0.737	0.680	0.611	0.525	0.458
3.00	0.754	0.735	0.678	0.609	0.523	0.456
3.50	0.753	0.735	0.678	0.609	0.523	0.456
4.01	0.754	0.735	0.678	0.608	0.523	0.456
4.50	0.753	0.734	0.677	0.608	0.522	0.455
4.74	0.752	0.735	0.677	0.608	0.522	0.455

Outer channel

Static-pressure ratios at s/l_s of -

NPR	0.524	0.744	0.839	0.912	0.973	0.986
1.50	0.859	0.766	0.697	0.680	0.636	0.639
1.80	0.831	0.697	0.604	0.581	0.505	0.503
2.00	0.824	0.670	0.569	0.547	0.461	0.432
2.20	0.821	0.656	0.552	0.532	0.449	0.411
2.50	0.820	0.650	0.544	0.526	0.445	0.403
3.00	0.819	0.647	0.541	0.524	0.443	0.401
3.50	0.819	0.646	0.540	0.523	0.442	0.401
4.01	0.819	0.646	0.539	0.523	0.442	0.401
4.50	0.819	0.645	0.537	0.522	0.442	0.401
4.74	0.818	0.644	0.536	0.522	0.442	0.401

Left instrumented sleeve

Static-pressure ratios at ϕ, deg, of -

NPR	0	45	90	135	180	225	270	315
1.50	0.808	0.806	0.844	0.894	0.910	0.900	0.853	0.812
1.80	0.776	0.774	0.820	0.877	0.897	0.884	0.828	0.783
2.00	0.768	0.766	0.813	0.873	0.892	0.880	0.821	0.775
2.20	0.763	0.761	0.810	0.870	0.890	0.877	0.818	0.771
2.50	0.760	0.758	0.809	0.869	0.890	0.876	0.815	0.769
3.00	0.759	0.756	0.807	0.868	0.889	0.876	0.815	0.768
3.50	0.757	0.754	0.806	0.868	0.889	0.875	0.813	0.767
4.01	0.757	0.754	0.806	0.868	0.889	0.875	0.813	0.768
4.50	0.756	0.753	0.805	0.868	0.889	0.875	0.813	0.767
4.74	0.756	0.753	0.805	0.868	0.889	0.875	0.813	0.767

Right instrumented sleeve

Static-pressure ratios at ϕ, deg, of -

NPR	0	45	90	135	180	225	270	315
1.50	0.826	0.814	0.846	0.896	0.908	0.894	0.843	0.809
1.80	0.801	0.789	0.822	0.880	0.894	0.879	0.819	0.780
2.00	0.794	0.782	0.815	0.875	0.891	0.875	0.813	0.772
2.20	0.791	0.777	0.812	0.873	0.889	0.872	0.810	0.768
2.50	0.790	0.776	0.811	0.872	0.888	0.872	0.808	0.767
3.00	0.789	0.774	0.808	0.871	0.888	0.871	0.807	0.765
3.50	0.789	0.773	0.808	0.871	0.887	0.870	0.807	0.765
4.01	0.789	0.773	0.808	0.872	0.888	0.870	0.806	0.765
4.50	0.789	0.772	0.807	0.871	0.887	0.870	0.806	0.765
4.74	0.788	0.772	0.807	0.871	0.887	0.870	0.806	0.765

Table 91. Static-Pressure Ratios in Nozzle and Instrumented Sleeves for Configuration $P_0C_MB_FN_3T$

Inner wall

Static-pressure ratios at s/l_s of -

NPR	0.429	0.859	0.905	0.926	0.943	0.959
1.51	0.930	0.442	0.462	0.615	0.630	0.643
1.81	0.918	0.334	0.346	0.489	0.503	0.522
2.00	0.915	0.301	0.299	0.424	0.439	0.463
2.21	0.914	0.281	0.267	0.371	0.385	0.412
2.50	0.913	0.265	0.239	0.319	0.332	0.359
3.00	0.912	0.253	0.213	0.262	0.273	0.297
3.50	0.912	0.247	0.199	0.224	0.234	0.256
4.00	0.912	0.244	0.191	0.194	0.204	0.226
4.51	0.912	0.242	0.187	0.171	0.179	0.203
5.00	0.912	0.241	0.185	0.154	0.160	0.186
6.02	0.912	0.239	0.182	0.128	0.131	0.160

Inner channel

Static-pressure ratios at s/l_s of -

NPR	0.723	0.837	0.885	0.922	0.953
1.51	0.850	0.819	0.772	0.741	0.721
1.81	0.821	0.781	0.724	0.686	0.657
2.00	0.811	0.769	0.709	0.669	0.638
2.21	0.804	0.761	0.699	0.659	0.628
2.50	0.800	0.755	0.693	0.654	0.623
3.00	0.794	0.749	0.688	0.650	0.620
3.50	0.789	0.746	0.685	0.647	0.619
4.00	0.788	0.746	0.684	0.648	0.619
4.51	0.787	0.746	0.684	0.647	0.618
5.00	0.786	0.745	0.684	0.646	0.618
6.02	0.784	0.745	0.683	0.646	0.618

Middle channel

Static-pressure ratios at s/l_s of -

NPR	0.673	0.817	0.878	0.924	0.963	0.982
1.51	0.821	0.808	0.771	0.729	0.679	0.648
1.81	0.780	0.761	0.717	0.660	0.587	0.536
2.00	0.767	0.748	0.701	0.639	0.557	0.494
2.21	0.762	0.743	0.693	0.629	0.544	0.477
2.50	0.760	0.739	0.690	0.626	0.540	0.471
3.00	0.760	0.740	0.691	0.625	0.540	0.470
3.50	0.761	0.740	0.690	0.624	0.539	0.469
4.00	0.761	0.741	0.691	0.625	0.539	0.470
4.51	0.762	0.741	0.691	0.625	0.539	0.470
5.00	0.761	0.740	0.690	0.624	0.539	0.469
6.02	0.761	0.741	0.690	0.623	0.538	0.469

Outer channel

Static-pressure ratios at s/l_s of -

NPR	0.524	0.744	0.839	0.912	0.973	0.986
1.51	0.854	0.770	0.701	0.681	0.636	0.636
1.81	0.827	0.701	0.609	0.585	0.510	0.501
2.00	0.821	0.678	0.577	0.554	0.471	0.440
2.21	0.819	0.668	0.563	0.542	0.458	0.418
2.50	0.818	0.662	0.555	0.536	0.455	0.413
3.00	0.818	0.658	0.551	0.534	0.454	0.411
3.50	0.818	0.658	0.551	0.534	0.453	0.411
4.00	0.818	0.654	0.545	0.532	0.453	0.411
4.51	0.818	0.651	0.540	0.530	0.452	0.411
5.00	0.818	0.650	0.539	0.530	0.452	0.411
6.02	0.818	0.648	0.534	0.529	0.451	0.412

Left instrumented sleeve

Static-pressure ratios at ϕ, deg, of -

NPR	0	45	90	135	180	225	270	315
1.51	0.802	0.800	0.850	0.899	0.911	0.902	0.850	0.808
1.81	0.770	0.768	0.828	0.882	0.898	0.885	0.827	0.779
2.00	0.762	0.758	0.822	0.879	0.894	0.881	0.820	0.771
2.21	0.758	0.755	0.819	0.877	0.893	0.880	0.816	0.768
2.50	0.755	0.752	0.817	0.875	0.892	0.878	0.815	0.766
3.00	0.754	0.750	0.816	0.874	0.892	0.878	0.814	0.765
3.50	0.752	0.749	0.816	0.874	0.892	0.877	0.813	0.764
4.00	0.753	0.748	0.815	0.874	0.891	0.877	0.812	0.764
4.51	0.753	0.747	0.814	0.873	0.891	0.877	0.811	0.763
5.00	0.752	0.746	0.813	0.873	0.891	0.877	0.811	0.763
6.02	0.751	0.745	0.813	0.873	0.891	0.876	0.811	0.763

Right instrumented sleeve

Static-pressure ratios at ϕ, deg, of -

NPR	0	45	90	135	180	225	270	315
1.51	0.813	0.813	0.858	0.903	0.913	0.899	0.850	0.808
1.81	0.785	0.782	0.834	0.887	0.899	0.883	0.826	0.776
2.00	0.778	0.775	0.827	0.882	0.895	0.878	0.818	0.768
2.21	0.775	0.771	0.824	0.881	0.893	0.876	0.815	0.764
2.50	0.773	0.768	0.822	0.880	0.892	0.875	0.812	0.761
3.00	0.772	0.768	0.820	0.879	0.892	0.874	0.811	0.759
3.50	0.772	0.767	0.819	0.879	0.891	0.874	0.810	0.758
4.00	0.771	0.767	0.820	0.878	0.891	0.873	0.809	0.757
4.51	0.770	0.766	0.819	0.878	0.891	0.873	0.809	0.756
5.00	0.770	0.765	0.818	0.877	0.891	0.873	0.808	0.756
6.02	0.769	0.764	0.818	0.877	0.890	0.872	0.807	0.755

Table 92. Static-Pressure Ratios in Nozzle and Instrumented Sleeves for Configuration $P_OC_MB_FN_3L$

Inner wall

Static-pressure ratios at s/l_s of -

NPR	0.429	0.859	0.905	0.926	0.943	0.959
1.50	0.920	0.437	0.475	0.624	0.642	0.650
1.80	0.908	0.313	0.332	0.500	0.518	0.533
2.00	0.904	0.276	0.282	0.430	0.449	0.470
2.20	0.903	0.253	0.249	0.377	0.397	0.421
2.50	0.901	0.234	0.218	0.319	0.338	0.362
3.01	0.902	0.221	0.189	0.255	0.274	0.303
3.51	0.901	0.216	0.175	0.215	0.231	0.261
3.99	0.901	0.215	0.167	0.188	0.201	0.232
4.51	0.902	0.214	0.163	0.168	0.178	0.211
4.75	0.901	0.215	0.162	0.160	0.170	0.204

Inner channel

Static-pressure ratios at s/l_s of -

0.723	0.837	0.885	0.922	0.953
0.807	0.790	0.748	0.727	0.716
0.773	0.752	0.699	0.667	0.647
0.758	0.735	0.679	0.646	0.622
0.753	0.729	0.671	0.638	0.612
0.745	0.721	0.663	0.630	0.604
0.743	0.718	0.659	0.627	0.601
0.741	0.716	0.657	0.625	0.600
0.741	0.716	0.656	0.625	0.600
0.743	0.718	0.658	0.626	0.601
0.743	0.718	0.657	0.625	0.601

Middle channel

Static-pressure ratios at s/l_s of -

NPR	0.673	0.817	0.878	0.924	0.963	0.982
1.50	0.818	0.800	0.759	0.715	0.668	0.644
1.80	0.776	0.754	0.701	0.640	0.568	0.525
2.00	0.762	0.739	0.683	0.615	0.531	0.472
2.20	0.755	0.734	0.677	0.607	0.519	0.455
2.50	0.752	0.730	0.674	0.603	0.516	0.449
3.01	0.750	0.730	0.673	0.602	0.515	0.448
3.51	0.750	0.730	0.672	0.602	0.515	0.448
3.99	0.750	0.730	0.673	0.602	0.515	0.448
4.51	0.748	0.730	0.672	0.602	0.516	0.449
4.75	0.748	0.730	0.672	0.602	0.516	0.449

Outer channel

Static-pressure ratios at s/l_s of -

0.524	0.744	0.839	0.912	0.973	0.986
0.867	0.777	0.706	0.685	0.639	0.640
0.841	0.713	0.616	0.588	0.511	0.506
0.833	0.687	0.581	0.552	0.464	0.435
0.830	0.676	0.566	0.536	0.450	0.411
0.828	0.669	0.557	0.529	0.444	0.402
0.827	0.667	0.554	0.527	0.443	0.400
0.827	0.665	0.553	0.526	0.442	0.399
0.826	0.663	0.551	0.525	0.442	0.400
0.825	0.661	0.549	0.525	0.442	0.400
0.825	0.660	0.548	0.525	0.442	0.401

Left instrumented sleeve

Static-pressure ratios at ϕ, deg, of -

NPR	0	45	90	135	180	225	270	315
1.50	0.810	0.807	0.842	0.890	0.909	0.899	0.846	0.811
1.80	0.779	0.777	0.818	0.874	0.896	0.884	0.823	0.781
2.00	0.770	0.767	0.809	0.868	0.890	0.878	0.814	0.772
2.20	0.766	0.764	0.807	0.867	0.890	0.877	0.812	0.769
2.50	0.764	0.760	0.805	0.865	0.889	0.875	0.809	0.767
3.01	0.762	0.758	0.804	0.865	0.888	0.875	0.809	0.766
3.51	0.761	0.756	0.803	0.865	0.888	0.875	0.809	0.765
3.99	0.760	0.755	0.803	0.865	0.888	0.875	0.809	0.765
4.51	0.759	0.754	0.802	0.865	0.888	0.875	0.809	0.765
4.75	0.759	0.754	0.802	0.865	0.888	0.875	0.809	0.764

Right instrumented sleeve

Static-pressure ratios at ϕ, deg, of -

0	45	90	135	180	225	270	315
0.832	0.817	0.845	0.894	0.905	0.887	0.833	0.811
0.807	0.792	0.821	0.879	0.892	0.871	0.807	0.782
0.800	0.784	0.814	0.873	0.888	0.865	0.798	0.772
0.798	0.781	0.811	0.871	0.886	0.863	0.795	0.769
0.796	0.778	0.809	0.870	0.885	0.862	0.792	0.767
0.795	0.776	0.807	0.870	0.885	0.861	0.791	0.765
0.795	0.775	0.807	0.870	0.884	0.859	0.790	0.765
0.795	0.775	0.807	0.870	0.884	0.858	0.789	0.766
0.795	0.775	0.807	0.871	0.883	0.857	0.787	0.765
0.795	0.774	0.807	0.870	0.883	0.857	0.787	0.765

Table 93. Static-Pressure Ratios in Nozzle and Instrumented Sleeves for Configuration $P_0C_LB_NN_3T$

Inner wall

Static-pressure ratios at s/l_s of -

NPR	0.429	0.859	0.905	0.926	0.943	0.959
1.52	0.931	0.425	0.450	0.613	0.629	0.639
1.81	0.919	0.321	0.335	0.492	0.508	0.526
2.00	0.916	0.287	0.286	0.424	0.441	0.465
2.20	0.915	0.267	0.255	0.371	0.388	0.415
2.49	0.914	0.250	0.226	0.314	0.331	0.360
3.00	0.913	0.239	0.200	0.254	0.269	0.299
3.50	0.913	0.234	0.187	0.217	0.230	0.256
4.02	0.913	0.232	0.180	0.189	0.200	0.225
4.51	0.913	0.230	0.176	0.169	0.178	0.204
5.01	0.913	0.230	0.174	0.154	0.161	0.188
6.01	0.912	0.228	0.171	0.131	0.135	0.166

Inner channel

Static-pressure ratios at s/l_s of -

NPR	0.723	0.837	0.885	0.922	0.953
1.52	0.837	0.812	0.764	0.734	0.716
1.81	0.812	0.779	0.721	0.683	0.656
2.00	0.801	0.767	0.706	0.665	0.635
2.20	0.795	0.759	0.697	0.656	0.626
2.49	0.789	0.753	0.690	0.651	0.621
3.00	0.784	0.747	0.684	0.646	0.617
3.50	0.780	0.744	0.681	0.644	0.616
4.02	0.779	0.743	0.680	0.644	0.616
4.51	0.778	0.742	0.680	0.643	0.616
5.01	0.778	0.742	0.680	0.644	0.616
6.01	0.775	0.740	0.678	0.643	0.615

Middle channel

Static-pressure ratios at s/l_s of -

NPR	0.673	0.817	0.878	0.924	0.963	0.982
1.52	0.820	0.805	0.766	0.720	0.669	0.641
1.81	0.783	0.764	0.716	0.656	0.582	0.533
2.00	0.771	0.751	0.700	0.635	0.552	0.491
2.20	0.765	0.745	0.693	0.626	0.541	0.475
2.49	0.763	0.743	0.690	0.623	0.537	0.469
3.00	0.761	0.742	0.689	0.622	0.535	0.467
3.50	0.761	0.742	0.689	0.621	0.535	0.467
4.02	0.761	0.742	0.689	0.621	0.535	0.467
4.51	0.760	0.741	0.689	0.621	0.535	0.466
5.01	0.759	0.741	0.688	0.620	0.535	0.466
6.01	0.759	0.741	0.687	0.619	0.533	0.465

Outer channel

Static-pressure ratios at s/l_s of -

NPR	0.524	0.744	0.839	0.912	0.973	0.986
1.52	0.856	0.763	0.693	0.674	0.627	0.628
1.81	0.831	0.693	0.599	0.578	0.501	0.495
2.00	0.826	0.669	0.566	0.548	0.463	0.434
2.20	0.823	0.657	0.551	0.535	0.454	0.415
2.49	0.823	0.649	0.541	0.529	0.450	0.408
3.00	0.822	0.646	0.539	0.527	0.449	0.407
3.50	0.823	0.647	0.538	0.527	0.449	0.407
4.02	0.823	0.646	0.535	0.527	0.449	0.407
4.51	0.823	0.644	0.533	0.526	0.448	0.408
5.01	0.822	0.642	0.530	0.525	0.448	0.408
6.01	0.823	0.640	0.528	0.524	0.448	0.408

Left instrumented sleeve

Static-pressure ratios at ϕ, deg. of -

NPR	0	45	90	135	180	225	270	315
1.52	0.804	0.801	0.849	0.898	0.912	0.901	0.849	0.806
1.81	0.776	0.771	0.825	0.882	0.899	0.887	0.827	0.781
2.00	0.767	0.762	0.818	0.878	0.895	0.881	0.820	0.773
2.20	0.763	0.758	0.816	0.876	0.894	0.880	0.816	0.769
2.49	0.761	0.755	0.814	0.875	0.893	0.879	0.814	0.768
3.00	0.759	0.753	0.812	0.873	0.892	0.878	0.812	0.766
3.50	0.757	0.752	0.812	0.873	0.892	0.877	0.810	0.765
4.02	0.757	0.751	0.811	0.873	0.891	0.877	0.810	0.765
4.51	0.757	0.750	0.811	0.873	0.891	0.877	0.810	0.764
5.01	0.756	0.750	0.810	0.873	0.892	0.877	0.810	0.765
6.01	0.756	0.749	0.809	0.873	0.891	0.876	0.810	0.764

Right instrumented sleeve

Static-pressure ratios at ϕ, deg. of -

NPR	0	45	90	135	180	225	270	315
1.52	0.816	0.811	0.854	0.900	0.913	0.901	0.844	0.804
1.81	0.787	0.783	0.832	0.886	0.900	0.885	0.819	0.774
2.00	0.780	0.776	0.826	0.881	0.896	0.880	0.812	0.766
2.20	0.778	0.771	0.822	0.880	0.894	0.878	0.810	0.763
2.49	0.775	0.768	0.820	0.878	0.893	0.877	0.807	0.758
3.00	0.774	0.767	0.818	0.877	0.892	0.876	0.805	0.757
3.50	0.775	0.766	0.817	0.878	0.892	0.876	0.806	0.758
4.02	0.775	0.765	0.816	0.877	0.892	0.875	0.805	0.757
4.51	0.774	0.765	0.816	0.877	0.892	0.875	0.805	0.757
5.01	0.773	0.764	0.815	0.876	0.891	0.874	0.803	0.756
6.01	0.773	0.763	0.815	0.875	0.891	0.873	0.803	0.755

Table 94. Static-Pressure Ratios in Nozzle and Instrumented Sleeves for Configuration $P_OC_LB_NN_3L$

Inner wall

Static-pressure ratios at s/l_s of -

NPR	0.429	0.859	0.905	0.926	0.943	0.959
1.52	0.922	0.431	0.458	0.612	0.632	0.644
1.80	0.910	0.312	0.329	0.494	0.511	0.530
2.01	0.907	0.279	0.280	0.423	0.441	0.465
2.20	0.905	0.261	0.249	0.371	0.388	0.416
2.51	0.904	0.246	0.219	0.312	0.330	0.358
3.00	0.903	0.234	0.196	0.253	0.270	0.299
3.50	0.903	0.230	0.183	0.214	0.228	0.256
4.00	0.903	0.228	0.177	0.186	0.198	0.227
4.52	0.903	0.227	0.174	0.164	0.174	0.206
4.75	0.903	0.226	0.174	0.156	0.165	0.198

Inner channel

Static-pressure ratios at s/l_s of -

NPR	0.723	0.837	0.885	0.922	0.953
1.52	0.831	0.807	0.762	0.733	0.717
1.80	0.798	0.769	0.712	0.676	0.651
2.01	0.789	0.758	0.698	0.657	0.628
2.20	0.780	0.748	0.687	0.647	0.617
2.51	0.772	0.739	0.677	0.638	0.609
3.00	0.762	0.730	0.668	0.631	0.603
3.50	0.767	0.734	0.671	0.634	0.605
4.00	0.764	0.731	0.669	0.632	0.604
4.52	0.763	0.730	0.668	0.632	0.604
4.75	0.763	0.731	0.668	0.632	0.604

Middle channel

Static-pressure ratios at s/l_s of -

NPR	0.673	0.817	0.878	0.924	0.963	0.982
1.52	0.816	0.803	0.763	0.719	0.671	0.643
1.80	0.777	0.760	0.708	0.649	0.579	0.532
2.01	0.763	0.745	0.690	0.624	0.543	0.482
2.20	0.758	0.739	0.683	0.615	0.530	0.463
2.51	0.755	0.736	0.679	0.610	0.524	0.456
3.00	0.753	0.734	0.677	0.607	0.521	0.454
3.50	0.753	0.735	0.678	0.609	0.524	0.455
4.00	0.753	0.734	0.677	0.608	0.523	0.455
4.52	0.752	0.734	0.677	0.608	0.523	0.455
4.75	0.751	0.734	0.677	0.608	0.523	0.455

Outer channel

Static-pressure ratios at s/l_s of -

NPR	0.524	0.744	0.839	0.912	0.973	0.986
1.52	0.853	0.762	0.693	0.674	0.630	0.632
1.80	0.826	0.696	0.605	0.581	0.507	0.504
2.01	0.818	0.668	0.567	0.545	0.458	0.430
2.20	0.815	0.656	0.552	0.531	0.447	0.409
2.51	0.815	0.650	0.545	0.524	0.442	0.400
3.00	0.813	0.649	0.544	0.522	0.440	0.397
3.50	0.812	0.644	0.539	0.520	0.440	0.398
4.00	0.812	0.644	0.538	0.520	0.440	0.398
4.52	0.812	0.643	0.536	0.520	0.440	0.398
4.75	0.811	0.642	0.535	0.519	0.439	0.398

Left instrumented sleeve

Static-pressure ratios at ϕ, deg, of -

NPR	0	45	90	135	180	225	270	315
1.52	0.803	0.801	0.842	0.892	0.910	0.898	0.850	0.809
1.80	0.773	0.772	0.818	0.876	0.896	0.882	0.827	0.781
2.01	0.763	0.763	0.811	0.871	0.892	0.878	0.821	0.773
2.20	0.759	0.759	0.808	0.869	0.890	0.875	0.817	0.770
2.51	0.757	0.756	0.806	0.868	0.889	0.874	0.814	0.767
3.00	0.754	0.753	0.804	0.867	0.888	0.872	0.812	0.765
3.50	0.753	0.751	0.804	0.867	0.889	0.873	0.813	0.766
4.00	0.752	0.750	0.803	0.867	0.888	0.873	0.812	0.765
4.52	0.752	0.750	0.803	0.866	0.888	0.872	0.811	0.765
4.75	0.751	0.750	0.803	0.866	0.888	0.872	0.812	0.765

Right instrumented sleeve

Static-pressure ratios at ϕ, deg, of -

NPR	0	45	90	135	180	225	270	315
1.52	0.826	0.811	0.841	0.894	0.904	0.888	0.836	0.808
1.80	0.801	0.785	0.818	0.879	0.891	0.873	0.812	0.779
2.01	0.794	0.779	0.811	0.874	0.886	0.867	0.804	0.770
2.20	0.791	0.775	0.808	0.872	0.885	0.865	0.801	0.767
2.51	0.790	0.773	0.806	0.871	0.884	0.865	0.801	0.765
3.00	0.789	0.771	0.804	0.870	0.884	0.864	0.801	0.764
3.50	0.788	0.769	0.803	0.869	0.882	0.862	0.798	0.762
4.00	0.788	0.769	0.803	0.869	0.882	0.862	0.798	0.762
4.52	0.788	0.769	0.803	0.869	0.883	0.862	0.799	0.762
4.75	0.787	0.769	0.803	0.869	0.882	0.862	0.798	0.762

Table 95. Static-Pressure Ratios in Nozzle and Instrumented Sleeves for Configuration $P_OC_LB_FN_3T$

Inner wall

Static-pressure ratios at s/l_s of -

NPR	0.429	0.859	0.905	0.926	0.943	0.959
1.51	0.927	0.452	0.464	0.609	0.628	0.642
1.81	0.915	0.338	0.348	0.489	0.504	0.522
2.00	0.913	0.307	0.303	0.428	0.443	0.464
2.20	0.911	0.289	0.272	0.377	0.392	0.415
2.50	0.909	0.274	0.244	0.324	0.338	0.361
3.01	0.909	0.263	0.219	0.264	0.276	0.297
3.52	0.909	0.258	0.207	0.223	0.235	0.255
4.00	0.909	0.255	0.203	0.193	0.204	0.225
4.50	0.908	0.253	0.200	0.169	0.178	0.203
5.01	0.908	0.252	0.198	0.149	0.158	0.184
6.00	0.907	0.251	0.196	0.123	0.128	0.159

Inner channel

Static-pressure ratios at s/l_s of -

0.723	0.837	0.885	0.922	0.953
0.850	0.819	0.774	0.742	0.724
0.825	0.781	0.727	0.688	0.660
0.814	0.769	0.711	0.669	0.639
0.810	0.762	0.704	0.663	0.631
0.807	0.756	0.698	0.658	0.625
0.802	0.751	0.693	0.653	0.622
0.798	0.749	0.691	0.652	0.621
0.796	0.748	0.690	0.651	0.620
0.794	0.747	0.689	0.650	0.619
0.793	0.747	0.689	0.650	0.619
0.790	0.746	0.687	0.648	0.617

Middle channel

Static-pressure ratios at s/l_s of -

NPR	0.673	0.817	0.878	0.924	0.963	0.982
1.51	0.813	0.805	0.777	0.737	0.687	0.656
1.81	0.769	0.757	0.724	0.671	0.597	0.548
2.00	0.760	0.745	0.707	0.648	0.566	0.504
2.20	0.749	0.736	0.699	0.640	0.554	0.488
2.50	0.747	0.733	0.695	0.634	0.548	0.479
3.01	0.747	0.732	0.694	0.632	0.546	0.476
3.52	0.746	0.731	0.693	0.631	0.545	0.475
4.00	0.748	0.732	0.692	0.630	0.544	0.475
4.50	0.747	0.731	0.691	0.629	0.543	0.474
5.01	0.747	0.731	0.691	0.629	0.543	0.473
6.00	0.746	0.730	0.689	0.627	0.542	0.472

Outer channel

Static-pressure ratios at s/l_s of -

0.524	0.744	0.839	0.912	0.973	0.986
0.845	0.758	0.691	0.675	0.635	0.636
0.816	0.684	0.591	0.572	0.507	0.502
0.812	0.665	0.560	0.543	0.465	0.438
0.807	0.647	0.535	0.523	0.449	0.410
0.807	0.641	0.527	0.518	0.444	0.402
0.807	0.637	0.523	0.516	0.443	0.401
0.807	0.634	0.520	0.515	0.443	0.401
0.807	0.634	0.519	0.515	0.443	0.401
0.807	0.631	0.515	0.513	0.442	0.401
0.807	0.629	0.512	0.512	0.442	0.402
0.807	0.626	0.509	0.511	0.441	0.402

Left instrumented sleeve

Static-pressure ratios at ϕ, deg, of -

NPR	0	45	90	135	180	225	270	315
1.51	0.799	0.798	0.848	0.894	0.909	0.899	0.849	0.805
1.81	0.765	0.765	0.824	0.877	0.895	0.882	0.825	0.775
2.00	0.758	0.758	0.820	0.874	0.891	0.879	0.818	0.767
2.20	0.754	0.752	0.816	0.871	0.889	0.876	0.816	0.765
2.50	0.751	0.750	0.814	0.870	0.888	0.875	0.814	0.763
3.01	0.749	0.748	0.813	0.869	0.888	0.874	0.813	0.762
3.52	0.748	0.746	0.812	0.869	0.887	0.874	0.812	0.761
4.00	0.747	0.745	0.812	0.869	0.887	0.874	0.811	0.761
4.50	0.746	0.744	0.811	0.868	0.886	0.873	0.811	0.760
5.01	0.746	0.744	0.811	0.868	0.887	0.873	0.810	0.760
6.00	0.745	0.743	0.810	0.868	0.886	0.872	0.809	0.760

Right instrumented sleeve

Static-pressure ratios at ϕ, deg, of -

0	45	90	135	180	225	270	315
0.821	0.813	0.855	0.903	0.916	0.903	0.851	0.809
0.793	0.784	0.831	0.887	0.901	0.886	0.826	0.778
0.787	0.777	0.824	0.882	0.897	0.883	0.820	0.770
0.785	0.773	0.822	0.882	0.896	0.881	0.817	0.767
0.782	0.771	0.820	0.880	0.895	0.879	0.815	0.764
0.781	0.769	0.818	0.880	0.894	0.878	0.813	0.762
0.781	0.767	0.817	0.879	0.894	0.877	0.813	0.761
0.780	0.767	0.817	0.878	0.893	0.877	0.812	0.760
0.780	0.766	0.816	0.878	0.893	0.876	0.811	0.759
0.779	0.766	0.816	0.878	0.893	0.876	0.811	0.759
0.779	0.764	0.816	0.877	0.892	0.875	0.810	0.758

Table 96. Static-Pressure Ratios in Nozzle and Instrumented Sleeves for Configuration $P_0C_LB_FN_3L$

Inner wall

Static-pressure ratios at s/l_s of -

NPR	0.429	0.859	0.905	0.926	0.943	0.959
1.51	0.914	0.444	0.467	0.614	0.631	0.643
1.81	0.902	0.330	0.346	0.491	0.508	0.526
2.00	0.898	0.298	0.302	0.426	0.443	0.467
2.20	0.897	0.278	0.269	0.373	0.390	0.416
2.50	0.897	0.260	0.239	0.318	0.333	0.360
3.00	0.896	0.245	0.211	0.259	0.273	0.299
3.51	0.896	0.239	0.195	0.218	0.229	0.257
4.01	0.896	0.236	0.188	0.189	0.199	0.228
4.51	0.896	0.236	0.186	0.167	0.175	0.206
4.76	0.896	0.236	0.185	0.158	0.166	0.197

Inner channel

Static-pressure ratios at s/l_s of -

NPR	0.723	0.837	0.885	0.922	0.953
1.51	0.828	0.803	0.759	0.732	0.717
1.81	0.798	0.767	0.712	0.676	0.651
2.00	0.788	0.753	0.695	0.657	0.629
2.20	0.783	0.746	0.686	0.648	0.619
2.50	0.778	0.740	0.679	0.642	0.613
3.00	0.771	0.732	0.673	0.637	0.609
3.51	0.770	0.732	0.672	0.637	0.610
4.01	0.767	0.730	0.670	0.636	0.609
4.51	0.770	0.732	0.672	0.637	0.610
4.76	0.771	0.733	0.673	0.638	0.610

Middle channel

Static-pressure ratios at s/l_s of -

NPR	0.673	0.817	0.878	0.924	0.963	0.982
1.51	0.809	0.798	0.759	0.716	0.668	0.641
1.81	0.767	0.754	0.704	0.645	0.574	0.527
2.00	0.752	0.739	0.687	0.623	0.541	0.481
2.20	0.746	0.734	0.680	0.614	0.530	0.464
2.50	0.744	0.732	0.677	0.610	0.526	0.458
3.00	0.743	0.731	0.677	0.609	0.525	0.457
3.51	0.742	0.731	0.677	0.610	0.526	0.458
4.01	0.742	0.731	0.677	0.610	0.525	0.457
4.51	0.740	0.731	0.677	0.610	0.526	0.459
4.76	0.739	0.730	0.677	0.610	0.526	0.459

Outer channel

Static-pressure ratios at s/l_s of -

NPR	0.524	0.744	0.839	0.912	0.973	0.986
1.51	0.860	0.770	0.698	0.678	0.631	0.633
1.81	0.833	0.704	0.609	0.583	0.505	0.498
2.00	0.825	0.679	0.576	0.550	0.463	0.432
2.20	0.822	0.666	0.559	0.535	0.451	0.412
2.50	0.820	0.659	0.550	0.528	0.446	0.403
3.00	0.819	0.657	0.547	0.525	0.444	0.401
3.51	0.818	0.654	0.544	0.525	0.444	0.401
4.01	0.817	0.653	0.542	0.524	0.443	0.401
4.51	0.816	0.650	0.539	0.523	0.443	0.402
4.76	0.816	0.649	0.538	0.523	0.444	0.402

Left instrumented sleeve

Static-pressure ratios at ϕ, deg. of -

NPR	0	45	90	135	180	225	270	315
1.51	0.800	0.802	0.841	0.886	0.904	0.898	0.849	0.803
1.81	0.769	0.772	0.817	0.869	0.891	0.882	0.826	0.775
2.00	0.760	0.763	0.810	0.864	0.885	0.877	0.820	0.766
2.20	0.756	0.759	0.807	0.862	0.885	0.875	0.817	0.763
2.50	0.753	0.756	0.806	0.861	0.884	0.875	0.816	0.762
3.00	0.752	0.753	0.804	0.860	0.883	0.874	0.814	0.761
3.51	0.750	0.752	0.804	0.860	0.884	0.874	0.814	0.761
4.01	0.750	0.751	0.803	0.860	0.883	0.874	0.813	0.761
4.51	0.749	0.750	0.803	0.860	0.883	0.874	0.814	0.761
4.76	0.748	0.750	0.803	0.860	0.883	0.873	0.813	0.760

Right instrumented sleeve

Static-pressure ratios at ϕ, deg. of -

NPR	0	45	90	135	180	225	270	315
1.51	0.826	0.814	0.843	0.892	0.906	0.896	0.842	0.806
1.81	0.801	0.789	0.821	0.877	0.892	0.881	0.820	0.778
2.00	0.794	0.782	0.814	0.872	0.887	0.876	0.812	0.769
2.20	0.791	0.778	0.811	0.870	0.886	0.874	0.810	0.766
2.50	0.790	0.776	0.809	0.868	0.885	0.873	0.808	0.764
3.00	0.789	0.774	0.807	0.867	0.884	0.872	0.807	0.762
3.51	0.788	0.773	0.806	0.867	0.884	0.872	0.807	0.762
4.01	0.788	0.773	0.806	0.867	0.884	0.872	0.807	0.762
4.51	0.788	0.772	0.806	0.866	0.884	0.871	0.805	0.761
4.76	0.787	0.772	0.806	0.866	0.883	0.871	0.805	0.761

Table 97. Static-Pressure Ratios in Nozzle and Instrumented Sleeves for Configuration $P_0C_LB_TN_3T$

Inner wall

Static-pressure ratios at s/l_s of -

NPR	0.429	0.859	0.905	0.926	0.943	0.959
1.53	0.929	0.427	0.452	0.610	0.626	0.636
1.80	0.919	0.324	0.338	0.492	0.507	0.526
2.02	0.917	0.285	0.283	0.414	0.431	0.458
2.20	0.915	0.268	0.254	0.367	0.384	0.414
2.51	0.915	0.253	0.226	0.308	0.325	0.355
3.00	0.914	0.243	0.202	0.252	0.266	0.295
3.51	0.914	0.238	0.190	0.214	0.227	0.253
4.02	0.915	0.236	0.183	0.188	0.199	0.223
4.50	0.914	0.234	0.180	0.169	0.177	0.201
5.02	0.915	0.233	0.178	0.152	0.159	0.184
6.02	0.915	0.232	0.175	0.128	0.132	0.159

Inner channel

Static-pressure ratios at s/l_s of -

NPR	0.723	0.837	0.885	0.922	0.953
1.53	0.845	0.815	0.766	0.735	0.715
1.80	0.818	0.782	0.723	0.684	0.656
2.02	0.805	0.767	0.705	0.664	0.634
2.20	0.801	0.761	0.697	0.657	0.626
2.51	0.794	0.754	0.690	0.651	0.621
3.00	0.789	0.748	0.684	0.646	0.618
3.51	0.785	0.746	0.682	0.645	0.617
4.02	0.784	0.745	0.682	0.645	0.617
4.50	0.782	0.744	0.681	0.644	0.616
5.02	0.783	0.744	0.681	0.644	0.617
6.02	0.781	0.744	0.680	0.644	0.617

Middle channel

Static-pressure ratios at s/l_s of -

NPR	0.673	0.817	0.878	0.924	0.963	0.982
1.53	0.816	0.804	0.768	0.724	0.671	0.641
1.80	0.780	0.764	0.719	0.662	0.588	0.537
2.02	0.768	0.751	0.701	0.638	0.554	0.491
2.20	0.764	0.746	0.696	0.631	0.545	0.479
2.51	0.762	0.744	0.693	0.627	0.540	0.472
3.00	0.762	0.743	0.692	0.625	0.539	0.470
3.51	0.763	0.744	0.692	0.625	0.539	0.470
4.02	0.763	0.744	0.692	0.625	0.538	0.470
4.50	0.762	0.743	0.691	0.624	0.538	0.469
5.02	0.761	0.743	0.691	0.624	0.539	0.469
6.02	0.760	0.742	0.690	0.623	0.537	0.469

Outer channel

Static-pressure ratios at s/l_s of -

NPR	0.524	0.744	0.839	0.912	0.973	0.986
1.53	0.851	0.761	0.692	0.671	0.626	0.626
1.80	0.827	0.699	0.607	0.583	0.508	0.500
2.02	0.821	0.676	0.574	0.550	0.466	0.433
2.20	0.819	0.666	0.560	0.540	0.457	0.417
2.51	0.818	0.661	0.554	0.535	0.453	0.410
3.00	0.819	0.660	0.551	0.534	0.453	0.409
3.51	0.819	0.660	0.550	0.534	0.453	0.410
4.02	0.819	0.658	0.547	0.533	0.452	0.410
4.50	0.819	0.657	0.546	0.533	0.452	0.411
5.02	0.819	0.654	0.542	0.531	0.452	0.411
6.02	0.819	0.652	0.539	0.531	0.451	0.411

Left instrumented sleeve

Static-pressure ratios at ϕ, deg. of -

NPR	0	45	90	135	180	225	270	315
1.53	0.802	0.797	0.849	0.897	0.913	0.902	0.851	0.807
1.80	0.773	0.768	0.828	0.883	0.901	0.887	0.829	0.781
2.02	0.765	0.759	0.821	0.878	0.897	0.882	0.822	0.772
2.20	0.762	0.755	0.819	0.877	0.896	0.881	0.819	0.769
2.51	0.760	0.753	0.818	0.876	0.895	0.880	0.818	0.768
3.00	0.758	0.750	0.816	0.875	0.894	0.879	0.816	0.766
3.51	0.757	0.749	0.815	0.876	0.894	0.878	0.815	0.765
4.02	0.757	0.749	0.815	0.875	0.894	0.878	0.814	0.765
4.50	0.756	0.747	0.814	0.875	0.893	0.878	0.813	0.765
5.02	0.756	0.747	0.814	0.875	0.894	0.878	0.813	0.765
6.02	0.755	0.747	0.813	0.875	0.894	0.878	0.813	0.765

Right instrumented sleeve

Static-pressure ratios at ϕ, deg. of -

NPR	0	45	90	135	180	225	270	315
1.53	0.818	0.808	0.851	0.901	0.913	0.900	0.848	0.807
1.80	0.795	0.782	0.830	0.888	0.901	0.886	0.827	0.781
2.02	0.788	0.775	0.823	0.883	0.897	0.882	0.821	0.773
2.20	0.786	0.772	0.821	0.882	0.896	0.880	0.818	0.770
2.51	0.785	0.770	0.820	0.881	0.895	0.880	0.817	0.768
3.00	0.784	0.769	0.818	0.881	0.895	0.879	0.816	0.766
3.51	0.784	0.768	0.817	0.880	0.894	0.878	0.815	0.765
4.02	0.783	0.768	0.817	0.880	0.894	0.878	0.815	0.765
4.50	0.783	0.767	0.816	0.880	0.894	0.877	0.814	0.764
5.02	0.783	0.767	0.816	0.879	0.894	0.877	0.814	0.764
6.02	0.782	0.766	0.816	0.879	0.893	0.877	0.813	0.763

Table 98. Static-Pressure Ratios in Nozzle and Instrumented Sleeves for Configuration $P_O C_L B_T N_3 L$

Inner wall
Static-pressure ratios at s/l_s of -

NPR	0.429	0.859	0.905	0.926	0.943	0.959
1.50	0.921	0.443	0.472	0.622	0.642	0.653
1.80	0.908	0.307	0.325	0.496	0.513	0.530
2.00	0.905	0.276	0.279	0.429	0.447	0.470
2.19	0.904	0.256	0.247	0.375	0.393	0.419
2.52	0.903	0.240	0.214	0.312	0.330	0.358
3.00	0.903	0.230	0.190	0.253	0.270	0.300
3.50	0.903	0.225	0.178	0.213	0.228	0.257
3.99	0.902	0.223	0.172	0.186	0.198	0.228
4.50	0.902	0.221	0.169	0.163	0.173	0.207
4.76	0.902	0.221	0.168	0.155	0.164	0.199

Inner channel
Static-pressure ratios at s/l_s of -

NPR	0.723	0.837	0.885	0.922	0.953
1.50	0.815	0.798	0.755	0.732	0.720
1.80	0.777	0.755	0.701	0.669	0.647
2.00	0.768	0.744	0.686	0.651	0.625
2.19	0.755	0.731	0.672	0.638	0.611
2.52	0.755	0.730	0.669	0.633	0.606
3.00	0.750	0.724	0.663	0.628	0.601
3.50	0.748	0.722	0.661	0.627	0.600
3.99	0.745	0.720	0.659	0.625	0.599
4.50	0.746	0.721	0.659	0.625	0.600
4.76	0.747	0.721	0.659	0.625	0.600

Middle channel
Static-pressure ratios at s/l_s of -

NPR	0.673	0.817	0.878	0.924	0.963	0.982
1.50	0.818	0.801	0.761	0.717	0.672	0.648
1.80	0.775	0.754	0.701	0.640	0.568	0.524
2.00	0.762	0.740	0.684	0.617	0.533	0.474
2.19	0.758	0.735	0.678	0.608	0.521	0.455
2.52	0.753	0.732	0.675	0.605	0.518	0.450
3.00	0.751	0.731	0.674	0.604	0.517	0.448
3.50	0.750	0.731	0.673	0.603	0.517	0.449
3.99	0.750	0.731	0.673	0.603	0.516	0.449
4.50	0.749	0.730	0.673	0.603	0.517	0.449
4.76	0.748	0.730	0.673	0.603	0.516	0.449

Outer channel
Static-pressure ratios at s/l_s of -

NPR	0.524	0.744	0.839	0.912	0.973	0.986
1.50	0.871	0.778	0.706	0.687	0.640	0.641
1.80	0.843	0.708	0.613	0.587	0.506	0.499
2.00	0.836	0.683	0.580	0.553	0.465	0.433
2.19	0.834	0.673	0.564	0.539	0.453	0.413
2.52	0.831	0.663	0.554	0.530	0.447	0.404
3.00	0.829	0.660	0.551	0.528	0.445	0.401
3.50	0.828	0.659	0.549	0.527	0.444	0.401
3.99	0.828	0.659	0.548	0.526	0.443	0.401
4.50	0.826	0.657	0.546	0.525	0.443	0.401
4.76	0.826	0.656	0.545	0.525	0.443	0.401

Left instrumented sleeve
Static-pressure ratios at ϕ, deg, of -

NPR	0	45	90	135	180	225	270	315
1.50	0.809	0.807	0.844	0.893	0.911	0.899	0.850	0.812
1.80	0.776	0.776	0.818	0.875	0.896	0.883	0.824	0.781
2.00	0.768	0.767	0.811	0.870	0.891	0.878	0.818	0.773
2.19	0.764	0.763	0.809	0.868	0.890	0.876	0.813	0.769
2.52	0.760	0.760	0.807	0.867	0.889	0.875	0.813	0.767
3.00	0.759	0.757	0.805	0.866	0.889	0.874	0.812	0.766
3.50	0.757	0.755	0.804	0.866	0.889	0.874	0.811	0.766
3.99	0.756	0.754	0.804	0.866	0.888	0.874	0.811	0.766
4.50	0.756	0.754	0.804	0.866	0.888	0.874	0.811	0.765
4.76	0.755	0.753	0.803	0.865	0.888	0.873	0.811	0.765

Right instrumented sleeve
Static-pressure ratios at ϕ, deg, of -

NPR	0	45	90	135	180	225	270	315
1.50	0.833	0.816	0.846	0.896	0.910	0.897	0.843	0.813
1.80	0.807	0.790	0.821	0.881	0.896	0.881	0.819	0.783
2.00	0.802	0.783	0.815	0.876	0.892	0.876	0.812	0.775
2.19	0.799	0.780	0.811	0.874	0.891	0.874	0.811	0.772
2.52	0.797	0.777	0.809	0.873	0.890	0.873	0.807	0.769
3.00	0.797	0.776	0.807	0.872	0.889	0.872	0.806	0.768
3.50	0.796	0.774	0.807	0.872	0.889	0.871	0.805	0.768
3.99	0.795	0.774	0.807	0.871	0.889	0.871	0.806	0.768
4.50	0.795	0.774	0.806	0.871	0.888	0.870	0.805	0.767
4.76	0.795	0.773	0.806	0.871	0.888	0.870	0.805	0.767

Table 99. Static-Pressure Ratios in Nozzle and Instrumented Sleeves for Configuration $P_OC_FB_NN_3T$

Inner wall

Static-pressure ratios at s/l_s of -

NPR	0.429	0.859	0.905	0.926	0.943	0.959
1.51	0.929	0.440	0.462	0.618	0.636	0.648
1.81	0.917	0.317	0.331	0.489	0.508	0.526
2.00	0.913	0.284	0.282	0.422	0.441	0.466
2.20	0.912	0.266	0.248	0.368	0.387	0.416
2.50	0.911	0.253	0.221	0.310	0.329	0.358
3.01	0.911	0.242	0.198	0.248	0.265	0.297
3.51	0.910	0.239	0.188	0.210	0.224	0.255
4.00	0.910	0.237	0.184	0.184	0.196	0.226
4.51	0.910	0.236	0.182	0.162	0.172	0.205
5.02	0.911	0.234	0.180	0.147	0.155	0.190
5.99	0.910	0.234	0.179	0.124	0.129	0.168

Inner channel

Static-pressure ratios at s/l_s of -

NPR	0.723	0.837	0.885	0.922	0.953
1.51	0.839	0.813	0.768	0.738	0.721
1.81	0.807	0.775	0.718	0.679	0.652
2.00	0.797	0.762	0.702	0.661	0.631
2.20	0.792	0.755	0.693	0.653	0.621
2.50	0.786	0.749	0.686	0.646	0.615
3.01	0.780	0.743	0.680	0.641	0.611
3.51	0.778	0.740	0.678	0.640	0.611
4.00	0.777	0.740	0.677	0.640	0.611
4.51	0.776	0.739	0.677	0.639	0.611
5.02	0.774	0.738	0.676	0.639	0.611
5.99	0.773	0.737	0.675	0.638	0.610

Middle channel

Static-pressure ratios at s/l_s of -

NPR	0.673	0.817	0.878	0.924	0.963	0.982
1.51	0.823	0.810	0.771	0.727	0.677	0.650
1.81	0.782	0.764	0.716	0.656	0.582	0.534
2.00	0.771	0.751	0.700	0.635	0.551	0.490
2.20	0.766	0.746	0.693	0.626	0.540	0.474
2.50	0.763	0.743	0.691	0.623	0.536	0.468
3.01	0.763	0.743	0.690	0.622	0.535	0.466
3.51	0.762	0.742	0.689	0.622	0.534	0.466
4.00	0.762	0.742	0.690	0.622	0.535	0.466
4.51	0.761	0.742	0.689	0.622	0.535	0.466
5.02	0.761	0.742	0.689	0.621	0.534	0.465
5.99	0.760	0.741	0.688	0.620	0.533	0.465

Outer channel

Static-pressure ratios at s/l_s of -

NPR	0.524	0.744	0.839	0.912	0.973	0.986
1.51	0.855	0.766	0.698	0.679	0.634	0.636
1.81	0.828	0.695	0.603	0.580	0.502	0.495
2.00	0.822	0.672	0.571	0.549	0.463	0.433
2.20	0.819	0.659	0.555	0.536	0.453	0.413
2.50	0.818	0.653	0.548	0.529	0.448	0.406
3.01	0.818	0.651	0.545	0.529	0.448	0.405
3.51	0.817	0.651	0.544	0.528	0.447	0.405
4.00	0.817	0.649	0.541	0.527	0.447	0.406
4.51	0.817	0.647	0.539	0.526	0.447	0.406
5.02	0.818	0.647	0.538	0.527	0.447	0.406
5.99	0.818	0.645	0.537	0.527	0.447	0.407

Left instrumented sleeve

Static-pressure ratios at ϕ, deg, of -

NPR	0	45	90	135	180	225	270	315
1.51	0.805	0.800	0.849	0.898	0.913	0.899	0.849	0.809
1.81	0.773	0.768	0.825	0.881	0.898	0.883	0.824	0.778
2.00	0.764	0.759	0.818	0.877	0.893	0.878	0.817	0.770
2.20	0.760	0.755	0.815	0.874	0.892	0.876	0.814	0.766
2.50	0.758	0.751	0.813	0.873	0.891	0.875	0.812	0.765
3.01	0.756	0.750	0.812	0.872	0.890	0.874	0.810	0.763
3.51	0.755	0.748	0.811	0.872	0.889	0.873	0.809	0.762
4.00	0.755	0.747	0.811	0.872	0.889	0.873	0.808	0.762
4.51	0.754	0.746	0.811	0.872	0.889	0.873	0.808	0.761
5.02	0.754	0.746	0.810	0.872	0.889	0.873	0.808	0.761
5.99	0.754	0.746	0.810	0.872	0.888	0.872	0.807	0.761

Right instrumented sleeve

Static-pressure ratios at ϕ, deg, of -

NPR	0	45	90	135	180	225	270	315
1.51	0.815	0.814	0.858	0.902	0.913	0.901	0.844	0.806
1.81	0.786	0.784	0.833	0.885	0.899	0.884	0.818	0.774
2.00	0.780	0.776	0.826	0.880	0.894	0.879	0.811	0.766
2.20	0.777	0.771	0.823	0.878	0.892	0.876	0.808	0.762
2.50	0.775	0.769	0.820	0.877	0.891	0.875	0.806	0.760
3.01	0.774	0.767	0.818	0.876	0.890	0.873	0.804	0.758
3.51	0.776	0.767	0.817	0.875	0.889	0.873	0.805	0.758
4.00	0.775	0.766	0.816	0.875	0.889	0.872	0.803	0.757
4.51	0.775	0.765	0.815	0.875	0.889	0.872	0.803	0.757
5.02	0.773	0.765	0.815	0.874	0.888	0.872	0.802	0.756
5.99	0.772	0.763	0.815	0.874	0.888	0.871	0.801	0.755

Table 100. Static-Pressure Ratios in Nozzle and Instrumented Sleeves for Configuration $P_OC_FB_NN_3L$

Inner wall
Static-pressure ratios at s/l_s of -

NPR	0.429	0.859	0.905	0.926	0.943	0.959
1.50	0.924	0.443	0.465	0.616	0.638	0.650
1.80	0.910	0.312	0.328	0.494	0.511	0.530
2.00	0.906	0.284	0.282	0.425	0.442	0.466
2.19	0.905	0.268	0.254	0.376	0.392	0.419
2.50	0.904	0.255	0.225	0.317	0.333	0.360
3.00	0.903	0.245	0.203	0.258	0.272	0.298
3.49	0.902	0.240	0.192	0.219	0.231	0.256
4.00	0.902	0.239	0.187	0.188	0.199	0.225
4.51	0.902	0.236	0.184	0.164	0.173	0.203
4.75	0.902	0.236	0.183	0.155	0.163	0.195

Inner channel
Static-pressure ratios at s/l_s of -

NPR	0.723	0.837	0.885	0.922	0.953
1.50	0.828	0.807	0.763	0.736	0.721
1.80	0.794	0.767	0.711	0.676	0.651
2.00	0.783	0.754	0.694	0.655	0.627
2.19	0.775	0.745	0.685	0.645	0.616
2.50	0.772	0.740	0.678	0.638	0.609
3.00	0.766	0.734	0.671	0.633	0.604
3.49	0.762	0.730	0.668	0.631	0.603
4.00	0.763	0.730	0.668	0.631	0.603
4.51	0.761	0.728	0.666	0.630	0.602
4.75	0.759	0.728	0.666	0.630	0.602

Middle channel
Static-pressure ratios at s/l_s of -

NPR	0.673	0.817	0.878	0.924	0.963	0.982
1.50	0.817	0.804	0.764	0.722	0.675	0.651
1.80	0.776	0.757	0.706	0.647	0.577	0.533
2.00	0.762	0.743	0.688	0.623	0.540	0.483
2.19	0.758	0.738	0.682	0.614	0.528	0.463
2.50	0.754	0.734	0.678	0.609	0.523	0.457
3.00	0.753	0.734	0.677	0.609	0.523	0.455
3.49	0.752	0.733	0.677	0.609	0.522	0.455
4.00	0.751	0.733	0.677	0.608	0.523	0.455
4.51	0.751	0.733	0.676	0.608	0.522	0.454
4.75	0.751	0.733	0.676	0.607	0.522	0.454

Outer channel
Static-pressure ratios at s/l_s of -

NPR	0.524	0.744	0.839	0.912	0.973	0.986
1.50	0.861	0.769	0.701	0.682	0.638	0.641
1.80	0.832	0.701	0.609	0.584	0.507	0.504
2.00	0.824	0.675	0.576	0.551	0.462	0.433
2.19	0.821	0.664	0.561	0.537	0.452	0.413
2.50	0.819	0.656	0.551	0.529	0.446	0.404
3.00	0.818	0.654	0.549	0.527	0.444	0.402
3.49	0.817	0.653	0.547	0.527	0.443	0.401
4.00	0.816	0.651	0.545	0.526	0.443	0.402
4.51	0.816	0.651	0.544	0.526	0.443	0.402
4.75	0.816	0.651	0.544	0.525	0.443	0.402

Left instrumented sleeve
Static-pressure ratios at ϕ, deg, of -

NPR	0	45	90	135	180	225	270	315
1.50	0.804	0.805	0.845	0.891	0.910	0.897	0.849	0.808
1.80	0.771	0.773	0.820	0.873	0.894	0.880	0.825	0.779
2.00	0.761	0.763	0.813	0.868	0.889	0.874	0.818	0.770
2.19	0.757	0.760	0.810	0.865	0.887	0.873	0.814	0.766
2.50	0.754	0.757	0.808	0.865	0.887	0.871	0.812	0.764
3.00	0.752	0.753	0.806	0.864	0.885	0.871	0.811	0.762
3.49	0.751	0.752	0.805	0.864	0.885	0.870	0.810	0.762
4.00	0.750	0.751	0.805	0.864	0.885	0.870	0.811	0.762
4.51	0.750	0.751	0.804	0.863	0.885	0.870	0.810	0.762
4.75	0.749	0.750	0.804	0.863	0.885	0.870	0.810	0.761

Right instrumented sleeve
Static-pressure ratios at ϕ, deg, of -

NPR	0	45	90	135	180	225	270	315
1.50	0.828	0.813	0.844	0.897	0.903	0.886	0.834	0.809
1.80	0.803	0.786	0.820	0.881	0.889	0.867	0.805	0.778
2.00	0.796	0.779	0.813	0.875	0.885	0.863	0.798	0.769
2.19	0.792	0.775	0.811	0.873	0.884	0.862	0.797	0.766
2.50	0.790	0.773	0.808	0.873	0.883	0.861	0.795	0.763
3.00	0.790	0.771	0.807	0.872	0.883	0.861	0.794	0.763
3.49	0.789	0.770	0.806	0.871	0.883	0.860	0.795	0.762
4.00	0.788	0.770	0.806	0.871	0.882	0.859	0.793	0.762
4.51	0.788	0.769	0.806	0.871	0.881	0.859	0.794	0.761
4.75	0.788	0.769	0.806	0.871	0.882	0.859	0.793	0.761

Table 101. Static-Pressure Ratios in Nozzle and Instrumented Sleeves for Configuration $P_O C_F B_F N_3 T$

Inner wall

Static-pressure ratios at s/l_s of -

NPR	0.429	0.859	0.905	0.926	0.943	0.959
1.50	0.931	0.445	0.467	0.621	0.639	0.651
1.80	0.918	0.317	0.331	0.492	0.509	0.527
2.01	0.915	0.281	0.278	0.418	0.437	0.463
2.21	0.914	0.264	0.246	0.364	0.382	0.412
2.50	0.914	0.252	0.219	0.306	0.324	0.356
3.00	0.913	0.243	0.198	0.246	0.262	0.295
3.51	0.914	0.239	0.188	0.207	0.222	0.252
4.00	0.914	0.237	0.183	0.181	0.194	0.223
4.50	0.914	0.235	0.181	0.164	0.174	0.202
5.00	0.914	0.234	0.179	0.149	0.157	0.186
6.01	0.914	0.233	0.176	0.126	0.130	0.162

Inner channel

Static-pressure ratios at s/l_s of -

NPR	0.723	0.837	0.885	0.922	0.953
1.50	0.840	0.817	0.770	0.740	0.723
1.80	0.808	0.777	0.718	0.680	0.652
2.01	0.796	0.763	0.701	0.660	0.630
2.21	0.791	0.756	0.693	0.652	0.621
2.50	0.785	0.750	0.685	0.645	0.614
3.00	0.781	0.744	0.679	0.640	0.611
3.51	0.778	0.742	0.677	0.639	0.610
4.00	0.776	0.740	0.676	0.639	0.610
4.50	0.774	0.739	0.675	0.638	0.610
5.00	0.774	0.739	0.675	0.638	0.610
6.01	0.772	0.738	0.674	0.637	0.610

Middle channel

Static-pressure ratios at s/l_s of -

NPR	0.673	0.817	0.878	0.924	0.963	0.982
1.50	0.829	0.813	0.774	0.731	0.682	0.654
1.80	0.789	0.768	0.718	0.658	0.585	0.536
2.01	0.777	0.755	0.701	0.635	0.552	0.490
2.21	0.773	0.750	0.696	0.628	0.541	0.475
2.50	0.772	0.749	0.693	0.624	0.537	0.469
3.00	0.771	0.748	0.693	0.624	0.536	0.468
3.51	0.771	0.748	0.693	0.624	0.536	0.468
4.00	0.771	0.748	0.693	0.623	0.536	0.467
4.50	0.770	0.748	0.692	0.623	0.536	0.467
5.00	0.770	0.748	0.692	0.623	0.535	0.466
6.01	0.769	0.747	0.691	0.622	0.535	0.466

Outer channel

Static-pressure ratios at s/l_s of -

NPR	0.524	0.744	0.839	0.912	0.973	0.986
1.50	0.855	0.771	0.705	0.686	0.640	0.640
1.80	0.827	0.702	0.611	0.585	0.508	0.500
2.01	0.821	0.678	0.579	0.553	0.465	0.434
2.21	0.818	0.668	0.565	0.541	0.455	0.415
2.50	0.818	0.664	0.559	0.537	0.452	0.409
3.00	0.819	0.662	0.557	0.537	0.452	0.409
3.51	0.819	0.661	0.555	0.536	0.451	0.409
4.00	0.820	0.660	0.554	0.535	0.451	0.410
4.50	0.820	0.659	0.553	0.535	0.451	0.411
5.00	0.820	0.658	0.552	0.535	0.451	0.411
6.01	0.819	0.656	0.549	0.534	0.451	0.411

Left instrumented sleeve

Static-pressure ratios at ϕ, deg, of -

NPR	0	45	90	135	180	225	270	315
1.50	0.807	0.803	0.852	0.899	0.914	0.901	0.851	0.809
1.80	0.773	0.769	0.828	0.881	0.900	0.884	0.825	0.778
2.01	0.765	0.760	0.821	0.877	0.895	0.879	0.818	0.770
2.21	0.761	0.757	0.819	0.875	0.894	0.878	0.815	0.767
2.50	0.759	0.754	0.817	0.875	0.893	0.877	0.813	0.765
3.00	0.758	0.752	0.816	0.874	0.892	0.876	0.812	0.764
3.51	0.757	0.751	0.816	0.874	0.893	0.876	0.811	0.764
4.00	0.756	0.750	0.815	0.874	0.892	0.876	0.810	0.763
4.50	0.756	0.750	0.815	0.874	0.892	0.875	0.810	0.763
5.00	0.756	0.749	0.815	0.874	0.892	0.875	0.809	0.763
6.01	0.755	0.748	0.814	0.873	0.892	0.875	0.809	0.762

Right instrumented sleeve

Static-pressure ratios at ϕ, deg, of -

NPR	0	45	90	135	180	225	270	315
1.50	0.823	0.811	0.852	0.900	0.910	0.900	0.848	0.809
1.80	0.795	0.781	0.827	0.884	0.896	0.882	0.823	0.779
2.01	0.788	0.774	0.820	0.880	0.892	0.878	0.817	0.771
2.21	0.785	0.771	0.818	0.878	0.890	0.876	0.814	0.768
2.50	0.784	0.769	0.817	0.878	0.890	0.875	0.813	0.766
3.00	0.784	0.768	0.815	0.878	0.890	0.875	0.812	0.764
3.51	0.782	0.767	0.815	0.877	0.890	0.874	0.811	0.763
4.00	0.783	0.767	0.814	0.877	0.890	0.874	0.811	0.763
4.50	0.782	0.766	0.814	0.877	0.889	0.874	0.810	0.763
5.00	0.782	0.766	0.814	0.877	0.889	0.874	0.810	0.763
6.01	0.782	0.765	0.814	0.876	0.889	0.874	0.809	0.762

Table 102. Static-Pressure Ratios in Nozzle and Instrumented Sleeves for Configuration $P_0C_FB_FN_3L$

Inner wall
Static-pressure ratios at s/l_s of -

NPR	0.429	0.859	0.905	0.926	0.943	0.959
1.50	0.922	0.443	0.467	0.616	0.637	0.650
1.80	0.910	0.307	0.324	0.492	0.509	0.530
2.01	0.906	0.279	0.277	0.423	0.440	0.465
2.20	0.905	0.264	0.247	0.371	0.387	0.415
2.50	0.905	0.251	0.220	0.315	0.331	0.360
3.01	0.904	0.241	0.197	0.254	0.268	0.297
3.50	0.904	0.237	0.187	0.216	0.229	0.256
3.99	0.904	0.236	0.183	0.187	0.198	0.226
4.50	0.904	0.234	0.180	0.162	0.172	0.204
4.76	0.904	0.234	0.180	0.153	0.161	0.195

Inner channel
Static-pressure ratios at s/l_s of -

NPR	0.723	0.837	0.885	0.922	0.953
1.50	0.820	0.802	0.758	0.733	0.720
1.80	0.783	0.761	0.706	0.671	0.649
2.01	0.772	0.747	0.688	0.651	0.625
2.20	0.766	0.740	0.680	0.642	0.614
2.50	0.759	0.732	0.671	0.634	0.606
3.01	0.756	0.729	0.666	0.630	0.603
3.50	0.754	0.726	0.664	0.629	0.602
3.99	0.753	0.725	0.663	0.628	0.601
4.50	0.753	0.725	0.663	0.628	0.601
4.76	0.752	0.724	0.662	0.627	0.601

Middle channel
Static-pressure ratios at s/l_s of -

NPR	0.673	0.817	0.878	0.924	0.963	0.982
1.50	0.817	0.801	0.761	0.717	0.672	0.647
1.80	0.775	0.755	0.703	0.642	0.570	0.526
2.01	0.762	0.740	0.685	0.618	0.534	0.475
2.20	0.756	0.735	0.678	0.610	0.524	0.457
2.50	0.754	0.734	0.677	0.607	0.520	0.452
3.01	0.752	0.732	0.675	0.606	0.519	0.451
3.50	0.752	0.732	0.675	0.606	0.519	0.451
3.99	0.751	0.732	0.675	0.605	0.519	0.451
4.50	0.750	0.732	0.675	0.605	0.519	0.451
4.76	0.750	0.732	0.674	0.605	0.519	0.451

Outer channel
Static-pressure ratios at s/l_s of -

NPR	0.524	0.744	0.839	0.912	0.973	0.986
1.50	0.870	0.777	0.704	0.686	0.637	0.639
1.80	0.843	0.709	0.614	0.588	0.506	0.498
2.01	0.836	0.685	0.582	0.556	0.466	0.433
2.20	0.832	0.672	0.566	0.542	0.455	0.414
2.50	0.832	0.666	0.559	0.535	0.450	0.406
3.01	0.829	0.663	0.555	0.532	0.448	0.404
3.50	0.829	0.662	0.553	0.531	0.447	0.404
3.99	0.827	0.660	0.551	0.530	0.446	0.404
4.50	0.826	0.659	0.550	0.529	0.446	0.404
4.76	0.826	0.659	0.549	0.529	0.445	0.404

Left instrumented sleeve
Static-pressure ratios at ϕ, deg, of -

NPR	0	45	90	135	180	225	270	315
1.50	0.804	0.803	0.846	0.892	0.910	0.898	0.850	0.809
1.80	0.772	0.771	0.821	0.875	0.896	0.882	0.826	0.780
2.01	0.763	0.762	0.814	0.869	0.891	0.876	0.819	0.771
2.20	0.759	0.758	0.811	0.868	0.889	0.875	0.815	0.768
2.50	0.757	0.755	0.809	0.867	0.889	0.874	0.814	0.766
3.01	0.754	0.752	0.807	0.866	0.888	0.873	0.813	0.765
3.50	0.754	0.751	0.807	0.866	0.888	0.873	0.812	0.764
3.99	0.753	0.750	0.806	0.866	0.888	0.873	0.812	0.764
4.50	0.752	0.749	0.806	0.866	0.888	0.872	0.812	0.764
4.76	0.751	0.749	0.805	0.866	0.887	0.872	0.811	0.764

Right instrumented sleeve
Static-pressure ratios at ϕ, deg, of -

NPR	0	45	90	135	180	225	270	315
1.50	0.830	0.816	0.846	0.898	0.910	0.896	0.844	0.811
1.80	0.805	0.789	0.822	0.883	0.896	0.879	0.819	0.782
2.01	0.798	0.782	0.815	0.877	0.892	0.875	0.813	0.774
2.20	0.795	0.778	0.812	0.875	0.890	0.872	0.810	0.770
2.50	0.794	0.776	0.810	0.874	0.890	0.872	0.809	0.768
3.01	0.793	0.775	0.808	0.874	0.889	0.871	0.807	0.767
3.50	0.793	0.774	0.808	0.873	0.889	0.870	0.807	0.767
3.99	0.793	0.773	0.807	0.873	0.888	0.869	0.806	0.766
4.50	0.792	0.773	0.807	0.873	0.888	0.869	0.805	0.766
4.76	0.792	0.772	0.807	0.873	0.888	0.869	0.805	0.766

Table 103. Static-Pressure Ratios in Nozzle and Instrumented Sleeves for Configuration $P_OC_FB_TN_3T$

Inner wall

Static-pressure ratios at s/l_s of -

NPR	0.429	0.859	0.905	0.926	0.943	0.959
1.51	0.928	0.446	0.470	0.620	0.638	0.648
1.80	0.916	0.323	0.340	0.493	0.512	0.531
2.00	0.913	0.283	0.282	0.420	0.441	0.466
2.20	0.912	0.265	0.247	0.364	0.384	0.414
2.51	0.911	0.253	0.220	0.305	0.326	0.357
3.00	0.910	0.245	0.200	0.245	0.264	0.298
3.51	0.910	0.241	0.191	0.207	0.223	0.256
4.00	0.911	0.239	0.186	0.183	0.196	0.228
4.51	0.910	0.237	0.184	0.164	0.174	0.210
5.01	0.910	0.237	0.182	0.149	0.157	0.195
6.01	0.910	0.235	0.180	0.129	0.132	0.174

Inner channel

Static-pressure ratios at s/l_s of -

NPR	0.723	0.837	0.885	0.922	0.953
1.51	0.830	0.810	0.765	0.737	0.721
1.80	0.796	0.772	0.715	0.679	0.652
2.00	0.785	0.758	0.698	0.659	0.630
2.20	0.777	0.749	0.688	0.649	0.618
2.51	0.772	0.744	0.681	0.642	0.612
3.00	0.766	0.738	0.675	0.638	0.608
3.51	0.764	0.736	0.673	0.636	0.608
4.00	0.762	0.734	0.671	0.636	0.607
4.51	0.761	0.733	0.671	0.635	0.607
5.01	0.760	0.732	0.670	0.635	0.607
6.01	0.759	0.732	0.669	0.634	0.607

Middle channel

Static-pressure ratios at s/l_s of -

NPR	0.673	0.817	0.878	0.924	0.963	0.982
1.51	0.829	0.808	0.768	0.723	0.675	0.648
1.80	0.792	0.765	0.715	0.653	0.580	0.533
2.00	0.781	0.753	0.698	0.631	0.547	0.486
2.20	0.776	0.748	0.693	0.623	0.536	0.471
2.51	0.774	0.746	0.690	0.621	0.533	0.465
3.00	0.774	0.746	0.691	0.620	0.533	0.465
3.51	0.774	0.747	0.691	0.621	0.534	0.465
4.00	0.774	0.747	0.691	0.620	0.533	0.465
4.51	0.773	0.747	0.691	0.620	0.533	0.464
5.01	0.772	0.747	0.691	0.620	0.533	0.464
6.01	0.771	0.746	0.690	0.619	0.532	0.463

Outer channel

Static-pressure ratios at s/l_s of -

NPR	0.524	0.744	0.839	0.912	0.973	0.986
1.51	0.862	0.772	0.704	0.685	0.636	0.637
1.80	0.837	0.705	0.614	0.589	0.507	0.498
2.00	0.831	0.682	0.583	0.558	0.469	0.434
2.20	0.831	0.672	0.570	0.547	0.459	0.418
2.51	0.830	0.665	0.562	0.542	0.456	0.413
3.00	0.830	0.664	0.559	0.541	0.455	0.412
3.51	0.831	0.664	0.558	0.540	0.455	0.413
4.00	0.831	0.664	0.557	0.541	0.455	0.414
4.51	0.831	0.661	0.553	0.539	0.455	0.414
5.01	0.831	0.660	0.552	0.539	0.455	0.414
6.01	0.831	0.658	0.550	0.538	0.455	0.415

Left instrumented sleeve

Static-pressure ratios at ϕ, deg, of -

NPR	0	45	90	135	180	225	270	315
1.51	0.808	0.802	0.851	0.899	0.913	0.900	0.849	0.810
1.80	0.775	0.771	0.828	0.883	0.899	0.883	0.824	0.780
2.00	0.767	0.762	0.822	0.879	0.895	0.879	0.818	0.772
2.20	0.764	0.759	0.819	0.877	0.893	0.878	0.813	0.769
2.51	0.761	0.755	0.817	0.876	0.892	0.876	0.811	0.767
3.00	0.760	0.753	0.816	0.875	0.892	0.875	0.810	0.765
3.51	0.759	0.753	0.816	0.875	0.891	0.875	0.808	0.764
4.00	0.759	0.752	0.816	0.875	0.891	0.875	0.807	0.764
4.51	0.758	0.751	0.815	0.875	0.891	0.874	0.807	0.764
5.01	0.758	0.751	0.815	0.875	0.891	0.874	0.806	0.763
6.01	0.757	0.750	0.814	0.875	0.891	0.873	0.806	0.763

Right instrumented sleeve

Static-pressure ratios at ϕ, deg, of -

NPR	0	45	90	135	180	225	270	315
1.51	0.823	0.812	0.853	0.900	0.910	0.899	0.845	0.810
1.80	0.796	0.784	0.830	0.885	0.896	0.883	0.821	0.781
2.00	0.790	0.777	0.824	0.881	0.893	0.879	0.815	0.773
2.20	0.787	0.774	0.821	0.880	0.892	0.878	0.813	0.770
2.51	0.785	0.771	0.819	0.879	0.890	0.876	0.810	0.767
3.00	0.785	0.770	0.818	0.878	0.890	0.875	0.809	0.766
3.51	0.784	0.770	0.818	0.878	0.890	0.875	0.809	0.765
4.00	0.785	0.770	0.817	0.878	0.890	0.875	0.809	0.765
4.51	0.784	0.769	0.817	0.878	0.890	0.875	0.808	0.764
5.01	0.784	0.769	0.817	0.877	0.889	0.875	0.807	0.764
6.01	0.783	0.768	0.817	0.877	0.890	0.874	0.807	0.764

Table 104. Static-Pressure Ratios in Nozzle and Instrumented Sleeves for Configuration $P_0C_FB_TN_3L$

Inner wall

Static-pressure ratios at s/l_s of -

NPR	0.429	0.859	0.905	0.926	0.943	0.959
1.50	0.923	0.445	0.470	0.619	0.639	0.651
1.80	0.911	0.305	0.324	0.492	0.512	0.532
2.00	0.907	0.272	0.270	0.419	0.439	0.466
2.20	0.907	0.257	0.238	0.363	0.383	0.415
2.50	0.906	0.245	0.213	0.303	0.324	0.357
3.00	0.905	0.237	0.194	0.242	0.261	0.297
3.50	0.905	0.233	0.184	0.206	0.221	0.255
4.00	0.905	0.231	0.180	0.182	0.194	0.227
4.51	0.905	0.231	0.178	0.162	0.171	0.205
4.75	0.905	0.230	0.176	0.154	0.163	0.198

Inner channel

Static-pressure ratios at s/l_s of -

NPR	0.723	0.837	0.885	0.922	0.953
1.50	0.817	0.799	0.757	0.732	0.720
1.80	0.783	0.760	0.706	0.672	0.650
2.00	0.770	0.746	0.688	0.652	0.626
2.20	0.764	0.739	0.679	0.642	0.614
2.50	0.759	0.733	0.671	0.635	0.607
3.00	0.753	0.726	0.665	0.630	0.602
3.50	0.749	0.722	0.662	0.627	0.600
4.00	0.749	0.722	0.661	0.627	0.600
4.51	0.751	0.723	0.662	0.628	0.601
4.75	0.750	0.723	0.661	0.627	0.600

Middle channel

Static-pressure ratios at s/l_s of -

NPR	0.673	0.817	0.878	0.924	0.963	0.982
1.50	0.815	0.799	0.759	0.716	0.670	0.646
1.80	0.773	0.752	0.701	0.641	0.570	0.527
2.00	0.759	0.738	0.683	0.617	0.533	0.474
2.20	0.754	0.733	0.676	0.608	0.522	0.456
2.50	0.751	0.730	0.674	0.605	0.518	0.450
3.00	0.750	0.730	0.673	0.604	0.517	0.449
3.50	0.749	0.730	0.673	0.603	0.517	0.448
4.00	0.748	0.730	0.672	0.603	0.516	0.448
4.51	0.747	0.729	0.672	0.603	0.517	0.449
4.75	0.747	0.729	0.672	0.602	0.516	0.448

Outer channel

Static-pressure ratios at s/l_s of -

NPR	0.524	0.744	0.839	0.912	0.973	0.986
1.50	0.873	0.778	0.704	0.685	0.637	0.638
1.80	0.845	0.711	0.614	0.588	0.505	0.498
2.00	0.838	0.686	0.582	0.556	0.466	0.432
2.20	0.836	0.675	0.568	0.543	0.456	0.415
2.50	0.834	0.669	0.560	0.536	0.451	0.407
3.00	0.833	0.667	0.557	0.534	0.449	0.405
3.50	0.833	0.667	0.557	0.533	0.449	0.405
4.00	0.832	0.666	0.555	0.533	0.448	0.405
4.51	0.830	0.664	0.554	0.532	0.448	0.405
4.75	0.830	0.664	0.553	0.532	0.447	0.405

Left instrumented sleeve

Static-pressure ratios at ϕ, deg, of -

NPR	0	45	90	135	180	225	270	315
1.50	0.807	0.803	0.846	0.895	0.911	0.899	0.852	0.811
1.80	0.775	0.771	0.822	0.877	0.897	0.882	0.827	0.782
2.00	0.765	0.762	0.814	0.873	0.893	0.877	0.820	0.773
2.20	0.762	0.758	0.812	0.871	0.891	0.875	0.817	0.770
2.50	0.759	0.754	0.810	0.870	0.890	0.874	0.815	0.768
3.00	0.757	0.751	0.808	0.870	0.890	0.873	0.814	0.767
3.50	0.755	0.749	0.807	0.869	0.890	0.873	0.813	0.767
4.00	0.754	0.748	0.807	0.869	0.889	0.872	0.813	0.766
4.51	0.754	0.747	0.806	0.869	0.889	0.872	0.813	0.765
4.75	0.753	0.746	0.806	0.869	0.889	0.872	0.813	0.765

Right instrumented sleeve

Static-pressure ratios at ϕ, deg, of -

NPR	0	45	90	135	180	225	270	315
1.50	0.830	0.811	0.846	0.899	0.909	0.896	0.844	0.815
1.80	0.805	0.784	0.822	0.884	0.896	0.879	0.820	0.786
2.00	0.798	0.776	0.815	0.879	0.891	0.874	0.813	0.779
2.20	0.795	0.773	0.812	0.878	0.891	0.873	0.811	0.776
2.50	0.793	0.770	0.811	0.877	0.889	0.871	0.809	0.773
3.00	0.793	0.768	0.809	0.876	0.889	0.870	0.807	0.772
3.50	0.792	0.768	0.808	0.876	0.889	0.870	0.808	0.772
4.00	0.792	0.767	0.808	0.875	0.888	0.869	0.807	0.771
4.51	0.791	0.766	0.807	0.875	0.888	0.869	0.806	0.771
4.75	0.791	0.766	0.807	0.875	0.887	0.868	0.806	0.770

Table 105. Static-Pressure Ratios in Nozzle and Instrumented Sleeves for Configuration $P_OC_SB_NN_4T$

Inner wall

Static-pressure ratios at s/l_s of -

NPR	0.318	0.637	0.779	0.840	0.888	0.928
1.50	0.910	0.648	0.599	0.444	0.502	0.586
1.80	0.905	0.624	0.573	0.358	0.400	0.480
2.01	0.905	0.621	0.569	0.316	0.333	0.407
2.20	0.906	0.621	0.568	0.289	0.301	0.352
2.50	0.906	0.620	0.568	0.274	0.278	0.301
3.00	0.907	0.621	0.568	0.272	0.272	0.269
3.51	0.908	0.622	0.568	0.272	0.273	0.267
4.00	0.907	0.622	0.567	0.272	0.272	0.266
4.50	0.907	0.622	0.567	0.272	0.272	0.266
5.01	0.907	0.622	0.566	0.272	0.271	0.265
6.00	0.907	0.622	0.566	0.271	0.270	0.264

Inner channel

Static-pressure ratios at s/l_s of -

0.552	0.730	0.817	0.884	0.940
0.636	0.692	0.704	0.684	0.674
0.583	0.637	0.644	0.605	0.577
0.573	0.627	0.634	0.592	0.556
0.566	0.620	0.630	0.587	0.552
0.564	0.621	0.630	0.588	0.553
0.562	0.621	0.631	0.588	0.554
0.557	0.618	0.629	0.587	0.553
0.554	0.617	0.629	0.588	0.553
0.553	0.618	0.630	0.588	0.554
0.551	0.617	0.630	0.587	0.554
0.549	0.618	0.631	0.588	0.554

Outer channel

Static-pressure ratios at s/l_s of -

NPR	0.402	0.658	0.765	0.846	0.916	0.956
1.50	0.840	0.770	0.716	0.684	0.647	0.649
1.80	0.825	0.743	0.669	0.615	0.544	0.529
2.01	0.823	0.740	0.663	0.603	0.511	0.471
2.20	0.823	0.741	0.665	0.604	0.511	0.454
2.50	0.823	0.742	0.664	0.604	0.511	0.440
3.00	0.824	0.743	0.666	0.605	0.512	0.430
3.51	0.824	0.744	0.667	0.606	0.514	0.425
4.00	0.824	0.744	0.667	0.606	0.514	0.422
4.50	0.824	0.744	0.667	0.606	0.514	0.420
5.01	0.824	0.744	0.667	0.605	0.514	0.418
6.00	0.825	0.744	0.667	0.605	0.514	0.418

Left instrumented sleeve

Static-pressure coefficients at ϕ, deg, of -

NPR	0	45	90	135	180	225	270	315
1.50	0.827	0.817	0.834	0.877	0.903	0.876	0.834	0.822
1.80	0.813	0.802	0.823	0.870	0.897	0.868	0.821	0.808
2.01	0.812	0.800	0.822	0.869	0.897	0.867	0.821	0.807
2.20	0.812	0.800	0.823	0.869	0.898	0.868	0.821	0.808
2.50	0.812	0.800	0.823	0.870	0.898	0.869	0.822	0.809
3.00	0.812	0.801	0.824	0.871	0.899	0.869	0.823	0.810
3.51	0.812	0.800	0.824	0.871	0.899	0.869	0.823	0.809
4.00	0.811	0.799	0.824	0.871	0.899	0.869	0.822	0.809
4.50	0.811	0.799	0.824	0.871	0.899	0.868	0.822	0.809
5.01	0.811	0.799	0.824	0.871	0.898	0.868	0.822	0.809
6.00	0.811	0.799	0.824	0.872	0.899	0.868	0.822	0.809

Right instrumented sleeve

Static-pressure ratios at ϕ, deg, of -

0	45	90	135	180	225	270	315
0.835	0.825	0.831	0.874	0.900	0.873	0.835	0.833
0.821	0.810	0.817	0.865	0.893	0.863	0.822	0.819
0.819	0.808	0.815	0.864	0.893	0.863	0.820	0.818
0.821	0.810	0.817	0.866	0.894	0.863	0.821	0.820
0.821	0.810	0.817	0.866	0.895	0.864	0.822	0.820
0.823	0.811	0.817	0.868	0.897	0.865	0.823	0.822
0.824	0.812	0.818	0.869	0.898	0.865	0.824	0.822
0.824	0.812	0.818	0.869	0.898	0.865	0.824	0.822
0.824	0.811	0.818	0.869	0.898	0.865	0.824	0.822
0.823	0.811	0.818	0.869	0.898	0.865	0.824	0.822
0.823	0.811	0.818	0.869	0.897	0.865	0.824	0.822

Table 106. Static-Pressure Ratios in Nozzle and Instrumented Sleeves for Configuration $P_OC_SB_NN_4L$

Inner wall

Static-pressure ratios at s/l_s of -

NPR	0.318	0.637	0.779	0.840	0.888	0.928
1.51	0.900	0.645	0.598	0.447	0.494	0.578
1.81	0.894	0.620	0.571	0.351	0.381	0.468
2.00	0.893	0.617	0.567	0.316	0.331	0.402
2.20	0.894	0.616	0.566	0.292	0.305	0.350
2.50	0.894	0.617	0.566	0.280	0.283	0.300
3.00	0.895	0.617	0.567	0.279	0.279	0.273
3.49	0.895	0.618	0.567	0.280	0.280	0.272
4.00	0.895	0.618	0.565	0.279	0.278	0.270
4.51	0.895	0.619	0.565	0.279	0.278	0.270
5.00	0.895	0.619	0.566	0.279	0.277	0.269

Inner channel

Static-pressure ratios at s/l_s of -

0.552	0.730	0.817	0.884	0.940
0.610	0.675	0.692	0.675	0.667
0.555	0.616	0.628	0.594	0.567
0.544	0.604	0.617	0.578	0.543
0.539	0.601	0.614	0.574	0.539
0.536	0.598	0.612	0.573	0.538
0.532	0.595	0.611	0.572	0.537
0.529	0.594	0.611	0.572	0.537
0.524	0.588	0.606	0.568	0.534
0.526	0.591	0.609	0.571	0.536
0.524	0.591	0.610	0.571	0.537

Outer channel

Static-pressure ratios at s/l_s of -

NPR	0.402	0.658	0.765	0.846	0.916	0.956
1.51	0.837	0.777	0.719	0.683	0.640	0.659
1.81	0.824	0.755	0.679	0.622	0.538	0.552
2.00	0.823	0.755	0.676	0.615	0.521	0.499
2.20	0.823	0.755	0.676	0.616	0.520	0.454
2.50	0.825	0.756	0.678	0.616	0.521	0.399
3.00	0.825	0.758	0.679	0.617	0.523	0.334
3.49	0.826	0.758	0.680	0.617	0.524	0.287
4.00	0.828	0.759	0.681	0.618	0.525	0.250
4.51	0.827	0.758	0.680	0.617	0.524	0.222
5.00	0.828	0.758	0.680	0.617	0.524	0.200

Left instrumented sleeve

Static-pressure coefficients at ϕ, deg, of -

NPR	0	45	90	135	180	225	270	315
1.51	0.828	0.816	0.833	0.874	0.897	0.872	0.832	0.820
1.81	0.815	0.801	0.822	0.867	0.892	0.864	0.820	0.808
2.00	0.815	0.800	0.822	0.866	0.892	0.864	0.819	0.807
2.20	0.815	0.800	0.822	0.867	0.892	0.864	0.820	0.807
2.50	0.815	0.800	0.822	0.867	0.893	0.865	0.821	0.808
3.00	0.815	0.800	0.823	0.868	0.893	0.865	0.821	0.808
3.49	0.815	0.799	0.823	0.869	0.894	0.865	0.821	0.808
4.00	0.814	0.798	0.822	0.868	0.893	0.865	0.821	0.808
4.51	0.814	0.798	0.822	0.869	0.893	0.865	0.821	0.808
5.00	0.813	0.798	0.823	0.869	0.893	0.864	0.821	0.808

Right instrumented sleeve

Static-pressure ratios at ϕ, deg, of -

0	45	90	135	180	225	270	315
0.837	0.829	0.831	0.871	0.895	0.870	0.833	0.821
0.823	0.815	0.818	0.862	0.888	0.861	0.819	0.806
0.823	0.814	0.816	0.861	0.888	0.861	0.818	0.804
0.823	0.814	0.816	0.862	0.888	0.860	0.818	0.804
0.825	0.815	0.817	0.863	0.889	0.861	0.819	0.805
0.826	0.815	0.817	0.864	0.890	0.862	0.819	0.806
0.827	0.816	0.818	0.865	0.890	0.862	0.820	0.806
0.828	0.816	0.819	0.866	0.892	0.863	0.821	0.807
0.828	0.816	0.818	0.865	0.891	0.863	0.820	0.807
0.828	0.816	0.818	0.865	0.891	0.863	0.820	0.807

Table 107. Static-Pressure Ratios in Nozzle and Instrumented Sleeves for Configuration $P_OC_SB_FN_4T$

Inner wall

Static-pressure ratios at s/l_s of -

NPR	0.318	0.637	0.779	0.840	0.888	0.928
1.51	0.909	0.646	0.596	0.441	0.504	0.587
1.81	0.904	0.622	0.571	0.356	0.402	0.479
2.01	0.903	0.619	0.566	0.313	0.333	0.409
2.20	0.903	0.618	0.566	0.287	0.300	0.355
2.50	0.904	0.619	0.566	0.269	0.274	0.299
3.00	0.905	0.619	0.566	0.267	0.269	0.265
3.49	0.904	0.619	0.565	0.268	0.269	0.264
4.02	0.904	0.620	0.565	0.268	0.269	0.263
4.50	0.904	0.621	0.565	0.269	0.269	0.263
5.00	0.904	0.621	0.564	0.268	0.268	0.262
6.01	0.904	0.620	0.564	0.268	0.267	0.262

Inner channel

Static-pressure ratios at s/l_s of -

0.552	0.730	0.817	0.884	0.940
0.626	0.686	0.700	0.681	0.673
0.577	0.634	0.641	0.605	0.576
0.570	0.625	0.632	0.592	0.556
0.566	0.620	0.628	0.587	0.552
0.563	0.619	0.628	0.587	0.552
0.557	0.617	0.627	0.587	0.552
0.556	0.617	0.628	0.587	0.552
0.553	0.615	0.628	0.587	0.552
0.554	0.617	0.629	0.588	0.553
0.550	0.615	0.628	0.586	0.552
0.550	0.617	0.629	0.587	0.553

Outer channel

Static-pressure ratios at s/l_s of -

NPR	0.402	0.658	0.765	0.846	0.916	0.956
1.51	0.840	0.770	0.715	0.681	0.644	0.646
1.81	0.827	0.744	0.670	0.614	0.539	0.524
2.01	0.824	0.741	0.664	0.604	0.511	0.471
2.20	0.824	0.741	0.664	0.604	0.511	0.454
2.50	0.825	0.742	0.665	0.605	0.512	0.441
3.00	0.825	0.744	0.667	0.607	0.513	0.432
3.49	0.825	0.743	0.667	0.606	0.514	0.427
4.02	0.826	0.744	0.668	0.607	0.514	0.424
4.50	0.825	0.743	0.667	0.605	0.514	0.421
5.00	0.826	0.744	0.668	0.606	0.515	0.420
6.01	0.826	0.744	0.667	0.606	0.514	0.419

Left instrumented sleeve

Static-pressure coefficients at ϕ, deg, of -

NPR	0	45	90	135	180	225	270	315
1.51	0.827	0.815	0.832	0.875	0.903	0.875	0.833	0.822
1.81	0.813	0.799	0.821	0.868	0.897	0.867	0.821	0.809
2.01	0.811	0.797	0.820	0.868	0.896	0.866	0.820	0.807
2.20	0.811	0.797	0.820	0.868	0.896	0.866	0.820	0.807
2.50	0.811	0.797	0.821	0.869	0.897	0.867	0.821	0.808
3.00	0.812	0.798	0.822	0.871	0.898	0.868	0.822	0.809
3.49	0.810	0.797	0.821	0.870	0.898	0.867	0.821	0.808
4.02	0.810	0.797	0.822	0.870	0.898	0.867	0.821	0.808
4.50	0.810	0.797	0.822	0.870	0.897	0.867	0.820	0.808
5.00	0.810	0.797	0.822	0.870	0.897	0.867	0.820	0.808
6.01	0.810	0.797	0.823	0.871	0.898	0.866	0.820	0.808

Right instrumented sleeve

Static-pressure ratios at ϕ, deg, of -

0	45	90	135	180	225	270	315
0.824	0.828	0.833	0.874	0.899	0.876	0.838	0.814
0.808	0.809	0.816	0.864	0.891	0.864	0.823	0.798
0.807	0.806	0.815	0.863	0.891	0.863	0.822	0.799
0.806	0.806	0.814	0.863	0.890	0.862	0.822	0.798
0.807	0.807	0.816	0.864	0.892	0.863	0.823	0.800
0.806	0.807	0.815	0.864	0.891	0.864	0.821	0.794
0.807	0.807	0.815	0.864	0.891	0.863	0.822	0.796
0.809	0.808	0.815	0.865	0.893	0.864	0.822	0.797
0.807	0.808	0.814	0.864	0.891	0.863	0.822	0.796
0.807	0.808	0.814	0.864	0.892	0.864	0.821	0.796
0.806	0.807	0.815	0.864	0.892	0.864	0.822	0.796

Table 108. Static-Pressure Ratios in Nozzle and Instrumented Sleeves for Configuration $P_OC_SB_FN_4L$

Inner wall

Static-pressure ratios at s/l_s of -

NPR	0.318	0.637	0.779	0.840	0.888	0.928
1.51	0.898	0.643	0.597	0.449	0.497	0.578
1.81	0.892	0.617	0.569	0.351	0.381	0.468
2.00	0.890	0.612	0.563	0.317	0.332	0.403
2.49	0.892	0.614	0.564	0.280	0.282	0.300
3.00	0.892	0.614	0.564	0.279	0.279	0.272
3.51	0.893	0.616	0.564	0.279	0.279	0.271
4.02	0.893	0.615	0.563	0.277	0.276	0.268
4.51	0.894	0.617	0.564	0.279	0.277	0.269
4.98	0.893	0.617	0.563	0.279	0.277	0.269

Inner channel

Static-pressure ratios at s/l_s of -

0.552	0.730	0.817	0.884	0.940
0.590	0.663	0.684	0.670	0.664
0.532	0.599	0.615	0.585	0.561
0.520	0.582	0.599	0.563	0.532
0.517	0.581	0.599	0.562	0.527
0.516	0.581	0.600	0.564	0.529
0.518	0.584	0.604	0.567	0.532
0.512	0.572	0.595	0.559	0.525
0.518	0.585	0.606	0.569	0.534
0.516	0.585	0.606	0.569	0.534

Outer channel

Static-pressure ratios at s/l_s of -

NPR	0.402	0.658	0.765	0.846	0.916	0.956
1.51	0.844	0.783	0.723	0.684	0.638	0.660
1.81	0.832	0.761	0.684	0.626	0.537	0.551
2.00	0.832	0.760	0.681	0.620	0.524	0.498
2.49	0.832	0.760	0.681	0.619	0.523	0.400
3.00	0.833	0.760	0.681	0.619	0.524	0.333
3.51	0.833	0.759	0.681	0.618	0.524	0.284
4.02	0.835	0.761	0.683	0.620	0.526	0.249
4.51	0.833	0.759	0.681	0.618	0.524	0.222
4.98	0.833	0.758	0.680	0.617	0.524	0.201

Left instrumented sleeve

Static-pressure coefficients at ϕ, deg, of -

NPR	0	45	90	135	180	225	270	315
1.51	0.828	0.814	0.830	0.870	0.896	0.872	0.831	0.819
1.81	0.815	0.800	0.820	0.863	0.890	0.864	0.818	0.806
2.00	0.813	0.797	0.818	0.863	0.889	0.863	0.816	0.805
2.49	0.814	0.798	0.820	0.864	0.891	0.864	0.818	0.806
3.00	0.813	0.797	0.820	0.864	0.891	0.864	0.818	0.806
3.51	0.813	0.797	0.820	0.865	0.891	0.864	0.819	0.806
4.02	0.813	0.796	0.820	0.865	0.891	0.863	0.818	0.807
4.51	0.813	0.796	0.821	0.866	0.891	0.864	0.820	0.806
4.98	0.812	0.796	0.820	0.866	0.891	0.864	0.819	0.806

Right instrumented sleeve

Static-pressure ratios at ϕ, deg, of -

0	45	90	135	180	225	270	315
0.837	0.825	0.825	0.868	0.881	0.851	0.827	0.826
0.823	0.808	0.809	0.858	0.874	0.841	0.810	0.809
0.822	0.807	0.806	0.857	0.876	0.842	0.808	0.806
0.823	0.806	0.806	0.857	0.876	0.841	0.808	0.806
0.823	0.806	0.807	0.858	0.876	0.842	0.809	0.806
0.823	0.806	0.807	0.858	0.875	0.841	0.810	0.806
0.824	0.807	0.809	0.859	0.878	0.844	0.811	0.807
0.824	0.805	0.807	0.858	0.875	0.840	0.809	0.806
0.824	0.806	0.807	0.859	0.877	0.842	0.809	0.807

Table 109. Static-Pressure Ratios in Nozzle and Instrumented Sleeves for Configuration $P_{()}C_MB_NN_4T$

Inner wall

Static-pressure ratios at s/l_s of -

NPR	0.318	0.637	0.779	0.840	0.888	0.928
1.51	0.906	0.642	0.594	0.447	0.507	0.586
1.81	0.901	0.617	0.566	0.359	0.401	0.477
2.00	0.900	0.613	0.562	0.316	0.336	0.409
2.20	0.900	0.613	0.561	0.289	0.302	0.356
2.51	0.901	0.612	0.561	0.273	0.277	0.299
3.01	0.902	0.613	0.560	0.271	0.272	0.269
3.50	0.902	0.613	0.560	0.273	0.274	0.268
4.01	0.903	0.615	0.560	0.272	0.273	0.267
4.51	0.903	0.615	0.560	0.272	0.272	0.267
5.00	0.902	0.615	0.559	0.272	0.272	0.266
6.01	0.902	0.615	0.559	0.271	0.270	0.265

Inner channel

Static-pressure ratios at s/l_s of -

0.552	0.730	0.817	0.884	0.940
0.650	0.698	0.705	0.684	0.672
0.596	0.644	0.647	0.607	0.576
0.589	0.636	0.638	0.595	0.557
0.583	0.631	0.634	0.591	0.554
0.581	0.631	0.635	0.592	0.554
0.578	0.631	0.636	0.592	0.556
0.577	0.632	0.637	0.593	0.556
0.573	0.630	0.636	0.593	0.556
0.572	0.630	0.637	0.593	0.556
0.571	0.631	0.638	0.594	0.557
0.570	0.631	0.638	0.594	0.557

Outer channel

Static-pressure ratios at s/l_s of -

NPR	0.402	0.658	0.765	0.846	0.916	0.956
1.51	0.836	0.768	0.716	0.687	0.651	0.646
1.81	0.820	0.738	0.665	0.615	0.547	0.521
2.00	0.818	0.733	0.657	0.599	0.507	0.457
2.20	0.818	0.733	0.657	0.599	0.506	0.451
2.51	0.819	0.734	0.658	0.599	0.506	0.447
3.01	0.819	0.735	0.659	0.599	0.507	0.447
3.50	0.819	0.735	0.659	0.599	0.508	0.447
4.01	0.820	0.736	0.660	0.600	0.509	0.448
4.51	0.820	0.736	0.660	0.600	0.509	0.448
5.00	0.821	0.736	0.660	0.600	0.509	0.448
6.01	0.821	0.736	0.660	0.600	0.509	0.449

Left instrumented sleeve

Static-pressure coefficients at ϕ, deg, of -

NPR	0	45	90	135	180	225	270	315
1.51	0.822	0.814	0.829	0.873	0.900	0.872	0.830	0.817
1.81	0.807	0.798	0.817	0.865	0.894	0.863	0.817	0.802
2.00	0.805	0.796	0.816	0.864	0.892	0.862	0.815	0.800
2.20	0.805	0.795	0.816	0.864	0.892	0.862	0.815	0.800
2.51	0.805	0.796	0.817	0.865	0.893	0.863	0.816	0.801
3.01	0.805	0.796	0.818	0.866	0.894	0.863	0.816	0.802
3.50	0.805	0.796	0.818	0.866	0.894	0.863	0.816	0.802
4.01	0.804	0.795	0.818	0.866	0.894	0.863	0.816	0.802
4.51	0.804	0.796	0.818	0.866	0.894	0.863	0.816	0.802
5.00	0.804	0.796	0.819	0.866	0.894	0.863	0.816	0.802
6.01	0.804	0.796	0.819	0.867	0.894	0.863	0.816	0.802

Right instrumented sleeve

Static-pressure ratios at ϕ, deg, of -

0	45	90	135	180	225	270	315
0.832	0.822	0.829	0.872	0.898	0.871	0.831	0.830
0.819	0.808	0.814	0.862	0.891	0.861	0.818	0.816
0.816	0.805	0.811	0.860	0.889	0.859	0.815	0.813
0.817	0.806	0.812	0.861	0.890	0.859	0.816	0.814
0.818	0.806	0.812	0.862	0.891	0.860	0.816	0.815
0.819	0.807	0.812	0.862	0.892	0.860	0.817	0.815
0.819	0.806	0.812	0.863	0.892	0.860	0.817	0.815
0.819	0.807	0.812	0.864	0.893	0.860	0.817	0.816
0.819	0.806	0.812	0.864	0.893	0.860	0.817	0.816
0.819	0.806	0.812	0.864	0.893	0.860	0.817	0.816
0.819	0.806	0.812	0.864	0.893	0.860	0.817	0.816

Table 110. Static-Pressure Ratios in Nozzle and Instrumented Sleeves for Configuration $P_OC_MB_NN_4L$

Inner wall

Static-pressure ratios at s/l_s of -

NPR	0.318	0.637	0.779	0.840	0.888	0.928
1.50	0.893	0.641	0.595	0.463	0.519	0.588
1.81	0.885	0.611	0.563	0.352	0.383	0.467
2.00	0.884	0.607	0.558	0.315	0.334	0.406
2.21	0.885	0.605	0.556	0.291	0.303	0.352
2.50	0.885	0.606	0.557	0.281	0.282	0.298
3.01	0.885	0.606	0.556	0.282	0.281	0.274
3.50	0.886	0.607	0.557	0.282	0.281	0.273
3.99	0.886	0.608	0.556	0.282	0.281	0.273
4.51	0.886	0.608	0.556	0.283	0.280	0.272
5.00	0.886	0.608	0.556	0.281	0.279	0.271

Inner channel

Static-pressure ratios at s/l_s of -

0.552	0.730	0.817	0.884	0.940
0.620	0.681	0.696	0.679	0.671
0.574	0.628	0.635	0.599	0.571
0.563	0.617	0.624	0.583	0.548
0.561	0.616	0.623	0.582	0.545
0.556	0.612	0.621	0.579	0.543
0.556	0.614	0.623	0.582	0.545
0.553	0.613	0.623	0.581	0.545
0.551	0.612	0.623	0.581	0.545
0.551	0.613	0.624	0.582	0.545
0.546	0.609	0.622	0.580	0.544

Outer channel

Static-pressure ratios at s/l_s of -

NPR	0.402	0.658	0.765	0.846	0.916	0.956
1.50	0.838	0.774	0.717	0.684	0.644	0.664
1.81	0.819	0.743	0.668	0.615	0.537	0.552
2.00	0.818	0.740	0.663	0.604	0.511	0.500
2.21	0.818	0.739	0.663	0.603	0.509	0.453
2.50	0.819	0.741	0.664	0.605	0.511	0.400
3.01	0.819	0.741	0.665	0.605	0.512	0.332
3.50	0.820	0.742	0.666	0.605	0.513	0.286
3.99	0.821	0.742	0.666	0.605	0.513	0.251
4.51	0.821	0.742	0.666	0.605	0.513	0.222
5.00	0.822	0.743	0.668	0.606	0.514	0.200

Left instrumented sleeve

Static-pressure coefficients at ϕ, deg, of -

NPR	0	45	90	135	180	225	270	315
1.50	0.825	0.811	0.830	0.870	0.894	0.869	0.830	0.816
1.81	0.809	0.795	0.818	0.862	0.888	0.860	0.816	0.801
2.00	0.807	0.792	0.816	0.861	0.886	0.858	0.814	0.799
2.21	0.807	0.792	0.817	0.861	0.886	0.859	0.814	0.800
2.50	0.807	0.791	0.817	0.862	0.886	0.858	0.815	0.800
3.01	0.806	0.791	0.817	0.863	0.887	0.859	0.815	0.801
3.50	0.806	0.792	0.817	0.863	0.887	0.859	0.816	0.801
3.99	0.806	0.792	0.817	0.863	0.887	0.859	0.815	0.801
4.51	0.805	0.791	0.817	0.864	0.888	0.859	0.815	0.801
5.00	0.805	0.791	0.817	0.863	0.887	0.859	0.815	0.802

Right instrumented sleeve

Static-pressure ratios at ϕ, deg, of -

0	45	90	135	180	225	270	315
0.835	0.829	0.830	0.871	0.894	0.870	0.833	0.820
0.820	0.812	0.814	0.858	0.884	0.857	0.815	0.802
0.818	0.810	0.812	0.857	0.883	0.856	0.814	0.800
0.819	0.810	0.811	0.857	0.884	0.856	0.813	0.799
0.820	0.810	0.812	0.858	0.885	0.857	0.815	0.800
0.820	0.810	0.812	0.858	0.885	0.857	0.815	0.800
0.821	0.810	0.812	0.859	0.885	0.857	0.815	0.800
0.821	0.810	0.812	0.859	0.885	0.857	0.815	0.800
0.821	0.810	0.812	0.859	0.886	0.857	0.815	0.800
0.821	0.810	0.813	0.859	0.885	0.857	0.815	0.800

Table 111. Static-Pressure Ratios in Nozzle and Instrumented Sleeves for Configuration $P_OC_MB_FN_4T$

Inner wall

Static-pressure ratios at s/l_s of -

NPR	0.318	0.637	0.779	0.840	0.888	0.928
1.51	0.905	0.643	0.593	0.447	0.518	0.590
1.81	0.897	0.617	0.565	0.360	0.412	0.481
2.00	0.897	0.613	0.561	0.313	0.344	0.417
2.20	0.897	0.612	0.559	0.281	0.299	0.361
2.51	0.898	0.612	0.559	0.262	0.268	0.298
3.00	0.899	0.613	0.559	0.261	0.263	0.261
3.52	0.900	0.614	0.559	0.262	0.264	0.259
4.01	0.899	0.614	0.559	0.264	0.265	0.260
4.50	0.899	0.614	0.558	0.263	0.264	0.259
5.00	0.899	0.615	0.559	0.264	0.265	0.259
6.00	0.899	0.615	0.558	0.263	0.263	0.258

Inner channel

Static-pressure ratios at s/l_s of -

0.552	0.730	0.817	0.884	0.940
0.633	0.689	0.701	0.683	0.672
0.596	0.643	0.647	0.609	0.578
0.584	0.632	0.635	0.594	0.557
0.579	0.627	0.631	0.589	0.553
0.577	0.627	0.632	0.589	0.553
0.576	0.627	0.633	0.590	0.554
0.571	0.624	0.632	0.589	0.553
0.573	0.628	0.635	0.591	0.555
0.568	0.624	0.633	0.589	0.554
0.571	0.629	0.636	0.592	0.555
0.568	0.628	0.636	0.591	0.555

Outer channel

Static-pressure ratios at s/l_s of -

NPR	0.402	0.658	0.765	0.846	0.916	0.956
1.51	0.840	0.772	0.718	0.686	0.649	0.643
1.81	0.821	0.737	0.664	0.615	0.546	0.521
2.00	0.819	0.733	0.656	0.599	0.507	0.458
2.20	0.819	0.733	0.657	0.598	0.506	0.451
2.51	0.819	0.734	0.658	0.599	0.507	0.448
3.00	0.819	0.734	0.659	0.600	0.507	0.447
3.52	0.821	0.736	0.661	0.601	0.509	0.448
4.01	0.821	0.735	0.660	0.600	0.509	0.448
4.50	0.823	0.737	0.661	0.602	0.510	0.449
5.00	0.821	0.735	0.659	0.600	0.509	0.449
6.00	0.822	0.735	0.660	0.600	0.509	0.450

Left instrumented sleeve

Static-pressure coefficients at ϕ, deg, of -

NPR	0	45	90	135	180	225	270	315
1.51	0.820	0.808	0.827	0.871	0.898	0.870	0.829	0.816
1.81	0.806	0.793	0.814	0.862	0.891	0.860	0.814	0.802
2.00	0.804	0.791	0.813	0.861	0.890	0.859	0.813	0.800
2.20	0.803	0.790	0.813	0.862	0.890	0.859	0.813	0.800
2.51	0.804	0.791	0.814	0.862	0.891	0.860	0.813	0.800
3.00	0.804	0.792	0.815	0.864	0.892	0.861	0.814	0.801
3.52	0.804	0.791	0.816	0.864	0.892	0.861	0.814	0.801
4.01	0.804	0.792	0.816	0.864	0.892	0.861	0.814	0.801
4.50	0.803	0.792	0.816	0.864	0.892	0.861	0.815	0.801
5.00	0.803	0.792	0.817	0.864	0.892	0.861	0.814	0.801
6.00	0.803	0.792	0.817	0.865	0.892	0.861	0.814	0.801

Right instrumented sleeve

Static-pressure ratios at ϕ, deg, of -

0	45	90	135	180	225	270	315
0.829	0.819	0.829	0.874	0.898	0.869	0.834	0.831
0.812	0.800	0.814	0.863	0.890	0.859	0.820	0.816
0.811	0.798	0.811	0.861	0.889	0.858	0.818	0.814
0.811	0.798	0.811	0.862	0.889	0.857	0.817	0.815
0.812	0.799	0.812	0.863	0.890	0.858	0.819	0.815
0.812	0.799	0.813	0.864	0.891	0.858	0.820	0.815
0.813	0.800	0.813	0.864	0.891	0.859	0.820	0.816
0.812	0.800	0.813	0.864	0.891	0.859	0.820	0.816
0.813	0.800	0.813	0.865	0.891	0.859	0.820	0.816
0.812	0.799	0.813	0.864	0.891	0.859	0.819	0.816
0.812	0.799	0.813	0.865	0.891	0.859	0.820	0.816

Table 112. Static-Pressure Ratios in Nozzle and Instrumented Sleeves for Configuration $P_OC_MB_FN_4L$

Inner wall

Static-pressure ratios at s/l_s of -

NPR	0.318	0.637	0.779	0.840	0.888	0.928
1.51	0.891	0.636	0.592	0.465	0.517	0.587
1.80	0.884	0.607	0.560	0.352	0.387	0.468
2.01	0.883	0.602	0.554	0.313	0.334	0.402
2.21	0.884	0.601	0.553	0.290	0.302	0.352
2.50	0.884	0.602	0.554	0.283	0.284	0.297
3.00	0.884	0.602	0.554	0.283	0.282	0.274
3.52	0.885	0.604	0.554	0.284	0.283	0.274
4.01	0.884	0.605	0.554	0.284	0.283	0.273
4.51	0.884	0.605	0.554	0.284	0.282	0.273
5.01	0.884	0.605	0.554	0.284	0.281	0.272

Inner channel

Static-pressure ratios at s/l_s of -

0.552	0.730	0.817	0.884	0.940
0.598	0.669	0.689	0.674	0.668
0.540	0.602	0.618	0.588	0.564
0.531	0.592	0.607	0.570	0.536
0.529	0.590	0.606	0.567	0.532
0.528	0.590	0.606	0.567	0.531
0.530	0.595	0.611	0.572	0.536
0.531	0.597	0.613	0.575	0.538
0.531	0.599	0.615	0.576	0.540
0.533	0.601	0.617	0.578	0.541
0.532	0.602	0.618	0.578	0.542

Outer channel

Static-pressure ratios at s/l_s of -

NPR	0.402	0.658	0.765	0.846	0.916	0.956
1.51	0.842	0.778	0.719	0.683	0.639	0.661
1.80	0.829	0.754	0.678	0.620	0.534	0.553
2.01	0.826	0.750	0.672	0.611	0.517	0.496
2.21	0.827	0.750	0.672	0.611	0.515	0.452
2.50	0.827	0.750	0.672	0.611	0.516	0.400
3.00	0.826	0.749	0.671	0.610	0.516	0.333
3.52	0.827	0.748	0.671	0.610	0.516	0.284
4.01	0.827	0.748	0.670	0.609	0.516	0.249
4.51	0.826	0.747	0.670	0.608	0.515	0.222
5.01	0.826	0.747	0.669	0.607	0.515	0.200

Left instrumented sleeve

Static-pressure coefficients at ϕ, deg, of -

NPR	0	45	90	135	180	225	270	315
1.51	0.824	0.811	0.825	0.867	0.892	0.869	0.827	0.814
1.80	0.809	0.795	0.813	0.859	0.886	0.860	0.813	0.800
2.01	0.807	0.792	0.812	0.859	0.885	0.859	0.812	0.798
2.21	0.807	0.793	0.813	0.859	0.885	0.859	0.812	0.798
2.50	0.807	0.792	0.813	0.860	0.886	0.859	0.812	0.798
3.00	0.807	0.792	0.813	0.860	0.887	0.860	0.813	0.799
3.52	0.807	0.792	0.814	0.861	0.888	0.860	0.815	0.799
4.01	0.806	0.792	0.814	0.862	0.887	0.860	0.815	0.799
4.51	0.806	0.791	0.814	0.862	0.887	0.860	0.815	0.799
5.01	0.805	0.791	0.815	0.862	0.887	0.859	0.815	0.800

Right instrumented sleeve

Static-pressure ratios at ϕ, deg, of -

0	45	90	135	180	225	270	315
0.836	0.826	0.826	0.867	0.890	0.865	0.826	0.818
0.823	0.810	0.810	0.856	0.882	0.855	0.810	0.800
0.820	0.807	0.808	0.853	0.881	0.853	0.807	0.798
0.822	0.808	0.807	0.854	0.882	0.853	0.808	0.798
0.822	0.807	0.807	0.854	0.882	0.853	0.807	0.798
0.822	0.808	0.808	0.854	0.882	0.853	0.808	0.799
0.824	0.807	0.807	0.855	0.883	0.853	0.808	0.799
0.824	0.807	0.807	0.856	0.882	0.852	0.807	0.800
0.824	0.807	0.807	0.855	0.882	0.852	0.807	0.799
0.824	0.807	0.807	0.855	0.882	0.852	0.807	0.799

Table 113. Static-Pressure Ratios in Nozzle and Instrumented Sleeves for Configuration $P_OC_LB_NN_4T$

Inner wall

Static-pressure ratios at s/l_s of -

NPR	0.318	0.637	0.779	0.840	0.888	0.928
1.50	0.904	0.641	0.593	0.448	0.510	0.587
1.80	0.899	0.614	0.564	0.357	0.401	0.479
2.00	0.898	0.611	0.560	0.315	0.337	0.411
2.21	0.898	0.609	0.558	0.286	0.301	0.352
2.50	0.898	0.609	0.558	0.272	0.276	0.299
2.99	0.899	0.610	0.558	0.272	0.273	0.268
3.51	0.899	0.611	0.558	0.272	0.273	0.266
4.00	0.899	0.611	0.558	0.272	0.273	0.266
4.51	0.899	0.612	0.557	0.272	0.272	0.265
5.00	0.899	0.612	0.557	0.271	0.271	0.264
6.00	0.899	0.612	0.556	0.271	0.270	0.264

Inner channel

Static-pressure ratios at s/l_s of -

0.552	0.730	0.817	0.884	0.940
0.639	0.694	0.704	0.685	0.674
0.586	0.638	0.644	0.607	0.576
0.575	0.627	0.633	0.592	0.555
0.570	0.623	0.630	0.589	0.552
0.567	0.622	0.629	0.588	0.552
0.566	0.623	0.631	0.589	0.553
0.563	0.622	0.631	0.590	0.554
0.561	0.622	0.632	0.590	0.553
0.559	0.621	0.631	0.589	0.553
0.557	0.619	0.631	0.589	0.553
0.557	0.622	0.633	0.590	0.554

Outer channel

Static-pressure ratios at s/l_s of -

NPR	0.402	0.658	0.765	0.846	0.916	0.956
1.50	0.836	0.767	0.714	0.683	0.647	0.644
1.80	0.819	0.738	0.664	0.612	0.541	0.518
2.00	0.817	0.734	0.656	0.598	0.506	0.455
2.21	0.816	0.733	0.656	0.597	0.505	0.449
2.50	0.817	0.735	0.658	0.598	0.506	0.446
2.99	0.817	0.735	0.658	0.599	0.506	0.445
3.51	0.818	0.735	0.659	0.599	0.507	0.446
4.00	0.818	0.736	0.659	0.599	0.507	0.446
4.51	0.818	0.736	0.660	0.599	0.507	0.447
5.00	0.819	0.736	0.660	0.599	0.508	0.447
6.00	0.819	0.736	0.659	0.598	0.508	0.447

Left instrumented sleeve

Static-pressure coefficients at ϕ, deg, of -

NPR	0	45	90	135	180	225	270	315
1.50	0.823	0.815	0.827	0.873	0.898	0.871	0.829	0.816
1.80	0.807	0.799	0.816	0.865	0.892	0.862	0.815	0.802
2.00	0.805	0.796	0.814	0.863	0.890	0.860	0.814	0.800
2.21	0.804	0.796	0.814	0.864	0.890	0.860	0.814	0.799
2.50	0.804	0.795	0.815	0.864	0.891	0.861	0.814	0.800
2.99	0.804	0.796	0.815	0.865	0.892	0.861	0.814	0.800
3.51	0.804	0.795	0.816	0.865	0.892	0.861	0.814	0.801
4.00	0.804	0.795	0.816	0.865	0.892	0.861	0.814	0.801
4.51	0.803	0.794	0.816	0.865	0.892	0.861	0.814	0.800
5.00	0.803	0.794	0.816	0.864	0.891	0.860	0.813	0.800
6.00	0.803	0.795	0.816	0.865	0.891	0.860	0.814	0.801

Right instrumented sleeve

Static-pressure ratios at ϕ, deg, of -

0	45	90	135	180	225	270	315
0.828	0.817	0.827	0.872	0.900	0.872	0.829	0.827
0.813	0.800	0.811	0.861	0.891	0.861	0.814	0.812
0.811	0.798	0.809	0.860	0.890	0.859	0.812	0.810
0.811	0.797	0.808	0.860	0.890	0.858	0.812	0.810
0.812	0.798	0.809	0.861	0.891	0.859	0.813	0.811
0.813	0.799	0.809	0.861	0.891	0.859	0.813	0.811
0.814	0.800	0.809	0.862	0.892	0.859	0.813	0.812
0.814	0.800	0.809	0.862	0.892	0.859	0.813	0.812
0.814	0.800	0.809	0.863	0.892	0.859	0.814	0.812
0.814	0.800	0.809	0.862	0.892	0.859	0.814	0.812
0.813	0.799	0.809	0.862	0.892	0.858	0.813	0.812

Table 114. Static-Pressure Ratios in Nozzle and Instrumented Sleeves for Configuration $P_OC_LB_NN_4L$

Inner wall

Static-pressure ratios at s/l_s of -

NPR	0.318	0.637	0.779	0.840	0.888	0.928
1.51	0.897	0.643	0.596	0.449	0.501	0.579
1.81	0.888	0.615	0.565	0.352	0.389	0.472
2.01	0.887	0.611	0.560	0.312	0.332	0.404
2.20	0.887	0.610	0.559	0.289	0.303	0.355
2.51	0.888	0.610	0.559	0.276	0.279	0.298
3.00	0.888	0.610	0.559	0.276	0.277	0.271
3.50	0.888	0.610	0.558	0.277	0.276	0.269
4.01	0.887	0.610	0.557	0.277	0.276	0.268
4.50	0.887	0.610	0.557	0.277	0.276	0.269
5.01	0.888	0.611	0.557	0.277	0.275	0.268

Inner channel

Static-pressure ratios at s/l_s of -

0.552	0.730	0.817	0.884	0.940
0.624	0.681	0.697	0.679	0.669
0.566	0.620	0.630	0.595	0.569
0.556	0.609	0.618	0.577	0.542
0.553	0.607	0.616	0.575	0.539
0.549	0.604	0.614	0.573	0.537
0.551	0.608	0.617	0.577	0.541
0.544	0.602	0.613	0.573	0.537
0.539	0.598	0.611	0.571	0.535
0.545	0.606	0.618	0.577	0.541
0.546	0.608	0.619	0.578	0.542

Outer channel

Static-pressure ratios at s/l_s of -

NPR	0.402	0.658	0.765	0.846	0.916	0.956
1.51	0.833	0.769	0.714	0.680	0.642	0.660
1.81	0.818	0.743	0.670	0.615	0.537	0.552
2.01	0.816	0.740	0.665	0.605	0.512	0.496
2.20	0.817	0.740	0.664	0.604	0.511	0.455
2.51	0.818	0.741	0.666	0.605	0.512	0.397
3.00	0.817	0.740	0.665	0.604	0.512	0.333
3.50	0.820	0.742	0.667	0.606	0.514	0.286
4.01	0.820	0.743	0.668	0.607	0.515	0.249
4.50	0.819	0.741	0.666	0.605	0.514	0.222
5.01	0.819	0.741	0.666	0.605	0.514	0.200

Left instrumented sleeve

Static-pressure coefficients at ϕ, deg, of -

NPR	0	45	90	135	180	225	270	315
1.51	0.821	0.810	0.827	0.869	0.892	0.867	0.829	0.815
1.81	0.806	0.794	0.814	0.860	0.885	0.857	0.815	0.800
2.01	0.804	0.791	0.813	0.859	0.884	0.855	0.813	0.798
2.20	0.805	0.791	0.814	0.860	0.884	0.856	0.814	0.798
2.51	0.804	0.790	0.813	0.860	0.884	0.856	0.813	0.799
3.00	0.804	0.790	0.814	0.861	0.886	0.856	0.814	0.799
3.50	0.804	0.789	0.814	0.861	0.886	0.856	0.813	0.799
4.01	0.804	0.789	0.813	0.861	0.885	0.856	0.813	0.799
4.50	0.803	0.788	0.814	0.861	0.886	0.856	0.813	0.799
5.01	0.803	0.788	0.814	0.862	0.886	0.856	0.814	0.799

Right instrumented sleeve

Static-pressure ratios at ϕ, deg, of -

0	45	90	135	180	225	270	315
0.832	0.823	0.824	0.867	0.888	0.862	0.824	0.816
0.818	0.807	0.809	0.857	0.879	0.851	0.808	0.798
0.817	0.805	0.807	0.855	0.879	0.850	0.807	0.795
0.817	0.805	0.807	0.856	0.879	0.850	0.807	0.796
0.818	0.805	0.807	0.855	0.879	0.850	0.807	0.795
0.818	0.805	0.806	0.855	0.879	0.850	0.807	0.795
0.819	0.806	0.808	0.856	0.881	0.852	0.809	0.796
0.819	0.806	0.808	0.857	0.882	0.852	0.810	0.796
0.819	0.805	0.807	0.856	0.880	0.851	0.808	0.796
0.819	0.805	0.807	0.856	0.880	0.851	0.808	0.796

Table 115. Static-Pressure Ratios in Nozzle and Instrumented Sleeves for Configuration $P_0C_LB_FN_4T$

Inner wall

Static-pressure ratios at s/l_s of -

NPR	0.318	0.637	0.779	0.840	0.888	0.928
1.51	0.900	0.651	0.601	0.444	0.514	0.587
1.81	0.893	0.625	0.573	0.358	0.409	0.480
2.01	0.894	0.622	0.568	0.310	0.340	0.414
2.21	0.894	0.620	0.567	0.280	0.297	0.357
2.50	0.893	0.620	0.567	0.263	0.269	0.300
3.01	0.894	0.620	0.566	0.262	0.263	0.262
3.51	0.895	0.620	0.566	0.263	0.265	0.260
4.00	0.894	0.621	0.566	0.264	0.265	0.260
4.50	0.893	0.622	0.566	0.264	0.265	0.260
5.01	0.893	0.621	0.565	0.264	0.265	0.260
6.01	0.892	0.621	0.564	0.263	0.263	0.258

Inner channel

Static-pressure ratios at s/l_s of -

0.552	0.730	0.817	0.884	0.940
0.644	0.694	0.703	0.684	0.673
0.593	0.639	0.643	0.607	0.577
0.582	0.627	0.631	0.590	0.553
0.578	0.624	0.628	0.586	0.550
0.578	0.624	0.629	0.586	0.550
0.575	0.624	0.629	0.587	0.551
0.573	0.624	0.630	0.588	0.551
0.572	0.625	0.631	0.588	0.552
0.573	0.626	0.632	0.588	0.552
0.571	0.625	0.632	0.588	0.552
0.567	0.624	0.631	0.588	0.551

Outer channel

Static-pressure ratios at s/l_s of -

NPR	0.402	0.658	0.765	0.846	0.916	0.956
1.51	0.835	0.766	0.716	0.688	0.652	0.647
1.81	0.819	0.735	0.664	0.617	0.549	0.524
2.01	0.818	0.732	0.657	0.600	0.509	0.460
2.21	0.817	0.731	0.656	0.599	0.507	0.453
2.50	0.817	0.731	0.656	0.599	0.508	0.450
3.01	0.818	0.731	0.657	0.600	0.508	0.450
3.51	0.819	0.731	0.658	0.600	0.509	0.450
4.00	0.819	0.731	0.658	0.600	0.509	0.450
4.50	0.819	0.731	0.657	0.600	0.509	0.450
5.01	0.819	0.731	0.658	0.600	0.509	0.450
6.01	0.820	0.731	0.658	0.599	0.509	0.451

Left instrumented sleeve

Static-pressure coefficients at ϕ, deg, of -

NPR	0	45	90	135	180	225	270	315
1.51	0.819	0.810	0.824	0.866	0.893	0.867	0.824	0.811
1.81	0.803	0.795	0.812	0.858	0.886	0.857	0.810	0.796
2.01	0.802	0.792	0.812	0.857	0.886	0.857	0.809	0.794
2.21	0.801	0.793	0.812	0.857	0.885	0.857	0.810	0.794
2.50	0.801	0.793	0.812	0.858	0.885	0.856	0.809	0.794
3.01	0.800	0.793	0.813	0.858	0.886	0.856	0.809	0.795
3.51	0.800	0.793	0.814	0.859	0.887	0.857	0.810	0.796
4.00	0.800	0.793	0.815	0.859	0.886	0.857	0.810	0.795
4.50	0.799	0.793	0.815	0.859	0.886	0.856	0.809	0.795
5.01	0.799	0.793	0.815	0.859	0.885	0.856	0.809	0.795
6.01	0.798	0.792	0.815	0.859	0.885	0.855	0.808	0.795

Right instrumented sleeve

Static-pressure ratios at ϕ, deg, of -

0	45	90	135	180	225	270	315
0.835	0.821	0.828	0.875	0.900	0.872	0.832	0.832
0.821	0.805	0.812	0.863	0.892	0.861	0.817	0.817
0.819	0.805	0.810	0.862	0.891	0.859	0.816	0.814
0.819	0.804	0.810	0.863	0.891	0.859	0.815	0.814
0.819	0.804	0.810	0.863	0.892	0.860	0.816	0.815
0.820	0.805	0.810	0.863	0.892	0.860	0.816	0.815
0.821	0.805	0.811	0.864	0.892	0.859	0.816	0.815
0.820	0.805	0.811	0.864	0.892	0.860	0.816	0.815
0.820	0.805	0.810	0.864	0.892	0.859	0.816	0.815
0.820	0.804	0.810	0.864	0.893	0.860	0.816	0.815
0.820	0.804	0.810	0.864	0.892	0.859	0.816	0.815

Table 116. Static-Pressure Ratios in Nozzle and Instrumented Sleeves for Configuration $P_OC_LB_FN_4L$

Inner wall

Static-pressure ratios at s/l_s of -

NPR	0.318	0.637	0.779	0.840	0.888	0.928
1.51	0.885	0.632	0.588	0.467	0.528	0.592
1.81	0.877	0.603	0.555	0.353	0.397	0.475
2.00	0.876	0.599	0.551	0.311	0.339	0.411
2.20	0.877	0.599	0.550	0.285	0.303	0.359
2.51	0.877	0.599	0.550	0.275	0.278	0.295
2.99	0.878	0.599	0.550	0.275	0.277	0.270
3.51	0.878	0.600	0.550	0.276	0.278	0.269
4.01	0.878	0.601	0.550	0.276	0.277	0.268
4.50	0.878	0.601	0.550	0.276	0.277	0.268
5.00	0.878	0.601	0.549	0.276	0.276	0.267

Inner channel

Static-pressure ratios at s/l_s of -

0.552	0.730	0.817	0.884	0.940
0.628	0.691	0.707	0.688	0.675
0.571	0.630	0.642	0.607	0.579
0.562	0.621	0.631	0.592	0.555
0.559	0.618	0.629	0.588	0.552
0.558	0.619	0.630	0.589	0.553
0.559	0.621	0.631	0.590	0.554
0.558	0.621	0.632	0.591	0.554
0.559	0.623	0.634	0.593	0.556
0.559	0.624	0.635	0.593	0.557
0.557	0.624	0.635	0.594	0.557

Outer channel

Static-pressure ratios at s/l_s of -

NPR	0.402	0.658	0.765	0.846	0.916	0.956
1.51	0.836	0.771	0.713	0.678	0.637	0.660
1.81	0.822	0.745	0.669	0.613	0.530	0.552
2.00	0.820	0.741	0.663	0.604	0.510	0.498
2.20	0.820	0.741	0.663	0.603	0.508	0.454
2.51	0.820	0.741	0.663	0.603	0.509	0.398
2.99	0.820	0.740	0.663	0.603	0.509	0.335
3.51	0.820	0.739	0.663	0.602	0.509	0.285
4.01	0.820	0.739	0.662	0.602	0.509	0.250
4.50	0.820	0.738	0.662	0.601	0.509	0.222
5.00	0.820	0.738	0.661	0.600	0.509	0.200

Left instrumented sleeve

Static-pressure coefficients at ϕ, deg, of -

NPR	0	45	90	135	180	225	270	315
1.51	0.820	0.810	0.825	0.863	0.887	0.866	0.829	0.812
1.81	0.805	0.794	0.812	0.853	0.880	0.856	0.815	0.797
2.00	0.803	0.792	0.812	0.853	0.879	0.855	0.814	0.795
2.20	0.803	0.791	0.812	0.854	0.879	0.855	0.815	0.795
2.51	0.803	0.791	0.813	0.854	0.881	0.856	0.815	0.796
2.99	0.803	0.791	0.813	0.855	0.882	0.856	0.815	0.797
3.51	0.803	0.790	0.813	0.856	0.882	0.857	0.815	0.797
4.01	0.802	0.790	0.813	0.855	0.882	0.857	0.815	0.797
4.50	0.802	0.790	0.813	0.856	0.882	0.857	0.815	0.797
5.00	0.801	0.789	0.813	0.856	0.882	0.857	0.814	0.797

Right instrumented sleeve

Static-pressure ratios at ϕ, deg, of -

0	45	90	135	180	225	270	315
0.833	0.827	0.827	0.867	0.891	0.871	0.831	0.816
0.820	0.812	0.813	0.856	0.882	0.860	0.817	0.800
0.818	0.810	0.812	0.855	0.881	0.859	0.815	0.797
0.819	0.810	0.812	0.855	0.882	0.859	0.815	0.797
0.819	0.810	0.812	0.856	0.882	0.860	0.816	0.798
0.820	0.811	0.812	0.856	0.882	0.860	0.816	0.798
0.821	0.810	0.812	0.856	0.883	0.860	0.816	0.798
0.821	0.810	0.812	0.856	0.883	0.860	0.816	0.798
0.821	0.810	0.812	0.856	0.883	0.860	0.816	0.798
0.821	0.810	0.812	0.856	0.883	0.860	0.816	0.798

Table 117. Static-Pressure Ratios in Nozzle and Instrumented Sleeves for Configuration $P_0C_LB_TN_4T$

Inner wall

Static-pressure ratios at s/l_s of -

NPR	0.318	0.637	0.779	0.840	0.888	0.928
1.51	0.905	0.639	0.589	0.441	0.509	0.585
1.81	0.900	0.614	0.563	0.358	0.408	0.479
2.00	0.899	0.610	0.559	0.313	0.338	0.413
2.20	0.900	0.610	0.558	0.283	0.299	0.356
2.50	0.900	0.610	0.558	0.265	0.272	0.298
3.00	0.900	0.610	0.558	0.265	0.267	0.263
3.50	0.901	0.612	0.558	0.266	0.268	0.261
4.01	0.901	0.612	0.557	0.266	0.267	0.261
4.51	0.902	0.612	0.557	0.266	0.267	0.261
4.99	0.902	0.612	0.556	0.266	0.266	0.260
6.01	0.902	0.612	0.556	0.264	0.264	0.259

Inner channel

Static-pressure ratios at s/l_s of -

0.552	0.730	0.817	0.884	0.940
0.639	0.693	0.703	0.683	0.671
0.587	0.639	0.645	0.607	0.576
0.577	0.628	0.634	0.593	0.556
0.575	0.625	0.632	0.590	0.553
0.570	0.623	0.630	0.589	0.553
0.568	0.624	0.632	0.590	0.554
0.564	0.622	0.631	0.589	0.554
0.565	0.624	0.633	0.591	0.555
0.566	0.625	0.634	0.591	0.556
0.567	0.627	0.635	0.592	0.556
0.563	0.626	0.635	0.592	0.556

Outer channel

Static-pressure ratios at s/l_s of -

NPR	0.402	0.658	0.765	0.846	0.916	0.956
1.51	0.837	0.765	0.712	0.681	0.645	0.641
1.81	0.822	0.737	0.663	0.612	0.541	0.517
2.00	0.820	0.734	0.657	0.599	0.507	0.455
2.20	0.819	0.734	0.657	0.599	0.505	0.450
2.50	0.820	0.735	0.658	0.599	0.506	0.448
3.00	0.820	0.735	0.659	0.599	0.507	0.446
3.50	0.821	0.736	0.660	0.600	0.508	0.447
4.01	0.821	0.736	0.660	0.600	0.508	0.447
4.51	0.822	0.736	0.660	0.600	0.508	0.448
4.99	0.822	0.736	0.660	0.599	0.508	0.448
6.01	0.823	0.736	0.660	0.599	0.508	0.449

Left instrumented sleeve

Static-pressure coefficients at ϕ, deg, of -

NPR	0	45	90	135	180	225	270	315
1.51	0.822	0.811	0.826	0.874	0.899	0.870	0.828	0.816
1.81	0.807	0.795	0.815	0.866	0.893	0.861	0.815	0.802
2.00	0.806	0.793	0.814	0.865	0.892	0.861	0.814	0.801
2.20	0.806	0.793	0.815	0.866	0.893	0.861	0.814	0.801
2.50	0.806	0.793	0.815	0.866	0.893	0.861	0.815	0.801
3.00	0.805	0.793	0.816	0.867	0.894	0.862	0.815	0.802
3.50	0.805	0.793	0.816	0.867	0.894	0.862	0.815	0.802
4.01	0.805	0.793	0.817	0.867	0.894	0.862	0.815	0.802
4.51	0.805	0.793	0.817	0.868	0.895	0.862	0.815	0.802
4.99	0.805	0.794	0.818	0.868	0.895	0.862	0.815	0.802
6.01	0.804	0.793	0.817	0.868	0.895	0.862	0.815	0.802

Right instrumented sleeve

Static-pressure ratios at ϕ, deg, of -

0	45	90	135	180	225	270	315
0.835	0.821	0.829	0.875	0.898	0.871	0.832	0.832
0.822	0.807	0.815	0.866	0.891	0.861	0.819	0.819
0.821	0.806	0.813	0.865	0.891	0.860	0.818	0.818
0.821	0.806	0.814	0.865	0.892	0.860	0.818	0.818
0.822	0.806	0.813	0.866	0.892	0.859	0.818	0.818
0.822	0.807	0.814	0.867	0.893	0.860	0.819	0.819
0.823	0.807	0.814	0.867	0.893	0.860	0.819	0.819
0.823	0.807	0.814	0.868	0.894	0.860	0.819	0.820
0.823	0.807	0.814	0.868	0.894	0.860	0.819	0.820
0.822	0.806	0.814	0.867	0.893	0.860	0.819	0.820
0.822	0.806	0.814	0.867	0.893	0.859	0.819	0.819

Table 118. Static-Pressure Ratios in Nozzle and Instrumented Sleeves for Configuration $P_OC_LB_TN_4L$

Inner wall

Static-pressure ratios at s/l_s of -

NPR	0.318	0.637	0.779	0.840	0.888	0.928
1.51	0.893	0.641	0.594	0.458	0.511	0.583
1.81	0.886	0.611	0.562	0.348	0.383	0.468
1.99	0.886	0.608	0.559	0.313	0.333	0.408
2.20	0.886	0.607	0.557	0.288	0.302	0.353
2.51	0.886	0.607	0.557	0.278	0.280	0.297
3.00	0.887	0.607	0.557	0.278	0.278	0.271
3.51	0.887	0.608	0.557	0.279	0.278	0.270
3.99	0.887	0.608	0.557	0.279	0.278	0.270
4.51	0.887	0.609	0.556	0.279	0.277	0.269
4.76	0.887	0.609	0.556	0.279	0.277	0.269

Inner channel

Static-pressure ratios at s/l_s of -

0.552	0.730	0.817	0.884	0.940
0.602	0.673	0.692	0.677	0.669
0.543	0.607	0.622	0.590	0.564
0.530	0.592	0.606	0.569	0.536
0.532	0.593	0.607	0.569	0.534
0.530	0.593	0.607	0.569	0.533
0.528	0.592	0.607	0.569	0.534
0.529	0.594	0.610	0.571	0.536
0.529	0.595	0.611	0.573	0.537
0.529	0.595	0.611	0.573	0.538
0.530	0.597	0.612	0.574	0.539

Outer channel

Static-pressure ratios at s/l_s of -

NPR	0.402	0.658	0.765	0.846	0.916	0.956
1.51	0.838	0.779	0.720	0.683	0.641	0.662
1.81	0.824	0.753	0.677	0.620	0.533	0.551
1.99	0.824	0.753	0.674	0.614	0.519	0.501
2.20	0.823	0.752	0.673	0.613	0.517	0.454
2.51	0.823	0.752	0.673	0.612	0.517	0.398
3.00	0.824	0.752	0.674	0.613	0.518	0.333
3.51	0.825	0.752	0.674	0.612	0.519	0.284
3.99	0.825	0.752	0.674	0.612	0.518	0.250
4.51	0.825	0.751	0.674	0.611	0.519	0.222
4.76	0.825	0.750	0.673	0.611	0.518	0.210

Left instrumented sleeve

Static-pressure coefficients at ϕ, deg. of -

NPR	0	45	90	135	180	225	270	315
1.51	0.823	0.811	0.826	0.867	0.891	0.867	0.828	0.814
1.81	0.808	0.795	0.814	0.859	0.884	0.858	0.815	0.799
1.99	0.807	0.792	0.813	0.858	0.883	0.857	0.814	0.798
2.20	0.807	0.792	0.813	0.858	0.884	0.857	0.814	0.798
2.51	0.806	0.791	0.814	0.859	0.884	0.857	0.814	0.798
3.00	0.806	0.791	0.814	0.859	0.885	0.858	0.814	0.799
3.51	0.806	0.790	0.814	0.861	0.886	0.858	0.815	0.799
3.99	0.806	0.790	0.814	0.861	0.886	0.858	0.815	0.799
4.51	0.805	0.789	0.814	0.861	0.886	0.858	0.815	0.799
4.76	0.805	0.789	0.814	0.861	0.886	0.858	0.815	0.799

Right instrumented sleeve

Static-pressure ratios at ϕ, deg. of -

0	45	90	135	180	225	270	315
0.837	0.827	0.829	0.870	0.892	0.869	0.830	0.818
0.823	0.812	0.814	0.859	0.885	0.859	0.816	0.801
0.822	0.810	0.813	0.858	0.885	0.858	0.814	0.800
0.823	0.811	0.813	0.858	0.885	0.858	0.814	0.799
0.824	0.810	0.813	0.858	0.885	0.858	0.815	0.800
0.824	0.811	0.813	0.859	0.886	0.859	0.815	0.800
0.825	0.811	0.813	0.860	0.887	0.859	0.816	0.800
0.825	0.811	0.813	0.860	0.887	0.859	0.815	0.800
0.825	0.810	0.813	0.859	0.887	0.859	0.816	0.800
0.825	0.810	0.813	0.859	0.886	0.859	0.815	0.800

Table 119. Static-Pressure Ratios in Nozzle and Instrumented Sleeves for Configuration $P_OC_FB_NN_4T$

Inner wall

Static-pressure ratios at s/l_s of -

NPR	0.318	0.637	0.779	0.840	0.888	0.928
1.51	0.905	0.643	0.594	0.442	0.503	0.584
1.80	0.898	0.619	0.567	0.356	0.401	0.480
2.01	0.896	0.615	0.564	0.312	0.334	0.409
2.20	0.896	0.614	0.562	0.286	0.301	0.354
2.51	0.897	0.614	0.563	0.272	0.277	0.299
3.01	0.897	0.614	0.562	0.271	0.272	0.268
3.50	0.897	0.615	0.562	0.273	0.273	0.267
4.00	0.898	0.616	0.562	0.273	0.273	0.267
4.50	0.897	0.616	0.562	0.272	0.272	0.266
5.01	0.898	0.617	0.562	0.271	0.270	0.264
6.01	0.897	0.616	0.560	0.271	0.269	0.264

Inner channel

Static-pressure ratios at s/l_s of -

0.552	0.730	0.817	0.884	0.940
0.627	0.685	0.701	0.680	0.671
0.575	0.630	0.639	0.602	0.575
0.564	0.618	0.627	0.585	0.550
0.561	0.615	0.624	0.582	0.547
0.559	0.614	0.624	0.582	0.547
0.554	0.612	0.623	0.582	0.547
0.554	0.614	0.624	0.583	0.549
0.553	0.615	0.626	0.585	0.549
0.552	0.614	0.625	0.584	0.549
0.547	0.611	0.624	0.583	0.548
0.548	0.614	0.626	0.584	0.549

Outer channel

Static-pressure ratios at s/l_s of -

NPR	0.402	0.658	0.765	0.846	0.916	0.956
1.51	0.836	0.765	0.711	0.681	0.643	0.661
1.80	0.819	0.737	0.664	0.613	0.542	0.555
2.01	0.816	0.733	0.657	0.600	0.508	0.497
2.20	0.816	0.733	0.657	0.599	0.506	0.454
2.51	0.816	0.734	0.658	0.600	0.507	0.399
3.01	0.816	0.735	0.659	0.600	0.507	0.333
3.50	0.816	0.735	0.659	0.600	0.508	0.286
4.00	0.817	0.736	0.660	0.600	0.508	0.250
4.50	0.817	0.736	0.660	0.599	0.508	0.222
5.01	0.818	0.738	0.661	0.601	0.509	0.200
6.01	0.818	0.736	0.660	0.599	0.508	0.167

Left instrumented sleeve

Static-pressure coefficients at ϕ, deg, of -

NPR	0	45	90	135	180	225	270	315
1.51	0.823	0.814	0.828	0.875	0.895	0.869	0.827	0.816
1.80	0.808	0.799	0.816	0.866	0.888	0.858	0.813	0.801
2.01	0.805	0.795	0.814	0.865	0.887	0.856	0.812	0.798
2.20	0.805	0.795	0.815	0.865	0.887	0.856	0.812	0.799
2.51	0.805	0.795	0.816	0.866	0.888	0.857	0.813	0.799
3.01	0.804	0.794	0.816	0.866	0.888	0.858	0.812	0.800
3.50	0.804	0.794	0.816	0.867	0.889	0.858	0.813	0.800
4.00	0.804	0.795	0.817	0.867	0.889	0.858	0.813	0.800
4.50	0.804	0.794	0.817	0.867	0.889	0.858	0.812	0.800
5.01	0.803	0.794	0.817	0.867	0.889	0.858	0.813	0.800
6.01	0.803	0.794	0.817	0.867	0.889	0.857	0.812	0.800

Right instrumented sleeve

Static-pressure ratios at ϕ, deg, of -

0	45	90	135	180	225	270	315
0.827	0.815	0.829	0.871	0.900	0.874	0.833	0.830
0.813	0.799	0.813	0.861	0.892	0.863	0.818	0.815
0.812	0.799	0.810	0.859	0.890	0.861	0.816	0.813
0.812	0.797	0.810	0.860	0.890	0.860	0.815	0.813
0.813	0.798	0.810	0.860	0.891	0.861	0.815	0.814
0.813	0.799	0.809	0.861	0.890	0.860	0.815	0.814
0.814	0.800	0.810	0.861	0.891	0.860	0.816	0.814
0.813	0.799	0.810	0.861	0.891	0.860	0.815	0.814
0.813	0.799	0.809	0.861	0.890	0.860	0.815	0.814
0.814	0.800	0.810	0.862	0.891	0.860	0.815	0.814
0.812	0.797	0.809	0.862	0.891	0.860	0.814	0.813

Table 120. Static-Pressure Ratios in Nozzle and Instrumented Sleeves for Configuration $P_0C_FB_NN_4L$

Inner wall

Static-pressure ratios at s/l_s of -

NPR	0.318	0.637	0.779	0.840	0.888	0.928
1.50	0.898	0.645	0.598	0.453	0.507	0.585
1.80	0.890	0.616	0.566	0.356	0.401	0.482
2.00	0.888	0.612	0.560	0.313	0.334	0.410
2.20	0.888	0.611	0.559	0.287	0.300	0.355
2.50	0.888	0.611	0.560	0.271	0.276	0.299
3.00	0.889	0.611	0.560	0.270	0.271	0.267
3.50	0.887	0.611	0.559	0.271	0.272	0.265
4.00	0.887	0.612	0.559	0.272	0.272	0.265
4.49	0.888	0.612	0.558	0.272	0.271	0.264
4.75	0.888	0.612	0.558	0.271	0.270	0.263

Inner channel

Static-pressure ratios at s/l_s of -

0.552	0.730	0.817	0.884	0.940
0.622	0.682	0.697	0.682	0.673
0.560	0.617	0.628	0.595	0.570
0.549	0.604	0.614	0.575	0.541
0.544	0.599	0.610	0.570	0.535
0.544	0.600	0.611	0.571	0.536
0.543	0.601	0.612	0.573	0.538
0.539	0.598	0.610	0.571	0.537
0.539	0.599	0.612	0.573	0.537
0.539	0.600	0.613	0.574	0.538
0.539	0.600	0.613	0.574	0.538

Outer channel

Static-pressure ratios at s/l_s of -

NPR	0.402	0.658	0.765	0.846	0.916	0.956
1.50	0.833	0.773	0.718	0.685	0.647	0.665
1.80	0.817	0.746	0.673	0.617	0.538	0.555
2.00	0.814	0.742	0.667	0.607	0.514	0.498
2.20	0.815	0.743	0.667	0.607	0.513	0.455
2.50	0.815	0.742	0.667	0.607	0.514	0.399
3.00	0.816	0.743	0.667	0.607	0.514	0.333
3.50	0.817	0.744	0.669	0.607	0.515	0.285
4.00	0.817	0.743	0.668	0.607	0.515	0.250
4.49	0.818	0.743	0.669	0.607	0.515	0.223
4.75	0.817	0.743	0.668	0.607	0.515	0.210

Left instrumented sleeve

Static-pressure coefficients at ϕ, deg, of -

NPR	0	45	90	135	180	225	270	315
1.50	0.822	0.811	0.827	0.867	0.892	0.867	0.829	0.815
1.80	0.806	0.794	0.813	0.857	0.884	0.857	0.815	0.800
2.00	0.804	0.791	0.812	0.856	0.881	0.855	0.813	0.797
2.20	0.804	0.790	0.812	0.856	0.882	0.855	0.813	0.797
2.50	0.803	0.790	0.813	0.856	0.883	0.855	0.813	0.798
3.00	0.803	0.789	0.813	0.857	0.884	0.855	0.813	0.799
3.50	0.803	0.788	0.813	0.856	0.883	0.855	0.813	0.798
4.00	0.802	0.788	0.813	0.857	0.883	0.855	0.813	0.798
4.49	0.802	0.788	0.813	0.858	0.884	0.856	0.813	0.798
4.75	0.802	0.788	0.813	0.857	0.884	0.855	0.813	0.798

Right instrumented sleeve

Static-pressure ratios at ϕ, deg, of -

0	45	90	135	180	225	270	315
0.836	0.825	0.827	0.869	0.888	0.863	0.824	0.816
0.820	0.808	0.811	0.859	0.880	0.853	0.808	0.799
0.818	0.806	0.808	0.856	0.879	0.850	0.806	0.796
0.818	0.805	0.808	0.857	0.879	0.851	0.807	0.796
0.819	0.806	0.809	0.857	0.880	0.851	0.807	0.796
0.820	0.806	0.809	0.857	0.881	0.852	0.808	0.796
0.820	0.806	0.809	0.857	0.881	0.852	0.808	0.796
0.819	0.806	0.809	0.857	0.881	0.852	0.809	0.796
0.820	0.806	0.808	0.857	0.881	0.852	0.808	0.796
0.820	0.805	0.808	0.857	0.881	0.851	0.808	0.796

Table 121. Static-Pressure Ratios in Nozzle and Instrumented Sleeves for Configuration $P_0C_FB_FN_4T$

Inner wall

Static-pressure ratios at s/l_s of -

NPR	0.318	0.637	0.779	0.840	0.888	0.928
1.50	0.905	0.646	0.597	0.447	0.509	0.589
1.80	0.899	0.620	0.568	0.355	0.402	0.480
2.00	0.898	0.616	0.564	0.312	0.333	0.410
2.21	0.898	0.615	0.563	0.284	0.298	0.353
2.50	0.899	0.616	0.563	0.270	0.275	0.300
3.00	0.899	0.616	0.563	0.269	0.270	0.267
3.51	0.900	0.616	0.562	0.270	0.271	0.265
4.00	0.899	0.617	0.562	0.270	0.271	0.265
4.50	0.900	0.617	0.562	0.270	0.270	0.264
5.00	0.900	0.617	0.561	0.270	0.269	0.264
6.01	0.900	0.617	0.561	0.269	0.268	0.262

Inner channel

Static-pressure ratios at s/l_s of -

0.552	0.730	0.817	0.884	0.940
0.624	0.685	0.701	0.683	0.676
0.566	0.623	0.633	0.598	0.572
0.557	0.612	0.622	0.583	0.549
0.552	0.609	0.619	0.579	0.546
0.551	0.608	0.619	0.579	0.546
0.549	0.608	0.620	0.580	0.547
0.549	0.609	0.622	0.582	0.548
0.546	0.608	0.622	0.582	0.548
0.545	0.609	0.623	0.582	0.548
0.544	0.610	0.623	0.583	0.549
0.541	0.609	0.623	0.583	0.549

Outer channel

Static-pressure ratios at s/l_s of -

NPR	0.402	0.658	0.765	0.846	0.916	0.956
1.50	0.837	0.769	0.714	0.684	0.650	0.666
1.80	0.821	0.741	0.666	0.613	0.541	0.552
2.00	0.819	0.738	0.660	0.601	0.510	0.498
2.21	0.818	0.738	0.660	0.601	0.508	0.452
2.50	0.819	0.738	0.661	0.601	0.509	0.400
3.00	0.819	0.739	0.662	0.602	0.510	0.333
3.51	0.819	0.739	0.662	0.602	0.510	0.285
4.00	0.819	0.740	0.663	0.602	0.511	0.250
4.50	0.820	0.739	0.663	0.602	0.511	0.222
5.00	0.820	0.740	0.663	0.602	0.511	0.200
6.01	0.821	0.740	0.664	0.602	0.511	0.166

Left instrumented sleeve

Static-pressure coefficients at ϕ, deg, of -

NPR	0	45	90	135	180	225	270	315
1.50	0.825	0.812	0.829	0.874	0.898	0.869	0.828	0.817
1.80	0.808	0.796	0.817	0.866	0.891	0.860	0.814	0.802
2.00	0.807	0.794	0.815	0.866	0.890	0.859	0.813	0.801
2.21	0.806	0.794	0.816	0.866	0.890	0.859	0.813	0.801
2.50	0.806	0.795	0.816	0.867	0.891	0.859	0.814	0.801
3.00	0.806	0.795	0.817	0.867	0.891	0.860	0.814	0.802
3.51	0.806	0.796	0.818	0.868	0.892	0.860	0.814	0.802
4.00	0.806	0.795	0.818	0.868	0.891	0.860	0.814	0.802
4.50	0.805	0.795	0.818	0.868	0.892	0.860	0.814	0.802
5.00	0.805	0.795	0.819	0.868	0.892	0.860	0.814	0.802
6.01	0.805	0.795	0.819	0.868	0.892	0.860	0.814	0.802

Right instrumented sleeve

Static-pressure ratios at ϕ, deg, of -

0	45	90	135	180	225	270	315
0.836	0.824	0.828	0.875	0.895	0.869	0.832	0.832
0.822	0.808	0.813	0.864	0.886	0.857	0.817	0.818
0.820	0.807	0.811	0.863	0.886	0.857	0.816	0.817
0.821	0.807	0.811	0.863	0.886	0.857	0.816	0.817
0.821	0.808	0.812	0.864	0.887	0.857	0.817	0.817
0.822	0.808	0.812	0.864	0.888	0.858	0.817	0.818
0.822	0.808	0.812	0.864	0.887	0.857	0.817	0.818
0.822	0.808	0.812	0.865	0.889	0.858	0.817	0.819
0.822	0.808	0.812	0.865	0.888	0.858	0.817	0.818
0.822	0.808	0.812	0.865	0.888	0.858	0.817	0.819
0.822	0.807	0.812	0.865	0.888	0.858	0.817	0.818

Table 122. Static-Pressure Ratios in Nozzle and Instrumented Sleeves for Configuration $P_OC_FB_FN_4L$

Inner wall

Static-pressure ratios at s/l_s of -

NPR	0.318	0.637	0.779	0.840	0.888	0.928
1.50	0.896	0.643	0.595	0.447	0.503	0.584
1.80	0.890	0.615	0.565	0.355	0.400	0.482
2.00	0.889	0.612	0.560	0.313	0.331	0.409
2.20	0.889	0.611	0.559	0.287	0.300	0.354
2.50	0.889	0.611	0.560	0.271	0.276	0.300
3.00	0.890	0.612	0.560	0.270	0.271	0.267
3.50	0.890	0.612	0.560	0.271	0.272	0.265
4.01	0.890	0.613	0.560	0.272	0.272	0.265
4.50	0.890	0.613	0.559	0.272	0.271	0.265
4.76	0.890	0.613	0.559	0.272	0.271	0.264

Inner channel

Static-pressure ratios at s/l_s of -

0.552	0.730	0.817	0.884	0.940
0.608	0.674	0.692	0.678	0.670
0.550	0.611	0.624	0.593	0.568
0.538	0.597	0.609	0.572	0.538
0.537	0.596	0.607	0.569	0.534
0.536	0.595	0.607	0.569	0.534
0.536	0.596	0.609	0.570	0.535
0.533	0.595	0.609	0.570	0.536
0.532	0.594	0.609	0.570	0.536
0.532	0.595	0.610	0.571	0.536
0.534	0.597	0.611	0.572	0.538

Outer channel

Static-pressure ratios at s/l_s of -

NPR	0.402	0.658	0.765	0.846	0.916	0.956
1.50	0.836	0.780	0.720	0.684	0.642	0.663
1.80	0.822	0.756	0.679	0.621	0.536	0.555
2.00	0.820	0.753	0.673	0.613	0.519	0.498
2.20	0.820	0.752	0.673	0.613	0.517	0.454
2.50	0.820	0.751	0.673	0.612	0.518	0.400
3.00	0.821	0.752	0.674	0.612	0.518	0.334
3.50	0.822	0.751	0.674	0.612	0.519	0.286
4.01	0.822	0.751	0.674	0.612	0.519	0.250
4.50	0.823	0.751	0.674	0.612	0.519	0.222
4.76	0.823	0.750	0.673	0.611	0.519	0.210

Left instrumented sleeve

Static-pressure coefficients at ϕ, deg, of -

NPR	0	45	90	135	180	225	270	315
1.50	0.823	0.810	0.827	0.866	0.893	0.867	0.830	0.816
1.80	0.808	0.794	0.815	0.858	0.885	0.858	0.817	0.802
2.00	0.806	0.792	0.814	0.857	0.884	0.857	0.816	0.800
2.20	0.806	0.791	0.814	0.857	0.884	0.857	0.815	0.800
2.50	0.805	0.790	0.814	0.858	0.884	0.857	0.815	0.800
3.00	0.806	0.791	0.815	0.858	0.886	0.858	0.816	0.800
3.50	0.805	0.790	0.815	0.859	0.886	0.858	0.816	0.800
4.01	0.805	0.790	0.815	0.859	0.886	0.858	0.816	0.800
4.50	0.805	0.789	0.815	0.859	0.886	0.858	0.816	0.800
4.76	0.805	0.789	0.815	0.859	0.886	0.858	0.816	0.801

Right instrumented sleeve

Static-pressure ratios at ϕ, deg, of -

0	45	90	135	180	225	270	315
0.835	0.828	0.828	0.871	0.895	0.869	0.831	0.819
0.822	0.812	0.814	0.861	0.887	0.859	0.817	0.802
0.820	0.810	0.813	0.859	0.886	0.858	0.815	0.799
0.821	0.810	0.812	0.859	0.886	0.857	0.815	0.799
0.821	0.811	0.813	0.860	0.887	0.858	0.815	0.799
0.822	0.810	0.813	0.860	0.887	0.858	0.816	0.800
0.822	0.810	0.813	0.861	0.888	0.858	0.816	0.800
0.823	0.810	0.813	0.861	0.888	0.858	0.817	0.800
0.823	0.810	0.813	0.861	0.888	0.859	0.817	0.800
0.823	0.810	0.813	0.861	0.888	0.859	0.817	0.800

Table 123. Static-Pressure Ratios in Nozzle and Instrumented Sleeves for Configuration $P_{()}C_FB_TN_4T$

Inner wall

Static-pressure ratios at s/l_s of -

NPR	0.318	0.637	0.779	0.840	0.888	0.928
1.50	0.901	0.644	0.596	0.450	0.513	0.588
1.80	0.896	0.620	0.569	0.352	0.395	0.477
2.00	0.894	0.616	0.564	0.311	0.331	0.409
2.20	0.893	0.615	0.563	0.286	0.300	0.351
2.51	0.893	0.615	0.564	0.276	0.279	0.298
2.99	0.895	0.617	0.564	0.275	0.276	0.273
3.50	0.894	0.617	0.564	0.277	0.278	0.273
4.00	0.894	0.618	0.565	0.277	0.277	0.272
4.50	0.894	0.618	0.564	0.277	0.277	0.272
4.99	0.893	0.618	0.563	0.277	0.276	0.271

Inner channel

Static-pressure ratios at s/l_s of -

0.552	0.730	0.817	0.884	0.940
0.620	0.680	0.693	0.676	0.669
0.562	0.619	0.628	0.593	0.566
0.554	0.610	0.617	0.578	0.545
0.550	0.606	0.615	0.576	0.542
0.546	0.605	0.615	0.575	0.542
0.541	0.601	0.614	0.575	0.543
0.540	0.602	0.615	0.576	0.543
0.536	0.600	0.615	0.576	0.543
0.536	0.601	0.616	0.577	0.543
0.537	0.602	0.616	0.577	0.543

Outer channel

Static-pressure ratios at s/l_s of -

NPR	0.402	0.658	0.765	0.846	0.916	0.956
1.50	0.837	0.769	0.712	0.681	0.644	0.644
1.80	0.822	0.742	0.667	0.613	0.541	0.517
2.00	0.819	0.738	0.660	0.600	0.508	0.456
2.20	0.818	0.737	0.660	0.599	0.507	0.451
2.51	0.818	0.739	0.660	0.600	0.508	0.448
2.99	0.818	0.740	0.662	0.601	0.509	0.448
3.50	0.818	0.740	0.663	0.601	0.509	0.448
4.00	0.818	0.741	0.663	0.601	0.510	0.448
4.50	0.818	0.741	0.663	0.601	0.510	0.449
4.99	0.818	0.740	0.663	0.601	0.510	0.450

Left instrumented sleeve

Static-pressure coefficients at ϕ, deg, of -

NPR	0	45	90	135	180	225	270	315
1.50	0.825	0.812	0.829	0.875	0.899	0.869	0.829	0.817
1.80	0.810	0.798	0.818	0.867	0.892	0.860	0.816	0.804
2.00	0.808	0.796	0.816	0.866	0.890	0.858	0.815	0.802
2.20	0.808	0.795	0.816	0.865	0.889	0.858	0.814	0.802
2.51	0.808	0.796	0.817	0.867	0.890	0.858	0.815	0.803
2.99	0.807	0.795	0.817	0.866	0.889	0.859	0.815	0.803
3.50	0.808	0.796	0.818	0.867	0.890	0.858	0.815	0.804
4.00	0.807	0.796	0.818	0.866	0.889	0.858	0.815	0.803
4.50	0.807	0.796	0.818	0.866	0.889	0.858	0.815	0.803
4.99	0.806	0.796	0.818	0.867	0.890	0.858	0.815	0.803

Right instrumented sleeve

Static-pressure ratios at ϕ, deg, of -

0	45	90	135	180	225	270	315
0.837	0.825	0.831	0.875	0.896	0.871	0.832	0.834
0.825	0.811	0.817	0.866	0.889	0.861	0.820	0.821
0.823	0.809	0.814	0.864	0.886	0.860	0.818	0.819
0.823	0.808	0.814	0.864	0.887	0.859	0.818	0.819
0.824	0.809	0.815	0.864	0.887	0.860	0.818	0.820
0.824	0.810	0.815	0.865	0.888	0.860	0.818	0.820
0.824	0.809	0.814	0.865	0.888	0.860	0.819	0.821
0.824	0.810	0.815	0.866	0.889	0.860	0.819	0.821
0.824	0.809	0.814	0.866	0.889	0.860	0.818	0.821
0.824	0.809	0.814	0.865	0.888	0.860	0.818	0.820

Table 124. Static-Pressure Ratios in Nozzle and Instrumented Sleeves for Configuration $P_OC_FB_TN_4L$

Inner wall

Static-pressure ratios at s/l_s of -

NPR	0.318	0.637	0.779	0.840	0.888	0.928
1.50	0.897	0.643	0.597	0.454	0.507	0.583
1.80	0.891	0.616	0.567	0.355	0.397	0.477
2.00	0.891	0.613	0.562	0.316	0.334	0.409
2.20	0.890	0.611	0.561	0.289	0.301	0.352
2.51	0.891	0.612	0.562	0.273	0.277	0.299
3.00	0.891	0.613	0.562	0.272	0.272	0.266
3.51	0.891	0.614	0.562	0.273	0.273	0.265
4.00	0.891	0.615	0.562	0.273	0.272	0.265
4.50	0.891	0.615	0.561	0.273	0.272	0.264
4.76	0.891	0.615	0.561	0.272	0.271	0.264

Inner channel

Static-pressure ratios at s/l_s of -

0.552	0.730	0.817	0.884	0.940
0.614	0.678	0.695	0.679	0.672
0.554	0.614	0.625	0.592	0.569
0.544	0.601	0.612	0.573	0.540
0.541	0.598	0.609	0.569	0.534
0.539	0.596	0.608	0.568	0.533
0.535	0.594	0.607	0.567	0.533
0.531	0.591	0.605	0.566	0.531
0.537	0.597	0.610	0.571	0.536
0.533	0.594	0.608	0.570	0.534
0.537	0.598	0.612	0.572	0.537

Outer channel

Static-pressure ratios at s/l_s of -

NPR	0.402	0.658	0.765	0.846	0.916	0.956
1.50	0.838	0.780	0.722	0.687	0.645	0.664
1.80	0.823	0.756	0.679	0.623	0.537	0.554
2.00	0.821	0.753	0.675	0.615	0.521	0.499
2.20	0.821	0.753	0.675	0.615	0.519	0.453
2.51	0.823	0.754	0.676	0.615	0.521	0.399
3.00	0.824	0.755	0.677	0.616	0.521	0.333
3.51	0.826	0.756	0.678	0.616	0.523	0.285
4.00	0.825	0.754	0.677	0.615	0.521	0.250
4.50	0.826	0.755	0.677	0.615	0.522	0.222
4.76	0.825	0.753	0.676	0.614	0.521	0.210

Left instrumented sleeve

Static-pressure coefficients at ϕ, deg. of -

NPR	0	45	90	135	180	225	270	315
1.50	0.823	0.809	0.828	0.868	0.894	0.868	0.830	0.815
1.80	0.808	0.794	0.815	0.861	0.888	0.859	0.817	0.801
2.00	0.806	0.791	0.814	0.860	0.886	0.858	0.816	0.799
2.20	0.806	0.790	0.814	0.859	0.887	0.858	0.816	0.800
2.51	0.806	0.791	0.815	0.861	0.888	0.858	0.817	0.801
3.00	0.806	0.789	0.815	0.861	0.888	0.858	0.817	0.800
3.51	0.805	0.789	0.815	0.862	0.888	0.858	0.817	0.801
4.00	0.805	0.789	0.815	0.862	0.888	0.858	0.818	0.801
4.50	0.804	0.789	0.815	0.862	0.888	0.859	0.817	0.801
4.76	0.804	0.789	0.815	0.862	0.889	0.858	0.818	0.801

Right instrumented sleeve

Static-pressure ratios at ϕ, deg. of -

0	45	90	135	180	225	270	315
0.836	0.827	0.830	0.874	0.894	0.871	0.833	0.819
0.823	0.812	0.816	0.864	0.887	0.859	0.818	0.803
0.822	0.810	0.814	0.863	0.887	0.859	0.817	0.801
0.822	0.809	0.814	0.863	0.887	0.858	0.816	0.800
0.823	0.810	0.815	0.864	0.888	0.859	0.817	0.801
0.823	0.810	0.814	0.864	0.888	0.859	0.818	0.801
0.823	0.809	0.814	0.864	0.889	0.859	0.818	0.801
0.823	0.809	0.814	0.864	0.889	0.859	0.817	0.801
0.824	0.809	0.814	0.864	0.889	0.859	0.818	0.801
0.823	0.809	0.813	0.864	0.888	0.858	0.817	0.801

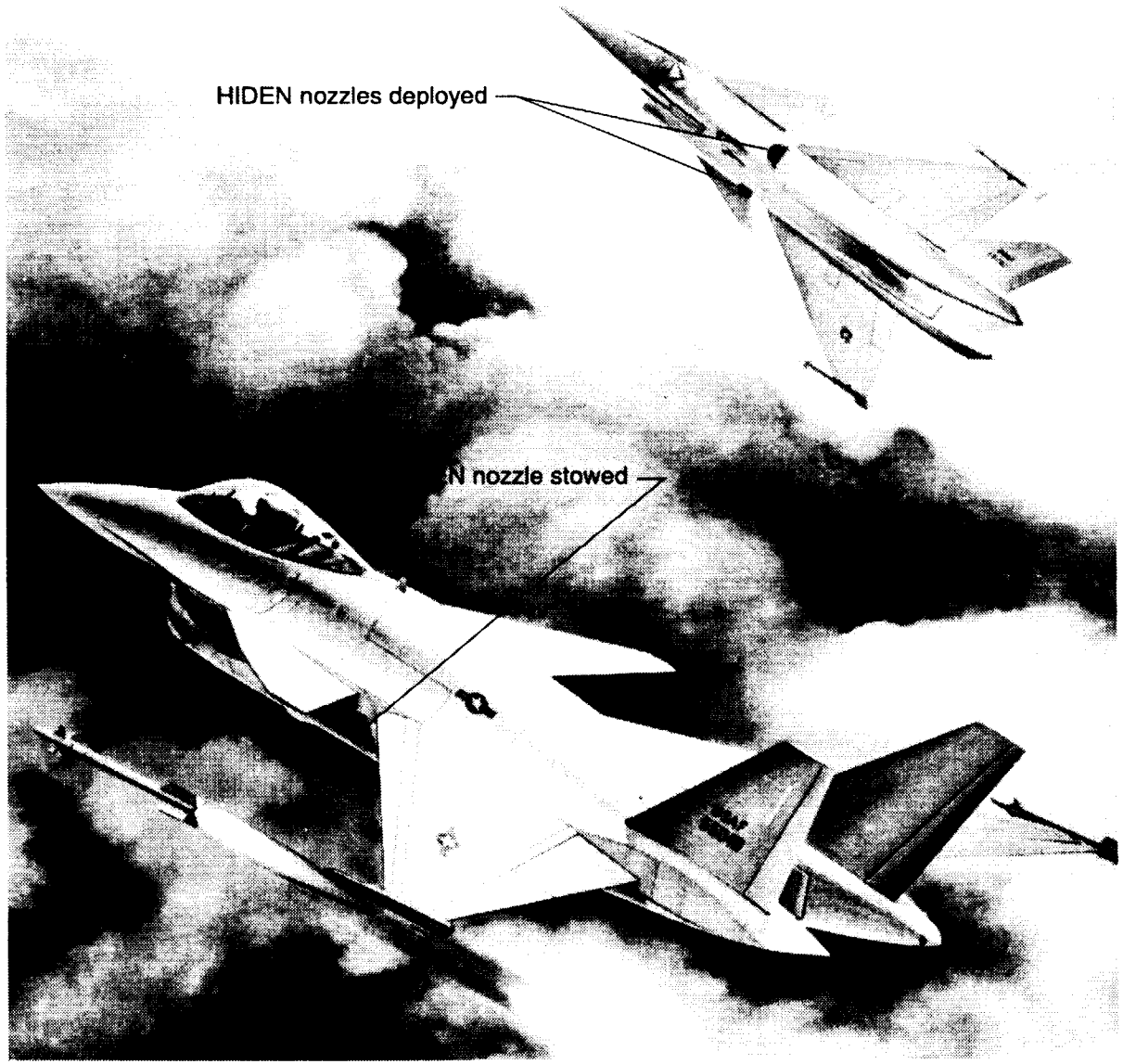

L-93-5265

Figure 1. Artist's concept of typical HIDEN nozzle installation.

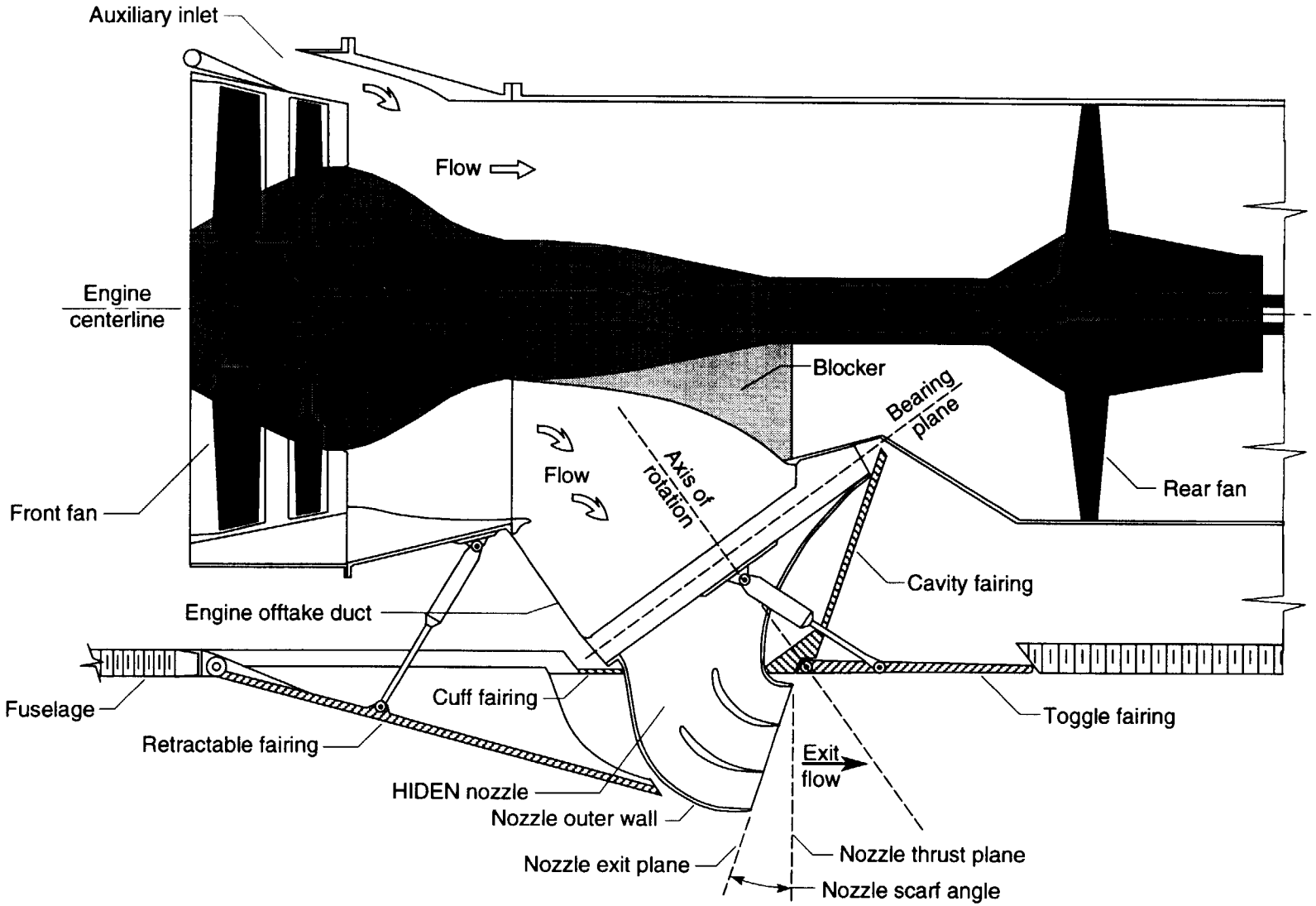

(a) HIDEN nozzle deployed in thrust mode.

Figure 2. Typical propulsion integration of HIDEN concept in fan section of HFVT engine.

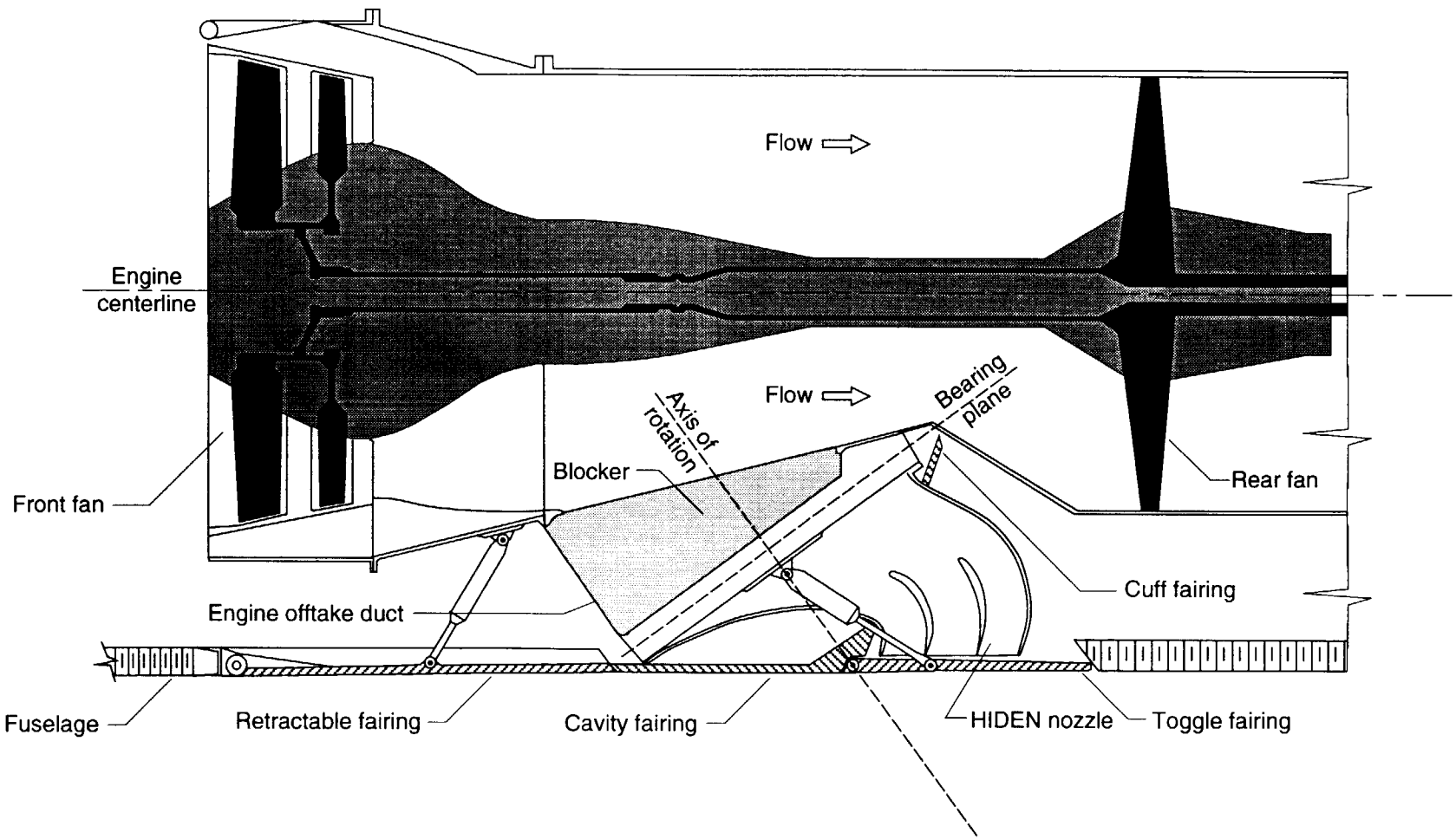

(b) HIDEN nozzle stowed.

Figure 2. Concluded.

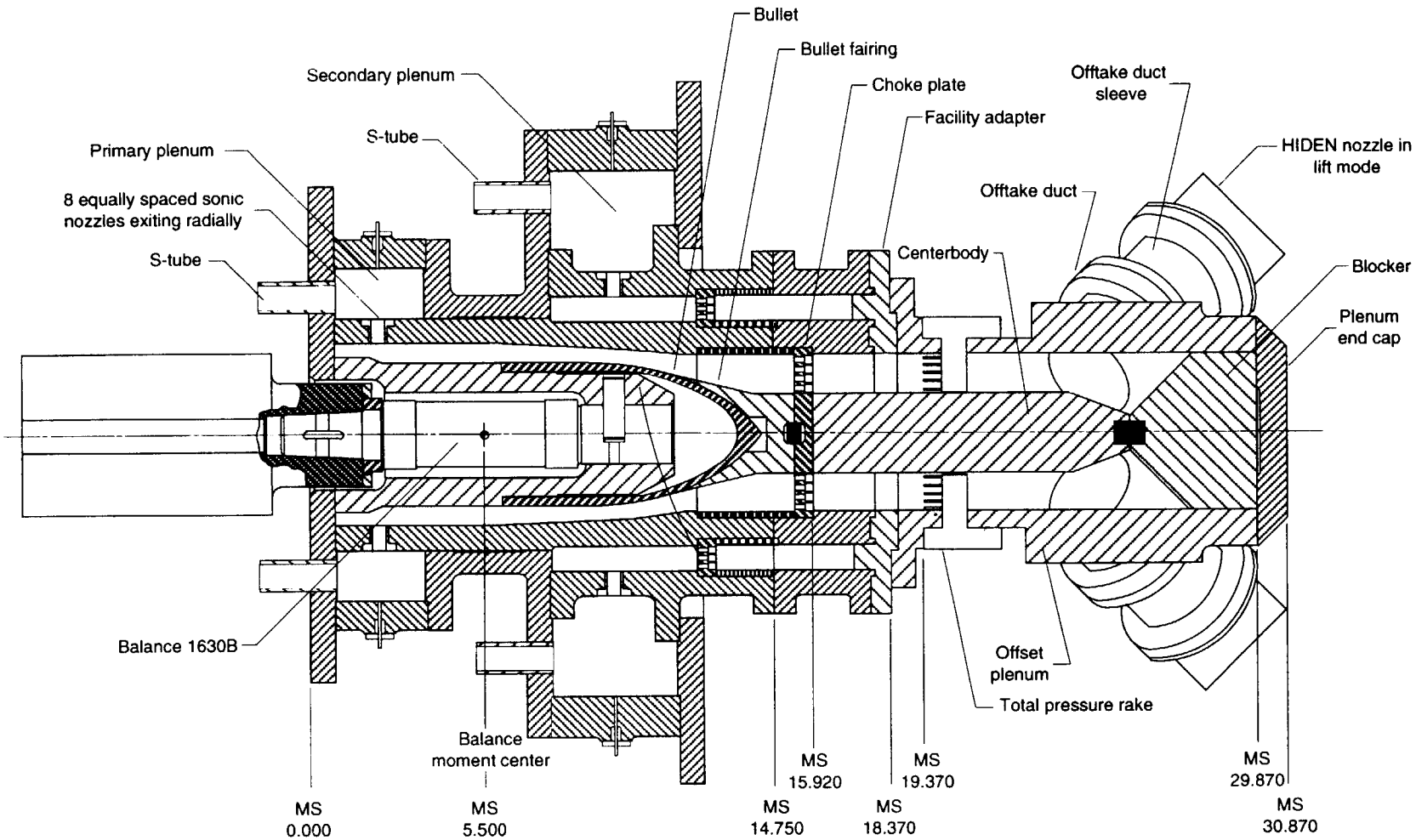

Figure 3. Top cutaway view of typical HIDEN installation on dual-flow single-engine propulsion simulation system. All model stations are in inches.

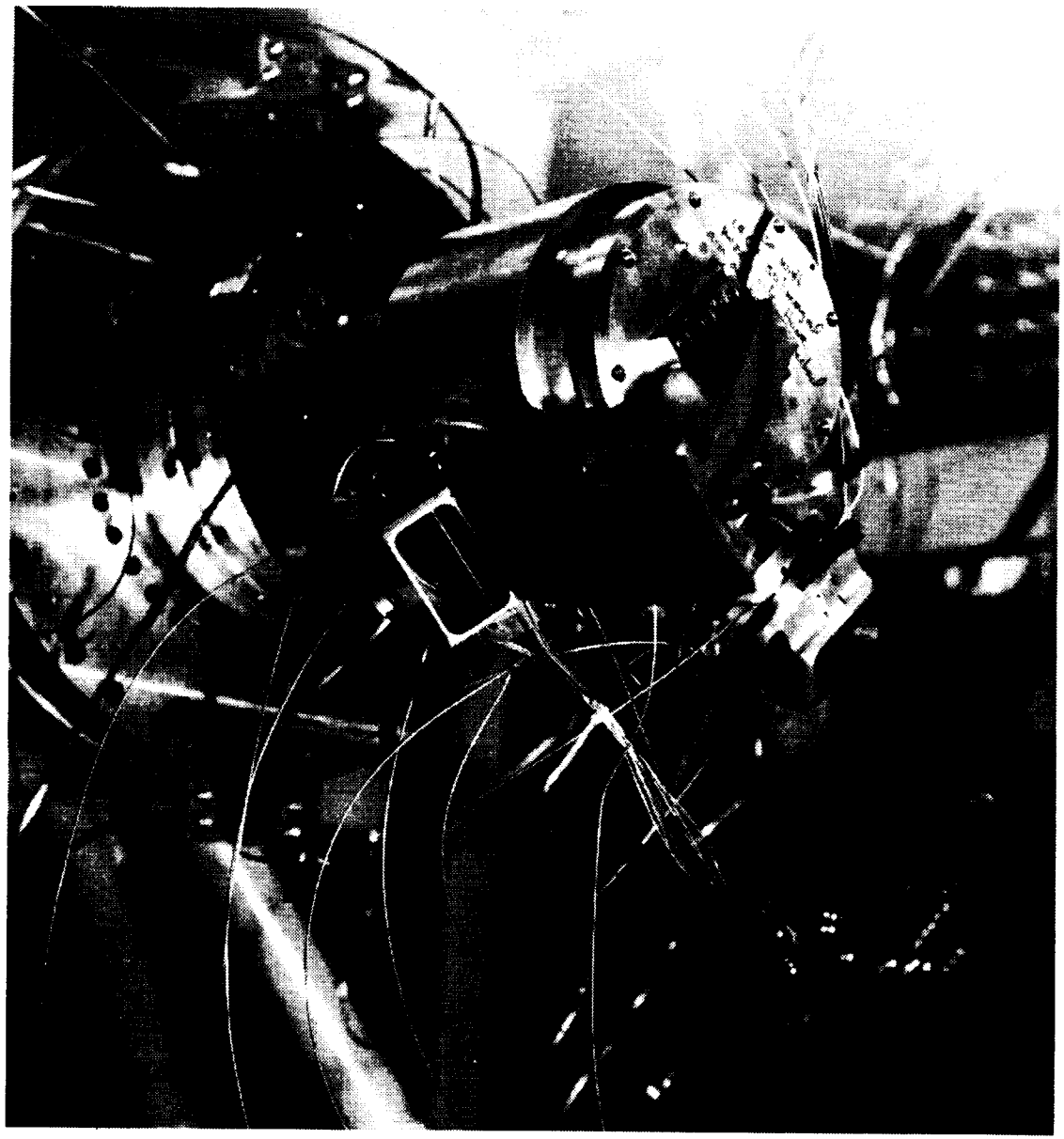

(a) HIDEN nozzles in thrust mode with instrumented ramp installed.

Figure 4. Offset plenum mounted on propulsion simulation system with 1.4 CR submerged nozzles installed.

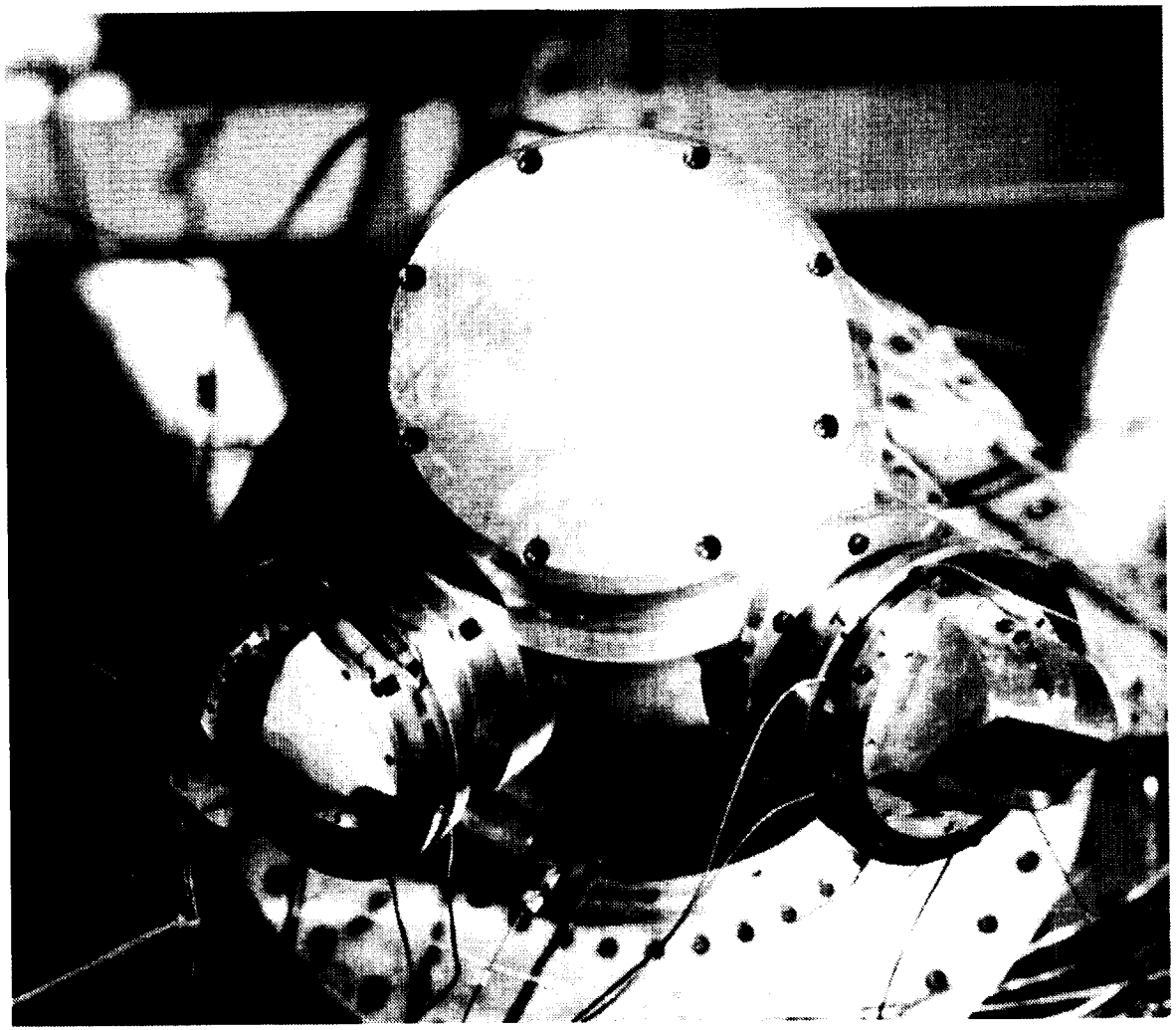

(b) HIDEN nozzles in lift mode.

Figure 4. Concluded.

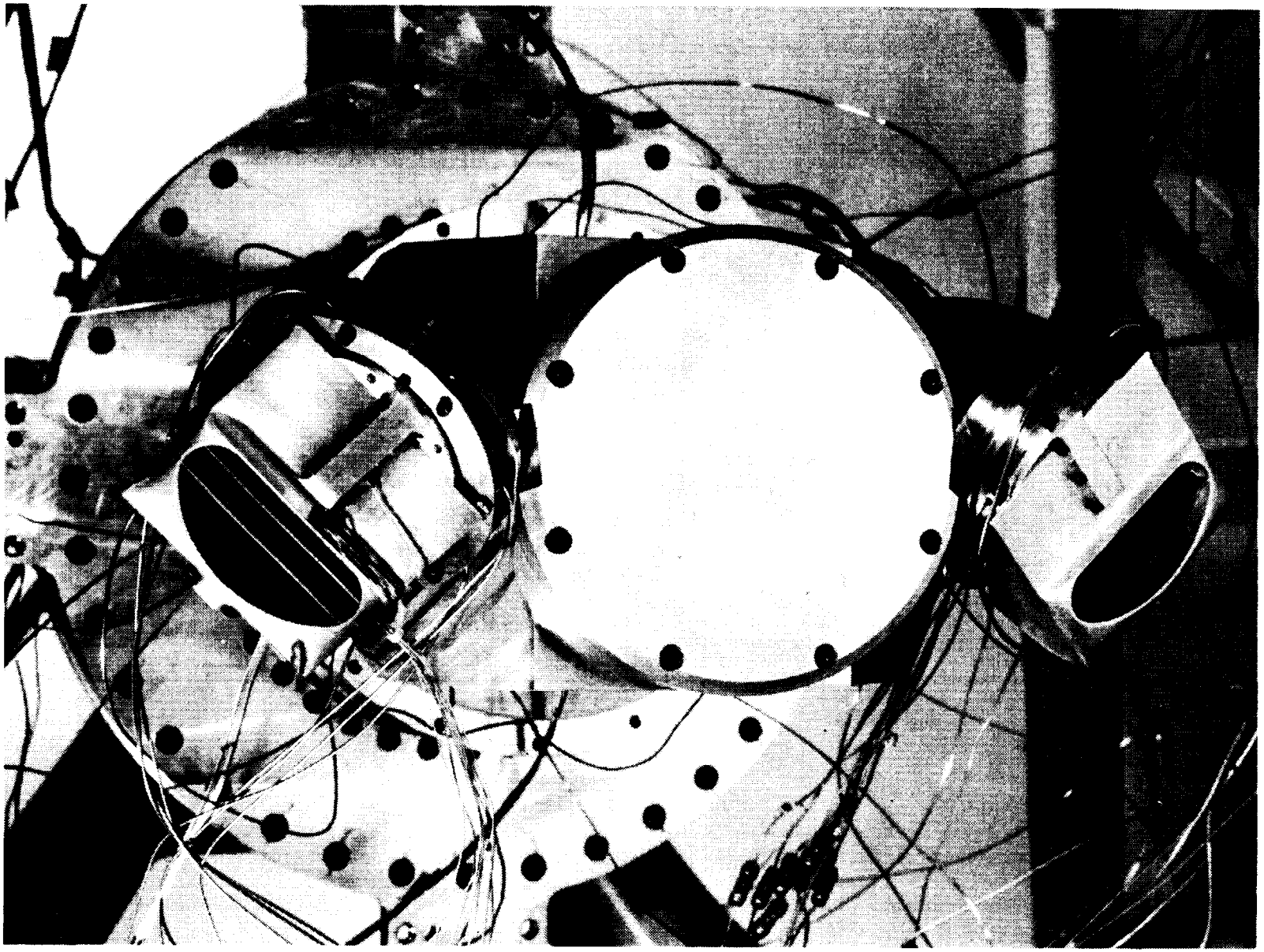

L-92-2825

(a) HIDEN nozzles in thrust mode.

Figure 5. Centerline plenum mounted on propulsion simulation system with 1.8 CR D-shaped nozzles installed.

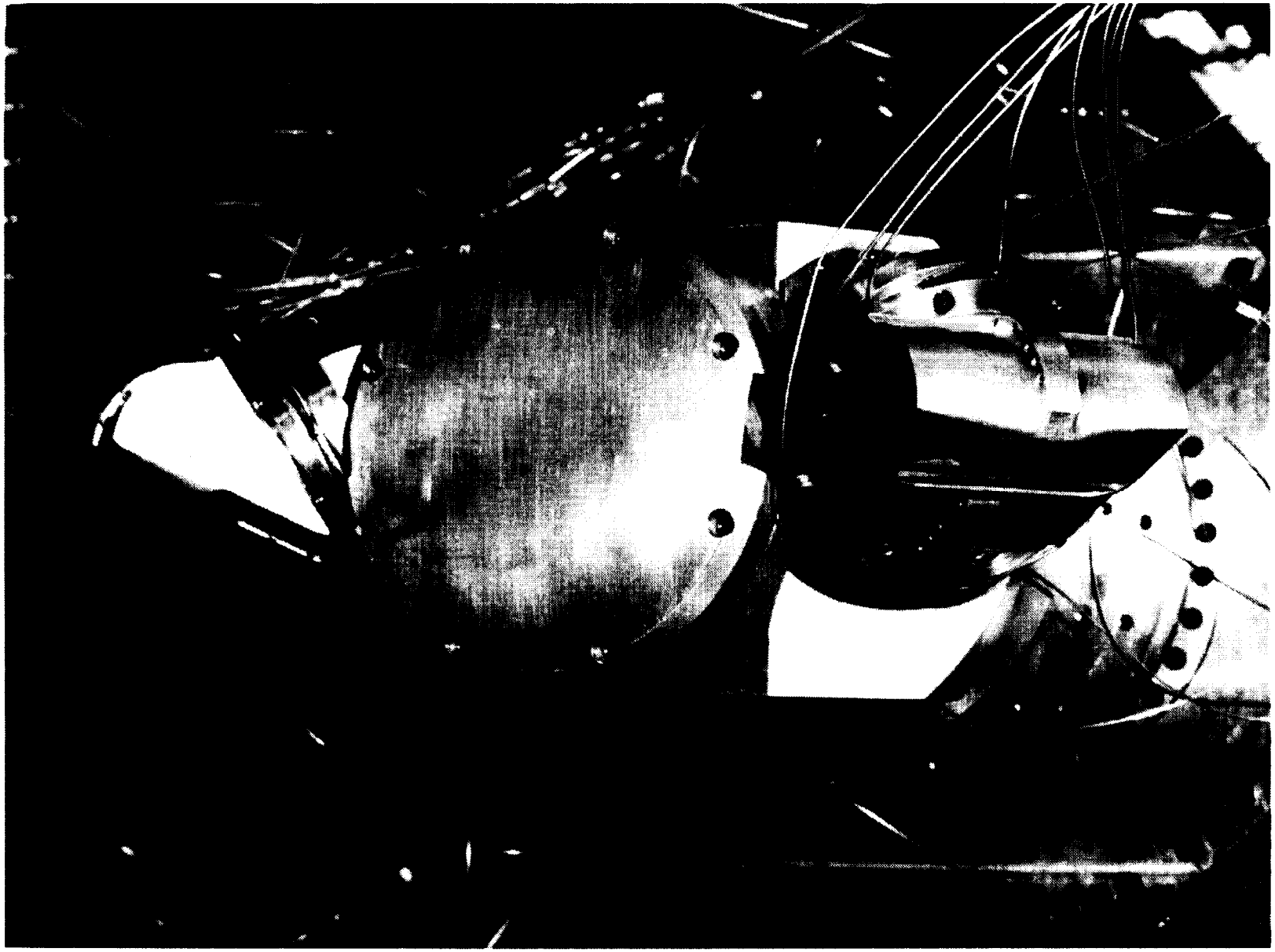

L-92-2911

(b) HIDEN nozzles in lift mode.

Figure 5. Concluded.

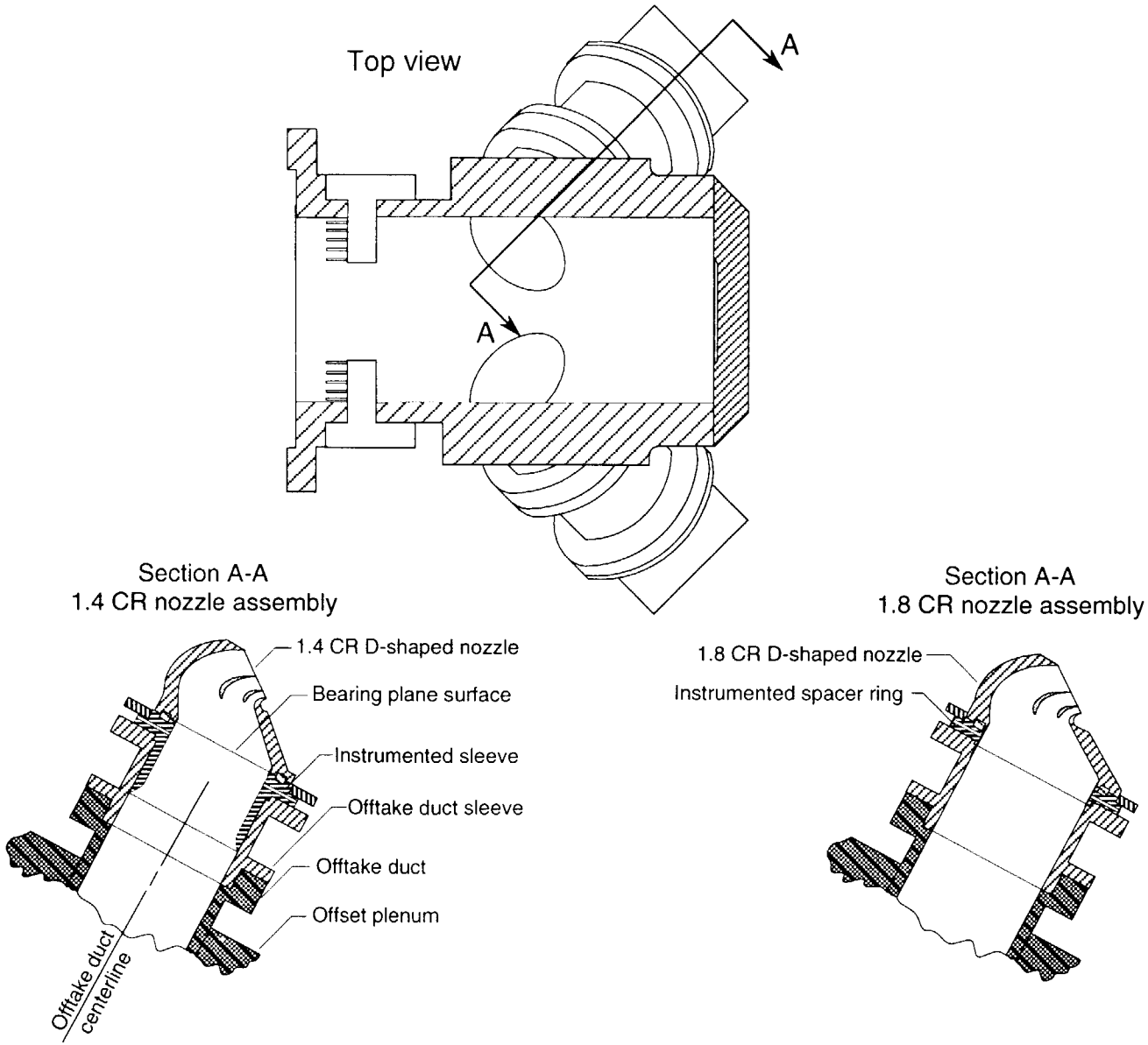

(a) Details of offset plenum assembly with centerbody and blocker removed.

Figure 6. Offset plenum geometry. All dimensions are in inches unless otherwise noted.

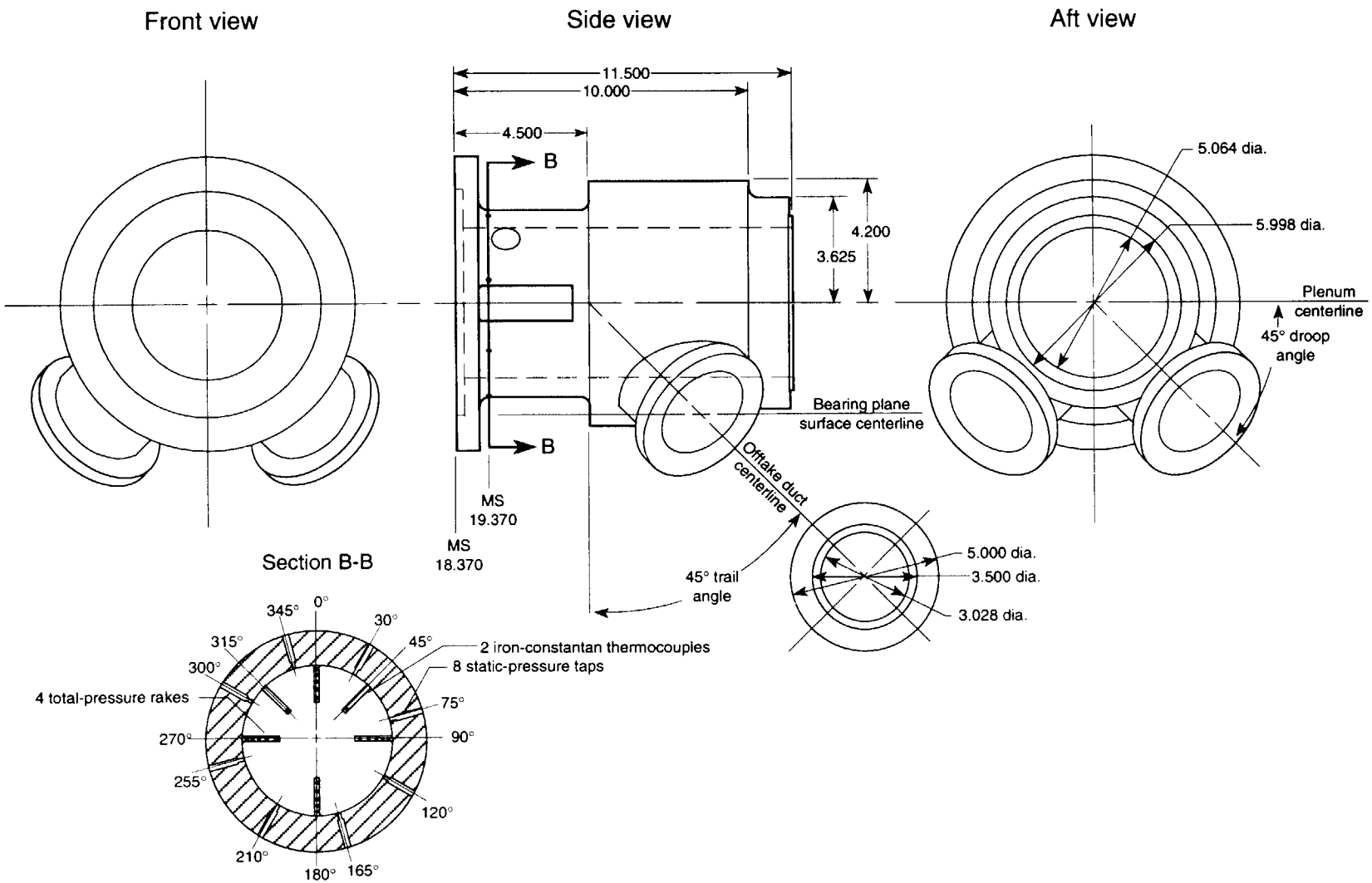

(b) Details of offset plenum.

Figure 6. Continued.

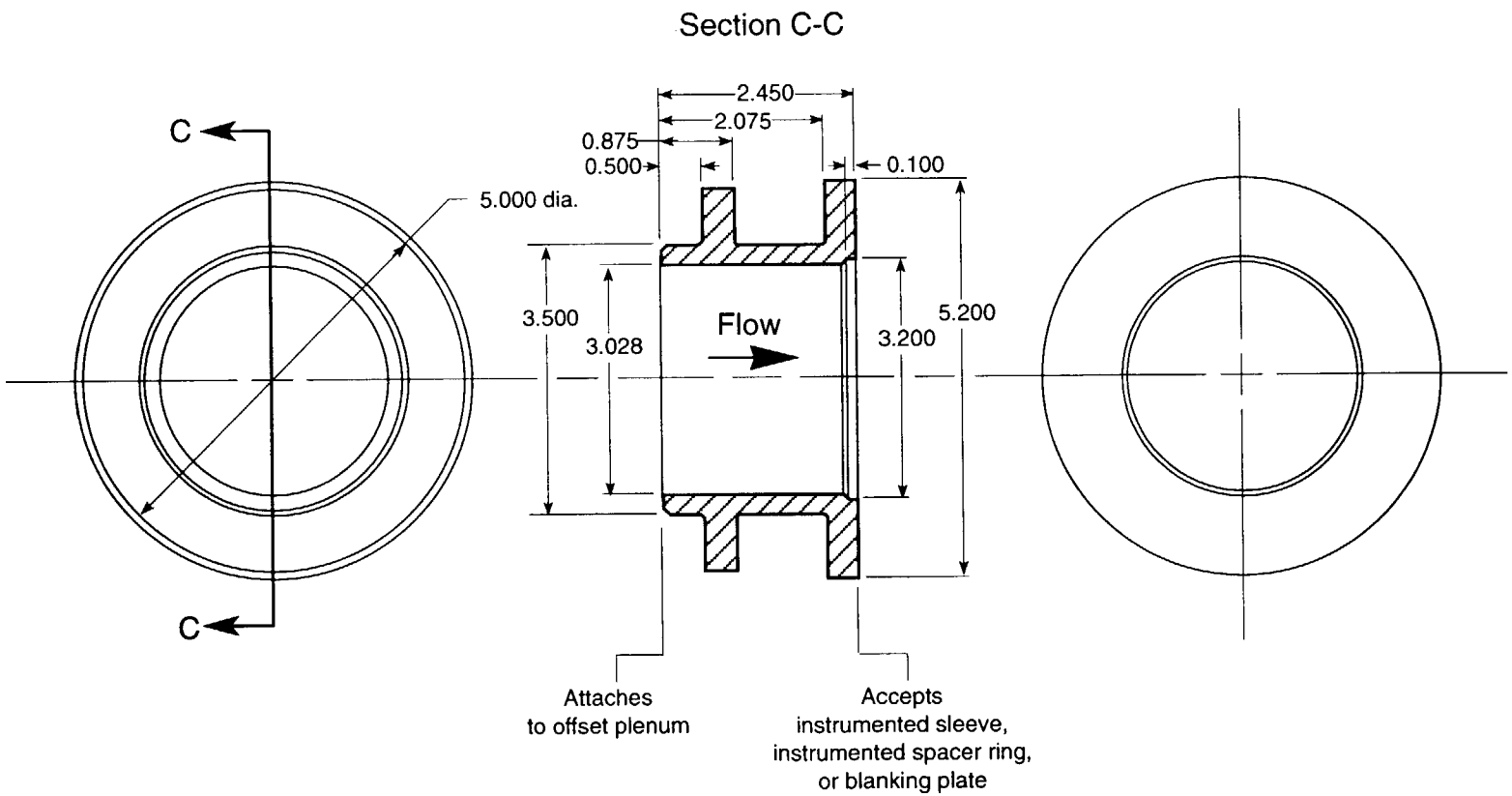

(c) Details of offtake duct sleeve.

Figure 6. Concluded.

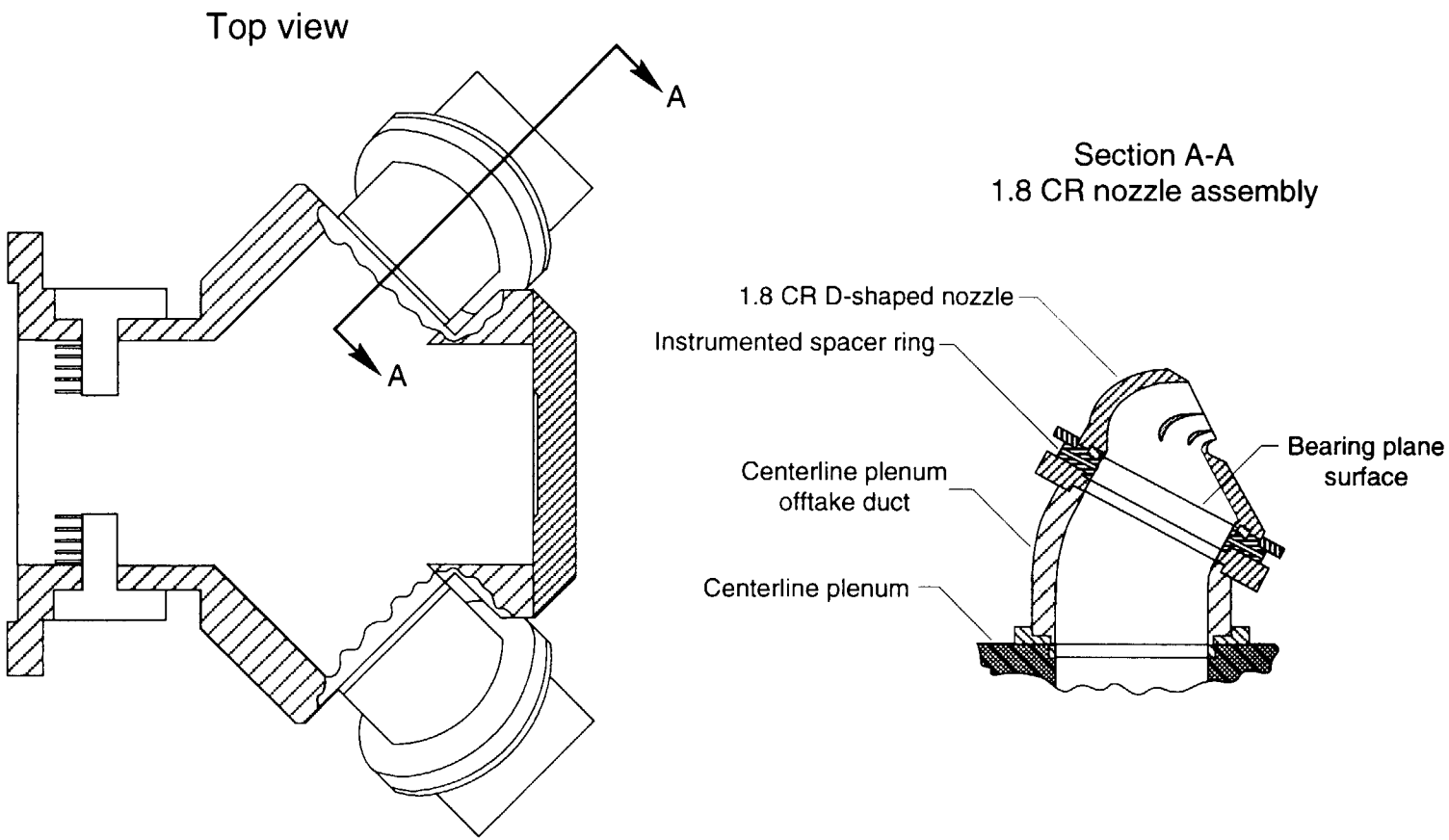

(a) Details of centerline plenum assembly with centerbody and blocker removed.

Figure 7. Centerline plenum geometry. All dimensions are in inches unless otherwise noted.

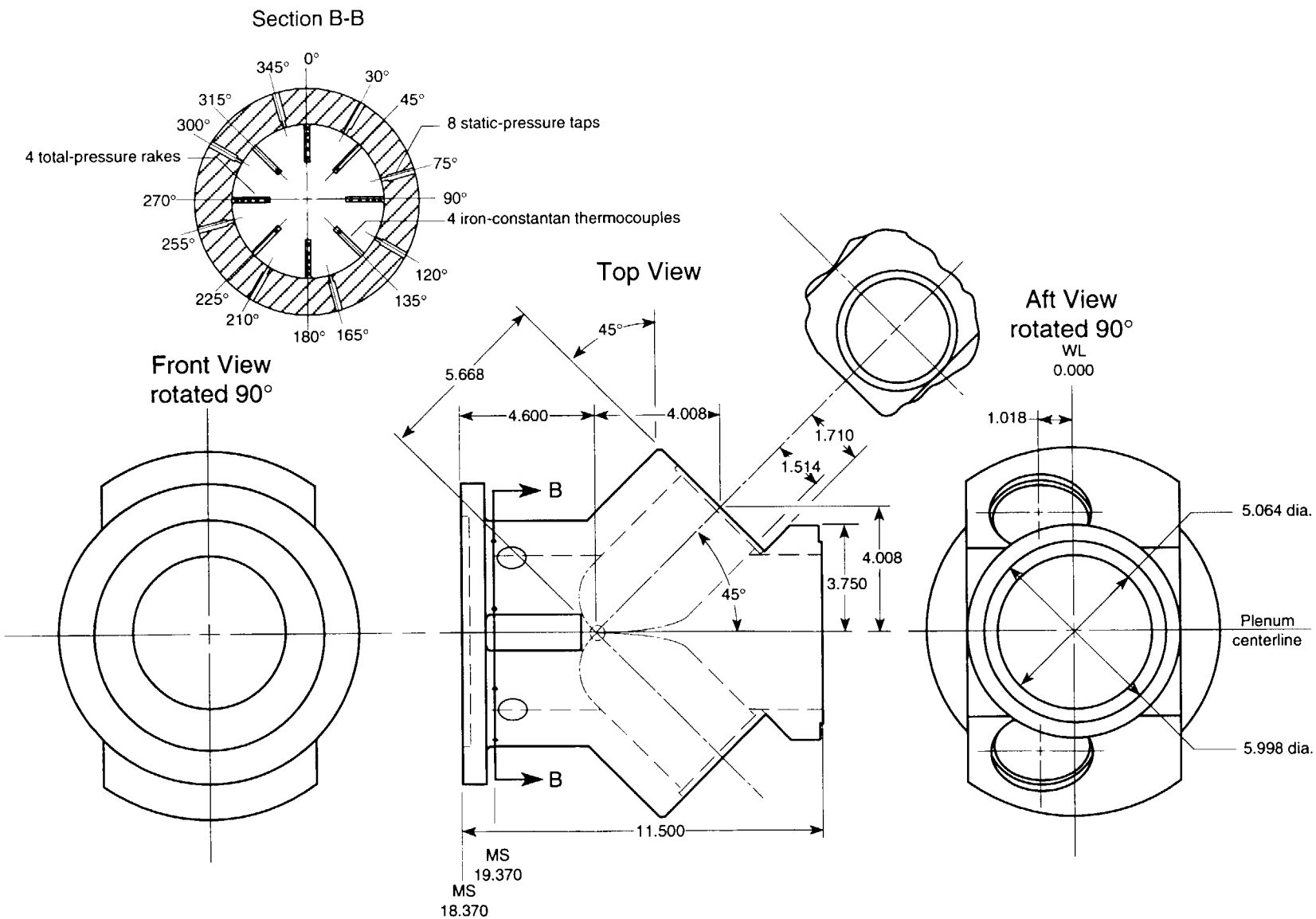

(b) Details of centerline plenum.

Figure 7. Continued.

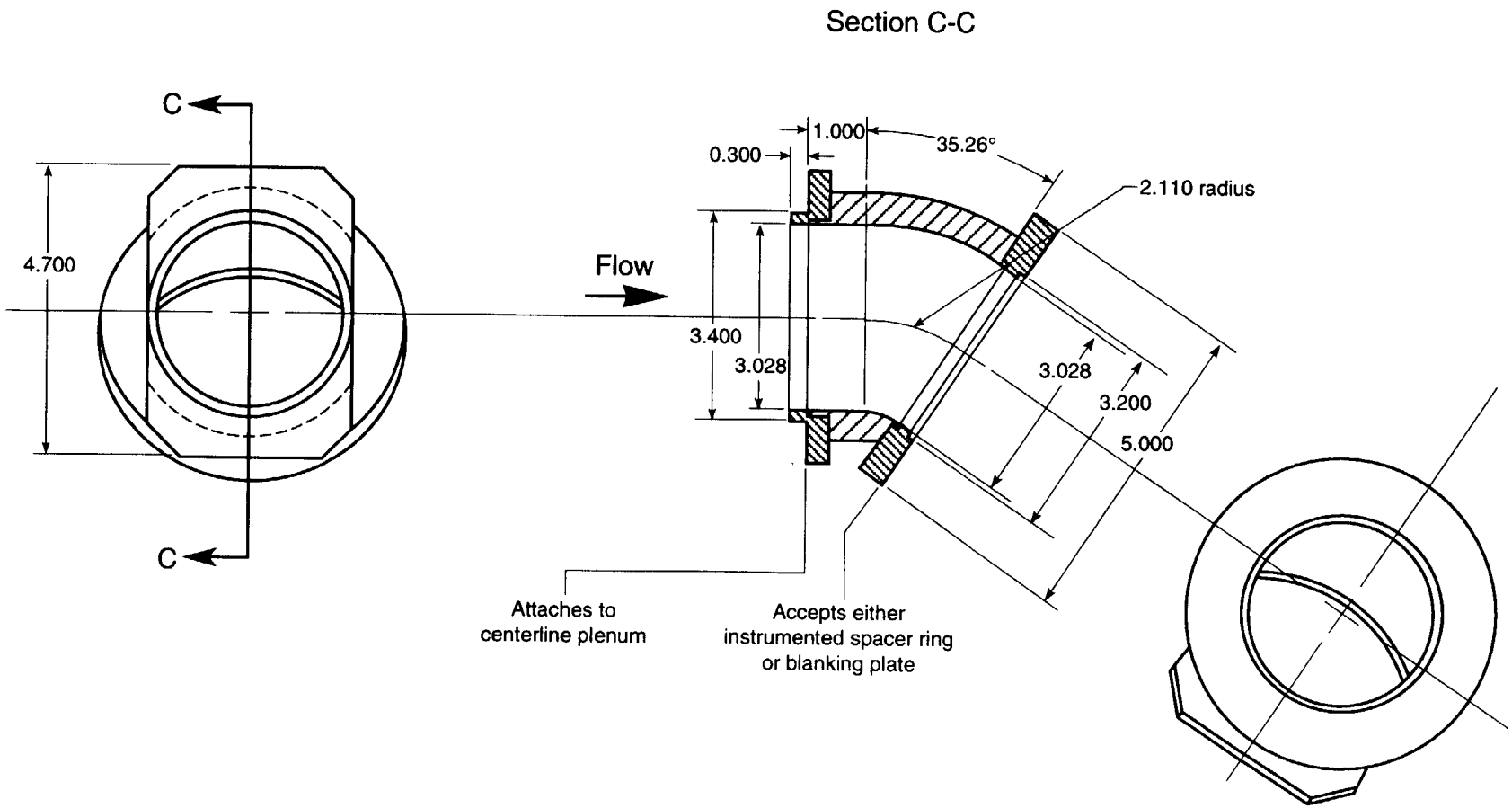

(c) Details of centerline plenum offtake duct.

Figure 7. Continued.

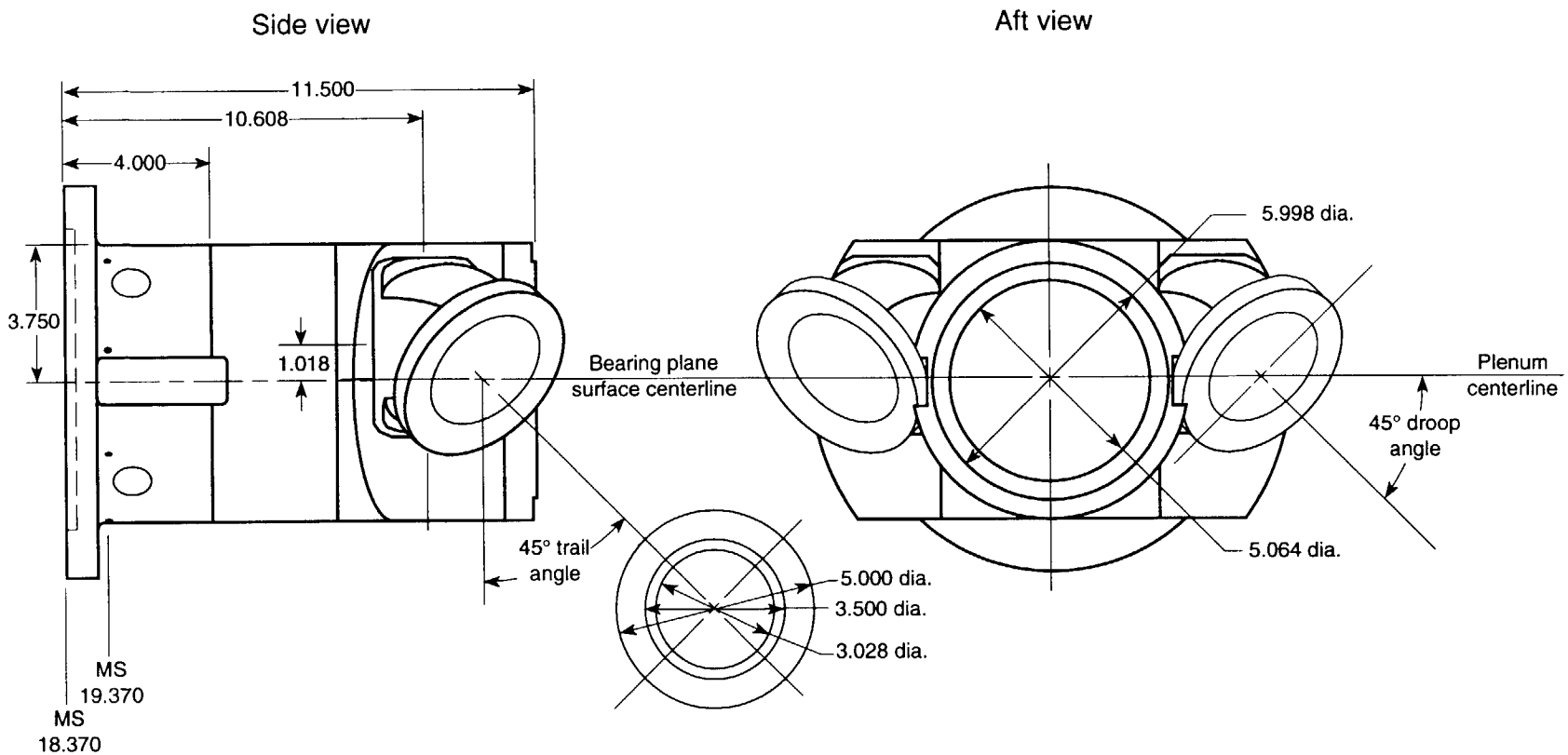

(d) Details of centerline plenum with offtake ducts installed.

Figure 7. Concluded.

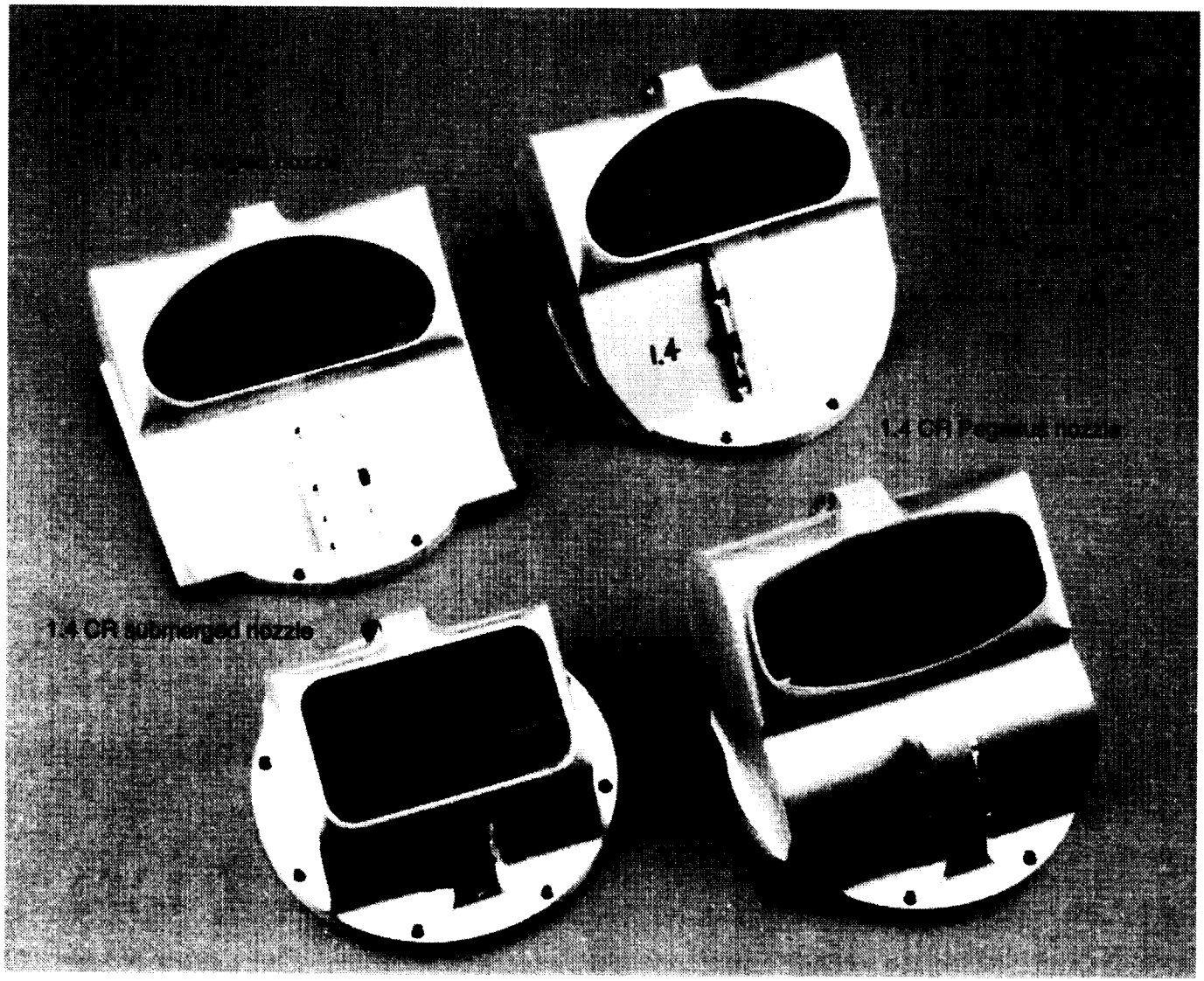

L-94-6643

(a) HIDEN nozzles.

Figure 8. Photographs of HIDEN nozzles.

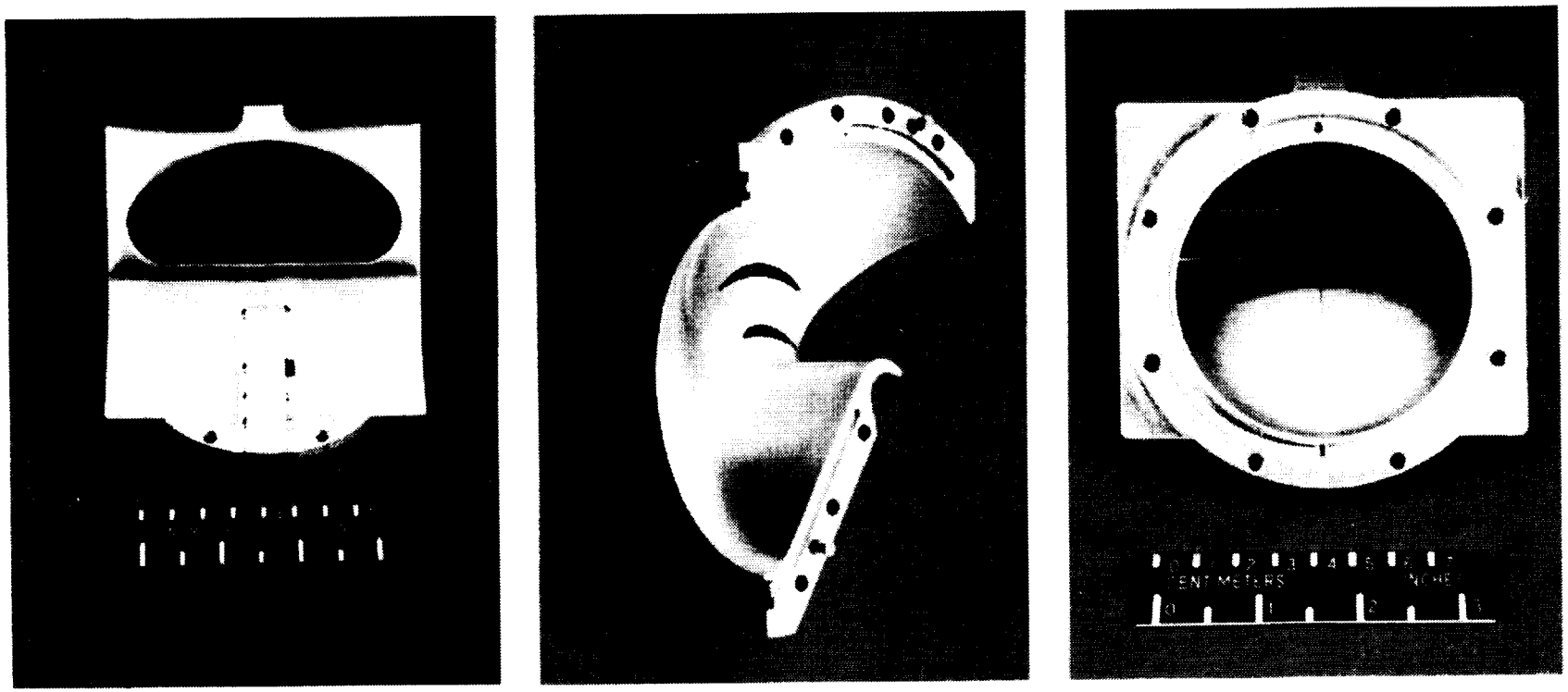

(b) The 1.8 CR D-shaped nozzle.

Figure 8. Continued.

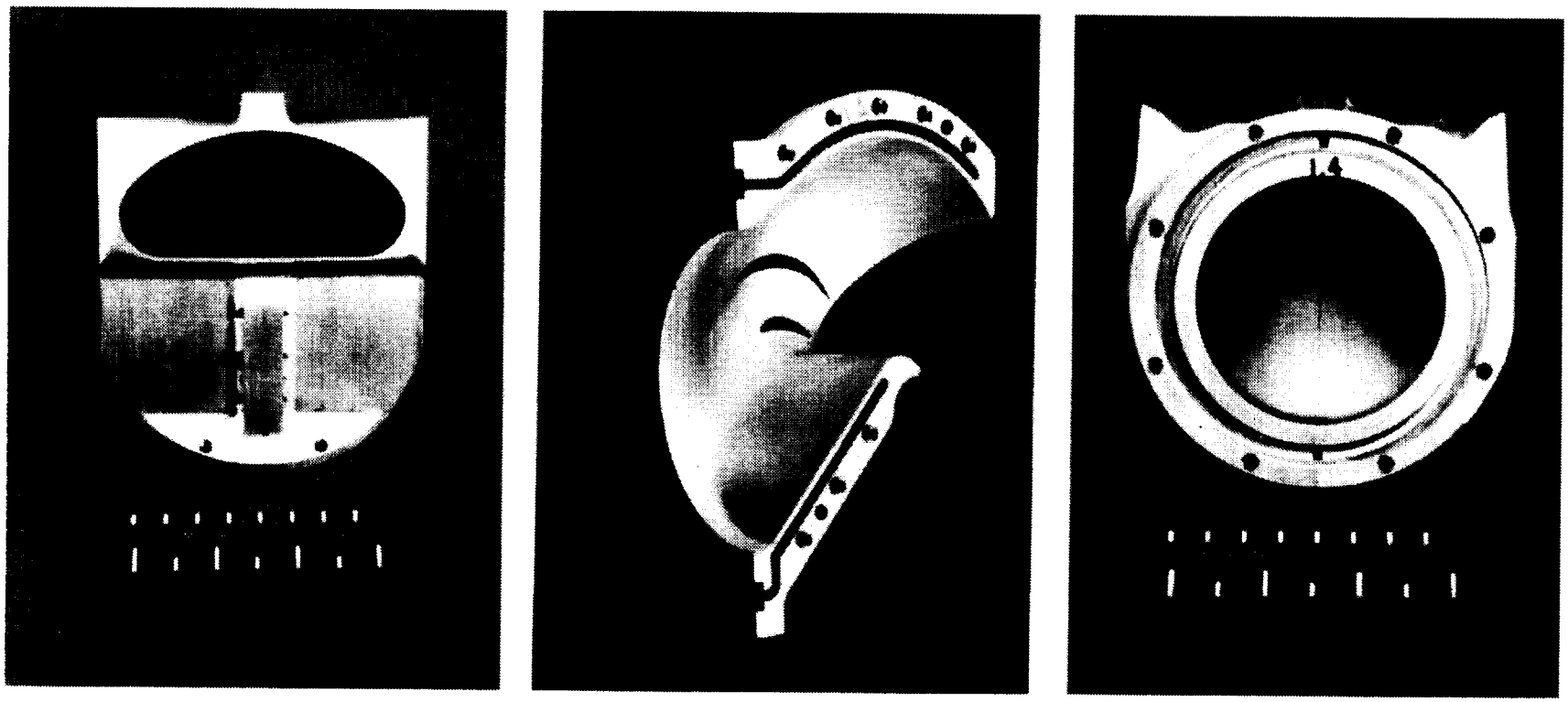

(c) The 1.4 CR D-shaped nozzle.

Figure 8. Continued.

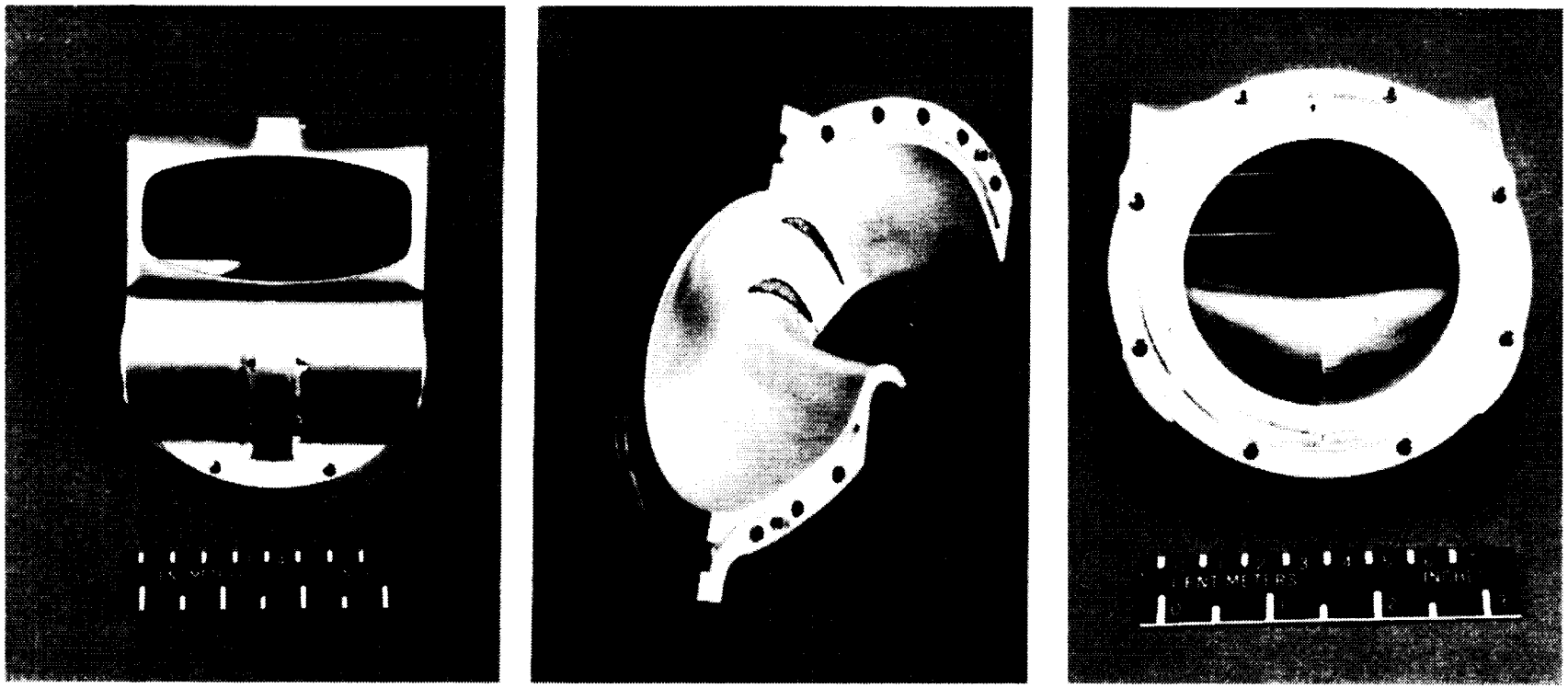

(d) The 1.4 CR Pegasus nozzle.

Figure 8. Continued.

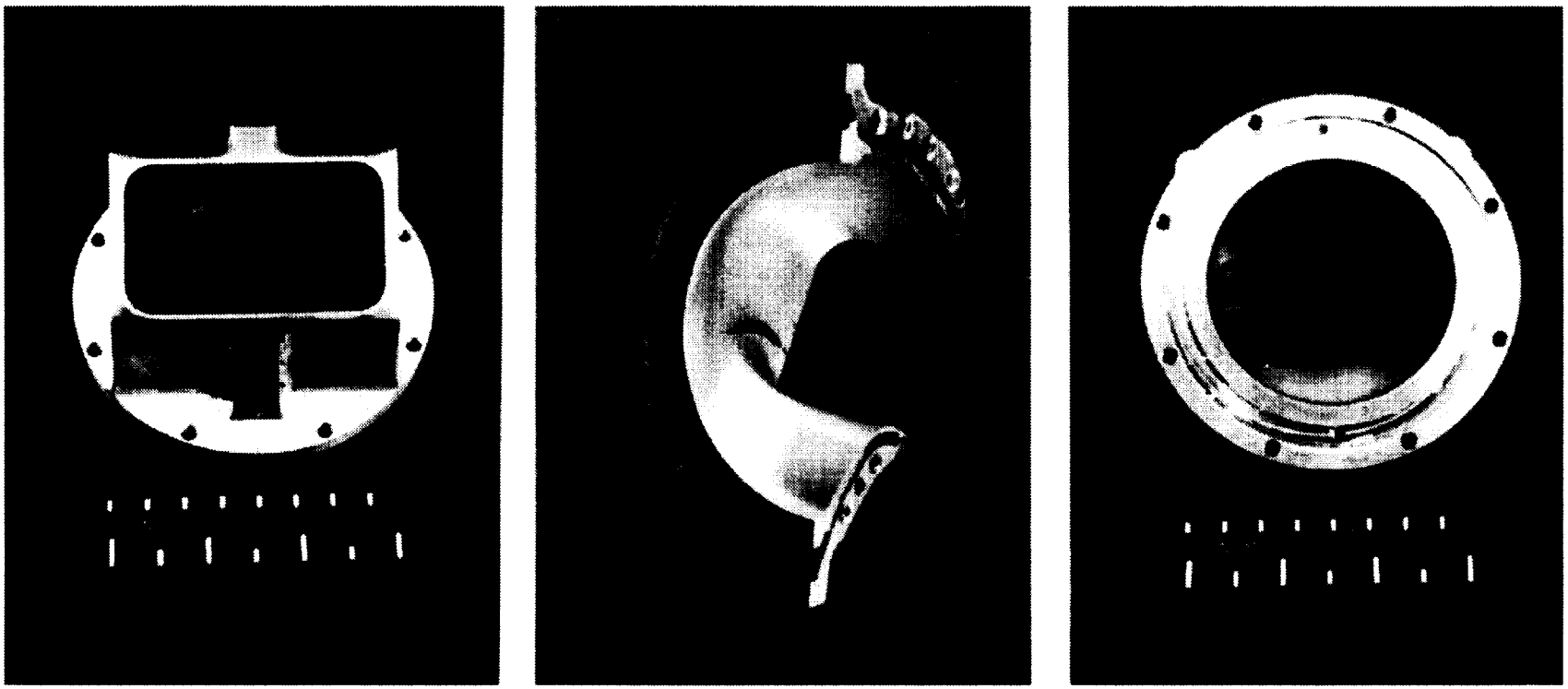

(e) The 1.4 CR submerged nozzle.

Figure 8. Concluded.

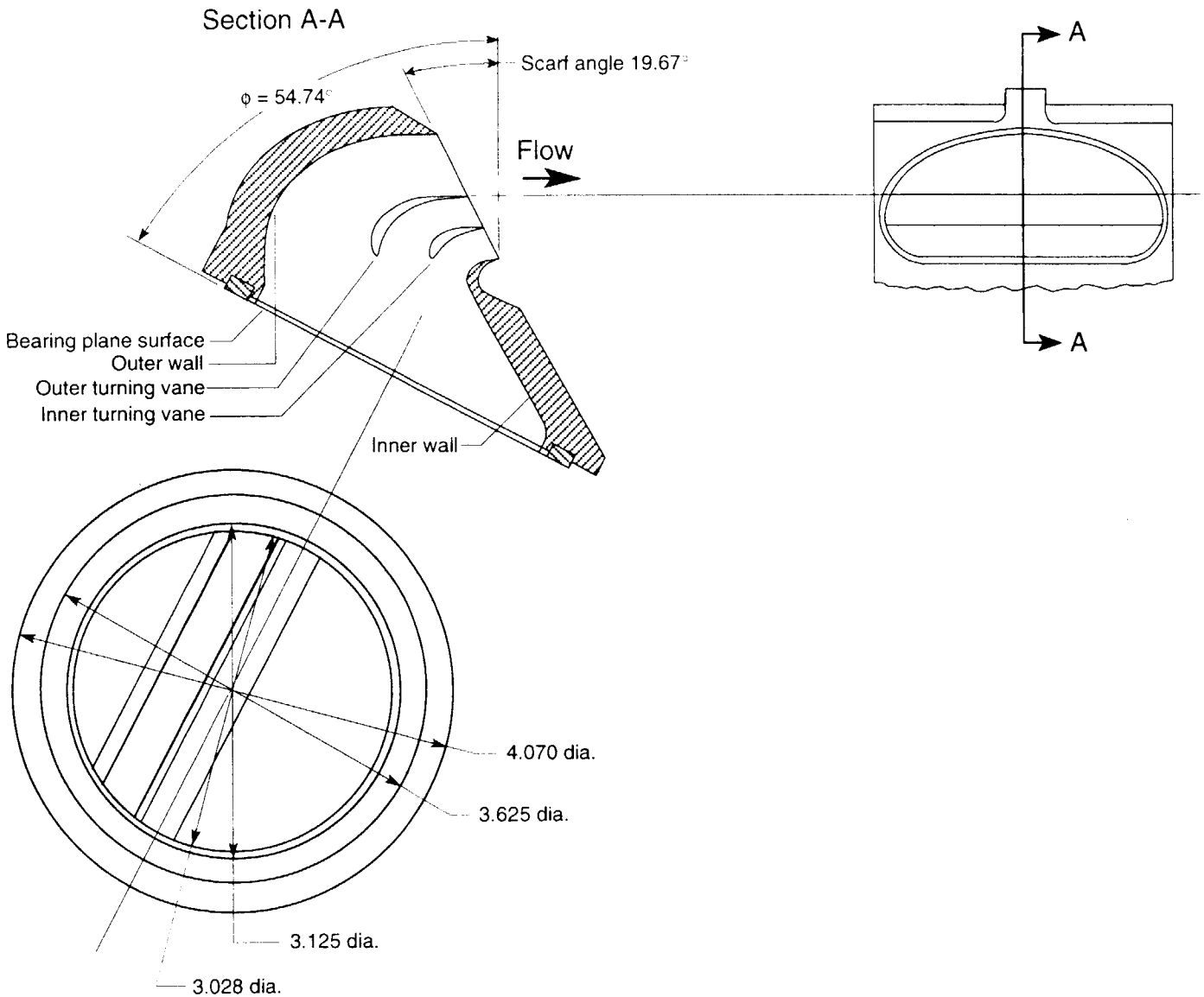

(a) The 1.8 CR D-shaped nozzle.

Figure 9. Details of HIDEN nozzles. All dimensions are in inches unless otherwise noted.

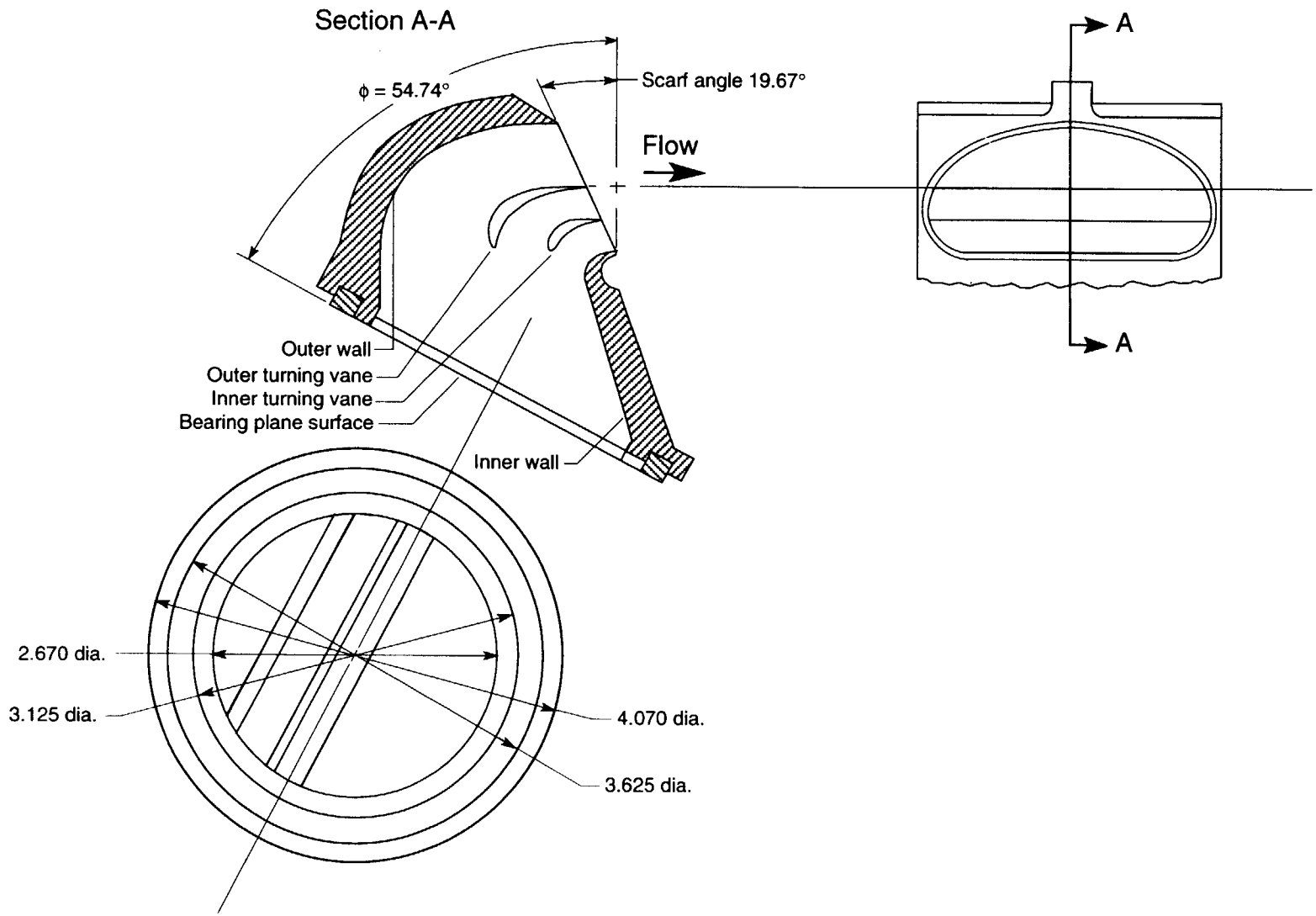

(b) The 1.4 CR D-shaped nozzle.

Figure 9. Continued.

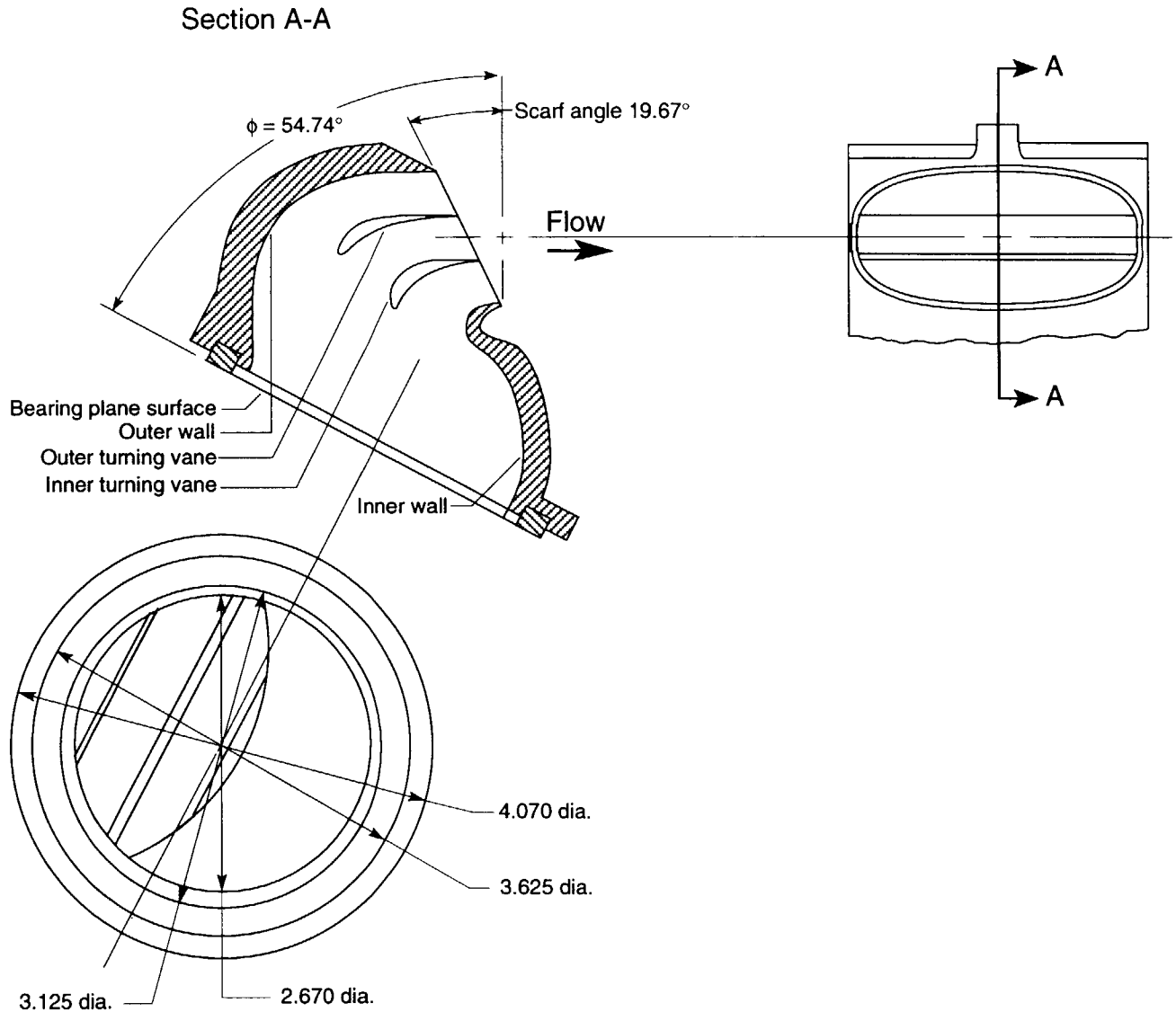

(c) The 1.4 CR Pegasus nozzle.

Figure 9. Continued.

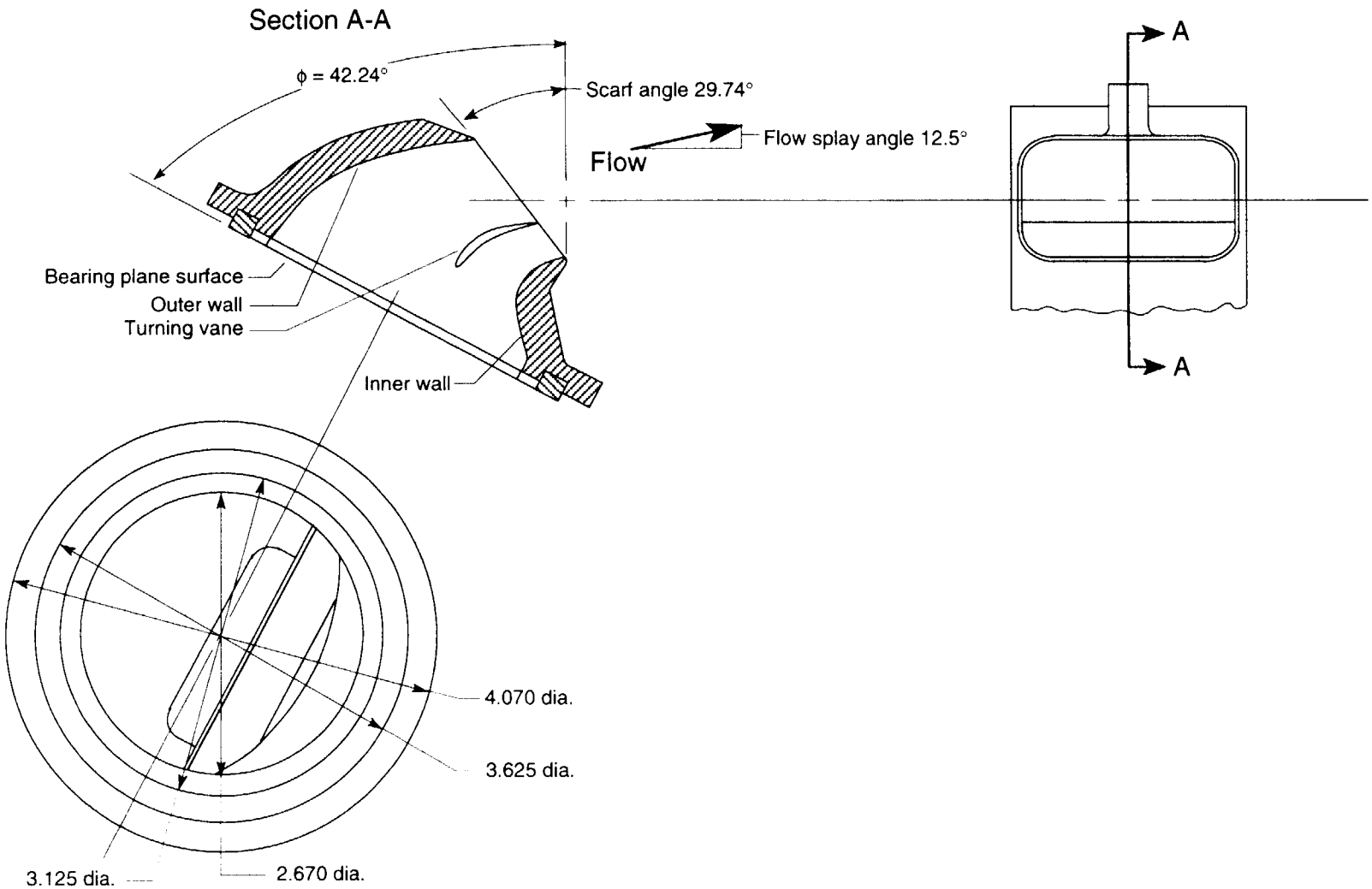

(d) The 1.4 CR submerged nozzle.

Figure 9. Continued.

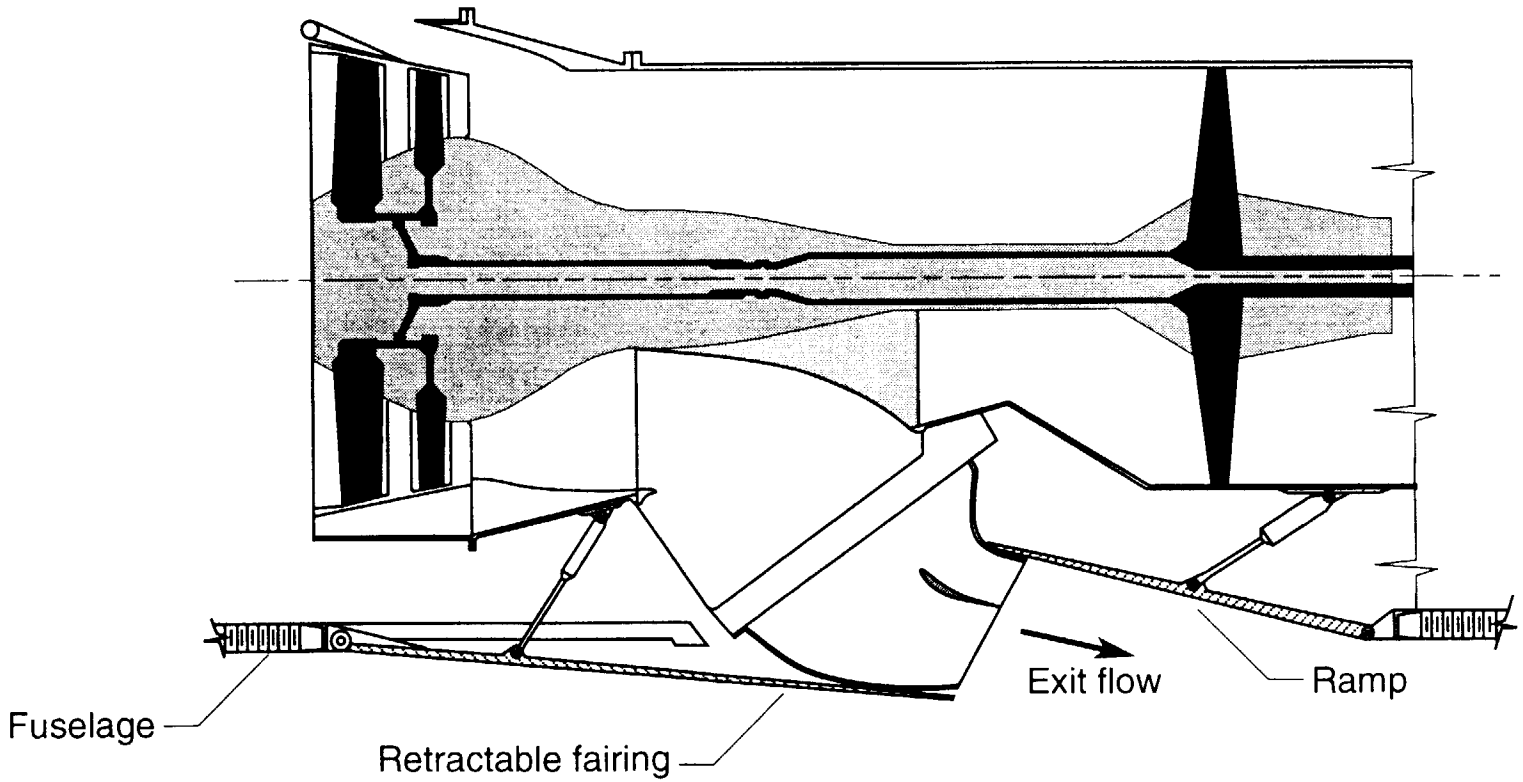

(e) Typical submerged nozzle installation in fan section of HFVT engine.

Figure 9. Concluded.

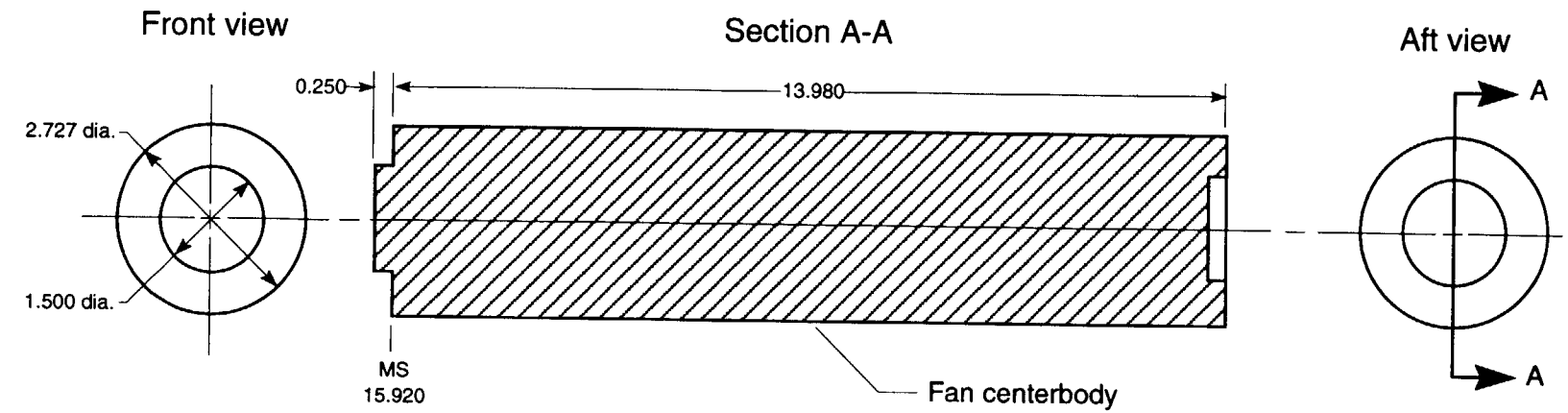

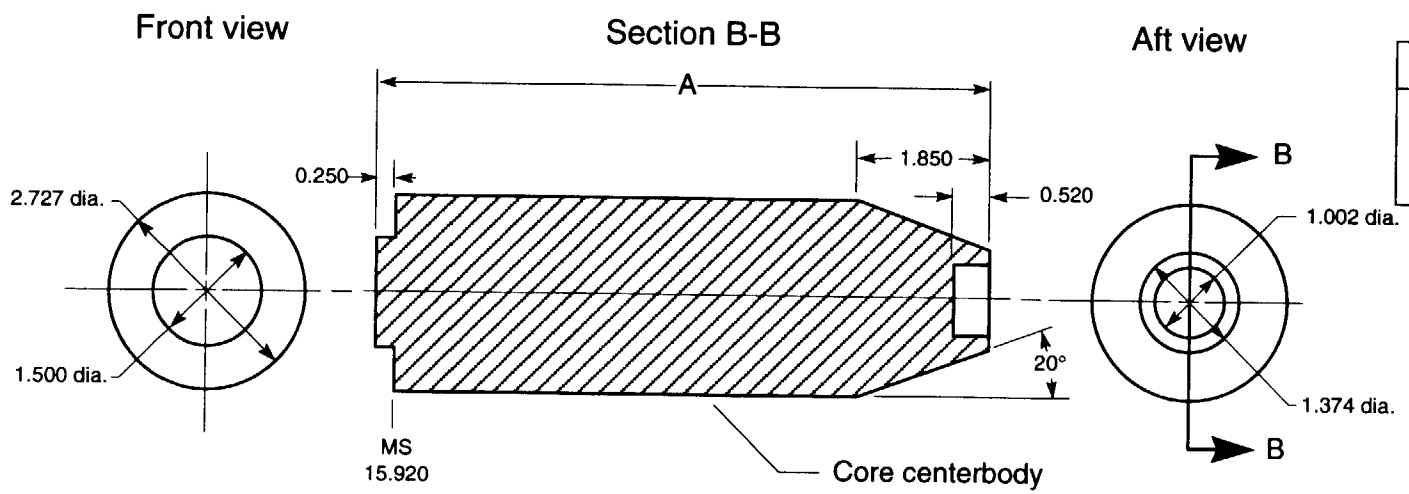

Centerbody	A
Short	6.729
Medium	8.224
Long	9.719

(a) Fan and core centerbody geometry.

Figure 10. Details of centerbody hardware. All dimensions are in inches unless otherwise noted.

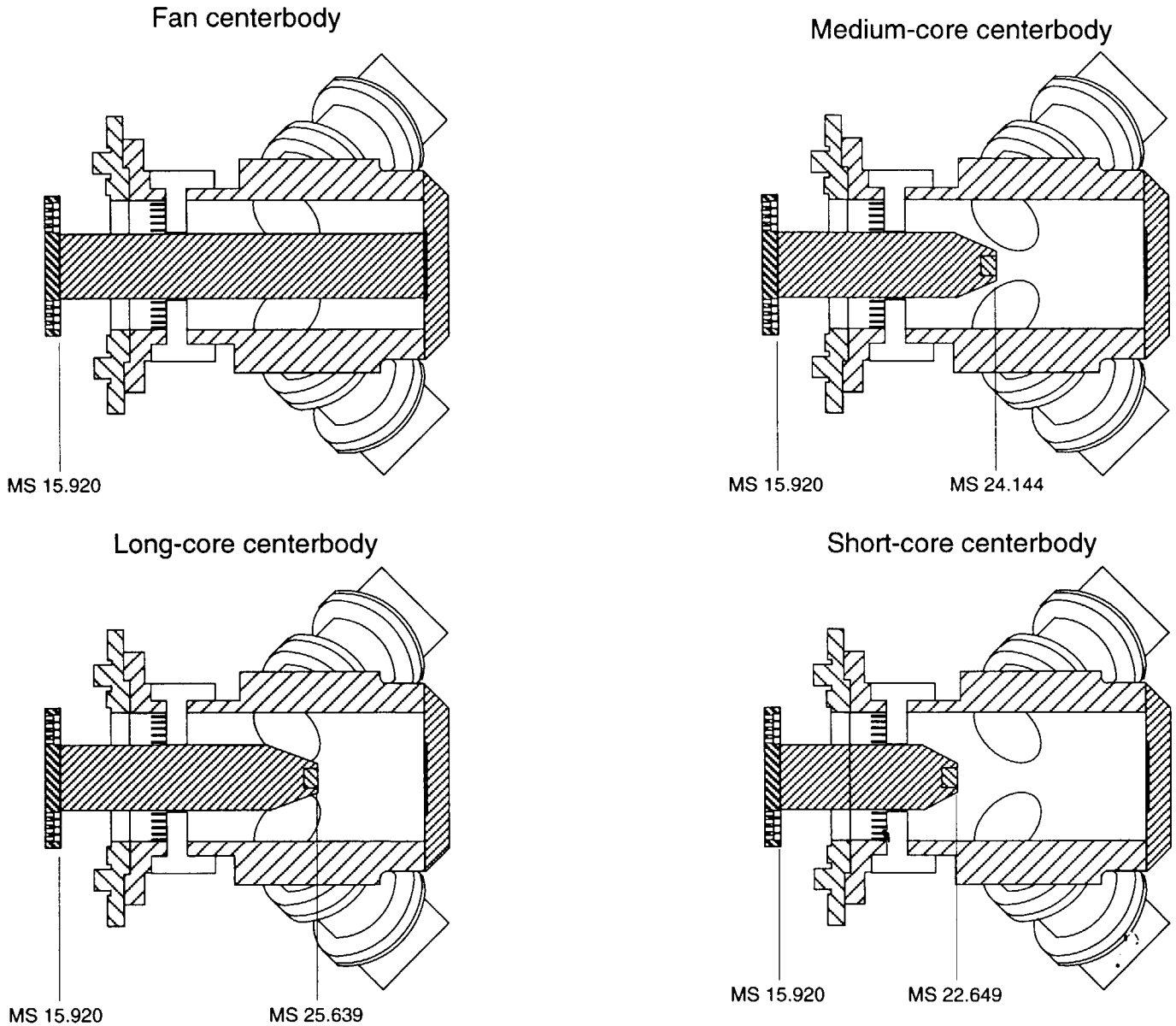

(b) Typical centerbody installations in offset plenum.

Figure 10. Concluded.

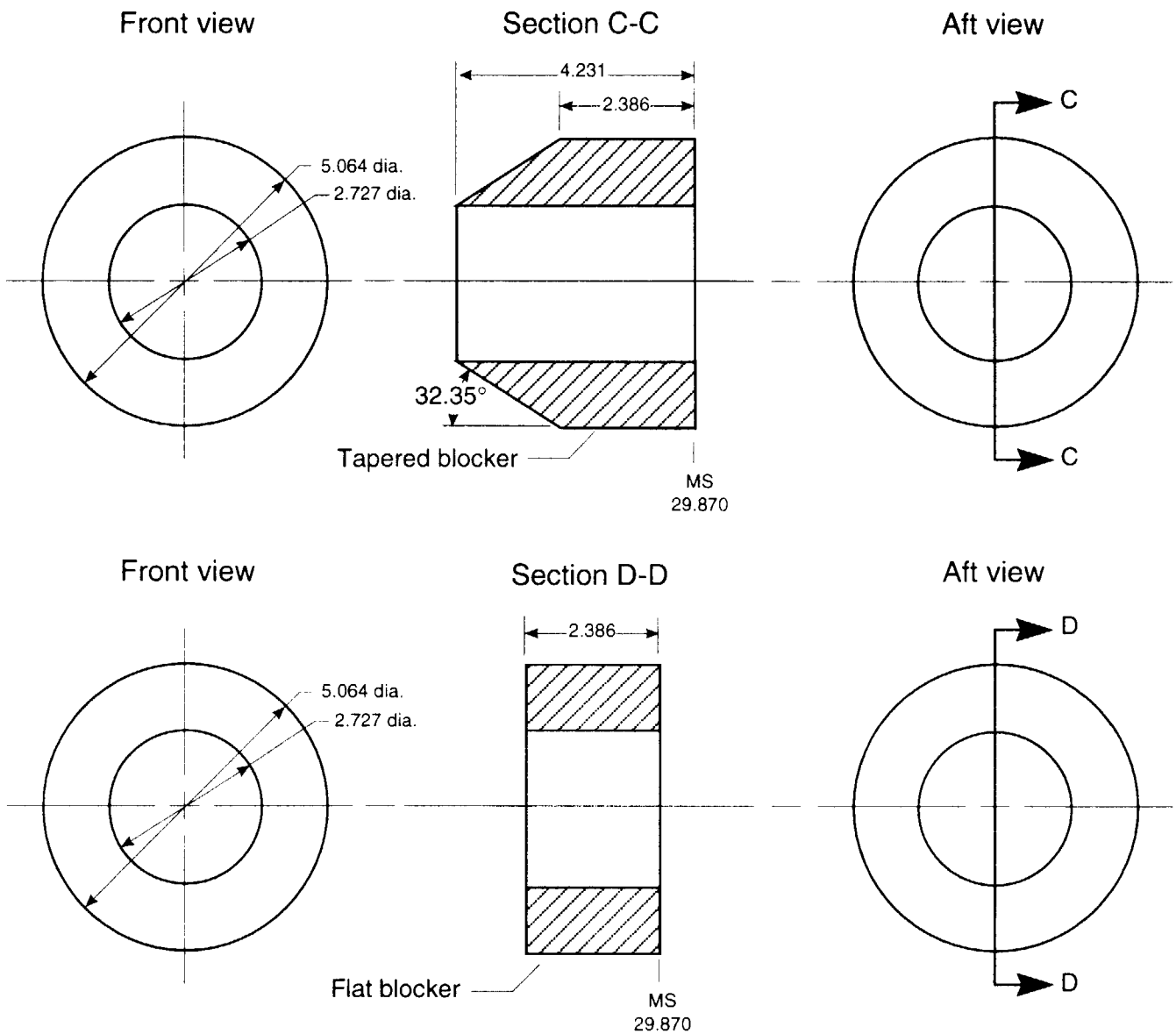

(a) Fan blocker geometry.

Figure 11. Details of fan and core blocker hardware. All dimensions are in inches unless otherwise noted.

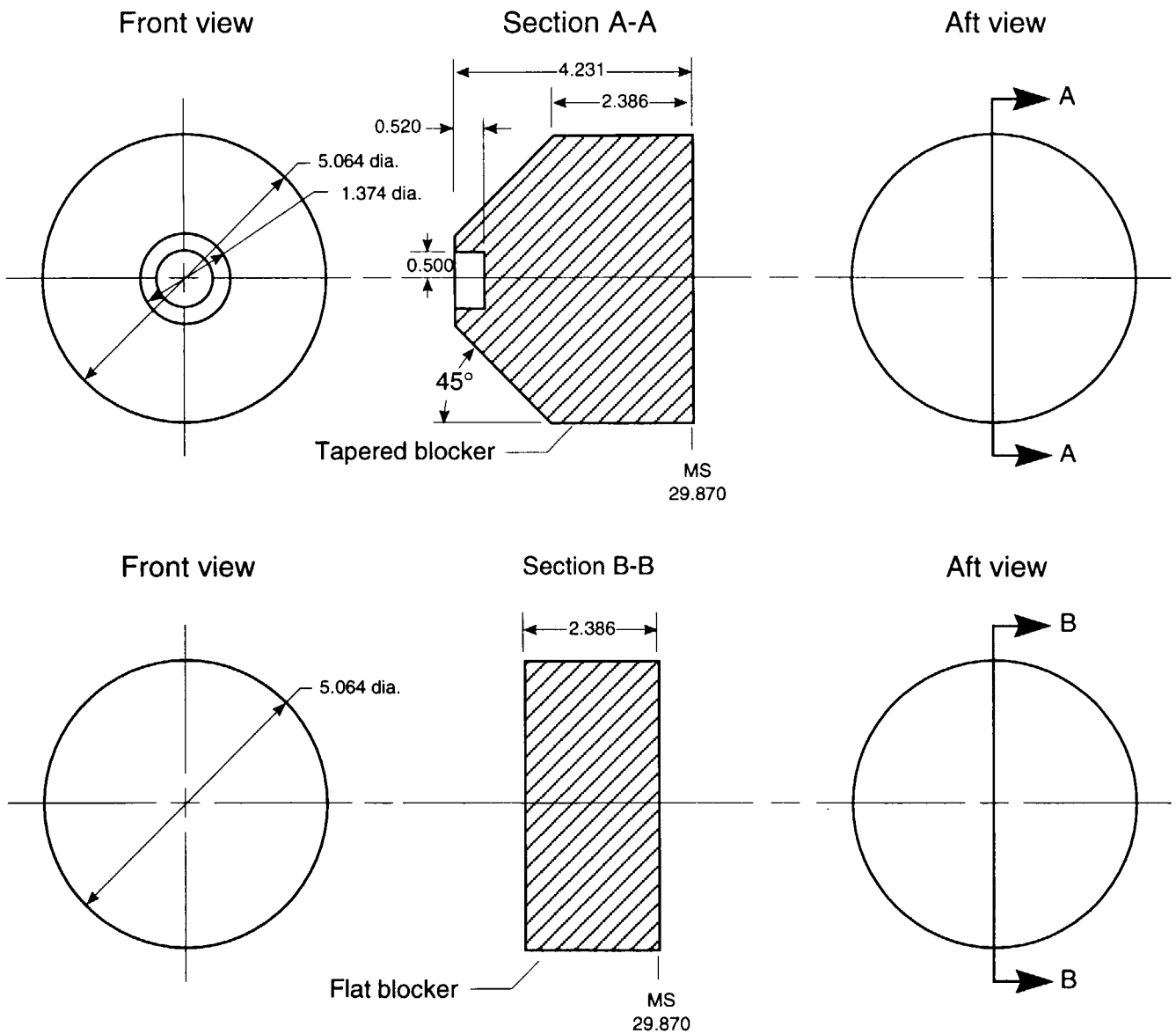

(b) Core blocker geometry.

Figure 11. Continued.

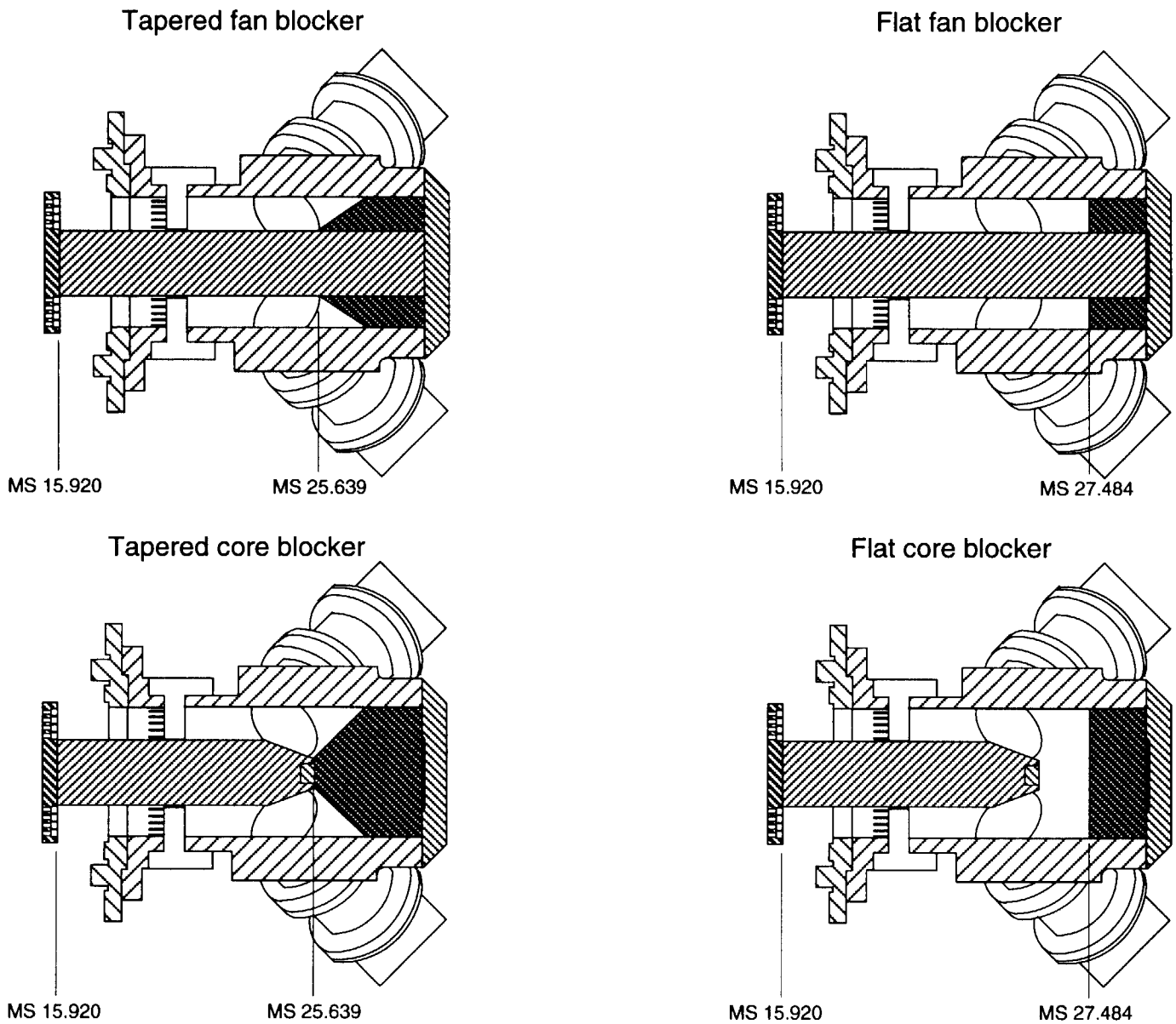

(c) Typical blocker installations in offset plenum.

Figure 11. Concluded.

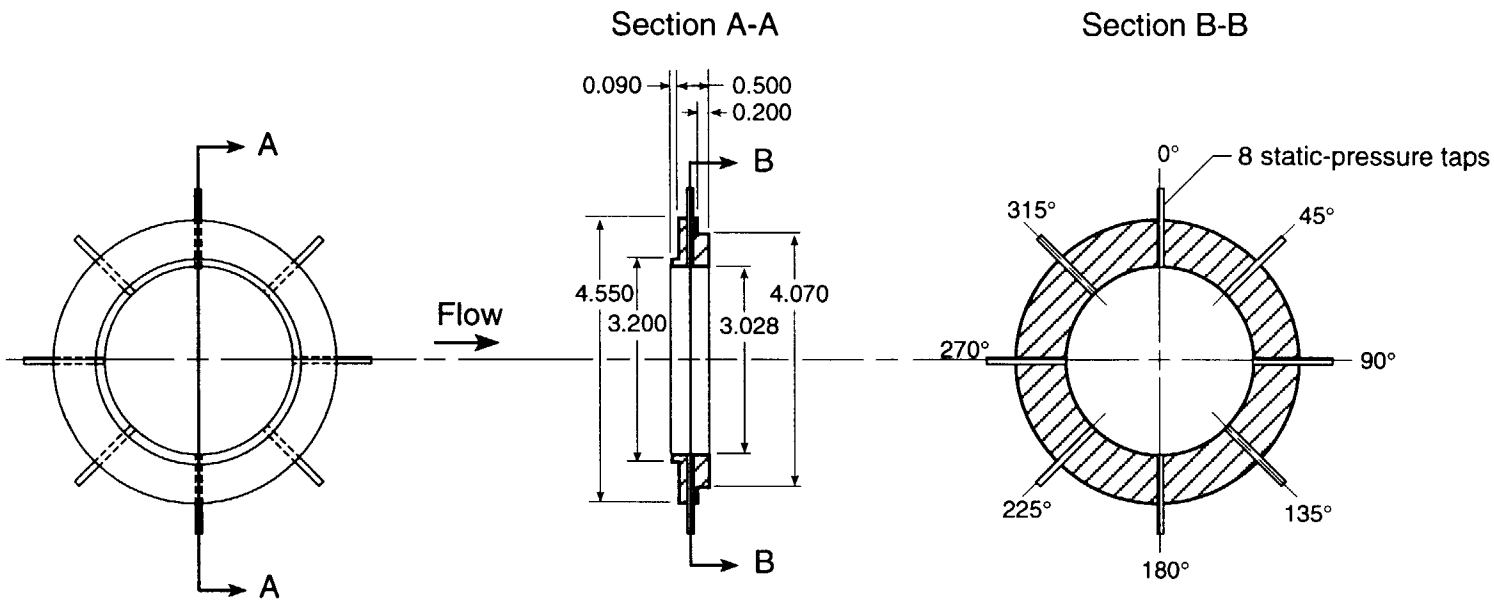

(a) Instrumented spacer ring.

Figure 12. Details of instrumented sleeves and instrumented spacer rings. All dimensions are in inches unless otherwise noted.

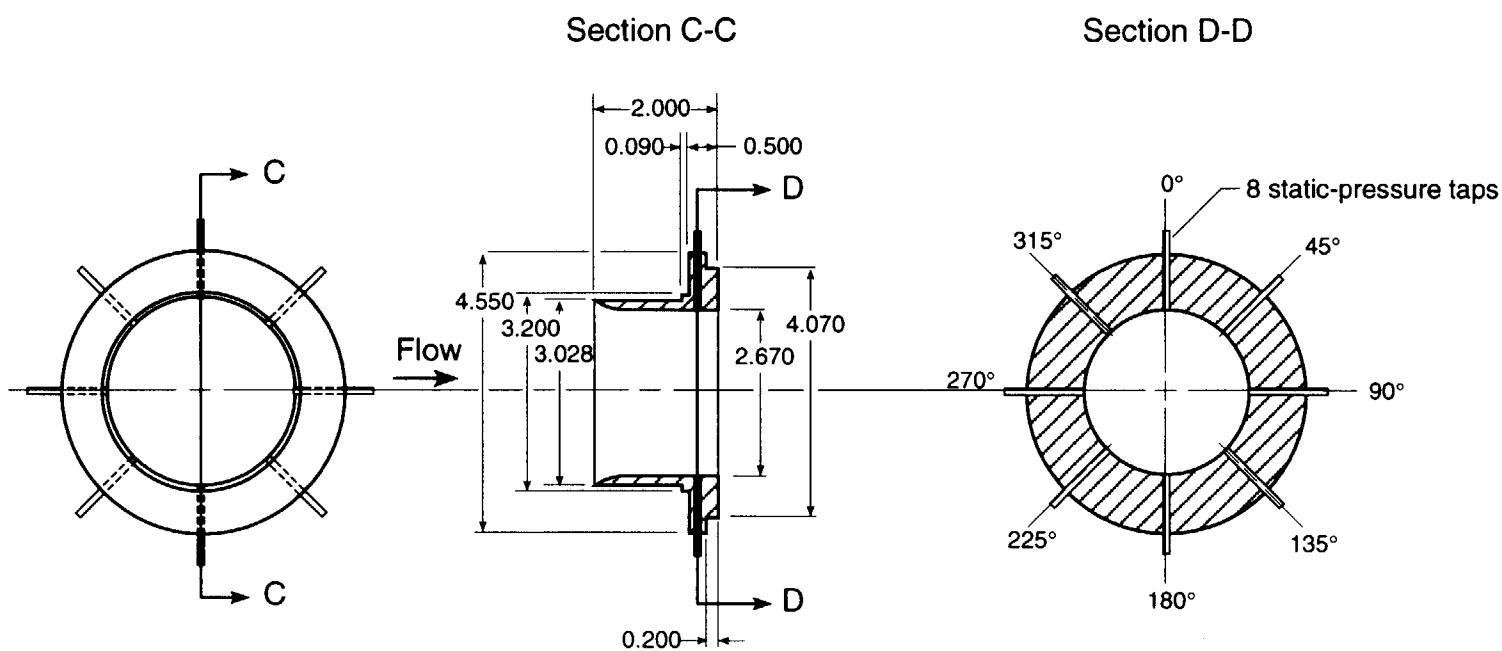

(b) Instrumented sleeve.

Figure 12. Concluded.

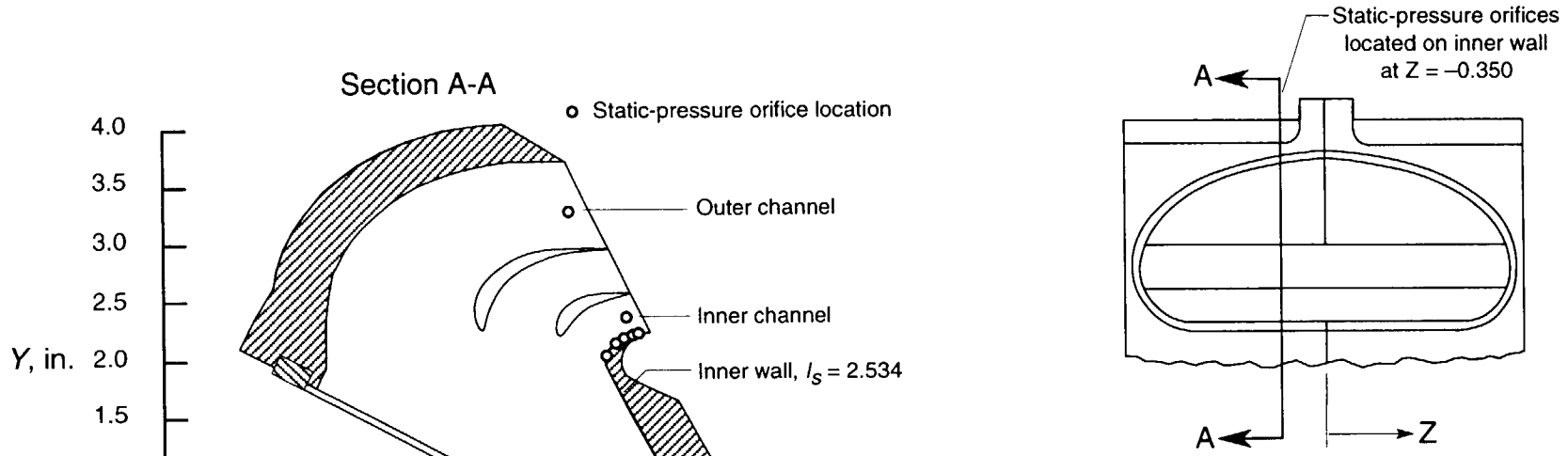

	Static-pressure orifice locations						
	X	Y	s/l_s	X	Y	s/l_s	
Inner wall	-0.267	1.103	0.429				
	-0.635	2.026	0.858				
	-0.560	2.140	0.913				
	-0.509	2.174	0.937				
	-0.465	2.194	0.956				
	-0.426	2.205	0.972				
Inner channel	-0.447	2.306	0.972	-0.880	3.273	0.972	Outer channel

(a) The 1.8 CR D-shaped nozzle.

Figure 13. Details of HIDEN nozzle instrumentation. All dimensions are in inches unless otherwise noted.

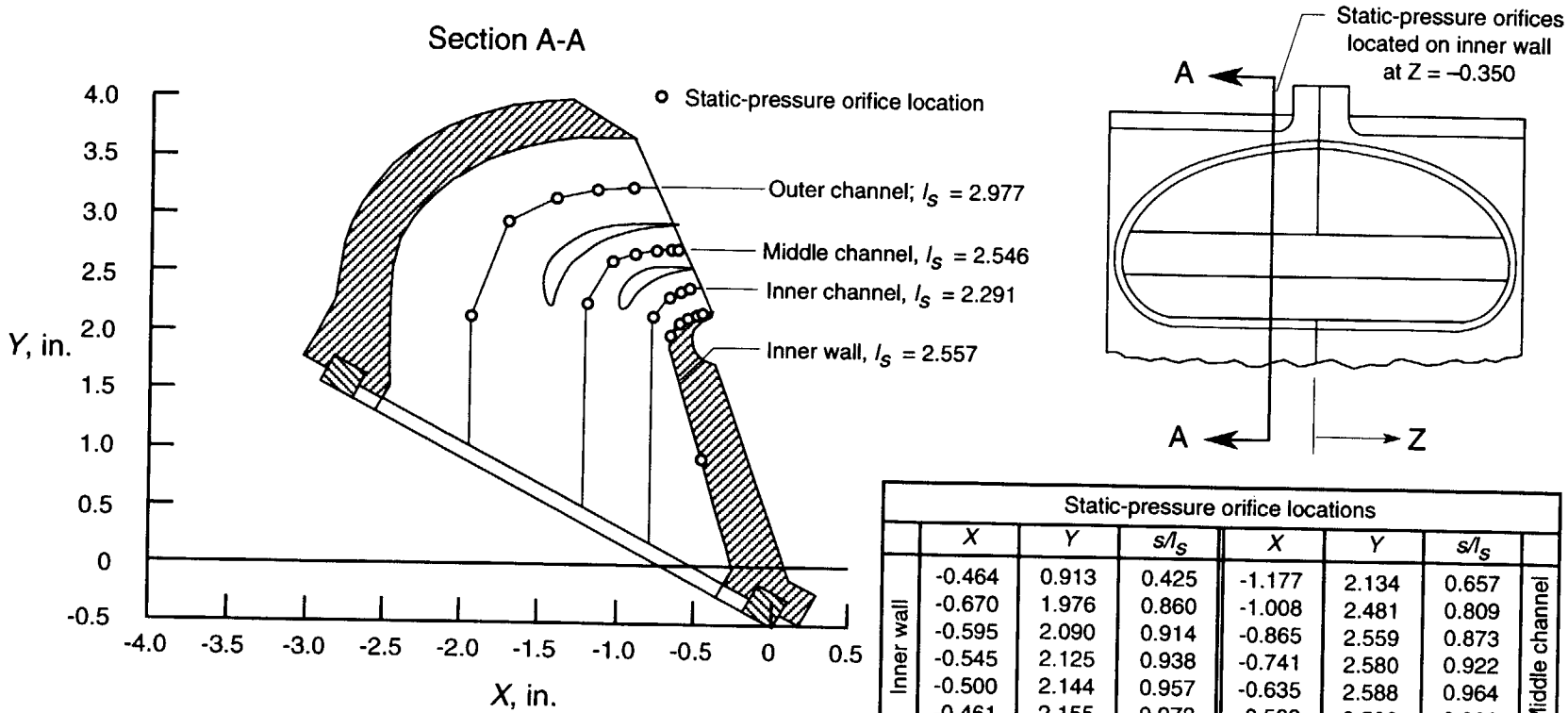

	Static-pressure orifice locations						
	X	Y	s/l_s	X	Y	s/l_s	
Inner wall	-0.464	0.913	0.425	-1.177	2.134	0.657	Middle channel
	-0.670	1.976	0.860	-1.008	2.481	0.809	
	-0.595	2.090	0.914	-0.865	2.559	0.873	
	-0.545	2.125	0.938	-0.741	2.580	0.922	
	-0.500	2.144	0.957	-0.635	2.588	0.964	
	-0.461	2.155	0.973	-0.589	2.588	0.982	
Inner channel	-0.781	2.009	0.798	-1.952	2.133	0.378	Outer channel
	-0.667	2.175	0.886	-1.713	2.937	0.659	
	-0.596	2.221	0.923	-1.416	3.137	0.780	
	-0.536	2.245	0.951	-1.148	3.209	0.873	
				-0.915	3.223	0.951	

(b) The 1.4 CR D-shaped nozzle.

Figure 13. Continued.

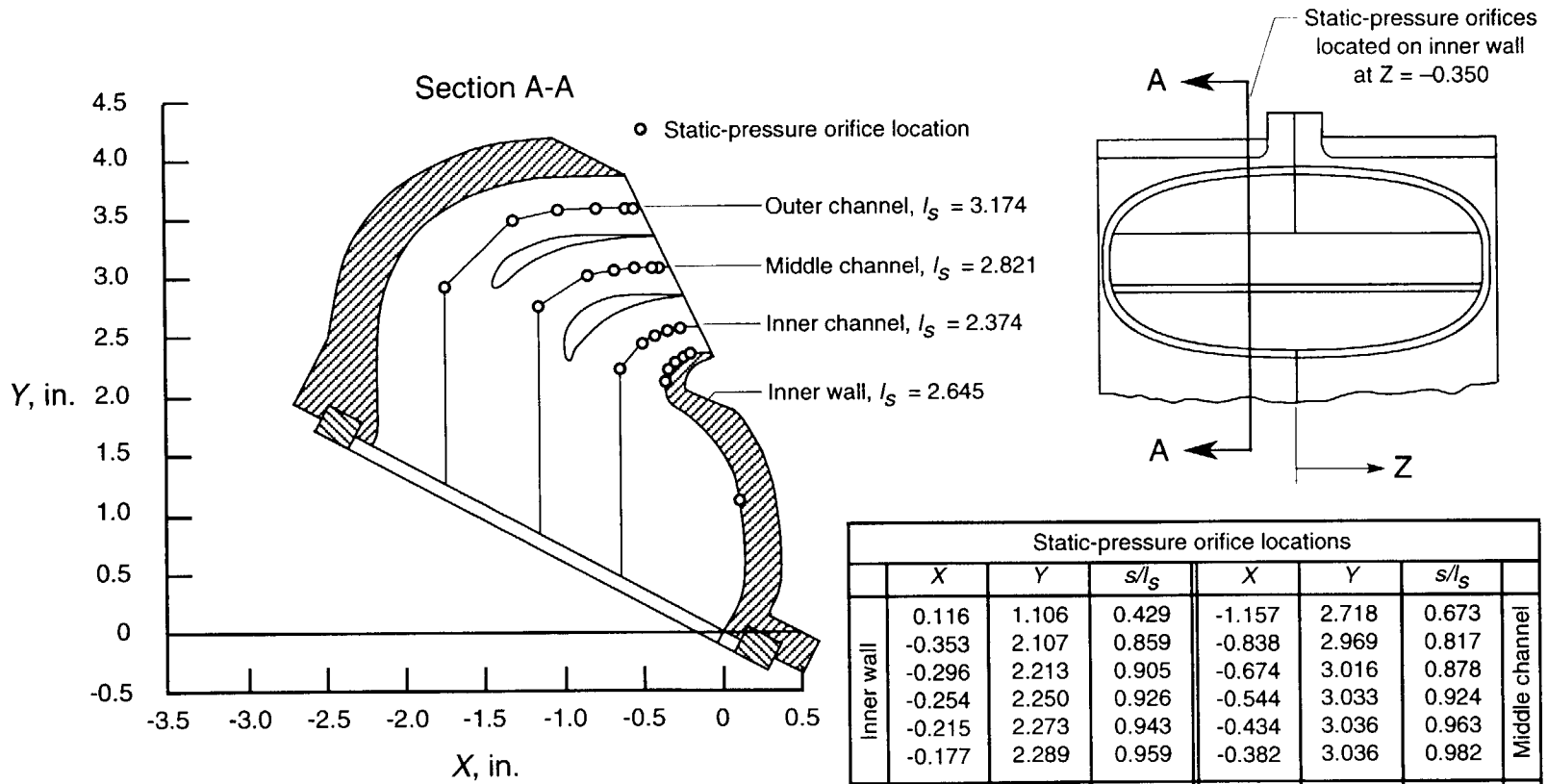

Static-pressure orifice locations							
	X	Y	s/l_s	X	Y	s/l_s	
Inner wall	0.116	1.106	0.429	-1.157	2.718	0.673	Middle channel
	-0.353	2.107	0.859	-0.838	2.969	0.817	
	-0.296	2.213	0.905	-0.674	3.016	0.878	
	-0.254	2.250	0.926	-0.544	3.033	0.924	
	-0.215	2.273	0.943	-0.434	3.036	0.963	
	-0.177	2.289	0.959	-0.382	3.036	0.982	
Inner channel	-0.644	2.172	0.723	-1.741	2.896	0.524	Outer channel
	-0.502	2.403	0.837	-1.311	3.446	0.744	
	-0.410	2.470	0.885	-1.020	3.518	0.839	
	-0.331	2.507	0.922	-0.789	3.532	0.912	
	-0.259	2.525	0.953	-0.594	3.535	0.973	
				-0.552	3.535	0.986	

(c) The 1.4 CR Pegasus nozzle.

Figure 13. Continued.

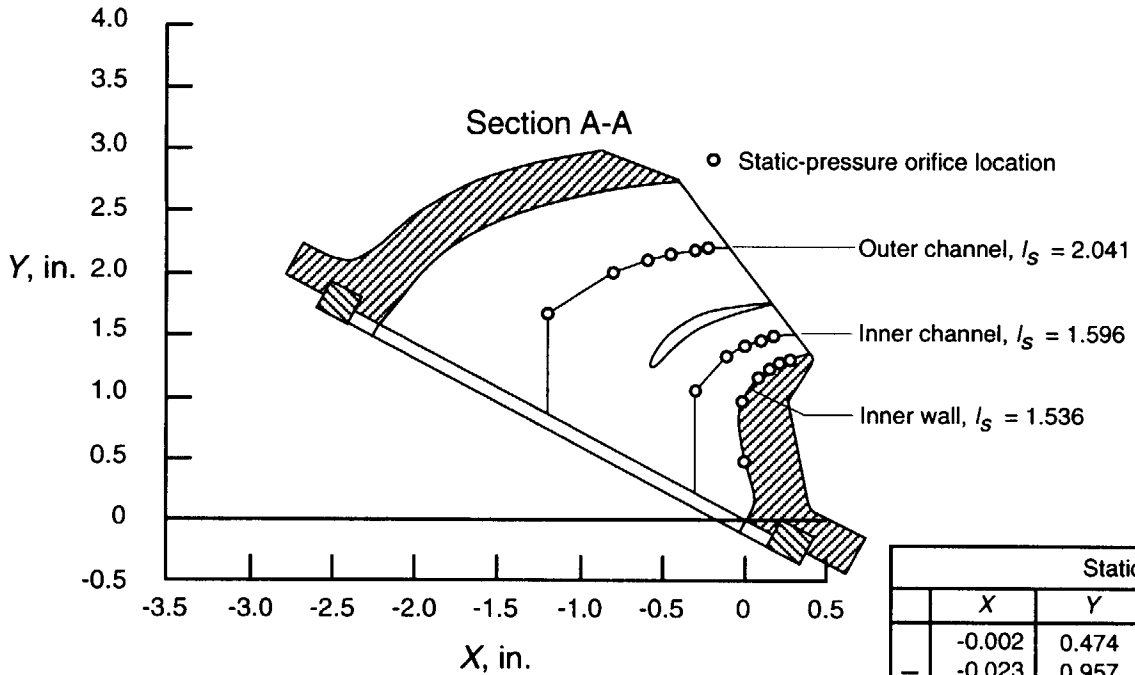

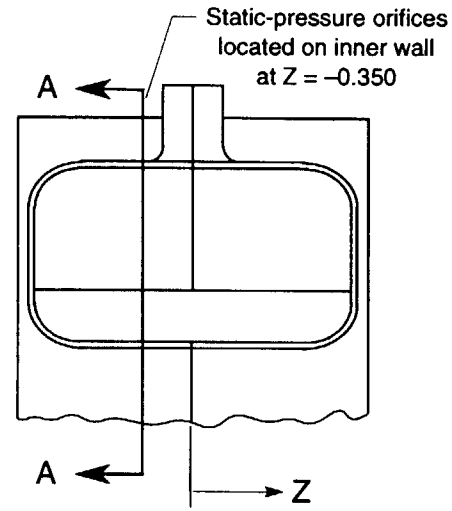

	Static-pressure orifice locations						
	X	Y	s/l_s	X	Y	s/l_s	
Inner wall	-0.002	0.474	0.318				
	-0.023	0.957	0.637				
	0.085	1.146	0.779				
	0.152	1.210	0.840				
	0.212	1.252	0.888				
	0.267	1.281	0.928				
Inner channel	-0.304	1.048	0.522	-1.202	1.671	0.402	Outer channel
	-0.114	1.321	0.730	-0.795	1.999	0.658	
	-0.003	1.404	0.817	-0.598	2.092	0.765	
	0.091	1.454	0.884	-0.442	2.148	0.846	
	0.174	1.487	0.940	-0.305	2.184	0.916	
				-0.225	2.202	0.956	

(d) The 1.4 CR submerged nozzle.

Figure 13. Concluded.

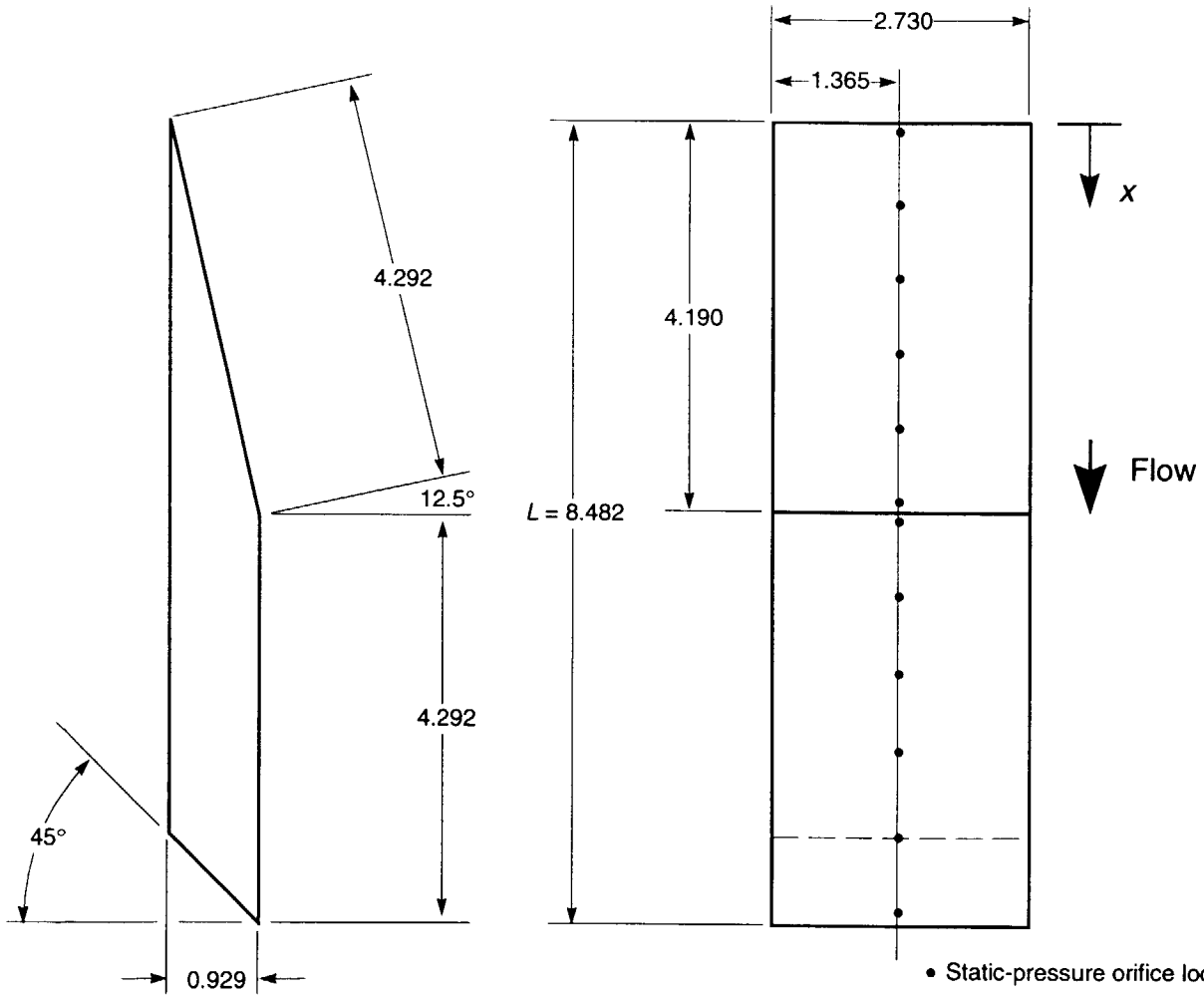

Static-pressure orifice location	
x, in.	x/L
0.098	0.012
0.897	0.106
1.696	0.200
2.495	0.294
3.294	0.388
5.110	0.602
5.928	0.699
6.746	0.795
7.564	0.892
8.382	0.988

Figure 14. Details of instrumented ramp. All dimensions are in inches unless otherwise noted.

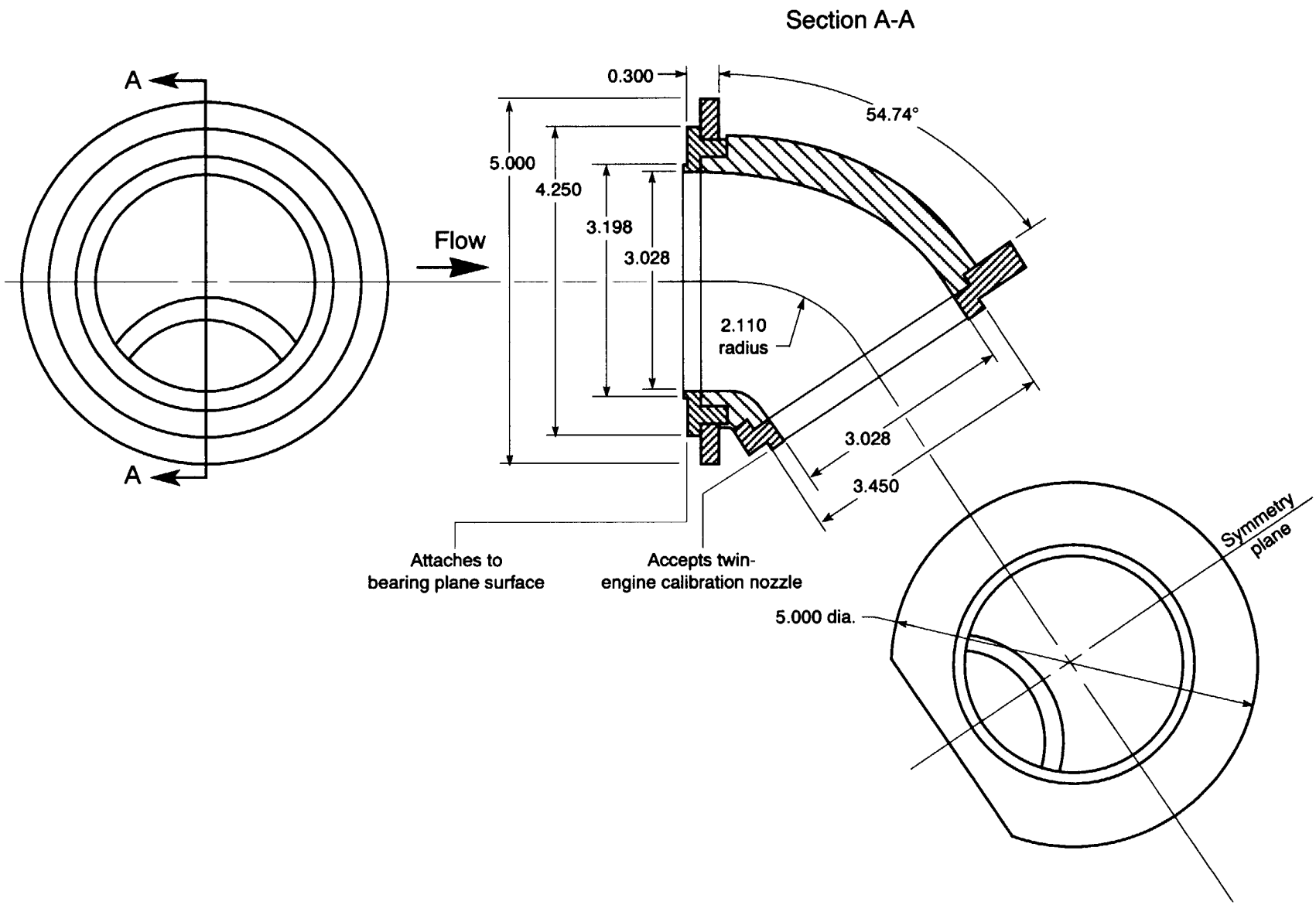

Figure 15. Details of calibration adapter assembly. All dimensions are in inches unless otherwise noted.

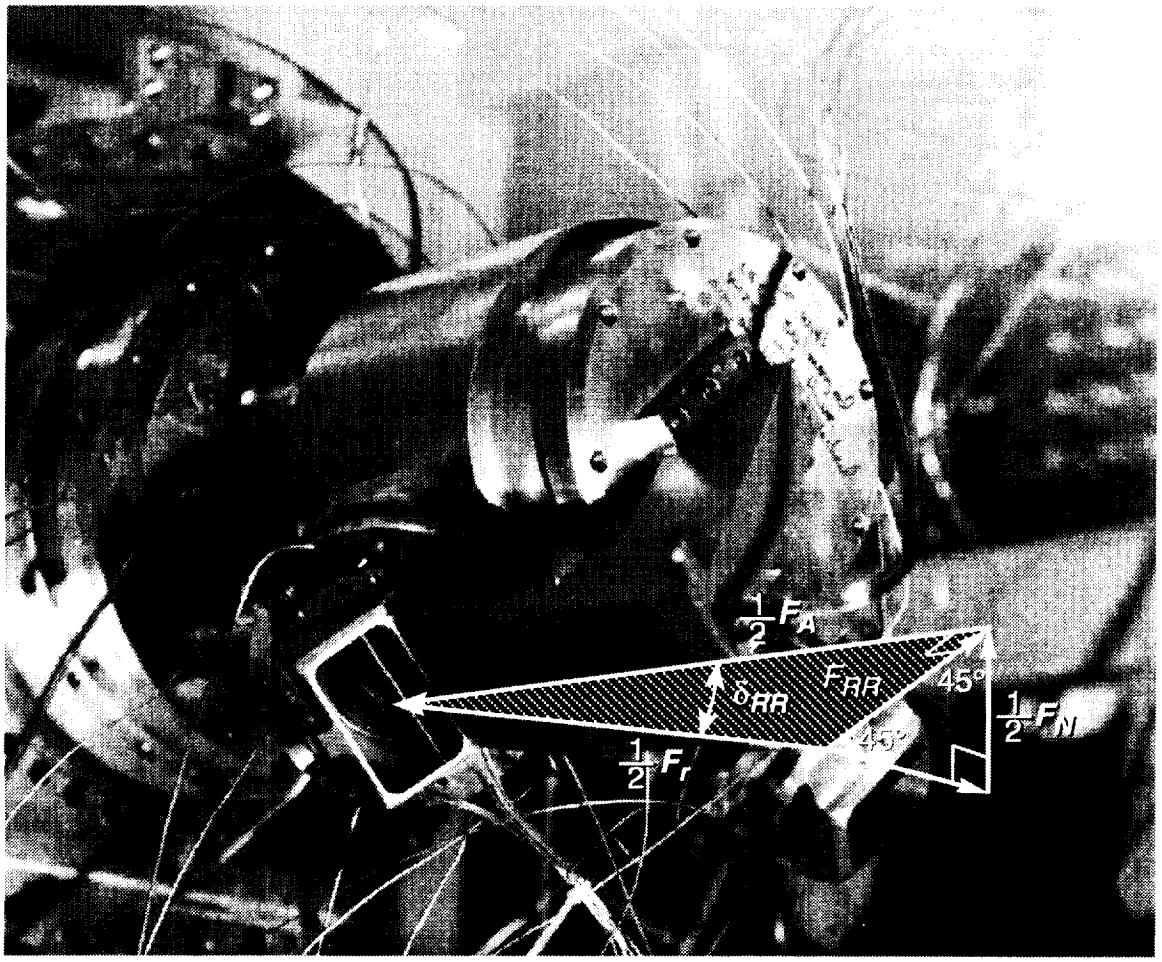

$$F_{RR} = \sqrt{\left(\frac{1}{2}F_N\right)^2 + \left(\frac{1}{2}F_N\right)^2} = \sqrt{\frac{1}{4}F_N^2 + \frac{1}{4}F_N^2} = \sqrt{\frac{1}{2}F_N^2} = \sqrt{\frac{1}{2}}F_N$$

$$\delta_{RR} = \tan^{-1}\left(\frac{F_{RR}}{\frac{1}{2}F_A}\right) = \tan^{-1}\left(\frac{\sqrt{\frac{1}{2}}F_N}{\frac{1}{2}F_A}\right) = \tan^{-1}\left(\frac{2\sqrt{\frac{1}{2}}F_N}{F_A}\right) = \tan^{-1}\left(\frac{\sqrt{2}F_N}{F_A}\right)$$

(a) The δ_{RR} in thrust mode.

Figure 16. Computed exhaust flow direction δ_{RR} in both thrust and lift modes.

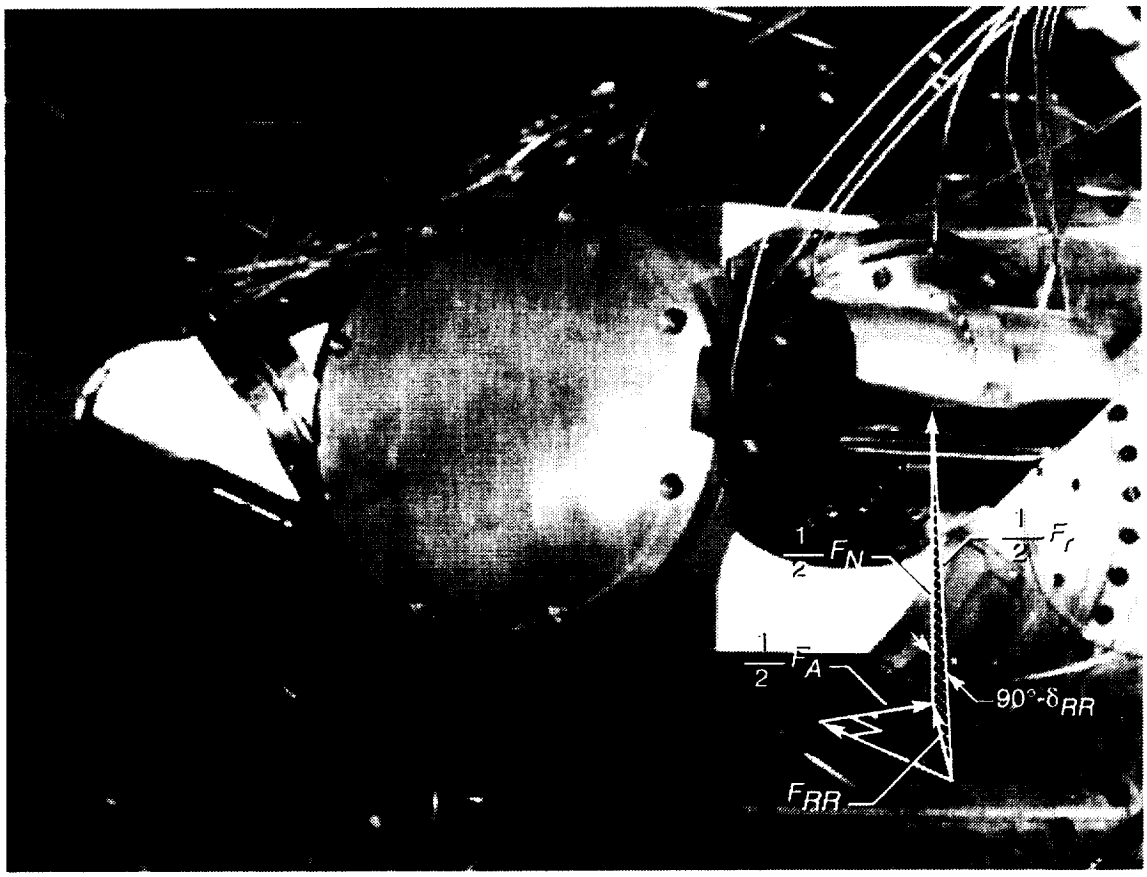

$$90° - \delta_{RR} = \tan^{-1}\left(\frac{F_{RR}}{\frac{1}{2}F_N}\right)$$

$$F_{RR} = \sqrt{\left(\frac{1}{2}F_A\right)^2 + \left(\frac{1}{2}F_A\right)^2} = \sqrt{\frac{1}{4}F_A^2 + \frac{1}{4}F_A^2} = \sqrt{\frac{1}{2}F_A^2} = \sqrt{\frac{1}{2}}F_A$$

$$\delta_{RR} = 90° - \tan^{-1}\left(\frac{F_{RR}}{\frac{1}{2}F_N}\right) = 90° - \tan^{-1}\left(\frac{\sqrt{\frac{1}{2}}F_A}{\frac{1}{2}F_N}\right) = 90° - \tan^{-1}\left(\frac{2\sqrt{\frac{1}{2}}F_A}{F_N}\right) = 90° - \tan^{-1}\left(\frac{\sqrt{2}F_A}{F_N}\right)$$

(b) The δ_{RR} in lift mode.

Figure 16. Concluded.

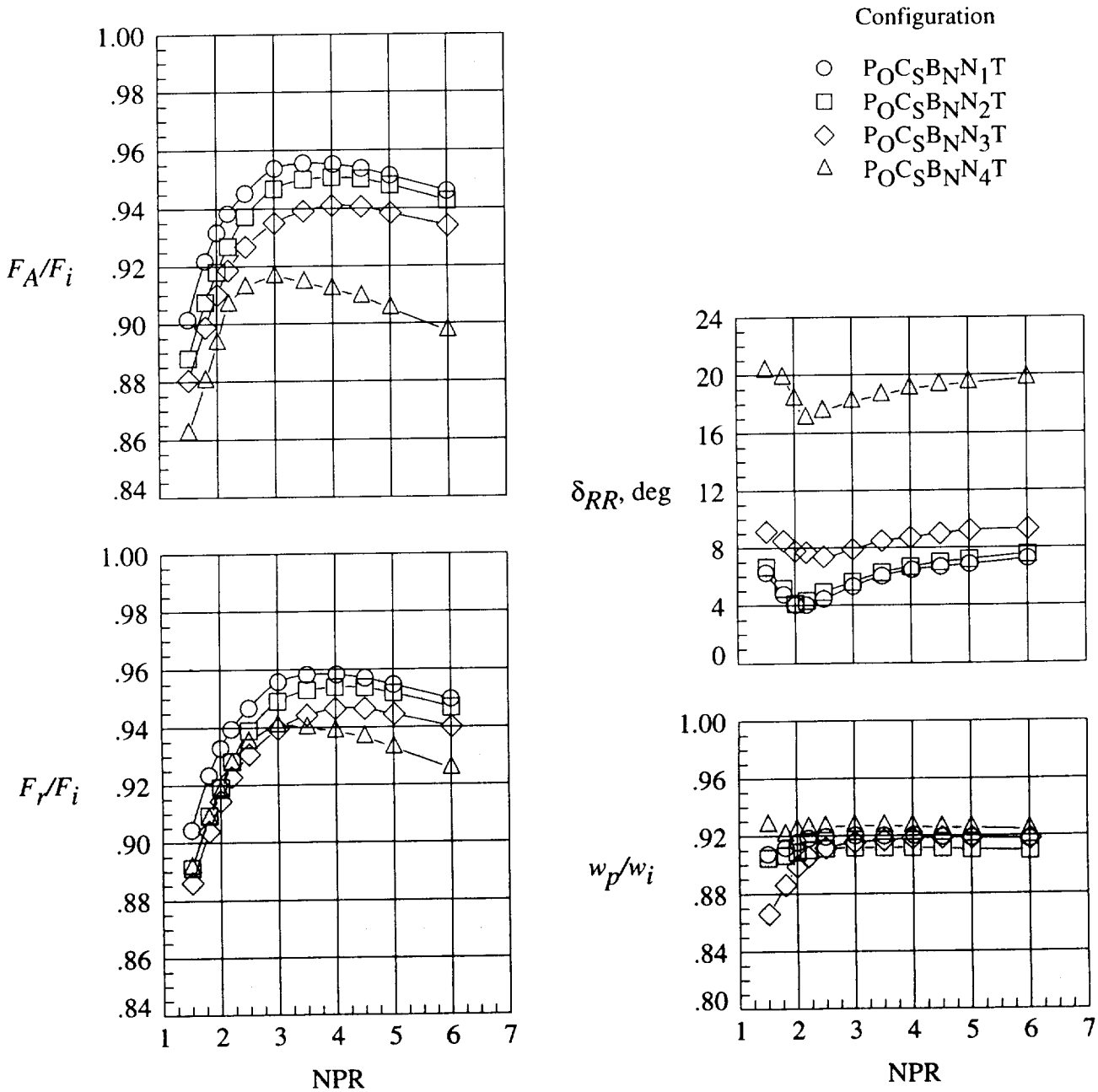

Figure 17. Internal performance characteristics of HIDEN nozzles in thrust mode installed on offset plenum with short-core centerbody and no blocker.

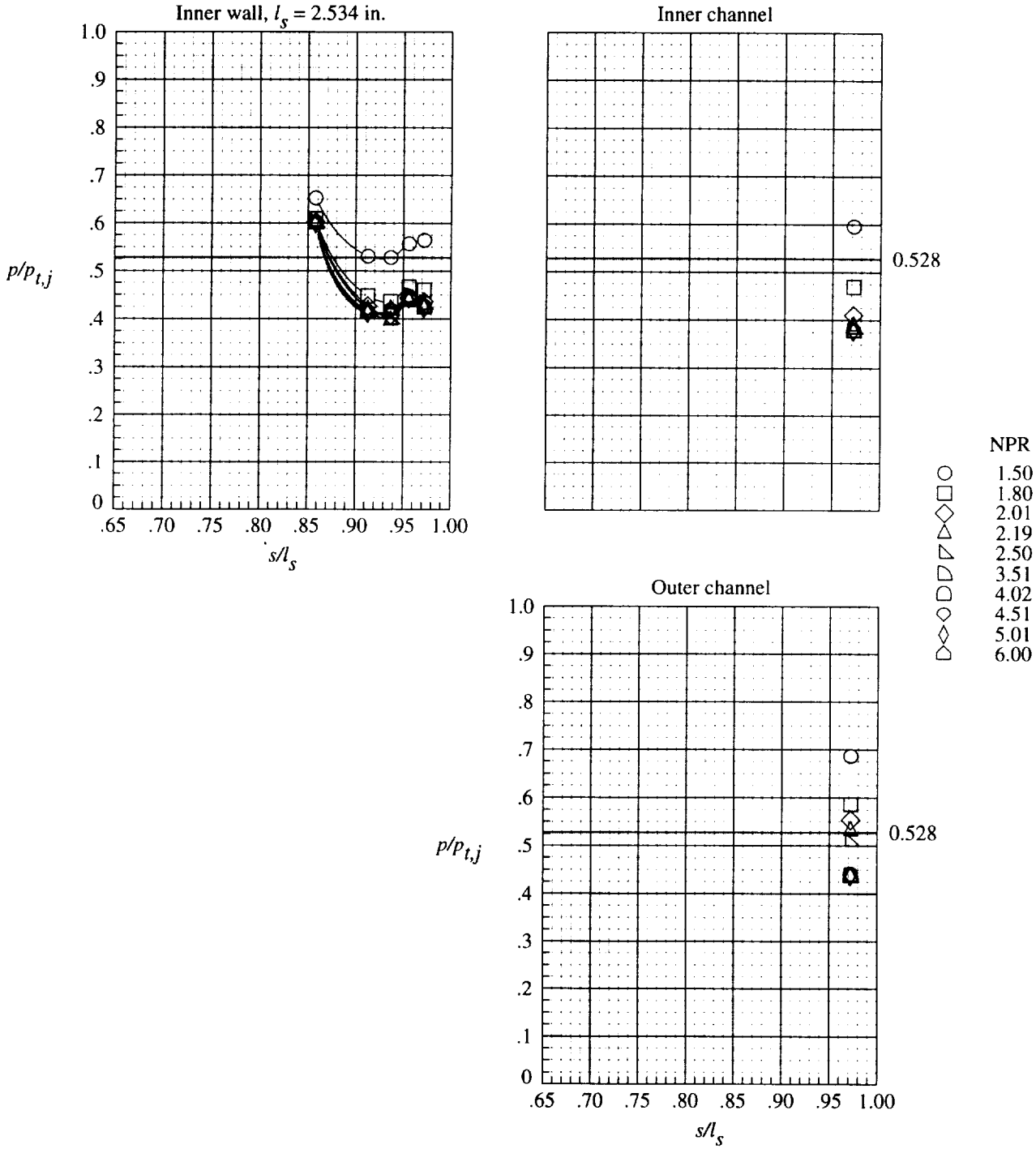

(a) The 1.8 CR D-shaped nozzles.

Figure 18. Internal static-pressure distributions $p/p_{t,j}$ of HIDEN nozzles in thrust mode installed on offset plenum with short-core centerbody and no blocker.

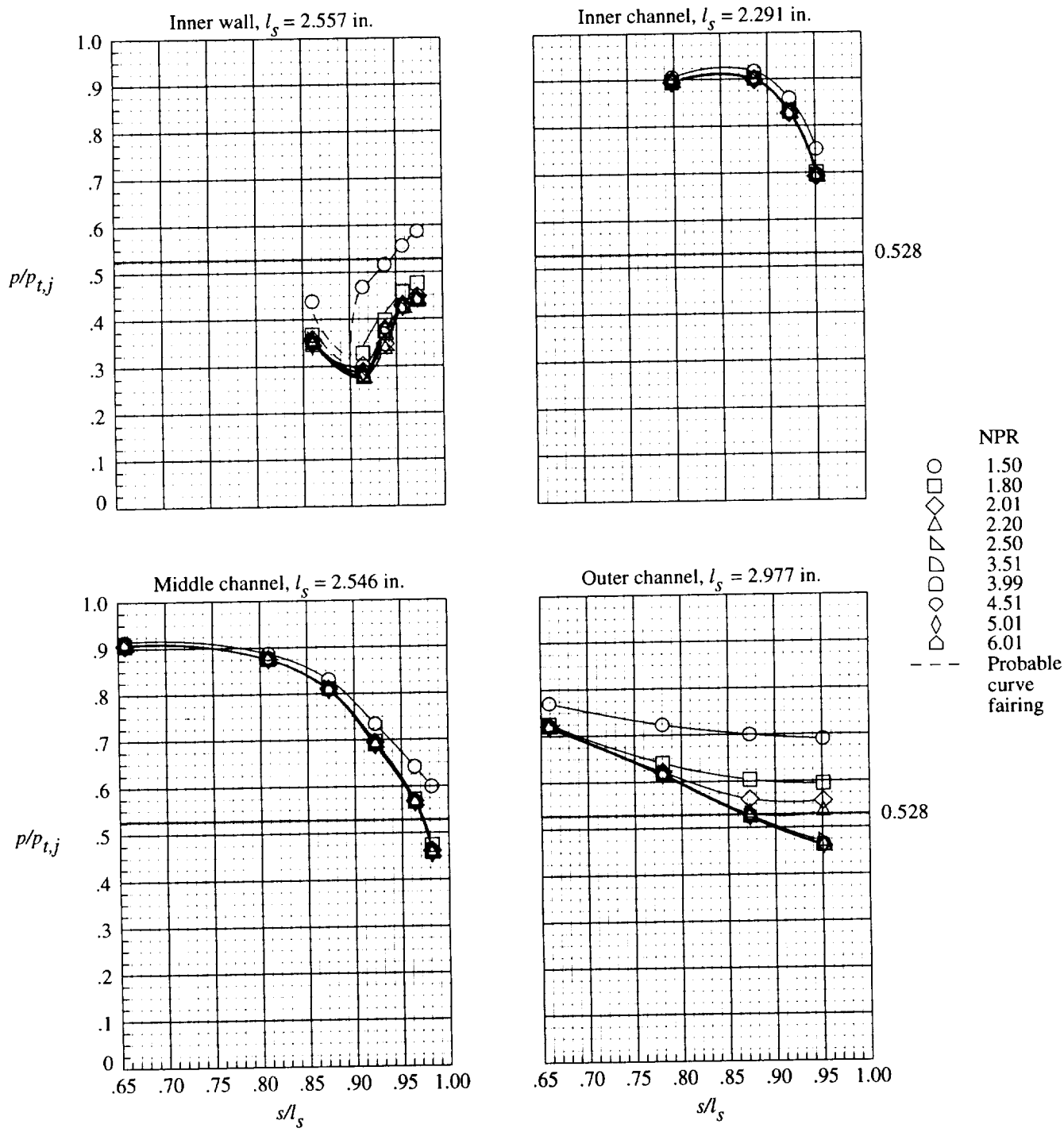

(b) The 1.4 CR D-shaped nozzles.

Figure 18. Continued.

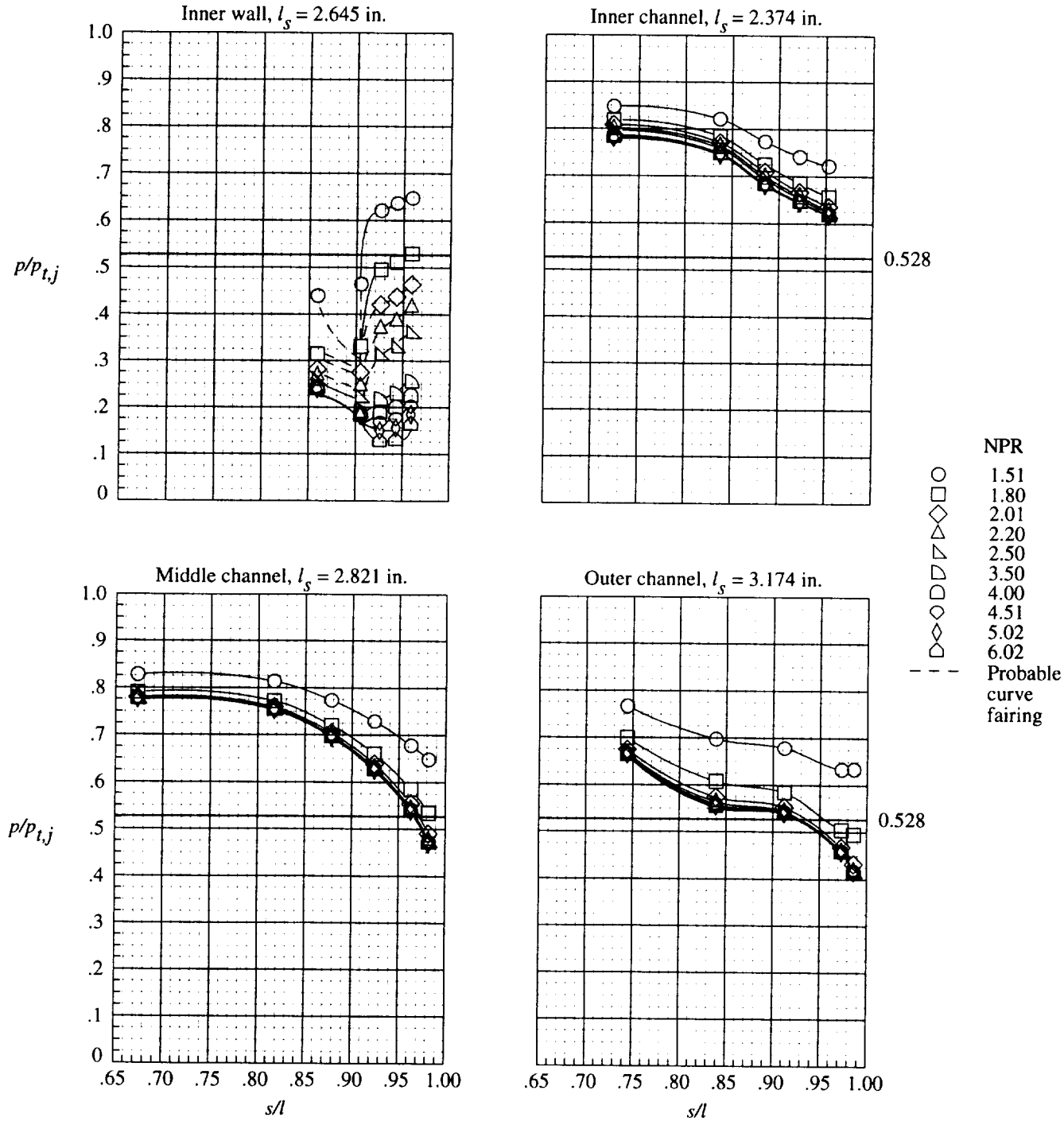

(c) The 1.4 CR Pegasus nozzles.

Figure 18. Continued.

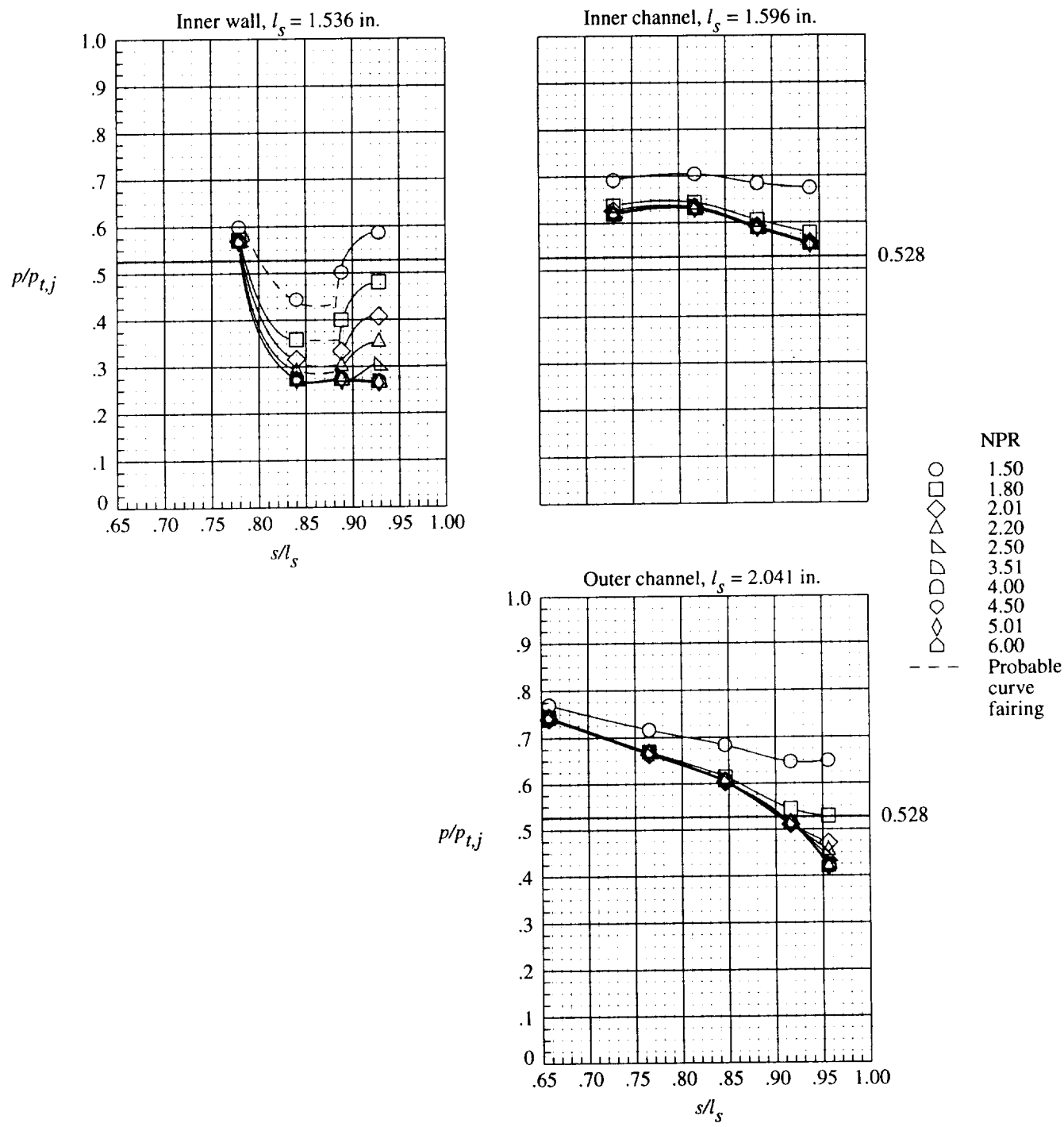

(d) The 1.4 CR submerged nozzles.

Figure 18. Concluded.

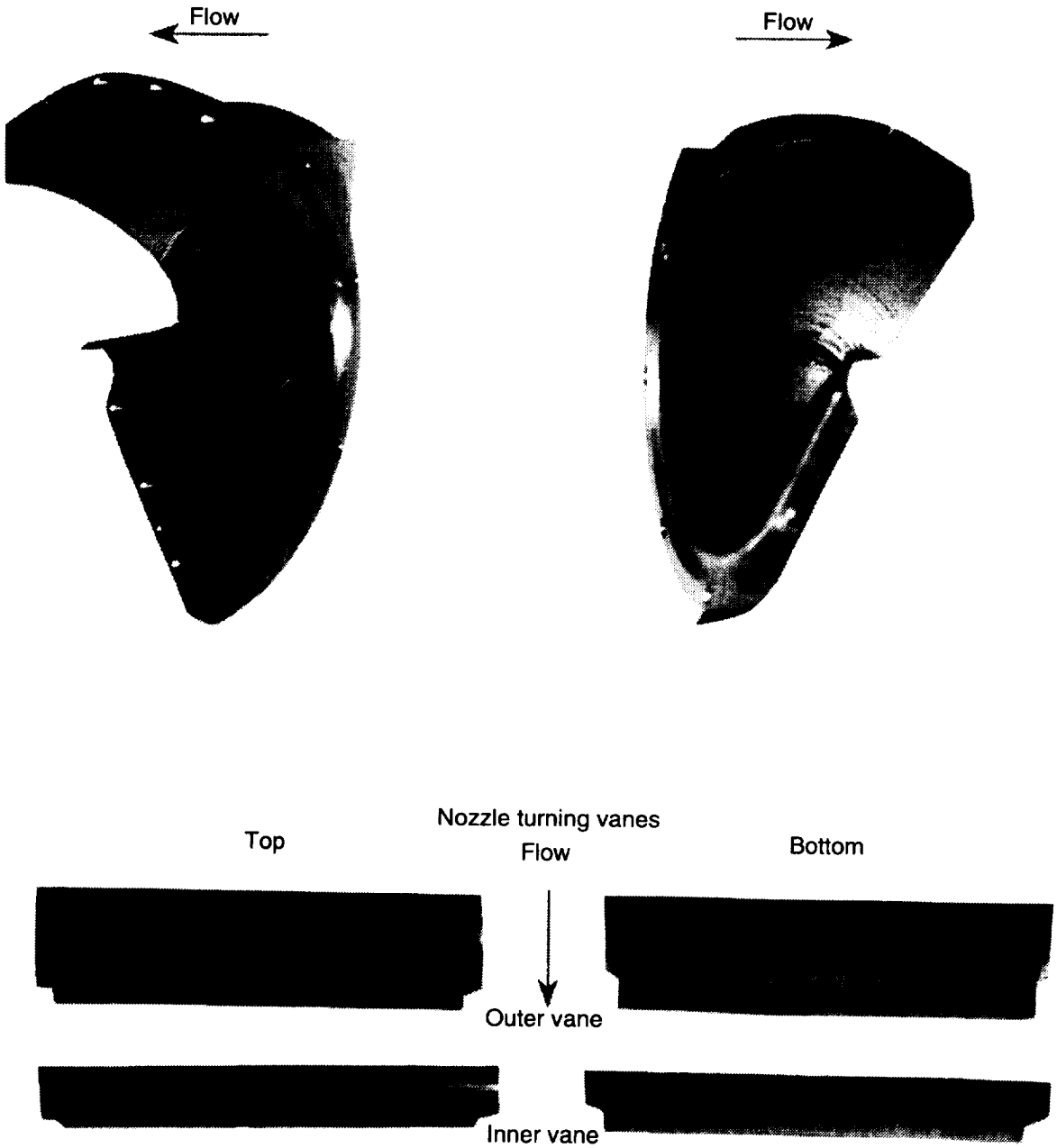

(a) The 1.8 CR D-shaped nozzle.

Figure 19. Flow visualization inside HIDEN nozzles in thrust mode installed on offset plenum with short-core center-body and no blocker. Nominal NPR = 4.0.

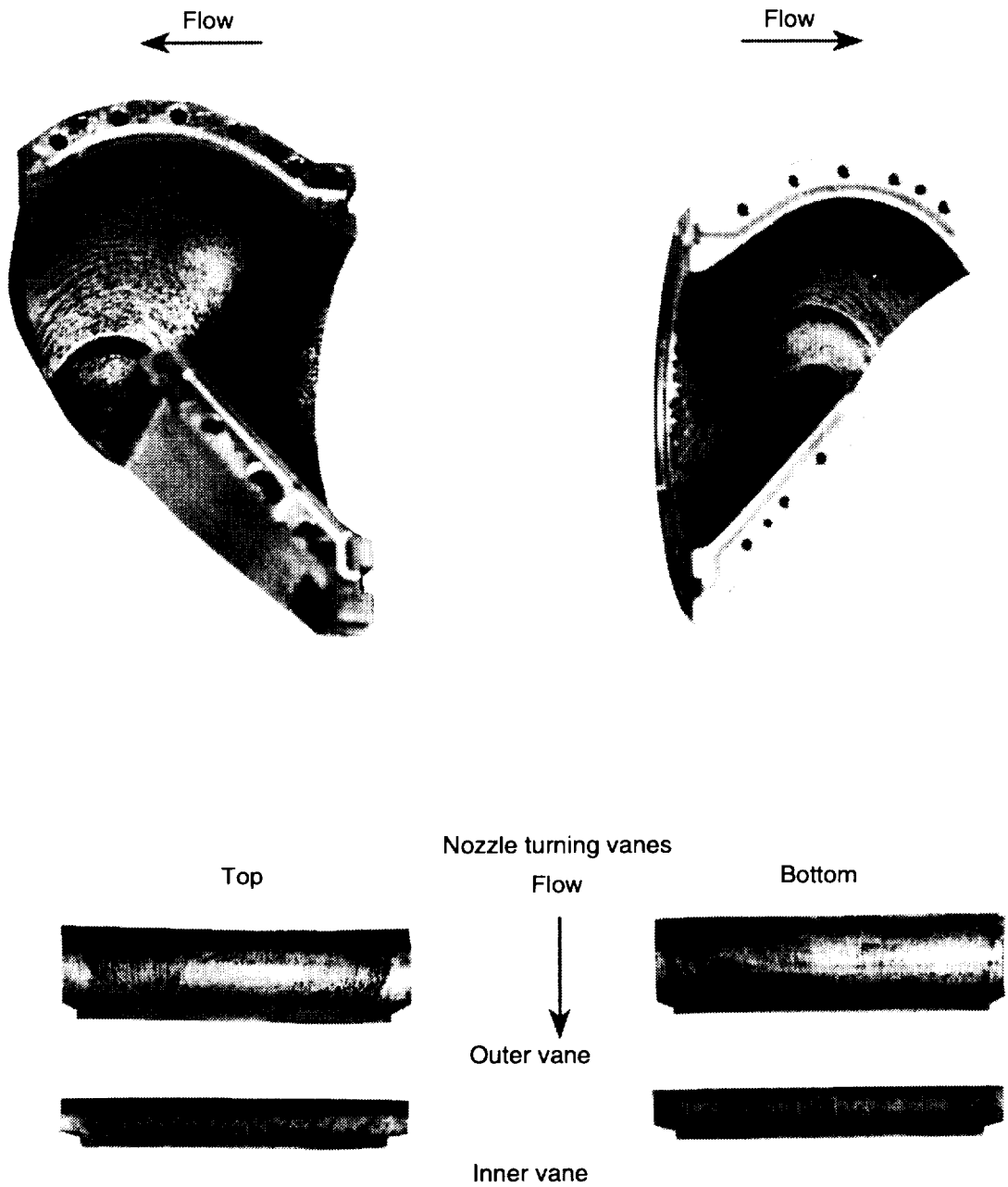

(b) The 1.4 CR D-shaped nozzle.

Figure 19. Continued.

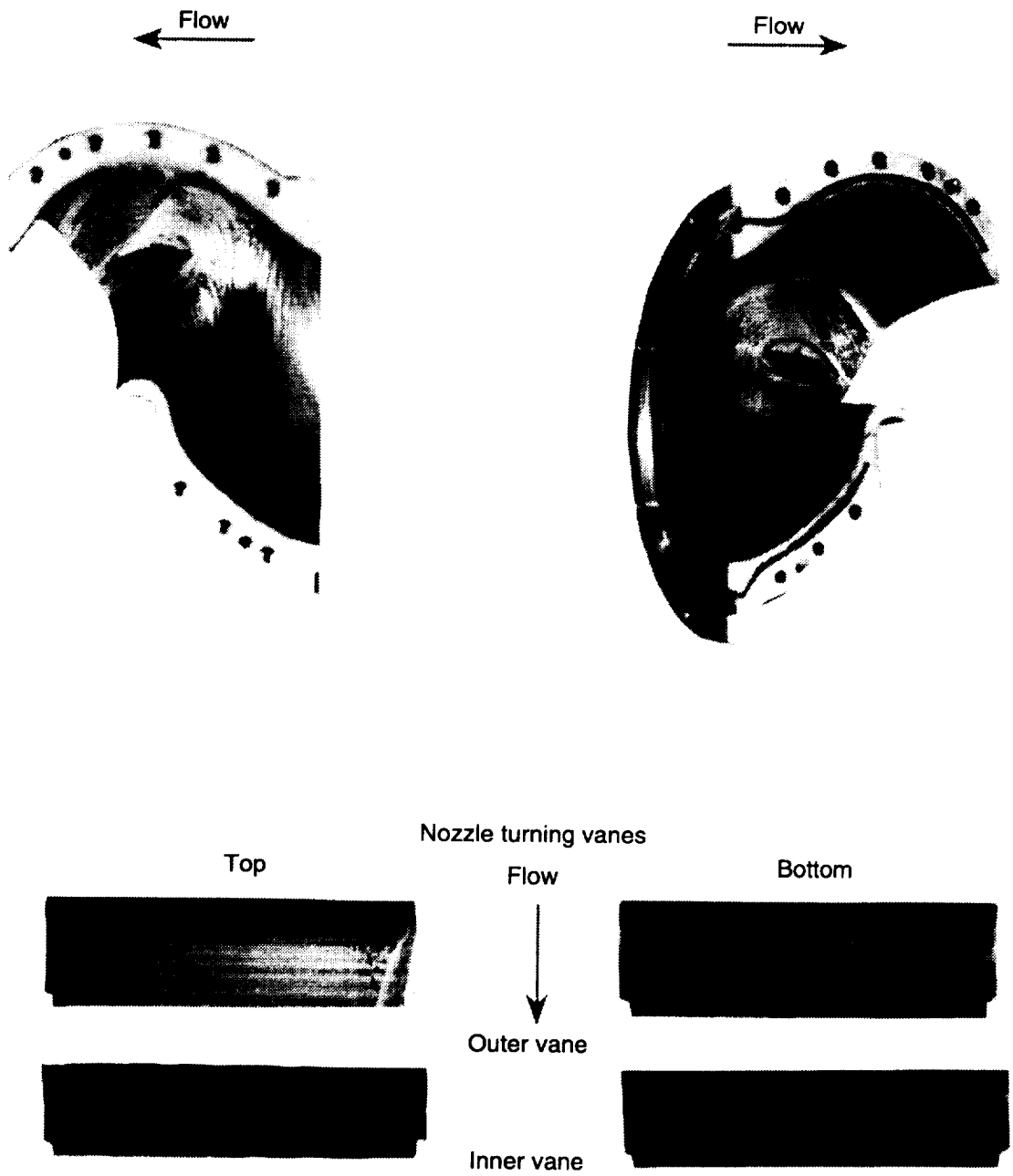

(c) The 1.4 CR Pegasus nozzle.

Figure 19. Continued.

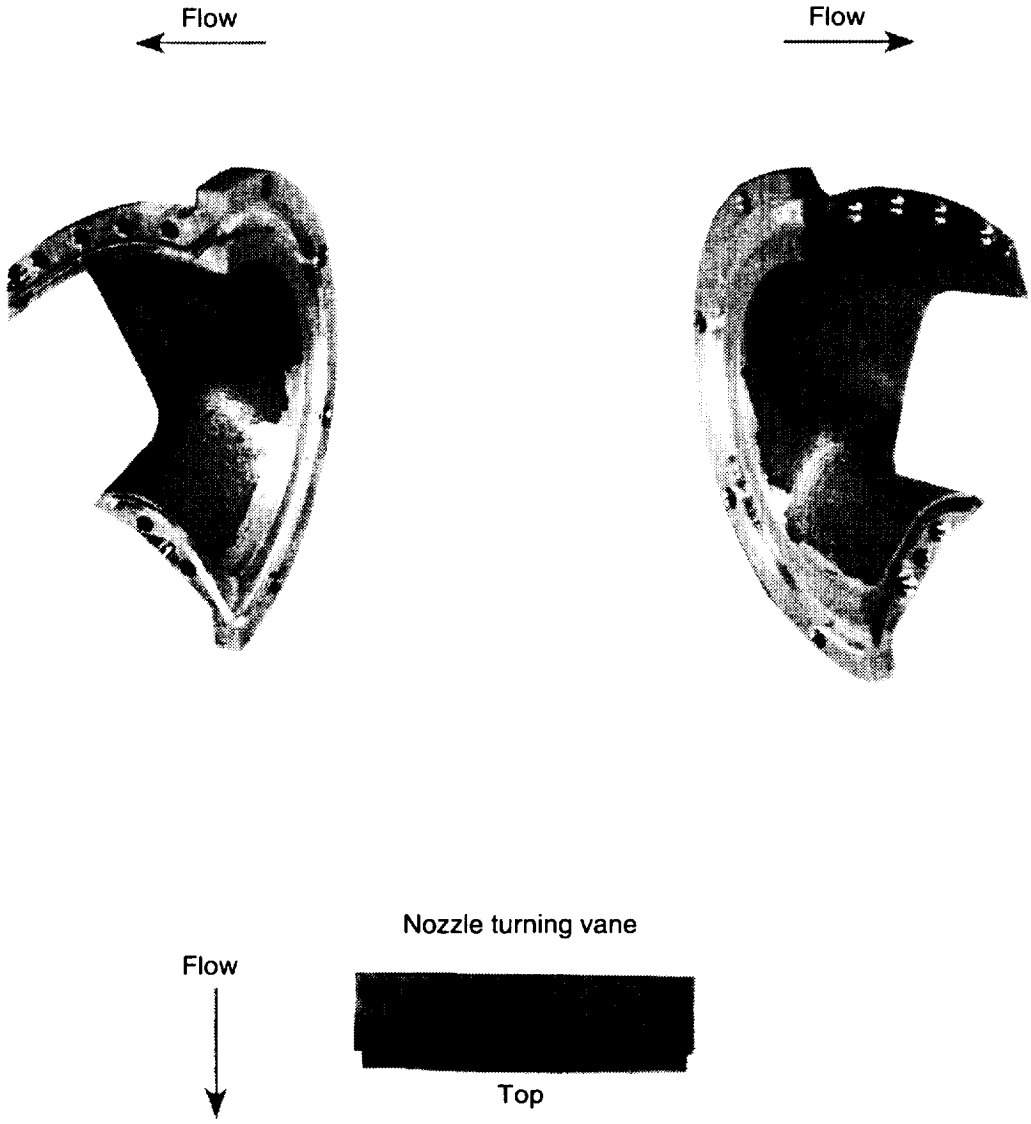

(d) The 1.4 CR submerged nozzle.

Figure 19. Concluded.

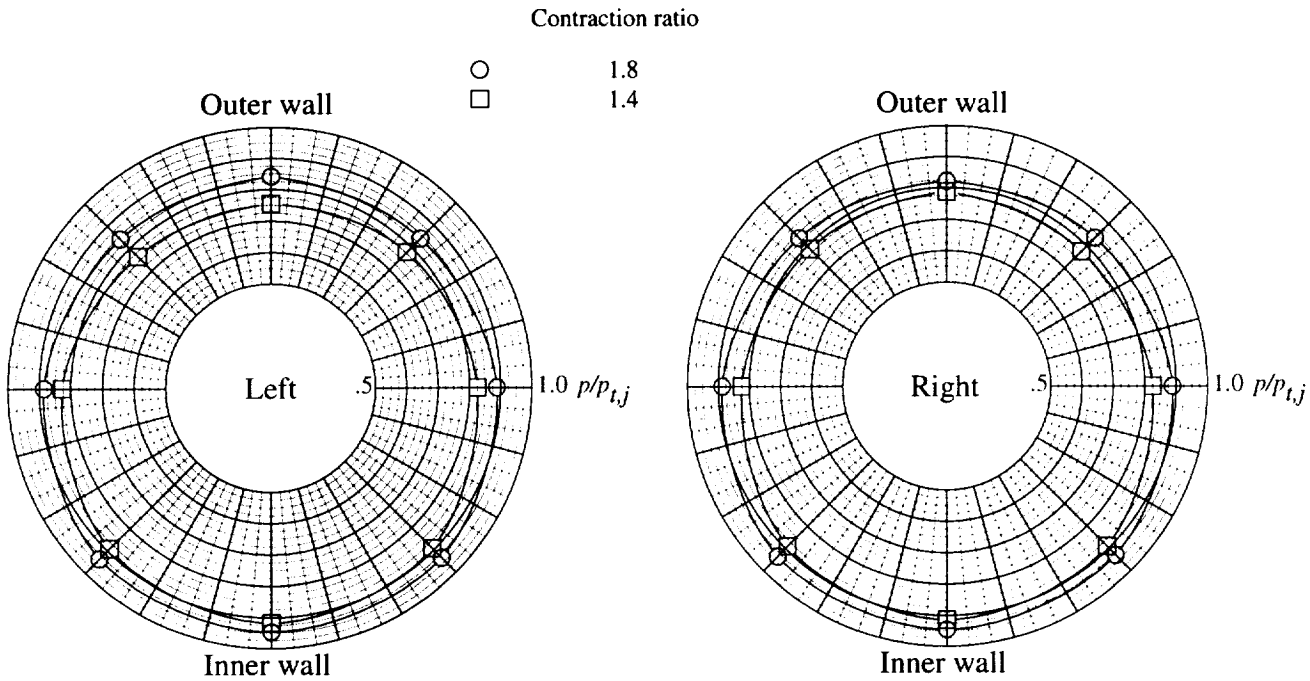

(a) Effect of CR. Nominal NPR = 4.0.

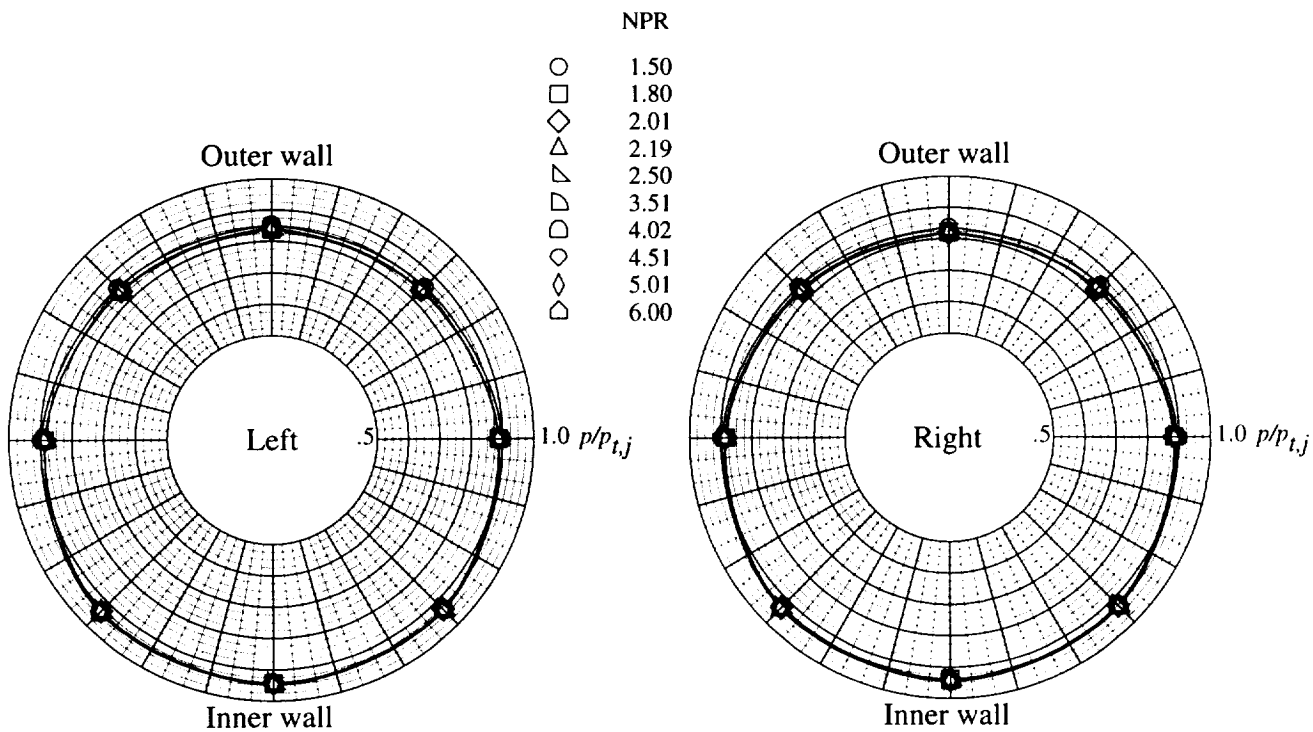

(b) Effect of NPR. CR = 1.8.

Figure 20. Effect of CR and NPR on offtake duct static-pressure ratios $p/p_{t,j}$ for offset plenum with short-core center-body, no blocker, and D-shaped nozzles in thrust mode.

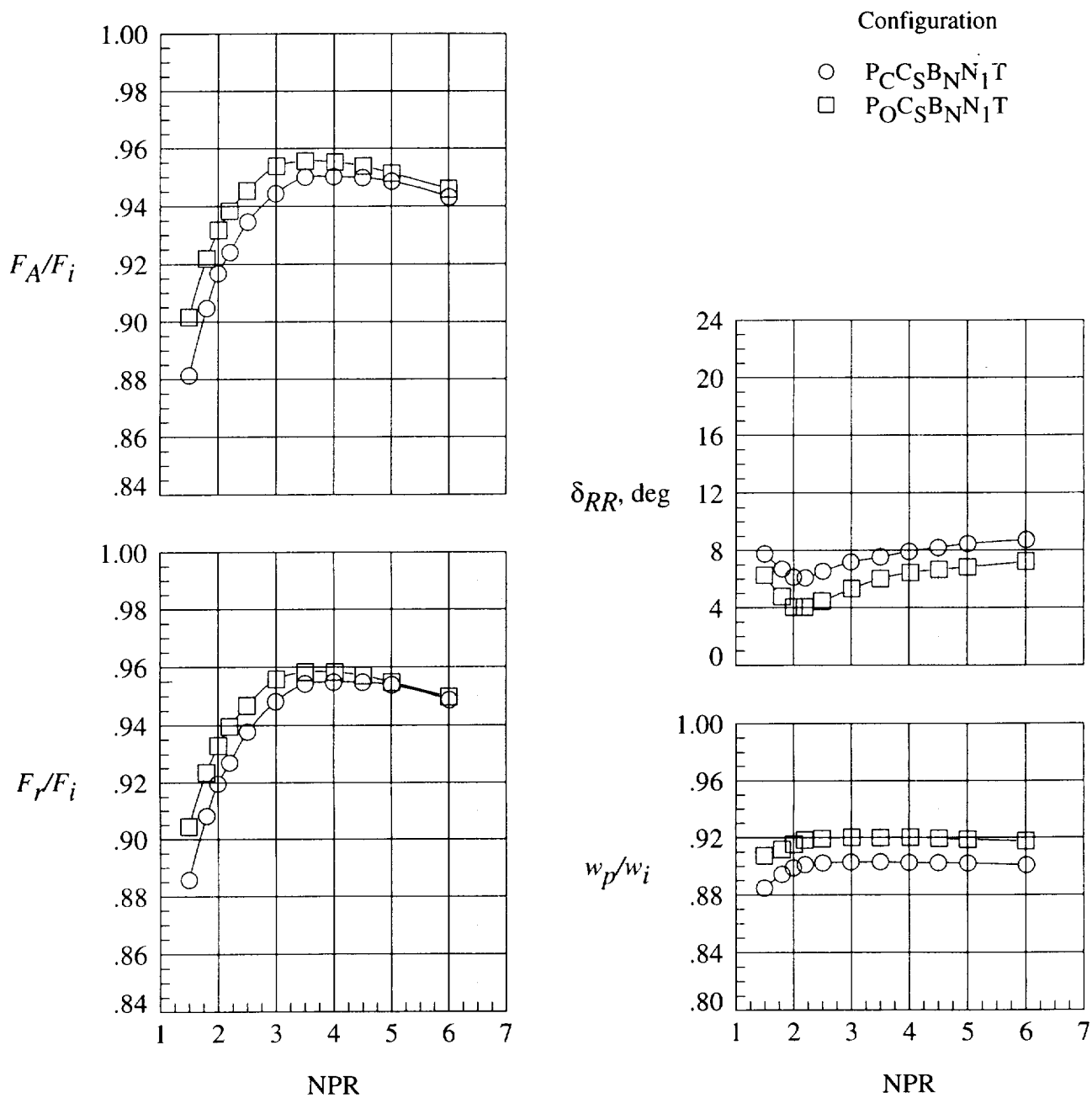

(a) Thrust mode.

Figure 21. Effect of plenum geometry on performance of 1.8 CR D-shaped nozzles with short-core centerbody and no blocker.

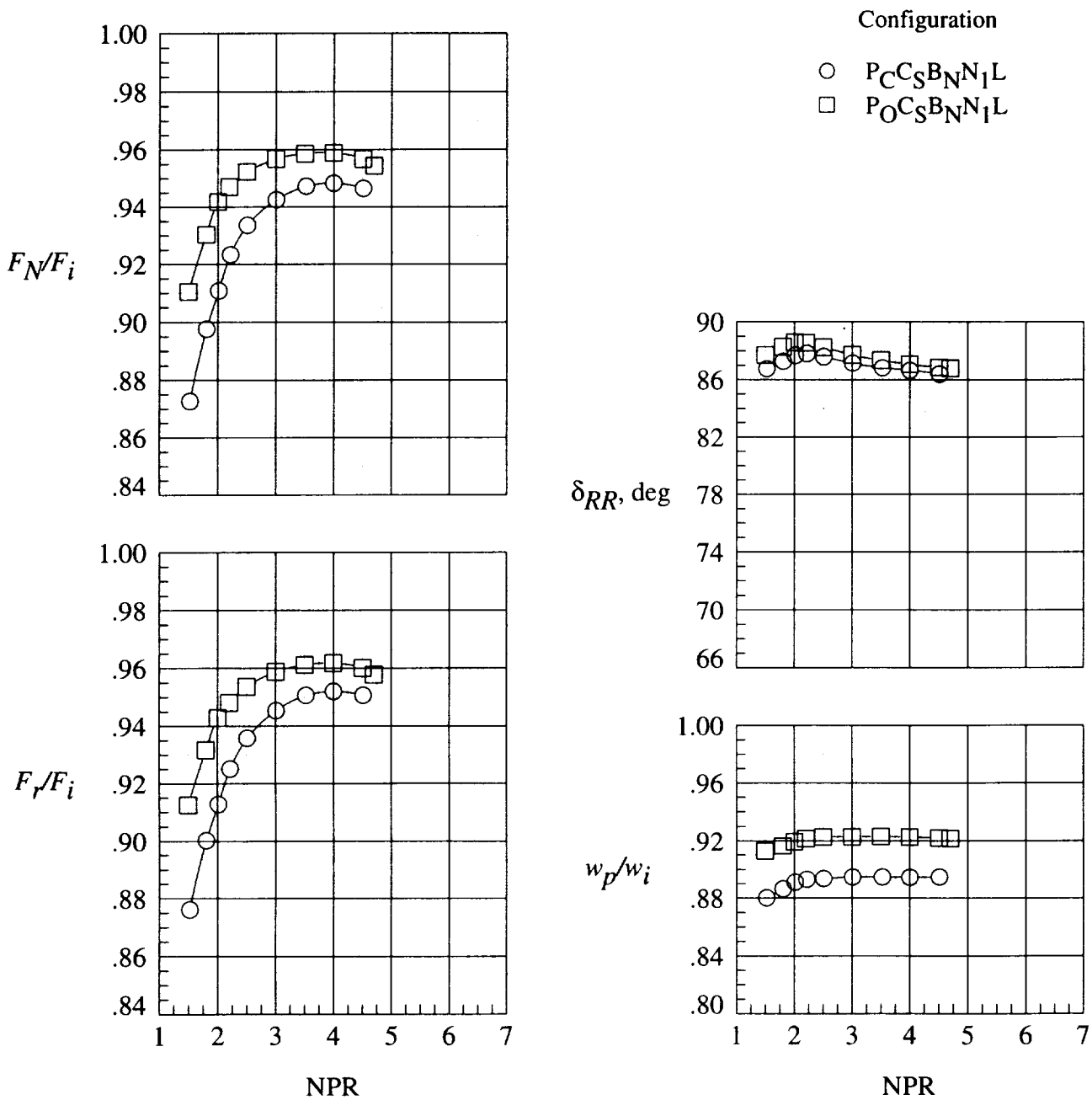

(b) Lift mode.

Figure 21. Concluded.

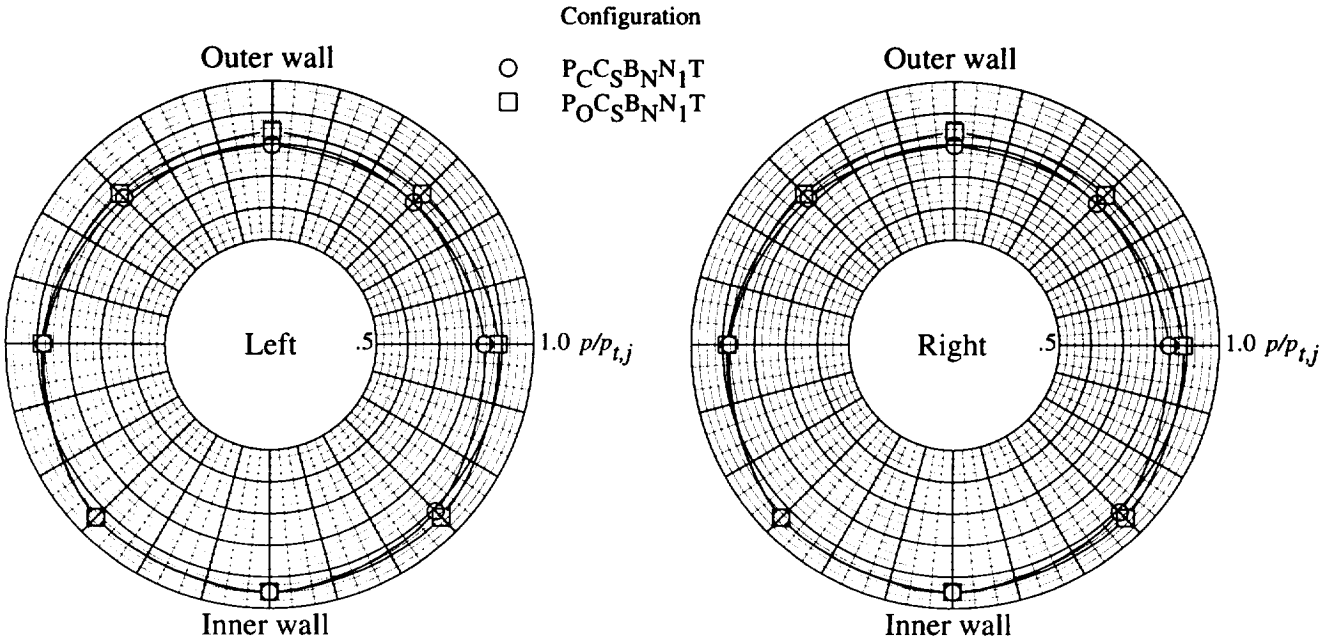

(a) Thrust mode.

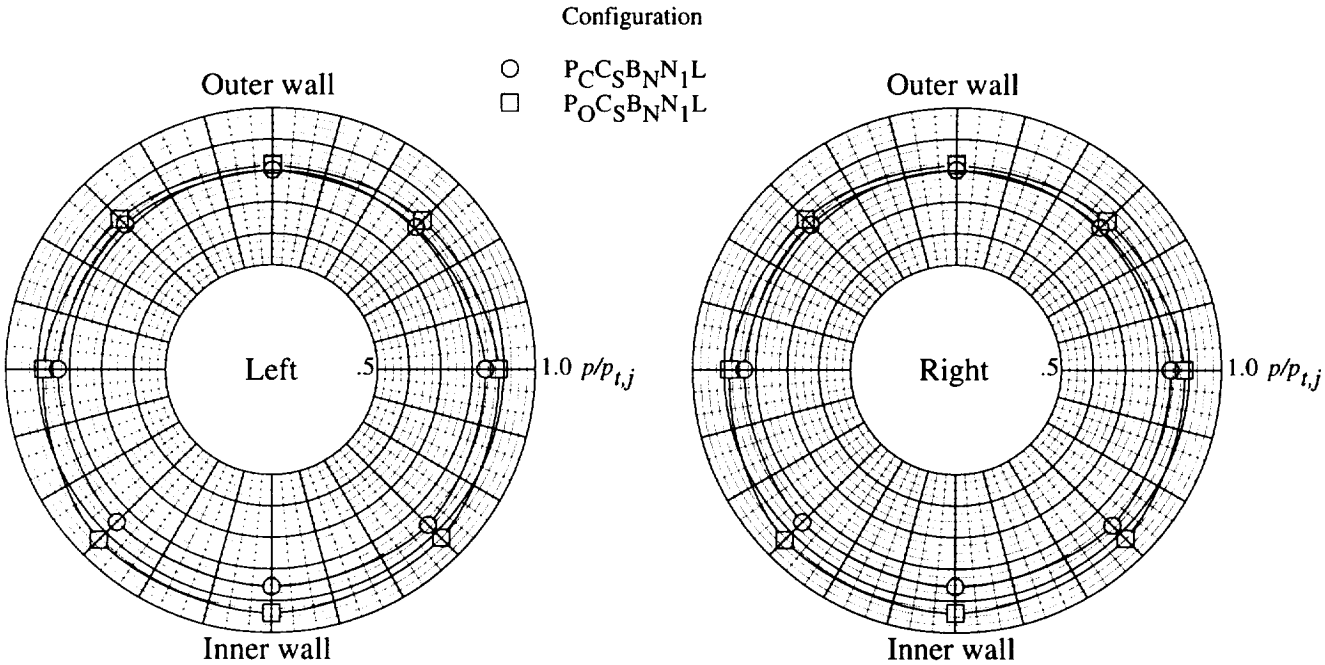

(b) Lift mode.

Figure 22. Effect of plenum geometry on offtake duct static-pressure ratios $p/p_{t,j}$ with short-core centerbody, no blocker, and 1.8 CR D-shaped nozzles. Nominal NPR = 4.0.

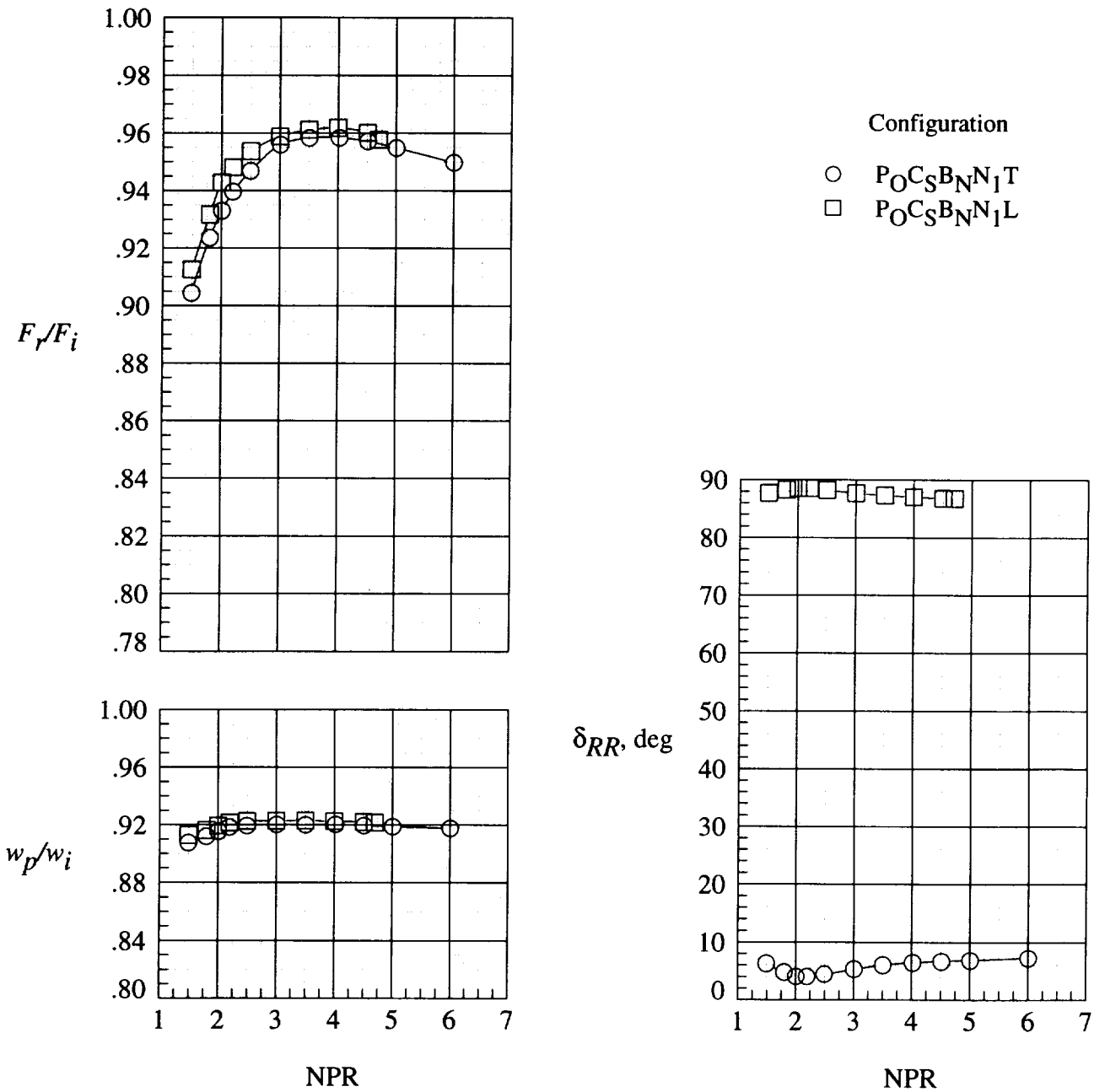

(a) Short-core centerbody with no blocker.

Figure 23. Effect of operation mode on performance of 1.8 CR D-shaped nozzles installed on offset plenum.

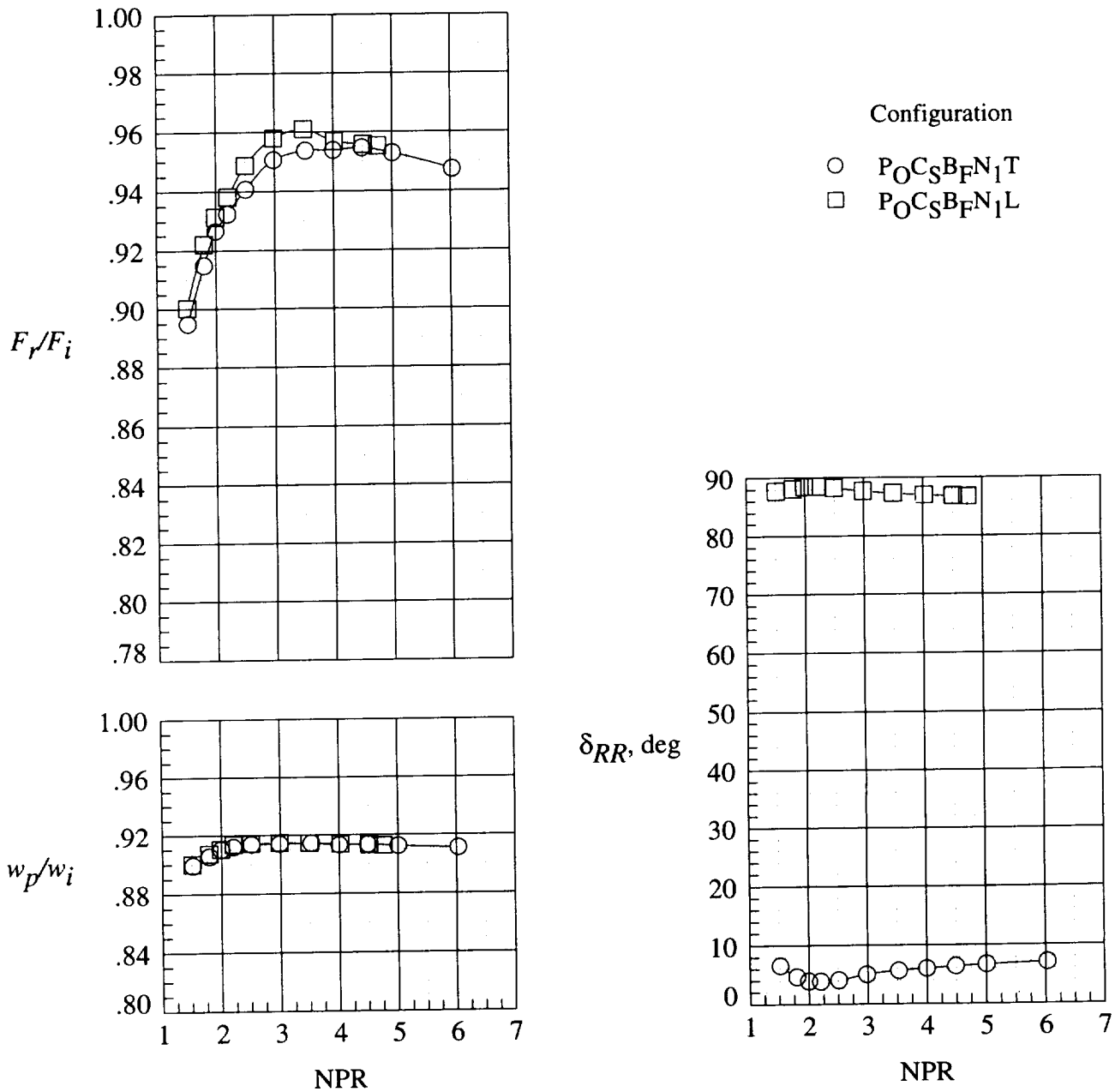

(b) Short-core centerbody with flat blocker.

Figure 23. Continued.

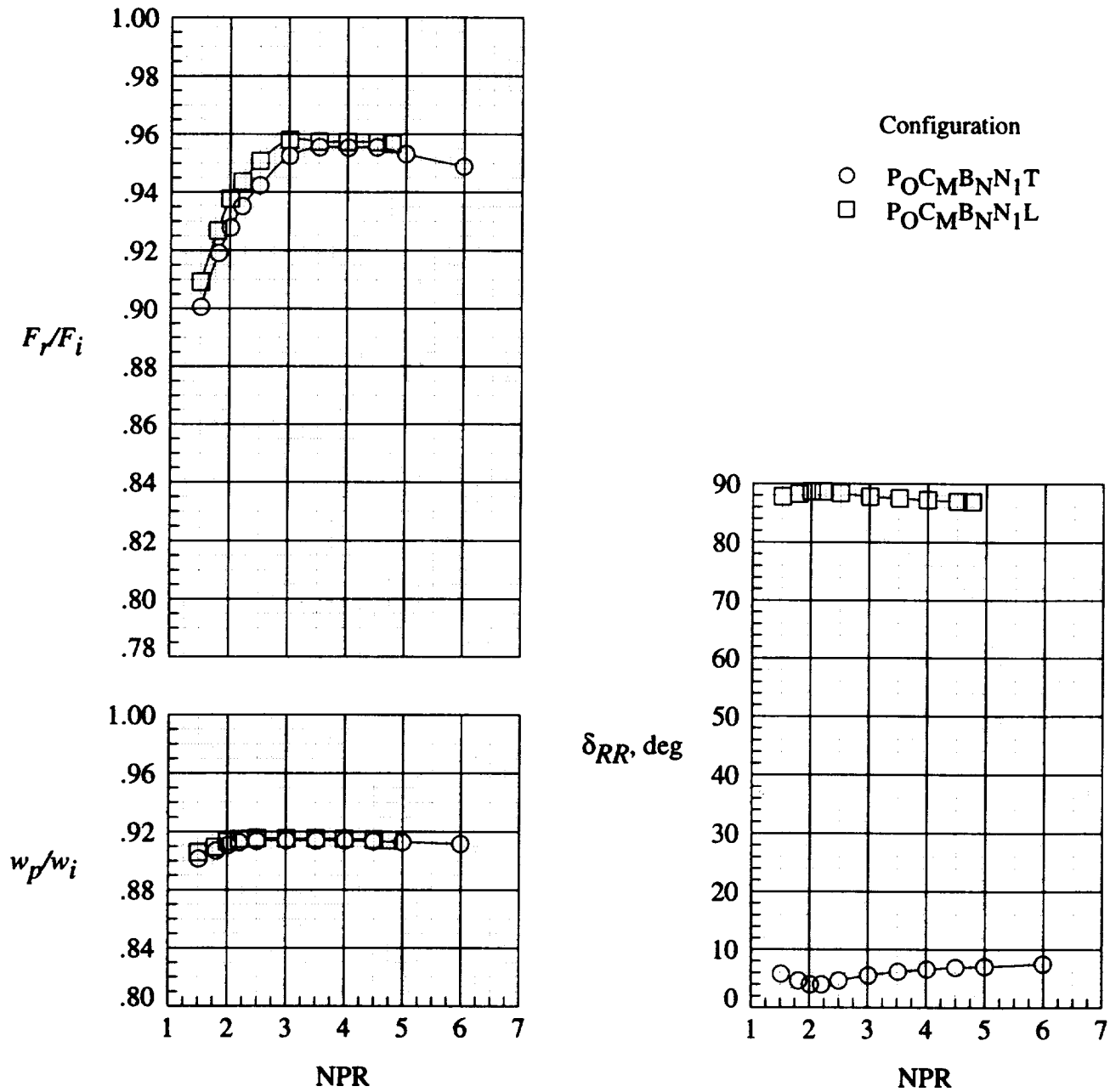

(c) Medium-core centerbody with no blocker.

Figure 23. Continued.

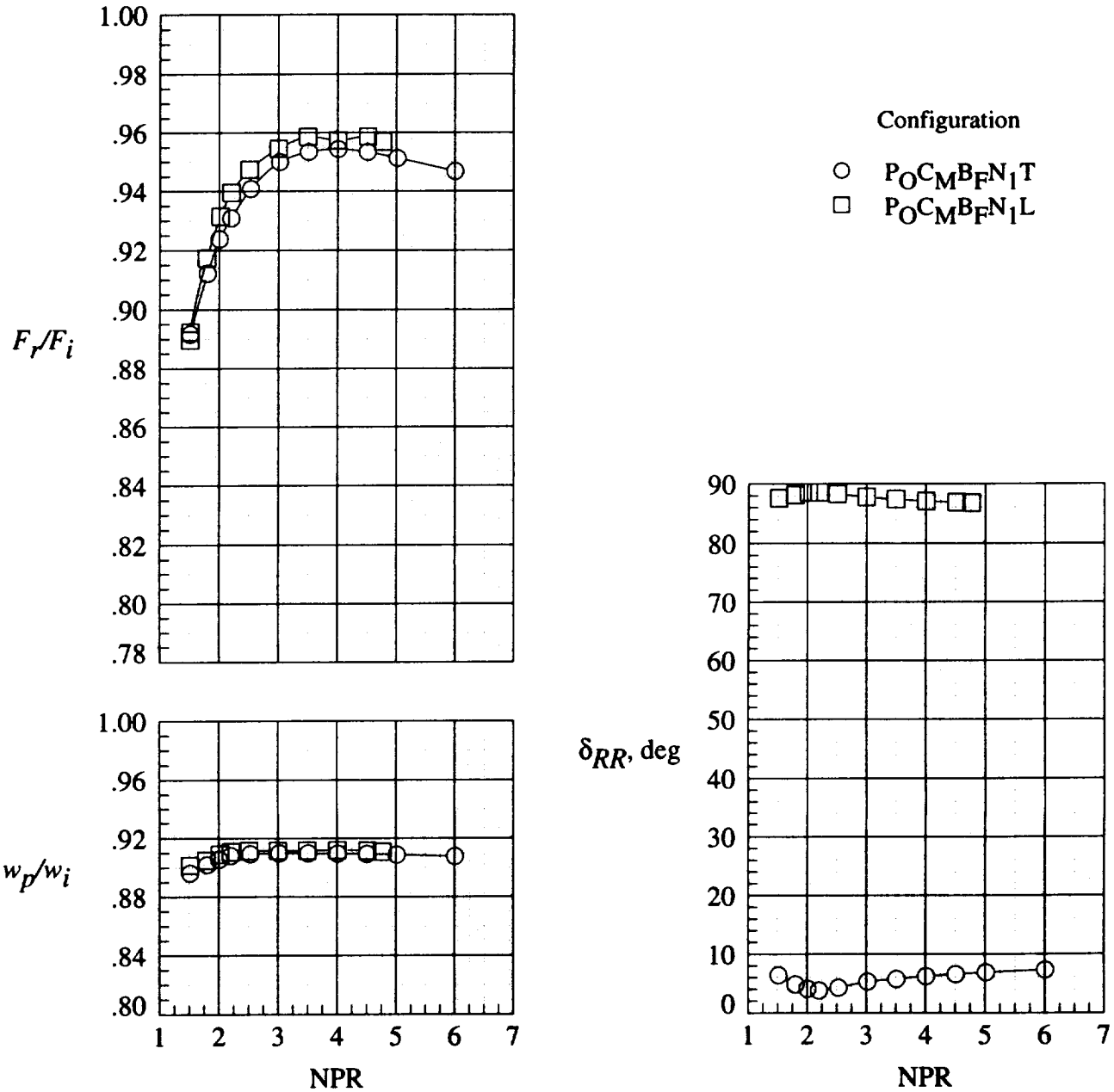

(d) Medium-core centerbody with flat blocker.

Figure 23. Continued.

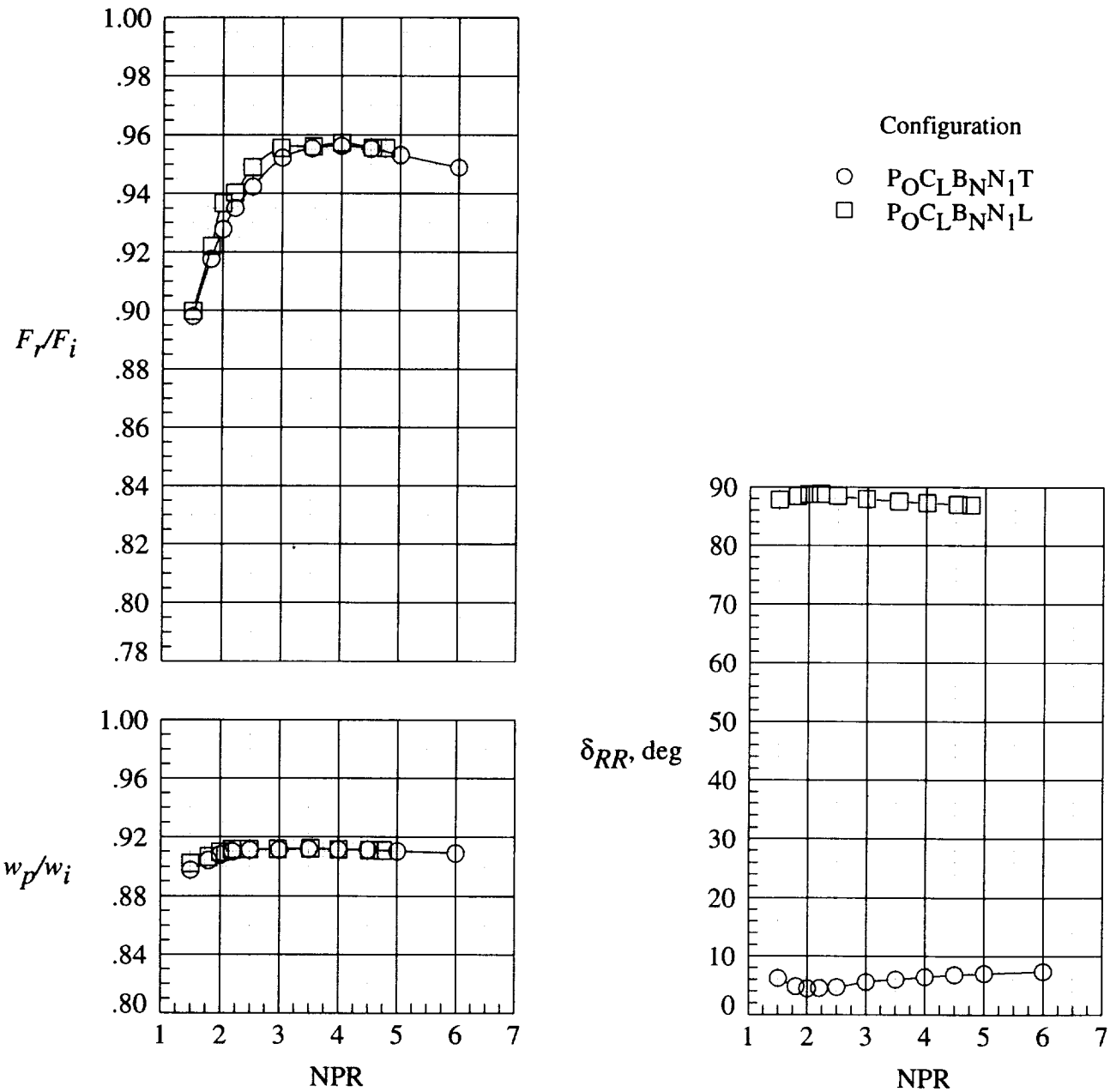

(e) Long-core centerbody with no blocker.

Figure 23. Continued.

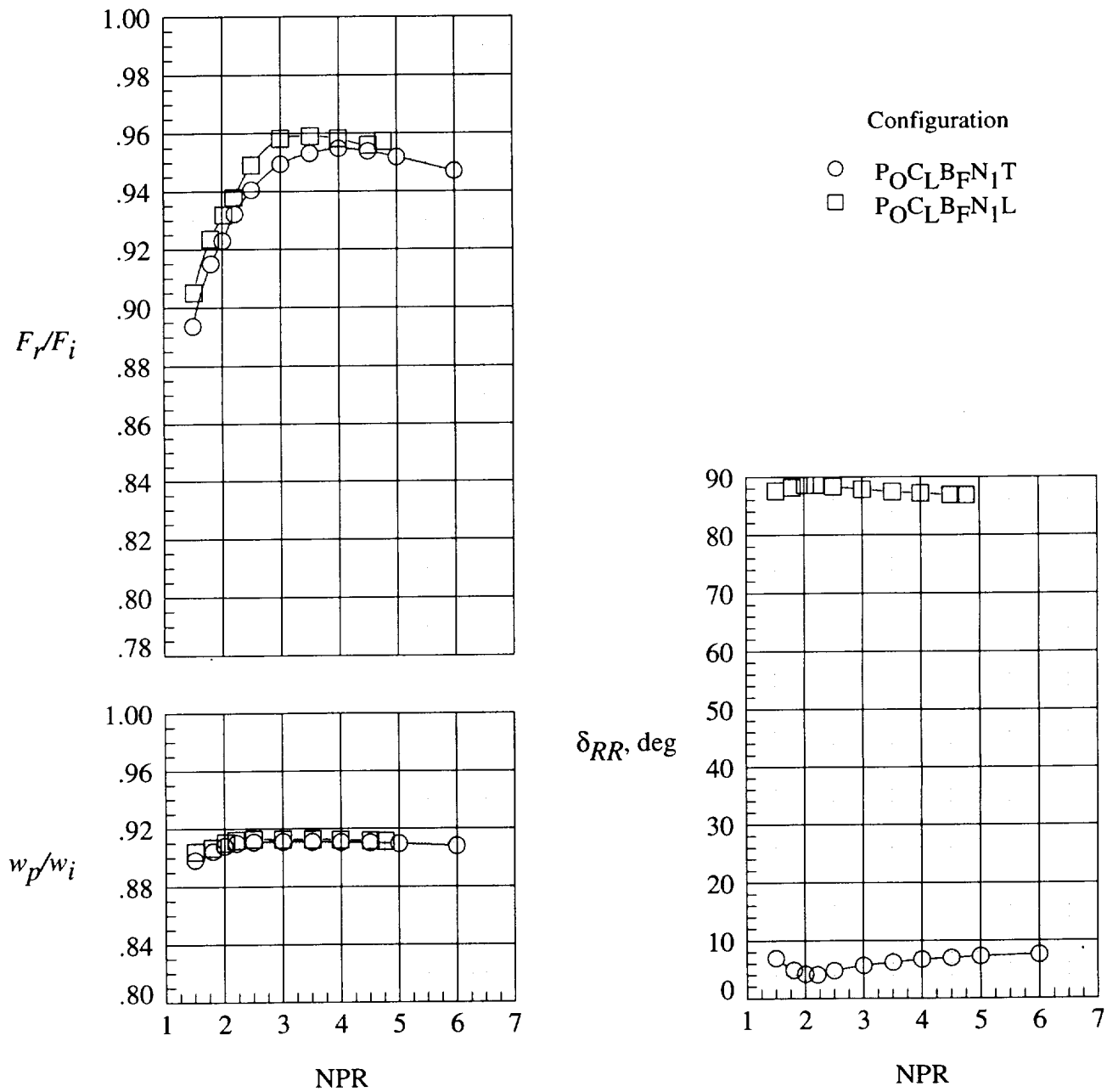

(f) Long-core centerbody with flat blocker.

Figure 23. Continued.

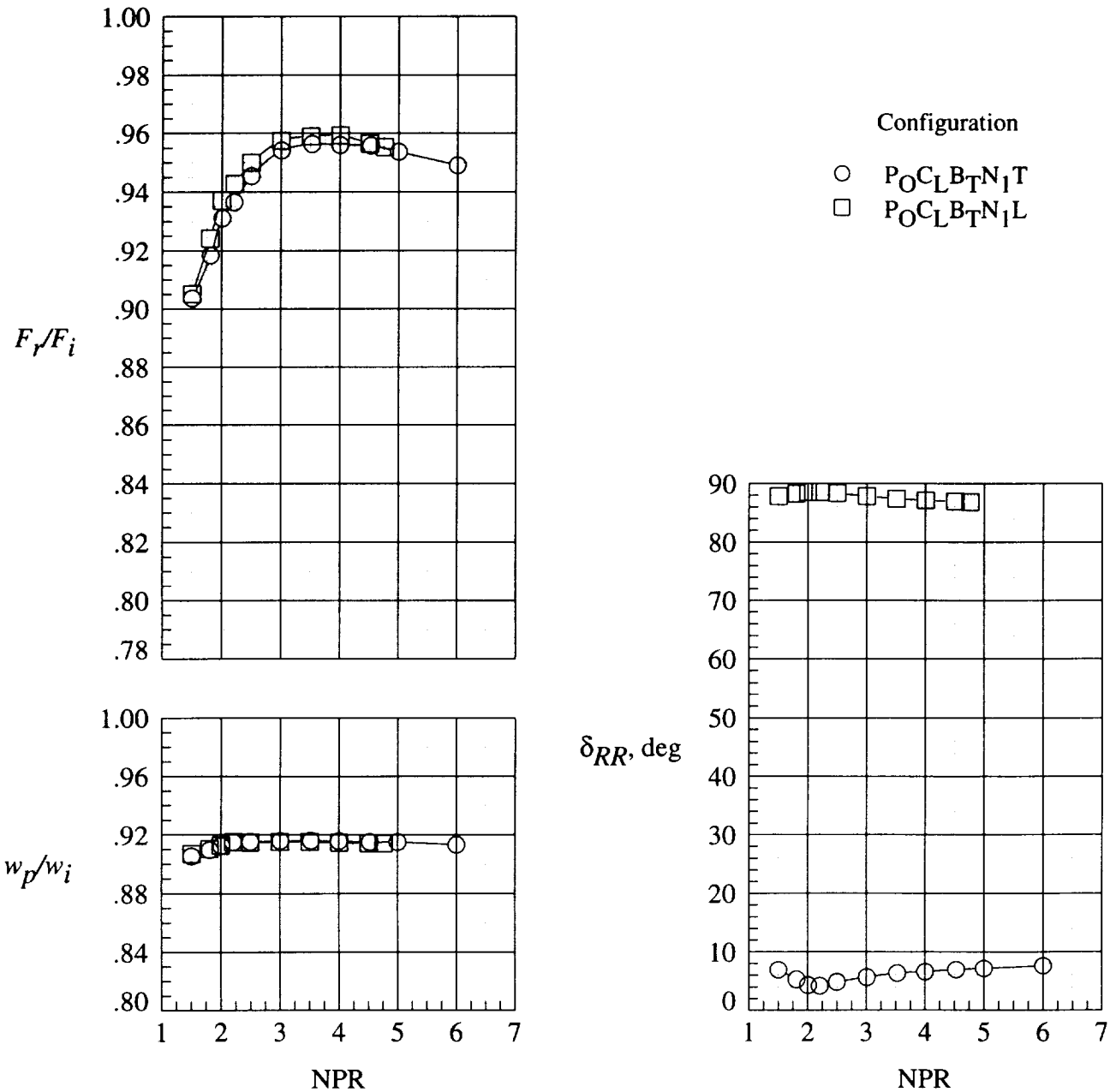

(g) Long-core centerbody with tapered blocker.

Figure 23. Continued.

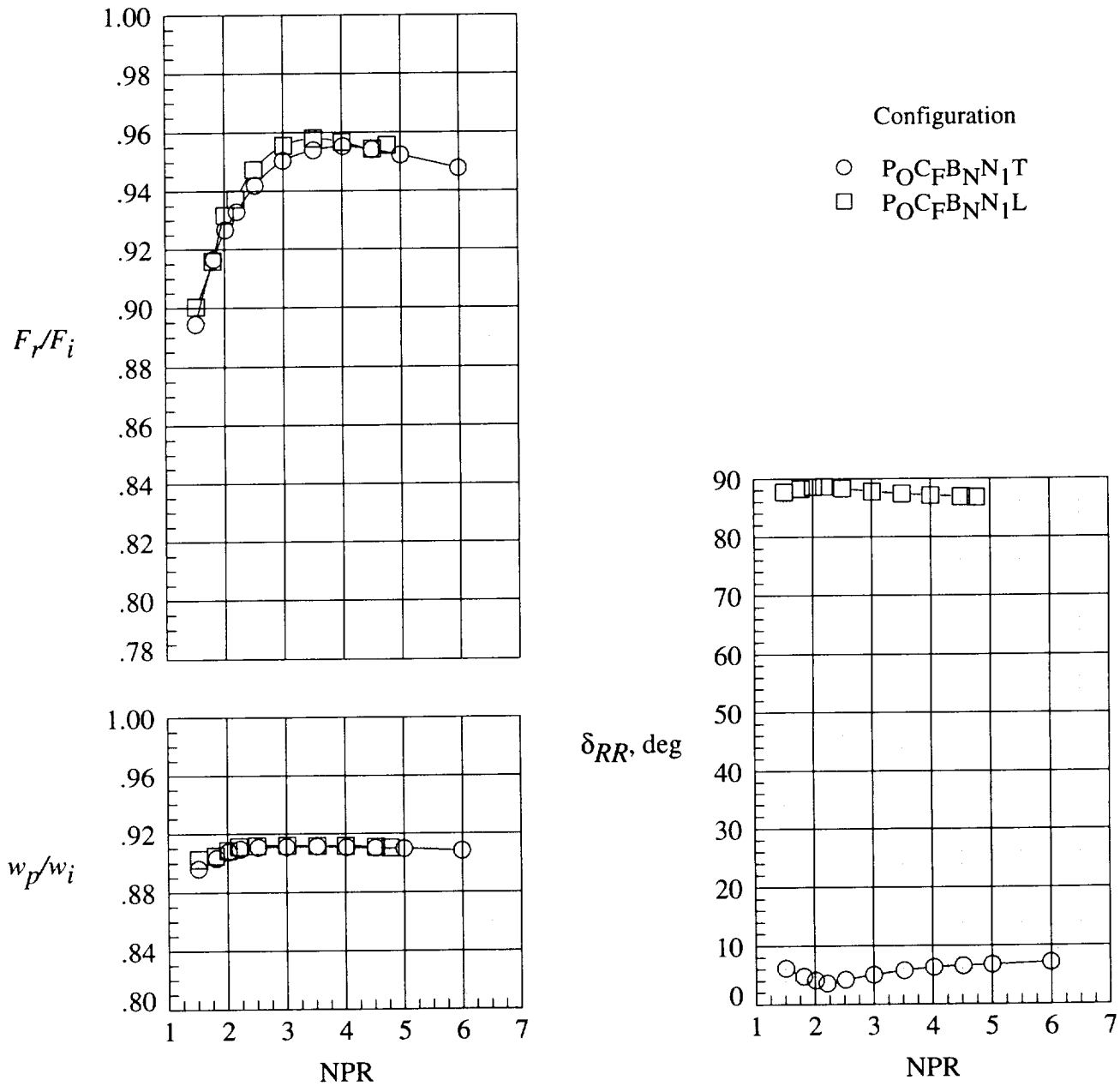

(h) Fan centerbody with no blocker.

Figure 23. Continued.

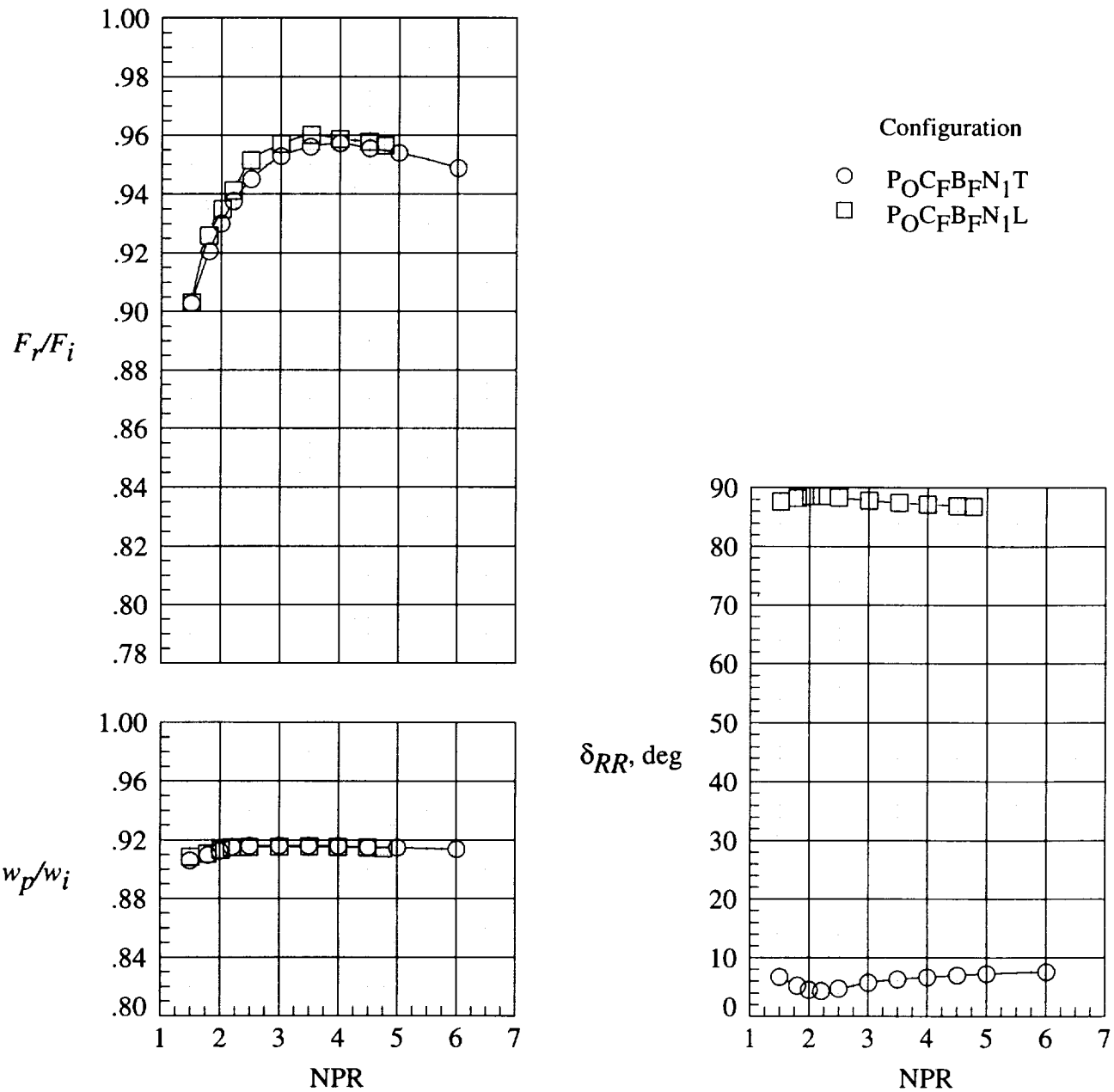

(i) Fan centerbody with flat blocker.

Figure 23. Continued.

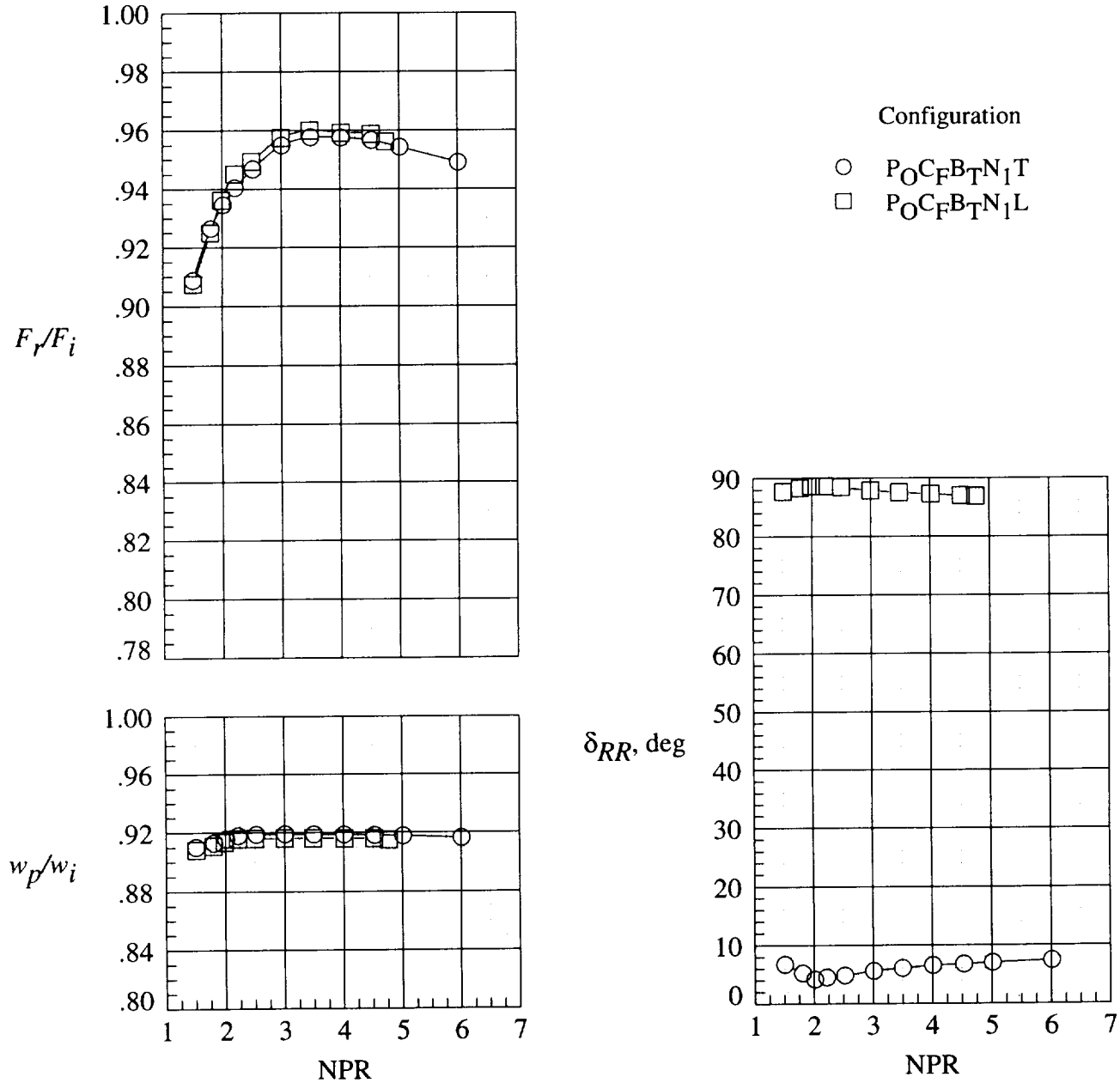

(j) Fan centerbody with tapered blocker.

Figure 23. Concluded.

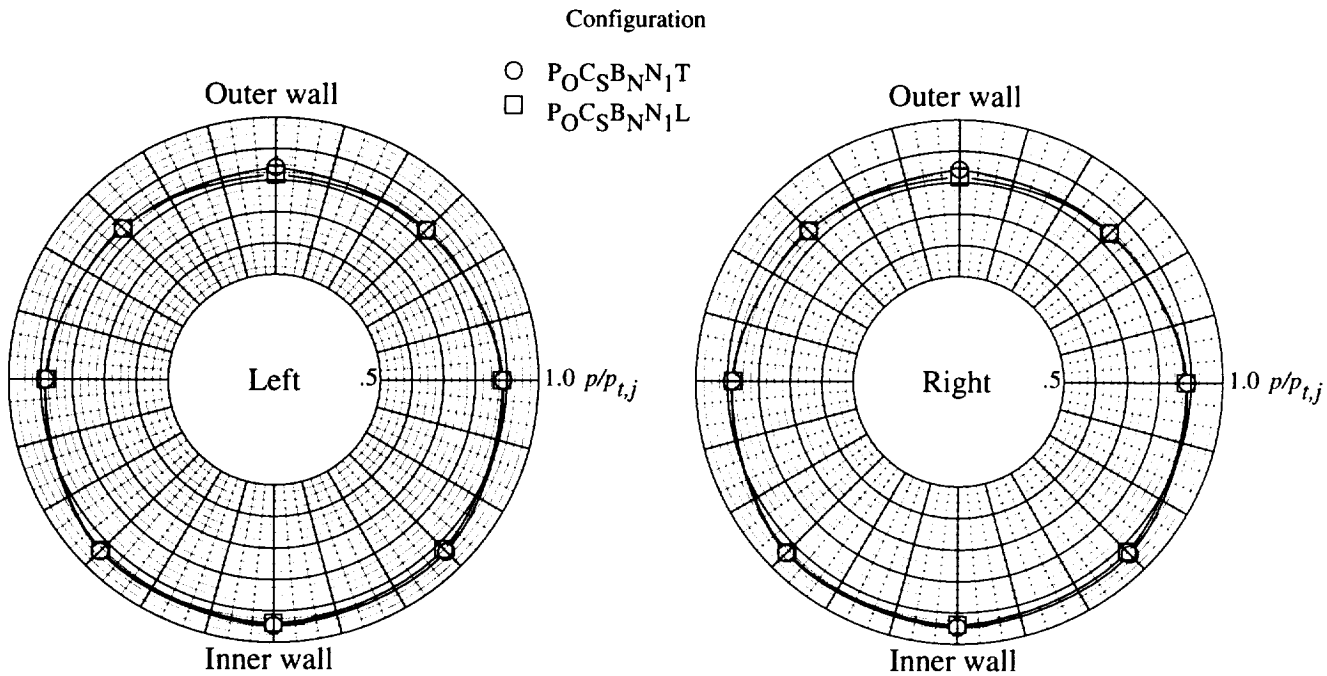

(a) Short-core centerbody and no blocker.

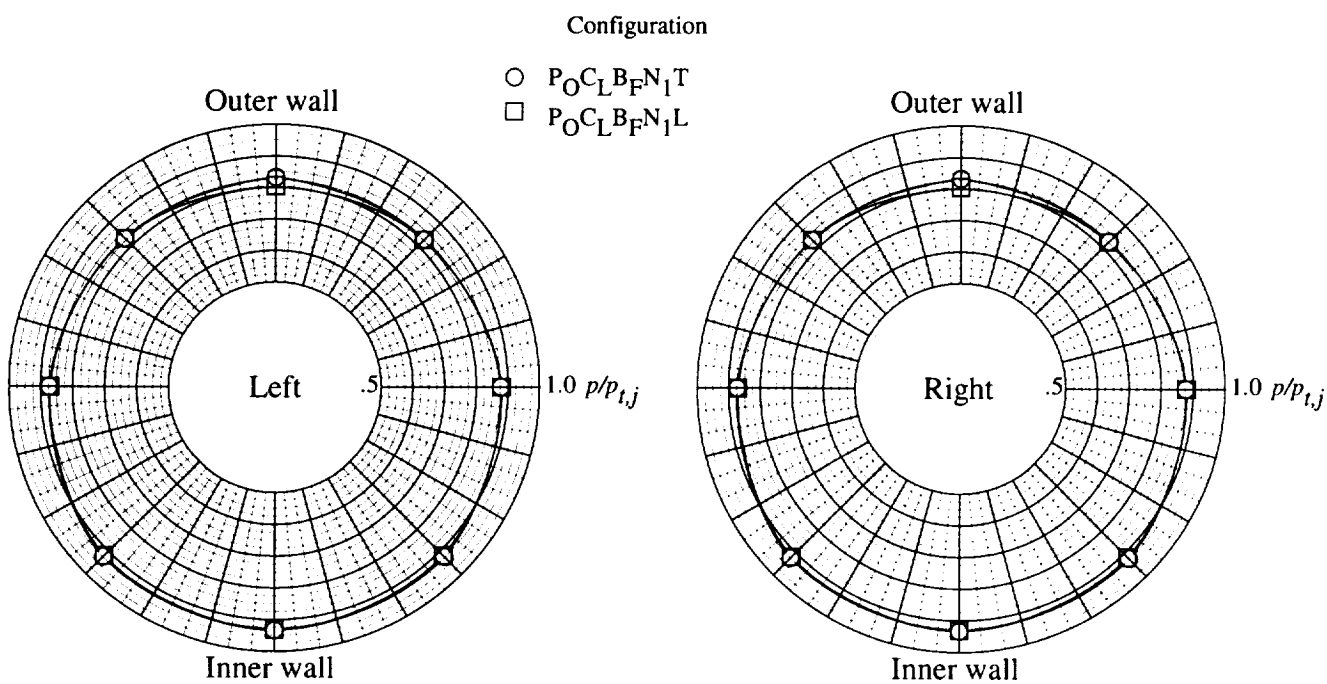

(b) Long-core centerbody with flat blocker.

Figure 24. Effect of operation mode on offtake duct static-pressure ratios $p/p_{t,j}$ for offset plenum with 1.8 CR D-shaped nozzles. Nominal NPR = 4.0.

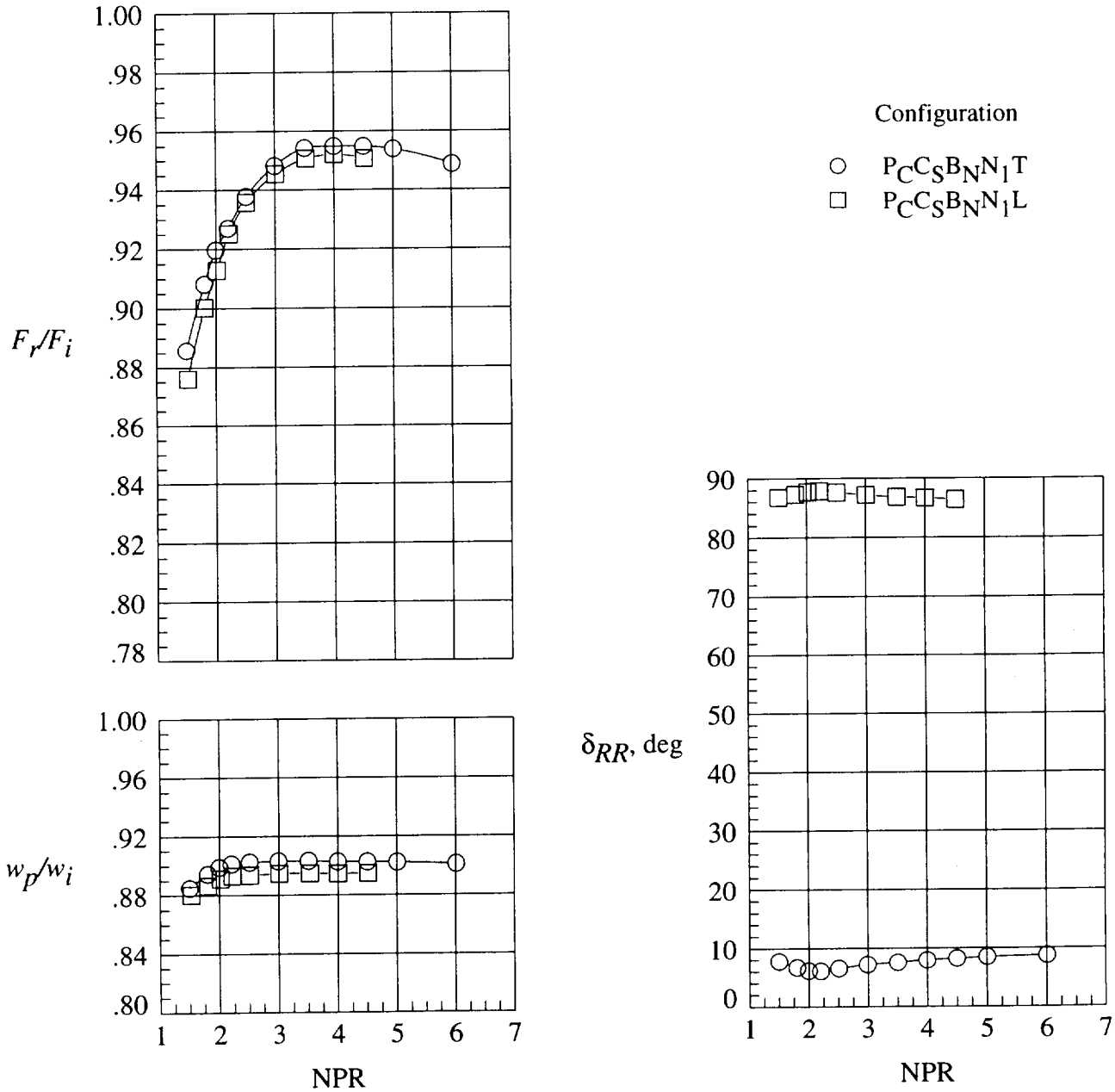

(a) Short-core centerbody with no blocker.

Figure 25. Effect of operation mode on performance of 1.8 CR D-shaped nozzles installed on centerline plenum.

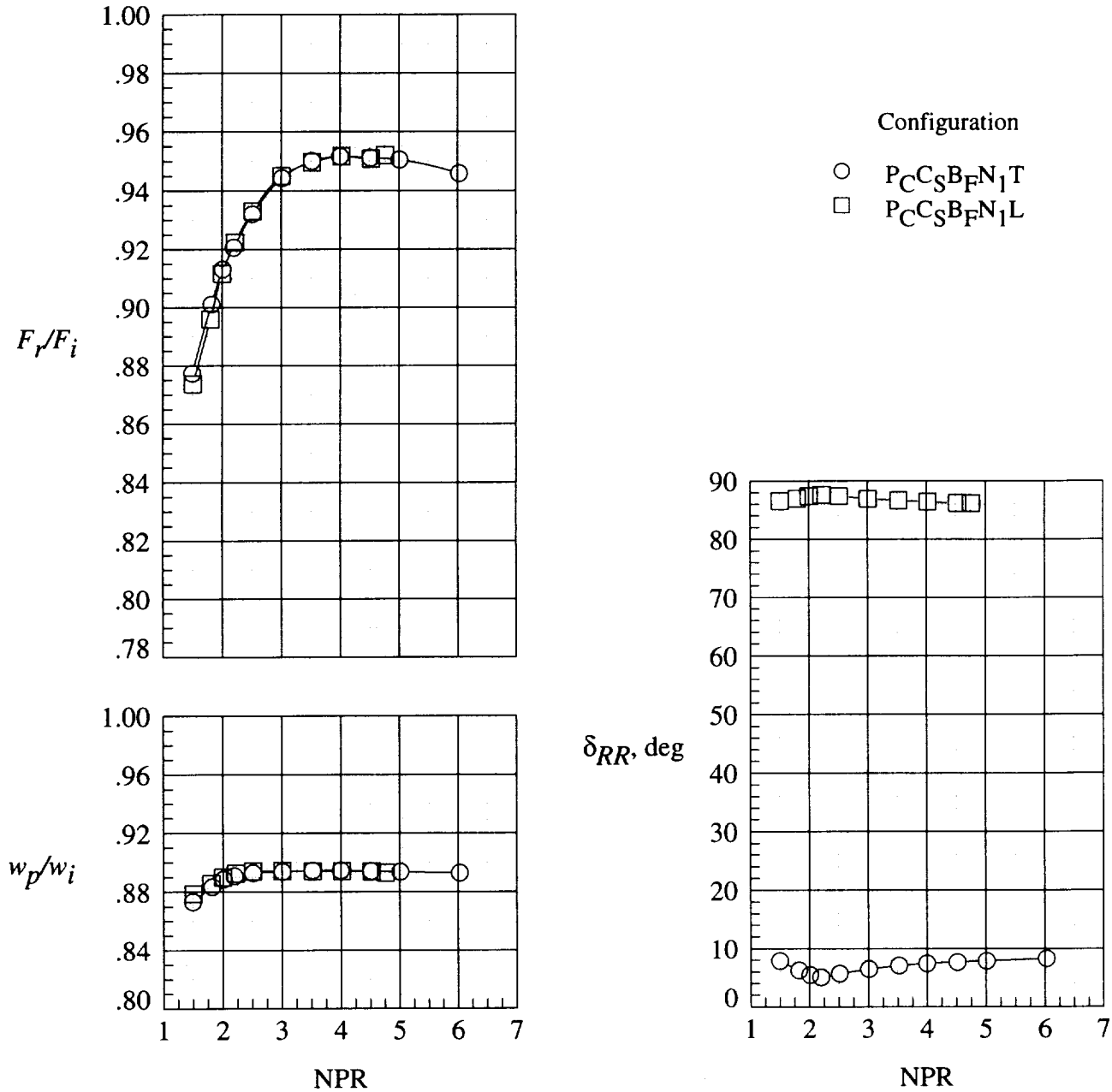

(b) Short-core centerbody with flat blocker.

Figure 25. Continued.

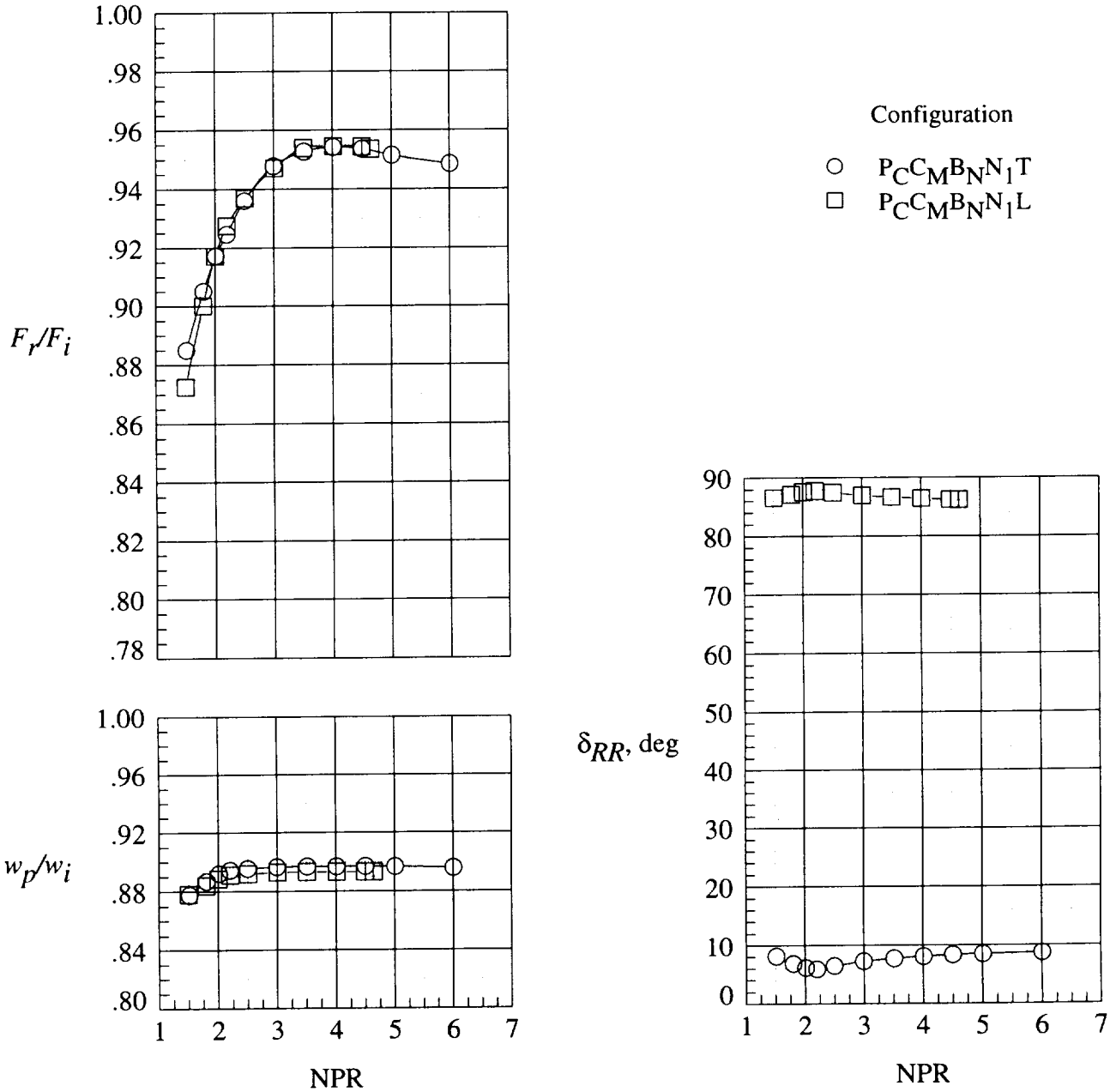

(c) Medium-core centerbody with no blocker.

Figure 25. Continued.

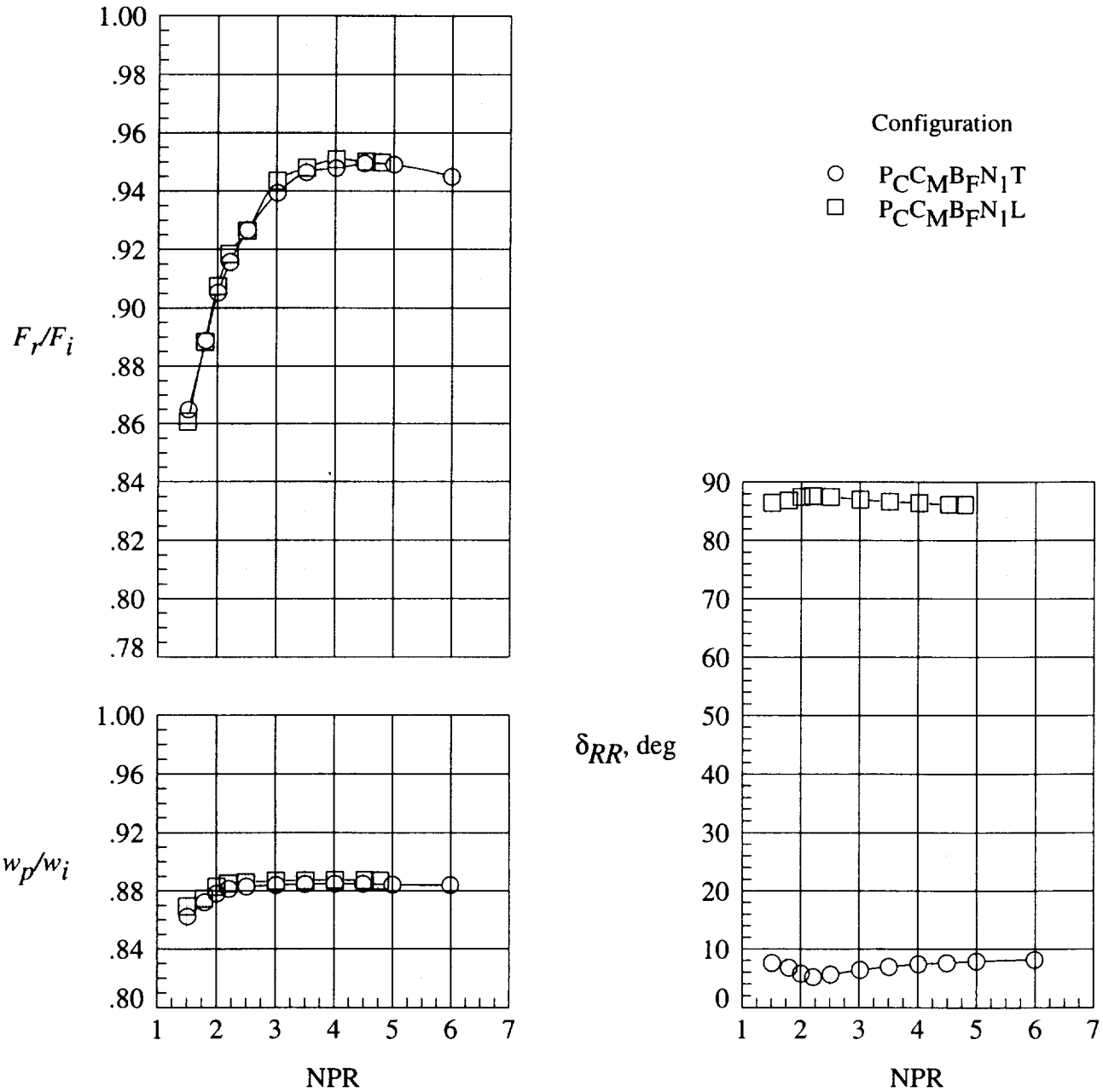

(d) Medium-core centerbody with flat blocker.

Figure 25. Continued.

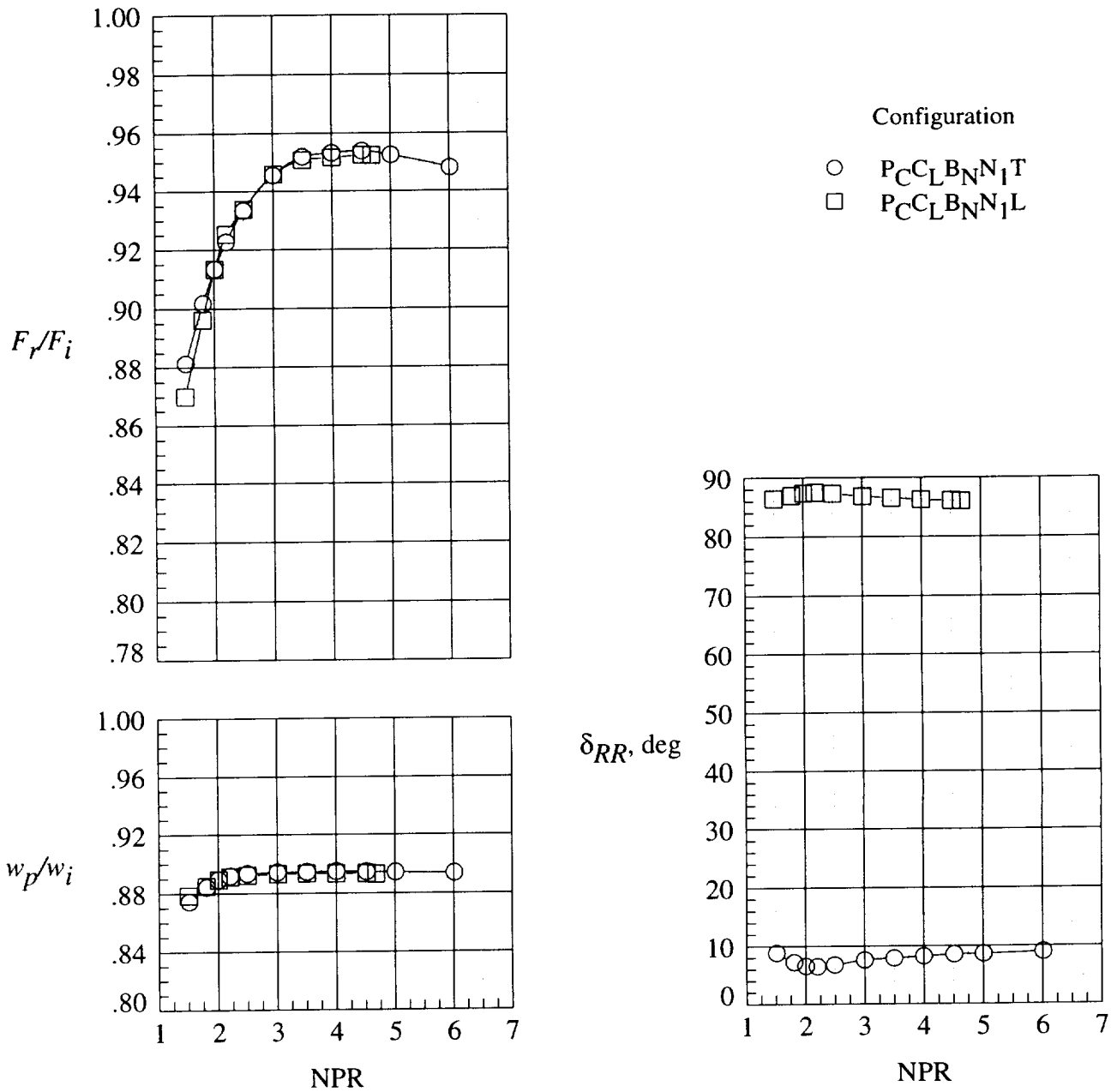

(e) Long-core centerbody with no blocker.

Figure 25. Continued.

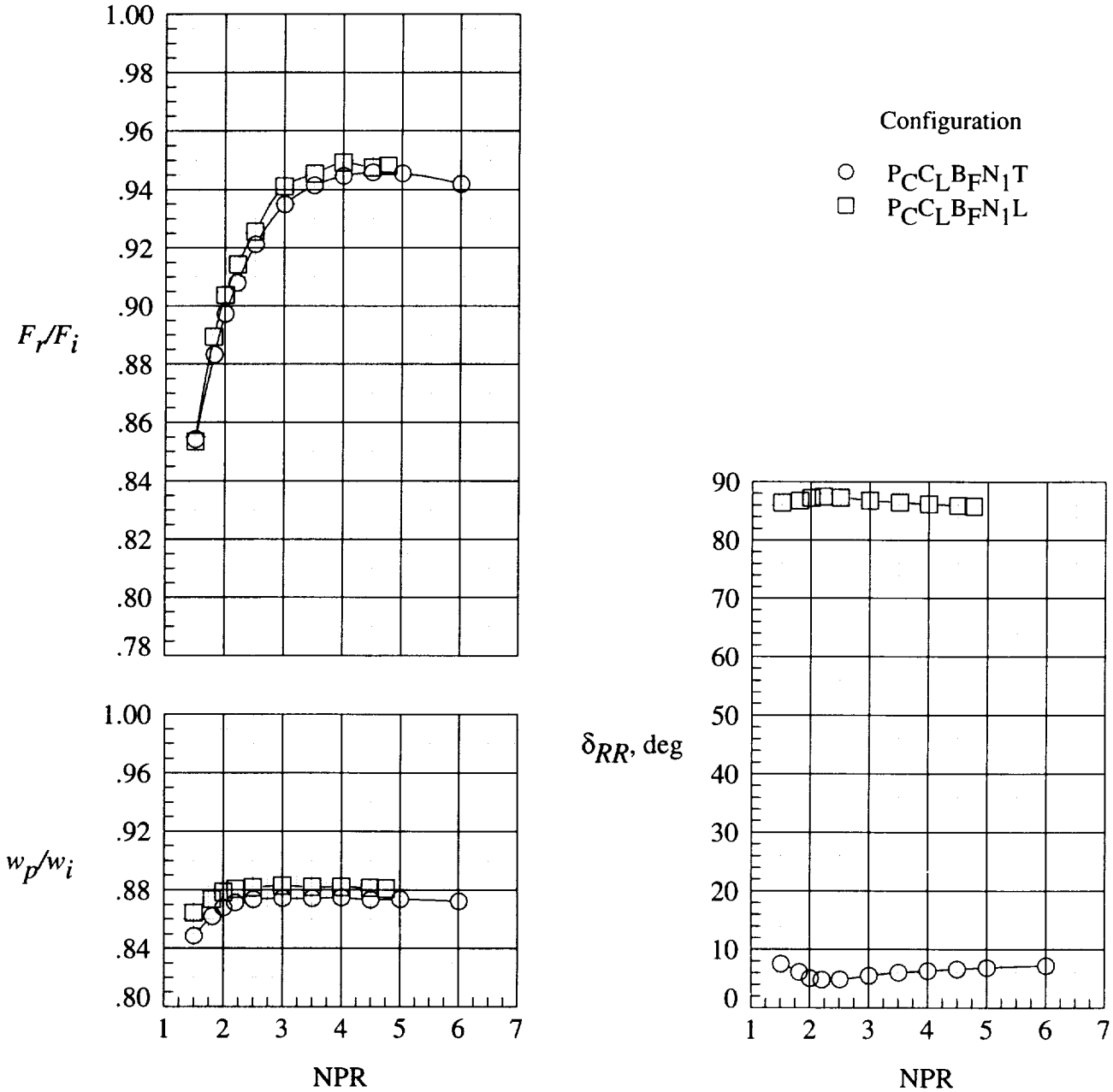

(f) Long-core centerbody with flat blocker.

Figure 25. Continued.

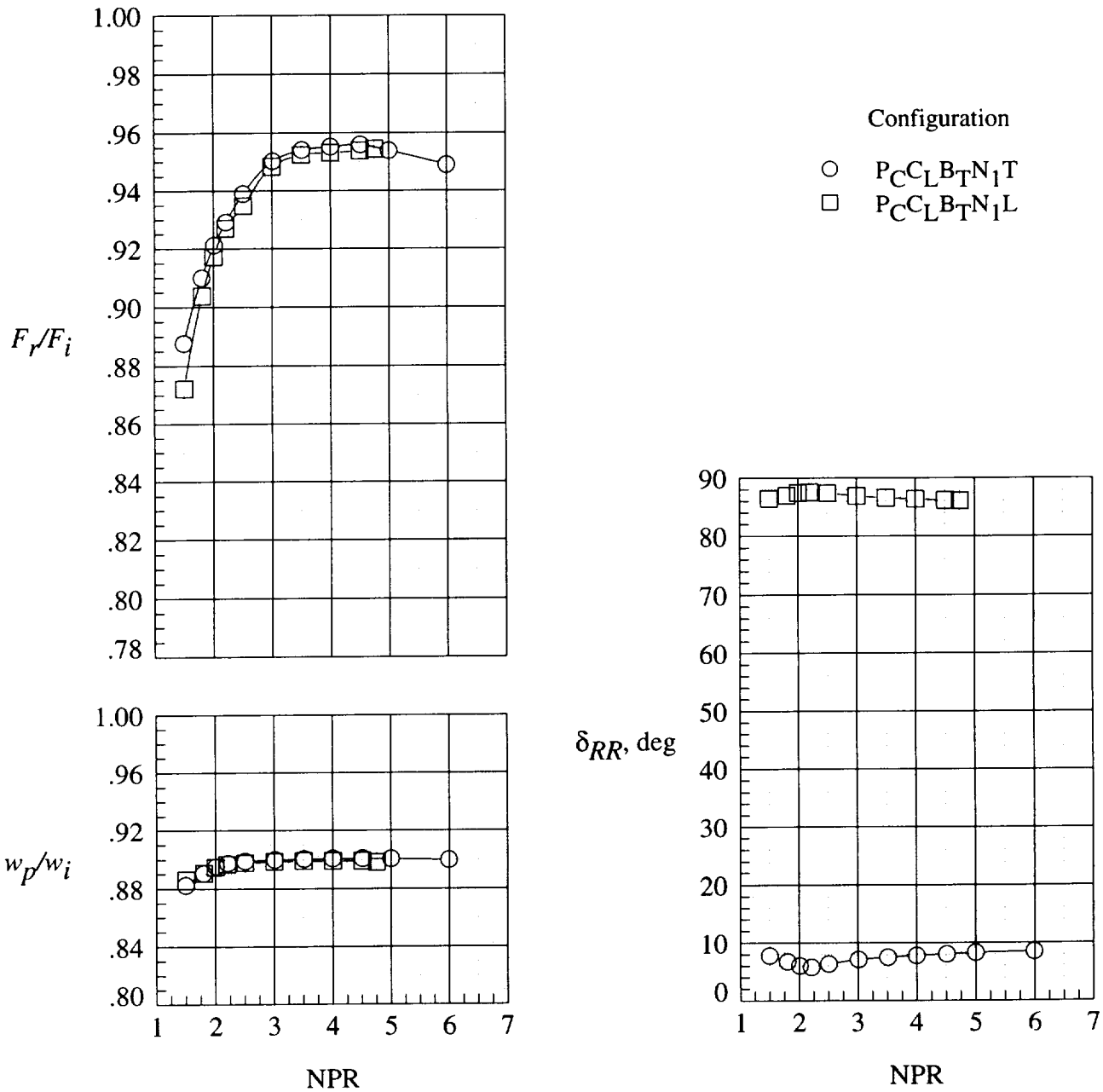

(g) Long-core centerbody with tapered blocker.

Figure 25. Continued.

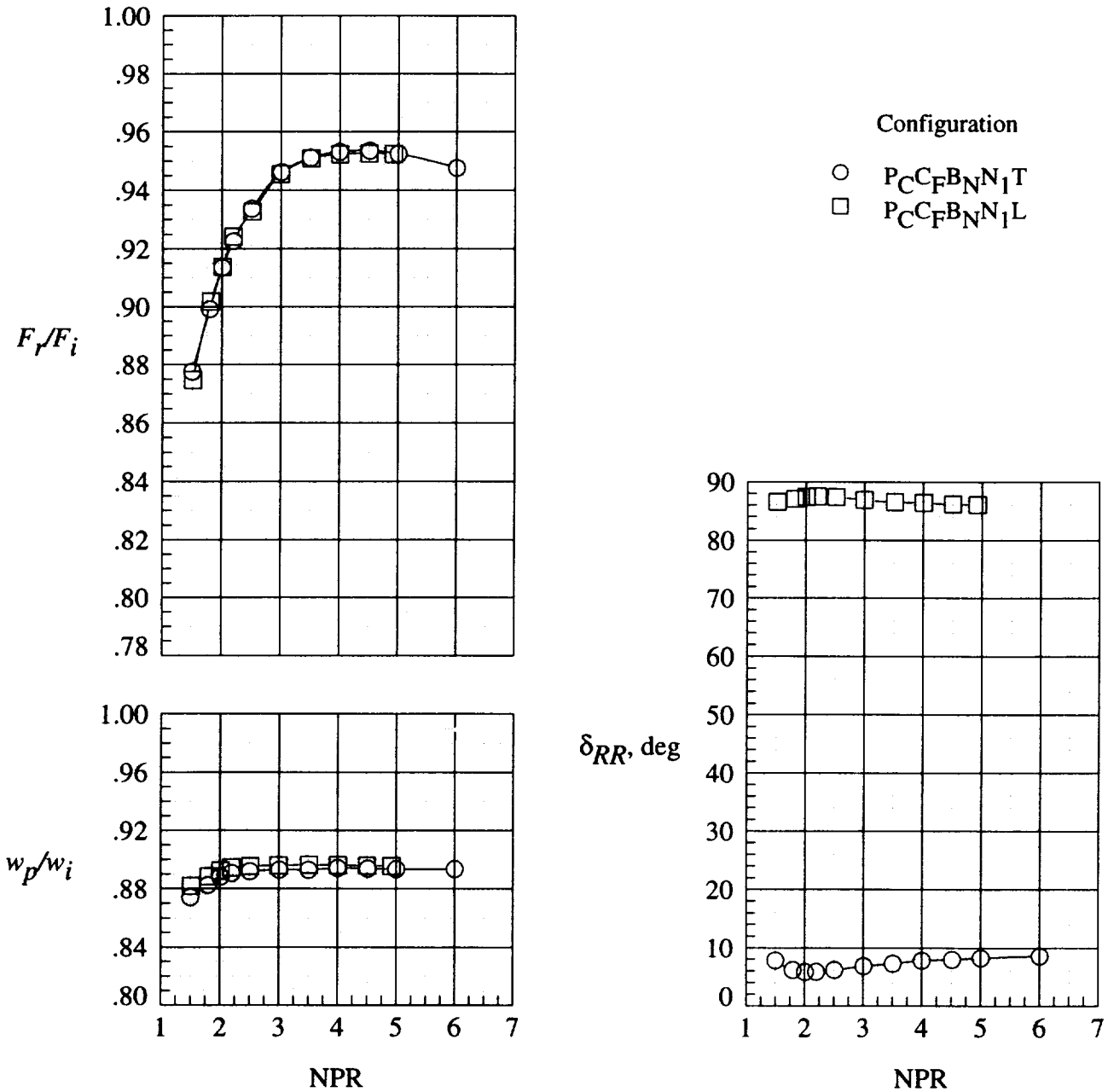

(h) Fan centerbody with no blocker.

Figure 25. Continued.

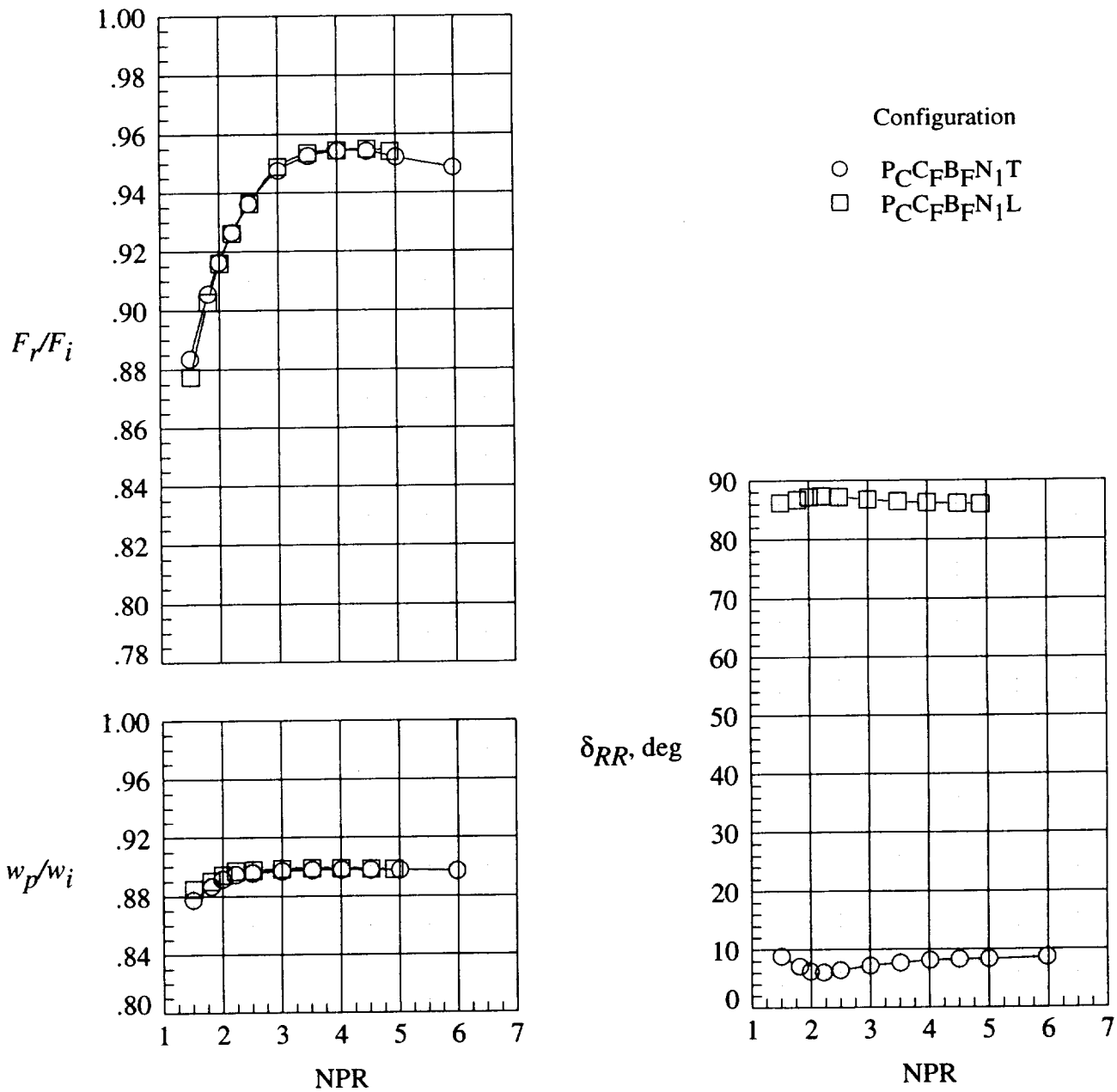

(i) Fan centerbody with flat blocker.

Figure 25. Continued.

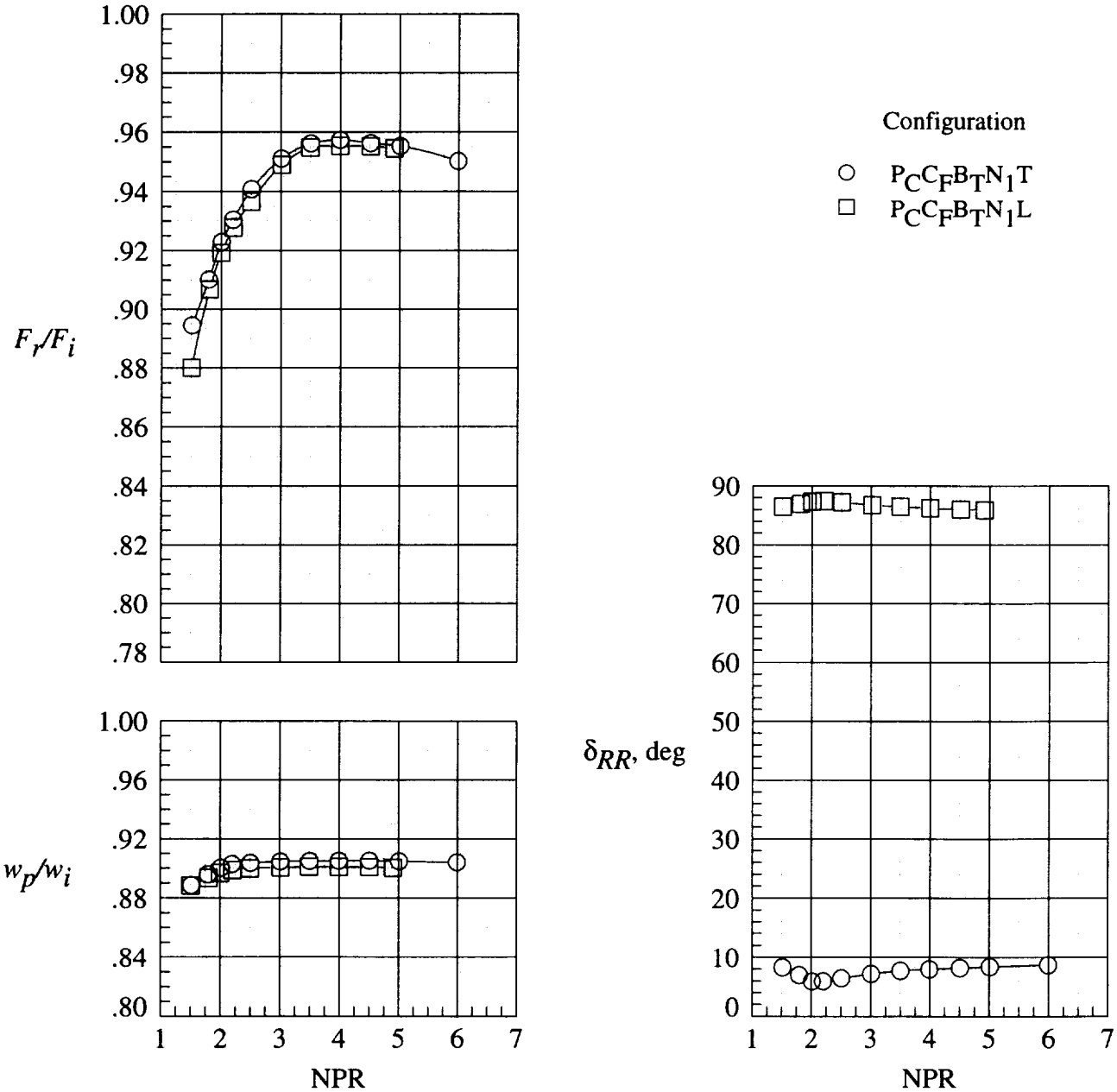

(j) Fan centerbody with tapered blocker.

Figure 25. Concluded.

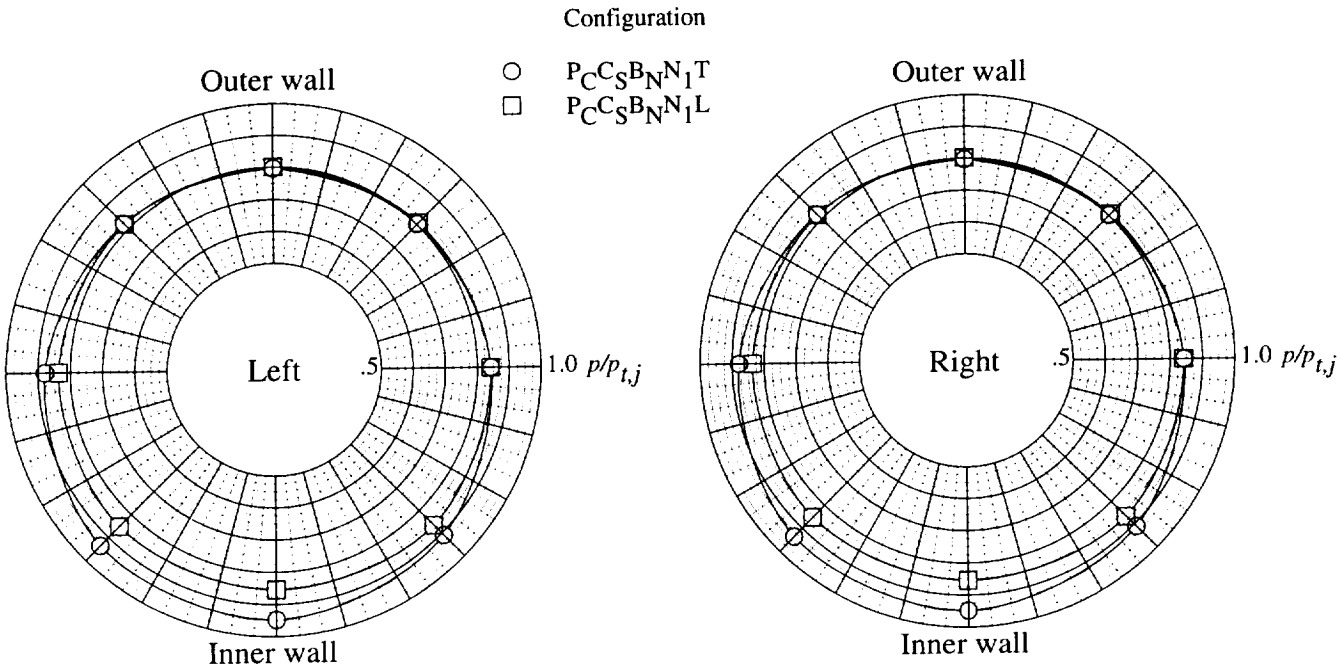

(a) Short-core centerbody with no blocker.

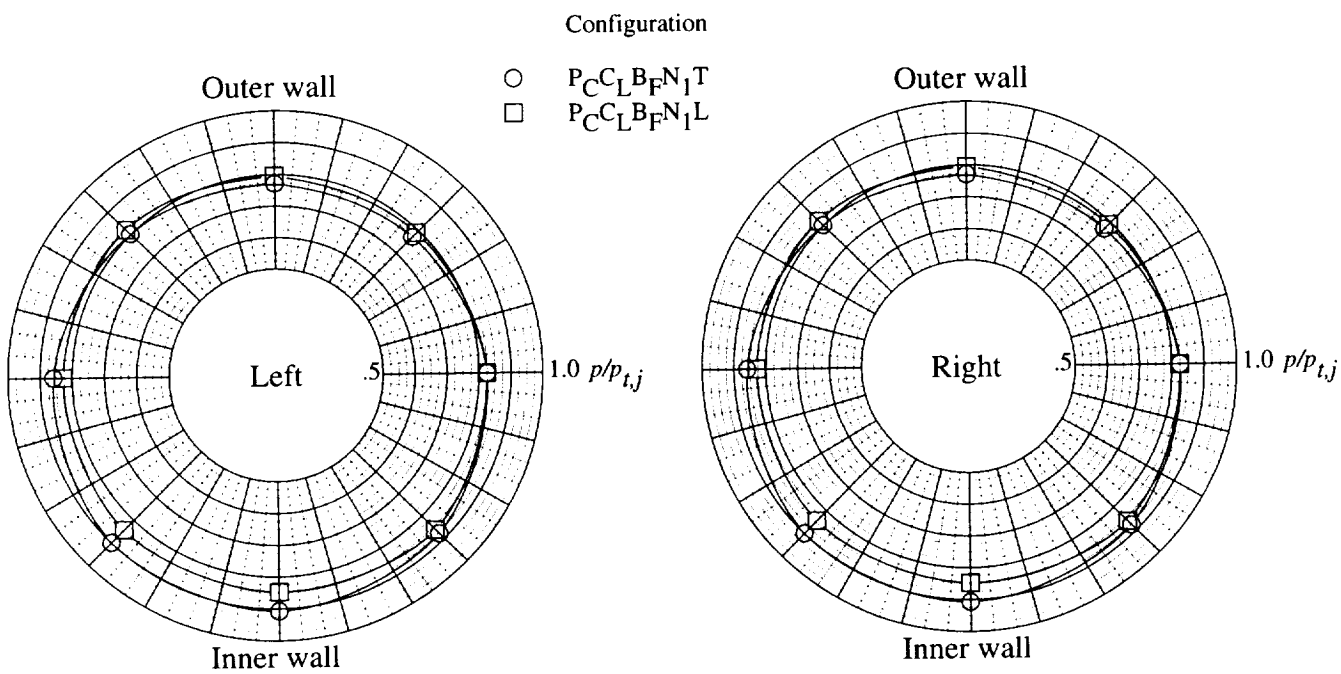

(b) Long-core centerbody with flat blocker.

Figure 26. Effect of operation mode on offtake duct static-pressure ratios $p/p_{t,j}$ for centerline plenum with 1.8 CR D-shaped nozzles. Nominal NPR = 4.0.

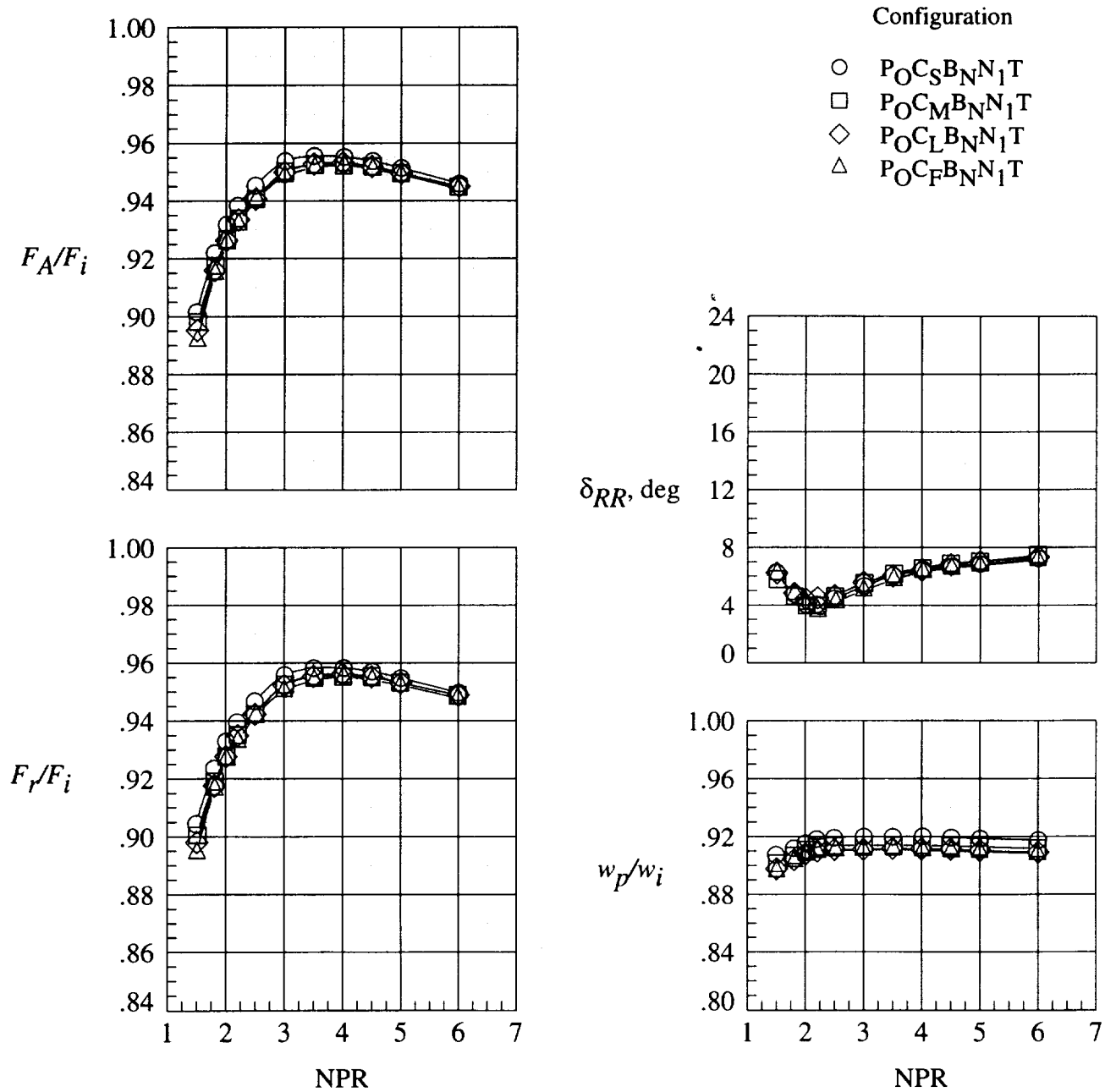

(a) No blocker.

Figure 27. Effect of centerbody type on performance of 1.8 CR D-shaped nozzles in thrust mode installed on offset plenum.

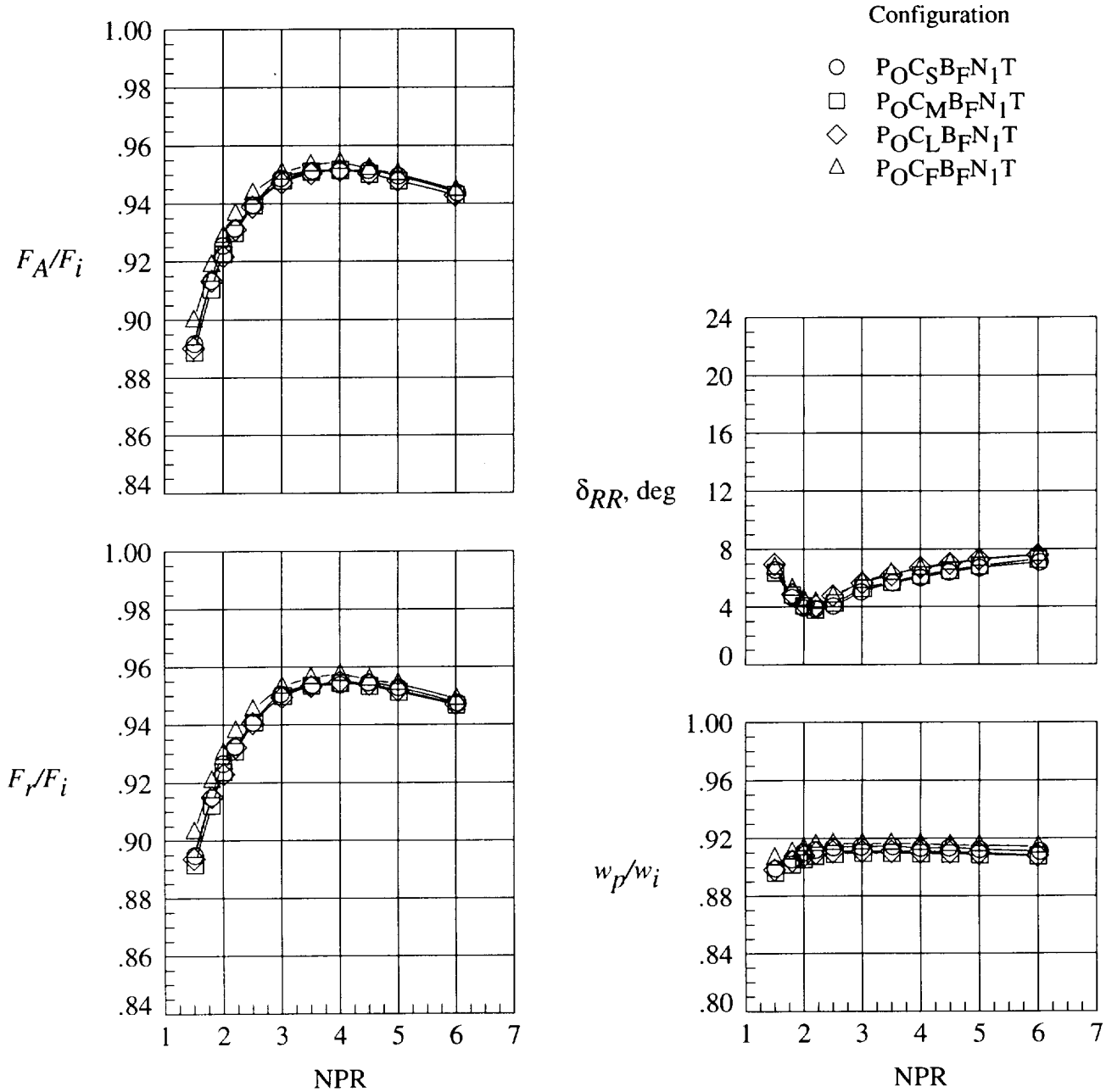

(b) Flat blocker.

Figure 27. Continued.

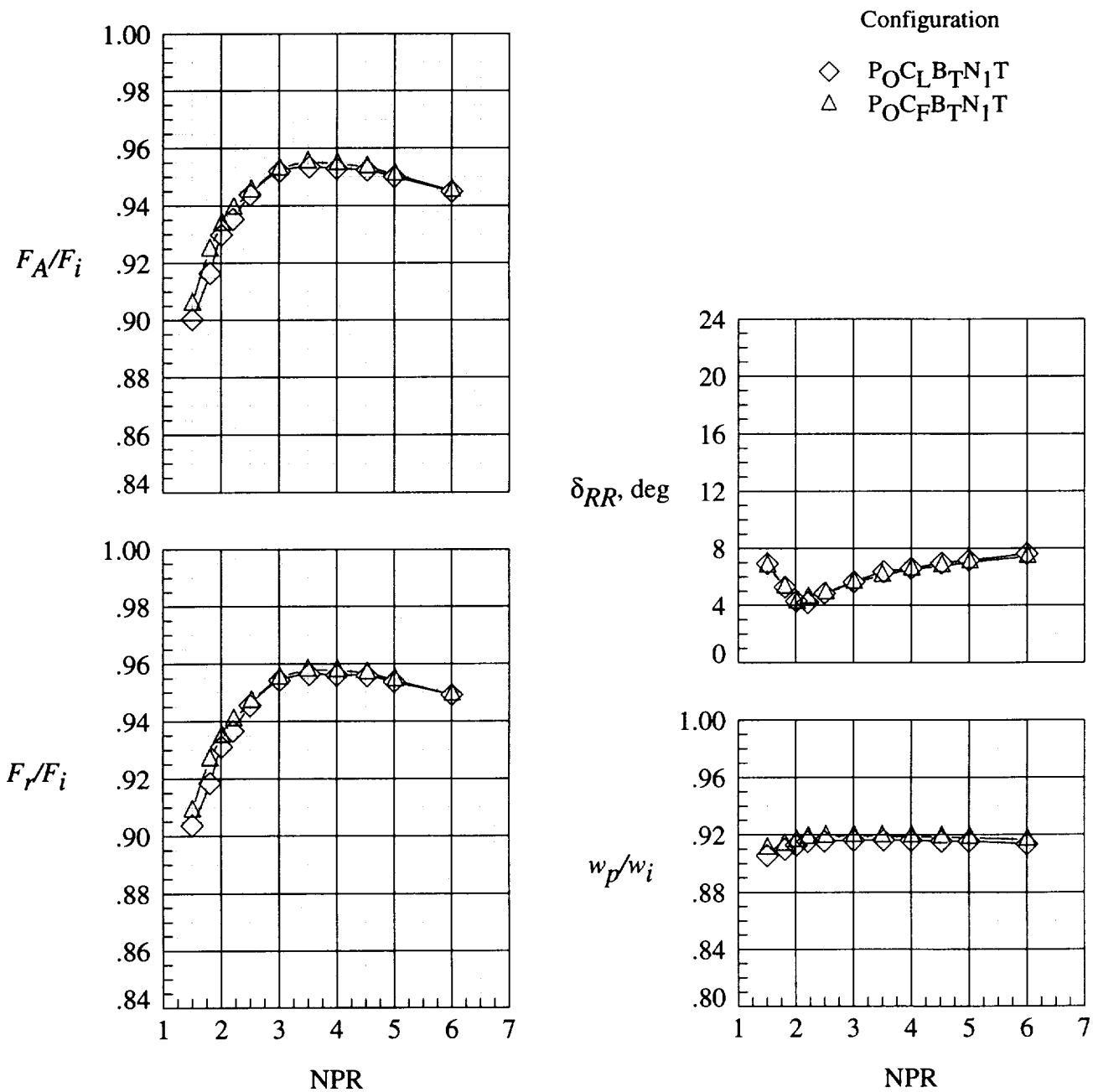

(c) Tapered blocker.

Figure 27. Concluded.

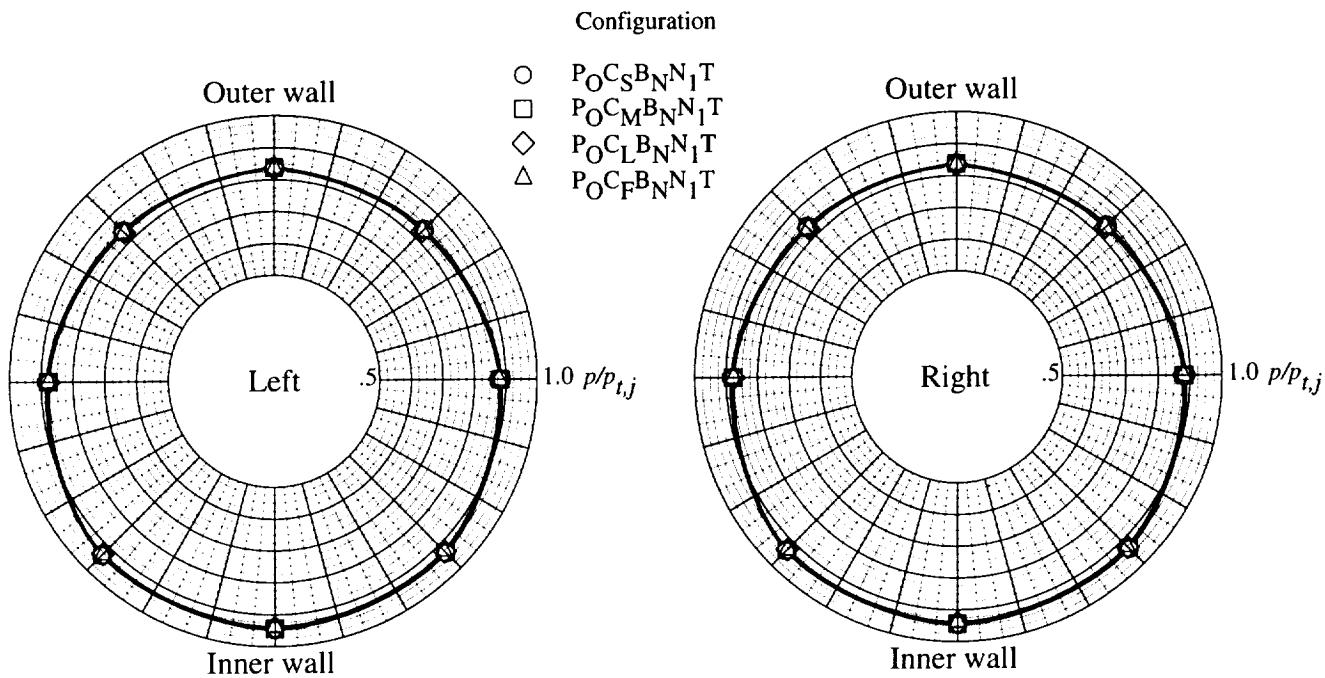

(a) No blocker.

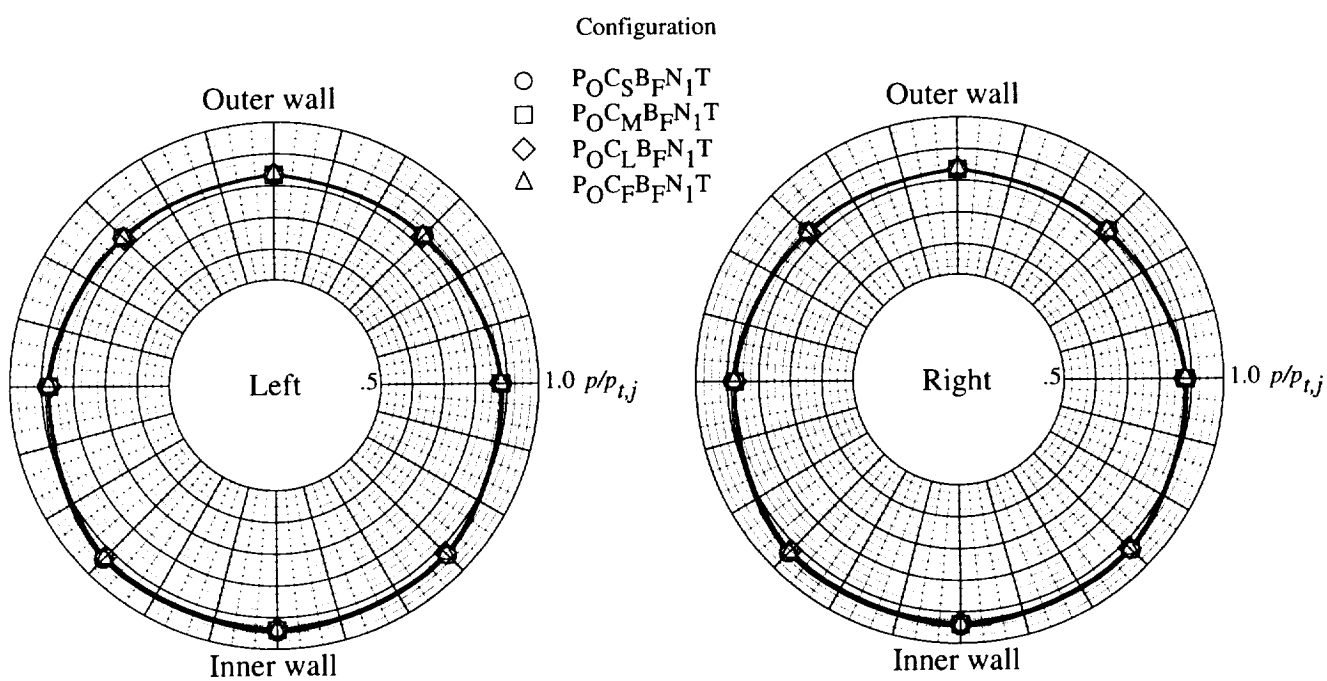

(b) Flat blocker.

Figure 28. Effect of centerbody type on offtake duct static-pressure ratios $p/p_{t,j}$ for offset plenum with 1.8 CR D-shaped nozzles in thrust mode. Nominal NPR = 4.0.

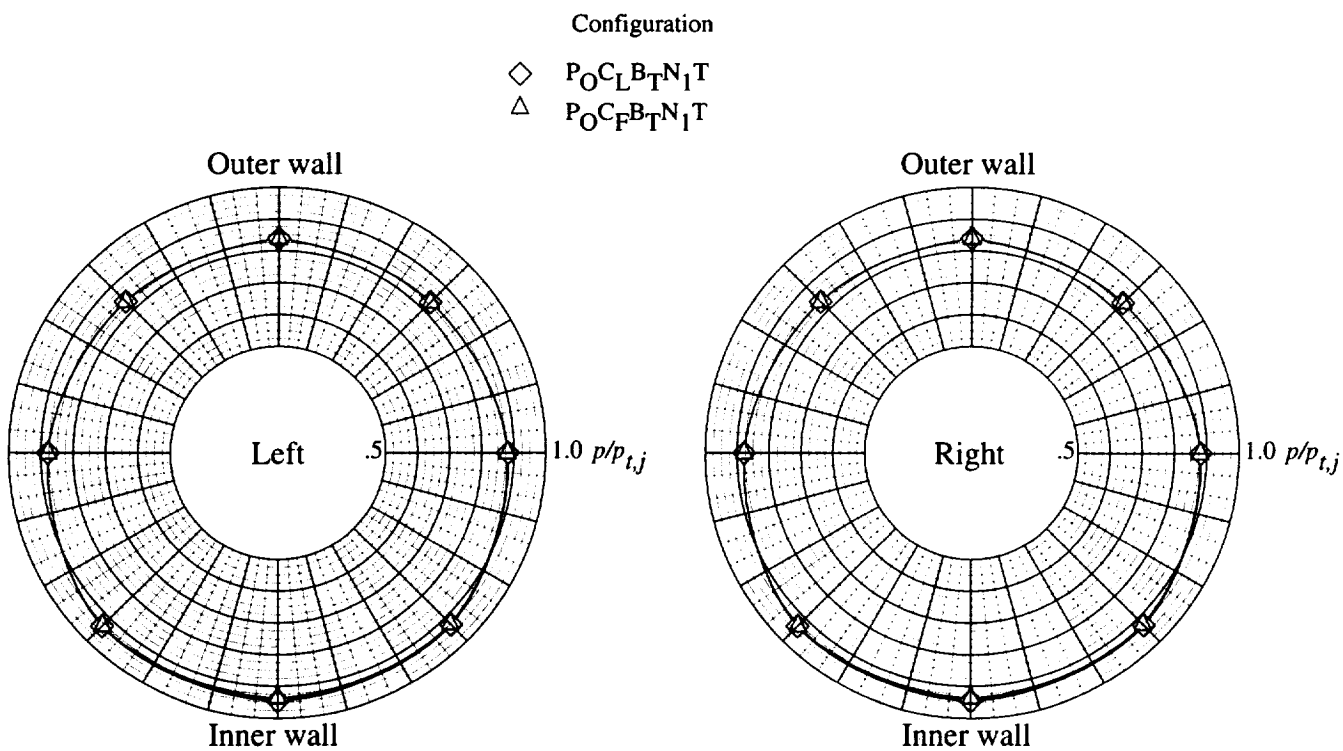

(c) Tapered blocker.

Figure 28. Concluded.

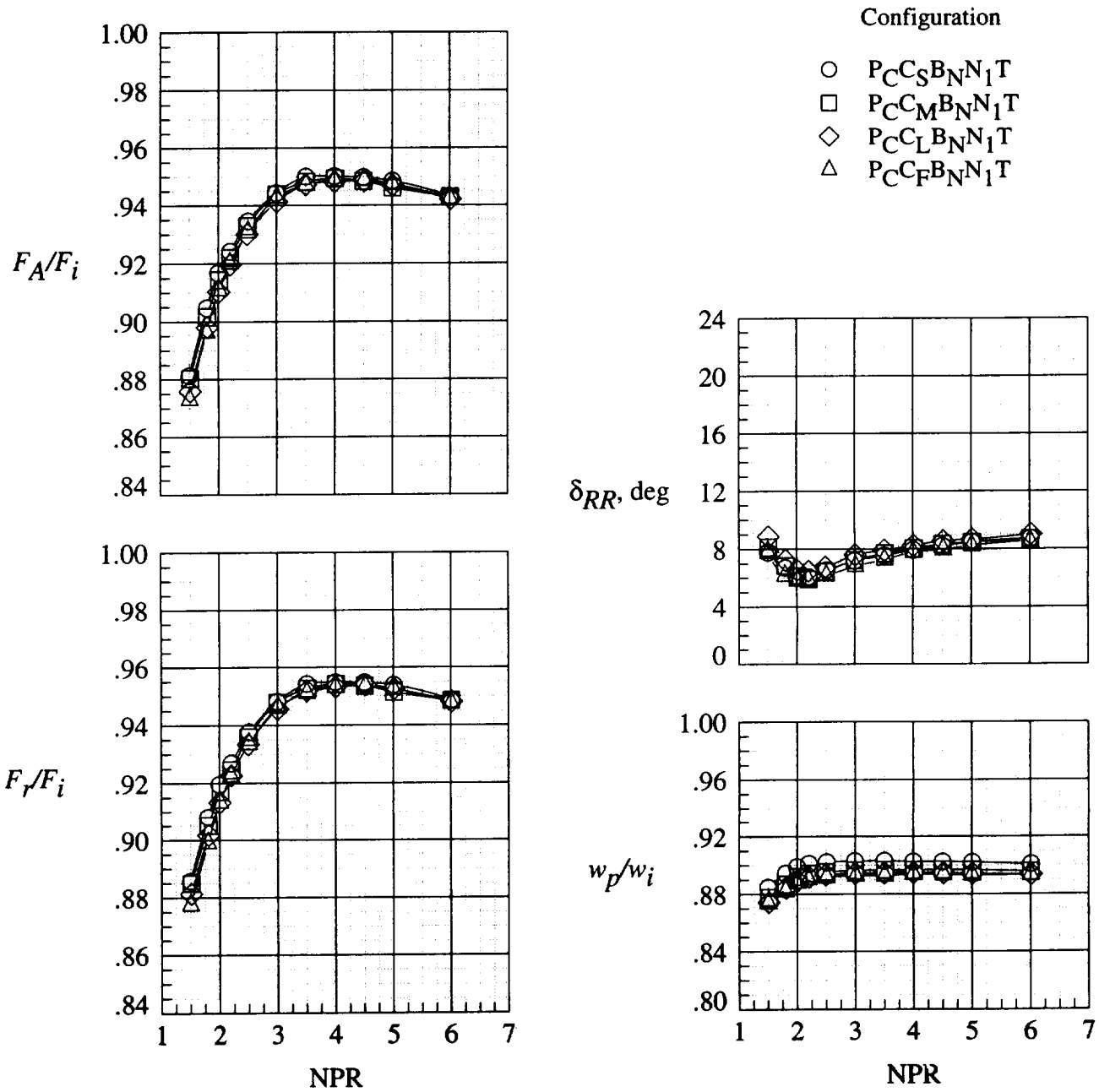

(a) No blocker.

Figure 29. Effect of centerbody type on performance of 1.8 CR D-shaped nozzles in thrust mode installed on centerline plenum.

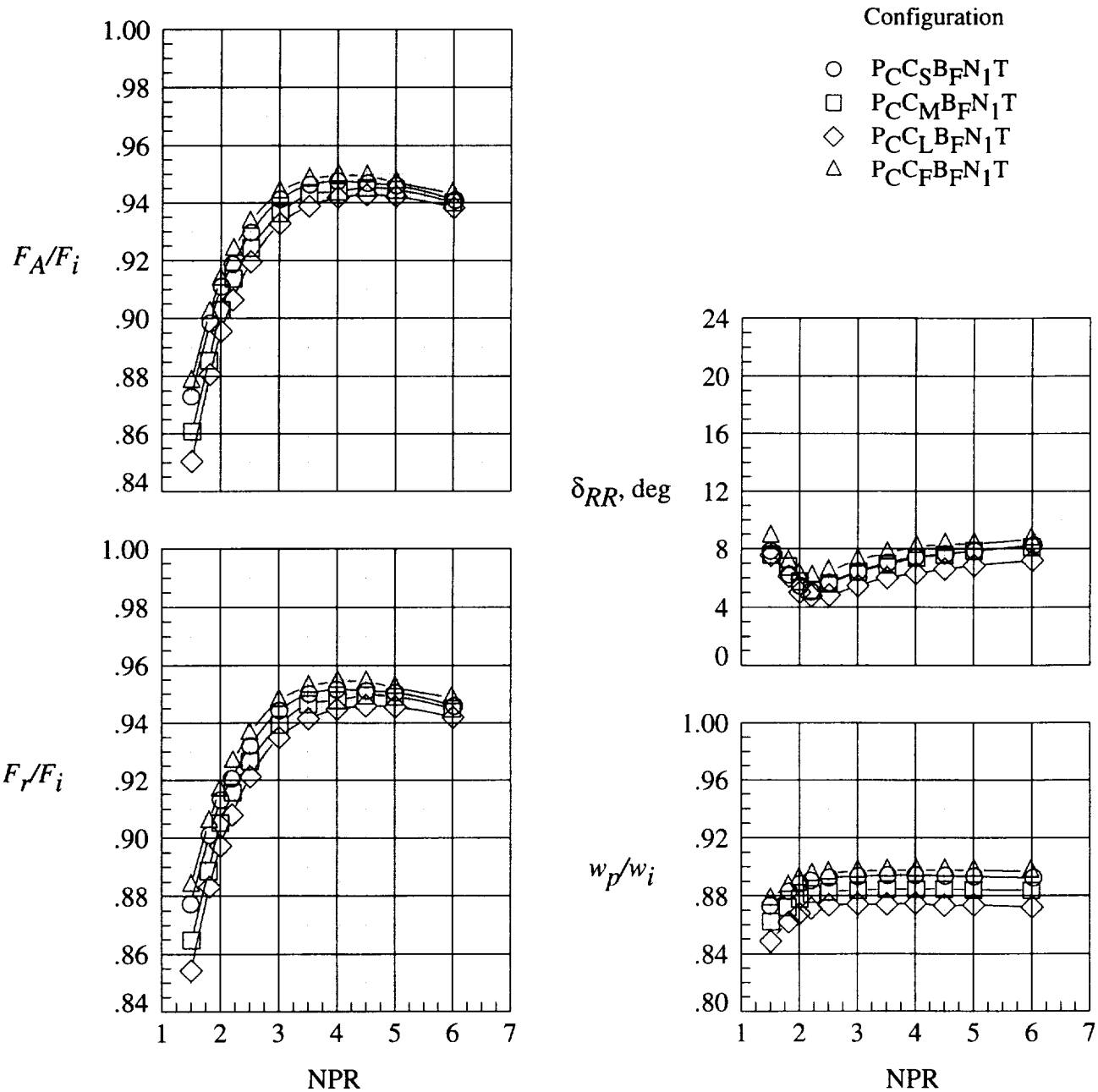

(b) Flat blocker.

Figure 29. Continued.

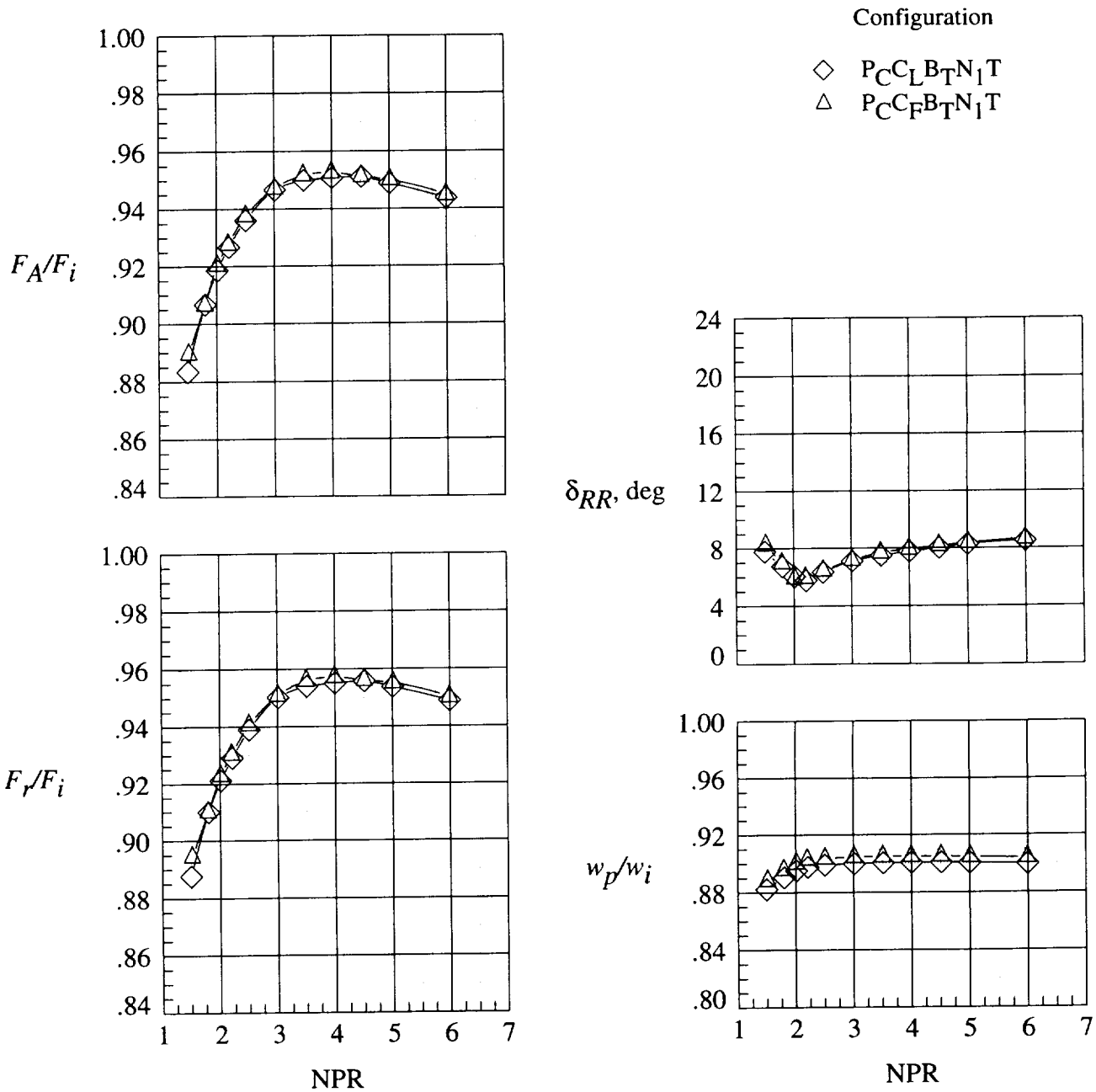

(c) Tapered blocker.

Figure 29. Concluded.

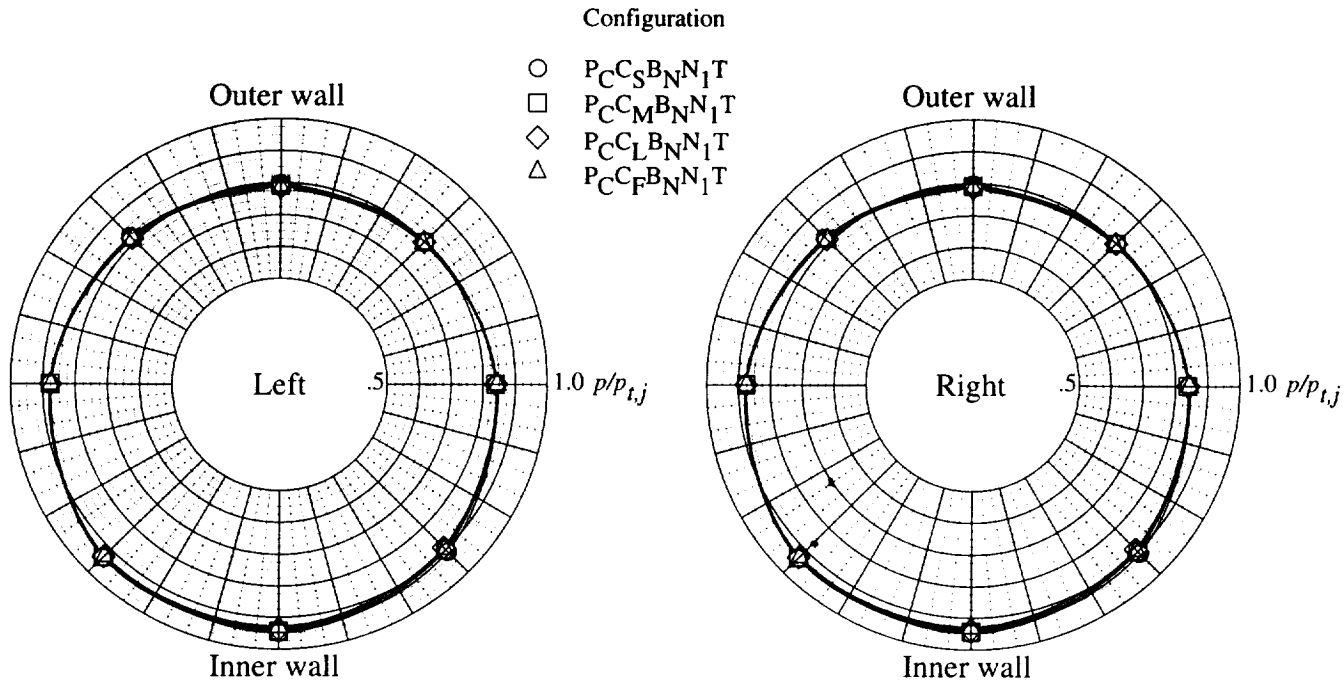

(a) No blocker.

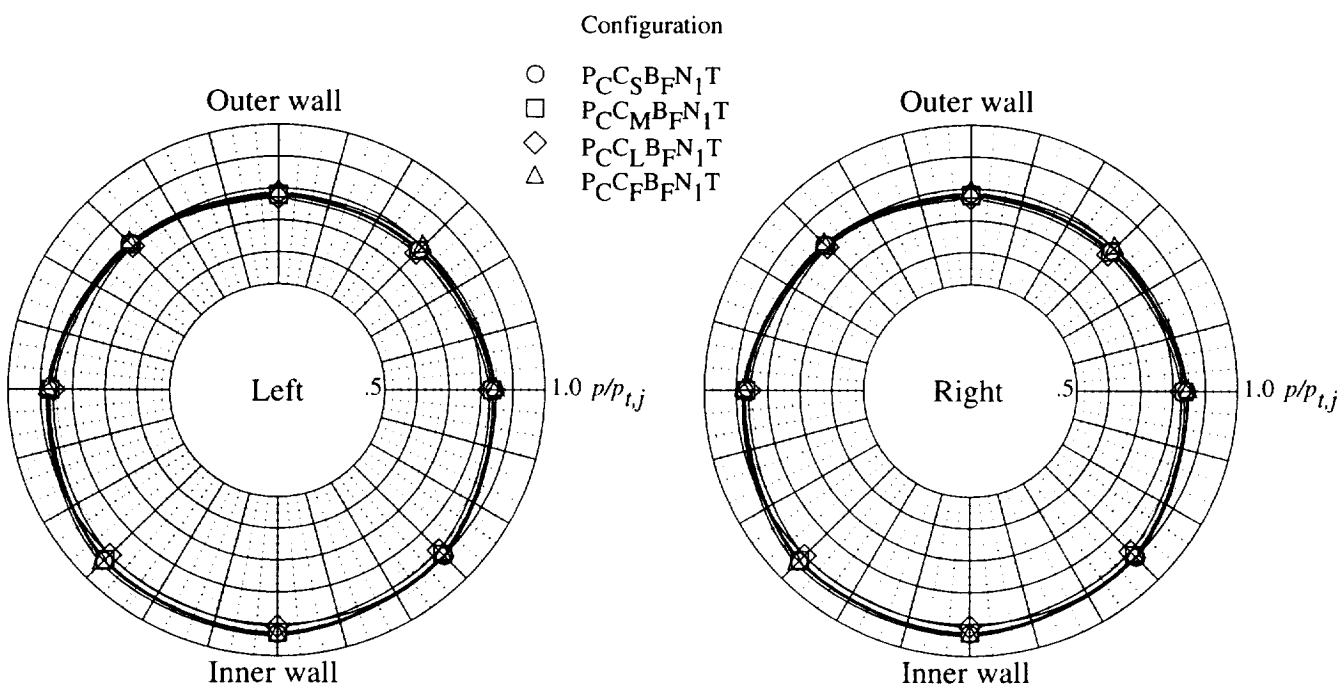

(b) Flat blocker.

Figure 30. Effect of centerbody type on offtake duct static-pressure ratios $p/p_{t,j}$ for centerline plenum with 1.8 CR D-shaped nozzles in thrust mode. Nominal NPR = 4.0.

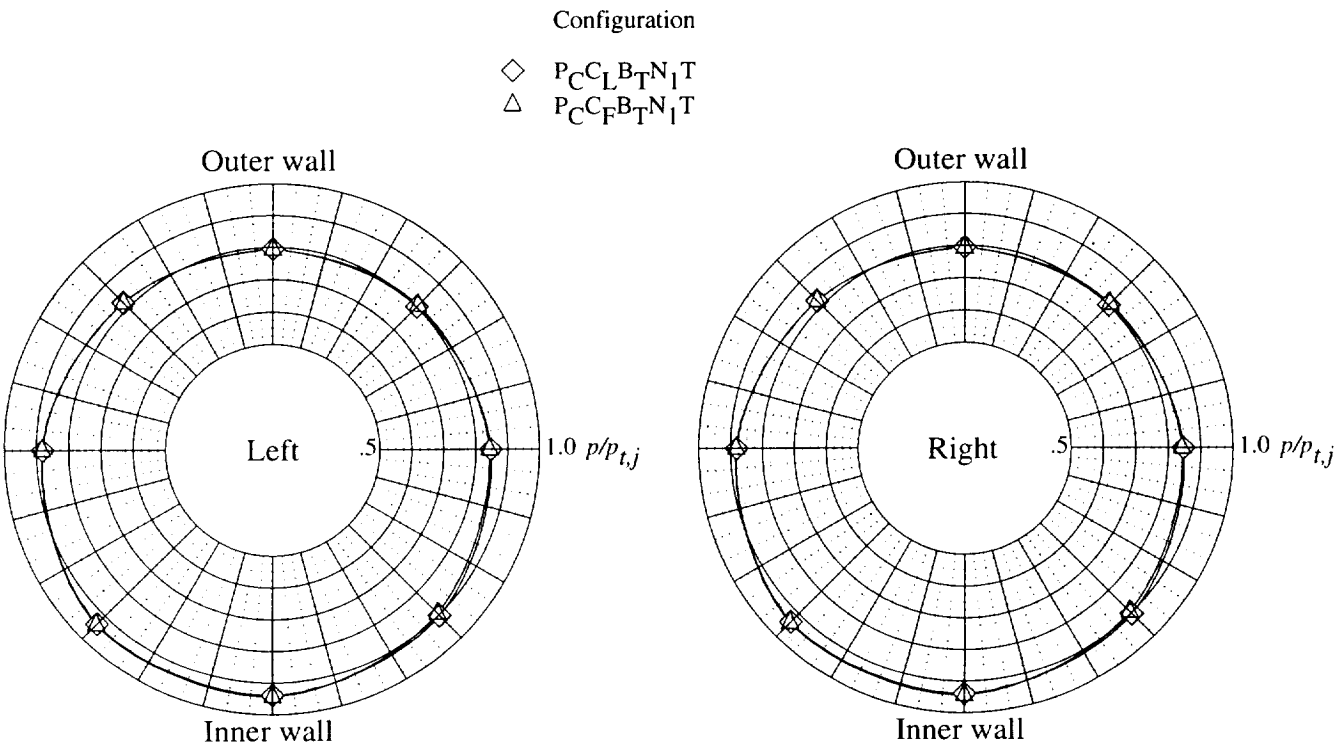

(c) Tapered blocker.

Figure 30. Concluded.

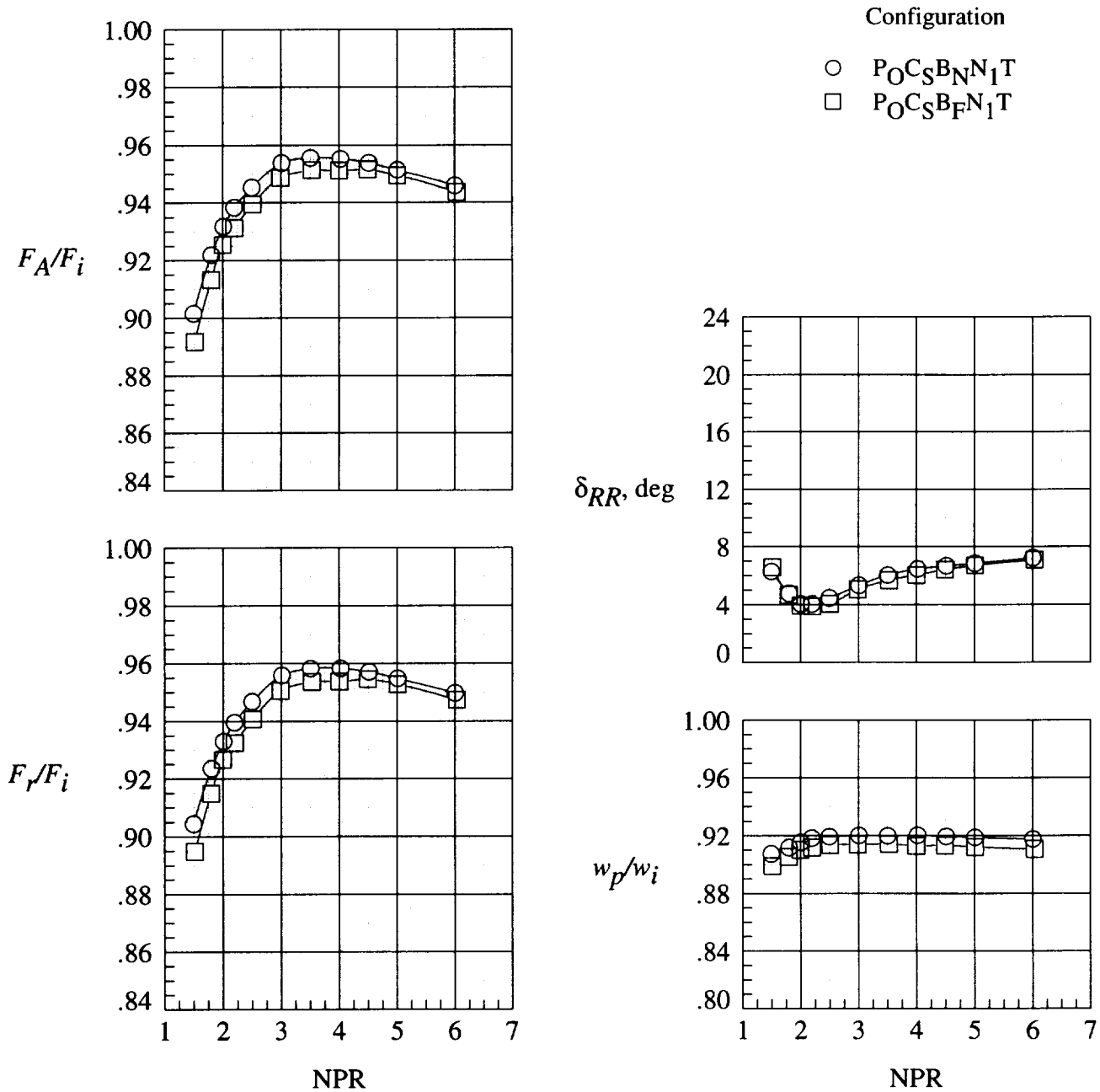

(a) Short-core centerbody.

Figure 31. Effect of blocker geometry on performance of 1.8 CR D-shaped nozzles in thrust mode installed on offset plenum.

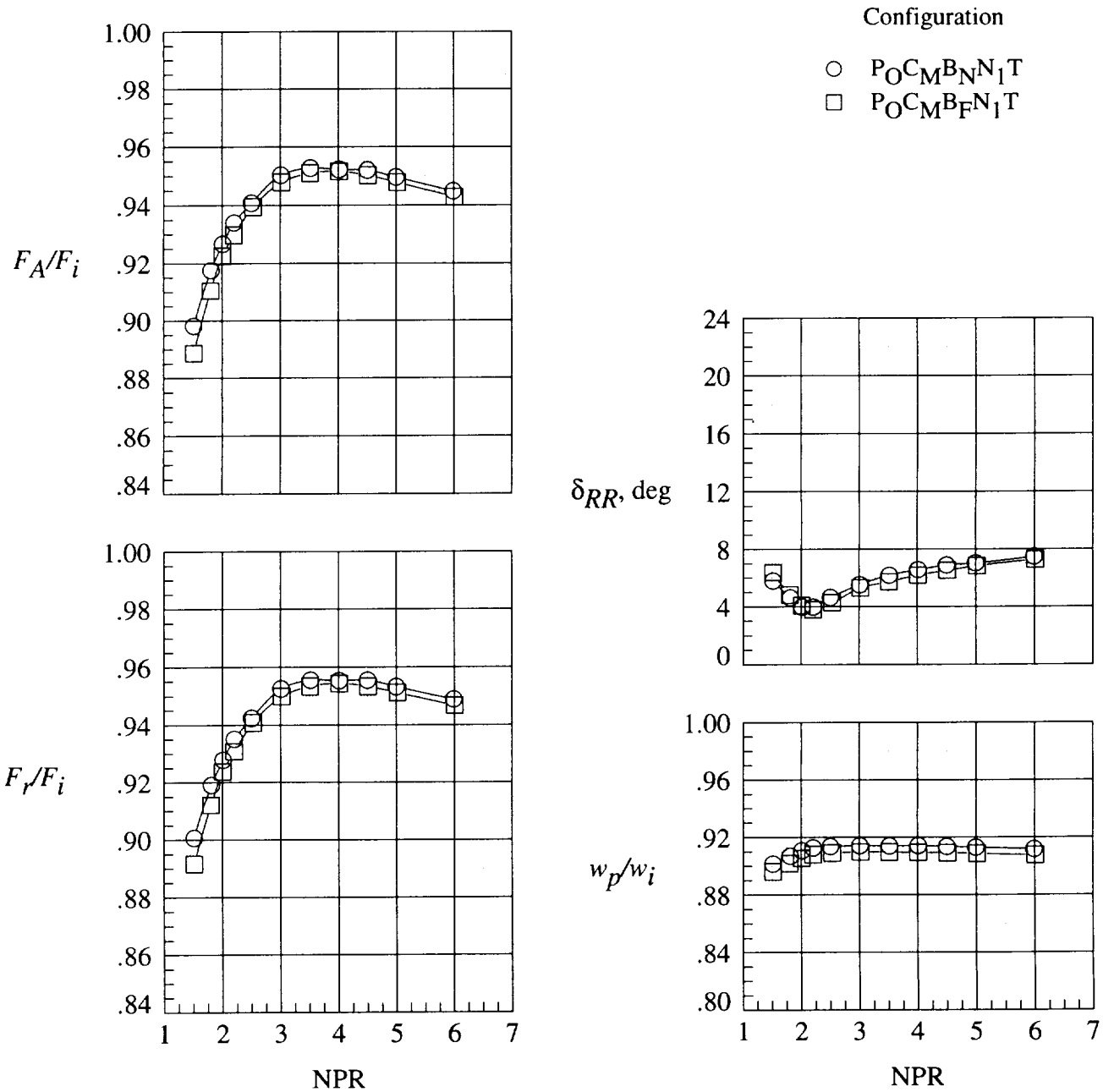

(b) Medium-core centerbody.

Figure 31. Continued.

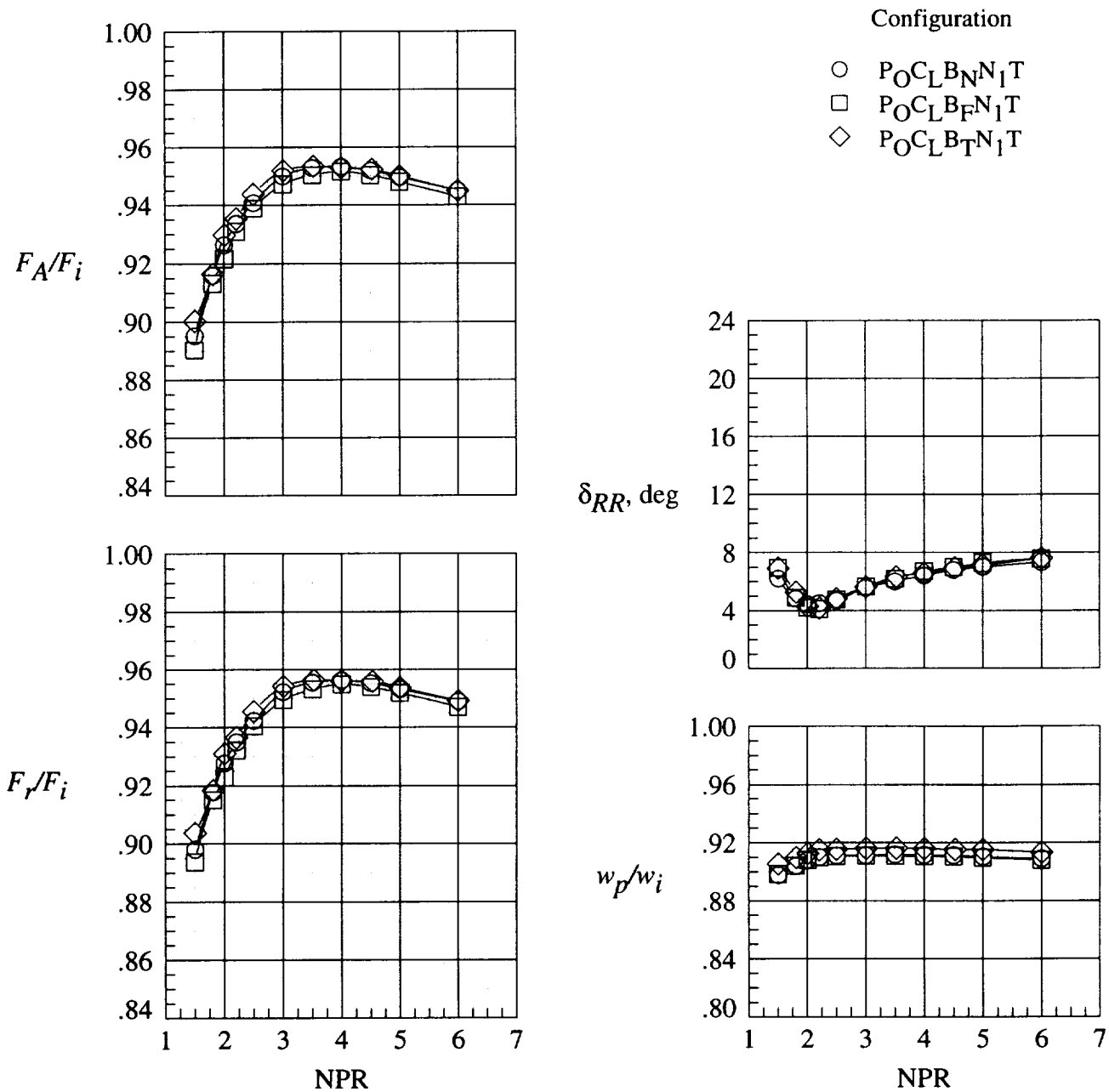

(c) Long-core centerbody.

Figure 31. Continued.

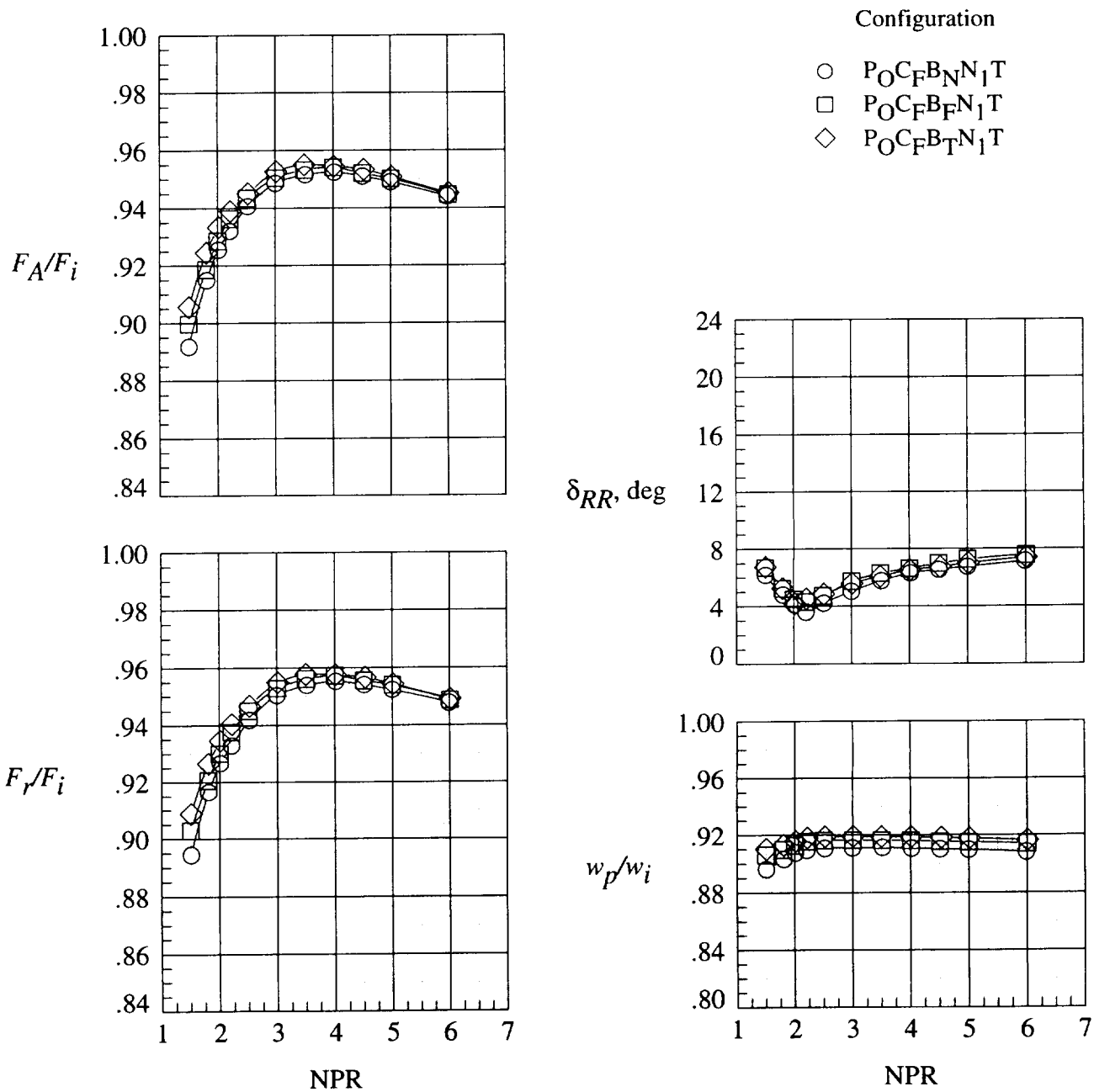

(d) Fan centerbody.

Figure 31. Concluded.

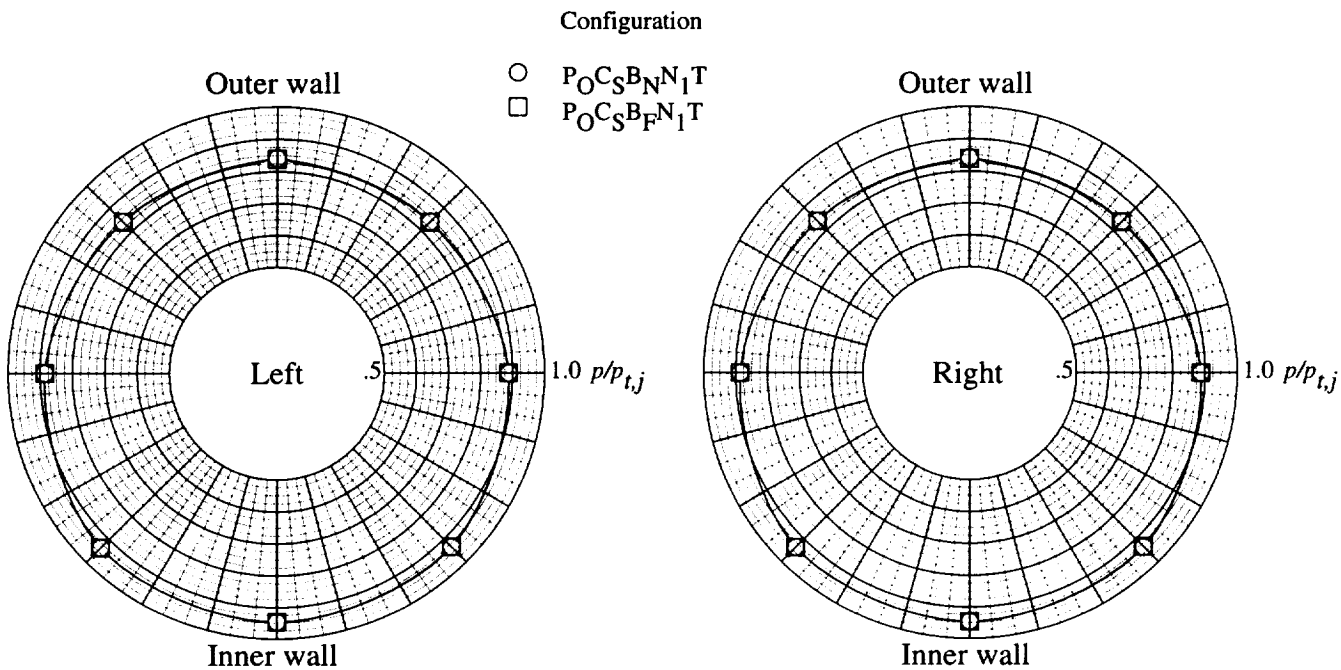

(a) Short-core centerbody.

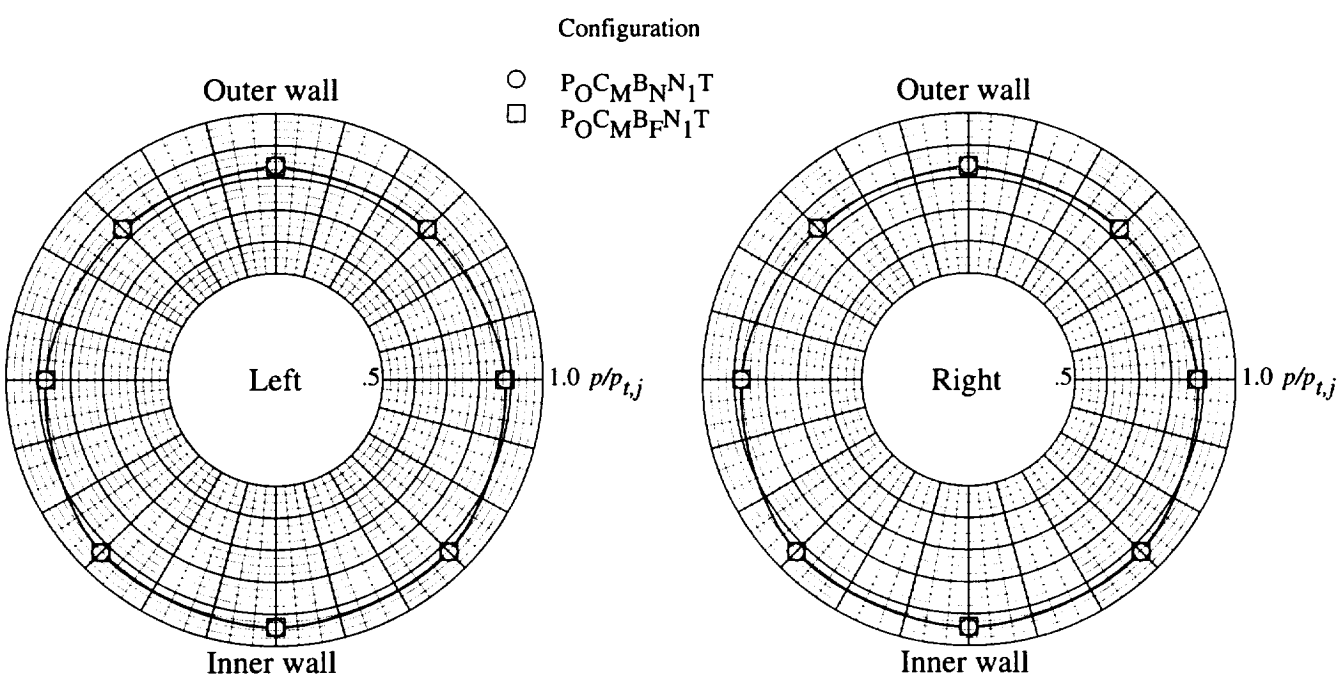

(b) Medium-core centerbody.

Figure 32. Effect of blocker geometry on offtake duct static-pressure ratios $p/p_{t,j}$ for offset plenum with 1.8 CR D-shaped nozzles in thrust mode. Nominal NPR = 4.0.

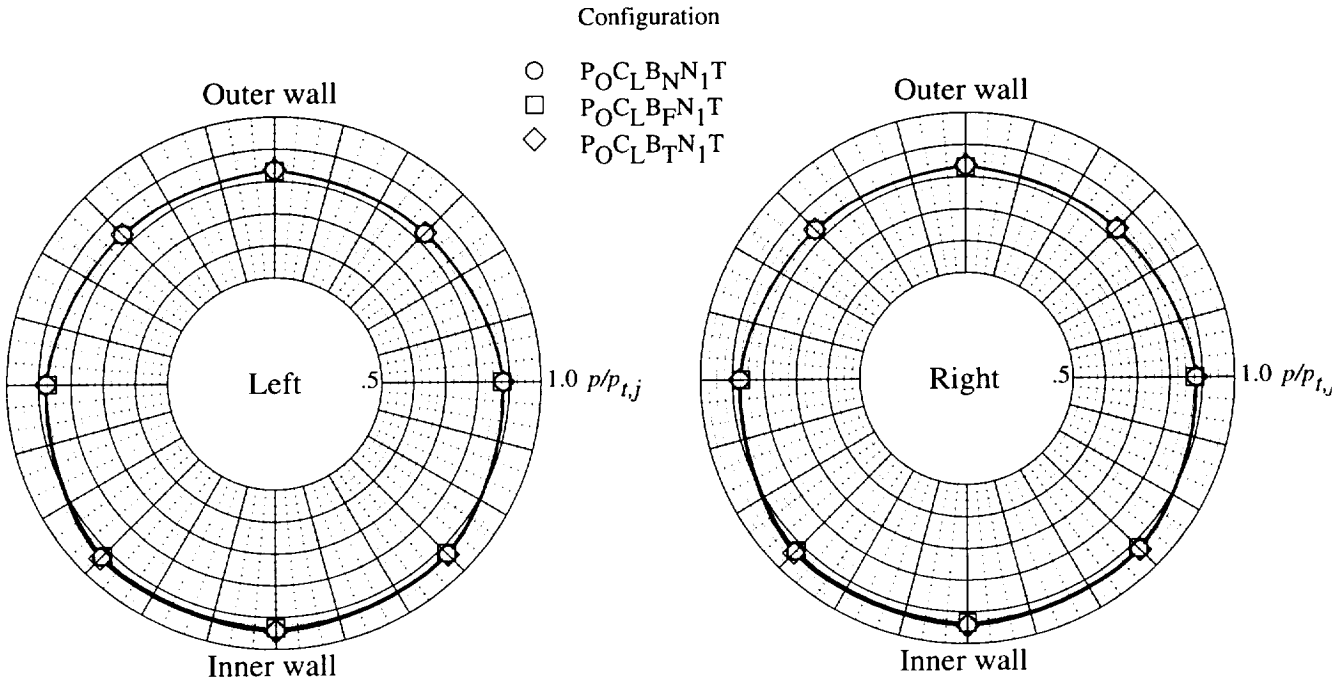

(c) Long-core centerbody.

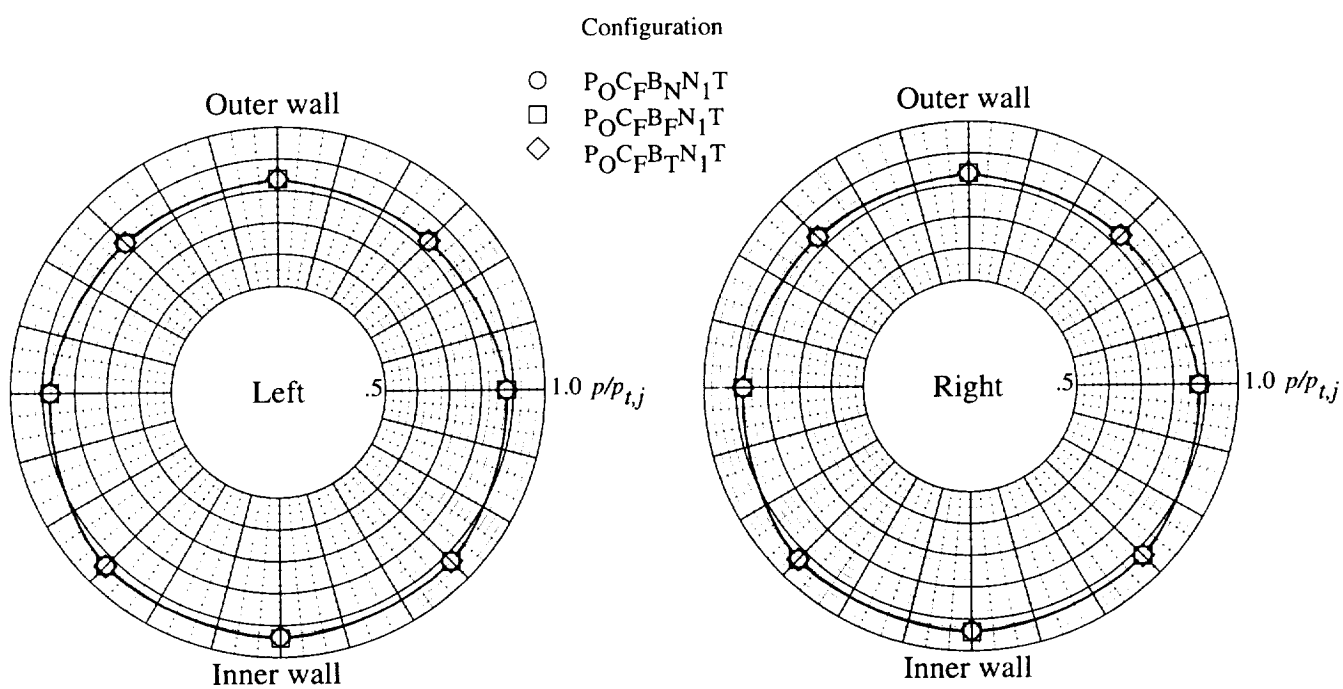

(d) Fan centerbody.

Figure 32. Concluded.

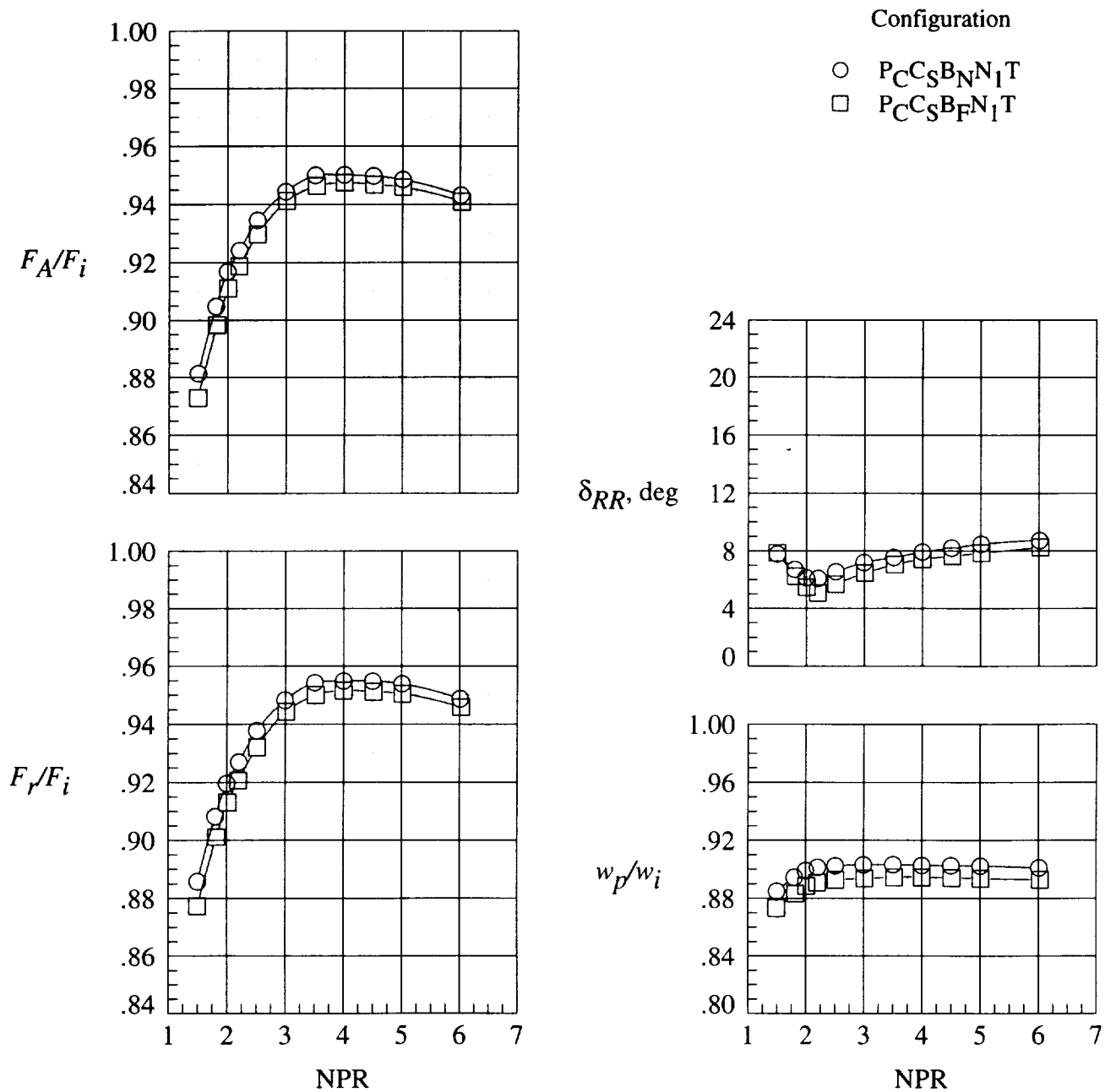

(a) Short-core centerbody.

Figure 33. Effect of blocker geometry on performance of 1.8 CR D-shaped nozzles in thrust mode installed on centerline plenum.

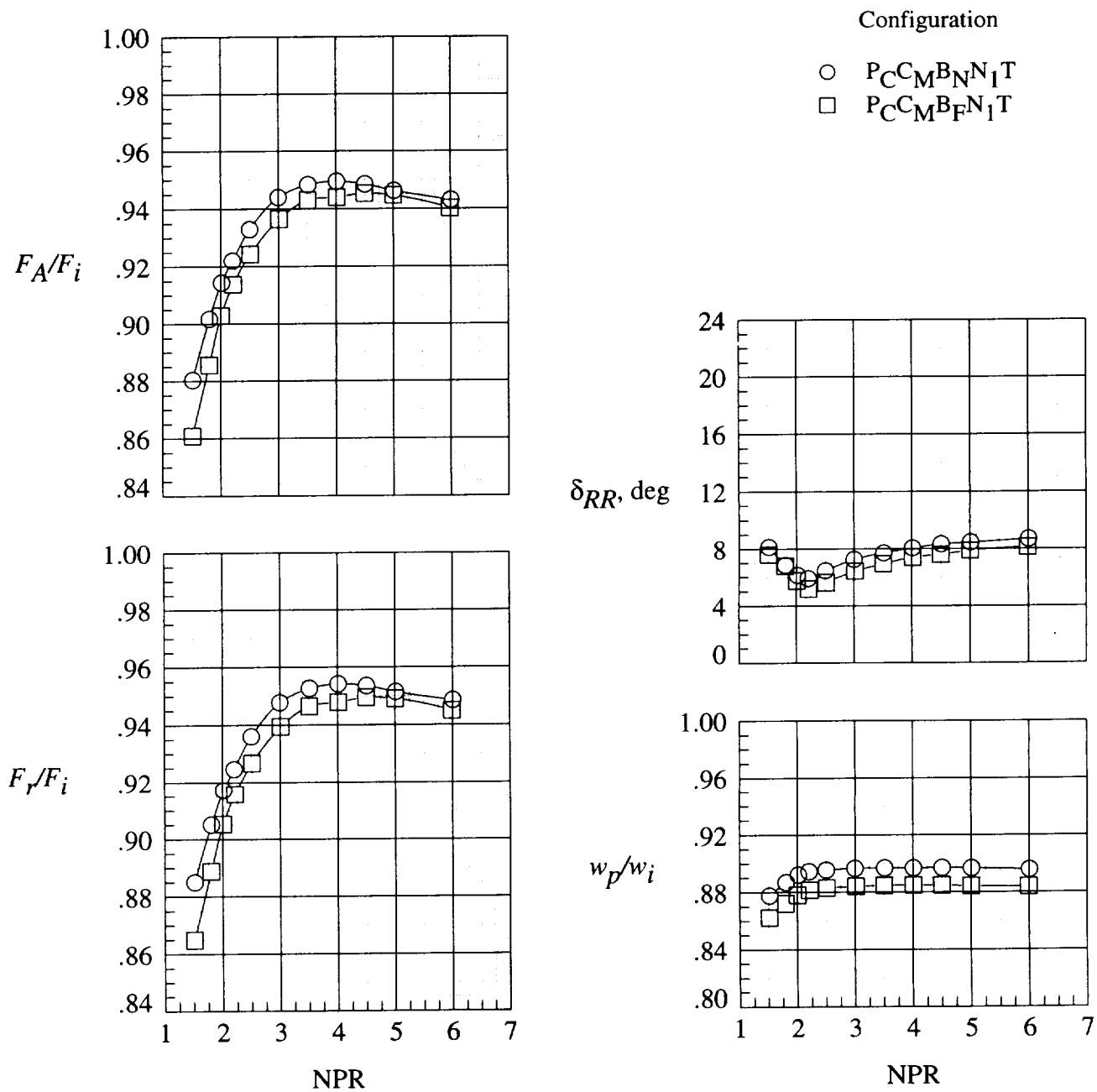

(b) Medium-core centerbody.

Figure 33. Continued.

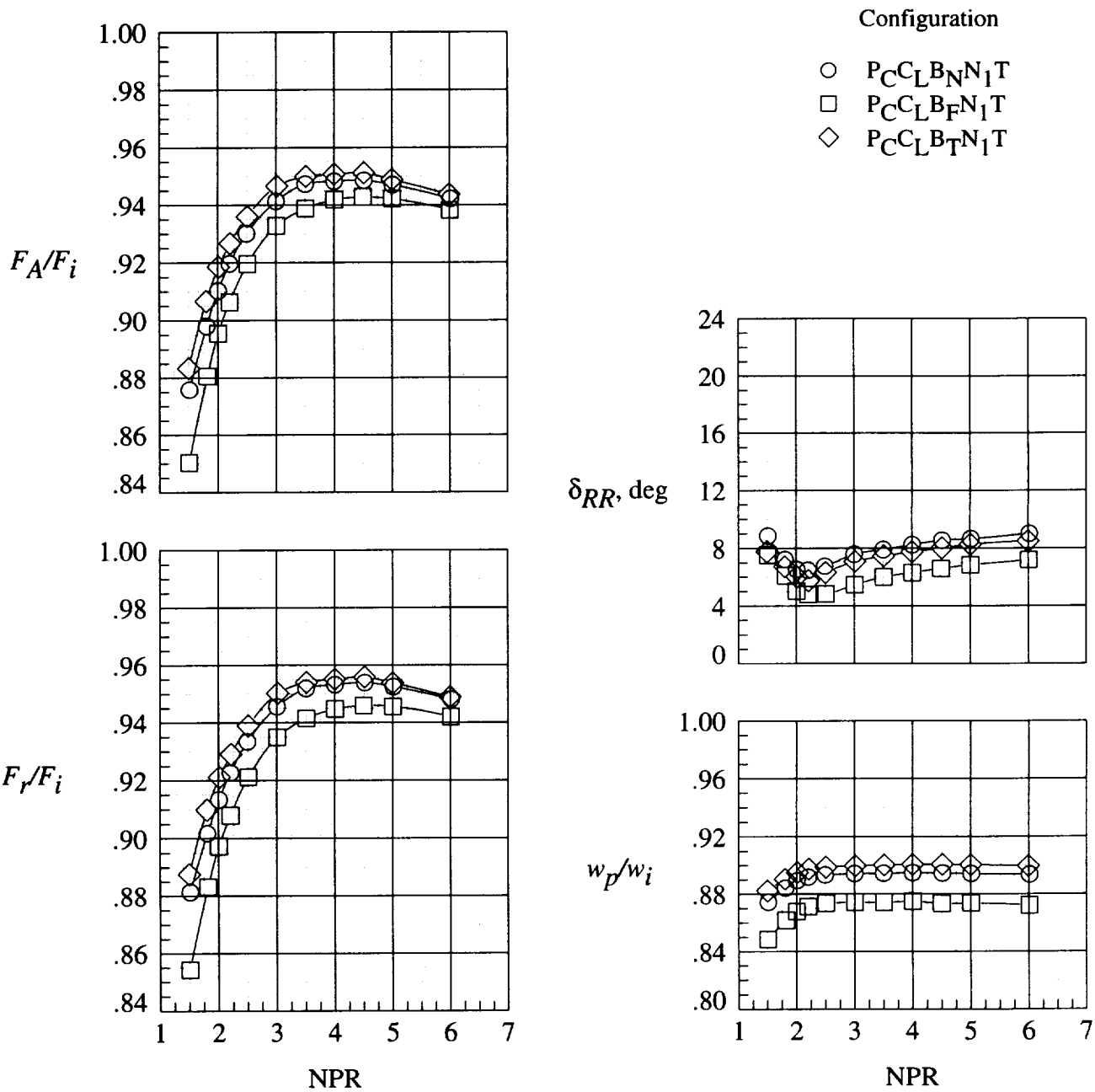

(c) Long-core centerbody.

Figure 33. Continued.

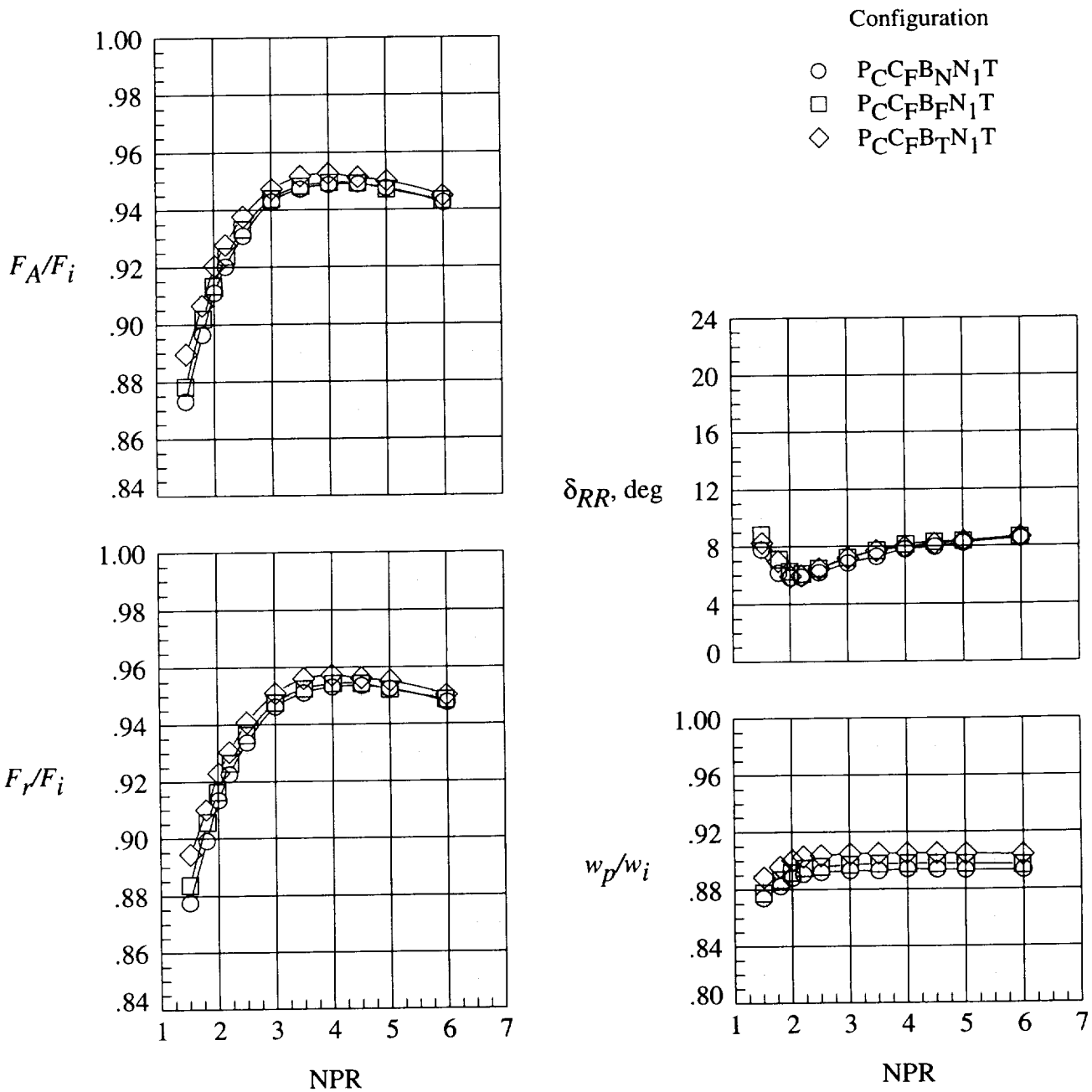

(d) Fan centerbody.

Figure 33. Concluded.

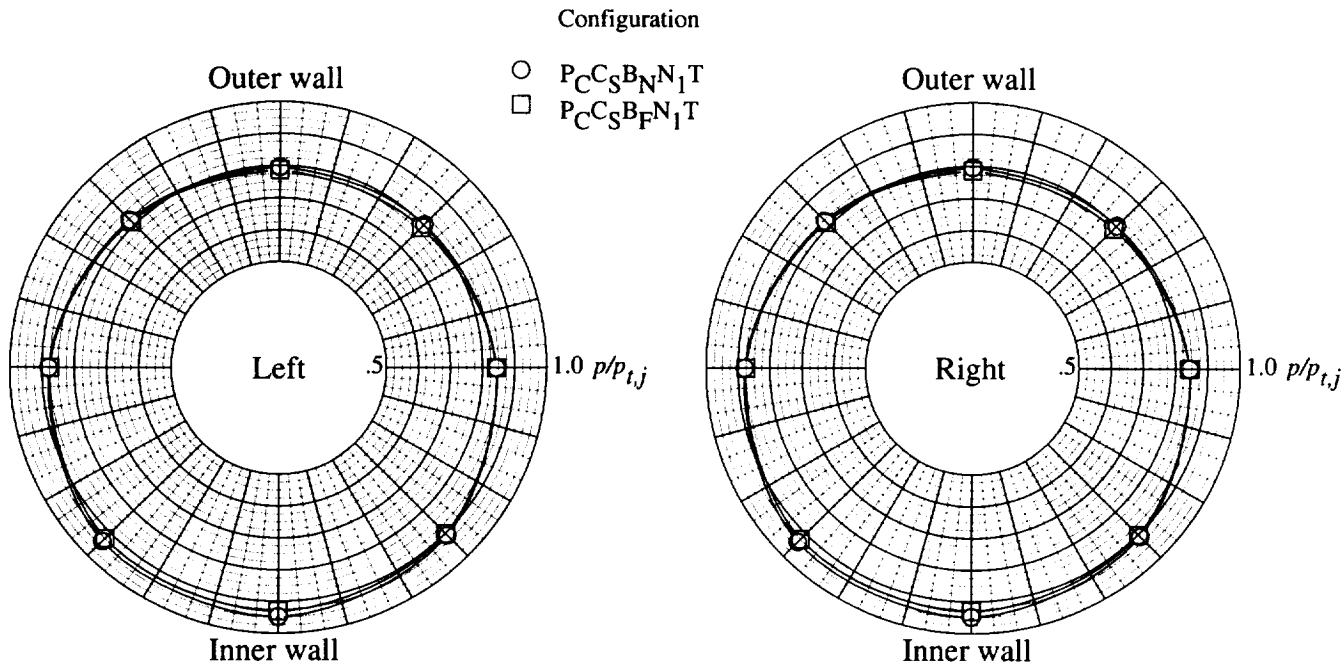

(a) Short-core centerbody.

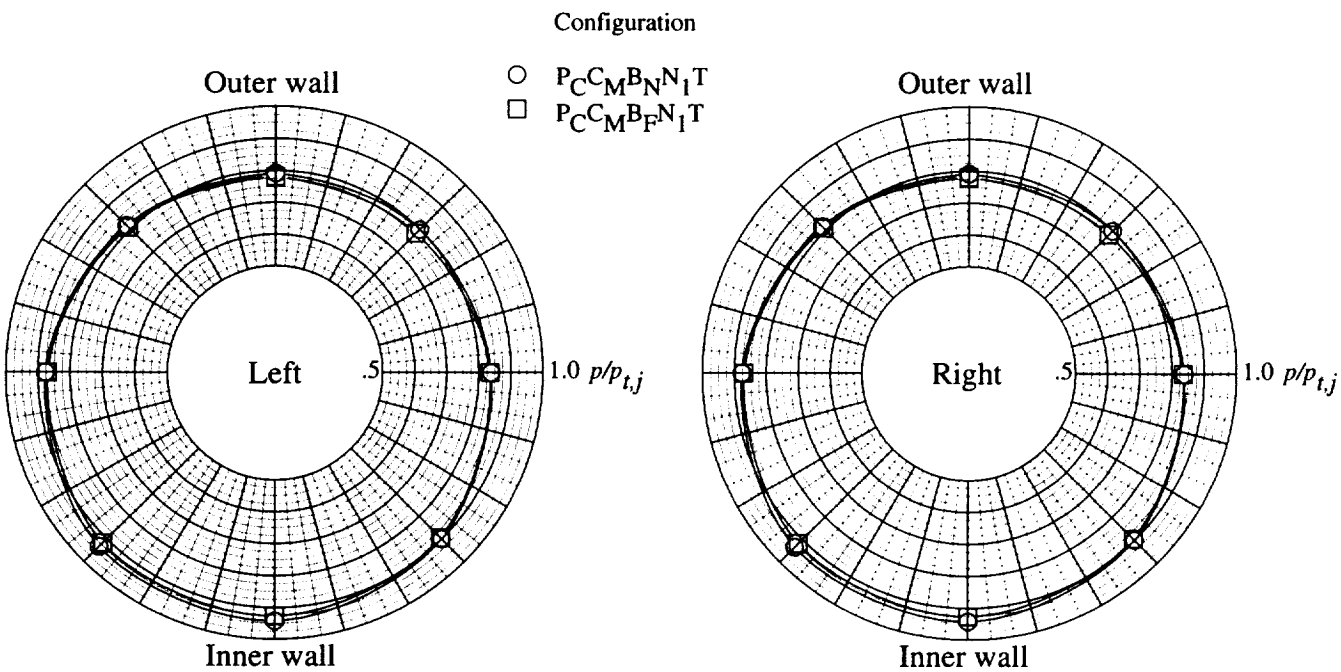

(b) Medium-core centerbody.

Figure 34. Effect of blocker geometry on offtake duct static-pressure ratios $p/p_{t,j}$ for centerline plenum with 1.8 CR D-shaped nozzles in thrust mode. Nominal NPR = 4.0.

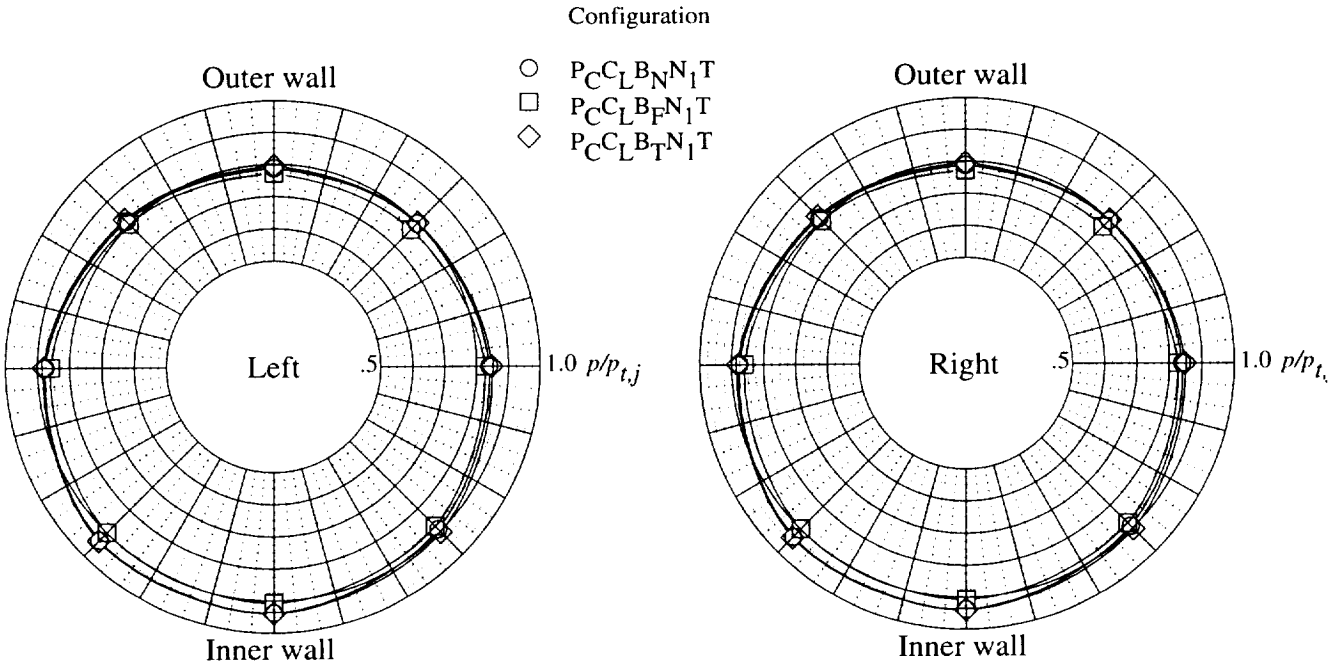

(c) Long-core centerbody.

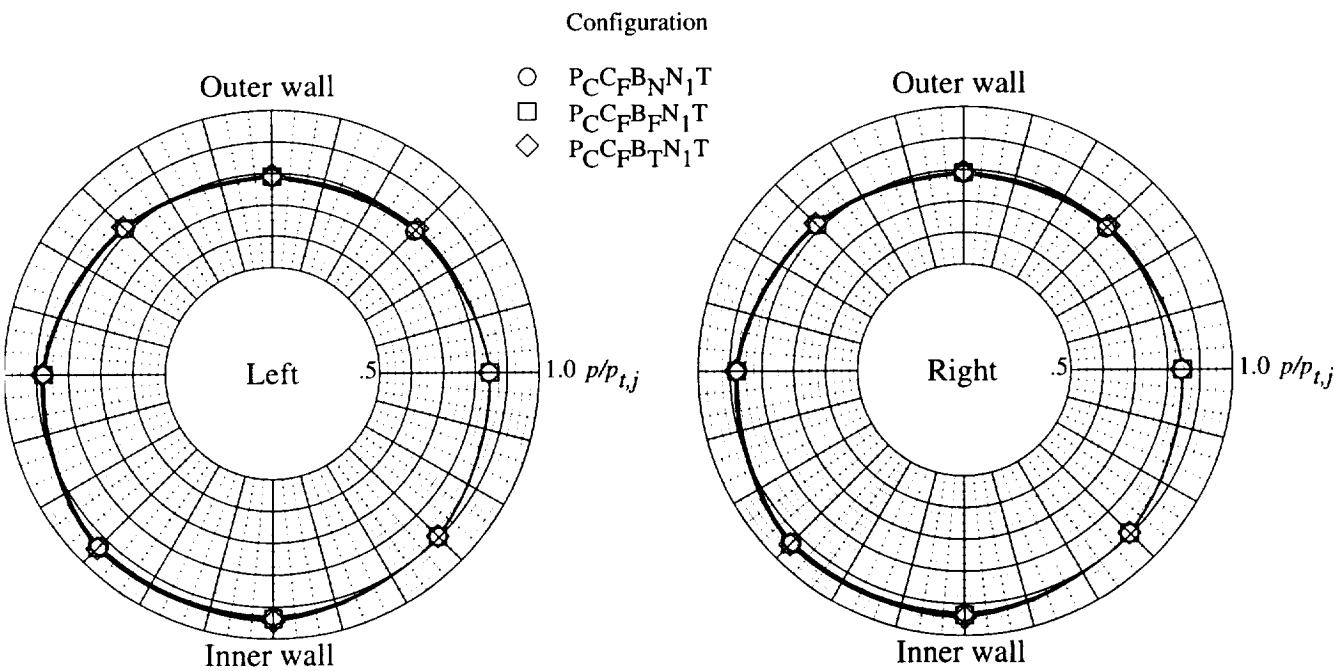

(d) Fan centerbody.

Figure 34. Concluded.

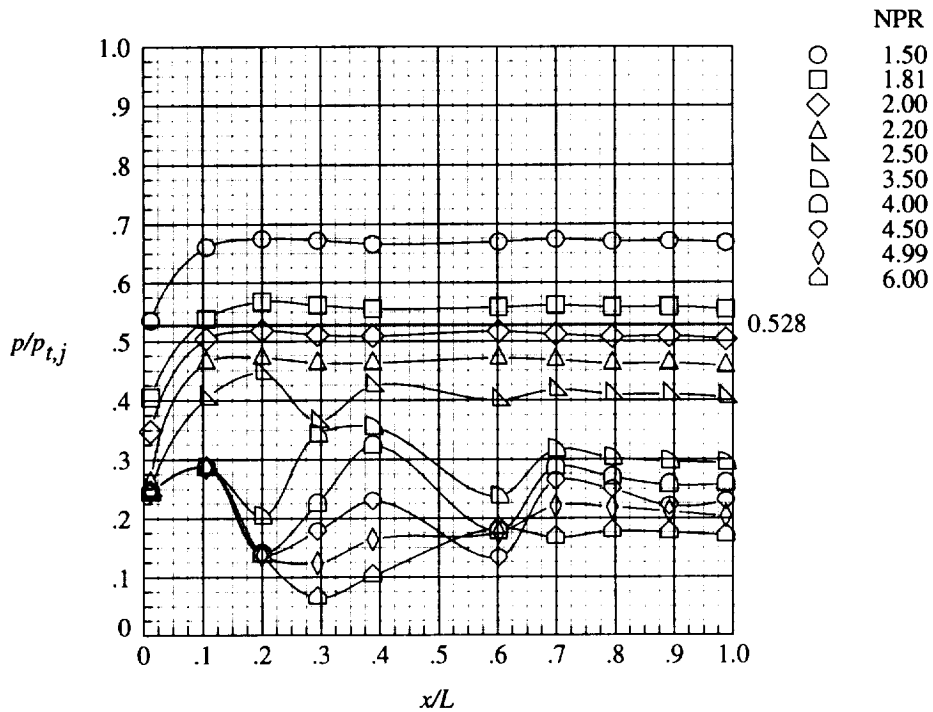

(a) No blocker.

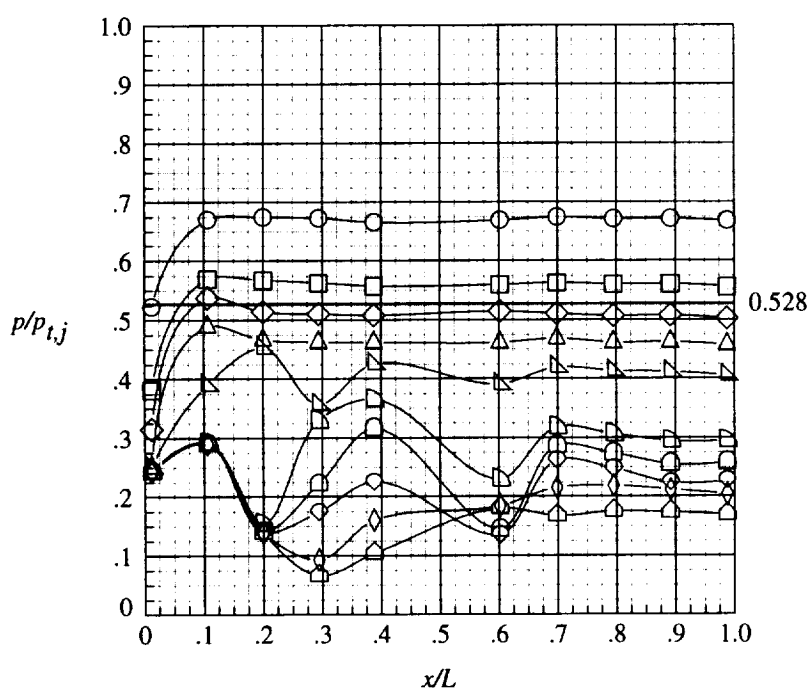

(b) Flat blocker.

Figure 35. Instrumented-ramp static-pressure ratios $p/p_{t,j}$ for 1.4 CR submerged nozzles in thrust mode installed on offset plenum with fan centerbody.

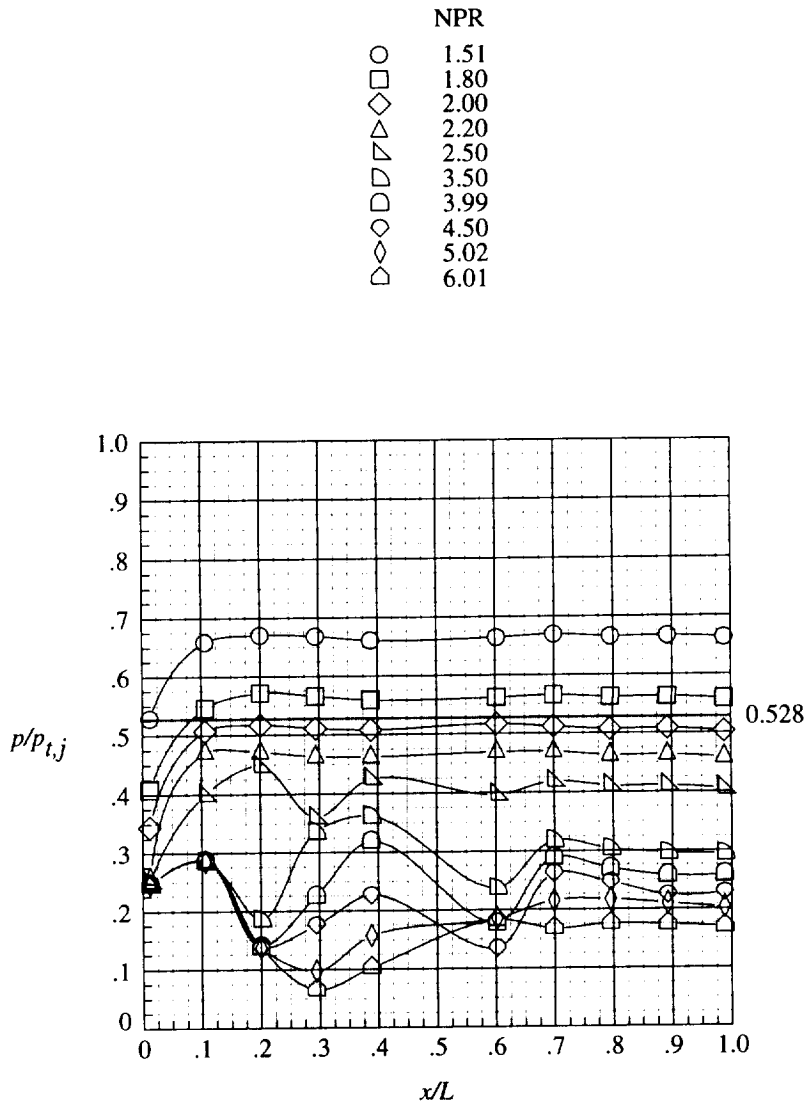

(c) Tapered blocker.

Figure 35. Concluded.

REPORT DOCUMENTATION PAGE

Form Approved
OMB No. 0704-0188

Public reporting burden for this collection of information is estimated to average 1 hour per response, including the time for reviewing instructions, searching existing data sources, gathering and maintaining the data needed, and completing and reviewing the collection of information. Send comments regarding this burden estimate or any other aspect of this collection of information, including suggestions for reducing this burden, to Washington Headquarters Services, Directorate for Information Operations and Reports, 1215 Jefferson Davis Highway, Suite 1204, Arlington, VA 22202-4302, and to the Office of Management and Budget, Paperwork Reduction Project (0704-0188), Washington, DC 20503.

1. AGENCY USE ONLY *(Leave blank)*

2. REPORT DATE
October 1995

3. REPORT TYPE AND DATES COVERED
Technical Paper

4. TITLE AND SUBTITLE
Internal Performance of Highly Integrated Deployable Exhaust Nozzles Applicable to Advanced Short-Takeoff and Vertical-Landing Aircraft

5. FUNDING NUMBERS
WU 505-59-70

6. AUTHOR(S)
Scott C. Asbury, Mary L. Mason, and Milton Lamb

7. PERFORMING ORGANIZATION NAME(S) AND ADDRESS(ES)
NASA Langley Research Center
Hampton, VA 23681-0001

8. PERFORMING ORGANIZATION REPORT NUMBER
L-17467

9. SPONSORING/MONITORING AGENCY NAME(S) AND ADDRESS(ES)
National Aeronautics and Space Administration
Washington, DC 20546-0001

10. SPONSORING/MONITORING AGENCY REPORT NUMBER
NASA TP-3542

11. SUPPLEMENTARY NOTES

12a. DISTRIBUTION/AVAILABILITY STATEMENT
Unclassified–Unlimited
Subject Category 02
Availability: NASA CASI (301) 621-0390

12b. DISTRIBUTION CODE

13. ABSTRACT *(Maximum 200 words)*

An investigation was conducted in the Jet-Exit Test Facility of the Langley 16-Foot Transonic Tunnel to evaluate the internal performance of highly integrated deployable exhaust nozzles (HIDEN) applicable to advanced short-takeoff and vertical-landing tactical aircraft. This investigation studied the performance of four HIDEN nozzle concepts in both the forward (thrust) and vertical (lift) operation modes. Two plenum designs with different offtake duct geometries varied the vertical distance between the plenum centerline and bearing plane surface centerline. Four plenum centerbodies with interchangeable blockers were tested to simulate engine fan- and core-mounted nozzle installations. All tests were conducted with no external flow and nozzle pressure ratio (NPR) was varied from 1.5 to approximately 6.0. Results indicate that the HIDEN nozzle concept has internal performance characteristics comparable to thrust-vectoring convergent-divergent nozzles. However, the exhaust flow was slightly underturned with each nozzle design, which resulted in a cosine thrust loss. Nozzles installed on the offset plenum had higher internal performance than the same nozzles installed on the centerline plenum throughout the entire NPR range investigated. Changing operation mode had only small effects on internal performance characteristics. Centerbody and blocker effects were also small.

14. SUBJECT TERMS
Short takeoff; STOVL; Thrust vectoring; Ventral nozzle; Vertical landing; V/STOL

15. NUMBER OF PAGES
278

16. PRICE CODE
A13

17. SECURITY CLASSIFICATION OF REPORT
Unclassified

18. SECURITY CLASSIFICATION OF THIS PAGE
Unclassified

19. SECURITY CLASSIFICATION OF ABSTRACT
Unclassified

20. LIMITATION OF ABSTRACT